Backbone *N*-modified peptides: beyond *N*-methylation

Ana Iris Fernández-Llamazares Onrubia

Programa de Doctorat en Química Orgànica

Tesi Doctoral

Backbone *N*-modified peptides: beyond *N*-methylation

Ana Iris Fernández-Llamazares Onrubia

Dirigida i revisada per:

Prof. Fernando Albericio
(Universitat de Barcelona)

Dr. Jan Spengler
(Institut de Recerca Biomèdica Barcelona)

Barcelona, 2013

Tesi Doctoral

Backbone *N*-modified peptides: beyond *N*-methylation

Ana Iris Fernández-Llamazares Onrubia

UNIVERSITAT DE BARCELONA

INSTITUTE
FOR RESEARCH
IN BIOMEDICINE

Departament de Química Orgànica

Facultat de Química

Universitat de Barcelona

2013

A la meva família. A tots els que han farcit aquesta etapa doctoral de moments feliços. I, per sobre de tot, al Marc.

"Without music, life would be a mistake."
Friedrich Nietzsche

"If music be the food of love, please play on..."
William Shakespeare

INDEX

ABBREVIATIONS 1

GENERAL OBJECTIVES 7

GENERAL INTRODUCTION 11

1. Peptides as drugs 13
2. Peptide backbone *N*-modification: an overview 16
   i. *N*-methylation 17
   ii. Backbone cyclization 19
   iii. Peptoids and peptide-peptoid hybrids 21
   iv. Modification with other *N*-alkyl groups 24

CHAPTER 1 – Synthesis of *N*-triethylene glycol (*N*-TEG) amino acids and use as solid-phase building blocks 29

1.1. Introduction 31
1.2. Objectives 32
1.3. Issues in the synthesis of peptides containing *N*-alkyl groups 33
1.4. Results and discussion 40
   1.4.1. Synthesis of Fmoc-*N*-TEG amino acids 40
   1.4.2. Use of Fmoc-*N*-TEG amino acids in SPPS 42
1.5. Summary and conclusions 49

CHAPTER 2 – *N*-triethylene glycol (*N*-TEG) as a surrogate for the *N*-methyl group. Application to Sansalvamide A peptide analogs. 51

2.1. Introduction 53
2.2. Objectives 54
2.3. Results and discussion 55
   2.3.1. Synthesis of the *N*-TEG and *N*-Me analogs of Sansalvamide A peptide 55
   2.3.2. Effect of *N*-TEG vs. *N*-Me on biological activity 60
   2.3.3. Effect of *N*-TEG vs. *N*-Me on lipophilicity 62
   2.3.4. Effect of *N*-TEG vs. *N*-Me on conformation 66
2.4. Summary and conclusions 68

CHAPTER 3 – Replacement of the *N*-methyl group of Cilengitide by *N*-oligoethylene glycol (*N*-OEG) chains of increasing length: effect on biological activity and lipophilicity. 69

3.1. Introduction 71
3.2. Objectives 73
3.3. Results and discussion 73
   3.3.1. Synthetic approach 73
   3.3.2. Synthesis of the Fmoc-*N*-OEG valine derivatives 74
   3.3.3. Synthesis of cyclo[RGDf*N*MeV] 75
   3.3.4. Synthesis of cyclo[RGDf(*N*-OEG_2)V] 76
   3.3.5. Synthesis of cyclo[RGDf(*N*-OEG_{11})V] 78
      SPPS of the *N*-OEG_{11} pentapeptide using the *N*-OEG_{11} Val derivative as building block 78
      SPPS of the *N*-OEG_{11} pentapeptide using a dipeptidic building block 79
      Cyclization and deprotection 82
   3.3.6. Synthesis of cyclo[RGDf(*N*-OEG_{23})V] 84
      SPPS of the *N*-OEG_{23} pentapeptide using the *N*-OEG_{23} Val derivative as building block 84

SPPS of the *N*-OEG_{23} pentapeptide using a dipeptidic building block . . . 85
Cyclization and deprotection . . . 86
Stereochemical validation of the *N*-OEG_{23} cyclopeptide . . . 87
3.3.7. Evaluation of the serum stability of the *N*-OEG cyclopeptide analogs . . . 88
3.3.8. Evaluation of the biological activity of the *N*-OEG cyclopeptide analogs . . . 89
3.3.9. Evaluation of the lipophilicity of the *N*-OEG cyclopeptide analogs . . . 90
3.4. Summary and conclusions . . . 93

CHAPTER 4 – The backbone *N*-(4-azidobutyl) linker for the preparation of peptide conjugates. Synthesis of an *N*-(4-azidobutylated) analog of Cilengitide and conjugation with PEG . . . 97

4.1. Introduction . . . 99
4.2. Objectives . . . 101
4.3. Results and discussion . . . 101
4.3.1. Synthesis of cyclo[RGDf(*N*-$CH_2CH_2CH_2CH_2N_3$)V] . . . 101
4.3.1.1. Synthetic approach . . . 101
4.3.1.2. Synthesis of 4-azidobutanal . . . 102
4.3.1.3. Synthesis of Fmoc-*N*-(4-azidobutyl) valine . . . 103
4.3.1.4. Synthesis of H-Asp(O^tBu)-D-Phe-(*N*-$CH_2CH_2CH_2CH_2N_3$)Val-Arg(Pbf)-Gly-OH . . . 104
Strategy A: SPPS using Fmoc-*N*-(4-azidobutyl) valine . . . 104
Strategy B: SPPS by reductive N^{α}-alkylation of resin-bound valine with 4-azidobutanal . . . 106
Strategy C: Synthesis by a combined solid-phase/solution approach . . . 109
4.3.1.5. Cyclization and deprotection . . . 111
4.3.2. Effect of *N*-(4-azidobutyl) vs. *N*-Me on conformation . . . 112
4.3.3. Synthesis of the PEG conjugates . . . 113
4.3.3.1. Synthetic approach . . . 113
4.3.3.2. Issues in the conjugation of peptides with polydisperse PEG . . . 114
4.3.3.3. Azide reduction . . . 116
4.3.3.4. Conjugation with PEG via amide bond formation . . . 117
4.3.3.5. Conjugation with PEG via reductive alkylation . . . 119
4.3.3.6. Conjugation with PEG via azide-alkyne cycloaddition . . . 121
4.3.3.7. A possible strategy to circumvent purification problems . . . 123
4.3.4. Evaluation of the biological activity of the PEG conjugates . . . 125
4.3.5. Evaluation of the lipophilicity of the PEG conjugates . . . 126
4.3.6. Study of conformational features of the PEG conjugates . . . 128
4.4. Summary and conclusions . . . 130

GLOBAL CONCLUSIONS . . . 133

EXPERIMENTAL SECTION . . . 137

RESUM DE LA MEMÒRIA . . . 187

BIBLIOGRAPHY . . . 211

ANNEXES . . . 231

Annex 1: Tables of amino acids, coupling reagents and protecting groups . . . 233
Annex 2: ^1H and ^{13}C-NMR assignment of the *N*-TEG and *N*-Me analogs of Sansalvamide A peptide . . . 235
Annex 3: ^1H and ^{13}C-NMR assignment of cyclo[RGDf*N*MeV] and its *N*-(4-azidobutylated) analog . . . 241
Annex 4: Cell adhesion inhibition curves of cyclo[RGDf*N*MeV] and the *N*-substituted cyclopeptides . . . 243
Annex 5: Publications . . . 245

ABBREVIATIONS

ABBREVIATIONS

δ	chemical shift
λ	wavelenght
ν	number of wavelenght
θ	ellipticity
$[\theta]_M$	molar ellipticity
$[\alpha]_D$	optical rotation
DMAP	4-dimethylaminopyridine
aa	amino acid
Ac-	acetyl
ACH	α-cyano-4-hydroxycinnamic acid
ACN	acetonitrile
AcOEt	ethyl acetate
AcOH	acetic acid
ADME	absorption, distribution, metabolism and excretion
Aib	α-aminoisobutyric acid
Alloc-	allyloxycarbonyl
anh.	anhydrous
aq.	aqueous
bs	broad signal
BTC	bis(trichloromethyl)carbonate, triphosgene
BTSA	*N*,*O*-bis(trimethylsilyl)acetamide
BSA	bovine serum albumin
c	concentration
calc.	calculated
CD	circular dichroism
COMU	1-[(1-(cyano-2-ethoxy-2-oxoethylideneaminooxy)-dimethylamino-morpholinomethylene)] methanaminiumhexafluorophosphate
conc.	concentrated
COSY	homonuclear correlation spectroscopy
CTC	2-chlorotrityl chloride (resin)
C18	octadecylsilane, octadecyl carbon chain-bonded silica
d	doublet

DCM	dichloromethane
dd	double doublet
DIEA	*N*,*N*-diisopropylethylamine
DIPCDI	*N,N'*-diisopropylcarbodiimide
DMEM	Dubelco's modified Eagle's medium
DMF	*N,N*-dimethylformamide
DMSO	dimethylsulfoxide
DSS	sodium 4,4-dimethyl-4-silapentane-1-sulfonate
dt	double triplet
EBM	endothelial basal medium
EDC·HCl	*N*-ethyl-*N'*-(3-dimethylaminopropyl)carbodiimide hydrochloride
EDTA	ethylenediaminetetraacetic acid
EP	expected product
ELISA	enzyme-linked immunosorbent assay
eq	equivalent
ESI	electrospray ionization
ES^+	electron single impact ionization in positive mode
e.g.	*exempli gratia*, for example
FB	fibrinogen
FBS	fetal bovine serum
FCS	fetal calf serum
FDA	Food and Drug Administration
Fmoc-	9-fluorenylmethoxycarbonyl
HATU	*O*-(7-azabenzotriazol-1-yl)-*N*,*N*,*N'*,*N'*-tetramethyluronium hexafluorophosphate
HBTU	*O*-(benzotriazol-1-yl)-*N*,*N*,*N'*,*N'*-tetramethyluronium hexafluorophosphate
HBSS	Hank's balanced salt solution
HOAt	1-hydroxy-7-azabenzotriazole
HOBt	1-hydroxybenzotriazole
HPLC	high pressure liquid chromatography
HPLC-MS	high pressure liquid chromatography coupled to an MS detector
HRMS	high ressolution mass spectrometry
HSQC	heteronuclear single-quantum correlation spectroscopy
IC_{50}	half maximal inhibitory concentration
IR	infrared

i.e.	*id est*, in other words, that is
J	coupling constant
m	multiplet
MALDI-TOF	matrix-assisted laser desorption ionization - time of flight
MeOH	methanol
MS	mass spectrometry
MTT	3-(4,5-dimethylthiazol-2-yl)-2,5-diphenyltetrazolium bromide
MW	microwave
NMR	nuclear magnetic ressonance
NOE	nuclear Overhauser effect
NOESY	nuclear Overhauser effect correlation spectroscopy
NPC	net peptide content
n.d.	non determined
OEG	oligoethylene glycol
OSu	*N*-hydroxysuccinimidyl ester
OxymaPure	ethyl-2-cyano-2-(hydroxyimino)acetate
P	partition coefficient
Pbf-	*2,2,4,6,7-pentamethyl-2,3-dihydrobenzofuran-5-sulfonyl*
PBS	phosphate buffered saline
PEG	polyethylene glycol
Pnb-	*p*-nitrobenzyl
ppm	parts per million
PyBOP	(benzotriazol-1-yl-oxy)tri(pyrrolidino)phosphonium hexafluorophosphate
q	quadruplet
RGD	peptide sequence arginine-glycine-aspartic acid
RP	reversed-phase
rpm	revolutions per minute
RPMI 1640	Roswell Park Memorial Institute medium
rt	room temperature
s	singlet
sat.	saturated
SM	starting material
SPPS	solid-phase peptide synthesis
t	triplet

T	temperature
$t_{1/2}$	half-life
TEG	triethylene glycol
TFA	trifluoroacetic acid
TFE	trifluoroethanol
TFFH	tetramethylfluoroformamidinium hexafluorophosphate
THF	tetrahydrofurane
TIS	triisopropylsilane
TLC	thin layer chromatography
TMS	trimethylsilane
TOCSY	total correlation spectroscopy
t_r	retention time
UV	ultraviolet
VN	vitronectin

GENERAL OBJECTIVES

GENERAL OBJECTIVES

The present Thesis is devoted to the synthesis of novel backbone *N*-substituted peptides, and to the study of their properties in comparison to *N*-Me peptides.

The specific objectives of each Chapter (1, 2, 3, and 4) are detailed in the corresponding Sections (1.2., 2.2., 3.2., 4.2., respectively).

Briefly:

- In **Chapter 1**, we sought to establish a synthetic methodology for the introduction of short *N*-oligoethylene glycol (*N*-OEG) chains into peptides on the solid-phase. In particular, we investigated the synthesis of Fmoc-amino acids bearing an *N*-triethylene glycol (*N*-TEG) group and their use as solid-phase building blocks.

- In **Chapter 2**, we sought to study the *N*-triethylene glycol (*N*-TEG) group as a surrogate for the *N*-Me group. For such an aim, we chose Sansalvamide A peptide as a model, and we sought to investigate how *N*-TEG vs. *N*-Me incorporation affects its biological activity, lipophilicity, and conformation.

- In **Chapter 3**, we sought to investigate upon which OEG chain length the acylation of an *N*-OEG amine is feasible. For such an aim, we chose Cilengitide as a model. A second objective of this Chapter was to investigate how *N*-Me-for-*N*-OEG substitution affects the biological activity and lipophilicity of our model peptide, and how these features are affected upon increasing the length of the OEG chain.

- In **Chapter 4**, we sought to study the *N*-(4-azidobutyl) group as a linker to support conjugation in peptides. For such an aim, we chose Cilengitide as a model, and we sought to apply our linker for the attachment of a polydisperse polyethylene glycol (PEG) chain. Other objectives of this Chapter were: i. to investigate the effect of *N*-Me-for-[*N*-(-azidobutyl)] substitution on the conformation of our model peptide, ii. to compare the biological activity, lipophilicity and conformation of the *N*-substituted cyclopeptide analogs with that of the unmodified peptide.

GENERAL INTRODUCTION

1. Peptides as drugs

Peptides are key regulators of a wide range of physiological processes and interact with numerous biological targets involved in pathological settings, thereby providing a vast opportunity for biomedical applications.[1] Currently, there are more than 100 peptide drugs on the market worldwide, around 140 in clinical phase trials, and more than 500 in preclinical phases.[2]

In recent years, the therapeutic potential of peptides has attracted growing attention from the pharmaceutical industry and academia.[3] Such a revival of interest may have been fuelled by the following fact: while the number of approved drugs is decreasing (as well as the number of small molecule drug candidates that enter clinical trials), an increasing number of peptide active pharmaceutical ingredients (APIs) have been approved for therapy in the past 10 years.

Indeed, peptides have a number of unique properties that make them potentially useful drugs (see Table 1).[3b] Many peptides are highly active and selective agonists or antagonists of different receptors involved in human diseases. These peptides have often undergone natural selection, and they can bind to their *in vivo* targets with exquisite specificity and great potency of action. Due to this high target specificity, peptide drug candidates offer potential for minimimum side-effects, which is a serious drawback of small molecule-based drugs. When compared to small molecules, another advantage of peptides is their low systemic toxicity (as their degradation products are only amino acids). Along these lines, peptides generally show a short half-life and do not accumulate in tissues, thereby minimizing the risk of possible complications from their metabolites. Remarkably, peptide drug candidates also offer various advantages over proteins and antibodies. Owing to their smaller size, peptides show a better penetration into tissues. In addition, they are generally less immunogenic, cheaper to manufacture (synthetic versus recombinant production), and more stable.

Table 1. Advantages and disadvantages of peptides as drugs. Adapted from [3b].

<table>
<tr><th colspan="2">Advantages</th><th>Disadvantages</th></tr>
<tr><td colspan="2">▪ High potency and selectivity towards a broad range of targets
▪ High chemical and biological diversity
▪ High target specificity
▪ Minimimum risk of systemic toxicity (i.e. the degradation products are amino acids)</td><td rowspan="2">▪ Poor metabolic stability
▪ Poor membrane permeability
▪ Poor oral bioavailability
▪ Rapid clearance
▪ Sometimes poor solubility
▪ High production costs (in comparison to small molecule drugs)</td></tr>
<tr><td>In comparison to small molecule drugs:
▪ Fewer side-effects (due to their high target specificity)
▪ Lower accumulation in tissues (due to their short half-life)
▪ Discoverable from the encoded nucleic acids</td><td>In comparison to protein and antibodies:
▪ Greater efficacy (i.e. higher activity per unit mass)
▪ Better penetration into tissues (owing to their smaller size)
▪ Potential for less immunogenicity
▪ Defined chemical structure that can be synthesized chemically
▪ Lower manufactoring costs (chemical versus recombinant production)
▪ Greater stability (lengthy storage at room temperature acceptable)
▪ Simpler intellectual property landscape</td></tr>
</table>

However, peptides present several disadvantages for their practical application in medicine.[3a] First, many peptides have a short *in vivo* half-life, owing to a fast degradation by proteolytic enzymes and a rapid renal clearance. Another

limitation is that most peptides show poor transport rates across biological barriers, such as the brush-border membranes in the intestinal tract or the blood-brain-barrier, and thus they are not suitable for oral delivery. In addition, many peptide agonists show low receptor subtype selectivity, which results in non-selective receptor binding.

Researchers have developed an array of strategies to overcome these issues.[3a,4] Many of them are based on chemical modification (see Table 2). Approaches to increase the enzymatic stability of peptides include cyclization, *N*-methylation, incorporation of non-natural amino acids (such as D- and β-amino acids), incorporation of peptide bond isosteres in those sites that are susceptible to proteolytic cleavage, and peptidomimetics. Among these modifications of a peptide structure, those that decrease the hydrogen-bonding potential and increase hydrophobicity (*e.g.* cyclization, *N*-methylation, incorporation of peptoid residues) generally enhance intestinal permeability, and can be used to gain oral bioavailability. Strategies to reduce the clearance rates of peptides are based on increasing their molecular size to prevent filtration by the kidneys. These strategies include modification with PEG, conjugation with albumin, and genetic fusion to the Fc domain of human gamma immunoglobin (IgC) antibody. Besides increasing overall size, these modifications also protect peptides from exopeptidases, thereby increasing metabolic stability. However, the conjugation of a peptide with a large moiety may lower its biological activity due to steric reasons. Finally, the receptor affinity of peptide ligands can be fine-tunned through conformational constraints, which can be imposed through cyclization, *N*-methylation, incorporation of non-natural amino acids (such as D-amino acids, β-amino acids, α,α-disubstituted amino acids), and peptidomimetics.

As can be seen in Table 2, some of the strategies to improve the therapeutic potential of peptides involve modification of their backbone by *N*-alkylation. Such modifications are highlighted in bold, and will be explained in the following Section.

Table 2. Some strategies to overcome the limitations of peptides as drugs. Adapted from [3a].
Highlighted in bold are those strategies that involve modification of the peptide backbone by *N*-alkylation.

Chemical modification	Effects	Aims
Cyclization of the peptide sequence ▪ Various cyclization modes: head to tail, side-chain to side-chain, head/end to side-chain, ***N*-backbone to *N*-backbone, *N*-backbone to head/end/side-chain**. ▪ Various types of linkage: amide, disulfide, lanthaionine, carba, hydrazine, lactam, alkene, and triazole, among others.	Conformational constraints. Less conformational flexibility. Decreased hydrogen-bonding potential. Increased hydrophobicity.	Optimized activity and/or selectivity to a biological target (as a result of conformational modulation). Increased proteolytic stability. Enhanced membrane permeability.
Replacement of natural amino acid residues by other unnatural amino acids ▪ D-amino acids ▪ β-amino acids ▪ conformationally constrained amino acids (*e.g.* α,α-dialkyl amino acids, α-trifuloromethyl amino acids) ▪ ***N*-alkyl amino acids** (mainly, *N*-Me amino acids) ▪ **Peptoid residues** (*N*-alkylated Gly derivatives)	Conformational constraints (*e.g.* D- and *N*-alkyl amino acids favour a *cis* configuration at the adjacent amide bond).	Increasing activity and/or selectivity to a biological target (as a result of conformational modulation). Increased proteolytic stability.
	<u>For *N*-alkyl amino acids and peptoid residues:</u> Decreased hydrogen-bonding potential. Increased hydrophobicity.	<u>For *N*-alkyl amino acids and peptoid residues:</u> Increased proteolytic stability. Enhanced membrane permeability.
Modification of amide bonds ▪ Modification of the CO group: -CH_2-NH- (reduced bond), -C(=S)-NH- (endothiopeptide bond), -P(=O)-OH-NH- (phosphonamide bond), and others. ▪ Modification of the NH group: -CO-O- (depsipeptide bond), -CO-S- (thioester bond), -CO-CH_2- (ketomethylene bond), **-CO-NR- (*N*-alkylated amide bond: peptoids)**, and others. ▪ Modification of both CO and NH groups: -NH-CO- (retro-inverso bond), -CH_2-S- (thiomethylene bond), -CH_2-CH_2- (carba bond), -CH=CH- (alkene bond), alkyne bond,-CHOH-CH_2- (hydroxyethylene bond), triazole, and others. ▪ Modification of CO and/or NH groups and also the α-carbon: oxazole-peptides, thiazole-peptides, aza-peptides, phosphonopeptides, and others. Modification of certain amide bonds within a peptide structure yields a <u>pseudo-peptide</u>; modification of all the amide bonds yields a <u>peptidomimetics</u> (*i.e.* a nonpeptide molecule).	Conformational constraints. Altered hydrogen-bonding potential. Altered hydrophobicity.	Optimized activity and/or selectivity to a biological target (as a result of conformational modulation). Increased proteolytic stability.
Modification of the *N*- or *C*-terminus ▪ by *N*-acylation, *N*-alkylation, *N*-pyroglutamate formation, *C*-amidation, *N*- or *C*-glycosilation (*i.e.* attachment of a carbohydrate moiety, such as glucose, xylose, or hexose), *N*-phosphoesterification, and others.		Increased proteolytic stability.
PEGylation ▪ Attachment of PEG moiety onto a peptide is usually achieved through its *N*- or *C*-terminus, or through its side-chain functional groups.	Shielding of backbone amide bonds. May shield certain peptide regions that are recognized by the immune system. Increase in molecular size. Drawback: risk of decreased or total loss of biological activity.	Increased proteolytic stability. Reduced immugenicity. Reduced renal and hepatic clearance (for conjugates >50 KDa).
Conjugation to a macromolecular carrier (*e.g.* serum albumin, the Fc fragment of IgG antibody)	Shielding of backbone amide bonds. May shield certain peptide regions that are recognized by the immune system. Increase in molecular size. Drawback: risk of decreased or total loss of biological activity.	Increased proteolytic stability. Reduced immugenicity. Reduced renal and hepatic clearance.

2. Peptide backbone *N*-modification: an overview

The amide bonds are intrinsic structural elements of peptides. In peptides, *N*-Me amino acids and Pro are the only naturally occurring residues in which the *NH* group is *N*-alkylated, and their presence in a peptide leads to a tertiary amide bond. Whereas Pro is incorporated into peptides by the usual ribosomal enzymatic machinery, *N*-methylated peptides are produced by large multifunctional enzymes in the non-ribosomal peptide synthetases.[5]

Remarkably, there are many bioactive peptides of natural origin that contain backbone *N*-Me groups within their structure.[6] Indeed, some of these peptides are highly *N*-methylated and exhibit excellent pharmacokinetic profiles (see Figure 1).

Figure 1. Structure of Cyclosporin A and Omphatolin A. Both are naturally occurring bioactive peptides that contain a high number of *N*-Me residues. Cyclosporin A is marketed as an orally active antiimmunopressive drug.

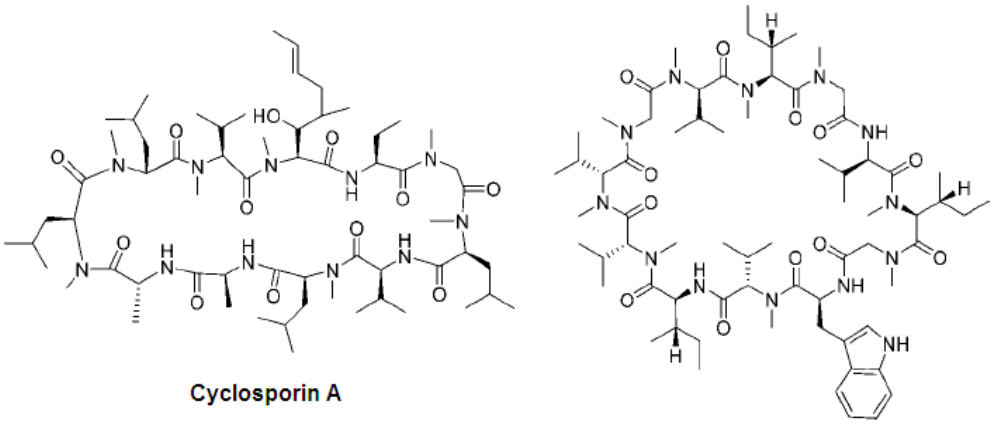

The willful introduction of *N*-Me groups in natural or *de novo*-designed peptides has resulted in numerous analogs with improved pharmacological properties.[6] Along these lines, medicinal chemists have investigated other modifications of the peptide backbone that also involve *N*-alkylation, such as backbone cyclization[7] and the introduction of peptoid residues.[8] Regardless of the nature of the *N*-alkyl group, its incorporation into a peptide generally affects its conformation and, hence, its biological activity. In addition, *N*-alkylation of a peptide decreases the number of amide protons that can act as hydrogen bond donors. This results in higher hydrophobicity, increased resistance to proteolytic cleavage, and –in most cases– enhanced instestinal permeability.[9]

In this Section, we sought to give a brief overview of those backbone *N*-modifications that are permanent: *N*-methylation, backbone cyclization, peptoids and peptide-peptoid hybrids, and modification with other *N*-alkyl groups different than *N*-Me. All these structural modifications are not only of interest from a medicinal chemistry point of view, but also for other specific applications.*

* *Note:* Other types of backbone *N*-modification are reported in which the *N*-substituent is only temporarily present. Protection of the backbone *NH* groups can be useful to prevent side-reactions and/or chain aggregation during solid-phase peptide synthesis. Reported backbone *N*-protectants include Hmb-, Dmb-, EDOTn-, MIM-, and Dcm-, (basically used for Gly and Ala), and pseudoprolines (only applicable for Thr, Ser and Cys).

i. *N*-Methylation

Backbone *N*-methylation is an established tool to improve various pharmacological properties of peptides drug candidates.[6] On one hand, it is a general method to impose conformational constraints on peptides with the aim of optimizing their activity and/or selectivity. On the other hand, the introduction of backbone *N*-Me groups in peptides increases their hydrophobicity, their enzymatic stability, and –in many cases– their intestinal permeability, thereby improving their bioavailability upon oral administration.

For the synthesis of peptides containing *N*-Me residues, there are two possible strategies to introduce the *N*-Me group: i. by using an *N*-Me amino acid derivative as building block, ii. by site-selective *N*-methylation of the α-amino group in solid-phase.

- In the first strategy, commercial *N*-Me building blocks can be used. Currently, all the Fmoc- and Boc-protected *N*-Me derivative of proteogenic amino acids can be purchased, but they are not available for certain protecting group combinations and, in general, they are expensive. Alternatively, the required *N*-Me amino acid derivatives can be prepared in solution through a plethora of methods,[10] among which the most generally applicable is the *N*-methylation of an *N*-arylsulfonamide-protected amino acid ester under Mitsunobu conditions.[11]

- In the second strategy, site-selective N^{α}-methylation of the resin-bound peptide is accomplished by a 3-step procedure that was originally developed by Miller and Scalman.[12] In this procedure, the α-amino group of the resin-bound peptide is activated with the *o*-nitrobenzenesulfonyl (*o*NBS) group, followed by *N*-methylation of the activated nitrogen via a direct nucleophilic substitution, and then removal of the sulfonamide group. Conditions for the nucleophilic step were optimized by Kessler and co-workers, who used dimethyl sulfate as methylating agent and DBU as base.[13] Alternatively, solid-phase *N*-methylation of the *o*NBS-protected amine can be performed via a Mitsunobu reaction (see Scheme 1).[14]

Scheme 1. Site-selective N^{α}-methylation of peptides on a solid support.[13]
A) Via Mitsunobu reaction. B) Via direct nucleophilic substitution.

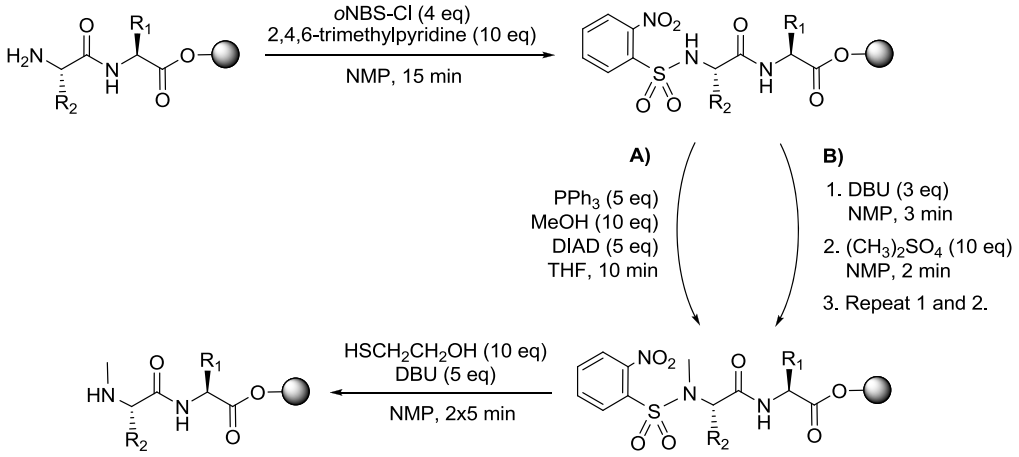

As previously mentioned, backbone *N*-methylation can have a strong impact on the conformation of a peptide. This can be due to various factors, or due to a combination of them. First, *N*-methylation lowers the energy difference between the *cis* and *trans* configuration of the *N*-methylated amide bond, favouring the *cis* configuration.[15] Thus, the *N*-methylated peptide may adopt conformations that would otherwise not be possible. Second, *N*-methylation eliminates one of the hydrogen bond donors of the peptide. This can alter its pattern of intramolecular hydrogen bonds, and may result in a distinct hydrogen-bonding pattern by which a different conformer is stabilized. Finally, *N*-

methylation can induce local backbone constraints due to steric reasons, thereby introducing some conformational rigidity.[16] Because of all these reasons, the introduction of backbone *N*-Me groups into a peptide is expected to affect its conformation and, hence, its biological activity.

For a target peptide sequence, a systematic method to identify those *N*-Me analogs that show the highest activity and/or other optimized properties (*i.e.* selectivity, enzymatic stability, membrane permeability) is the *N*-Me scan. In this approach, a library of peptides with *N*-Me residues at different positions is synthesized and tested. Since the library consists of *N*-Me peptides having the same sequence but differing in their conformation, peptides selected based on their activity are likely to have the best conformation for interacting with the chosen target receptor. Along these lines, it is important to note that the presence of a an *N*-Me group may also decrease biological activity by sterically interfering with the peptide-receptor interaction. Therefore, unless details of the peptide-receptor interaction are known, a decreased biological activity for a given *N*-Me analog of the library can not be unambiguously attributed to a conformation in which the pharmacophoric groups are not well-oriented for binding.

Early on, the introduction of backbone *N*-Me groups in a trial-and-error manner led to metabollically stable analogs of numerous bioactive peptides, resulting in some cases in enhanced activity and selectivity. With the *N*-Me scan approach, a great number of *N*-methylated analogs with improved activity and/or pharmacokinetics have been discovered from peptide leads. In addition to library-based strategies, conformational design approaches have also yield success. For examples on the discovery of *N*-methylated peptide analogs with improved pharmacological properties, refer to Sagan *et al.*[17]

Figure 2. Structures of three peptides that contain *N*-Me groups and are currently in clinical phase trials for cancer treatment. Aplidine is a natural product, whereas TZT-1027 and Cilengitide are non-naturally occurring.

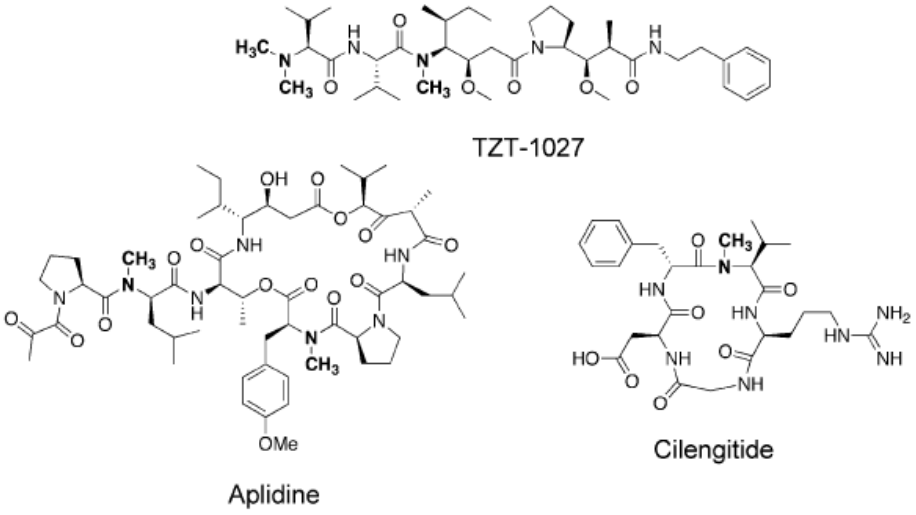

Besides the well-known effects of backbone *N*-methylation on conformation, hydrophobicity, and enzymatic stability, recent studies on *N*-methylated cyclic peptides cleary suggest that *N*-methylation enhances the intestinal permeability of peptides[9,18] and can improve their oral bioavailability.[19] The presence of *N*-Me groups in peptides increases their transport across membranes by favouring passive transcellullar diffusion. This has been attributed to the decreased hydrogen-bonding potential and increased hydrophobicity of *N*-methylated peptides,[20] and also to certain conformational features upon *N*-methylation.[9,18a,19b]

Current research within the *N*-methylation field is aimed at understanding how the incorporation of multiple *N*-Me groups into bioactive peptides affects their conformation, activity, and intestinal permeability. Very recently, the

Kessler group has reported various interesting findings on these issues.[6] First, they found that there is a regular pattern in the way how multiple *N*-methylation modulates the conformation of cyclic pentapeptides,[21] and that the conformational effects induced by the presence of various *N*-Me residues are similar to those induced by Pro.[22] Second, Kessler *et al.* showed that multiple *N*-methylation of a bioactive cyclic peptide can greatly enhance its activity and selectivity towards different receptor subtypes.[23] By varying the positions of the *N*-Me groups, the selectivity of a cyclic peptide towards different subtypes of receptors can be fine-tunned. The high selectivity achievable is due to the conformational rigidity imposed by cyclization and multiple *N*-methylation, and cannot be achieved by any of these two structural modifications alone.[24] Finally, it has been shown that multiple *N*-methylation introduces remarkable metabolic stability,[19a,25] makes the peptide substantially more hydrophobic, and can result in a markedly enhanced intestinal permeability.[18a]

ii. Backbone cyclization

Backbone cyclization is a general method to impose conformational constraints on peptides with the aim of achieving higher activity and/or selectivity. In this type of cyclization, which was first introduced by Gilon,[7] ring formation is accomplished by interconnecting a backbone nitrogen with: a. another backbone nitrogen, b. a side-chain functionality, c. the *N*- or the *C*-terminus (see Figure 3). The resulting conformationally constrained peptides can differ in the position of the backbone bridge, in the ring size, and in the chemistry of the linkage. Therefore, with backbone cyclization, a variety of cyclic structures can be prepared for any target peptide sequence without altering its original side-chains. This is not possible with other cyclization modes (*i.e.* ends to side-chain, side-chain to side-chain) that can also be applied for conformational constriction and/or for increasing metabolic stability.

Figure 3. Various modes of backbone *N*-cyclization.

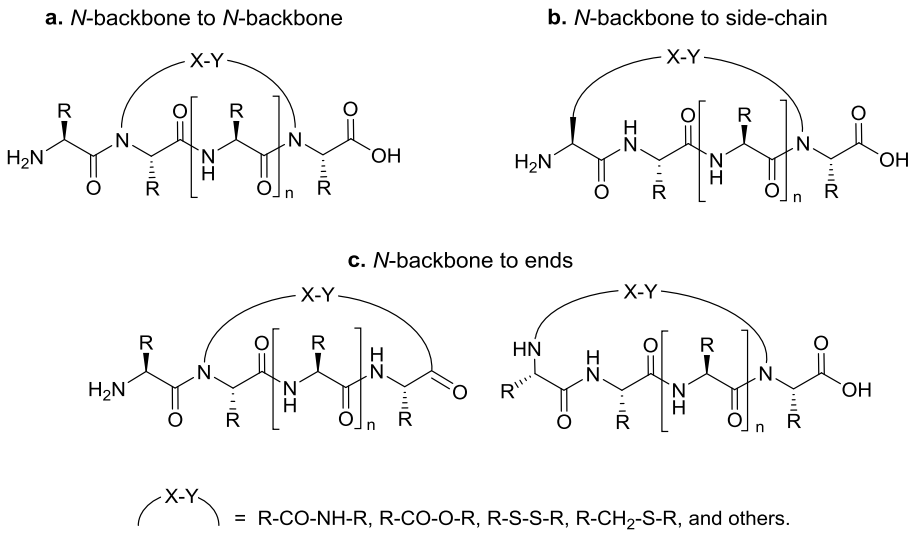

Notably, backbone cyclization combines two structural modifications that are known to improve proteolytic stability and intestinal permeability: cyclization and backbone *N*-alkylation. The increased proteolytic resistance of backbone cyclic peptides with respect to linear peptides is well-known, and their enhanced intestinal permeability via membrane passive diffusion has been recently demonstrated in a systematic study.[26]

The synthesis of backbone cyclic peptides relies on *N*-functionalized building blocks bearing amino, carboxy, alkenyl, or sulfanyl moieties. These building blocks have to be prepared in advance,[27] and their incorporation into a peptide

sequence requires special activation methods, since the acylation of secondary amines is hampered by steric hindrance.[28] After assembling the *N*-functionalized linear precursor, its cyclization is performed in solution.

In order to identify the most bioactive backbone cyclic analog from a given peptide sequence, Gilon *et al.* developed a method called "cycloscan".[29] In this selection method, a combinatorial library of backbone cyclic peptides is prepared and then screened for biological activity. Possible variations in such library include: i. mode of backbone cyclization, ii. positioning of the backbone bridge along the peptide sequence, iii. ring size, and iv. ring chemistry. Since the library consists of backbone cyclic peptides having the same sequence but differing in their conformation, peptides selected based on their activity are likely to have the best conformation for interacting with the target receptor.

Backbone cyclization in combination with cycloscan has been applied to improve the activity and selectivity of numerous peptides.[30] A successful example is the discovery of peptide PTR 3046, a backbone cyclic analog of Somatostatin-14 (SRIF) that shows enhanced selectivity for receptor-5 (see Figure 4).[30c] Along these lines, the backbone cyclization-cycloscan approach has been extensively used to improve the metabolic stability of known peptides, such as Substance P,[30a] pheromone biosynthesis-activating neuropeptide,[31] Somatostatin,[32] and Tat.[33] More recently, the backbone cyclization-cycloscan approach has been applied to improve the oral availability of peptide drug candidates.[34]

Figure 4. A) Structure of cyclo[(*N*-aminoethyl)Phe-Tyr-D-Trp-Lys-Val-(*N*-carboxypropyl)Phe]-Thr-NH_2 (PTR 3046), a backbone cyclic Somatostatin analog developed by Kessler and co-workers.[30c] **B)** Structure of Somatostatin-14 (SRIF).

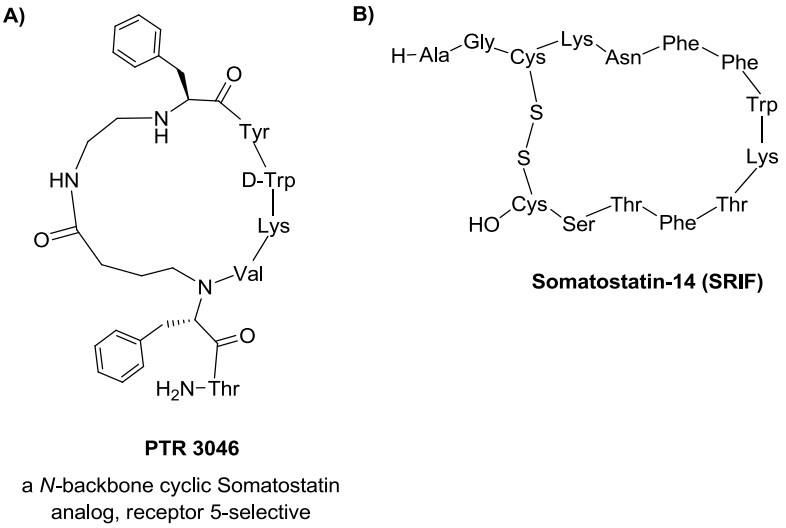

Current research within the backbone cyclization field is also aimed at the development of peptides that can mimic secondary structures of proteins.[33,35] In these proteinomimetic strategies, backbone cyclization is used to constrain a protein epitope into a well-defined secondary structure, and cycloscan allows to identify those backbone cyclic peptide-based proteinomimetics that can interact with a chosen protein receptor.

iii. Peptoids and peptide-peptoid hybrids

Peptoids are a class of biomimetic oligomers that are made of *N*-substituted Gly units.[36] They can be regarded as peptide mimics in which the side-chains are connected to the backbone nitrogens, instead being appended to the α-carbons (see Figure 5). These oligomers were initially proposed as an accessible class of molecules from which lead compounds could be identified for drug discovery. They can be efficiently synthesized in solid-phase by a modular

submonomer approach,[37] and such an approach allows the incorporation of a wide range of side-chain substituents that can be arranged in any particular sequence.

Figure 5. Generic structure of a peptide and a peptoid.

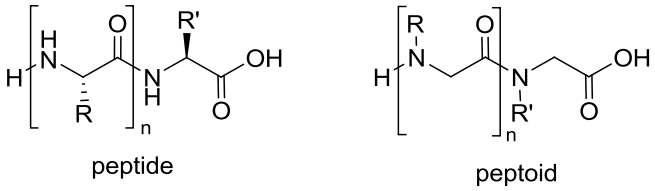

As peptides, peptoids can form stable secondary structures and can interact with a wide range of biological targets.[38] Due to the absence of amide protons, they are highly resistant to proteolytic degradation[39] and show enhanced membrane permeabilities compared to peptides.[40] Therefore, peptoids provide a vast opportunity for biomedical applications.

In general, peptoid oligomers show less conformational rigidity than peptides.[36] The lack of stereogenicity facilitates the *trans/cis* isomerization of the amide bonds and, due to the absence of amide protons, the peptoid secondary structure cannot be stabilized through backbone hydrogen-bonding in the same manner as in peptides. Likewise, the presence of *N*-alkyl groups lowers the energy of the *cis* configuration of *N*-alkylated amide bonds, thereby favouring their *trans*-to-*cis* isomerization. All these characteristics make peptoid oligomers highly flexible structures.

For molecular recognition applications in which conformational ordering is desired, several methods have been developed for stabilizing helical, loop and turn motifs in peptoids by incorporating side-chains that restrict their backbone conformation.[38] For instance, the presence of bulky chiral side-chains can induce helical structures.[41] Further research has shown that peptoid folding can be stabilized by several types of non-covalent interactions. This knowledge has been applied for the rational design of peptoids that mimic well-defined secondary structures of bioactive peptides.[42]

For the solid-phase synthesis of peptoids, two main approaches have been described. The first method is based on the coupling of bromoacetic acid onto the free amine of the growing peptide, followed by nucleophilic reaction with a primary amine to obtain the desired *N*-alkylated Gly derivative (Scheme 2A).[37] The second method is based on the coupling of Fmoc-Gly-OH onto the peptidyl-resin, followed by N^{α}-deprotection and reductive alkylation with an appropriate aldehyde (Scheme 2B).[43] The first approach is often preferred, as: i. it avoids the N^{α}-deprotection step, ii. DIPCDI-activated bromoacetic acid is a highly reactive acylating species, due to its small size and the electron-withdrawing effect of the Br atom. This submonomer approach is very unexpensive and allows straightforward incorporation of a wide range of chemical functionalities. In addition to the intrinsic chemical diversity obtained through oligomer synthesis, strategies have also been developed for the preparation of suitably functionalized peptoids that can be chemically modified post-synthetically.[44]

Scheme 2. Two main synthetic strategies for the solid-phase synthesis of peptoids.
A) Submonomer approach using bromo acetic acid.
B) Submonomer approach involving reductive N^{α}-alkylation.

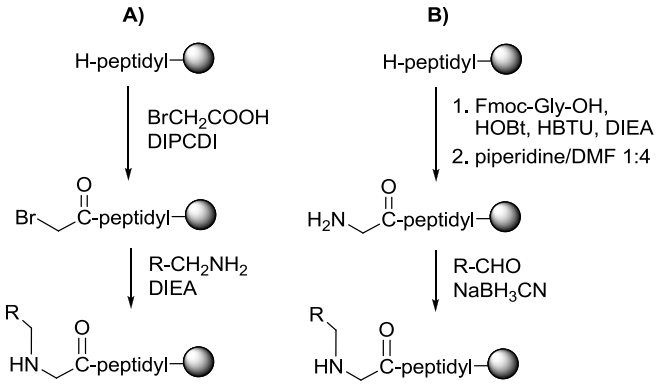

The ease of peptoid synthesis and their potential for a large chemical diversity makes peptoids ideal candidates for the combinatorial discovery of novel peptidomimetic drug candidates. Early on, the synthesis of combinatorial peptoid libraries allowed for the discovery of high-affinity ligands to pharmaceutically relevant receptors.[45] More recently, molecular design approaches have been successfully applied to generate peptoids that exhibit an array of biological activities.[38,46] Numerous peptoids have been developed as highly active and selective ligands for protein targets involved in human diseases, such as the Vascular Endothelial Growth Factor (VEGF) receptor 2[47] or the Src Homology 3 (SH3) domain[48] (see Figure 6). Along these lines, a peptoid that binds to the antibody IgG has been recently reported, and it was used as biomarker for the identification of Alzeimer's disease.[45d] Other rationally designed peptoids include α-helical mimics of antimicrobial peptides,[42b,45b,49] mimics of lung surfactant proteins,[50] and peptoids with cell-penetrating properties.[51]

Figure 6. Examples of peptoid ligands that bind to pharmacologically relevant receptors. **A)** Ligand for the VEGF receptor 2, Kodadek and co-workers.[47] **B)** Inhibitor of the HMD2-p53 interaction, Appella and co-workers.[42a]

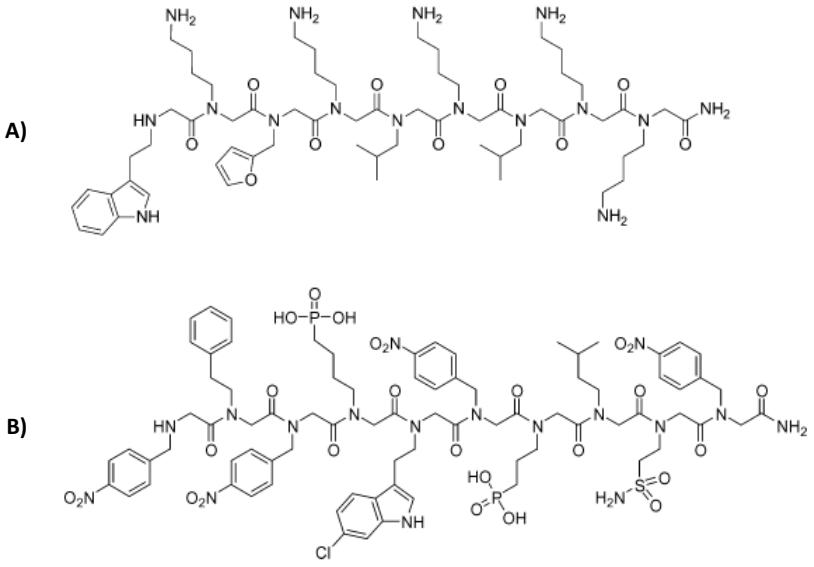

Along with the development of peptoid mimics, researchers have also designed numerous hybrid peptide-peptoid oligomers, often called "peptomers", for various biomedical applications (see Figure 7).[8] Examples include ligands for disrupting RNA-protein interactions,[52] ligands that bind to somatostatin-,[53] melanocortin-,[54] and opiod-receptors,[55] and a variety of antimicrobial peptomers.[56]

Figure 7. Examples of hybrid peptide-peptoid ligands that bind to RNA or protein targets of pharmacological interest. **A)** Inhibitor of the Tat-TAR RNA interaction, Hamy and co-workers.[52] **B)** Ligand for the Grb2 SH3 domain, Lim and co-workers.[48] **C)** Ligand for the EVH1 domain, Ball and co-workers.[57b]

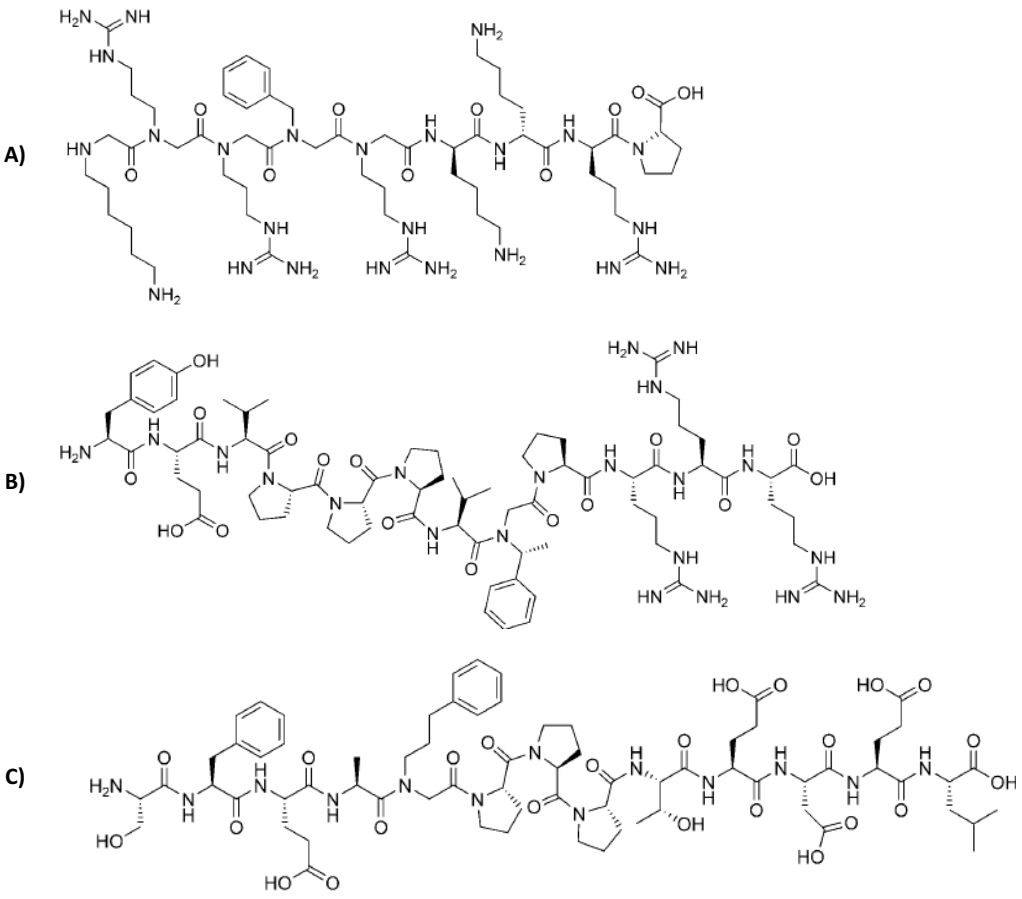

As peptoids, peptide-peptoid oligomers hold significant promise as therapeutic agents due to their enhanced enzymatic stability and membrane permeability. The incorporation of one or more *N*-alkylated Gly monomers into naturally occurrring peptides has led to analogs with improved pharmacological properties.[57] However, the transformation of a therapeutic peptide into a peptide-peptoid analog with equivalent biological activity is not straightforward, as biological activity can be substantially affected by minimal structural changes. For peptide-to-peptomer transformation, several analogs have to be synthesized, tested and further optimized, and such laborious trial-and-error approaches may yield limited success in the discovery of bioactive molecules.[58]

It is important to note that the replacement of all the amino acids of a peptide sequence by peptoid monomers with identical or similar side-chains is unlikely to yield a compound with analogous activity as the original peptide. The monomer-to-monomer substitution of peptide residues by peptoid residues alters the tridimensional arrangement of the pharmaphoric groups, and the conformational constraints imposed by *N*-alkylated Gly residues can drastically change the secondary structure of the oligomer.

Very recently, Barron *et al.* developed an applicable strategy for the identification of peptoid-replaceable residues in a target peptide sequence by combining Ala, Pro and Sar scans.[59] This method explores the conformational tolerance and the importance of each of the individual side-chains, providing information that cannot be obtained from NMR or X-ray structural studies. Along these lines, Hoffmann *et al*. proposed a systematic method for the discovery of bioactive peptoids from peptide leads.[60] The reported procedure is based on a peptidomimetic array in which each position of the peptide is exchanged by a set of different peptoid monomers. After probing the array towards protein binding, the best binding peptomer are selected and subjected to a successive transformation.

iv. Modification of the peptide backbone with other *N*-alkyl groups

Besides peptide-peptoid oligomers (in which the *N*-alkyl groups are exclusively placed at Gly residues) and backbone cyclic peptides, modification of the peptide backbone with other *N*-alkyl substituents different than the *N*-Me group has rarely been investigated. The only examples of other *N*-backbone-modified peptides so far described are limited to small *N*-alkyl groups.

Before reviewing such few examples, some remarks about their synthesis should be made. The synthesis of *N*-alkylated peptides through solution-phase methodologies generally involves the use of *N*-alkyl amino acid derivatives. For the preparation of such building blocks, only a few methods are described, and they are not general nor without problems.[27f,61] Specific routes to various *N*-ethyl amino acid derivatives have been developed.[62] For the synthesis of *N*-alkyl-containing peptides on a solid support, the *N*-substituent can be introduced by *o*NBS-activation of the α-amino group followed by Mitsunobu reaction with a suitable alcohol.[14]

Wenger *et al.* described the solution-phase synthesis of various *N*-ethyl analogs of Cyclosporin A (see Figure 8).[63] The substitution of the *N*-Me group at the fourth position of this cyclopeptide by an *N*-ethyl group was aimed to reduce immunosuppressive activity without affecting its potential anti-HIV activity. Examples in which *N*-ethyl peptides have been obtained by solid-phase methodologies are also reported, such as the *N*-ethyl scan of Leu-enkephalin performed by Liskamp *et al.* [14]

Figure 8. Structure of Cyclosporin A (CsA) and the *N*-ethyl analogs synthesized by Wenger and co-workers.[63]

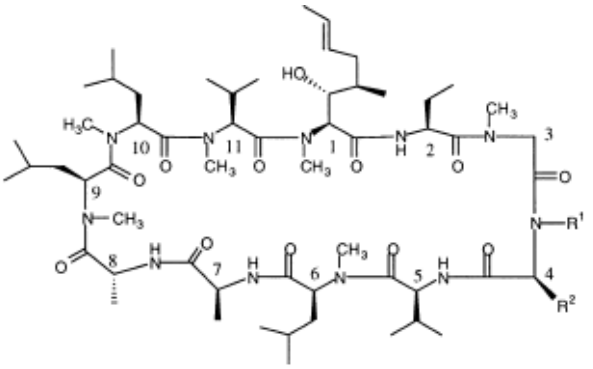

Compound	Residue 4	
	***N*-R^1**	**R^2**
CsA	*N*-Me	-CH_2-$CH(CH_3)_2$
(*N*-Et)Leu^4-CsA	*N*-Et	-CH_2-$CH(CH_3)_2$
(*N*-Et)Val^4-CsA	*N*-Et	-$CH(CH_3)_2$
(*N*-Et)Ile^4-CsA	*N*-Et	-$CH(CH_3)$-CH_2-CH_3
(*N*-Et)Thr^4-CsA	*N*-Et	-CH_2OH-CH_3

In a different study, Liskamp *et al.* reported the synthesis of an *N*-butylated derivative of human Amylin (25-29) (see Figure 9).[64] This peptide was designed to interfere with the aggregation of β-sheets that ultimately leads to the formation of amyloid fibrils. The introduction of an *N*-butyl group at the Ser position of human Amylin (25-29) alters its intermolecular hydrogen-bonding pattern, either as a result of steric hindrance or due to the absence of an essential amide proton, and this prevents further growth of the antiparallel β-sheet.

Figure 9. A) Structure of human Amylin (25-29) and the *N*-butylated derivative developed by Liskamp and co-workers as a β-sheet breaker.[64] **B)** Rationale for the design of β-sheet breaker peptides based on human Amylin (25-29). Adapted from [64].

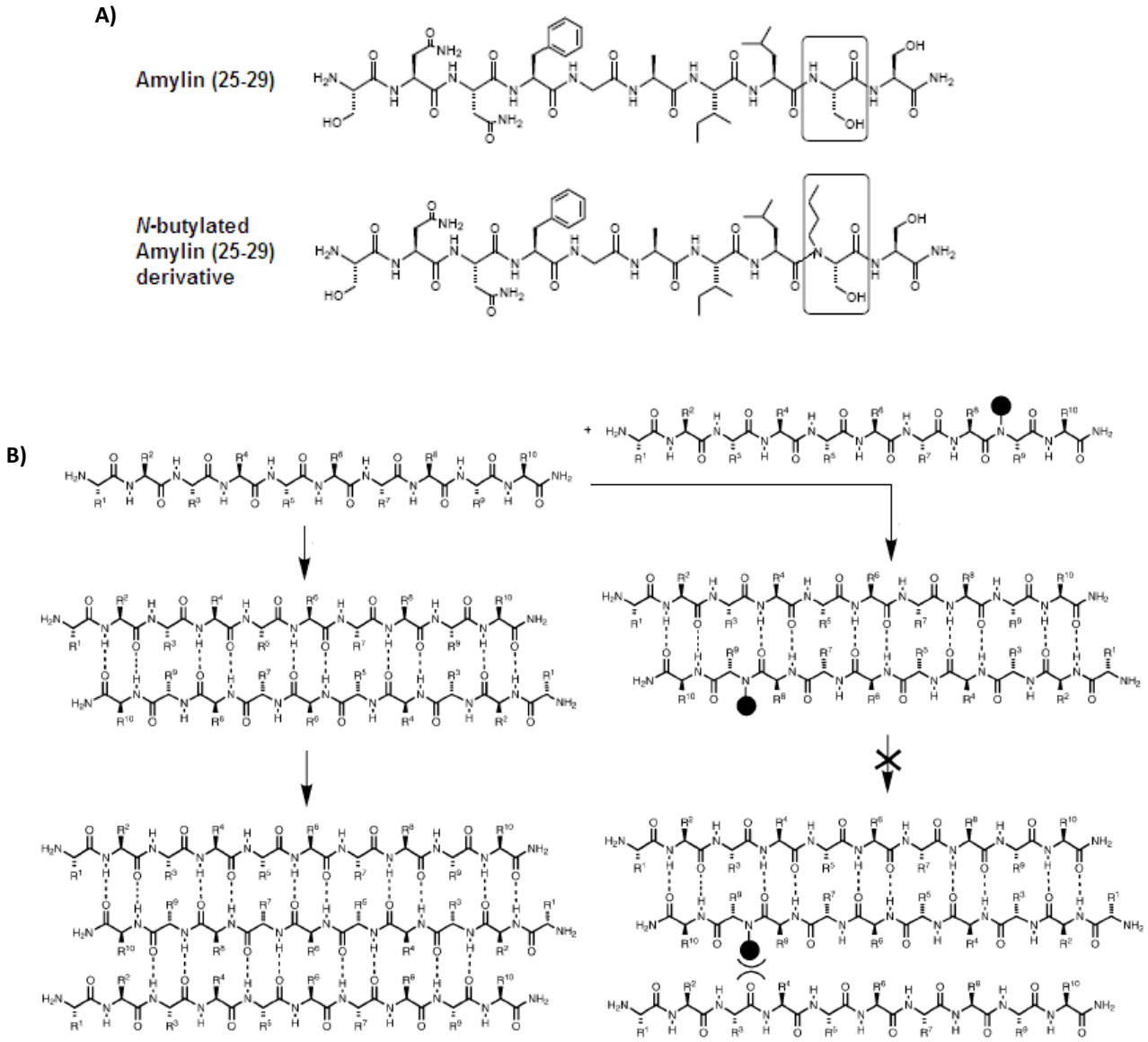

An impressive paper published by Aurora *et al.* described the synthesis several *N*-allyl-containing peptides and their ring-closing methatesis (RCM) (see Figure 10).[65] The resulting carbon-carbon bonds can stabilize short peptide sequences in a helical conformation, acting as hydrogen bond surrogates. If the *N*-allyl groups are placed at the appropriate positions of the peptide chain, the artificial α-helices derived from RCM can fully reproduce the conformation of a canonical α-helix,[66] and they can bind to target protein receptors in cell-free and cell-culture assays.[67]

Figure 10. Synthesis of hydrogen bond surrogate helixes by RCM of an *N*-allyl-containing peptide.[65]

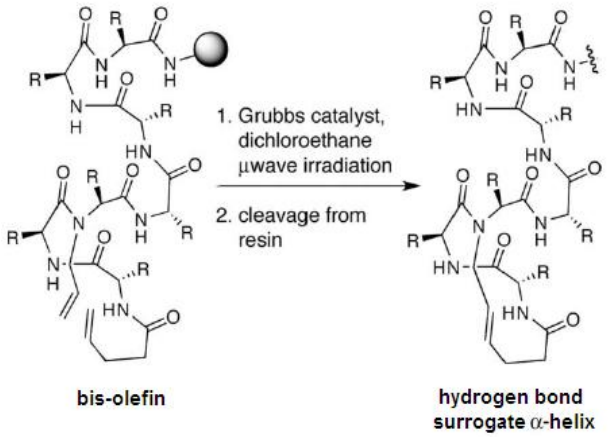

With the solid-phase synthesis of Ac-[Cys-His-D-Phe-(*N*-guanidylbutyl)Cys]-Trp-NH_2, Hruby *et al.* showed that an N-guanidylbutyl group can be introduced into a peptide by Mitsunobu N^{α}-alkylation with *N,N'*-diBoc-guanidinylbutanol (see Figure 11).[68] This *N*-guanidylbutyl-containing cyclopeptide is as a highly active and selective peptide ligand for the melanocortin 4 receptor (MC4R). It was discovered from MTII, another peptide-based antagonist for MC4R, by applying conformational constraints via ring contraction. The *N*-guanidylbutyl group was introduced to mimic the Arg side-chain originally present in MTII, which is an important pharmacophoric element.

Figure 11. Structure of Ac-[Cys-His-D-Phe-(*N*-guanidylbutyl)Cys]-Trp-NH_2, a highly active and selective ligand for the MC4R receptor, and MTII, the lead peptide from which it was discovered by Hruby and co-workers.[68]

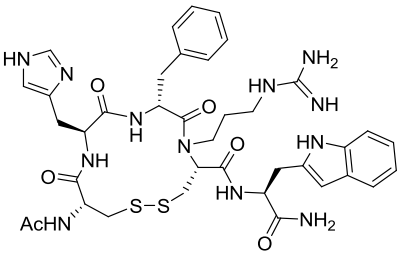

Ac-[Cys-His-D-Phe-(*N*-guanidylbutyl)Cys]-Trp-NH_2

IC_{50} = 1.8 nM for binding to MC4R

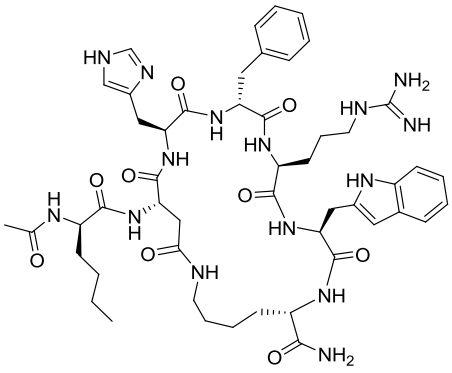

MTII

IC_{50} = 1.1 nM for binding to MC4R

Regarding the preparation of *N*-alkyl-containing peptides through combinatorial approaches, there is only one example reported. Houghten *et al.* described the synthesis of a combinatorial library of dipeptide amides *N*-alkylated at two positions: at the *C*-terminal backbone nitrogen and at the *C*-terminal amide function (see Figure 12).[69] This library was prepared by a split-and-mix approach. The synthesis was performed on the solid-phase by alternating amino acid attachment and *N*-alkylation of the previously formed amide bonds. The non support-bound library mixtures were screened in solution in antimicrobial, enzyme inhibition and radio-receptor assays.

Figure 12. General structure of the compounds of the combinatorial library synthesized by Houghten and coworkers.[69]

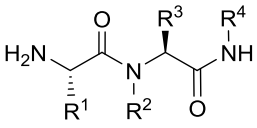

R^1 = >50 L, D- and unnatural amino acids
R^2 = methyl, ethyl, allyl, benzyl, naphthylmethyl
R^3 = >46 L, D- and unnatural amino acids
R^4 = methyl, ethyl, allyl, benzyl, naphthylmethyl

57500 compounds

CHAPTER 1

Synthesis of *N*-triethylene glycol (*N*-TEG) amino acids and use as solid-phase building blocks

---

Abstract: We have developed a scalable route to prepare Fmoc-protected *N*-TEG amino acids with satisfying yields. These building blocks are straightforward to obtain through reductive N^{α}-alkylation with 3,6,9-trioxadecanaldehyde, and they can be coupled onto a resin-bound peptide using standard activation methods. The acylation of *N*-TEG amines is hampered due to steric reasons, but can be achieved in solid-phase using triphosgene as activating reagent.

1.1. Introduction

As has been explained in the General Introduction, *N*-alkylation of the peptide backbone is of interest due to its conformational and physichochemical effects. However, modification of peptides with other *N*-alkyl groups different than *N*-Me has rarely been investigated. Besides peptoids (in which the *N*-substituents are only attached to Gly),[36] the only reported examples are limited to small *N*-alkyl groups (*i.e.* *N*-ethyl,[14,63] *N*-allyl,[14,65] *N*-butyl,[64] *N*-guanidylbutyl,[68] and short *N*-functionalized chains for backbone cyclization[7]).

This lack of precedents can be attributed to several issues concerning the synthesis of *N*-alkylated peptides.[70] The main difficulty is the acylation of *N*-alkyl amino acids, which is hampered by steric hindrance. In adddition, *N*-alkyl amino acids are prone to α-epimerization upon *COOH*-activation, and their presence in a growing peptide favours DKP formation. These and other side-reactions can become problematic in slow coupling reactions.

In the present Thesis, we sought to investigate the synthetic viability of modifiying the peptide backbone with larger *N*-substituents than the *N*-Me group. To investigate this, we focused on oligoethylene glycol (OEG) as *N*-substituting chemical moiety.

OEG is an oligomeric linear structure comprising between 2 and 24 ethylene oxide units, whereas polymers comprising more than 24 units are referred to as polyethylene glycol (PEG) (see Figure 13). OEG and PEG are frequently employed to optimize peptides for specific biomedical applications.[71] Their widespread use stems from their low toxicity, excellent aqueous solubility, and low antigenicity. Depending on their length and structure, they can serve as pharmacokinetic modifiers,[72] linkers to support conjugation with a desired molecule,[73] spacers to avoid non-specific interactions with the biological target, or scaffolds to create multimeric constructs that can simultaneously target different receptors.[74]

Figure 13. Structure of linear OEG and PEG.

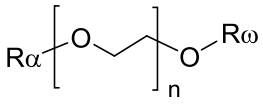

OEG: n = 2-24

PEG: n >24

In general, OEG and PEG are attached onto peptides post-synthetically.[75] A wide range of OEG and PEG derivatives are commercially available, differing in size, structure (linear or branched), functionalization (monofunctional, bifunctional…), and in the nature of the α- and ω-terminal groups. Since most PEG reagents are obtained by a polimerization process, they are polydisperse.[76] This means that, instead of having an exact number of ethylene oxide units, they have a distribution of polymer chain lengths around an average MW. In recent years, various OEG and PEG reagents of discrete length have become commercially available. However, these monodisperse reagents are very expensive, specially upon increasing OEG chain length.

In biomedical applications, polydispersity is not desirable. The attachment of a polydisperse PEG chain onto a peptide leads to a population of peptide-PEG conjugates of various sizes which may have different biological properties (*i.e.* biological activity, *in vivo* half-life, immunogenicity). Such mixtures of PEGylated products are difficult to analyze, purify, and characterize.[75b] Along these lines, the bioanalytical heterogenicity of polydisperse PEGylated products complicates their FDA approval of as drugs for clinical use.[77]

To avoid polydispersity issues, we sought to investigate peptide *N*-modification with an OEG substituent of discrete size. For this aim, we chose triethylene glycol (TEG). The reason for this choice is that triethyelene glycol monomethyl ether is commercially available at inexpensive price. We envisioned that amino acids bearing an *N*-TEG group could be obtained by reductive alkylation of the α-amino group with 3,6,9-trioxadecanaldehyde, which is accessible from the aforementioned alcohol (see Scheme 3).

Scheme 3. Retrosynthetic desconnection of a *COOH*-protected *N*-TEG amino acid.

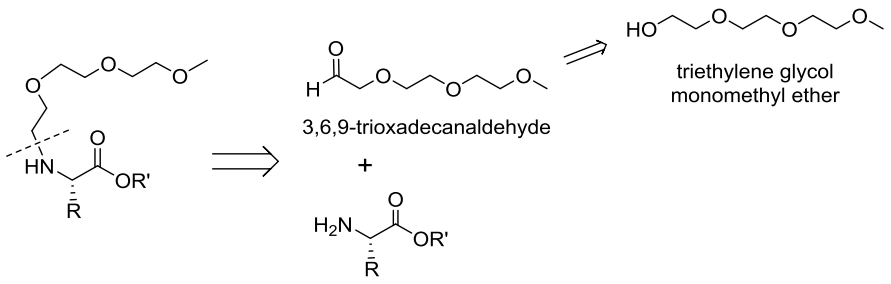

Having conceived this synthetic route towards *N*-TEG building blocks, we sought to optimize a protocol for the preparation of Fmoc-protected *N*-TEG amino acids, and then find conditions for their incorporation into peptides using solid-phase methodology (see Figure 14).

Figure 14. A) Structure of an Fmoc-*N*-TEG amino acid. **B)** Structure of an *N*-TEG peptide.

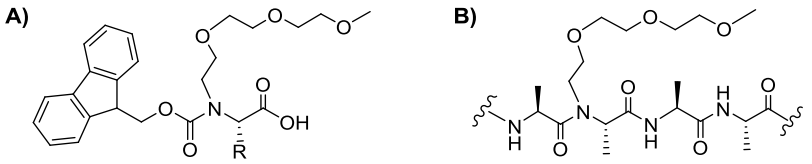

1.2. Objectives

The objectives of this Chapter were:

1. To develop a synthetic methodology to prepare Fmoc-protected amino acids bearing an *N*-TEG chain at the α-amino group.

2. To investigate the use of Fmoc-*N*-TEG amino acids as building blocks in SPPS and find conditions for the acylation of *N*-TEG residues.

1.3. Issues in the synthesis of peptides containing *N*-alkyl groups

The synthesis of *N*-alkylated peptides presents several issues.[70] The main difficulty is the acylation of *N*-alkyl amino acids, which is hampered by steric hindrance. This is not only reflected in poor coupling yields unless special activation methods are employed, but also in a number of side-reactions that become more problematic as coupling rates decrease. In addition, *N*-alkyl amino acids are very prone to α-epimerization upon *COOH*-activation, and their presence in peptides favours DKP formation. Furthermore, peptides containing *N*-alkyl residues may undergo fragmentation under acidic conditions, mainly due to the lability of *N*-alkylated amide bonds.

Nowadays, many of the difficulties concerning the synthesis of *N*-methylated peptides have been overcome, and a few peptides containing short *N*-alkyl groups have been accessed. However, the preparation of *N*-alkylated peptides is not a routine task, and often requires a special design of the synthetic strategy.

This Section summarizes the main issues in the synthesis of *N*-alkylated peptides and possible solutions to overcome them.

1.3.1. Couplings onto *N*-alkyl residues

Due to steric hindrance, couplings onto *N*-alkyl amino acids generally proceed in low yields under standard conditions. This is especially true for syntheses on a solid support, as the reactivity of resin-bound secondary amines towards activated amino acids is lower than in solution.[78]

Although several activating reagents are reported as efficient for the acylation of *N*-Me amines, they do not always work for couplings between consecutive *N*-Me residues and/or residues with bulky amino acid side-chains. Upon increasing the size of the *N*-substituent, formation of the *N*-alkylated amide bond becomes more difficult, and strong activating reagents may fail to provide good yields.

Besides the **use of strong activation methods**, other ways to improve the efficiency of couplings onto *N*-alkyl residues include **MW heating** and the **use of non-carbamate protection at the α-amino group**, which prevents oxazolone formation from the activated amino acid species.

i. Activating reagents recommended for couplings onto *N*-alkyl residues

Until recently, the most promising reagents for the acylation of *N*-Me residues in solid-phase were DIPCDI/HOAt, HATU/HOAt, PyAOP, PyBrOP and PyBOP/HOAt. The superiority of such **HOAt-based reagents** for couplings onto hindered *N*-Me residues was shown in several studies.[78,79] Another established method for couplings onto *N*-Me residues was to activate the following amino acid as a symmetrical anhydride. This method was employed for couplings between adjacent *N*-Me residues in the SPPS of several Cyclosporin analogues.[80] The SPPS of such Cyclosporin peptides was also accomplished by employing HATU or DIPCDI/HOAt for the construction of *N*-alkylated amide bonds.[81] However, both approaches required multiple coupling cycles to obtain adequate yields.

In addition to the aforementioned activation methods, another traditional approach to perform couplings onto *N*-Me residues was to use an acid halide as acylating species.[82] Due to their high reactivity, **Fmoc-amino acid chlorides** have been successfully applied for couplings onto hindered *N*-Me residues in solution.[83] However, couplings via acid chlorides are hampered by their base-catalized conversion to an oxazolone, which is prone to racemization and less

susceptible to be aminolized (see Scheme 4 in Subsection iii).[82] The formation of such oxazolone limits the effectiveness of Fmoc-amino acid chlorides in solid-phase.[84] Further disadvantages of Fmoc-amino acid chlorides as coupling reagents are their limited shelf-stability and their uncompatibility with acid-labile protecting groups (*e.g.* ^{t}Bu-, Trt-).

In contrast to Fmoc-amino acid chlorides, **Fmoc-amino acid fluorides** are more resistant to base-catalyzed oxazolone formation and have been extensively used in solid-phase.[82,85] Their most impressive application is the coupling of adjacent α,α-dialkyl amino acids such as Aib,[86] as demonstrated by the first successful SPPS of peptaibols.[87] However, although Fmoc-amino acid fluorides are excellent reagents for couplings between moderately hindered amino acids *(e.g.* Aib-to-Aib), they are not suitable for significantly more hindered systems *(e.g.* Aib-to-*N*MeAib) under standard conditions.[88] In couplings via acid fluorides, higher yields can be achieved if the amino component is previously treated with a silylating reagent such as *N*,*O*-bis(trimethylsilyl)acetamide (BTSA).[89] The resulting *N*-silylamine shows increased nucleophilicity and is easier to acylate. This modification allowed for the coupling of several Fmoc-amino acid fluorides onto *N*MeAib in solution, though in moderate yields.[90]

In recent years, the use of **bis(trichloromethylcarbonate) (BTC)** as activating reagent has become a reliable method to achieve couplings onto *N*-Me residues. Activation of an Fmoc-amino acid with BTC is likely to proceed through the corresponding acid chloride.[28] Alternatively, mixed anhydrides may be formed. This method was first reported by Gilon *et al*.[28] They used BTC in the presence of 2,4,6-trimethylpyridine for the *in situ*-generation of several Fmoc-amino acid chlorides both from non-alkylated and *N*-alkylated amino acids. Such amino acid chlorides were then added to various Rinkamide 4-methylbenzhydrylamine (MBHA) resin-bound peptides, and couplings were allowed to proceed for 1 hour at 50 ºC. These conditions allowed for the coupling of a wide range of Fmoc-amino acids onto several functionalized *N*-alkyl residues [*e.g. N*-Me, *N*-$(CH_2)_{n=2-4}$-NHAlloc, *N*-$(CH_2)_{n=2-3}$-COOAll]. All the couplings proceeded in high yield and with no detectable epimerization. Furthermore, Fmoc-amino acids bearing acid-labile side-chain protecting groups are stable to these conditions.

The high effectiveness of the BTC method for couplings onto hindered *N*-Me residues was demonstrated by comparison with other activating reagents, such as DIPCDI/HOAt and TFFH.[91] However, the original protocol by Gilon *et al*. was found to be innappropriate for the SPPS of large peptides on the CTC resin.[91a] Under the original BTC-coupling conditions, premature cleavage of the peptide from the highly acid-labile CTC resin takes place. This was attributted to 2,4,6-trimethylpyridine not being enough basic to neutralize the HCl formed in the BTC activation step. Jung *et al.* showed that premature peptide cleavage could be avoided by treating the resin with DIEA before adding the *in situ*-generated Fmoc-amino acid chloride.[91a] Remarkably, the presence of DIEA appeared to accelerate the reaction, and thus the elevated temperature employed in the original procedure were no longer necessary.

This modified BTC procedure was applied in the total SPPS of Cyclosporin O[91a] and Omphatolin A[91b] on the CTC resin. In the total SPPS of Petriellin A, which was also performed on the CTC resin, BTC activation was used for coupling a depsipeptide segment onto *N*MeVal.[92] Other examples in which BTC has been applied to achieve couplings onto *N*-alkyl residues are reported.[65,93]

Very recently, our group developed **4-di(4,6-[2,2,2-trifluoroethoxy]-1,3,5-triazyn-2-yl)-4-methylomorpholinium tetrafluoroborate (DFET/NMM/BF_4)** as a very efficient reagent to perform couplings between sterically hindered *N*-Me residues.[94] The effectiveness of this coupling reagent was demonstrated in the SPPS of several Leu-enkephaline pentapeptides, which involved very difficult couplings, such as *N*MeVal-to-*N*MeVal and *N*MeLeu-to-*N*MeLeu. For such couplings, DFET/NMM/BF_4 showed superior performance relative to TBTU, regardless of the reaction conditions.

Also very recently, our group reported the use of COMU in the total SPPS of *N*Me-IB-01212, a highly *N*-methylated cyclic peptide.[95] In this synthesis, **COMU/OxymaPure** was employed for the *N*MeLeu-to-*N*MePhe and Dap(Alloc)-to-*N*MeLeu coupling steps. This coupling system allowed for a complete acylation of the peptidyl-resin and proved to be advantageous to HATU/HOAt, since DKP formation was prevented. The efficiency of COMU for the coupling onto hindered *N*-Me residues was demonstrated in a comparative study conducted by Jensen *et al*. In this study, COMU proved to superior to other coupling reagents, such as DIPCDI/HOAt and HATU, all of which were tested in combination with MW heating.[96]

ii. Use of MW heating to promote couplings onto *N*-alkyl residues

The use of MW irradiation is an established tool to promote difficult couplings in solid-phase.[97] Several reports especulate that MW-assisted SPPS reactions are not only accelerated due to an increased temperature, but also due to the alternating electric field from MW irradiation, to which the polar backbone of the peptide continuously tries to align.[98] This mechanism is useful for preventing chain aggregation and facilitating the access of reagents to the solid-phase reaction matrix, thereby improving the coupling efficiency.

Several examples are reported in which the acylation of sterically hindered non-alkylated residues can hugely benefit from MW irradiation.[99] However, only a few reports describe the use of MW heating to achieve couplings onto *N*-alkyl residues.

Recently, our group published a protocol for the SPPS of short peptides containing adjacent *N*-Me residues using MW irradiation (35 ºC, 20 min) and **DIPCDI/HOAt** as coupling reagents in DCM.[98c] The use of MW was found to be advantageous, as it dramatically reduced the coupling times and increased the purity of the products. Remarkably, two of the peptides synthesized involved the acylation of an *N*-Me residue bearing a β-branched side-chain. These two peptides could not be obtained by conventional methods at room temperature even when performing several coupling cycles. At the same time, Jensen *et al.* reported very similar findings.[100] MW irradiation (75 ºC, 2x10 min) was applied to the SPPS of short *N*-Me-rich peptides using DIPCDI/HOAt activation and DMF as solvent. The use of MW tremendously increased the coupling yields, specially for those couplings that involved β-branched *N*-Me residues.

More recently, Jensen *et al.* described the combination of **COMU** and MW heating (75 ºC, 20 min) as a very efficient approach to perform couplings onto sterically hindered *N*-Me residues in solid-phase.[96] COMU displayed higher efficiency than DIPCDI/HOAt and HATU, which were also tested under MW irradiation.

MW heating has also been applied to achieve difficult couplings onto *N*-alkyl amino acids using **BTC** activation, but only three examples are reported.[65,101] In the most remarkable one, MW heating (45 ºC, 1 h) in combination with BTC allowed for the acylation of several resin-bound *N*-allyl residues, though three treatments were required for an almost complete conversion.[65]

iii. Alternative N^{α}-protecting groups to facilitate couplings onto *N*-alkyl residues

In peptide synthesis, the protecting groups that are most frequently employed to protect the α-amino function are carbamate-type protectants.[102] Besides Fmoc- and Boc-, which are the most common for SPPS, there is the Alloc-group, which allows a fully orthogonal protection in combination with Fmoc- and Boc-, and several other carbamate-type N^{α}-protecting groups have also been described. Among them, benzyloxycarbonyl (Z-), *p*-nitrobenzyloxycarbonyl (pNZ-), and [2-(4-biphenyl)isopropoxycarbonyl)] (Bpoc-) of particular interest for the synthesis of peptides in solution, as their specific features make them potentially useful in combination with ^{t}Bu-type side-chain protection.[103]

A major disadvantage of the use of carbamate-protected aminoacids is their base-catalyzed conversion to an oxazolone upon *COOH*-activation, specially if *N*-alkyl groups are present (see Scheme 4).[104] The resulting oxazolone, which is still an acylating species, is less reactive than the original activated amino acid, and this limits the usefulness of certain coupling methods that are reported as highly potent. For instance, despite the high reactivity of acid chlorides, couplings via Fmoc-amino acid chlorides do not proceed efficiently, because such derivatives are readily converted to their less reactive oxazolones in the presence of base.[84] This base is required to trap the HCl that is formed during the coupling step.

Scheme 4. Mechanism for base-catalyzed conversion of carbamate-protected amino acid chlorides to their corresponding oxazolones, which are less reactive acylating species and prone to racemization.

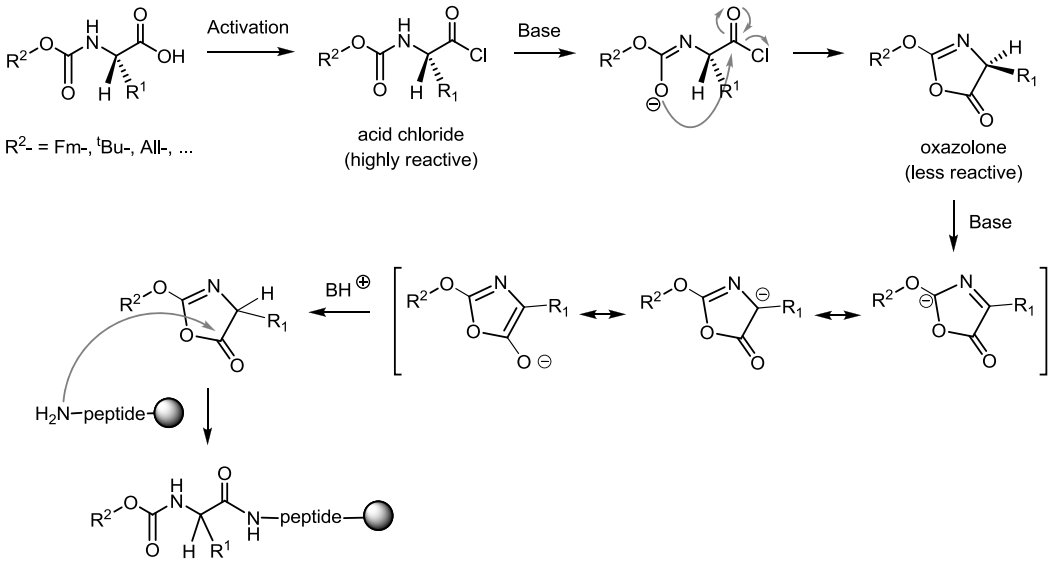

For hindered couplings that demand the reactivity of an acid chloride, oxazolone formation can be avoided by using sulfonamide-protection at the α-amino group (see Figure 15). **Arylsulfonamide-protected amino acid chlorides** are recommended as practical reagents for difficult couplings in solution,[88] and have allowed the preparation of extremely hindered *N*-methylated peptides.[105] Such arylsulfonamide-protected amino acid chlorides have also been used in solid-phase, and proved to be efficient in cases where the analogous Fmoc-amino acid chlorides failed to couple well.[106]

Figure 15. Structure of several arylsulfonyl N^{α}-protecting groups: *o*-nitrobenzenesulfonyl (*o*NBS), dinitrobenzenesulfonyl (dNBS), and *N*-benzothiazole-2-sulfonyl (Bts).

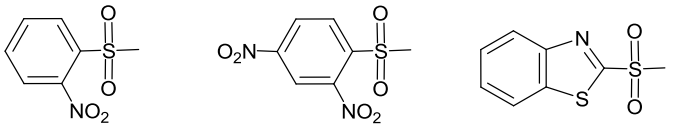

*o*NBS-

Removal conditions:
a. $PhSH/K_2CO_3$
(only for 1ary amines)
b. b-mercaptoetanol/DBU
(only for 2ary amines)

*d*NBS-

Removal conditions:
$HSCH_2COOH/NEt_3$

Bts-

Removal conditions:
a. PhSH/base
(K_2CO_3, DIPEA, ^tBuOK)
b. Al/Hg or Zn
c. H_3PO_2
d. $NaBH_4$
(only for 2ary amines)

Another N^{α}-protecting group for which oxazolone formation is precluded is the azide group. The concept of azides as temporary α-amino protecting groups for SPPS was introduced by Meldal *et al.*[107] They described the use of DTT and

other thiols for the efficient reduction of resin-bound azido groups, and they developed a novel method for SPPS in which α-azido acids are used as building blocks. Incorporation of α-azido acids into peptides synthesized by the Fmoc-protocol is straightforward, and the possibility of activating the carboxyl group as a highly reactive acid chloride allows sterically hindered couplings to be achieved. The efficiency **α-azido acid chlorides** as solid-phase coupling reagents has also been attributed to the decreased size of the α-azido group with respect to other N^{α}-protecting groups.[108]

1.3.2. Racemization

During the coupling of *N*-alkyl amino acids, epimerization can readily take place (see Scheme 5). The enhanced epimerization of *N*-alkyl amino acids upon *COOH*-activation is due to different reasons. The presence of an *N*-alkyl group: i. induces a *cis* configuration at the *N*-alkylated amide bond (which is more easily α-deprotonated than in the *trans* amido conformer), and ii. stabilizes the α-deprotonated carbanion by hyperconjugation.[109] As a consequence, activated *N*-alkyl amino acids are very prone to undergo base-catalized enolization (path A). In addition, activated *N*-alkyl amino acids can also racemize through an oxazolonium ion (path B), whose tautomerization gives rise to pseudoaromatic structures.[70] The presence of an electron-donating *N*-alkyl group favours amino acid racemization through this mechanism, as it stabilizes the positively charged nitrogen atom of the oxazolonium ion intermediate.

Scheme 5. Mechanisms for the racemization of *N*-alkyl amino acids upon *COOH*-activation:
A) via base-catalized enolization, **B)** via formation of an oxazolonium ion.

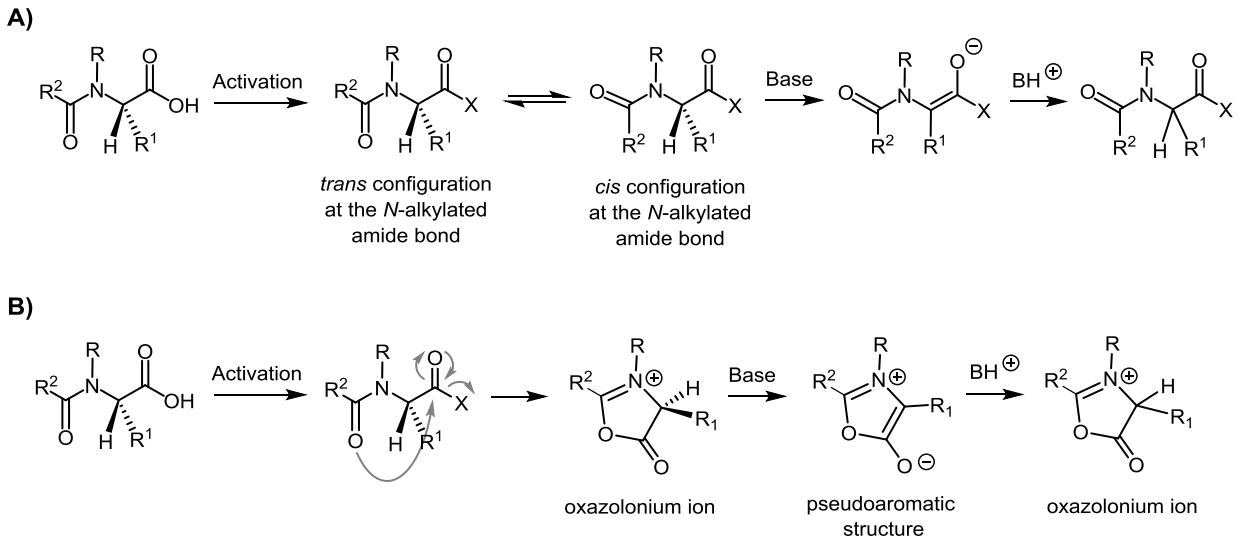

Furthermore, epimerization is also likely to occur during couplings onto *N*-alkyl residues, since the slow rates of these couplings provide an increased opportunity the activated amino acid to racemize.

In order to minimize the risk of epimerization, several factors must be taken into consideration. For the amino acid undergoing activation, racemization via an oxazolone or an oxozolonium ion can be suppressed by carbamate-protection at the α-amino group, whereas N^{α}-acyl protection facilitates the process.[110] When carbodiimides are used as coupling reagents, racemization can be reduced by the presence of additives such as HOBt, HOAt or OxymaPure.[110] Such additives convert the highly reactive *O*-acyl isourea intermediate, which can suffer racemization, to the corresponding active ester. A further isue to decrease epimerization is the basicity and nature of the tertiary amine that may be used during the coupling reaction. Those bases that are greatly hindered jeopardize α-proton abstraction.[111]

1.3.3. DKP formation

During the SPPS of peptides containing *N*-alkyl amino acids, peptide chain elongation may be hampered by spontaneous DKP formation (see Scheme 6). In this side-reaction, the amino group released after *N*-terminal deprotection nucleophilically attacks the carbonyl group of the adjacent amino acid whilst forming a cyclic dipeptide that is cleaved off from the resin. This side-reaction is very common in Fmoc-based SPPS and is particularly prone to occur at the dipeptide and tripeptide stage. The reaction is both base- and acid-catalyzed, and its extent depends on the dipeptidic sequence at the *N*-terminus (*i.e.* bulky amino acid side-chains hamper intramolecular aminolysis). In particular, the formation of DKPs is strongly favoured by the presence of of *N*-alkyl residues (which induce a *cis* configuration at the *N*-alkylated amide bond, rendering the carbonyl group more accessible) and by the presence of L- and D- amino acids (which leads to the more stable six-membered ring DKP).[112]

Scheme 6. DKP formation in a resin-bound tripeptide containing an *N*-alkyl group.

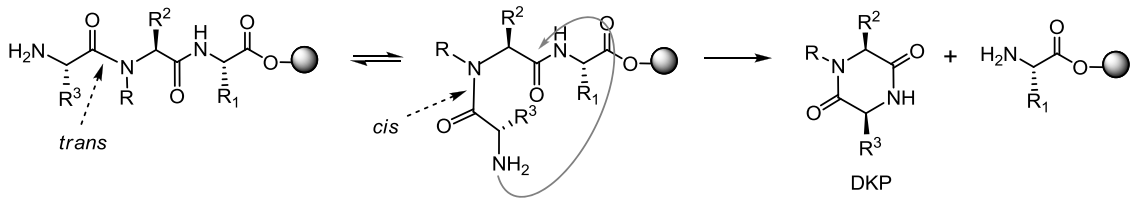

Since peptide sequences containing *N*-alkyl residues are prone to DKP formation, the occurrance of this side-reaction should be carefully checked. DKP formation during peptide elongation can be detected by: i. a decreased resin loading after assembly of the following amino acid, ii. the appearance of peptide sequences lacking the DKP-prone dipeptidic segment in the HPLC-MS spectra of a cleaved resin sample. It is important to note that DKP formation can also occur during the final cleavage step, as this reaction is also acid-catalyzed. In that case, DKPs will be present in the HPLC-MS spectra of the cleaved peptide. Along these lines, the presence of DKPs in the HPLC-MS spectra of a cleaved resin sample is not indicative of DKP formation during peptide elongation.

In order to minimize the risk of DKP formation during the SPPS of peptides containing *N*-alkyl residues, the use of the CTC resin as solid support is recommended[113] and, if possible, positioning of *N*-alkyl residues at the *C*-terminal and penultimate positions of the peptide sequence should be avoided.

1.3.4. Presence of multiple peaks in the HPLC spectra

Fmoc-protected *N*-alkyl amino acids often show two peaks in their HPLC spectra.[70] This is due to the slow conversion between the two conformers differing at the configuration of the *N*-alkylated amide bond. Multiple HPLC peaks are also often seen for peptides containing an *N*-alkyl amino acid at the *C*-terminus. In contrast, the HPLC chromatograms of *N*-alkylated peptides in which the *N*-alkyl group is located at the *N*-terminus or in the middle of the sequence usually exhibit a single peak.

1.3.5. Peptide fragmentation during cleavage

Peptides containing *N*-alkyl groups are not very stable under acidic conditions, and various side-reactions can take place during their cleavage from resin.[70] In peptides that have an Ac-*N*-alkyl amino acid at the *N*-terminus, this residue is lost during TFA cleavage (see Scheme 7A).[114] Peptide acids that have an *N*-alkyl residue at the *C*-terminus are also

prone to acid-catalyzed fragmentation (see Scheme 7B).[115] This reaction normally proceeds slowly and is only detected in small amounts during standard acidolytic Boc- or *tert*-butyl ester deprotections.

Scheme 7. Acid-catalyzed fragmentation of peptides containing *N*-alkyl residues. **A)** Cleavage of an *N*-terminal Ac-*N*-alkyl residue. **B)** Cleavage of a *C*-terminal *N*-alkyl residue. Both in A) and B), R^2 represents the remaining peptide sequence.

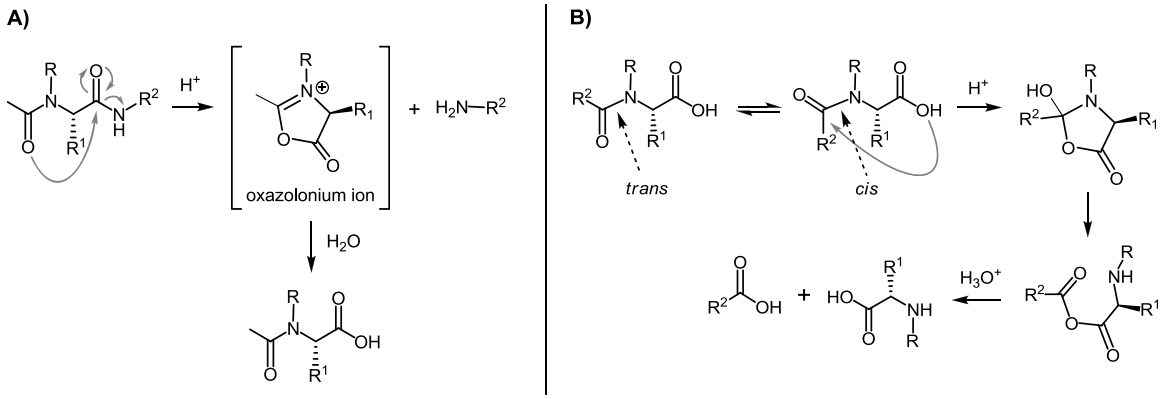

In a related side-reaction, the *C*-terminal *N*-alkyl amino acid of a sequence of three consecutive *N*-alkyl residues is readily cleaved by acid.[116] Anteunis and Van der Auwera proposed that cleavage between the two *N*-alkyl residues at the *C*-terminus may proceed through a diketopiperazinium ion (see Scheme 8A). Fragmentation between *N*-alkyl residues has also been observed when there are only two consecutive *N*-alkyl amino acids (instead of three), and without the requirement of such residues being located at the *C*-terminus. Urban *et al.* postulated that cleavage between consecutive *N*-alkyl amino acids occurs via an oxazolonium ion.[114] This mechanism, which is based on evidence from H-D exchange experiments using NMR and MS techniques (see Scheme 8B), may also account for the high lability of the *C*-terminal *N*-alkyl residue of a triad of *N*-alkyl groups.

Scheme 8. Acid-catalyzed fragmentation between consecutive *N*-alkyl residues. **A)** Mechanism for the cleavage of the *C*-terminal *N*-alkyl residue in a triad of *N*-alkyl amino acids via a diketopiperazinium ion, as proposed by Anteunis and Van der Auwera (X = OH, NH_2 or resin).[116] **B)** Mechanism for the cleavage of between two *N*-alkyl residues via an oxozolonium ion, as postulated by Urban *et al*.[114] Both in A) and B), R' and R'' represent the remaining peptide sequence.

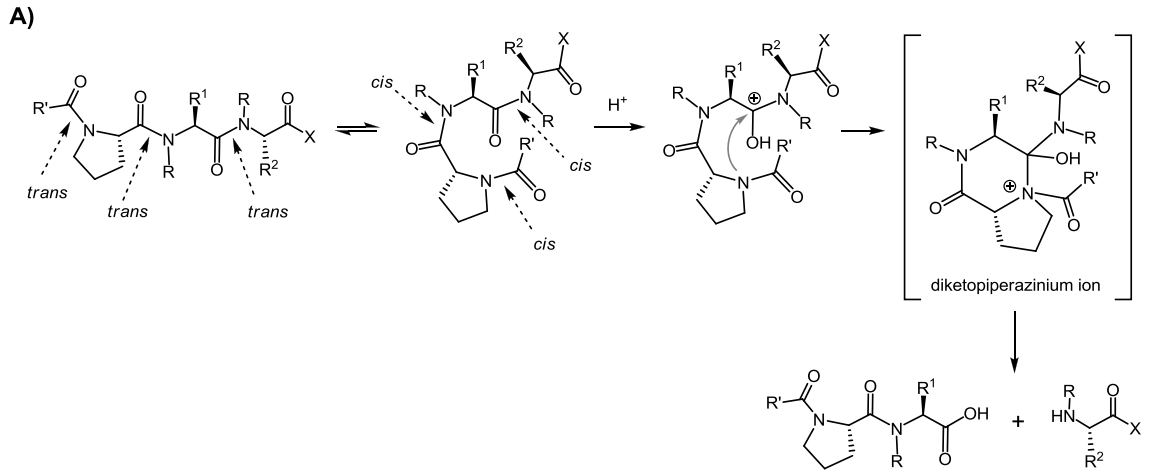

B)

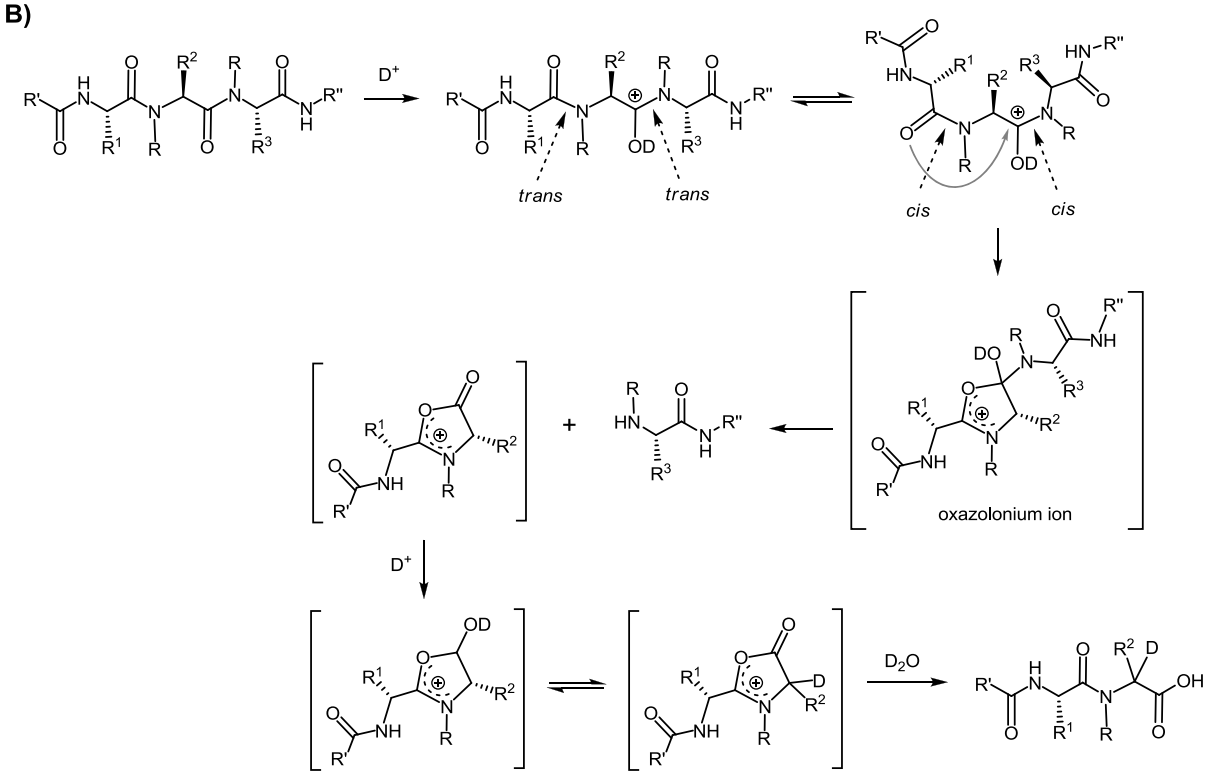

In order to minimize fragmentation of *N*-alkyl-containing peptides, the use of the CTC resin is recommended, as it can be cleaved with very mild acid conditions. For other solid supports that are not so acid-labile, the time of cleavage and the composition of the cleavage cocktail (with or without H_2O as scavenger) should be carefully optimized.

1.4. Results and discussion

1.4.1. Synthesis of Fmoc-*N*-TEG amino acids

In the literature there is only one example in which the synthesis of an *N*-TEG amino acid is reported. Prato *et al.* described the preparation of *N*-TEG glycine by reductive alkylation with 3,6,9-trioxadecanaldehyde using Z-/Bn-protection (see Scheme 9).[117] The required aldehyde can be easily prepared by Swern oxidation of triethylene glycol monomethyl ether, which is inexpensive and commmercially available.

Scheme 9. A) Synthesis of 3,6,9-trioxadecanaldehyde. **B)** Synthesis of *N*-TEG glycine, as described by Prato *et. al.*[117] Although the authors prepared *N*-TEG glycine, its use as solid-phase building block has not been investigated.

A)

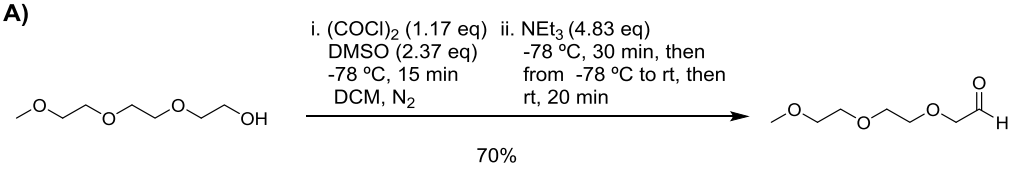

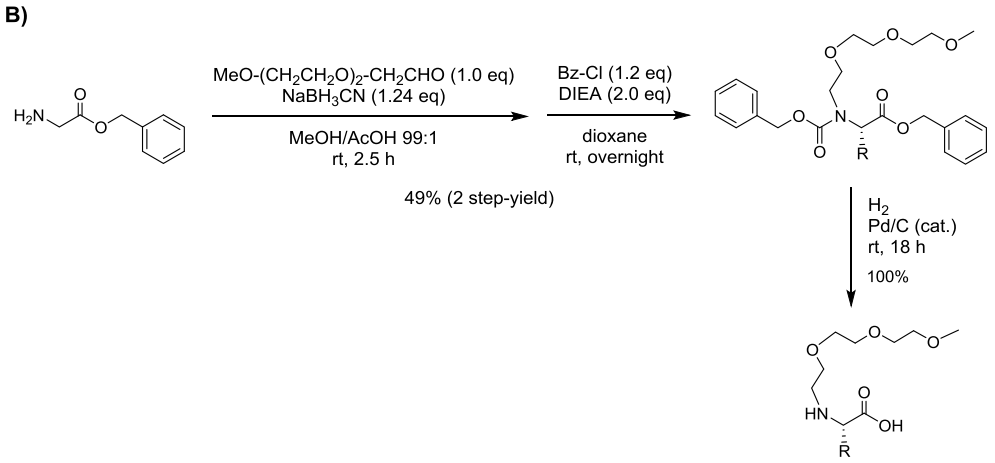

For our aim, we adapted this strategy to prepare Fmoc-*N*-TEG amino acids (see Scheme 10). Our protocol for the synthesis of such derivatives starts from the corresponding amino acid *tert*-butyl ester and has three steps: i. reductive alkylation with 3,6,9-trioxadecanaldehyde, ii. Fmoc-protection of the *N*-alkylated amino group, iii. acidic cleavage of the *tert*-butyl ester. This facile method allows access to Fmoc-*N*-TEG amino acids in an efficient and inexpensive manner. As a proof-of-principle, the Fmoc-*N*-TEG analogs of Ala, Val, Leu and Phe (**5-8**) were prepared up to a 5 g scale in 40-70% overall yields. In all cases, reductive alkylation yielded a mixture of unreacted starting material, *N*-monoalkylated product, and *N,N*-dialkylated product in which the last two were found to be inseparable; however, after Fmoc-protection of the amino group, the desired products (**1-4**) were easy to isolate by flash chromatography.

Scheme 10. Synthesis of Fmoc-*N*-TEG amino acids (**5-8**).[a]

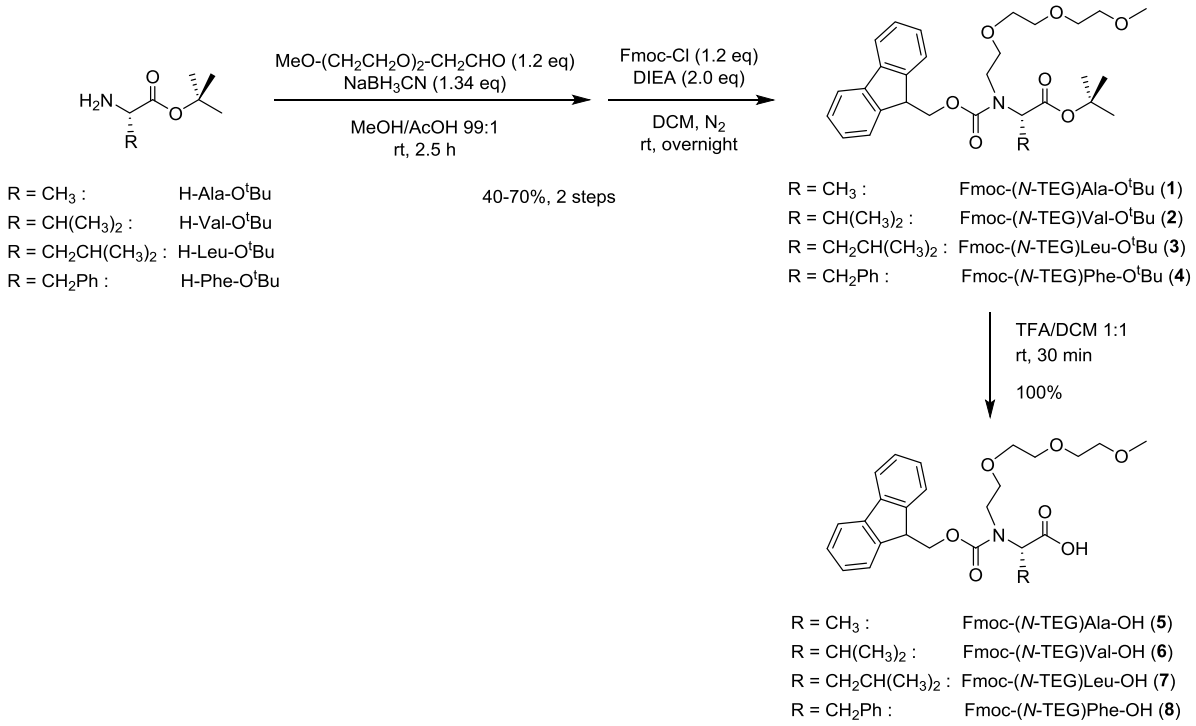

[a] Fmoc-*N*-TEG amino acids are stable on storage at room temperature over several months.

1.4.2. Use of Fmoc-*N*-TEG amino acids in SPPS

Preliminary observations

We found that Fmoc-*N*-TEG amino acids can be coupled to a peptidyl-resin using standard activating reagents (see Scheme 11). In a preliminary experiment, the dipeptidic sequence Leu-Phe was assembled on the CTC resin and then acylated with either Fmoc-(*N*-TEG)Ala-OH (**5**) or Fmoc-(*N*-TEG)Leu-OH (**7**). These building blocks were coupled in a 3-fold excess using DIPCDI/OxymaPure activation. After 1 hour, the peptidyl-resin was completely acylated and no racemization was detected (as confirmed by HPLC analysis of cleaved resin samples).

Scheme 11. Preliminar studies on the use of Fmoc-*N*-TEG amino acids in SPPS.

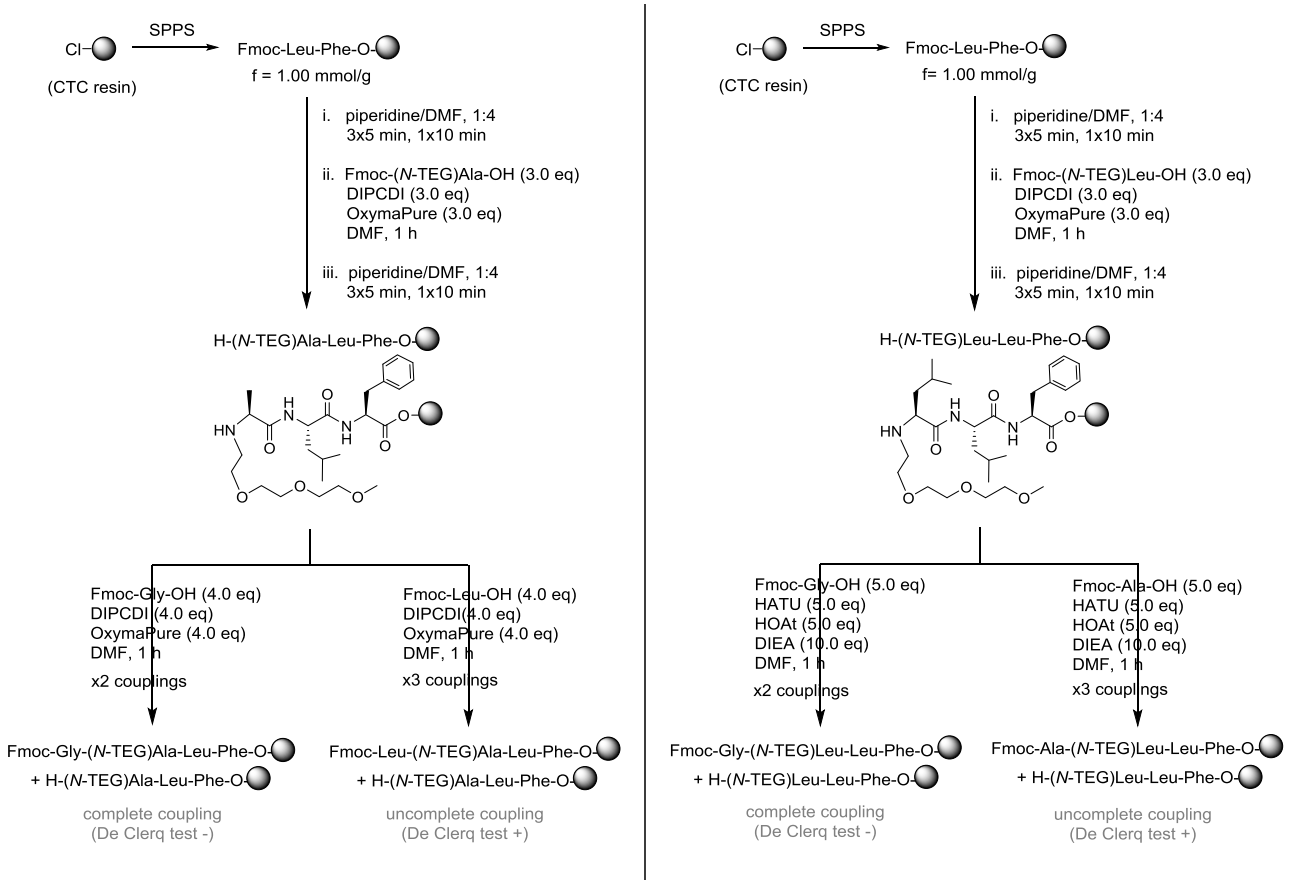

As expected, coupling of the following amino acid onto the resin-bound *N*-TEG residue was hampered by steric hindrance. For the (*N*-TEG)Ala peptidyl-resin, complete acylation with Fmoc-Gly-OH using DIPCDI/OxymaPure required two treatments with a 4-fold excess of the activated amino acid, but these conditions resulted in an uncomplete acylation with Fmoc-Leu-OH. For the couplings onto the (*N*-TEG)Leu peptidyl-resin, we investigated the use of HATU/HOAt as a stronger activation method.[78,79,118] Performing two HATU/HOAt-mediated couplings in a 5-fold excess of reagents allowed for the efficient coupling of Fmoc-Gly-OH, but the yield was not satisfactory for Fmoc-Ala-OH.

Model to investigate conditions for solid-phase coupling onto *N*-TEG residues

In order to identify a method under which the solid-phase couplings onto *N*-TEG residues proceed efficiently, we undertook the study of a wide range of coupling conditions. As a model reaction, we studied the coupling of Fmoc-Ala-OH onto (*N*-TEG)Leu (see Scheme 12).

Scheme 12. Model to investigate conditions for an efficient coupling onto *N*-TEG residues in solid-phase.

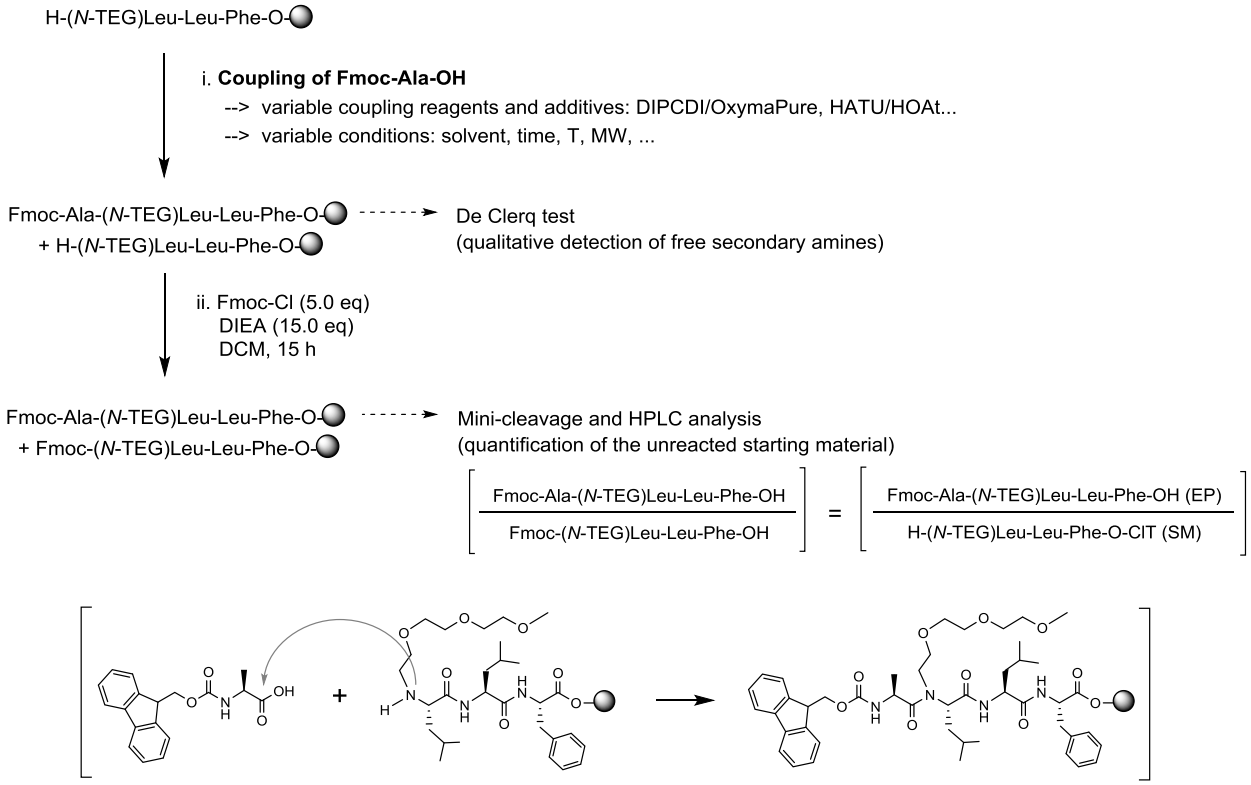

After a test coupling, unreacted *N*-TEG amino groups can be detected by performing a De Clerq test, which reveals the presence of primary and secondary amines.[119] However, the % of unreacted starting material cannot be directly estimated from the HPLC spectra of a cleaved resin sample. Since the Fmoc- group of the product absorbs strongly in the UV, the relation between the areas of the HPLC peaks of the starting material and the product does not reflect the true proportion between these two species.

We found that a quantitative interpretation of the HPLC spectra was possible if the unreacted resin-bound peptide was protected with Fmoc- prior to cleavage and HPLC analysis. Acylation of the (*N*-TEG)Leu-peptidyl-resin with 5.0 equivalents of Fmoc-Cl takes place quantitatively in 1.5 hours (as confirmed by HPLC-MS). Since the UV absorption of the Fmoc-protected starting material and the product is mainly due to the contribution of the Fmoc- group, it can be assumed that both species will have similar UV-absorption coefficients. Based on this assumption, we used the relation between their HPLC peak areas to estimate the conversion of our test coupling reactions.

Study of the effectiveness of several activation methods

After having defined our model system, we run a series of test reactions with various activation methods and conditions, followed by HPLC analysis with regard to coupling efficiency (see Table 3). In all experiments, Fmoc-Ala-OH was coupled in a 5-fold excess.

Table 3. Evaluation of the efficiency of several activation methods.

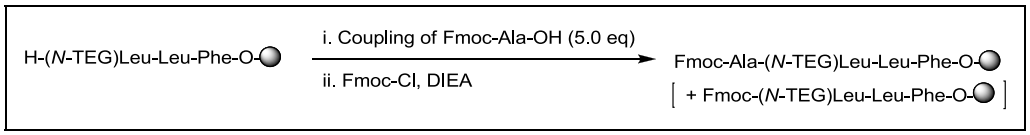

Entry	Coupling method	Solvent	Time (h)	Coupling efficiency
1	DIPCDI (5.0 eq)/OxymaPure (5.0 eq)	DMF	1	2%
		DMF	15	33%
2	DIPCDI (5.0 eq)/HOBt (5.0 eq)	DMF	1	9%
		DMF	15	16%
3	DIPCDI (5.0 eq)/HOAt (5.0 eq)	DMF	1	10%
		DMF	15	**63%**
4	HATU (5.0 eq)/HOAt (5.0 eq)/DIEA (10.0 eq)	DMF	1	8%
		DMF	15	27%
5	COMU (5.0 eq)/DIEA (10.0 eq)	DMF	1	0%
		DMF	15	14%
6[a]	DIPCDI (5.0 eq)/DMAP (0.2 eq)	DCM	1	0%
		DCM	15	0%
7[b]	Fmoc-Ala-Cl (5.0 eq)/DIEA (5.0 eq)	DMF	1	0%
		DMF	15	0%
8[b]	Fmoc-Ala-Cl (5.0 eq)/HOBt (5.0 eq)/DIEA (5.0 eq)	DMF	1	3%
		DMF	15	28%
9	TFFH (5.0 eq)/DIEA (5.0 eq) a. No base for the coupling step. b. + DIEA (2.0 eq)	THF	1	0%
		THF	15	0%
10	TFFH (5.0 eq)/DIEA (5.0 eq) [*N*-silylation with BTSA (5.0 eq) prior to coupling]	THF	1	0%
		THF	15	0%
11	BTC (1.65 eq)/2,4,6-trimethylpyridine (14.0 eq)	THF	1	59%
		THF	15	**87%**

[a] For the symmetric anhydryde method, we used a 10-fold excess of Fmoc-Ala-OH, so that Fmoc-aa-OH/DIPCDI 2:1.

[b] For the acid chloride method, Fmoc-Ala-Cl was prepared in a prior step by chlorination of Fmoc-Ala-OH with $SOCl_2$.

For DIPCDI-mediated couplings using OxymaPure, HOBt or HOAt as additives (entries 1-3), almost no product was formed after 1 hour. A similarly low conversion was observed for HATU/HOAt activation (entry 4). When these couplings were allowed to proceed overnight, the best results were obtained with DIPCDI/HOAt (entry 3), which afforded a 63% conversion. The superiority of HOAt-based coupling reagents (DIPCDI/HOAt and HATU/HOAt) to HOBt in terms of coupling efficiency is in agreement with previous studies on the acylation of sterically hindered *N*-Me residues.[78,79,118] Unlike -OBt esters, -OAt active esters exhibit good reactivity towards *N*-Me amines, mainly through intramolecular base catalysis, and have generated excellent results both in solution and in solid-phase synthesis. The better performance of DIPCDI/HOAt in comparison with HATU/HOAt is also in agreement with literature data: extremely hindered secondary amines are reported to be less amenable to acylation by HATU.[120]

The use of COMU, the uronium salt of OxymaPure, did not provide a good conversion (entry 5). Activation of Fmoc-Ala-OH as symmetrical anhydride failed to give the desired peptide (entry 6), even in the presence of DMAP.[121]

We then explored the use of pre-made Fmoc-Ala-Cl as acylating species. Due to their high reactivity, Fmoc-amino acid chlorides have been successfully applied to perform sterically hindered couplings onto *N*-Me residues in solution.[83] However, Fmoc-amino acid chlorides show sluggish reactivity in solid-phase due to their base-catalyzed conversion to an oxazolone, which is prone to racemization and aminolized at a slower rate.[84] This side-reaction can readily occur upon mixing the acid chloride and the necessary base. Taking this into consideration, it is not surprising that an overnight treatment of the *N*-TEG peptidyl-resin with a solution of Fmoc-Ala-Cl and DIEA failed to give the desired peptide (entry 7).

Carpino *et al.* reported that Fmoc-amino acid chlorides can be used as solid-phase reagents by treatment with a 1:1 mixture of HOBt and DIEA, which converts them into the corresponding HOBt esters.[84] This allows to prevent oxazolone formation, but the resulting HOBt ester is considerably less reactive than the original acid chloride. When the *N*-TEG peptidyl-resin was treated with Fmoc-Ala-Cl in the presence of HOBt, the coupling took place, but only in 28% conversion (entry 8).

At this stage, we sought to investigate the use of an acid fluoride for the acylation of the *N*-TEG residue. Although Fmoc-amino acid fluorides are less reactive than the chlorides,[88] they are more resistant to base-catalyzed oxazolone formation and have been extensively used in SPPS.[82,85] Remarkably, Fmoc-amino acid fluorides have proved to be efficient for solid-phase couplings between sterically hindered amino acids such as Aib and Iva.[86] Along those lines, it is important to note that couplings via acid fluorides are equally efficient in the absence or in the presence of base.[82] While couplings via acid chlorides require a base to trap the HCl that would convert the amino group into its unreactive protonated form, in couplings via acid fluorides this base is not necessary.

To test the effectiveness of the acid fluoride method, Fmoc-Ala-OH was converted into its acid fluoride by treatment with TFFH in the presence of DIEA, and then added to the *N*-TEG peptidyl-resin.[122] The use of TFFH is advantageous to other fluorinating reagents, such as cyanuric fluoride or diethylaminosulfur trifluoride (DAST), as it allows for the *in situ*-generation of Fmoc-amino acid fluorides that do not have to be isolated before use.[82]

The TFFH-mediated free-base coupling of Fmoc-Ala-OH onto the *N*-TEG residue did not take place (entry 9a). The same coupling was tested in the presence of 2.0 equivalents of DIEA, since this modification was reported to accelerate the coupling of Fmoc-*N*MeAib-F and Fmoc-(3-aminopentanoyl)-F onto H-Aib-OMe in solution.[88] However, the desired product was not formed either (entry 9b). These results are in agreement with a report by Carpino *et al.*, which states that although Fmoc-amino acid fluorides are excellent reagents for the coupling of moderately hindered amino acids *(e.g.* Aib-to-Aib), they are not suited for significantly more hindered systems *(e.g.* Aib-to-*N*MeAib) under standard conditions.[88]

In a different study, Carpino *et al.* reported that the coupling of Fmoc-amino acid fluorides onto *N*MeAib proceeds more efficiently if this residue is previously treated with *N*,*O*-bis(trimethylsilyl)acetamide (BTSA).[90] The increased reactivity of *N*-silylamines towards acid fluorides has also been shown for less hindered systems.[89] Wishing to form the desired amide bond, the (*N*-TEG)Leu-peptidyl-resin was subjected to *N*-silylation conditions prior to addition of the *in situ*-generated Fmoc-Ala-F. The coupling was allowed to proceed overnight, but no product was detected either (entry 10).

Finally, we investigated the use of BTC for our model coupling reaction. In recent years, the *in situ*-generation of an acid chloride using BTC has become a reliable method to achieve difficult couplings onto *N*-alkyl residues.[28,91,92] To prevent cleavage of the acid-labile *O*-trityl ester bond during the BTC-mediated coupling, the peptidyl-resin was pretreated with DIEA. With this precaution, an 87% conversion was reached after an overnight coupling (entry 11). The product was formed in high purity and, in agreement with previous reports on BTC-mediated couplings, [28,91a] no

epimerization was detected. In terms of coupling efficiency, BTC activation proved to be superior to all the other methods tested, and the low cost of this reagent is an advantageous feature.

Study of the effectiveness of several activation methods under MW heating

At this stage, we sought to investigate the use of MW heating to promote the acylation of *N*-TEG residues. As has been explained in Section 1.3.1., MW irradiation improves the efficiency of couplings onto *N*-Me amino acids in solid-phase, as it increases yields and purities and also reduces reaction times.[96,98c]

In order to find suitable conditions for the MW-assisted coupling onto *N*-TEG residues, we initially focused on the DIPCDI/OxymaPure activation method (see Table 4). To optimize this reaction, we varied several parameters, such as temperature, reaction time, solvent and excess of reagents. In our first experiments, almost no product was formed when the coupling was carried out at 80 or 100 ºC (entries 7-10). At these temperatures, decomposition of the activated amino acid may have occurred, as evidenced by the change in the initial colour of the reaction mixture. When the temperature was set at 60 ºC, coupling times below 1 hour were found to be insufficient for an optimum conversion (entries 3-6). A 1 hour-coupling at 60 ºC afforded 53% conversion (entry 6), and an almost same coupling yield was obtained at 50 ºC (entry 1). This lower temperature was considered as preferrable to minimize possible side-reactions. At 50 ºC, raising the reaction time from 60 minutes to 90 minutes did not lead to a significant increase in yield (entry 2). We then explored the effect of solvent, but none of the solvents tested gave better results than DMF (see entries 1b-1f). Using a higher excess of reagents did not improve the coupling efficiency either (entry 1g). Therefore, the best conditions for the DIPCDI/OxymaPure-mediated coupling under MW heating were established as the following: DMF as solvent, a 5-fold excess of reagents, a temperature of 50 ºC, and a coupling time of 1 hour.

Table 4. Optimization of the DIPCDI/OxymaPure-mediated coupling under MW heating.

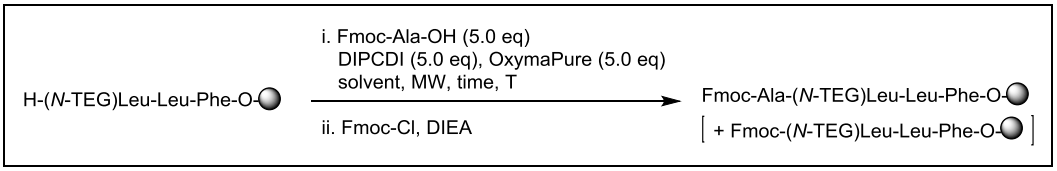

A) Effect of time and temperature

Entry	Solvent	T (ºC)	Time (min)	Coupling efficiency
1	DMF	50	60	51%
2	DMF	50	90	54%
3	DMF	60	5	5%
4	DMF	60	10	10%
5	DMF	60	20	30%
6	DMF	60	60	53%
7	DMF	80	5	Almost 0%
8	DMF	80	10	Almost 0%
9	DMF	80	20	Almost 0%
10	DMF	100	5	0%

B) Effect of solvent

Entry	Solvent	T (ºC)	Time (min)	Coupling efficiency
1	DMF	50	60	51%
1b	THF	50	60	50%
1c	DMSO	50	60	55%
1d	diglyme	50	60	36%
1e	ACN	50	60	33%
1f	dioxane	50	60	21%

C) Effect of amino acid excess

Entry	Fmoc-Ala-OH (eq)	Solvent	T (ºC)	Time (min)	Coupling efficiency
1	5.0	DMF	50	60	51%
1g	10.0	DMF	50	60	51%

We investigated if performing several MW-assisted coupling cycles would allow for a complete acylation of the *N*-TEG residue (see Table 5). The best results were obtained when performing two couplings of 90 minutes, but conversion was not increased to the desired extent. Nevertheless, the 51% conversion reached after a single 1 hour-coupling was

a positive result. In comparison with the overnight coupling in the absence of MW, irradiation with MW and heating at 50 ºC shortened the reaction time to 1 hour and rose conversion from 33% to 51%.

Table 5. Optimization of the DIPCDI/OxymaPure-mediated coupling under MW heating. Effect of coupling cycles.

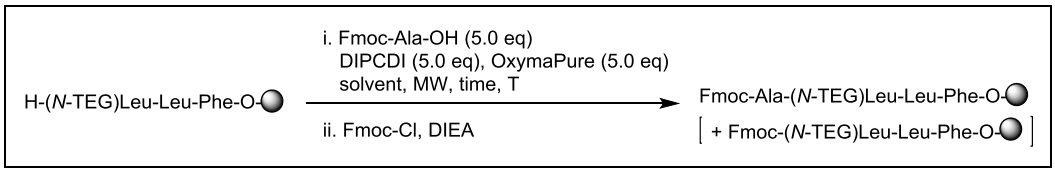

Entry	Solvent	MW	T (ºC)	Time (min)	Coupling cycles	Coupling efficiency
1	DMF	MW	50	60	1	51%
2	DMF	MW	50	60	2	56%
3	DMF	MW	50	60	3	67%
4	DMF	MW	50	90	1	54%
5	DMF	MW	50	90	2	72%
6	DMF	-	rt	overnight	1	33%

At this stage, we tested the effectiveness of other activating reagents under MW heating for our model coupling reaction (see Table 6). In these experiments, we applied the conditions optimized for DIPCDI/OxymaPure. The coupling yields were compared with those obtained in the absence of MW for overnight couplings at room temperature. For DIPCDI/HOAt, the use of MW increased conversion from 63% to 82% (entry 2). In the case of HATU/HOAt and COMU, MW irradiation did not improve the coupling yield (entres 3 and 4). When the amino acid was activated as its symmetric anhydride, MW heating promoted the coupling, but the yield was not satisfactory (entry 5). The same happened for TCFH and TFFH (entries 6 and 7). These reagents were used for the *in situ*-generation of Fmoc-Ala-Cl or Fmoc-Ala-F, respectively, which only reacted with the resin-bound (*N*-TEG)Leu when MW heating was applied. The yields observed reflect the superiority of the acid chloride to the acid fluoride for the acylation of *N*-alkyl residues,[88] but none of the two methods provided a good conversion. Surprisingly, in the case of BTC activation, the coupling under MW heating proceeded in lower efficiency than in the absence of MW (entry 8). This result was not expected, since the use of BTC in combination with MW heating has proved to be efficient for the acylation of hindered *N*-Me residues in solid-phase[101] and has also been applied for couplings onto *N*-allyl residues.[65]

Table 6. Evaluation of the efficiency of several coupling methods with and without MW heating.

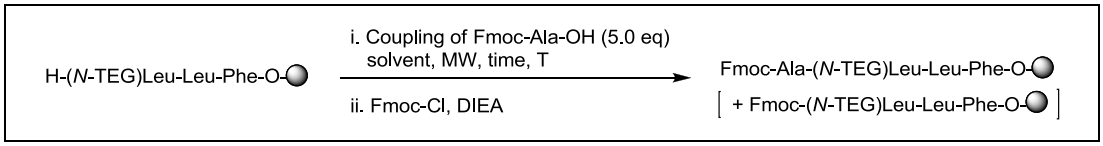

Entry	Coupling method	Solvent	MW	T (ºC)	Time (min)	Coupling efficiency
1[a,b]	DIPCDI (5.0 eq)/OxymaPure (5.0 eq)	DMF	-	rt	overnight	33%
		DMF	MW	50	60	51%
2[a,b]	DIPCDI (5.0 eq)/HOAt (5.0 eq)	DMF	-	rt	overnight	63%
		DMF	MW	50	60	82%
3	HATU (5.0 eq)/HOAt (5.0 eq)/DIEA (10.0 eq)	DMF	-	rt	overnight	27%
		DMF	MW	50	60	11%
4	COMU (5.0 eq)/DIEA (10.0 eq)	DMF	-	rt	overnight	14%
		DMF	MW	50	60	13%
5[c]	DIPCDI (5.0 eq)/DMAP (0.2 eq)	DCM	-	rt	overnight	0%
		DMF	MW	50	60	25%
6[d]	TCFH (5.0 eq)/DIEA (5.0 eq) + DIEA (2.0 eq)	THF	-	rt	overnight	0%
		THF	MW	50	60	25%

7[d]	TFFH (5.0 eq)/DIEA (5.0 eq) + DIEA (5.0 eq)	THF	-	rt	overnight	0%
		THF	MW	50	60	7%
8	BTC (1.65 eq)/2,4,6-trimethylpyridine (14.0 eq)	THF	-	rt	overnight	87%
		THF	MW	45	60	51%

[a] For the DIPCDI-mediated couplings using HOAt or OxymaPure, we preactivated the amino acid for 3 min prior to addition to the peptidyl-resin for the MW-assisted coupling. When this reaction was tested without preactivation of the Fmoc-aa-OH, we only observed traces of product.

[b] For the DIPCDI-mediated couplings using HOAt or OxymaPure, we investigated the addition of 5.0 equiv. of DIEA to the preactivation mixture. This led to a lower coupling efficiency (26%) after performing the coupling under the same conditions (MW, 50 ºC, 60 min).

[c] For the symmetric anhydryde method, we used a 10-fold excess of Fmoc-Ala-OH, so that Fmoc-aa-OH/DIPCDI 2:1.

[d] For TCFH and TFFH-mediated couplings, we did not test the effectiveness of performing *N*-silylation prior to coupling.

Method of choice for solid-phase couplings onto *N*-TEG residues

Taking all the results into consideration, we concluded that the best methods for the acylation of *N*-TEG residues in solid-phase were: a) to use BTC activation and allow the coupling to proceed overnight at room temperature, b) to use DIPCDI/HOAt activation and perform a 1 hour-coupling under MW heating at 50 ºC (see Figure 16).

Figure 16. Comparison of the coupling efficiency of the BTC method vs. the MW-assisted DIPCDI/HOAt method. HPLC analyses of cleaved samples after coupling Fmoc-Ala-OH onto the H-(*N*-TEG)Leu-peptidyl-resin and subsequent Fmoc- protection, linear gradient from 40% to 100% ACN over 8 min.

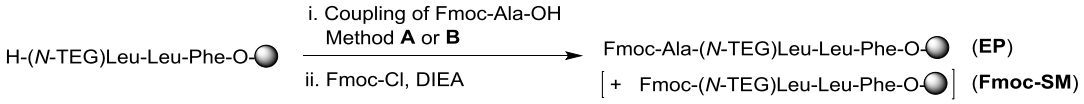

A) Coupling conditions:
Fmoc-Ala-OH (5.0 eq)
BTC (1.65 eq)
2,4,6-trimethylpyridine (14.0 eq)
THF, rt, 15 h

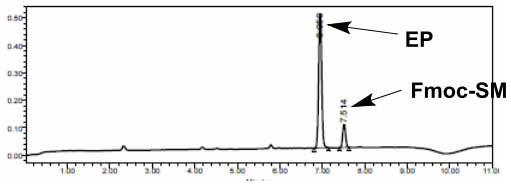

coupling efficiency = 87%

B) Coupling conditions:
Fmoc-Ala-OH (5.0 eq)
DIPCDI (5.0 eq)
HOAt (5.0 eq)
DMF, MW, 50 ºC, 60 min

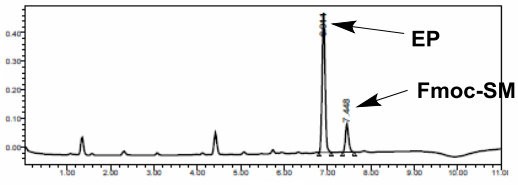

coupling efficiency = 82%

Among these two methods, the BTC procedure is preferrable. This method proved to be efficient for the coupling of other amino acids different than Fmoc-Ala-OH (see Table 7). In contrast, the coupling of such amino acids using DIPCDI/HOAt under MW heating took place in lower yields, and differences in yield were considerable for Fmoc-Val-OH (data not shown).

Table 7. Evaluation of the efficiency of the BTC method for the coupling of various Fmoc-aa-OH.

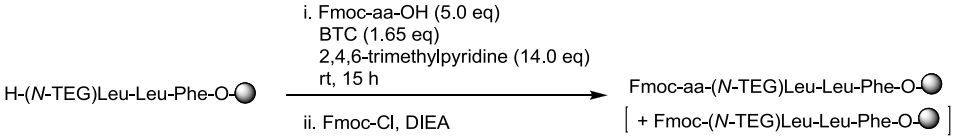

Entry	Fmoc-aa-OH[a]	Coupling cycles	Coupling efficiency
1	Fmoc-Ala-OH	1	87%
		2	98%
2	Fmoc-Leu-OH	1	90%
		2	100%
3	Fmoc-Phe-OH	1	94%
		2	100%
4	Fmoc-Val-OH	1	74%
		2	91%

[a] Although no Fmoc-amino acid bearing acid-labile side-chain protecting groups was tested, its stability under under BTC coupling conditions is well-established.[28]

1.5. Summary and conclusions

In this Chapter, we have established a methodology to synthesize peptides bearing a short *N*-OEG chain. Modification of the peptide backbone with this chemical moiety has not been previously reported.

Our methodology involves the use of Fmoc-protected *N*-TEG amino acids as solid-phase building blocks. We found that these derivatives can be easily obtained from their corresponding amino acid *tert*-butyl esters by reductive N^{α}-alkylation with 3,6,9-trioxadecanaldehyde, followed by Fmoc-protection and *tert*-butyl ester cleavage. With this scalable protocol, we prepared several Fmoc-*N*-TEG derivatives with satisfying yields.

We found that Fmoc-*N*-TEG amino acids are efficiently coupled to a peptidyl-resin under standard coupling conditions, but subsequent acylation of the *N*-TEG amine is hampered by steric hindrance. This coupling can be achieved in solid-phase using BTC activation, a method that is very low-cost and experimentally simple. We also evaluated other activating reagents recommended for difficult couplings and, in many cases, the use of MW heating dramatically reduced the reaction time and increased the purity of the product. However, in terms of coupling efficiency, the use of BTC as activating reagent proved to be superior to all the methods tested, including activation with HATU/HOAt or the use of a pre-made Fmoc-amino acid chloride. After two BTC-mediated couplings, the acylation of a resin-bound *N*-TEG amino acid is complete or almost complete.

In conclusion, Fmoc-*N*-TEG amino acids can be easily prepared from readily available starting materials, and they are valuable building blocks to prepare *N*-TEG peptides in rapid and inexpensive manner. The feasibility of introducing the *N*-TEG group into peptides may be useful for modifying physichochemical properties of pharmacological interest.

CHAPTER 2

N-triethylene glycol (*N*-TEG) as a surrogate for the *N*-Me group. Application to Sansalvamide A peptide analogs.

Abstract: We have studied the *N*-triethylene glycol (*N*-TEG) group as a surrogate for the *N*-Me group in the example of Sansalvamide A peptide. The five *N*-TEG and *N*-Me analogs of this cyclic pentapeptide were synthesized, and their biological activity, hydrophobicity, and conformational features were compared.

2.1. Introduction

In medicinal chemistry, backbone *N*-methylation is one of the most attractive modifications of a peptide structure.[6] The replacement of natural amino acids for *N*-Me residues in biologically active peptides has resulted in analogs with improved pharmacological properties. Peptides containing *N*-Me residues show higher hydrophobicity, increased metabolic stability, and –in some cases– more membrane permeability, which can enhance their bioavailability, thus amplifying their therapeutic potential. Furthermore, the introduction of backbone *N*-Me groups in bioactive peptides can have a substantial impact on their conformation and, as a result, higher activity and selectivity may be achieved.

Surprisingly, little attention has been devoted to the comparison of the synthesis and properties of *N*-methylated peptides with other *N*-alkylated peptides. We hypothesized that modification of a peptide with the *N*-triethylene glycol (*N*-TEG) group would be comparable to modification with the *N*-Me group in terms of structural and biological effects, whilst providing some of the features associated with oligoethylene glycol (see Figure 17). In both cases, *N*-alkylation of the peptide backbone decreases the number of hydrogen bonds that can be formed and is expected to have an impact on the original backbone conformation. These changes may affect the biological activity and certain physicochemical properties.

Figure 17. The *N*-TEG unit as a surrogate for the *N*-Me group in a cyclic peptide backbone.

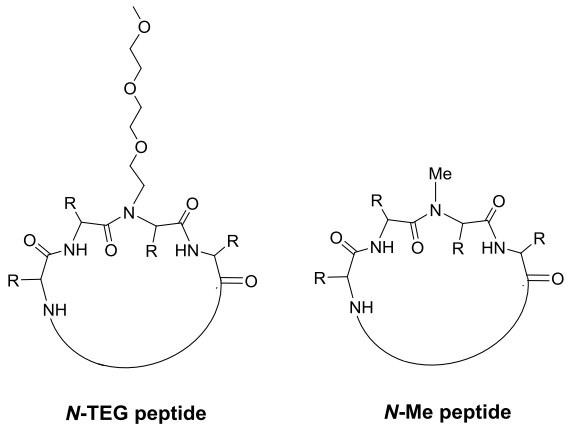

To test this notion, we sought to incorporate *N*-TEG amino acids at the different positions of Sansalvamide A peptide (**1**), a cyclic pentapeptide that shows anti-tumor activity against a variety of cancer cell lines (see Figure 18).[123] This cyclic peptide was considered a good model because it has a simple structure and well-characterized conformational and biological properties. Its five *N*-Me analogs (**1b-5b**) have already been synthesized and some of them are cytotoxic against certain cancer cell lines.[123a]

Figure 18. Structure of Sansalvamide A peptide (**1**).

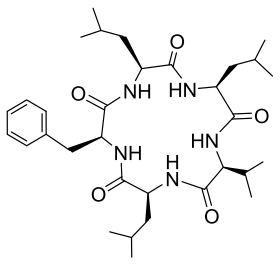

1

The structures of the target *N*-TEG and *N*-Me analogs (**1a-5a** and **1b-5b**) of Sansalvamide A peptide (**1**) are shown in Figure 19. Replacement of the *N*-Me groups present in **1b-5b** by an *N*-TEG group does not alter the amide proton pattern of their cyclic backbone, and is expected to provide a minimal perturbation of their conformational state. However, due to the amphiphilic nature of oligoethylene glycol, an alteration of certain physicochemical properties, such as hydrophobicity, was expected.

Figure 19. Structure of the target *N*-TEG (**1a-5a**) and *N*-Me (**1b-5b**) analogs.

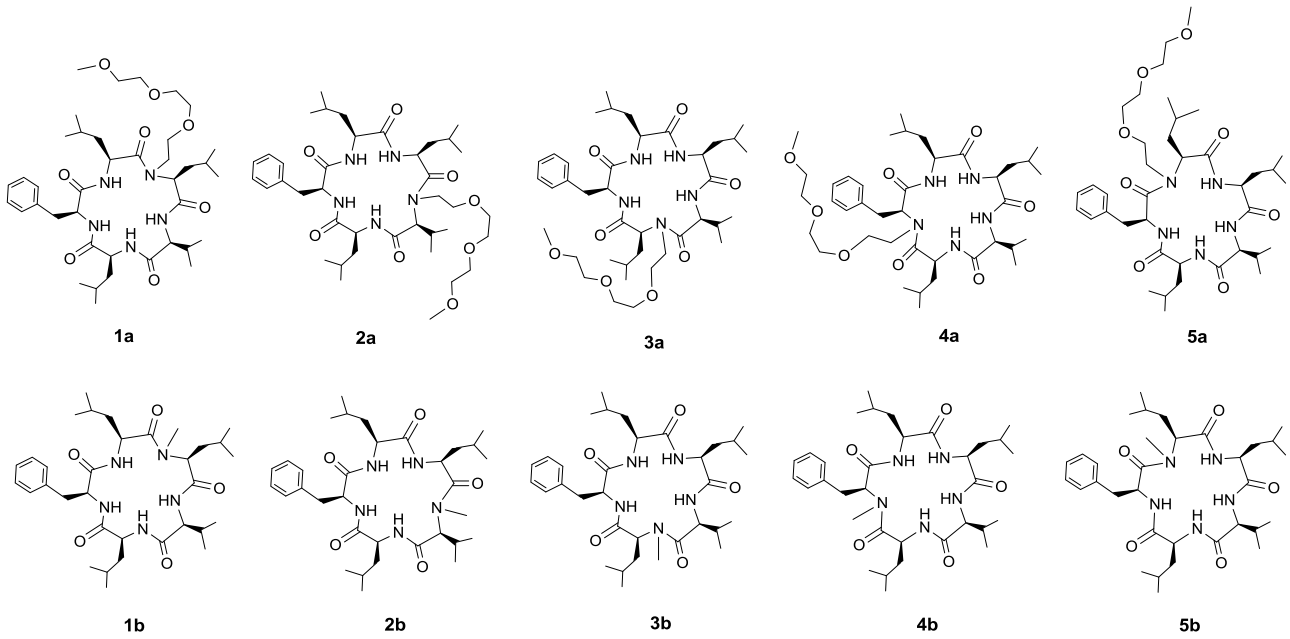

2.2. Objectives

The objectives of this Chapter were:

1. To synthesize the five analogs of Sansalvamide A peptide (**1**) bearing an *N*-TEG chain at the different backbone positions, and study the effect of *N*-TEG modification on the biological activity, lipophilicity, and conformational state of the original peptide.

2. To compare the five *N*-TEG Sansalvamide A peptide analogs (**1a-5a**) and their *N*-Me homologues (**1b-5b**) with respect to biological activity, hydrophobicity, and conformational features.

2.3. Results and discussion

2.3.1. Synthesis of the *N*-TEG and *N*-Me analogs of Sansalvamide A peptide

Our synthetic strategy to obtain the five *N*-TEG and *N*-Me analogs of the Sansalvamide A peptide (**1a-5a** and **1b-5b**) is shown in Scheme 13. We sought to prepare their linear pentapeptide precursors (**p1a-p5a** and **p1b-p5b**) by SPPS and cyclize them in solution. In all the pentapeptides, the *N*-substituted residue was placed in the middle of the sequence, which minimizes steric hindrance during cyclization and is expected to facilitate this process due to the turn-inducing properties of *N*-alkyl amino acids.[124]

Scheme 13. Synthetic approach to obtain the *N*-TEG and the *N*-Me analogs (**1a-5a** and **1b-5b**).

	SPPS		Cyclization	
Cl—	⟶	H-Phe-Leu-(*N*-TEG)Leu-Val-Leu-OH (**p1a**)	⟶	cyclo[Phe-Leu-(*N*-TEG)Leu-Val-Leu] (**1a**)
Cl—	⟶	H-Leu-Leu-(*N*-TEG)Val-Leu-Phe-OH (**p2a**)	⟶	cyclo[Leu-Leu-(*N*-TEG)Val-Leu-Phe] (**2a**)
Cl—	⟶	H-Leu-Val-(*N*-TEG)Leu-Phe-Leu-OH (**p3a**)	⟶	cyclo[Leu-Val-(*N*-TEG)Leu-Phe-Leu] (**3a**)
Cl—	⟶	H-Val-Leu-(*N*-TEG)Phe-Leu-Leu-OH (**p4a**)	⟶	cyclo[Val-Leu-(*N*-TEG)Phe-Leu-Leu] (**4a**)
Cl—	⟶	H-Leu-Phe-(*N*-TEG)Leu-Leu-Val-OH (**p5a**)	⟶	cyclo[Leu-Phe-(*N*-TEG)Leu-Leu-Val] (**5a**)
Cl—	⟶	H-Phe-Leu-*N*MeLeu-Val-Leu-OH (**p1b**)	⟶	cyclo[Phe-Leu-*N*MeLeu-Val-Leu] (**1b**)
Cl—	⟶	H-Leu-Leu-*N*MeVal-Leu-Phe-OH (**p2b**)	⟶	cyclo[Leu-Leu-*N*MeVal-Leu-Phe] (**2b**)
Cl—	⟶	H-Leu-Val-*N*MeLeu-Phe-Leu-OH (**p3b**)	⟶	cyclo[Leu-Val-*N*MeLeu-Phe-Leu] (**3b**)
Cl—	⟶	H-Val-Leu-*N*MePhe-Leu-Leu-OH (**p4b**)	⟶	cyclo[Val-Leu-*N*MePhe-Leu-Leu] (**4b**)
Cl—	⟶	H-Leu-Phe-*N*MeLeu-Leu-Val-OH (**p5a**)	⟶	cyclo[Leu-Phe-*N*MeLeu-Leu-Val] (**5b**)

For the SPPS of the *N*-TEG pentapeptides (**p1a-p5a**), we applied the synthetic methodology developed in Chapter 1. Thus, we prepared the required Fmoc-*N*-TEG amino acids (**6-8**) following the 3-step protocol that has been explained in Section 1.4.1: the amino acid *tert*-butyl ester precursors were subjected to reductive N^{α}-alkylation with 3,6,9-trioxadecanaldehyde, followed by Fmoc-protection and *tert*-butyl removal. The structures of such *N*-TEG building blocks are shown in Figure 20. For the SPPS of the *N*-Me pentapeptides (**p1b-p5b**), we used commercially available Fmoc-*N*-Me amino acids as building blocks.

Figure 20. Structure of the Fmoc-*N*-TEG derivatives of Val, Leu and Phe (**6**-**8**).

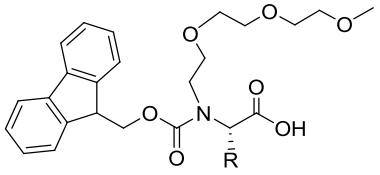

R = $CH(CH_3)_2$: Fmoc-(*N*-TEG)Val-OH (**6**)
R = $CH_2CH(CH_3)_2$: Fmoc-(*N*-TEG)Leu-OH (**7**)
R = CH_2Ph : Fmoc-(*N*-TEG)Phe-OH (**8**)

The synthesis of pentapeptides **p1a-p5a** and **p1b-p5b** was performed on the CTC resin by stepwise assembly of the corresponding Fmoc-amino acids (see Scheme 14). For standard couplings, we used a 3-fold excess of amino acid activated with DIPCDI/OxymaPure, and acylation was complete after 1 hour (ninhydrin test). These conditions were also found to work well for the couplings of Fmoc-*N*-TEG (**6-8**) and Fmoc-*N*Me amino acids, and the absence of

epimerization was confirmed by HPLC. For couplings onto *N*-substituted residues, the following amino acid was activated with BTC in the presence of a 2,4,6-trimethylpyridine excess. Activation was performed slowly at 0 ºC to avoid undesired side-reactions, and the resin-bound peptide was pretreated with 20% DIEA in THF to prevent peptide cleavage from the acid-labile CTC resin.[91] With these precautions, the BTC procedure provided a clean coupling in all cases, and no epimerization was detected. In the case of BTC-mediated couplings onto *N*-Me residues, no unreacted peptide was detected in cleaved samples after a single treatment with the activated amino acid (as checked by HPLC-MS). For the couplings onto the *N*-TEG residues, complete conversion was achieved after two treatments. Further elongation and final cleavage afforded the desired pentapeptides (**p1a-p5a** and **p1b-p5b**), which were found to be sufficiently pure to be directly cyclized.

Scheme 14. SPPS of the *N*-TEG and *N*-Me pentapeptides (**p1a-p5a** and **p1b-p5b**).

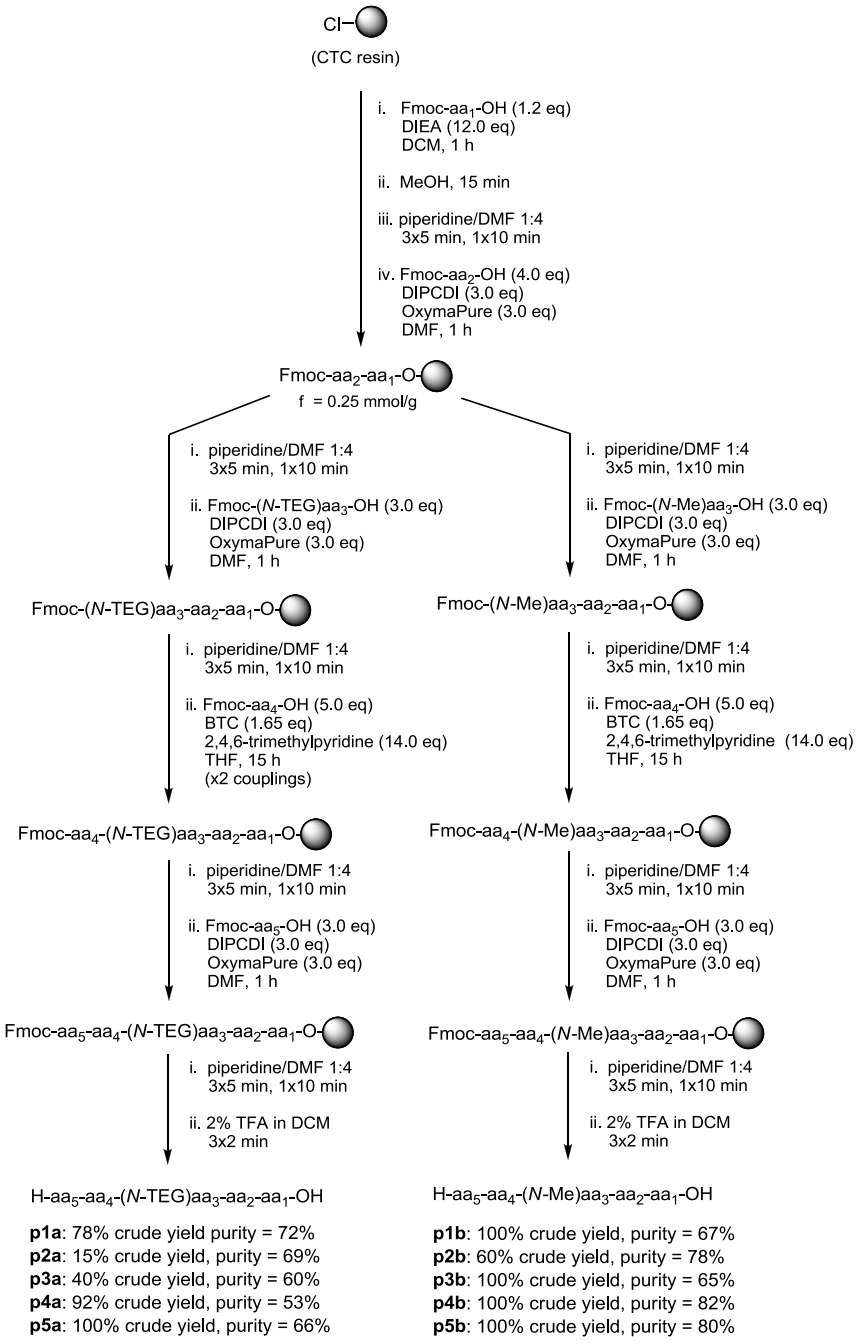

Before cyclizing our pentapeptides (**p1a-p5a** and **p1b-p5b**), we were aware of certain issues. The cyclization of pentapeptides is often difficult because dimerization to a cyclodecapeptide can easily occur.[125] To prevent this, the linear peptide precursor should be cyclized in highly dilute conditions (10^{-3}-10^{-4} M), but then the cyclization may take several hours or days to complete unless a highly efficient coupling reagent is used. Furthermore, for such slow cyclizations, the increased lifetime of the activated peptide intermediate provides an opportunity for α-epimerization at its *C*-terminal residue.

Taking these issues into consideration, we checked different cyclization protocols using H-Phe-Leu-Leu-Val-Leu-OH (**p1**) as model substrate (see Table 8). For all the conditions tested, reactions were monitorized by HPLC and HPLC-MS. Cyclization was initially assayed with HATU (0.7 eq)/DEPT (0.7 eq)/TBTU (0.7 eq)/DIEA (entry 1) at a 7 mM substrate concentration. These cyclization conditions are reported as high-yielding for obtaining Sansalvamide A peptide derivatives.[126] With this method, the cyclization proceeded extremely fast, with no remaining starting material after 1 hour, but the crude cyclic peptide was obtained in very low purity and the non-desired cyclodimer was also formed. Similarly rapid cyclizations were observed with PyBOP (5.0 eq)/DIEA and HATU (5.0 eq)/DIEA (entries 2-3), but cyclization was accompanied by the formation of a considerable amount of by-products. Perfoming the reaction at more dilute conditions led to better results in terms of purity (entries 4-8). When the pentapeptide was cyclized at 0.5 mM using HATU (1.1 eq)/DIEA or PyAOP (1.1 eq)/DIEA (entries 4-5), the lowered concentration of linear precursor decreased cyclodimerization, but the reaction was not complete after 20 hours. With these coupling reagents, more than 1.1 equivalents seem to be required for an efficient cyclization at high dilution. Among all the conditions tested, the best results were obtained with HBTU (4.0 eq)/DMAP and EDC·HCl (10.0 eq)/DMAP (entries 6-7). For these methods, we investigated the reaction with a low concentration of linear precursor (0.5 mM) and a higher concentration of coupling reagents (2-5 mM). Cyclizations proceeded slowly, but the desired cyclic pentapeptide was formed with excellent purity and, for the EDC-mediated coupling (entry 7), the formation of the cyclodecapeptide was totally suppressed.

Table 8. Conditions investigated for the cyclization of **p1**.

H-Phe-Leu-Leu-Val-Leu-OH (**p1**) ⟶ cyclo[Phe-Leu-Leu-Val-Leu] **(1)**

Entry	Coupling reagents	Solvent	Conc. of substrate	Conditions	Result
1	HATU (0.7 eq) DEPBT (0.7 eq) TBTU (0.7 eq) DIEA (6.0 eq)	THF/ACN/DCM 2 :2 :1	7 mM	rt, 1 h	No remaining starting material. Considerable formation of by-products.
2	PyBOP (5.0 eq) DIEA (15.0 eq)	NMP	9 mM	rt, 2 h	No remaining starting material. Considerable formation of by-products.
3	HATU (5.0 eq) DIEA (15.0 eq)	DMF	9 mM	rt, 2 h	No remaining starting material. Considerable formation of by-products.
4	HATU (1.1 eq) DIEA (3.0 eq)	DMF	0.5 mM	rt, 20 h	Remaining starting material. Cyclodimer only detected at trace level. Crude cyclopeptide obtained in good purity.
5	PyAOP (1.1 eq) DIEA (3.0 eq)	DMF	0.5 mM	rt, 20 h	Remaining starting material. Cyclodimer only detected at trace level. Crude cyclopeptide obtained in good purity.
6[a]	HBTU (4.0 eq) DMAP (6.0 eq)	DCM/DMF 9:1	0.5 mM	rt, 20 h	No remaining starting material. Cyclodimer only detected at trace level. Crude cyclopeptide obtained in excellent purity
7[a]	EDC·HCl (10.0 eq) DMAP (4.0 eq)	DCM/DMF 9:1	0.5 mM	rt, 20 h	No remaining starting material. No cyclodimerization. Crude cyclopeptide obtained in excellent purity.

[a] In a study on the synthesis of cyclic pentapeptides and the factors that influence cyclization yield, Gao *et. al.* investigated the effect of the DMAP proportion in the cyclizations mediated by HBTU and EDC·HCl. A 2:3 HBTU/DMAP ratio and a 5:2 EDC·HCl/DMAP ratio were stated as optimal for the cyclization of linear pentapeptide precursors.[125c]

Therefore, we concluded that cyclization with EDC·HCl/DMAP was the preferrable method, as it combines the strong activating power of EDC with the possibility of washing out the resultant urea by aqueous extraction. With these conditions (entry 7 in Table 8), all the linear pentapeptides (**p1a-p5a** and **p1b-p5b**) were efficiently cyclized in small scale (0.036 mmol). In all cases, the reactions were complete, almost no by-products were formed and, at a concentration of 0.5 mM, cyclodimerization was prevented. However, epimerization of the *C*-terminal residue took place in some cases. In particular, the highest degree of epimerization was observed in the cyclization of pentapeptide **p2a**, for which a 25% of non-desired epimer was formed.

This model reaction was used to check for epimerization during the EDC-mediated cyclization under various conditions (see Table 9). Decreasing the amount of DMAP (entries 2-3) or increasing the excess of coupling reagent (entry 4) did not lead to any substantial reduction in the degree of epimerization detected. When lowering the temperature, no significant improvement was observed either (entries 5-6). Since the prolonged existence of the activated carboxy group increases the possibility of *C*-terminal epimerization, we investigated if the use of a stronger base could preserve chiral integrity by accelerating the cyclization process. Replacement of DMAP by DIEA totally suppressed epimerization, but more than 50% of the pentapeptide was consumed in the formation of the non-desired cyclodecapeptide (entry 7). The extent of epimerization may be diminished by application of the azide method or its modification using DPPA,[125b] but these conditions were not assayed.

Table 9. Conditions investigated to minimize epimerization during the cyclization of **p2a**.

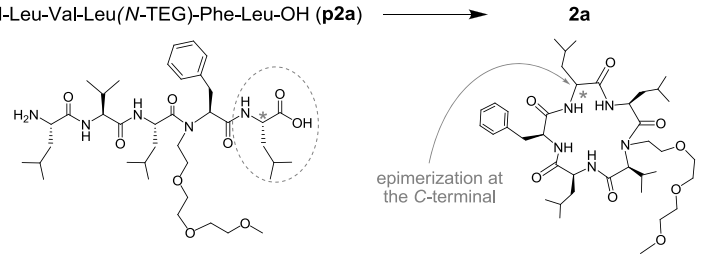

Entry	Coupling reagents	Solvent	Conc. of substrate	Conditions	desired product : epimer[a]
1	EDC·HCl (10.0 eq) DMAP (4.0 eq)	DCM/DMF 9:1	0.5 mM	rt, 20 h	0.75 : 0.25
2	EDC·HCl (10.0 eq) DMAP (2.0 eq)	DCM/DMF 9:1	0.5 mM	rt, 20 h	0.77 : 0.23
3	EDC·HCl (10.0 eq) DMAP (1.0 eq)	DCM/DMF 9:1	0.5 mM	rt, 20 h	0.72 : 0.28
4	EDC·HCl (25.0 eq) DMAP (10.0 eq)	DCM/DMF 9:1	0.5 mM	rt, 20 h	0.69 : 0.31
5	EDC·HCl (25.0 eq) DMAP (10.0 eq)	DCM/DMF, 9:1	0.5 mM	0 ºC, 2 h → rt, 20 h	0.72 : 0.28
6	EDC·HCl (25.0 eq) DMAP (10.0 eq)	DCM/DMF 9:1	0.5 mM	-15 ºC, 2 h → rt, 20 h	0.72 : 0.28
7	EDC·HCl (10.0 eq) DIEA (10.0 eq)	DCM/DMF 9:1	0.5 mM	rt, 20 h	No epimer detected, but a significant amount of cyclodimer (>50%) was formed.

[a] As determined by HPLC.

In our attempts to supress epimerization, we found that the amount of DMAP could be reduced from 4.0 to 2.0 equivalents without affecting the coupling efficiency (entry 2 in Table 9). Therefore, for the cyclization of pentapeptides **p1a-p5a** and **p1b-p5b** in a larger scale, we only employed 2.0 equivalents of DMAP (see Scheme 15). All the cyclization reactions proceeded smoothly, and the crude cyclopeptides (**1a-5a** and **1b-5b**) were easily purified by semipreparative RP-HPLC (see Figures 21 and 22). In those cases in which epimerization had taken place during the

cyclization step, the non-desired epimer was separated without difficulties. After purification, the *N*-Me and *N*-TEG cyclopeptides (**1a-5a** and **1b-5b**) were isolated in >95% purity.

Scheme 15. Cyclization to obtain the *N*-TEG and the *N*-Me analogs (**1a-5a** and **1b-5b**).[a]

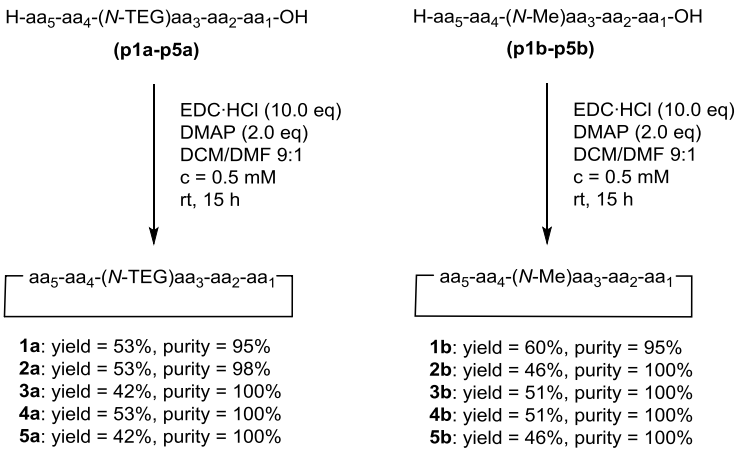

1a: yield = 53%, purity = 95%
2a: yield = 53%, purity = 98%
3a: yield = 42%, purity = 100%
4a: yield = 53%, purity = 100%
5a: yield = 42%, purity = 100%

1b: yield = 60%, purity = 95%
2b: yield = 46%, purity = 100%
3b: yield = 51%, purity = 100%
4b: yield = 51%, purity = 100%
5b: yield = 46%, purity = 100%

[a] Yields of the isolated cyclic peptides (**1a-5a** and **1b-5b**), calculated with respect to the linear precursors (**p1a-p1b** and **p1b-p5b**).

Figure 21. HPLC analysis of the crude and purified *N*-TEG cyclopeptides (**1a-5a**), linear gradient from 40 to 100% ACN over 8 min.

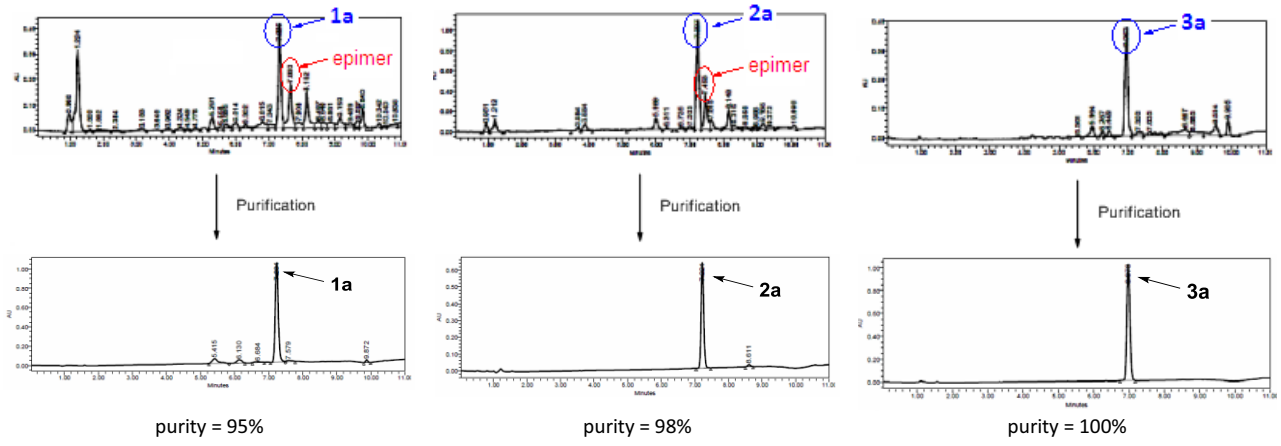

purity = 95% purity = 98% purity = 100%

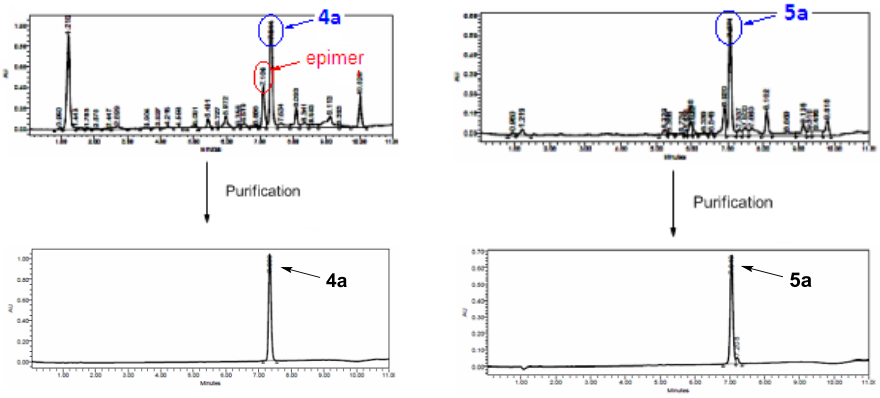

purity = 100% purity >99%

Figure 22. HPLC analysis of the crude and purified *N*-Me cyclopeptides (**1b-5b**), linear gradient from 40 to 100% ACN over 8 min.

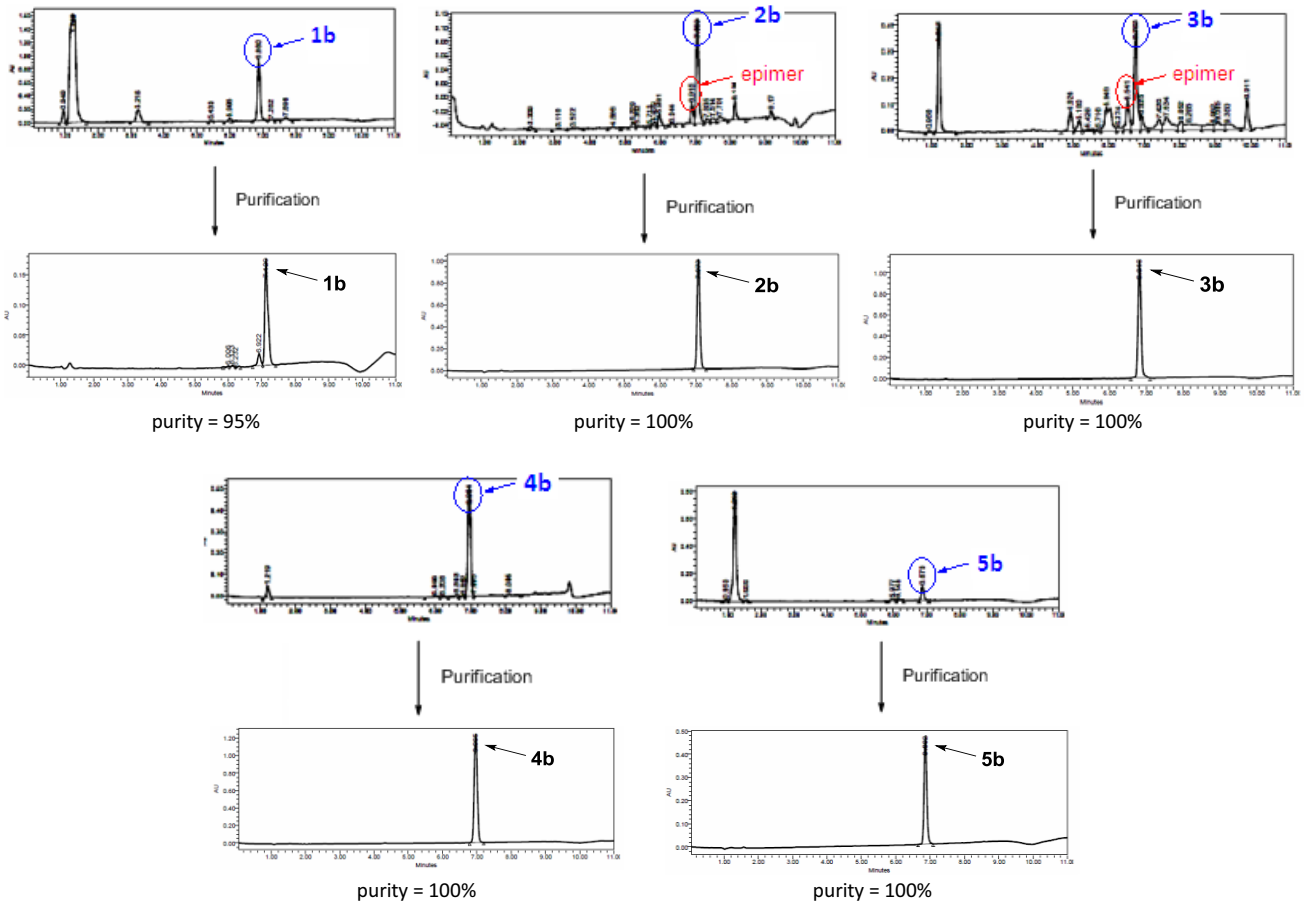

In all cases, sufficient amounts of pure peptide were obtained in yields that are commonly achieved for cyclic pentapeptides. Except for compound **2a**, the overall yields of the syntheses of the *N*-TEG cyclopeptides (**1a-5a**) and were not dramatically lower than those of the *N*-Me cyclopeptides (**1a-5a**). Thus, *N*-TEG peptides are accessible by the same synthetic repertoire as that already established for *N*-Me peptides.

2.3.2. Effect of *N*-TEG vs. *N*-Me on biological activity

Sansalvamide A peptide (**1**) and its *N*-Me analogs (**1b-5b**) are reported to have modest or little activity against various cancer cell lines.[123] In order to investigate how *N*-Me-for-*N*-TEG substitution affects their anti-cancer activities, we tested our compounds (**1**, **1a-5a** and **1b-5b**) for their cytotoxicity against GLC-4 (small cell lung cancer), MDA-MB-231 (breast cancer) and SW-480 (colon cancer) cells.

Cytotoxicity was evaluated through cell viability assays. For each each cancer cell line, cells were seeded into 96-well plates and treated with the compounds of study at different concentrations and, after a certain period of time, the % of cell viability was determined through MTT assay.[204] Each experiment was performed 3 times (seeding the 3 plates at 3 different times) and, for each plate, test conditions were assayed in triplicate wells. This work was carried out at the Cancer Cell Biology Research Group of the UB Faculty of Medicine (Bellvitge campus), under the supervision of Prof. Ricardo Pérez and Dr. Vanessa Soto-Cerrato.

At a concentration of 10 µM, none of our compounds showed significant cytotoxicity (*i.e.* >70% reduction of cell viability) against any of the cancer cell lines. At a concentration of 50 µM, we performed time-course experiments with GLC-4 cells, and the highest cytotoxic effects were observed after a 72 hour-treatment (see Figure 23).

Figure 23. Cell viability of GLC-4 cancer cells after 50 µM treatment of **1**, **1a-5a** and **1b-5b** for 24/48/72 h.

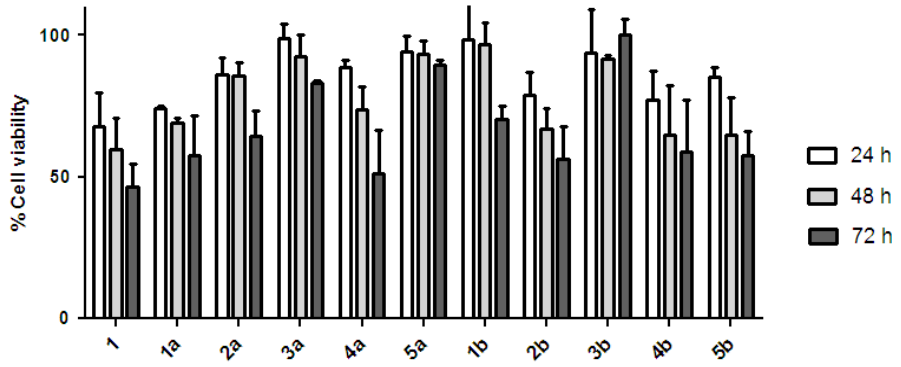

Treatment of GLC-4, MDA-MB-231 and SW-480 cells with 50 µM of some compounds for 72 hours decreased the viability of GLC-4 (**1, 1a, 2a**, **4a, 2b**, **4b**, **5b**) and MDA-MB-231 (**1a**, **4a, 3b**) cells up to 50-60%, whereas the only compound that reduced viability of SW-480 cells below 60% was **2b** (see Figure 24). Indeed, this colon cancer cell line is reported to be strongly resistant against several anti-cancer agents.[127]

Figure 24. Cell viability of GLC-4, MDA-MB-231 and SW-480 cancer cells after 50 µM treatment of **1**, **1a-5a** and **1b-5b** for 72 h.

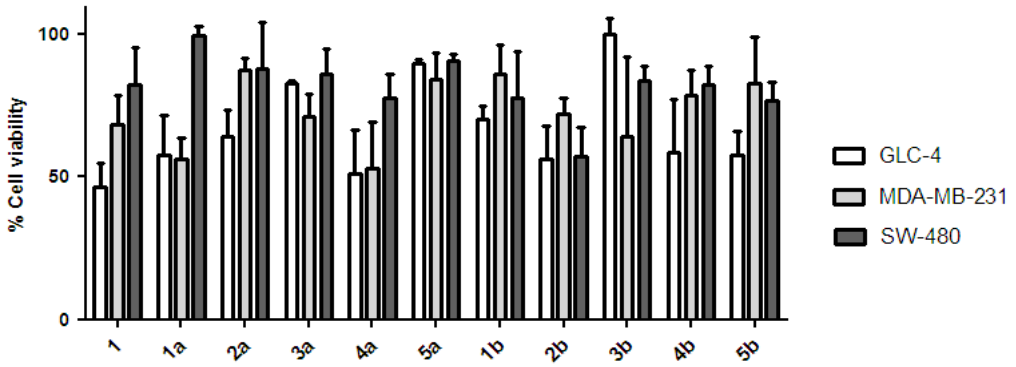

Although the cytotoxic effects observed were rather modest, the activities of the *N*-TEG analogs **1a** and **4a** were very similar to that of the parent peptide (**1**) against both GLC-4 and MDA-MB-231 cells. For **1** and these most potent *N*-TEG analogs (**1a** and **4a**), we estimated their IC_{50} (72 h) value. Such value is the compound concentration that reduces cell viability to 50% after a 72 hour-treatment, and can be calculated by interpolation from the corresponding dose-response curve. Sansalvamide A peptide (**1**) showed an IC_{50} around 85 µM against GLC-4 cells and superior to 100 µM against MDA-MB-231 cells, whereas the IC_{50} values of **1a** and **4a** were lower than 90 µM against these two cell types (see Table 10).

Table 10. Estimation of IC_{50} (72 h) of **1**, **1a** and **4a** against GLC-4 and MDA-MB-231 cancer cells. IC_{50} (72 h) values are given in μM.[a]

Peptide	IC_{50} (72 h) against GLC-4	IC_{50} (72 h) against MDA-MB-231
1	85	>100
1a	55	87
4a	74	67

As shown in Figure 24, the cytotoxic activities of the certain *N*-TEG analogs are within the same range of those of their *N*-Me homologues for the tested cancer cell lines. These findings suggest that specific amino acid constituents may be amenable to *N*-Me-for-*N*-TEG substitution without a loss in biological activity.

2.3.3. Effect of *N*-TEG vs. *N*-Me on lipophilicity

The incorporation of *N*-TEG or *N*-Me groups was expected to affect the lipophilicity of Sansalvamide A peptide (**1**). This peptide is very hydrophobic, as it lacks ionizable *N*- and *C*-terminus and it is exclusively composed of non-polar amino acids. The introduction of an *N*-alkyl group into a peptide decreases the number of amide protons that can act as hydrogen bond donors and, hence, increases hydrophobicity. However, since TEG is an amphiphilic moiety, we envisioned that *N*-TEG and *N*-Me could affect hydrophobicity/lipophilicity in a different manner.

Hydrophobicity and lipophilicity: definitions

Prior to discuss our results, we would like to make an explanatory comment concerning the terms “hydrophobicity” and “lipophilicity”. Although both terms are widely used in relation to the sorption of organic compounds from water, their exact meaning is somewhat vague or confused.[128a]

The following definitions have been suggested by the IUPAC:[129]

- **Hydrophobicity** refers to the tendency of a non-polar molecule to prefer a non-aqueous environment over an aqueous environment. The term “hydrophobicity” is related to the term “hydrophobic effect”, which is the association of non-polar moieties/molecules in an aqueous environment. The driving force for this process is the preference of water to form an ordered structure, thereby excluding non-polar moieties/molecules.

- **Lipophilicity** refers to the affinity of a molecule for a lipophilic environment, and encodes several types of intermolecular interactions. It is commonly measured by the distribution behaviour of such a molecule between two phases, either liquid-liquid (*e.g.* partition in octanol/water) or solid-liquid (*e.g.* retention in RP-HPLC, permeation across biomembranes).

Measurements of lipophilicity express the net result of all the intermolecular forces involving the solute and the two phases between which it partitions.[128b] Several equations have been proposed to factorize lipophilicity into a number of parameters.[130] As a result of such equations, it is common to factorize lipophilicity into two (or three) sets of terms, namely: hydrophobicity (which accounts for hydrophobic and dispersion forces), polarity (which accounts for hydrogen bonds, and orientation and induction forces), and ionic interactions (either attractive or repulsive).[128b,130a] When measured in isotropic systems (*i.e*. octanol/water, RP-HPLC), lipophilicity mainly expresses the balance of

hydrophobic and polar interactions [see "a)" below]. When measured in anisotropic systems (*i.e.* liposome/water, membrane-like systems), it also encodes the influence of ionic interactions [see "b)" below].

a) Isotropic system: Lipophilicity = Hydrophobicity - Polarity

b) Anisotropic system: Lipophilicity = Hydrophobicity - Polarity + Ionic interactions

Therefore, hydrophobicity is not synonymous with lipophilicity, but a mere component of it. For a series of compounds with similar functional and ionizable groups, the more hydrophic the compound, the higher its lipophilicity.

Throughout this Thesis, we will use the terms "lipophilicity" and "hydrophobicity" in the broad sense of their meaning. However, for measurements from partition experiments and for refering to transport across biological membranes, we will only use the term "lipophilicity".

Methods to measure lipophilicity

One of the most common parameters to measure lipophilicity is the partition coefficient (logP), which is the ratio of distribution of a compound between two immiscible solvents (usually octanol and water). This value can be determined by the shake-flask method (see Figure 25).[131] In this method, the compound is dissolved in the organic solvent, water is added, the mixture is shaken for 2-3 days so that compound partition reaches equilibrium, and then fraction of compound in each phase is assessed (*e.g.* UV detection). However, logP determination of poorly soluble compounds by the shake-flask method is problematic. Along these lines, logP determination by the shake flask method is prone to errors if the compound is extremely hydrophilic or hydrophobic, as its concentration in one of the phases will be exceedingly small and thus difficult to quantify.

Figure 25. Determination of logP by the shake-flask method.
$A_{octanol}$ and A_{water} refer to the HPLC peak areas of the compound in the octanol and aqueous phase, respectively.

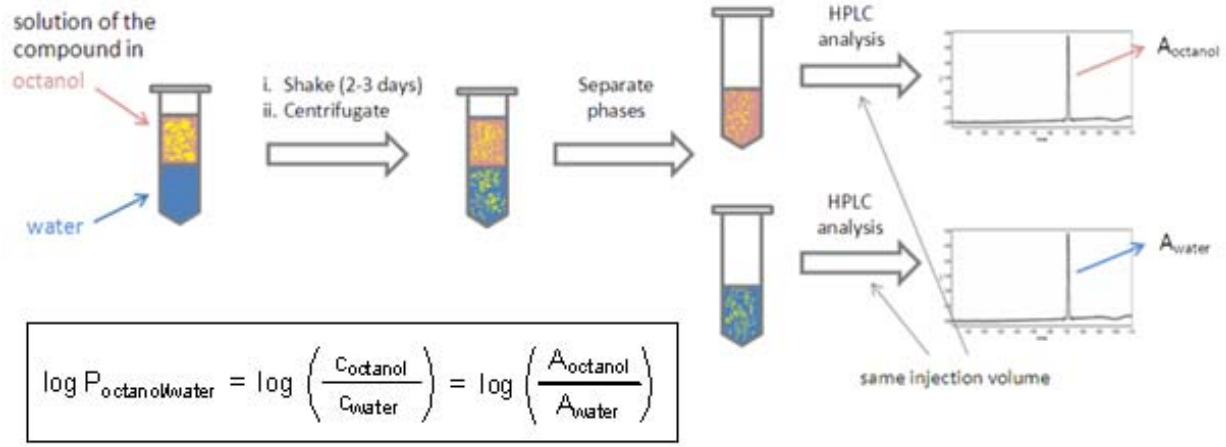

Besides the shake flask method, logP can be indirectly determined by chromatographic methods.[132] These methods are based on the putative correlation of logP with chromatographic retention parameters, such as those derived from RP-HPLC. The correlation equation is constructed from a set of reference compounds with known log P values. Several RP-HPLC-based equations for logP estimation are reported, comprising a wide range of stationary and mobile phases. However, most equations based on chemically bonded stationary phases do not work for logP estimation of a wide range of compounds of diverse structure.[128c] This is because the fundamental properties responsible for chromatographic retention tend to be different to those responsible for partition between octanol and water,

especially the contribution from hydrogen bonding interactions. Therefore, for new classes of compounds for which there are no comparable reference structures, logP determination from chromatographic parameters is not suitable.

Despite this issue, for a series of modified analogs of similar MW, comparison of their RP-HPLC retention times is a valid method to rank their hydrophobicities.[133] The RP-HPLC behaviour of a compound depends on its interactions with the non-polar stationary phase: the more hydrophobic a compound is, the stronger its retention on the column. This does not allow to measure lipophilicity (logP) or hydrophobicity in an absolute manner, but allows to determine the relative hydrophobicity of a series of compounds that are similar in size and structure.

Evaluation of the lipophilicity of our compounds

As previously mentioned, the incorporation of *N*-TEG or *N*-Me groups into Sansalvamide A peptide (**1**) was expected to affect its lipophilicity in a different manner.

To investigate this, we attempted to determine the logP of our compounds (**1**, **1a-5a** and **1b-5b**) by the shake flask method (see Table 11). First, we investigated their partition in octanol/water, for which we performed several experiments changing the proportions between the two phases. In all cases, no compound was detected in the aqueous phase and thus logP's could not be calculated. Indeed, since the amide protons can form hydrogen bonds with octanol, determination of the logP's of peptides is often very difficult or even impossible.[128d] This is specially true for very hydrophobic peptides that are poorly soluble in water. Wishing to overcome this issue, we investigated partition in other solvent systems with different hydrogen-bonding capacities, such as dodecane/ethyleneglycol or dodecane/water. However, these solvent mixtures did not allow for logP determination either. With dodecane/ethyleneglycol, all the compound went to the ethylene glycol phase, pressumably due to the capability of this solvent to form hydrogen bonds. With dodecane/water, compounds separated between both phases, but the experiments were not reproducible.

Table 11. Some of our attemps to determine logP by the shake-flask method.[a]

Peptide	octanol/water	Result	log P
1	1:1, 1:2, 2:1	No compound in the aqueous phase.	-
5a	1:1, 1:2, 2:1, 1:4		
Peptide	dodecane/ethyleneglycol	Result	log P
1	1:1	No compound in the dodecane phase.	-
5a	1:1		
Peptide	dodecane/water	Result	log P
1	1:1	Partition takes place, but results are not reproducible.	0.60 ± 0.83
5a	1:1	Partition takes place, but results are not reproducible.	0.43 ± 0.66
5b	1:1	Partition takes place, but results are not reproducible.	0.63 ± 0.42

[a] LogP determination experiments were performed as triplicates.Increasing the equilibration time from 2 to 4 days did lead to any change in the results, and no difference was observed when using different types of shakers to mix the phases till partition.

Since we were not able to determine logP's by the shake flask method, we evaluated the relative hydrophobicities of **1**, **1a-5a** and **1b-5b** by comparing their RP-HPLC retention times (see Table 12). The increase in time at which the *N*-TEG and the *N*-Me analogs (**1a-5a** and **1b-5b**) eluted indicates that these analogs are more hydrophobic than Sansalvamide A peptide (**1**). This can be attributed to the fact that *N*-alkylation with TEG or Me eliminates one amide proton, which is a strong hydrogen bond donor.

Table 12. RP-HPLC retention times of **1**, **1a-5a**, **1b-5b**, linear gradient from 10% to 90% ACN over 8 min, C18 column.

t_r (min)	
1: 5.97	
1a: 7.29	**1b:** 7.12
2a: 7.22	**2b:** 7.07
3a: 6.98	**3b:** 6.82
4a: 7.34	**4b:** 6.97
5a: 7.05	**5b:** 6.86

Interestingly, all the *N*-TEG analogs (**1a-5a**) were found to be slightly more hydrophobic than their corresponding *N*-Me homologues (**1b-5b**). A possible explanation for this will be given in Section 3.3.9 of the next Chapter. However, herein we would like to note that OEG oligomers, such as TEG, are amphiphilic moieties.[135] Their ether oxygen atoms are weak hydrogen bond acceptors, whereas the presence of two methylene units *per* each ether functionality and the lack of ionizable groups account for a certain hydrophobic character. Along these lines, we would like to make another remark: although OEG-modified peptides often show better aqueous solubility than their corresponding non-modified peptides, this is not due to a higher hydrophilicity; it is due to to their OEG chain preventing intermolecular aggregation.[76,136] Because of this same reason, the attachment of OEG onto peptides can also improve their solubility in organic solvents.[76,137]

Potential effect of *N*-TEG modification of peptides on their membrane permeability

Lipophilicity is one of the most influencing molecular properties in determining transport across biological barriers (*e.g.* intestinal epithelium layer, blood-brain-barrier, skin).[138] In particular, it favours passive diffusion through the phospholipidic cell membranes, and thus favours crossing via passive transcellular diffusion, which is the most common transport mechanism for the majority of drugs.

Since peptide modification with *N*-TEG increases hydrophobicity, it should influence permeability across biological membranes. However, such an effect is difficult to predict. On one hand, the greater lipophilicity upon *N*-TEG incorporation should enhance permeability by favouring passive diffusion. On the other hand, incorporation of *N*-TEG increases the overall molecular size, which is disfavourable for passive diffusion and could offset the lipophilicity effect.

N-methylated peptides generally show enhanced intestinal permeability with respect to their non-alkylated homologues.[9,18,19a] This has been attributed to their decreased hydrogen-bonding potential and increased hydrophobicity –which enhance passive permeation–,[20] and to certain conformational features which facilitate passive permeation as well.[9,18a,19b] As *N*-methylation, peptide modification with *N*-TEG eliminates a strong hydrogen bond donor (*i.e.* a backbone amide proton), but it also introduces three weak hydrogen bond acceptors (*i.e*. the ether oxygen atoms of the TEG chain).

It would be very interesting to evaluate the intestinal permeability of *N*-TEG vs. *N*-Me and/or unmodified peptides in Caco-2 cell-based assays or parallel artificial membrane permeability (PAMPA) assays. However, this was beyond the scope of the present PhD project.

2.3.4. Effect of *N*-TEG vs. *N*-Me on conformation

The incorporation of *N*-TEG or *N*-Me groups was expected to perturbate the conformational state of Sansalvamide A peptide (**1**). In small cyclic peptides, conformation is mainly dictated by the backbone stereochemistry and the presence of *N*-alkyl groups, rather than by interactions with or among the amino acid side-chains.[21] The introduction of an *N*-alkyl group into a peptide: i. eliminates one hydrogen bond donor, ii. lowers the energy barrier for the *trans*-to-*cis* isomerization of the *N*-alkylated amide bond,[15] iii. can induce local backbone constraints to minimize steric interactions, thereby providing conformational rigidity.[16] These restraints can affect the original peptide conformation by modulating its backbone torsional preferences due to steric reasons and/or by altering its intramolecular hydrogen-bonding pattern.

To study if the effect the *N*-TEG group on the conformational state of **1** was similar to that of an *N*-Me group, we analyzed all the compounds (**1**, **1a-5a** and **1b-5b**) by ^{1}H and ^{13}C-NMR spectroscopy, and we compared their H^{N}, H^{α}, and C^{α} resonances, which are sensitive to conformational changes. An overlay of the ^{1}H-NMR spectra of **1**, **1a-5a** and **1b-5b** in the H^{N}- and H^{α}-regions clearly showed that *N*-alkylation induced changes in the backbone conformation of the parent peptide (see Figure 26). Depending on the position of *N*-alkylation, different signal patterns were observed; however, the *N*-TEG and the *N*-Me analogs (**1a-5a** and **1b-5b**) bearing the *N*-substituent at the same position were found to have similar H^{N}- and H^{α}-resonances, which indicates a similar backbone conformation regardless of the nature of the *N*-substituent. The resemblance of their C^{α}-chemical shifts gives further evidence of similar conformational preferences for a same *N*-alkylation pattern (see Table 13).

Figure 26. ^{1}H-NMR spectra (in $CDCl_3$) of **1**, **1a-5a** and **1b-5b** in the 8.5-6.0 ppm region (A) and in the 5.5-3.5 ppm region (B).[a]

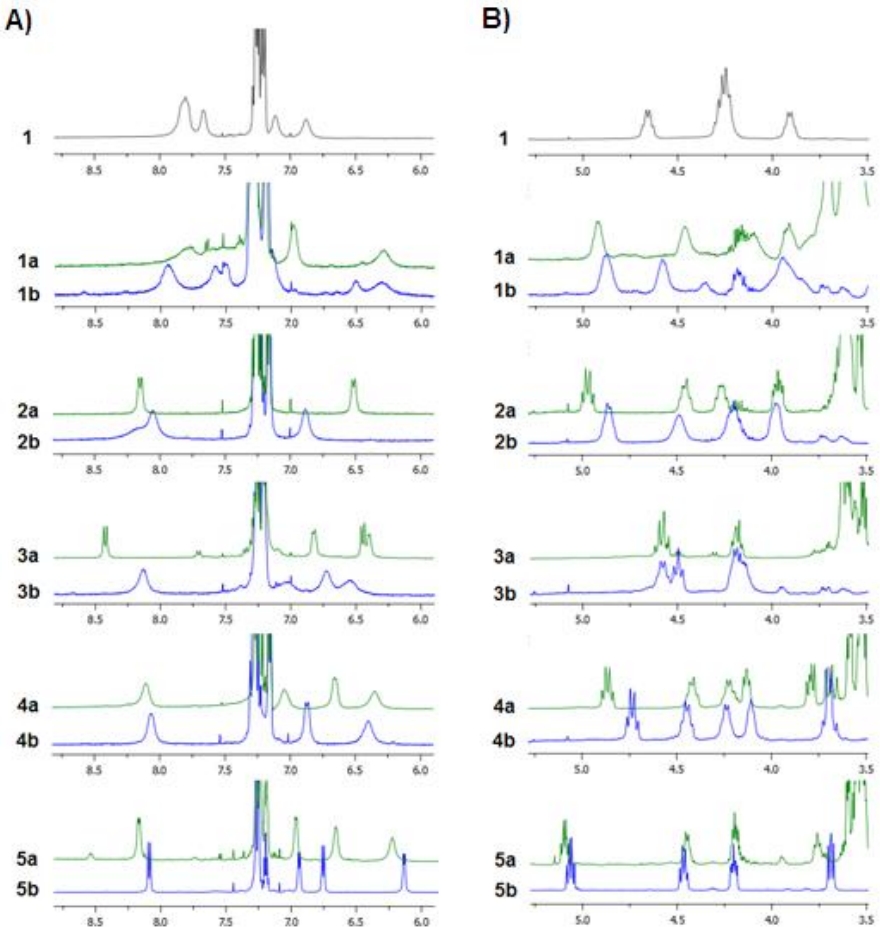

[a] The partial assignment of the proton resonances of **1**, **1a-5a** and **1b-5b** is shown in Annex 2.

Table 13. C^{α}-chemical shifts (ppm) of **1**, **1a-5a** and **1b-5b** in $CDCl_3$.[a]

1	1a	1b	2a	2b	3a	3b	4a	4b	5a	5b
51.7	48.6	49.2	48.3	48.3	51.9	52.1	48.5	48.3	51.2	51.2
53.7	52.6	55.0	50.9	51.5	53.9	54.3	51.5	51.7	51.4	51.5
55.3	56.1	56.0	53.5	53.2	54.4	54.6	52.8	53.0	53.6	53.4
57.9	59.8	59.1	56.6	57.5	55.4	55.3	60.2	60.2	60.7	61.2
58.8	66.4	65.0	66.4	65.1	67.9	68.9	70.8	72.1	68.4	70.0

[a] The partial assignment of the carbon resonances of **1**, **1a-5a** and **1b-5b** is shown in Annex 2.

As depicted in Figure 26, Sansalvamide A peptide (**1**) was found to exist as a single conformer on the NMR time scale of chemical shift separation. The *N*-TEG and *N*-Me analogs (**1a-5a** and **1b-5b**) also showed a clearly preferred backbone conformation (*i.e.* for each peptide, only one set of H^N-, H^{α}- and C^{α}-signals was detected under measurement conditions). However, for peptides **1a** and **1b**, a minor set of certain H^N- and H^{α}-signals was also present in their ^{1}H-NMR spectra together with the major one. This indicates that for these peptides there are two conformers in slow chemical exchange on the NMR time scale of chemical shift separation.

It is important to note that the single set of signals observed for **1**, **2a-5a** and **2b-5b** (as the major set of signals observed for **1a** and **1b**) could be the average of signals from various conformers in fast chemical exchange. To rule out this possibility, we analyzed peptides **1**, **5a** and **5b** by ^{1}H-NMR at 5, 15, 25, 35 and 45 ºC. For the three peptides, no evidence of conformational equilibria was found in this temperature range.

For peptides **5a** and **5b**, we performed a more detailed NMR study in comparison with the parent peptide (**1**). For each peptide, two-dimensional NMR experiments (COSY, TOCSY, NOESY and HSQC) were performed and their H^N-, H^{α}- and C^{α}-signals were unequivocally assigned (see Table 14). The temperature coefficients of the amide protons were determined from the variable temperature ^{1}H-NMR experiments, and the NOEs between the amide protons were analyzed (see Table 15). These experimental parameters, which are sensitive to conformational changes, were almost identical for the *N*-TEG and *N*-Me analogs **5a** and **5b**, whilst considerably differing from those of the unmodified Sansalvamide A peptide (**1**). These findings corroborate that *N*-TEG and *N*-Me groups exert similar constraints on the backbone conformation of **1** when incorporated at the same residue.

Table 14. H^N-, H^{α}- and C^{α}-chemical shifts (ppm) of **1**, **5a** and **5b** in $CDCl_3$ at 298 K.

Peptide	δ (H^N) [ppm]					δ (H^{α}) [ppm]				
	H^N [Leu^3]	H^N [Leu^2]	H^N [Val]	H^N [Phe]	H^N [Leu^1]	H^{α} [Phe]	H^{α} [Leu^2]	H^{α} [Leu^1]	H^{α} [Val]	**1:** H^{α} [Leu^3] **5a**: H^{α} [(*N*-TEG)Leu] **5b**: H^{α} [*N*MeLeu]
cyclo[Leu^1-Phe-Leu^3-Leu^2-Val] (**1**)	7.12	7.51	7.70	6.81	7.65	4.63	3.90	4.24	4.22	4.24
cyclo[Leu^1-Phe-(*N*-TEG)Leu-Leu^2-Val] (**5a**)	-	8.15	6.96	6.66	6.23	5.09	4.45	4.20	3.76	3.55
cyclo[Leu^1-Phe-*N*MeLeu-Leu^2-Val] (**5b**)	-	8.07	6.93	6.75	6.14	5.06	4.46	4.20	3.69	3.43

Peptide	δ (C^{α}) [ppm]				
	1: C^{α} [Leu^3] **5a**: C^{α} [(*N*-TEG)Leu] **5b**: C^{α} [*N*MeLeu]	C^{α} [Val]	C^{α} [Leu^1]	C^{α} [Phe]	C^{α} [Leu^2]
cyclo[Leu^1-Phe-Leu^3-Leu^2-Val] (**1**)	51.8 or 53.2[a]	58.7	51.8 or 53.2[a]	55.4	57.7
cyclo[Leu^1-Phe-(*N*-TEG)Leu-Leu^2-Val] (**5a**)	68.4	60.7	53.6	51.4	51.2
cyclo[Leu^1-Phe-*N*MeLeu-Leu^2-Val] (**5b**)	70.0	61.3	53.4	51.5	51.2

[a] For Sansalvamide A peptide (**1**), the ^{13}C-NMR signals at 51.8 and 53.2 ppm could not be unambiguosly assigned to C^{α} [Leu^3] and C^{α} [Leu^1], since the ^{1}H-NMR signals associated to H^{α} [Leu^3] and H^{α} [Leu^1] overlapped at 4.24 ppm. The HSQC spectra showed cross-peaks at (4.24, 51.8) and (4.24, 53.2) ppm.

Table 15. Temperature coefficients (ppb K^{-1}) and NOE data for for the amide protons of **1**, **5a** and **5b** in $CDCl_3$.

Peptide	Δδ/ΔT [ppb K^{-1}]					Significant NOEs
	H^N [Leu^3]	H^N [Leu^2]	H^N [Val]	H^N [Phe]	H^N [Leu^1]	
cyclo[Leu^1-Phe-Leu^3-Leu^2-Val] (**1**)	-3.5	-6.8	-4.8	-6.1	-10.3	-[a]
cyclo[Leu^1-Phe-(*N*-TEG)Leu-Leu^2-Val] (**5a**)	-	<0.1	-8.7	-6.3	-6.0	H^N [Phe] - H^N [Leu^2] H^N [Phe] - H^N [Leu^1] H^N [Val] - H^N [Leu^2]
cyclo[Leu^1-Phe-*N*MeLeu-Leu^2-Val] (**5b**)	-	<0.1	-10.6	-6.3	-6.0	H^N [Phe] - H^N [Leu^2] H^N [Phe] - H^N [Leu^1] H^N [Val] - H^N [Leu^2]

[a] For Sansalvamide A peptide (**1**), NOEs between the amide protons could not be detected under measurement conditions. McAlpine *et al.* studied the conformation of **1** in DMSO-*d*6/H_2O 4:1 and observed NOEs between H^N [Phe] - H^N [Leu^1] and H^N [Val] - H^N [Leu^2].[123e]

On the basis of this study, replacement of a backbone *N*-Me group of a cyclic peptide by an *N*-TEG chain is expected to provide a minimal perturbation of its backbone conformation.

2.4. Summary and conclusions

In this Chapter, we have investigated the *N*-TEG group as a surrogate for the *N*-Me group on the example of Sansalvamide A peptide. For that, we synthesized five analogs of this cyclopentapeptide in which the *N*-TEG group was incorporated at the different backbone positions. Such *N*-TEG chain was introduced during the SPPS of the peptide using Fmoc-*N*-TEG amino acids as building blocks. Formation of the amide bond betweeen the *N*-TEG residue and the following amino acid was achieved in solid-phase using BTC as activating reagent.

We studied how modification of Sansalvamide A peptide with *N*-TEG and *N*-Me affects its biological activity, hydrophobicity, and conformational features. Several *N*-TEG and *N*-Me analogs exhibited low cytotoxic effects against GLC-4 and MDA-MB-231 cancer cells. Although none of our compounds was highly active against any of the cell lines tested, the activities of certain *N*-TEG analogs were within the same range as those of their *N*-Me homologues. The introduction of *N*-TEG or *N*-Me groups into Sansalvamide A peptide led to analogs with increased hydrophobicity, as indicated by their higher RP-HPLC retention times. Indeed, the *N*-TEG analogs were slightly more hydrophobic than their *N*-Me counterparts. As expected, NMR data showed that the incorporation of *N*-TEG or *N*-Me residues at the different positions of Sansalvamide A peptide altered its conformation in solution. Those *N*-TEG and *N*-Me analogs bearing the *N*-substituent at the same position had similar H^N-, H^α- and C^α-resonances, which gives evidence of a similar backbone conformation. On the basis of these findings, the *N*-TEG group is expected to provide similar conformational restraints as a backbone *N*-Me group when incorporated into a cyclic peptide.

In conclusion, peptides in which the backbone *N*-Me group has been replaced by a short *N*-OEG chain are accessible by the same synthetic repertoire as that already established for *N*-Me peptides. The ten-atom chain of *N*-TEG does not considerably alter the conformational preferences with respect to an *N*-Me group, and provides a slightly enhanced hydrophobicity. Considering the high abundance of *N*-Me amino acids in biologically active peptides, modication at this position may be a valuable alternative to introduce chemical diversity when modification at any other position of the peptide is not sought or possible, and may be useful to optimize physichochemical properties that are of pharmacological interest.

CHAPTER 3

Replacement of the *N*-methyl group of Cilengitide by *N*-oligoethylene glycol (N-OEG) chains of increasing length: effect on biological activity and lipophilicity.

Abstract: We have synthesized three analogs of cyclo[RGDf*N*MeV] (Cilengitide) in which the *N*-Me group has been replaced by *N*-oligoethylene glycol (*N*-OEG) chains of increasing length; namely, *N*-OEG_2, *N*-OEG_{11} and *N*-OEG_{23}, which are respectively composed of 2, 11 and 23 repeating ethylene oxide monomer units. These three *N*-OEG cyclopeptides were compared with Cilengitide with respect to biological activity and lipophilicity, as *N*-Me-for-*N*-OEG substitution and OEG chain length were expected to affect these features.

3.1. Introduction

In Chapter 2, we described that peptides bearing a short *N*-TEG chain are accessible using standard solid-phase techniques. The formation of the amide bond between the *N*-TEG residue and the following amino acid can be achieved in solid-phase using BTC as activating reagent.

We wanted to investigate if peptides modified with a larger *N*-OEG chain could also be prepared. To investigate this, we chose Cilengitide (**1**) as a model (see Figure 27). This peptide is an Arg-Gly-Asp (RGD) peptide of sequence cyclo[RGDf*N*MeV] that shows antagonistic activity for the $\alpha_v\beta_3$, $\alpha_v\beta_5$ and $\alpha_v\beta_1$ integrin receptors.[139] These receptors belong to the $\alpha_v\beta$ integrin family, a family of transmembrane receptors that bind to several extracellular matrix (ECM) proteins with the exposed RGD-tripeptide sequence.[148] By interacting with ECM proteins, integrins play a crucial role in controlling crucial events such as cell adhesion, growth, differentiation and apoptosis;[149] hence, they are attractive therapeutic targets for a number of diseases.[195] Antagonists for the $\alpha_v\beta_3$ integrin, such as Cilengitide, hold significant potential as anti-angiogenic drugs.[196] Furthermore, since the $\alpha_v\beta_3$, $\alpha_v\beta_5$ and $\alpha_v\beta_1$ integrins are overexpressed in several types of cancers,[140] RGD-cyclopeptides with high affinity for these receptors have been extensively used as targeting vectors for tumor imaging and therapeutics.[141] Along these lines, RGD-peptides are also employed for surface modification of biomaterials, with a view to elicit selective cellular responses.[197]

Figure 27. Structure of cyclo[RGDf*N*MeV] (**23**).

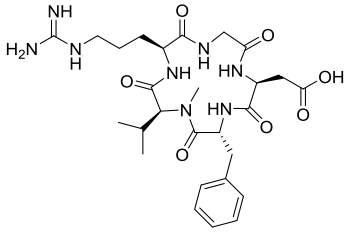

23

For specific biomedical applications, RGD-based cyclopeptide ligands are often optimized by attachment of an OEG-based polymer.[142] Depending on their length and structure, these polymers can serve as pharmacokinetic modifiers, linkers to support conjugation with a desired molecule, spacers to avoid non-specific interactions with the RGD motif, and scaffolds to create multimeric constructs that can simultaneously target different receptors.

We sought to synthesize three analogs of cyclo[RGDf*N*MeV] (**23**) in which the *N*-Me group of Val was replaced by *N*-OEG chains of increasing length, namely *N*-OEG_2, *N*-OEG_{11} and *N*-OEG_{23}, which are respectively composed of 2, 11 and 23 repeating ethylene oxide monomer units (see Figure 28). The synthesis of these *N*-OEG cyclopeptides (**24-26**) involves the coupling of D-Phe onto (*N*-OEG)Val. This coupling is not only hampered by the *N*-OEG substituent, but also by the additional steric hindrance exerted by β-branched side-chain of Val. Therefore, this coupling reaction is a very good model to investigate up to which OEG chain length the acylation of an *N*-OEG residue is feasible.

Figure 28. Structure of the target *N*-OEG cyclopeptide analogs (**24-26**).

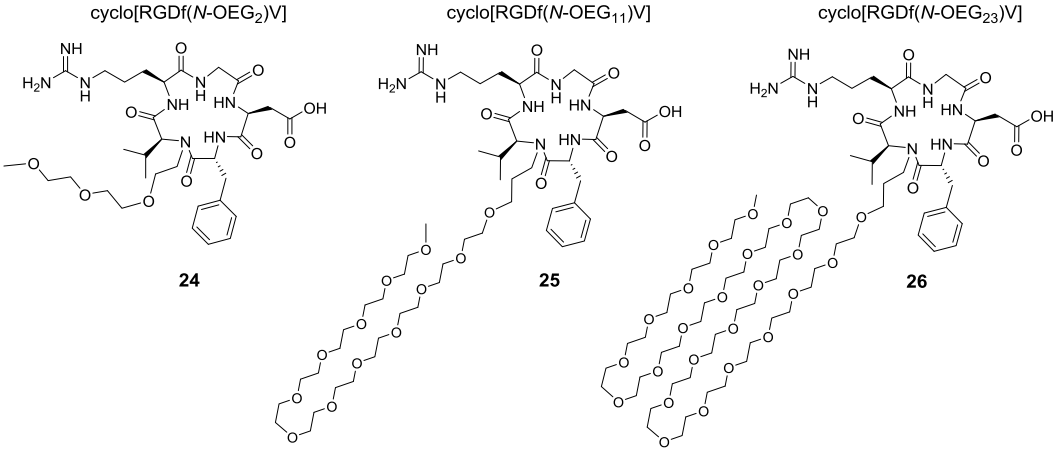

As a second objective, we wanted to investigate how *N*-Me-for-*N*-OEG substitution affects the biological activity and hydrophobicity of cyclo[RGDf*N*MeV] (**23**), and also the impact of OEG chain length on these two features. For this aim, cyclo[RGDf*N*MeV] (**23**) can also be considered a good model, as its conformational and biological properties are well-characterized.[139]

The RGD-tripeptide sequence is a common regnition motif for various receptor subtypes of the $\alpha_v\beta$ integrin family.[148] Several RGD-cyclopentapeptides bind to certain integrins with high affinity because their cyclic structure constrains the RGD sequence in a suitable orientation for binding.[143] A receptor model for their optimal interaction with the $\alpha_v\beta_3$ integrin is postulated (see Figure 29).[144] This model highlights the pharmacophoric features of cyclo[RGDfV], the lead peptide from which **23** was discovered by *N*-Me scan.[145] According to this model, Arg and Asp are involved in ionic interactions with the receptor, Gly imposes steric restrictions, and position 4 requires a hydrophobic residue at the D-configuration (*i.e.* D-Phe) for optimal side-chain orientation and interaction with the receptor. The amide bond between residues 3 and 4 also participates in the binding, probably as a hydrogen bond donor. Position 5 does not make contact with the integrin surface, and can accommodate a number of residues without an impact on the biological activity.

Figure 29. Receptor model for the binding of RGD-cyclopentapeptides to the $\alpha_v\beta_3$ integrin, postulated by Kessler *et al.*[144] This Figure has been adapted from [139], and highlights the main pharmacophoric features of c[RGDfV] for $\alpha_v\beta_3$-binding.

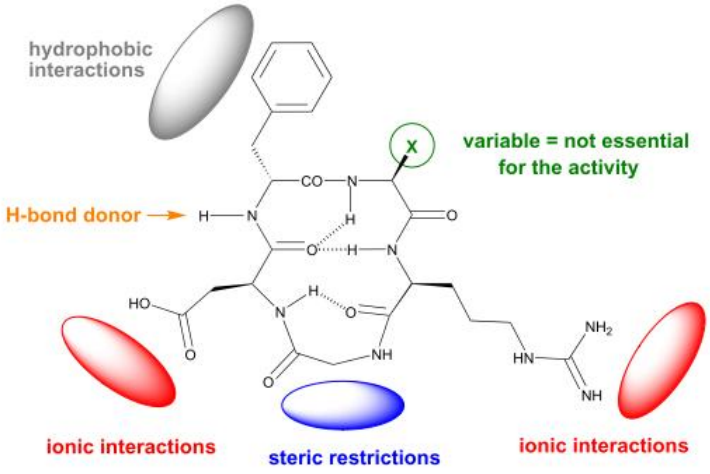

Since the fifth residue of the cyclo[RGDx_4X_5] scaffold for is not essential for $\alpha_v\beta_3$-binding, *N*-Me-for-*N*-OEG substitution in cyclo[RGDf*N*MeV] (**23**) may not result in a loss of biological activity. However, the affinity of RGD-cyclopeptides

towards the distinct integrin subtypes is strongly dependant on their conformation.[182] In the case of cyclo[RGDf*N*MeV] (**23**), the *N*-Me group at Val promotes conformational constraints that stabilize the RGD motif into its optimal orientation for $\alpha_v\beta_3$-binding; as a result, cyclo[RGDf*N*MeV] (**23**) is much more active and selective towards this integrin than its non-methylated homologue, cyclo[RGDfV].[145]

3.2. Objectives

The objectives of this Chapter were:

1. To synthesize three analogs of cyclo[RGDf*N*MeV] (**23**) in which the *N*-Me group has been replaced by *N*-OEG chains of increasing length (namely *N*-OEG_2, *N*-OEG_{11} and *N*-OEG_{23}), in order to investigate upon which OEG chain length the acylation of an *N*-OEG amine is feasible.

2. To compare the *N*-OEG cyclopeptide analogs (**24-26**) and parent peptide (**23**) with respect to biological activity and hydrophobicity in order to investigate how an increased OEG chain length affects these features.

3.3. Results and discussion

3.3.1. Synthetic approach

Our synthetic strategy to obtain cyclo[RGDf*N*MeV] (**23**) and the *N*-OEG cyclopeptides (**24-26**) is shown in Scheme 16. We sought to prepare their linear pentapeptide precursors (**p19**-**p22**) by SPPS using an *N*-substituted Val derivative as building block, and then cleave them for subsequent cyclization in solution and removal of side-chain protecting groups.

Scheme 16. Synthetic approach to obtain cyclo[RGDf*N*MeV] (**23**) and its *N*-OEG cyclopeptide analogs (**24-26**).

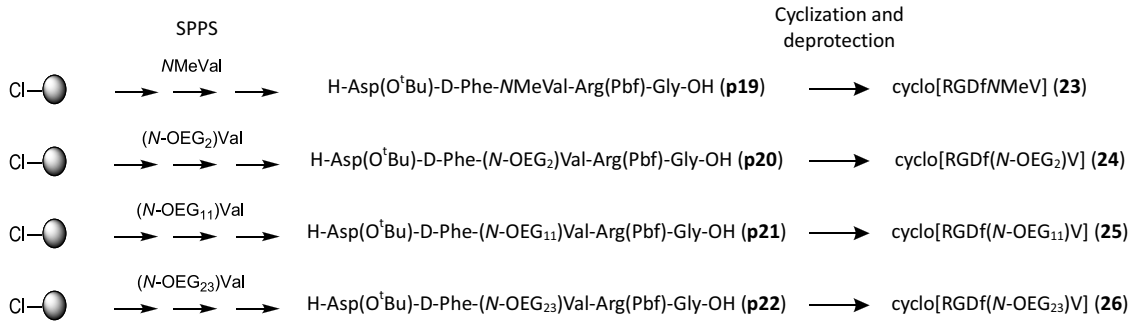

In all the pentapeptides (**p19**-**p22**), the *N*-substituted Val residue was placed in the middle of the sequence. This renders Gly at the *C*-terminus, which minimizes steric hindrance during cyclization and rules out the possibility of epimerization taking place during this process. In addition, positioning of *N*-alkyl groups in the middle of a peptide sequence is expected to facilitate its cyclization due to the turn-inducing properties of *N*-alkyl amino acids.[124]

For the solid-phase synthesis of these pentapeptides (**p19**-**p22**), we used the CTC resin. This resin was chosen as solid support because it can be cleaved with very mild acid conditions that enable to obtain fully protected peptide acids. In

all cases, we used a low functionalization (0.1-0.4 mmol/g resin), since it may facilitate the hindered coupling step by increasing the accessibility of the α-amino group.[146]

As has been explained in the introduction of this Chapter, the syntheses of pentapeptides **p19**-**p22** involves the coupling of D-Phe onto *N*-substituted Val. This coupling is not only hampered by the *N*-substituent, but also by the β-branched side-chain of Val (see Figure 30).

Figure 30. Solid-phase coupling of Fmoc-D-Phe-OH onto the *N*-substituted Val residue.

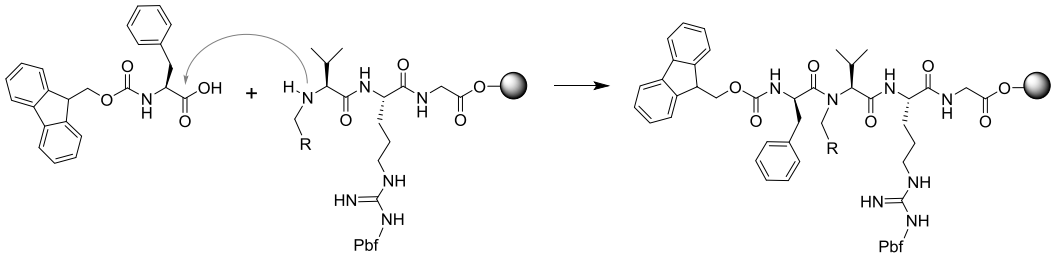

3.3.2. Synthesis of the Fmoc-*N*-OEG valine derivatives

Our methodology for the synthesis *N*-OEG peptides relies on Fmoc-protected *N*-OEG building blocks. To prepare the required Fmoc-*N*-OEG valine derivatives (**12-14**), we followed the 3-step protocol previously described in Section 1.4.4.1. Thus, *tert*-butyl valinate was subjected to reductive N^{α}-alkylation with a suitable OEG-containing aldehyde, followed by Fmoc-protection and *tert*-butyl removal (see Scheme 17). Remarkably, the increased length of the *N*-OEG chain did not prevent the acylation of *tert*-butyl protected *N*-OEG Val with Fmoc-Cl, and still allowed for the purification of **10** and **11** by flash chromatography. After acidic cleavage of the *tert*-butyl ester, the desired building blocks (**12**-**14**) were isolated in 45-54% overall yields.

Scheme 17. Synthesis of the Fmoc-*N*-OEG valine derivatives (**12**-**14**).[a]

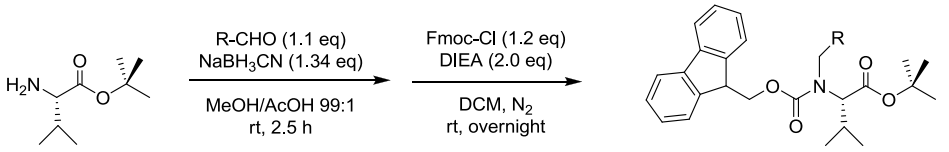

45-54%, 2 steps

Fmoc-(*N*-OEG$_2$)Val-O^{t}Bu (**9**), R- = $CH_3O(CH_2CH_2O)_2CH_2$-
Fmoc-(*N*-OEG$_{11}$)Val-O^{t}Bu (**10**), R- = $CH_3O(CH_2CH_2O)_{11}CH_2CH_2$-
Fmoc-(*N*-OEG$_{23}$)Val-O^{t}Bu (**11**), R- = $CH_3O(CH_2CH_2O)_{23}CH_2CH_2$-

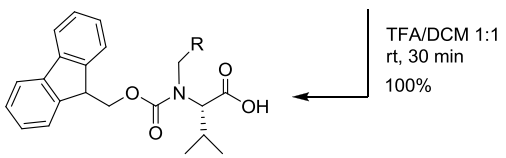

Fmoc-(*N*-OEG$_2$)Val-OH (**12**), R- = $CH_3O(CH_2CH_2O)_2CH_2$-
Fmoc-(*N*-OEG$_{11}$)Val-OH (**13**), R- = $CH_3O(CH_2CH_2O)_{11}CH_2CH_2$-
Fmoc-(*N*-OEG$_{23}$)Val-OH (**14**), R- = $CH_3O(CH_2CH_2O)_{23}CH_2CH_2$-

[a] CH_3O-$(CH_2CH_2O)_2$-CH_2-CHO was obtained by Swern oxidation of triethylene glycol monomethyl ether, which is readily available at low cost. CH_3O-$(CH_2CH_2O)_{11}$-CH_2CH_2-CHO and CH_3O-$(CH_2CH_2O)_{23}$-CH_2CH_2-CHO were purchased, but -as most monodisperse PEG reagents- they are very expensive.

3.3.3. Synthesis of cyclo[RGDf*N*MeV]

To obtain cyclo[RGDf*N*MeV] (**23**), we prepared its linear pentapeptide precursor (**p19**) on the CTC resin through Fmoc-/^{t}Bu- chemistry (see Scheme 18). The *N*MeVal residue was introduced in the middle of the peptide sequence using commercially available Fmoc-*N*MeVal-OH. For couplings onto non-alkylated residues, we used DIPCDI/OxymaPure activation. Acylation of *N*MeVal required HATU/HOAt as stronger coupling reagents. In a prior test, we found that activation of Fmoc-D-Phe-OH with DIPCDI/OxymaPure resulted in an uncomplete acylation of *N*MeVal after two treatments with a 3-fold excess of activated amino acid. In contrast, when 3.0 equivalents of Fmoc-D-Phe-OH were activated with HATU/HOAt, acylation was complete after two treatments. Peptide chain elongation and cleavage with 2% TFA in DCM afforded pentapeptide **p19** with all side-chain protecting groups.

Scheme 18. SPPS of H-Asp(O^{t}Bu)-D-Phe-*N*MeVal-Arg(Pbf)-Gly-OH (**p19**).

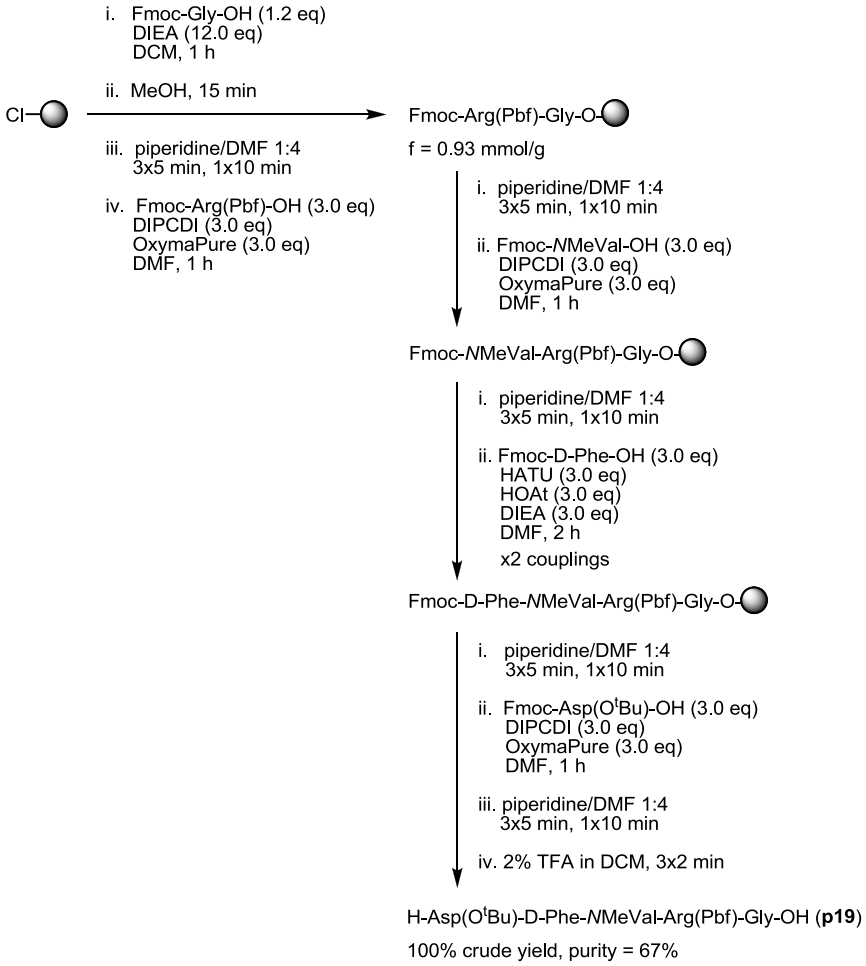

The crude linear pentapeptide (**p19**) was cyclized with EDC·HCl/DMAP (see Scheme 19). This method is particularly suitable for the cyclization of peptides in solution, because the urea from EDC can be removed by simple aqueous washings. To prevent cyclodimerization of **p19**, cyclization was carried out in very dilute conditions (1 mM) and allowed to proceed overnight. After this time, the reaction was complete and the cyclopeptide **19** was obtained in 95% crude yield. Then, the Pbf- and ^{t}Bu- groups were cleaved with 95% TFA in the presence of H_2O and TIS, and the unprotected peptide was precipitated in cold *tert*-butyl methyl ether. After purification by semipreparative RP-HPLC, cyclo[RGDf*N*MeV] (**23**) was isolated in 100% purity (see Figure 31).

Scheme 19. Cyclization of **p19** and deprotection to obtain cyclo[RGDf*N*MeV] (**23**).

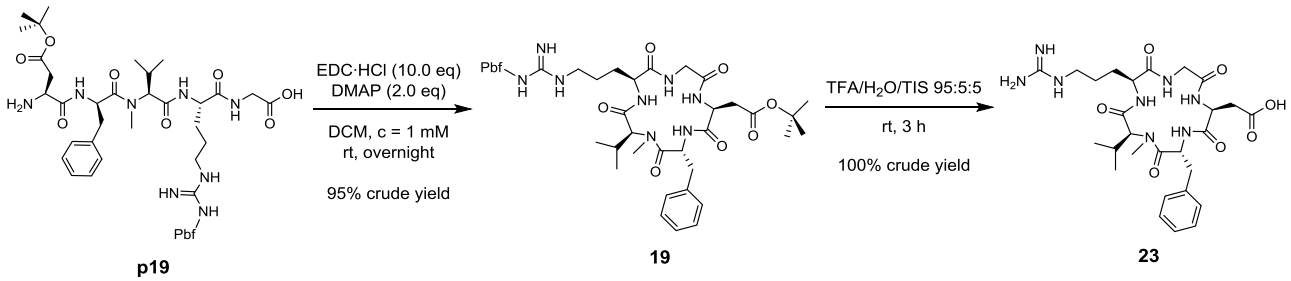

Figure 31. A) HPLC analysis of crude cyclo[RGDf*N*MeV] (**23**) obtained after deprotection, linear gradient from 30% to 100% ACN over 8 min. **B)** HPLC analysis of purified cyclo[RGDf*N*MeV] (**23**), linear gradient from 10% to 50% ACN over 8 min.

A)

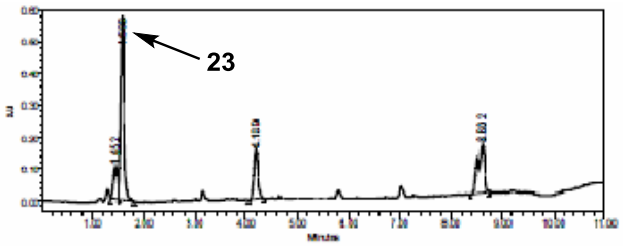

purity = 51%

B)

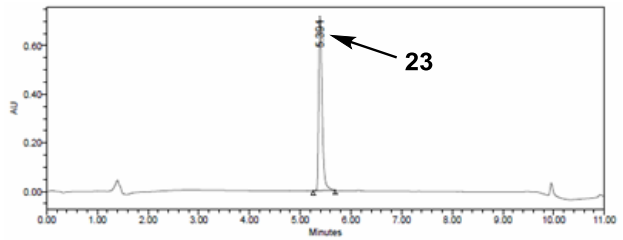

purity = 100%

3.3.4. Synthesis of cyclo[RGDf(*N*-OEG$_2$)V]

To obtain cyclo[RGDf(*N*-OEG$_2$)V] (**24**), we prepared its linear pentapeptide precursor (**p20**) by stepwise assembly of the corresponding Fmoc-amino acids on the CTC resin (see Scheme 20). Standard couplings were performed with DIPCDI/OxymaPure. Coupling of Fmoc-*N*-OEG$_2$ valine (**12**) with this activation method took place efficiently and with no detectable racemization. The small amount of unreacted peptide was capped with Ac_2O prior to the Fmoc-D-Phe-OH coupling step. This coupling was found feasible using BTC as activating reagent. After two BTC-mediated couplings, acylation of resin-bound *N*-OEG$_2$ Val was almost complete and no epimerization was observed. Traces of unreacted *N*-OEG$_2$ peptide were detected by HPLC-MS, but since the *N*-terminal residue of this peptide is not acylated under standard conditions, this species cannot lead to any deleition sequence which would compromise the purification of the final product. Thus, we continued with the synthesis and, after cleavage with 2% TFA in DCM, pentapeptide **p20** was obtained in 62% purity (see Figure 32).

Scheme 20. SPPS of H-Asp(O^{t}Bu)-D-Phe-(*N*-OEG$_2$)Val-Arg(Pbf)-Gly-OH (**p20**).

Cl–[resin]

↓ SPPS

Fmoc-Arg(Pbf)-Gly-O-[resin]

f = 0.27 mmol/g

↓
- i. piperidine/DMF 1:4 3x5 min, 1x10 min
- ii. Fmoc-(*N*-OEG$_2$)Val-OH (**12**, 4.0 eq) DIPCDI (4.0 eq) OxymaPure (4.0 eq) DMF, 2 h
- iii. Ac$_2$O (10.0 eq) DIEA (10.0 eq) DCM, 15 min

Fmoc-(*N*-OEG$_2$)Val-Arg(Pbf)-Gly-O-[resin]

↓
- i. piperidine/DMF 1:4 3x5 min, 1x10 min
- ii. Fmoc-D-Phe-OH (5.0 eq) BTC (1.65 eq) 2,4,6-trimethylpyridine (14.0 eq) THF, overnight x2 couplings

Fmoc-D-Phe-(*N*-OEG$_2$)Val-Arg(Pbf)-Gly-O-[resin]

↓
- i. piperidine/DMF 1:4 3x5 min, 1x10 min
- ii. Fmoc-Asp(O^{t}Bu)-OH (3.0 eq) DIPCDI (3.0 eq) OxymaPure (3.0 eq) DMF, 1 h
- iii. piperidine/DMF 1:4 3x5 min, 1x10 min
- iv. 2% TFA in DCM, 3x2 min

H-Asp(O^{t}Bu)-D-Phe-(*N*-OEG$_2$)Val-Arg(Pbf)-Gly-OH (**p20**)

100% crude yield, purity = 62%

Figure 32. A) HPLC analysis of a cleaved sample of peptidyl-resin after the two BTC-mediated couplings of Fmoc-D-Phe-OH, linear gradient from 40% to 100% ACN over 8 min. **B)** HPLC analysis of crude pentapeptide **p20**, linear gradient from 20% to 70% ACN over 8 min.

A)

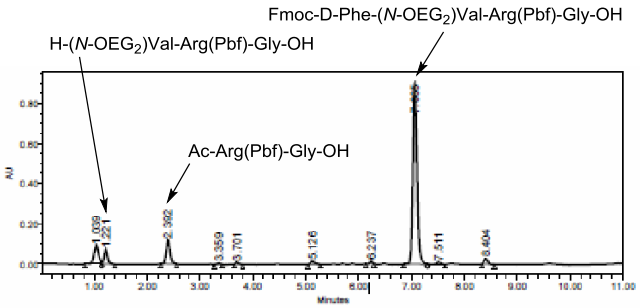

B)

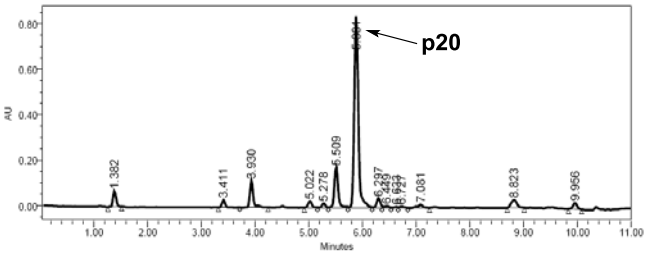

purity = 62%

Crude pentapeptide **p20** was cyclized with EDC·HCl in the presence of catalytic amounts of DMAP (see Scheme 21). After 15 h, the reaction was complete and no cyclodimer was detected (as checked by HPLC-MS). After removing the urea of EDC by aqueous washings, cyclopeptide **20** was obtained in high purity. Then, the side-chain protecting groups were removed with TFA:TIS:H$_2$O 95:5:5, and the unprotected peptide was precipitated in cold *tert*-butyl methyl ether. After purification by semipreparative RP-HPLC, cyclo[RGDf(*N*-OEG$_2$)V] (**24**) was isolated in >99% purity (see Figure 33).

Scheme 21. Cyclization of **p20** and deprotection to obtain cyclo[RGDf(*N*-OEG$_2$)V] (**24**).

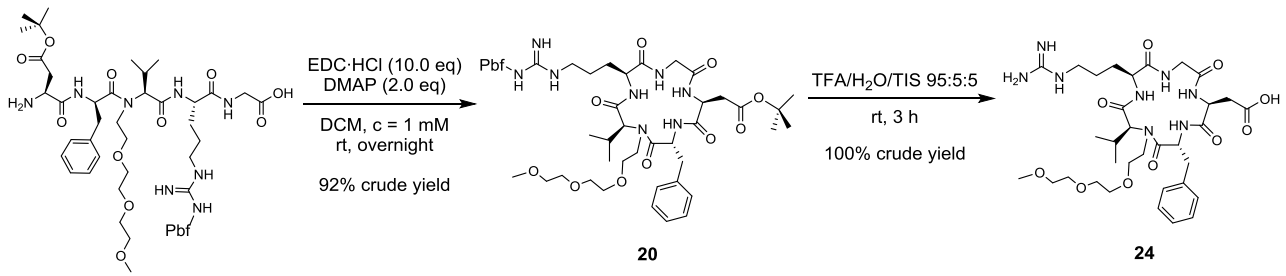

Figure 33. A) HPLC analysis of the crude cyclo[RGDf(*N*-OEG$_2$)V] (**24**) obtained after deprotection, linear gradient from 10% to 50% ACN over 8 min. **B)** HPLC analysis of the purified cyclo[RGDf(*N*-OEG$_2$)V] (**24**), linear gradient from 10% to 50% ACN over 8 min.

A)

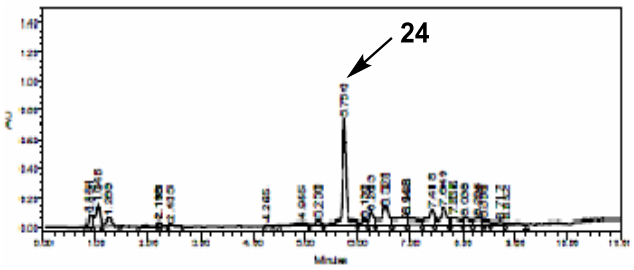

purity = 31%

B)

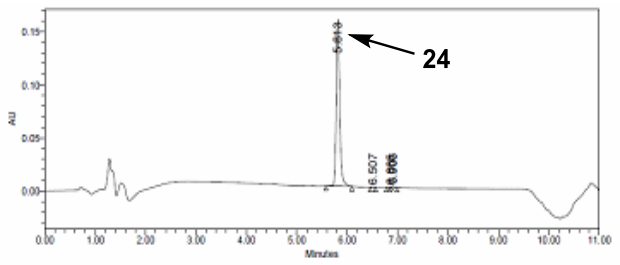

purity >99%

3.3.5. Synthesis of cyclo[RGDf(*N*-OEG$_{11}$)V]

SPPS of the *N*-OEG$_{11}$ pentapeptide using the *N*-OEG$_{11}$ Val derivative as building block

To obtain cyclo[RGDf(*N*-OEG$_{11}$)V] (**25**), we sought to synthesize its linear pentapeptide precursor (**p21**) using Fmoc-*N*-OEG$_{11}$ valine (**13**) as building block (see Scheme 22). The synthesis of **p21** was carried out on the CTC resin using DIPCDI/OxymaPure for standard couplings. Coupling of Fmoc-*N*-OEG$_{11}$ valine (**13**) with DIPCDI/OxymaPure activation took place efficiently and without racemization. The small amount of unreacted resin-bound peptide was capped with Ac_2O, and we proceeded to couple Fmoc-D-Phe-OH onto resin-bound *N*-OEG$_{11}$ Val. In order to define a method under which this coupling proceeds efficently, the peptidyl-resin was split into several portions and we tested several reagents and conditions. In terms of coupling efficiency, the best results were obtained with BTC activation, with the acid chloride of Fmoc-D-Phe-OH in the presence of DIEA and HOBt, and with DIPCDI/HOAt activation under MW heating at 50 ºC. These three methods gave very similar coupling yields, but the BTC and the acid chloride method provided higher purities and were preferrable due to their low-cost and experimental simplicity. To avoid the prior preparation of an Fmoc-amino acid chloride, the BTC protocol was selected as the method of choice for coupling Fmoc-D-Phe-OH onto *N*-OEG$_{11}$ Val. However, complete acylation of the secondary amine could not be achieved. After two BTC-mediated couplings, a considerable amount of unreacted peptidyl-resin was detected in cleaved samples and, after a third coupling using BTC activation, conversion did not improve (see Figure 34). Despite the unefficiency of this coupling, we continued with the synthesis. Peptide elongation and clevage afforded pentapeptide **p21** in its stereochemically pure form (see Figure 34). However, the residue obtained after cleavage also contained a considerable amount of unacylated H-(*N*-OEG$_{11}$)-Val-Arg(Pbf)-Gly-OH and, since several samples of peptidyl-resin were taken for the coupling optimization experiments, a low amount of crude **p21** was obtained.

Scheme 22. SPPS of H-Asp(O^{t}Bu)-D-Phe-(*N*-OEG$_{11}$)Val-Arg(Pbf)-Gly-OH (**p21**) using Fmoc-(*N*-OEG$_{11}$)Val-OH (**13**) as building block.

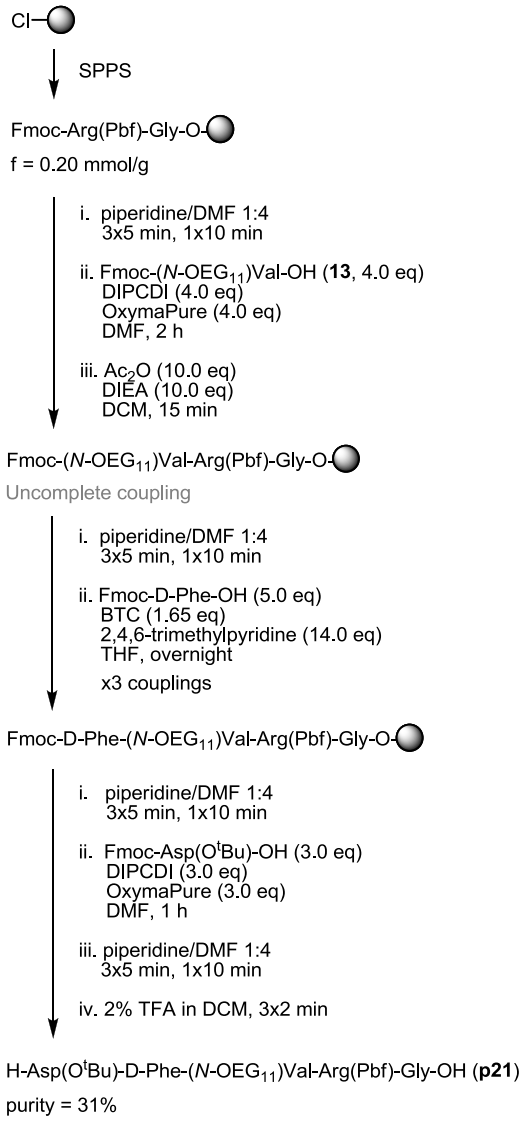

Figure 34. A) HPLC analysis of a cleaved sample of peptidyl-resin after the three BTC-mediated couplings of Fmoc-D-Phe-OH, linear gradient from 40% to 100% ACN over 8 min. **B)** HPLC analysis of crude pentapeptide **p21**, linear gradient from 20% to 70% ACN over 8 min.

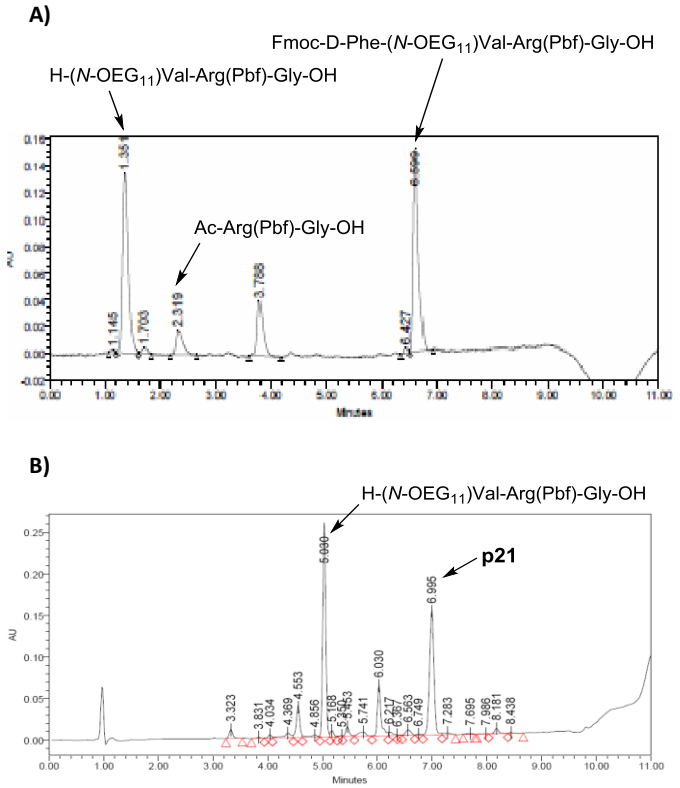

purity = 62%

<u>SPPS of the *N*-OEG$_{11}$ pentapeptide using a dipeptidic building block</u>

The stepwise synthesis of pentapeptide **p21** using Fmoc-*N*-OEG$_{11}$ valine as building block is limited by the unefficiency of the D-Phe-(*N*-OEG$_{11}$)Val coupling step. To circumvent this issue, we sought to prepare a D-Phe-(*N*-OEG$_{11}$)Val dipeptide (**17**) in solution and use it as solid-phase building block. In this way, the difficult formation of the D-Phe-(*N*-OEG$_{11}$)Val amide bond in solid-phase is avoided. Achieving this coupling in solution was expected to be less difficult, since the reactivity of secondary amines towards activated amino acids is lower when they are bound to a solid support.[147]

To prepare the required dipeptide (**17**), valine *tert*-butyl ester was subjected to reductive alkylation with a suitable OEG-aldehyde (see Scheme 23), for which we employed the conditions established in Section 1.4.4.1. For the subsequent coupling of Fmoc-D-Phe-OH onto the *N*-OEG$_{11}$ Val derivative, we sought to use an acid chloride: acid chlorides are highly reactive acylating species and have been successfully applied for hindered couplings between *N*-Me residues in solution.[83b] Thus, the acid chloride of Fmoc-D-Phe-OH was prepared in a prior step and then reacted

with *tert*-butyl protected *N*-OEG_{11} Val in the presence of DIEA, which is required to trap the HCl released upon acylation. This method enabled us to obtain dipeptide **15** with no detectable epimerization. Acidic cleavage of its *tert*-butyl ester yielded the required Fmoc-protected dipeptide (**17**).

Scheme 23. Synthesis of the D-Phe-(*N*-OEG_{11})Val dipeptide (**17**).
Fmoc-D-Phe-Cl was prepared by refluxing Fmoc-D-Phe-OH and $SOCl_2$ in DCM.

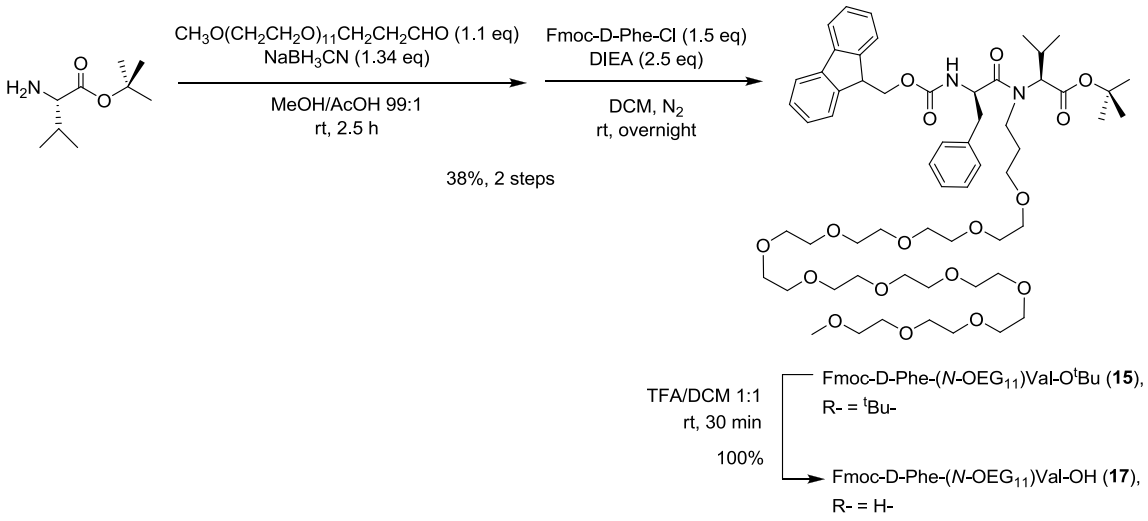

For the synthesis of pentapeptide **p21** (see Scheme 24), dipeptide **17** was coupled onto the Arg(Pbf)-Gly-resin with PyBOP/HOAt in the presence of DIEA. Since **17** is a very valuable building block, only 1.0 equivalent was used. The efficiency of the coupling was acceptable, but considerable epimerization took place at the Val residue. The occurrence of epimerization after dipeptide coupling was confirmed by the appearance of two HPLC peaks with the mass of the desired product (see Figure 35). These two peaks were present in a 34:56 proportion, and the major one was associated to the desired product by comparison with HPLC data from the synthesis of **p21** using Fmoc-(*N*-OEG_{11})Val-OH, in which no epimerization was observed. Further peptide elongation and cleavage from resin yielded the desired pentapeptide, which was obtained as a mixture of diastereomers (**p21** and **p21***) differing at the configuration of the Val residue (see Figure 35).

Scheme 24. SPPS of H-Asp(O^{t}Bu)-D-Phe-(*N*-OEG$_{11}$)Val-Arg(Pbf)-Gly-OH (**p21**) using Fmoc-D-Phe-(*N*-OEG$_{11}$)Val-OH (**17**) as building block.

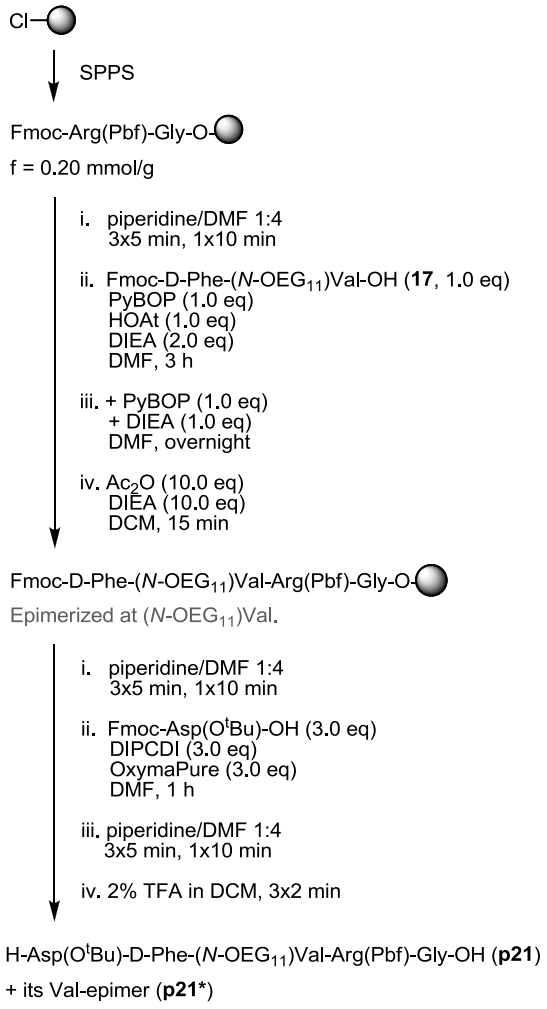

Figure 35. A) HPLC analysis of a cleaved sample of peptidyl-resin after the coupling of dipeptide **17**, linear gradient from 40% to 100% ACN over 8 min. **B)** HPLC analysis of crude pentapeptide **p21**, linear gradient from 20% to 70% ACN over 8 min.

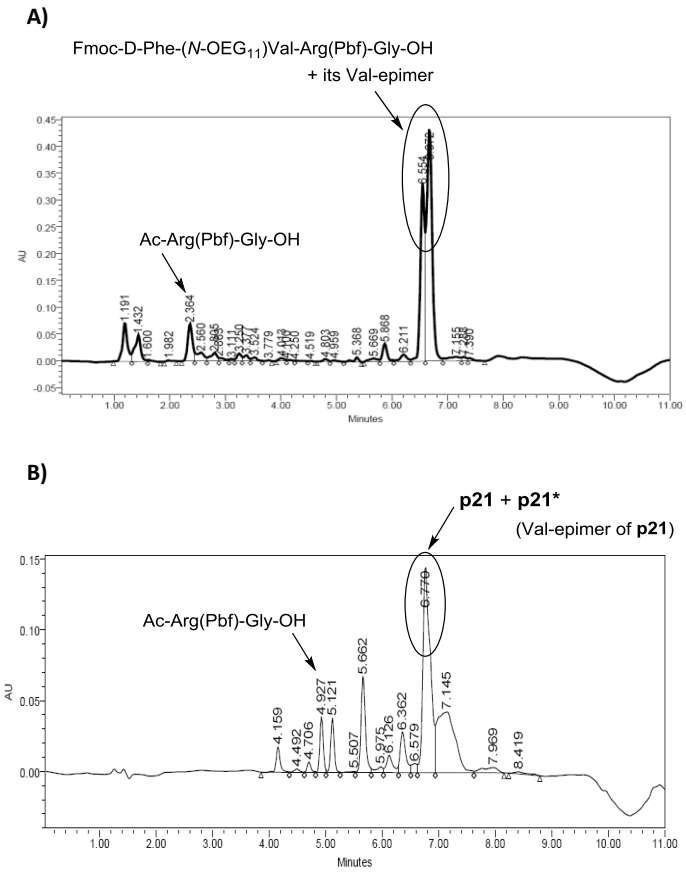

The occurrence of epimerization during the coupling of dipeptide **17** was a predictable issue. Activated dipeptides are very prone to *C*-terminal epimerization. This is because the dipeptidic residue undergoing activation is *N*-acylated, which favours its base-catalyzed conversion to an oxazolone (see path B in Scheme 25), whereas in *N*-carbamate-protected amino acids this process is less favoured.[110] The resulting oxazolone undergoes fast epimerization in basic media, specially when *N*-alkylated.[109] Along these lines, the presence of *N*-alkyl groups in dipeptides also facilitates their epimerization via direct enolization (see path A in Scheme 25). This is due to: i. hyperconjugative stabilization of the α-deprotonated carbanion, and ii. *cis* configuration favoured at the *N*-alkylated amide bond (α-proton abstraction in a *cis* amido conformer requires less energy than in a *trans*).[109] Taking into consideration that dipeptide **17** has an *N*-alkyl group, the degree of epimerization observed is not surprising.

Scheme 25. Mechanisms for the epimerization of dipeptides upon *COOH*-activation.
A) Via direct enolization. **B)** Via oxazolone formation.

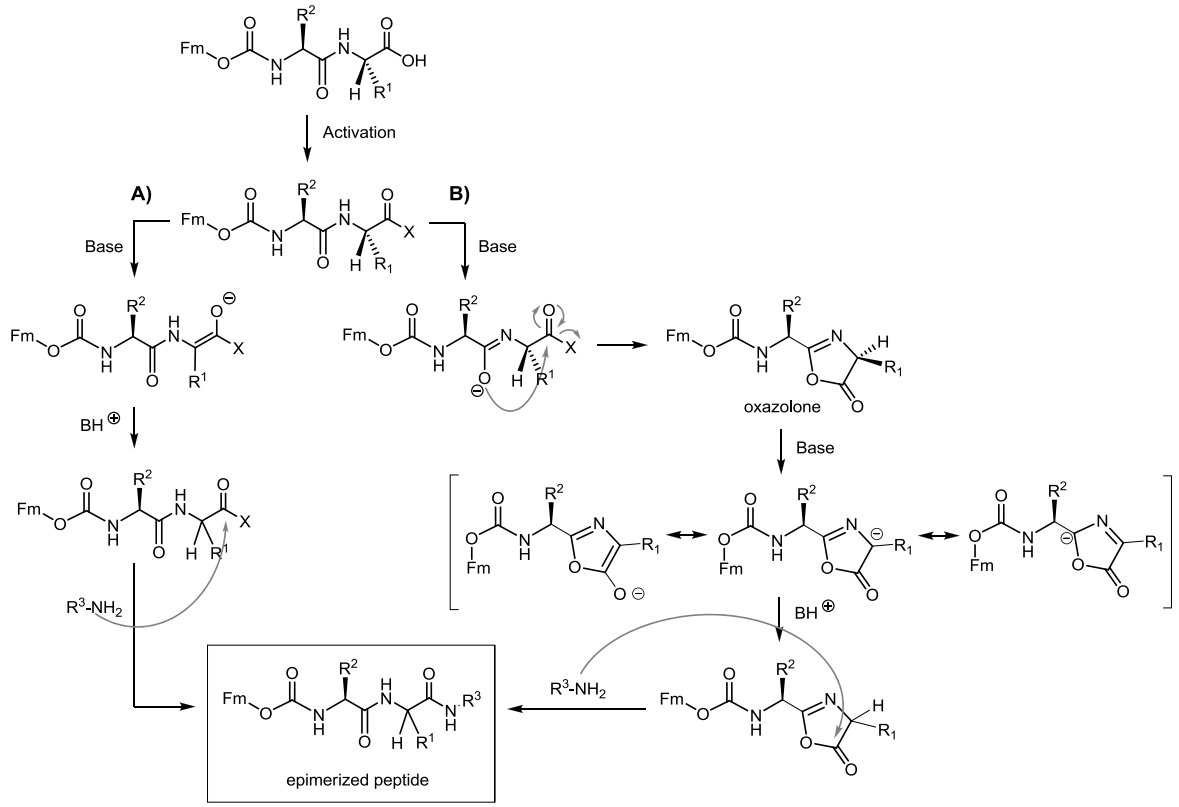

Cyclization and deprotection

The small amount of stereochemically pure *N*-OEG_{11} pentapeptide (**p21**) that was obtained using Fmoc-*N*-OEG_{11} valine as building block, was cyclized with EDC·HCl/DMAP (see Scheme 26). After side-chain deprotection with TFA:TIS:H_2O 95:5:5 and precipitation with cold *tert*-butyl methyl ether, semipreparative RP-HPLC rendered traces of the desired product, cyclo[RGDf(*N*-OEG_{11})V] (**25**).

Scheme 26. Cyclization of **p21** and deprotection to obtain cyclo[RGDf(*N*-OEG_{11})V] (**25**).

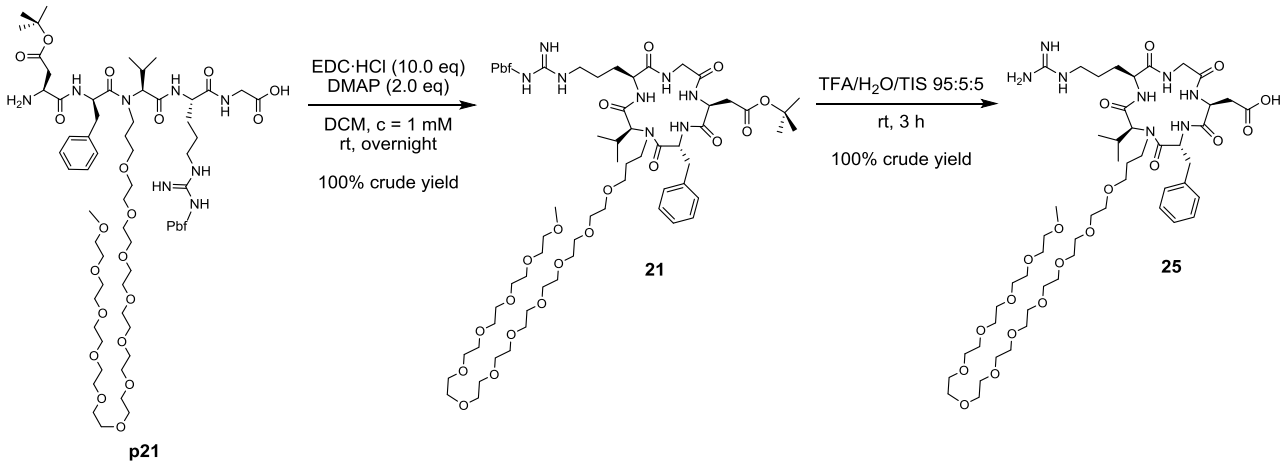

For the crude *N*-OEG$_{11}$ pentapeptide epimerized at Val (**p21** and its Val-epimer, **p21***), EDC-mediated cyclization proceeded smoothly. After side-chain deprotection and precipitation with cold *tert*-butyl methyl ether, HPLC analysis of the resulting residue showed two different peaks with the mass of the desired product, **25** and **25*** (see Figure 36). The desired *N*-OEG$_{11}$ cyclopeptide (**25**) and its non-desired Val-epimer (**25***) were separated by semipreparative RP-HPLC. The isolated product having a lower retention time (**25**) was found to co-elute with stereochemically pure cyclo[RGDf(*N*-OEG$_{11}$)V] (**25**), confirming that this species was the product with the desired stereochemistry.

Figure 36. A) HPLC analysis of the crude stereoisomeric mixture of *N*-OEG$_{11}$ cyclopeptides (**25** and **25***) obtained after cyclization deprotection, linear gradient from 10% to 50% ACN over 8 min. **B)** HPLC analysis of the isolated *N*-OEG$_{11}$ cyclopeptide having the desired stereochemistry, cyclo[RGDf(*N*-OEG$_{11}$)V] (**25**), linear gradient from 10% to 50% ACN over 8 min. **C)** HPLC analysis of the isolated *N*-OEG$_{11}$ cyclopeptide epimerized at Val (**25***), linear gradient from 10% to 50% ACN over 8 min.

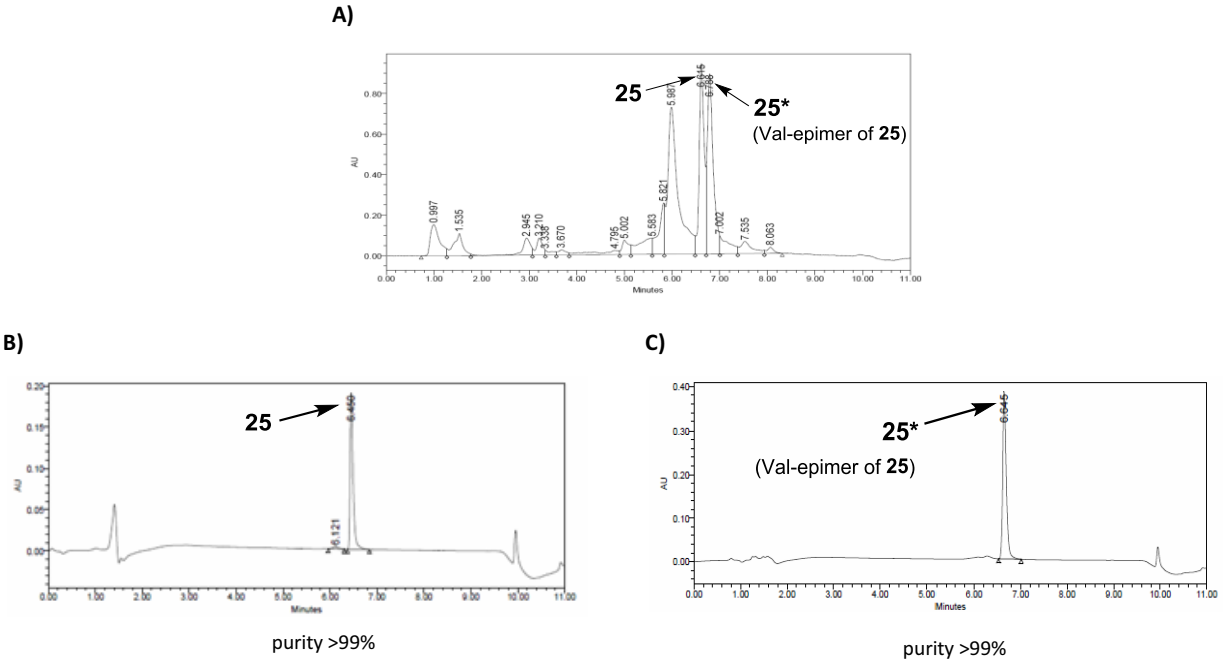

However, it shoud be noted that separation of the desired *N*-OEG$_{11}$ cyclopeptide (**25**) from its Val-epimer (**25***) was difficult to accomplish. First, due to the small amount of crude residue to be purified, the conditions used for the RP-HPLC purification of **23** and **24** (*i.e.* the use of a Sunfire™ C18 semipreparative column at a flow rate of 15.0 mL/min) were not applicable in this case. For the purification of the crude mixture containing **25** and **25***, working at an analytical scale was mandatory. Furthermore, finding a suitable gradient to separate **25** and **25*** was not straightforward. After performing several tests with different columns, the best conditions were found to be the use of an Xbridge™ C18 column and a linear gradient from 25% to 33% ACN over 11 min at a 3.0 mL/min flow rate. With these conditions, **25** and **25*** were almost baseline-separated. Since complete baseline-separation could not be achieved, fractions had to be collected manually, and only those fractions containing pure **25** or **25*** were pooled together. In this way, we were able to isolate the desired *N*-OEG$_{11}$ cyclopeptide (**25**) and its Val-epimer (**25***) in >99% purity, but the whole purification process was time-consuming and, due to the fact that fractions containing mixtures of **25** and **25*** were discarded, a low amount of **25** was obtained.

3.3.6. Synthesis of cyclo[RGDf(*N*-OEG$_{23}$)V]

SPPS of the *N*-OEG$_{23}$ pentapeptide using the *N*-OEG$_{23}$ Val derivative as building block

We attempted to synthesize of the *N*-OEG$_{23}$ pentapeptide (**p22**) using Fmoc-*N*-OEG$_{23}$ valine as building block. Although the stepwise synthesis of the *N*-OEG$_{11}$ pentapeptide (**p21**) was limited by the uncomplete acylation of the *N*-OEG$_{11}$ residue, the synthesis of **p21** by using a dipeptidic building block took place with epimerization, which was an issue. Taking into account an expectably low conversion for the coupling Fmoc-D-Phe-OH onto resin-bound *N*-OEG$_{23}$ Val, the feasibility of this coupling would perhaps allow us to obtain sufficient amount of **p22** in its stereopure form, and to avoid extensive RP-HPLC purification of the final cyclic product.

In preliminary experiments, we observed that the coupling of Fmoc-*N*-OEG$_{23}$ valine (**14**) onto the Arg(Pbf)-Gly-loaded resin was hampered by its *N*-OEG$_{23}$ chain. Activation of **14** with DIPCDI/OxymaPure resulted in an uncomplete acylation after performing two couplings (1 h) with a 3-fold excess of reagents. Using PyBOP/HOAt for the coupling of **14** (4.0 equivalents, 15 h) led to a higher conversion, but the reaction was still not complete.

In the synthesis of pentapeptide **p22**, we used PyBOP/HOAt for coupling Fmoc-*N*-OEG$_{23}$ valine (**14**) onto the Arg(Pbf)-Gly-resin, and then we capped the unreacted resin-bound peptide with Ac_2O (see Scheme 27). To investigate the coupling of Fmoc-D-Phe-OH onto *N*-OEG$_{23}$ Val, we splitted the peptidyl-resin into several portions and we tested several coupling methods, such as the BTC procedure or the DIPCDI/HOAt-mediated coupling under MW irradiation. However, none of the methods tested enabled us to form the desired amide bond. With steric hindrance of this magnitude, the practical limit of carbamate-protected amino acid coupling in solid-phase appears to have been reached.

Scheme 27. SPPS of H-Asp(O^{t}Bu)-D-Phe-(*N*-OEG$_{11}$)Val-Arg(Pbf)-Gly-OH (**p22**) using Fmoc-(*N*-OEG$_{23}$)Val-OH (**14**) as building block.

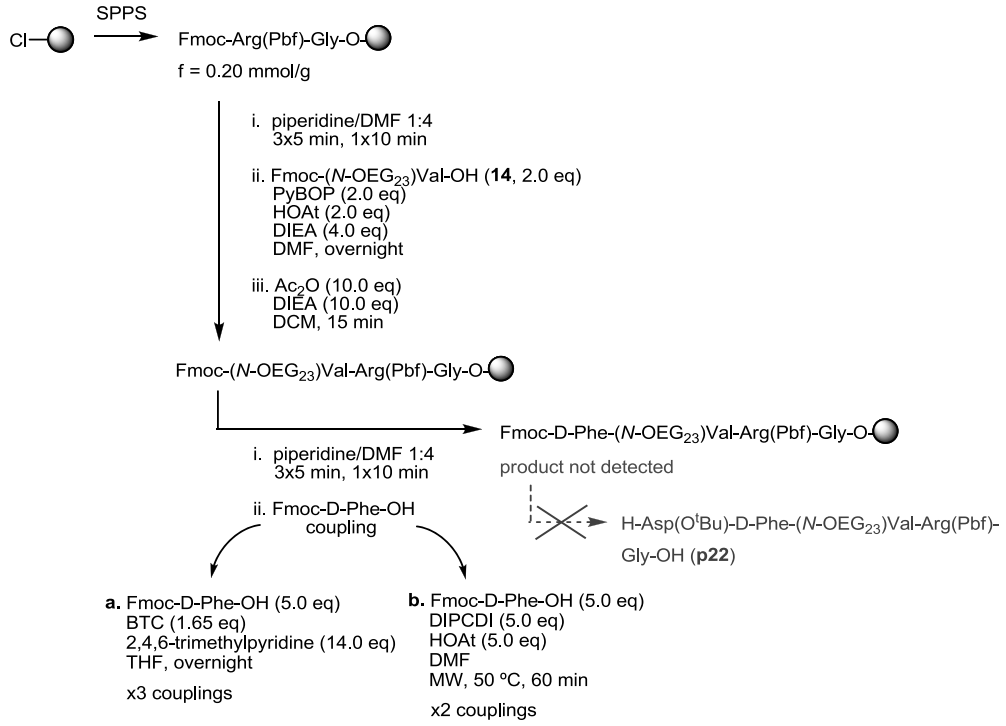

A possible approach for the difficult formation of the D-Phe-(*N*-OEG_{23})Val amide bond in solid-phase would be to use an α-amino acid protecting group for which oxazolone formation is precluded, thereby allowing activation of D-Phe as a highly reactive acid chloride.[88,103] For instance, *o*-nitrobenzylsulfonyl (*o*NBS)-protected amino acid chlorides have been used for difficult solid-phase couplings in cases where the analogous Fmoc-amino acid chlorides failed to couple well.[106] Similarly, α-azido acid chlorides do not suffer from oxazolone formation and have been successfully used for hindered couplings in solid-phase.[107,108] However, since after three BTC-mediated couplings no product had been formed, it seemed highly unlikely that coupling via a sulfonamide- or azido-protected D-Phe acid chloride would led to an acceptable conversion. Therefore, these methods were not tested, and we discontinued the synthesis of **p22** by this stepwise approach.

SPPS of the *N*-OEG_{23} pentapeptide using a dipeptidic building block

Since no coupling could be achieved between Fmoc-D-Phe-OH and resin-bound *N*-OEG_{23} Val, the synthesis of **p22** required the use of an Fmoc-protected D-Phe-(*N*-OEG_{23})Val building block. To prepare this dipeptide (**18**), we used the same 3-step procedure with which we had obtained the D-Phe-(*N*-OEG_{11})Val dipeptide of Section 3.3.5., but we employed a distinct OEG-aldehyde in the reductive alkylation step (see Scheme 28). The solution-phase coupling between the acid chloride of Fmoc-D-Phe-OH and *tert*-butyl protected *N*-OEG_{23} Val took place, though in low conversion. The yield of this coupling reaction may be improved by using a larger excess of acylating species. Alternatively, this yield could be improved by several modifications of the acid chloride method that are reported to prevent oxazolone formation. Such variations include performing the reaction in a two-phase system of DCM-aqueous carbonate (Schotten-Baumann conditions) or using the potassium salt of HOBt instead of DIEA.[82] Nevertheless, since we had obtained enough amount of dipeptide, conditions for the difficult coupling step were not optimized, and the Fmoc-protected D-Phe-(*N*-OEG_{23})Val dipeptide (**18**) was obtained in 26% overall yield.

Scheme 28. Synthesis of the D-Phe-(*N*-OEG_{23})Val dipeptide (**18**).
Fmoc-D-Phe-Cl was prepared by refluxing Fmoc-D-Phe-OH and $SOCl_2$ in DCM.

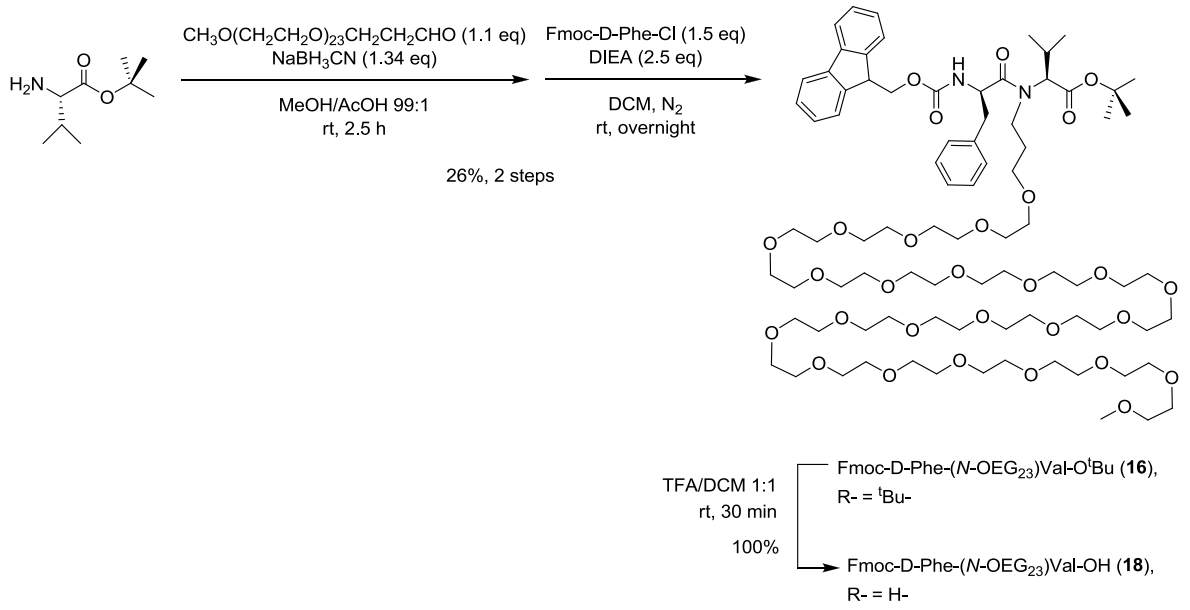

To synthesize pentapeptide **p22**, dipeptide **18** was coupled onto the Arg(Pbf)-Gly-resin with PyBOP/HOAt in the presence of DIEA (see Scheme 29). Since **18** is a very valuable building block, we only used 1.0 equivalent. The coupling proceeded with acceptable efficiency, but considerable epimerization took place at the Val residue. The

occurrence of epimerization after dipeptide coupling was confirmed by the appearance of two peaks with the mass of the desired product in the HPLC spectra of a cleaved peptidyl-resin sample (see Figure 37). Further assembly of the peptide and cleavage from resin yielded the desired pentapeptide, which was obtained as a mixture of diastereomers (**p22** and **p22***) differing at the configuration of the Val residue (see Figure 37).

Scheme 29. SPPS of H-Asp(O^{t}Bu)-D-Phe-(*N*-OEG$_{23}$)Val-Arg(Pbf)-Gly-OH (**p22**) using Fmoc-D-Phe-(*N*-OEG$_{23}$)Val-OH (**18**) as building block.

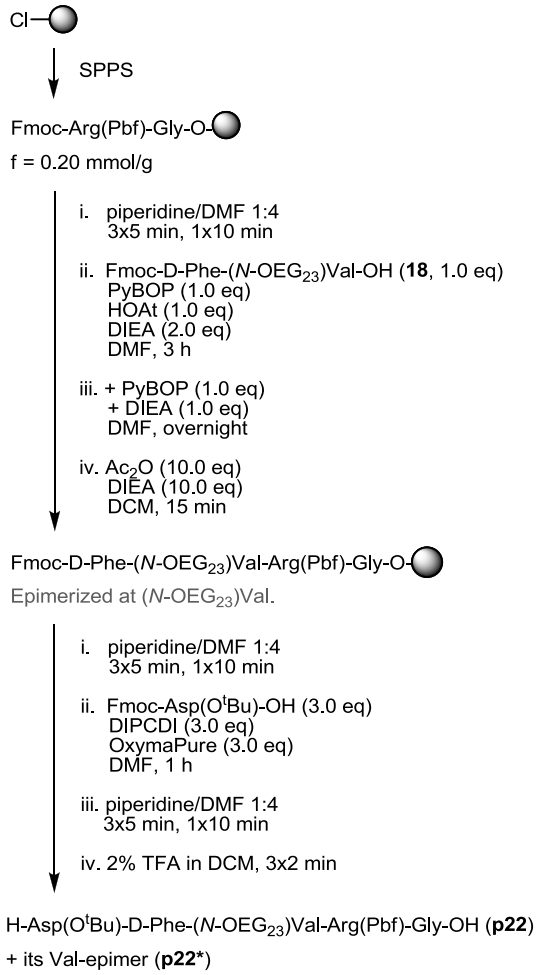

Figure 37. A) HPLC analysis of a cleaved sample of peptidyl-resin after the coupling of dipeptide **18**, linear gradient from 40% to 100% ACN over 8 min. **B)** HPLC analysis of crude pentapeptide **p22**, linear gradient from 20% to 70% ACN over 8 min.

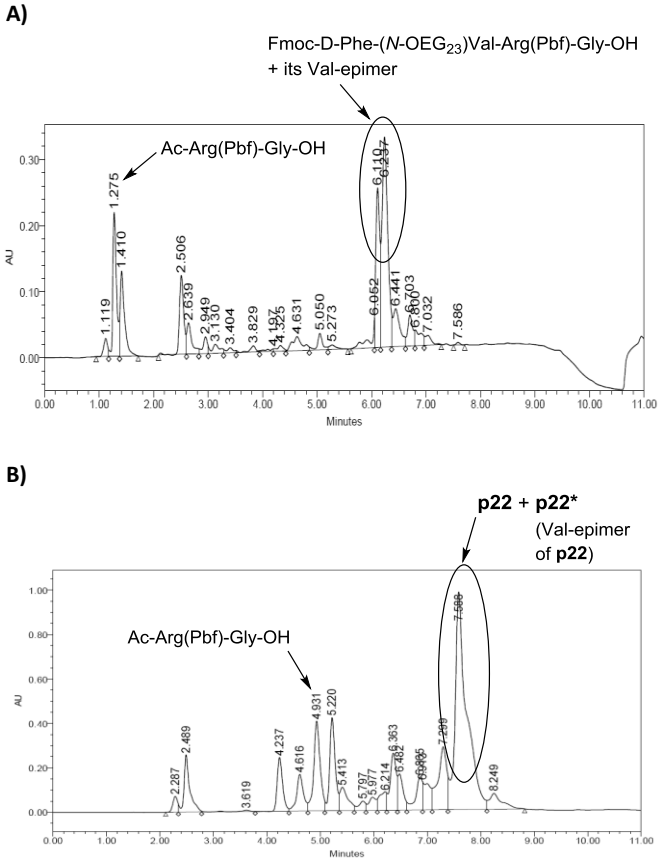

purity = 45%
(considering both diastereomers)

Cyclization and deprotection

The crude mixture of stereoisomeric *N*-OEG$_{23}$ pentapeptides (**p22** and **p22***) was cyclized with EDC·HCl and catalytic amounts of DMAP (see Scheme 30). Then, the side-chain protecting groups were removed with 95% TFA and the deprotected peptide was washed with cold *tert*-butyl methyl ether. HPLC analysis of the resulting residue showed two different peaks with the mass of the desired product, **26** and **26*** (see Figure 38).

The desired isomer of cyclo[RGDf(*N*-OEG$_{23}$)V] (**26**) was separated from its Val-epimer (**26***) by semipreparative RP-HPLC. Complete base-line separation of **26** and **26*** could not be achieved but, at least, the use of an Xbridge™ C18 column and an appropriate gradient enabled us to isolate the two *N*-OEG$_{23}$ cyclopeptides (**26** and **26***) (see Figure 38). HPLC analysis of pure **26** and **26*** gave a single peak with the same mass and different retention time, and co-injection of the two diastereomers into the HPLC apparatus gave two separate peaks. However, the whole purification process was very tedious and, in the end, a very low amount of the desired peptide (**26**) was obtained.

Scheme 30. Cyclization of **p22** and deprotection to obtain cyclo[RGDf(*N*-OEG$_{23}$)V] (**26**).

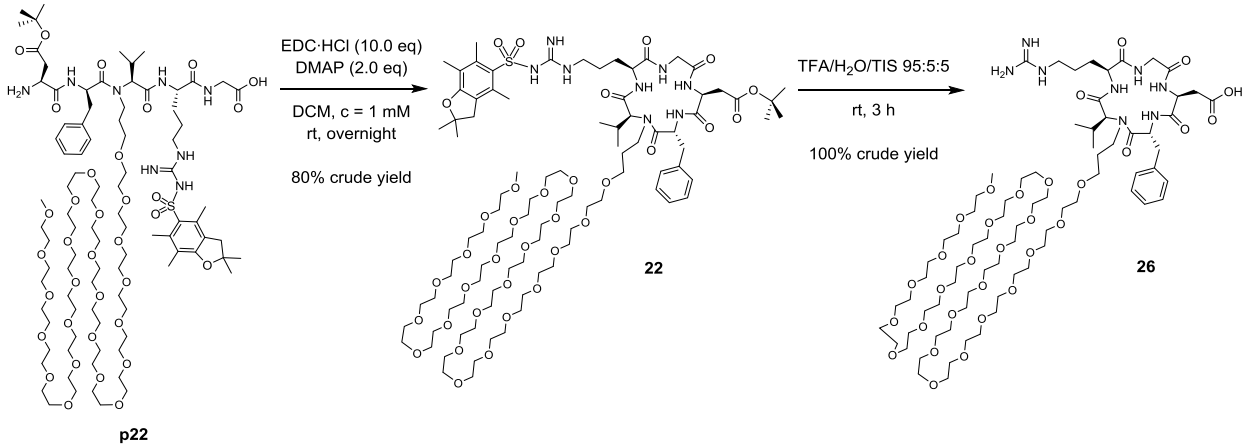

Figure 38. A) HPLC analysis of the crude stereoisomeric mixture of *N*-OEG$_{23}$ cyclopeptides (**26** and **26***) obtained after cyclization deprotection, linear gradient from 10% to 50% ACN over 8 min. **B)** HPLC analysis of the isolated *N*-OEG$_{23}$ cyclopeptide having the desired stereochemistry, cyclo[RGDf(*N*-OEG$_{23}$)V] (**26**), linear gradient from 10% to 50% ACN over 8 min. **C)** HPLC analysis of the isolated *N*-OEG$_{23}$ cyclopeptide epimerized at Val (**26***), linear gradient from 10% to 50% ACN over 8 min.

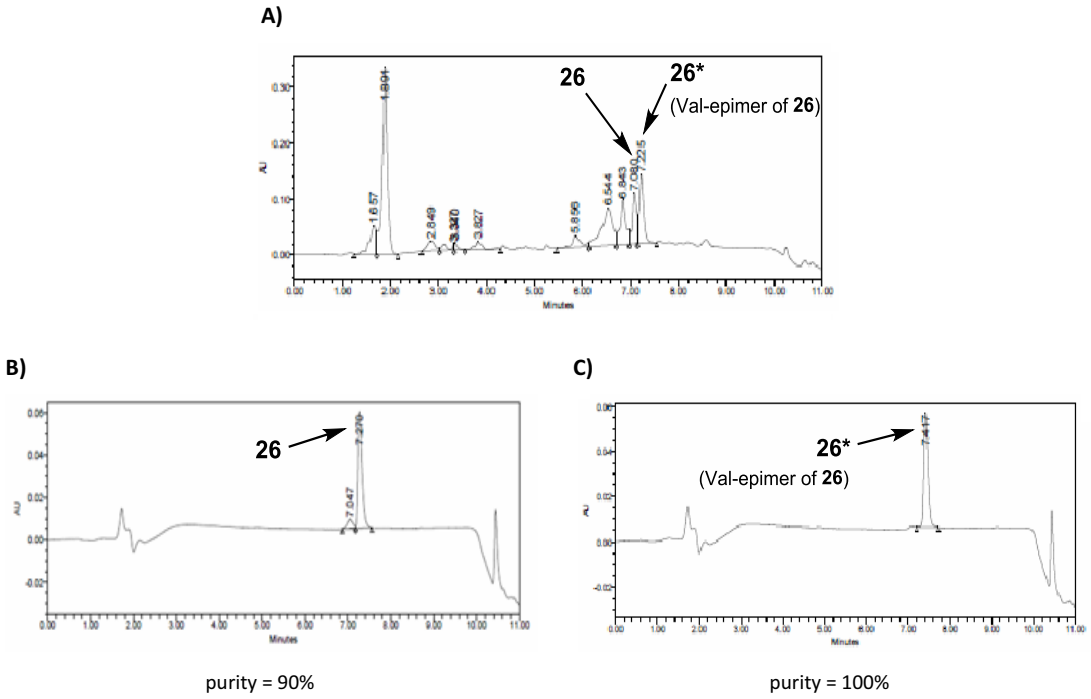

Stereochemical validation of the *N*-OEG$_{23}$ cyclopeptide

Since we did not have any sample of stereochemically pure cyclo[RGDf(*N*-OEG$_{23}$)V], the stereochemistry of the two isolated *N*-OEG$_{23}$ cyclopeptides (**26** and **26***) could not be assessed by RP-HPLC co-elution experiments. Despite this, we assumed that the isolated cyclopeptide having a lower retention time (**26**) was the desired stereisomer, as we had confirmed for cyclo[RGDf(*N*-OEG$_{11}$)V] (**25**). This assumption is reasonable, since the the crude residues corresponding to the different *N*-OEG$_{23}$ and *N*-OEG$_{11}$ intermediates had very similar HPLC spectra.

Besides, comparison of ^{1}H-NMR data of the two isolated *N*-OEG$_{23}$ cyclopeptides (**26** and **26***) versus the two isolated *N*-OEG$_{11}$ cyclopeptides (**25** and **25***) gave further evidence to our consideration of **26** as the desired product (see Figure 39). For both *N*-OEG$_{11}$ and *N*-OEG$_{23}$ cyclopeptides, ^{1}H-NMR analysis of the isolated compounds with lower retention times (**25** and **26**) showed two major signals for the two Me- groups of the Val side-chain (*i.e.* two doublets in the 1.3-0.2 ppm region). In contrast, ^{1}H-NMR analysis of the isolated compounds with higher retention times (**25*** and **26***) showed several sets of signals in the 1.3-02 ppm region, suggesting the existence of more than one conformer in the NMR time scale of chemical shift separation. The splitting of signals associated to the Me- groups of Val had not been observed for cyclo[RGDf*N*MeV] (**24**) and cyclo[RGDf(*N*-OEG$_2$)V] (**24**), which were obtained in its stereochemically pure form. Thus, it is reasonable to assume that among the two isolated *N*-OEG$_{23}$ cyclopeptides (**26** and **26***) that may correspond to the desired product, the one showing only 2 main peaks in the 1.3-0.2 ppm region of its ^{1}H-NMR spectra is the product with the desired stereochemistry, cyclo[RGDf(*N*-OEG$_{23}$)V] (**26**).

Figure 39. A) ^{1}H-NMR spectra (in CD_3OD) of **25** and **26** in the 4.5-0.0 ppm region.
B) ^{1}H-NMR spectra (in CD_3OD) of **25*** and **26*** in the 4.5-0.0 ppm region.[a]

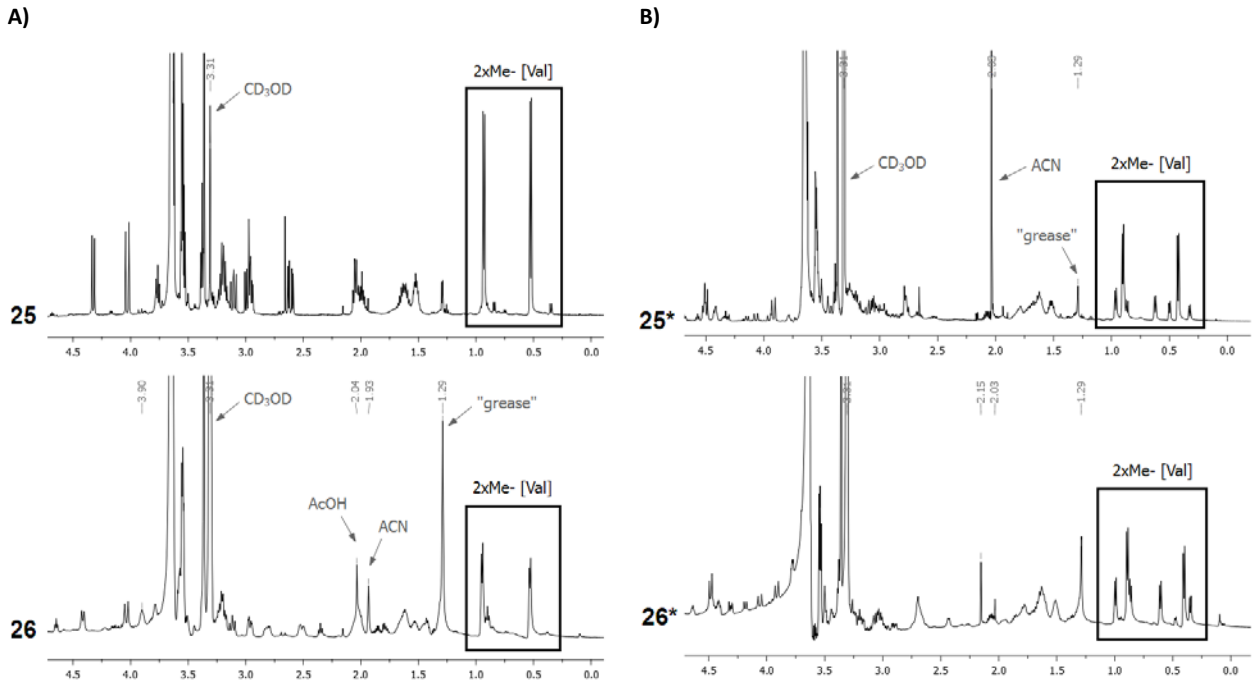

[a] Note: The ^{1}H-NMR spectrum of **26** showed in panel A corresponds to a sample of **26** of 90% purity (HPLC spectrum of such sample shown in Figure 38B).

3.3.7. Evaluation of the serum stability of the *N*-OEG cyclopeptide analogs

After having synthesized cyclo[RGDf*N*MeV] (**23**) and its *N*-OEG analogs (**24-26**), we evaluated their stability in human serum. This assay provides a general measure of the stability of compounds towards proteolytic enzimes. All our compounds showed no degradation when incubated at 37 ºC over a period of 48 hours (see Figure 40). Such a high degree of stability was expectable, as cyclic peptides show increased resistance to proteolytic cleavage, and the presence of D- and *N*-alkyl residues confers them further stability.[4]

Figure 40. Stability of cyclo[RGDf*N*MeV] (**23**) and the *N*-OEG cyclopeptides (**24-26**) in human serum. Time-course evolution of the integration areas of the HPLC peaks corresponding to **23-26** upon injection of an aliquot of serum-incubated sample.

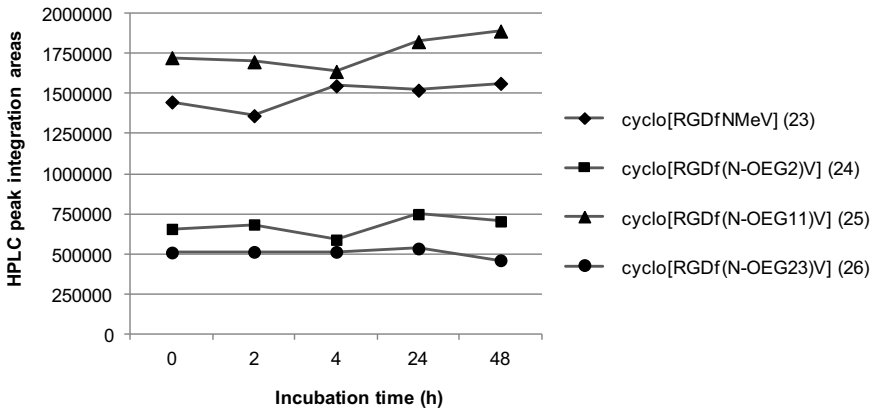

3.3.8. Evaluation of the biological activity of the *N*-OEG cyclopeptide analogs

The biological activity of cyclo[RGDf*N*MeV] (**23**) and the *N*-OEG analogs (**24-26**) was evaluated in cell adhesion inhibition assays (see Table 16). These assays were performed by Dr. Jaume Adan, from Leitat technological center. Compounds were tested for their capacity to inhibit the integrin-mediated adhesion of various cell lines onto two immobilized ligands: vitronectin (VN) and fibrinogen (FN).[150] The cell lines used in this study were: HUVEC (endothelial), DAOY (glioblastoma), and HT-29 (colon cancer). The first two overexpress the $\alpha_v\beta_3$ and $\alpha_v\beta_5$ receptors of the α_v-integrin family, whereas HT-29 cells only overexpresses the $\alpha_v\beta_5$ subtype. In the experiments using VN as ligand, both HUVEC and DAOY cells use integrins $\alpha_v\beta_3$ and $\alpha_v\beta_5$ for adhering, whereas the adhesion of HT-29 cells is only $\alpha_v\beta_5$-dependent. In the experiments with FB, the adhesion of HUVEC and DAOY cells to this ligand is only mediated by integrin $\alpha_v\beta_3$. In this assay, compounds that bind to $\alpha_v\beta_3$ and/or $\alpha_v\beta_5$ receptors, which are present at the cell surface, inhibit the adhesion of cells onto their endogenous integrin ligands (*i.e.* VN and FB). Therefore, the inhibitory activities of our RGD-cyclopeptides (**23-26**) provide an indirect measurement of their antagonistic activities towards the distinct integrin suptypes.

Table 16. Adhesion inhibition assays of cyclo[RGDf*N*MeV] (**23**) and the *N*-OEG cyclopeptides (**24-26**). EC_{50} values are given in μM. Standard deviations are between parentheses.[a]

Compound	Vitronectin (VN) $\alpha_v\beta_3 + \alpha_v\beta_5$			Fibrinogen (FB) $\alpha_v\beta_3$	
	HUVEC on VN	DAOY on VN	HT-29 on VN ($\alpha_v\beta_5$ only)	HUVEC on FB	DAOY on FB
cyclo[RGDf*N*MeV] (**23**)	0.37 (0.05)	2.69 (0.09)	3.11	0.076 (0.06)	0.44 (0.05)
cyclo[RGDf(*N*-OEG_2)V] (**24**)	0.42 (0.03)	3.62 (0.02)	2.17	0.036 (0.10)	0.14 (0.06)
cyclo[RGDf(*N*-OEG_{11})V] (**25**)	12.42 (0.07)	171.5 (0.39)	n.d.	1.38 (0.06)	4.55 (0.04)
cyclo[RGDf(*N*-OEG_{23})V] (**26**)	22.30 (0.23)	143.1 (0.57)	n.d.	0.28 (0.09)	2.31 (0.05)

[a] The parent peptide, cyclo[RGDf*N*MeV] (**23**), was used as reference control in all the assays performed and, its activity correlated well with existing data.[151] Cell adhesion inhibition curves are shown in Annex 4.

For all the cell/ligand systems, all the compounds inhibited cell adhesion in a concentration-dependent manner, resulting in the expected sigmoid curves. The inhibitory activities of the *N*-OEG_2 cyclopeptide (**24**) were very similar to

those of cyclo[RGDf*N*MeV] (**23**), which indicates that replacement of its *N*-Me group by a short *N*-OEG_2 chain does not affect binding affinity. In contrast, the *N*-OEG_{11} and *N*-OEG_{23} analogs (**25** and **26**) inhibited cell adhesion with less potency, which is probably due their longer OEG chains interfering with the RGD-receptor interaction. Indeed, the reduced biological activity of peptides upon attachment of a bulky OEG chain is an issue of major concern, especially in the case of small peptides.[152]

3.3.9. Evaluation of the lipophilicity of the *N*-OEG cyclopeptide analogs

The attachment of OEG chain onto a molecule should have an impact on its lipophilicity. Predicting this effect is of interest, as lipophilicity plays a crucial role in determining the ADMET (absorption, distribution, metabolism, excretion, and toxicity) properties and the overall suitability of drug candidates.[153]

To the far of our knowledge, there is no study on how modification of a molecule with OEG chains of varying length affects its lipophilicity. We sought to investigate how replacement of a backbone *N*-Me group of a peptide by *N*-OEG chains of increasing size affects this molecular property. For that, we evaluated the relative hydrophobicity of cyclo[RGDf*N*MeV] (**23**) and the *N*-OEG cyclopeptides (**24-26**) from their RP-HPLC retention times. As mentioned in Section 2.3.3., comparison of RP-HPLC retention parameters is as a valid method to rank the hydrophobicities of a series of modified analogs.[133] Upon co-injection onto a C18 column, all the *N*-OEG cyclopeptides (**24-26**) showed higher retention times than the parent peptide (**23**), and their retention was systematically increased with the length OEG chain (see Figure 41). In contrast, for Fmoc-*N*MeVal-OH and its *N*-OEG derivatives (**12-14**), the opposite trend was observed: *N*-Me-for-*N*-OEG substitution decreased hydrophobicity, and *N*-OEG chains of increasing size provided an less hydrophobic character (see Figure 42).[†]

Figure 41. HPLC chromatogram obtained after co-injection of cyclo[RGDf*N*MeV] (**23**) and the *N*-OEG cyclopeptides (**24-26**), linear gradient from 10% to 50% ACN over 8 min, C18 column.

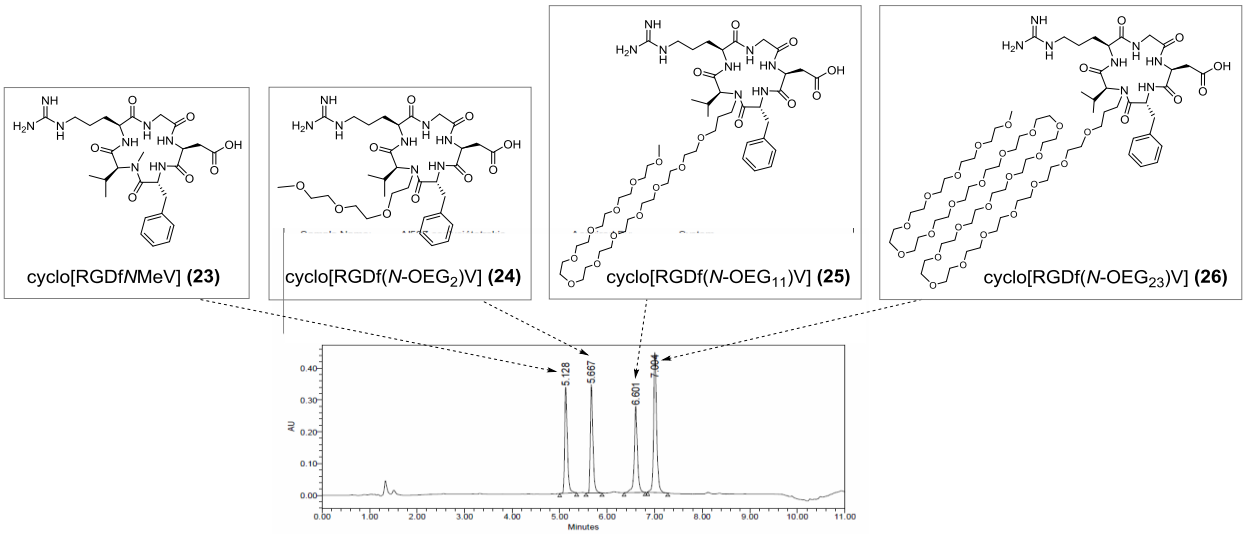

[†] *Note:* The RP-HPLC retention of a compound depends on its hydrophobicity and, to a lesser extent, molecular size. An increase in any of these two parameters should increase retention. In our case, it is very unlikely that size effects play an important role in determining the RP-HPLC retention of the *N*-OEG cyclopeptides (**24-26**), as the correlation between their retention times and OEG chain length was the opposite to that observed for the Fmoc-*N*-OEG Val derivatives (**12-14**). Thus, it is reasonable to assume that the distinct retention times of our compounds are due to their different hydrophobicity.

Figure 42. HPLC chromatogram obtained after co-injection of Fmoc-*N*MeVal-OH and the Fmoc-*N*-OEG Val derivatives (**12-14**), isocratic flow of 50% ACN over 15 min, C18 column.

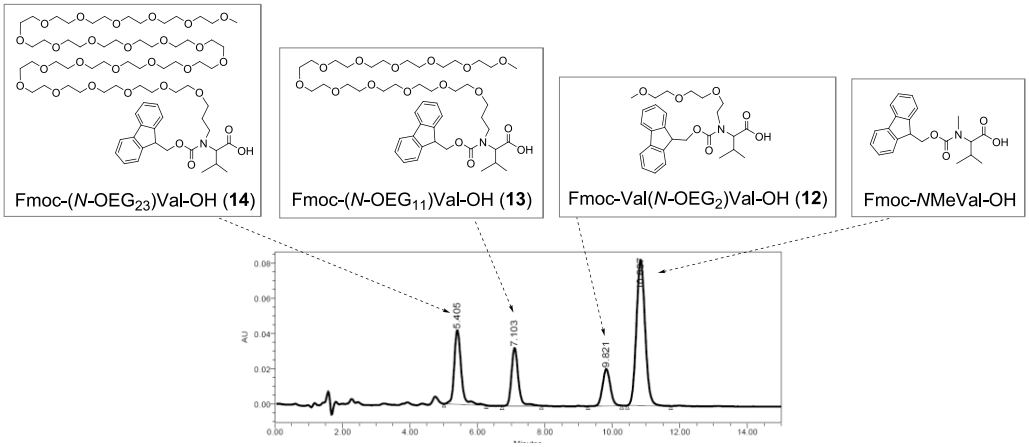

Our findings upon *N*-Me-for-*N*-OEG substitution in cyclo[RGDf*N*MeVal] (**23**), which has two ionizable side-chain functionalities, are consistent with our findings for the *N*-Me vs. *N*-OEG_2 analogs of the totally aliphatic Sansalvamide A peptide (see Section 2.3.3.): for both model peptides, replacement of a backbone *N*-Me group by an amphiphilic *N*-OEG chain provides a higher hydrophobicity.

Wishing to understand why *N*-Me-for-*N*-OEG substitution in peptides leads to more hydrophobic analogs, whereas in an Fmoc-amino acid results in the opposite effect, we classified the structural elements of the compounds of study in two different classes: those elements that can interact with the non-polar stationary phase (*e.g.* C18 column), and those that can interact with the polar mobile phase (*e.g.* H_2O/ACN containing 0.036-0.045% TFA). Such classification is shown in Table 17.

Table 17. Structural elements of the *N*-Me vs. *N*-OEG derivatives of **A)** Fmoc-Val-OH, **B)** Cilengitide, **C)** Sansalvamide A peptide. Classification based on their interactions with the stationary and mobile phases of RP-HPLC.

Compound		Structural elements that interact with the non-polar stationary phase	Structural elements that interact with the polar mobile phase		
			Ionizable groups	Potential hydrogen bond donors	Potential hydrogen bond acceptors
A) Fmoc-Val-OH derivatives	Fmoc-*N*MeVal-OH	▪ aliphatic side-chain ▪ Fm- ▪ ***N*-Me**	▪ COOH	-	▪ 2 carbonyl *O* atoms [COOH, Fmoc-] ▪ Urethane *O* atom [Fmoc-]
	Fmoc-(*N*-OEG_2)Val-OH (**12**) Fmoc-(*N*-OEG_{11})Val-OH (**13**) Fmoc-(*N*-OEG_{23})Val-OH (**14**)	▪ aliphatic side-chain ▪ Fm- ▪ ***CH_2* from *N*-OEG**	▪ COOH	-	▪ 2 carbonyl *O* atoms [COOH, Fmoc-] ▪ Urethanel *O* atom [Fmoc-] ▪ ***O* from *N*-OEG**
B) Cilengitide derivatives	cyclo[RGDf*N*MeV] (**23**)	▪ aliphatic side-chains [Val, D-Phe] ▪ ***N*-Me**	▪ COOH [Asp] ▪ guanidyl [Arg]	▪ 4 amide protons [4xCONH]	▪ 5 carbonyl *O* atoms [4xCONH + CONR]
	cyclo[RGDf(*N*-OEG_2)V] (**24**) cyclo[RGDf(*N*-OEG_{11})V] (**25**) cyclo[RGDf(*N*-OEG_{23})V] (**26**)	▪ aliphatic side-chains [Val, D-Phe] ▪ ***CH_2* from *N*-OEG**	▪ COOH [Asp] ▪ guanidyl [Arg]	▪ 4 amide protons [4xCONH]	▪ 5 carbonyl *O* atoms [4xCONH + CONR] ▪ ***O* from *N*-OEG**
C) Sansalvamide A peptide derivatives	*N*-Me analogs of Sansalvamide A peptide (**1b-5b**)	▪ Side-chains ▪ ***N*-Me**	-	▪ 4 amide protons [4xCONH]	▪ 5 carbonyl *O* atoms [4xCONH + CONR]
	N-OEG_2 analogs of Sansalvamide A peptide (**1a-5a**)	▪ Side-chains ▪ ***CH_2* from *N*-OEG**	-	▪ 4 amide protons [4xCONH]	▪ 5 carbonyl *O* atoms [4xCONH + CONR] ▪ ***O* from *N*-OEG**

For any *N*-methylated compound, *N*-Me-for-*N*-OEG substitution introduces ether oxygen atoms, which are weak hydrogen bond acceptors. These oxygen atoms that can form hydrogen bonds with the aqueous mobile phase, and/or with suitable hydrogen bond donors present in the molecule.

- For the *N*-Me vs. *N*-OEG Val derivatives (Fmoc-*N*MeVal-OH vs. **12-14**), the lowered retention time of **12-14** may be attributed to the interaction between their *N*-OEG chains and the aqueous mobile phase through hydrogen-bonding. The fact that increasing the length of the OEG chain decreases the retention of **12-14** is consistent with this hypothesis: those derivatives that can form more hydrogen bonds with the mobile phase are the first ones to be eluted.

- For the *N*-Me vs. *N*-OEG derivatives of our two model peptides (Cilengitide: **23** vs. **24-26**, and Sansalvamide A peptide: **1b-5b** vs. **1a-1b**), there is a different scenario. In contrast to the *N*-substituted Val derivatives, these *N*-substituted peptides contain backbone amide protons, which are strong hydrogen bond donors. Considering the increased retention time of our *N*-OEG peptides with respect to their *N*-Me homologues, it seems reasonable to assume that *N*-Me-for-*N*-OEG substitution leads to an interaction between the oxygen atoms from the OEG chain (hydrogen bond acceptors) and the backbone amide protons (hydrogen bond donors). This intramolecular interaction decreases the potential for hydrogen-bonding with the RP-HPLC mobile phase, thereby resulting in a higher retention time, which -in turn- is indicative of an enhanced hydrophobicity. The fact that increasing the length of the OEG chain enhances the retention of **24-26** is consistent with this hypothesis: those derivatives with a larger *N*-OEG chain can potentially provide a better shielding of the backbone amide protons, and thus lower their interaction with the aqueous mobile phase.

As previously mentioned in Section 2.3.3., lipophilicity is one of the most influencing properties in determining the permeability of a molecule across biological barriers, such as the intestinal epithelium layer, the blood-brain-barrier, or the skin. In particular, lipophilicity favours passive diffusion through the phospholipidic cell membrane; hence, it favours transport across biological barriers via passive transcellullar diffusion,[138] which is the most common transport mechanism for the majority of drugs.

Unfortunately, many peptide drug candidates are highly hydrophilic, and this limits their passive membrane permeation. Unless such hydrophilic peptides can cross biological barriers through other mechanisms (*e.g.* passive paracellullar diffusion through the tight junctions, carrier-mediated transport), they generally show poor transport rates, and they are not suitable for oral delivery due to poor gastrointestinal absorption.[154] This is the case of Cilengitide, cyclo[RGDf*N*MeV] (**23**), which recently failed to meet primary endpoint in clinical phase III trials for the treatment of glioblastoma and is currently in clinical phase II for the treatment of other cancers.[139] Although Cilengitide displays remarkable metabolic stability and is highly soluble in water, it suffers from low intestinal permeability. Thus, 50% of the drug is excreted in 3-5 hours when administered orally.[155]

Providing membrane permeability to peptides is a major academic and industrial challenge. A possible approach to do so is to increase the lipophilicity of the peptide itself.[154] In several reported examples, the covalent modification of peptides by attaching lipophilic moieties proved to be effective to improve their intestinal permeability[156] and oral bioavailability.[157] A relevant example is hexyl-insulin monoconjugate-2 (HIM2), an insulin-oligomer conjugate formed by attachment of a low-MW amphiphilic OEG chain to the Lys moiety at position b-29 (see Figure 43).[157b] This covalently modified insulin product was developed by NOBEX Corporation as an orally active drug for diabetes treatment. Clinical assays showed that oral administration of a liquid formulation of HIM2 can therapeutically affect glucose levels of type I and type II diabetics, whereas formulations of insulin are not orally active.

Figure 43. Structure of insulin and hexyl-insulin monoconjugate-2 (HIM2). Insulin is shown in black, whereas HIM2 is shown in grey.

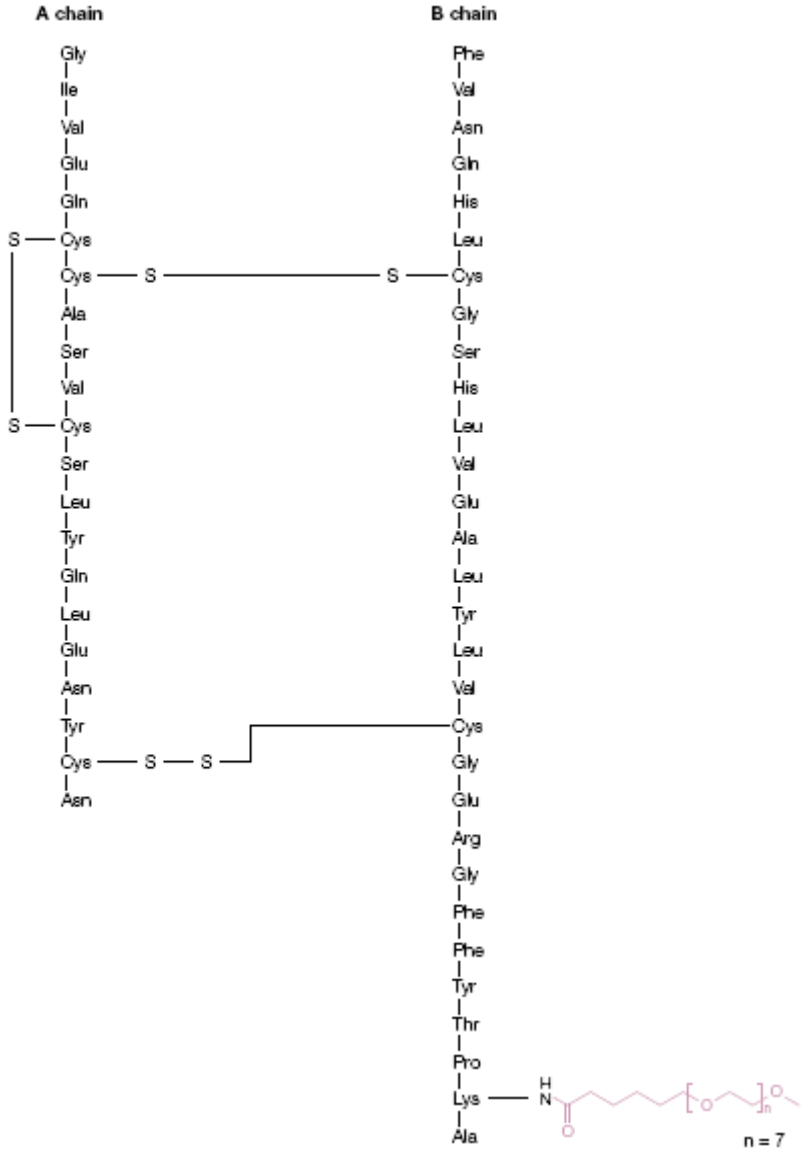

3.4. Summary and conclusions

In this Chapter, we have investigated upon which length of an OEG chain the acylation of an *N*-OEG residue is feasible. To investigate this, we synthesized three analogs of cyclo[RGDf*N*MeV] (Cilengitide) in which the *N*-Me group of Val was replaced by *N*-OEG chains of increasing size; namely, *N*-OEG_2, *N*-OEG_{11} and *N*-OEG_{23}, which are respectively composed of 2, 11 and 23 repeating ethylene oxide monomer units.

To obtain these *N*-OEG cyclopeptides, we synthesized their linear pentapeptide precursors on the CTC resin and we cyclized them in solution, followed by side-chain deprotection.

We initially investigated the synthesis of the target *N*-OEG peptides using an Fmoc-*N*-OEG amino acid as solid-phase building block. For that, we prepared the required Fmoc-protected *N*-OEG_2, *N*-OEG_{11} and *N*-OEG_{23} Val derivatives in solution by reductive N^{α}-alkylation of *tert*-butyl valinate with a suitable OEG-aldehyde, followed by Fmoc- protection

and *tert*-butyl ester cleavage. Remarkably, the increased length of the *N*-OEG chain did not prevent the acylation of *N*-alkylated Val with Fmoc-Cl, and still allowed to purify the *N*-OEG building blocks by flash chromatography.

We found that the Fmoc-protected *N*-OEG_2 and *N*-OEG_{11} Val derivatives can be efficiently coupled to a peptidyl-resin using DIPCDI/OxymaPure as activating reagents. In contrast, the coupling of Fmoc-*N*-OEG_{23} Val required the use of PyBOP/HOAt as a stronger activation method, and still did not proceed to completion.

The use of Fmoc-*N*-OEG_2 Val as solid-phase building block enabled us to obtain cyclo[RGDf(*N*-OEG_2)V]. Coupling of Fmoc-D-Phe-OH onto resin-bound *N*-OEG_2 Val was achieved using BTC as activating reagent. After two BTC-mediated couplings, acylation of *N*-OEG_2 Val was almost complete. Further peptide elongation and cleavage afforded the linear *N*-OEG_2 pentapeptide. After cyclization and side-chain deprotection, the desired *N*-OEG_2 cyclopeptide was isolated by semipreparative RP-HPLC.

In contrast, the efficient preparation of cyclo[RGDf(*N*-OEG_{11})V] and cyclo[RGDf(*N*-OEG_{23})V] using the corresponding Fmoc-*N*-OEG Val derivatives was not possible, because the acylation of the *N*-OEG Val residue is severely hampered. In the case of resin-bound *N*-OEG_{11} Val, a method under which Fmoc-D-Phe-OH couples efficiently could not be found. The best results in terms of yield were obtained with BTC activation, but performing three coupling cycles provided a poor conversion. Despite the unefficiency of this coupling step, we continued with the synthesis and we isolated the *N*-OEG_{11} cyclopeptide, though in low amount. In the case of resin-bound *N*-OEG_{23} Val, the D-Phe-(*N*-OEG_{23})Val amide bond could not be formed. With steric hindrance of this magnitude, the practical limit of carbamate-protected amino acid coupling in solid-phase appears to have been reached.

To avoid the difficult formation of the D-Phe-(*N*-OEG_{11})Val or D-Phe-(*N*-OEG_{23})Val amide bonds in solid-phase, the synthesis of the *N*-OEG_{11} and *N*-OEG_{23} peptides required the use of a dipeptidic building block. The required Fmoc-protected D-Phe-(*N*-OEG)Val dipeptides could be prepared, as the difficult coupling step was found feasible in solution by using an acid chloride as acylating species. However, when these dipeptides were coupled to the Arg(Pbf)-Gly-resin using PyBOP/HOAt, considerable epimerization took place at their dipeptidic *C*-terminus. Thus, further peptide elongation and cleavage yielded the *N*-OEG_{11} and *N*-OEG_{23} pentapeptides epimerized at the Val residue. After cyclization and deprotection, the desired *N*-OEG_{11} and *N*-OEG_{23} cyclopeptides were separated from their non-desired Val-epimers by semipreparative RP-HPLC. In the case of cyclo[RGDf(*N*-OEG_{11})V], the stereochemistry of the two isolated products was assessed by RP-HPLC co-elution experiments with a sample of stereochemically pure peptide. In the case of cyclo[RGDf(*N*-OEG_{23})V], the product having the desired stereochemistry was identified by comparison of RP-HPLC and ^{1}H-NMR data of the *N*-OEG_{23} versus the *N*-OEG_{11} derivatives. However, the whole purification process was tedious, and only rendered traces of the desired products.

We compared the three *N*-OEG cyclopeptides and cyclo[RGDf*N*MeV] (Cilengitide) with respect to lipophilicity and biological activity. The RP-HPLC retention times of the *N*-OEG analogs were found to be higher than that of the parent *N*-Me cyclopeptide, and increased with the OEG chain length. To explain this observation, we reasoned that *N*-Me-for-*N*-OEG substitution leads to an interaction between the oxygen atoms of the OEG chain (hydrogen bond acceptors) and the backbone amide protons (hydrogen bond donors). This intramolecular interaction decreases the potential for hydrogen-bonding with the aqueous RP-HPLC mobile phase, thereby resulting in a higher retention time, which -in turn- indicates a greater hydrophobicity. Remarkably, the *N*-OEG_2 cyclopeptide displayed the same capacity as Cilengitide to inhibit integrin-mediated cell adhesion. In contrast, the inhibitory activities of the *N*-OEG_{11} and *N*-OEG_{23} cyclopeptides were one order of magnitude lower. Taken together, these results show that, in the case of the cyclic pentapeptide Cilengitide, substitution of a backbone *N*-Me group by a short *N*-OEG chain provides a more lipophilic analog with analogous biological activity.

With these observations, we conclude that replacement of a suitable backbone *N*-Me group by a short *N*-OEG chain is a feasible strategy to confer lipophilicity whilst preserving biological activity, whereas for larger *N*-substituents synthetic yields drop and receptor binding may be hampered.

CHAPTER 4

The backbone *N*-(4-azidobutyl) linker for the preparation of peptide conjugates. Synthesis of an *N*-(4-azidobutylated) analog of Cilengitide and conjugation with PEG.

Abstract: We have developed a robust protocol for the introduction of the *N*-(4-azidobutyl) group into peptides using standard SPPS techniques. The introduction of this linker into a peptide allows conjugation of a desired molecule either via click chemistry or -after azide reduction- via acylation or reductive alkylation. To demonstrate the appliccability of our strategy, we synthesized an analog of cyclo[RGDf*N*MeV] (Cilengitide) in which the *N*-Me group of Val was replaced by an *N*-(4-azidobutyl) group, which provided a minimal perturbation of its conformation. By preparing various PEG conjugates from this *N*-(4-azidobutylated) cyclopeptide, we show that this linker allows conjugation onto peptides under full conservation of their amino acid side-chains.

4.1. Introduction

The site-specific covalent attachment of "unnatural" moieties, such as fluorophores, radiolabels, affinity labels or polymers, to peptides has proved to be useful for a wide variety of applications.[158] The conjugation of peptides with a desired molecule is typically performed at the *N*-terminus or at naturally occurring side-chain functional groups.[159] Cyclic peptides or even some linear peptides without derivatizable groups require the introduction of additional residues to support side-chain-selective conjugation (*i.e.* Lys, Cys, unnatural amino acid with a bioorthogonal functionality). Bioorthogonal conjugation methods that target unnatural amino acids are becoming valuable alternatives to the more commonly used Lys- and Cys-based strategies, as they do not involve cumbersome protection and deprotection protocols.[160]

However, in many cyclic peptides that lack conjugation sites, additional residues cannot be introduced, and finding a suitable position for amino acid replacement is not straightforward. In particular: i. certain amino acid constituents are essential for biological activity, ii. conformational changes upon amino acid substitution may cause a loss in biological activity.

We envisaged that modification of the backbone amide groups with a functionalized *N*-substituent may be a valuable addition to the chemist's toolbox to perform peptide conjugation. With this aim, we sought to investigate the *N*-(4-azidobutyl) group as a linker for the attachment of molecules (see Scheme 31). This *N*-substituent can be introduced into a resin-bound peptide by reductive alkylation with 4-azidobutanal, providing an azide onto which alkyne-functionalized molecules can be grafted by Cu(I)-catalyzed 1,3-dipolar cycloaddition. Alternatively, the azide group can be reduced to an amine, onto which molecules can be conjugated via amide bond formation or via reductive alkylation. The azide function is stable to common deprotection protocols used in peptide synthesis and chemically inert to side-chain functional groups, thereby minimizing side-reactions and simplifying protection schemes.[161]

Scheme 31. Peptide modification through the backbone *N*-(4-azidobutyl) linker.

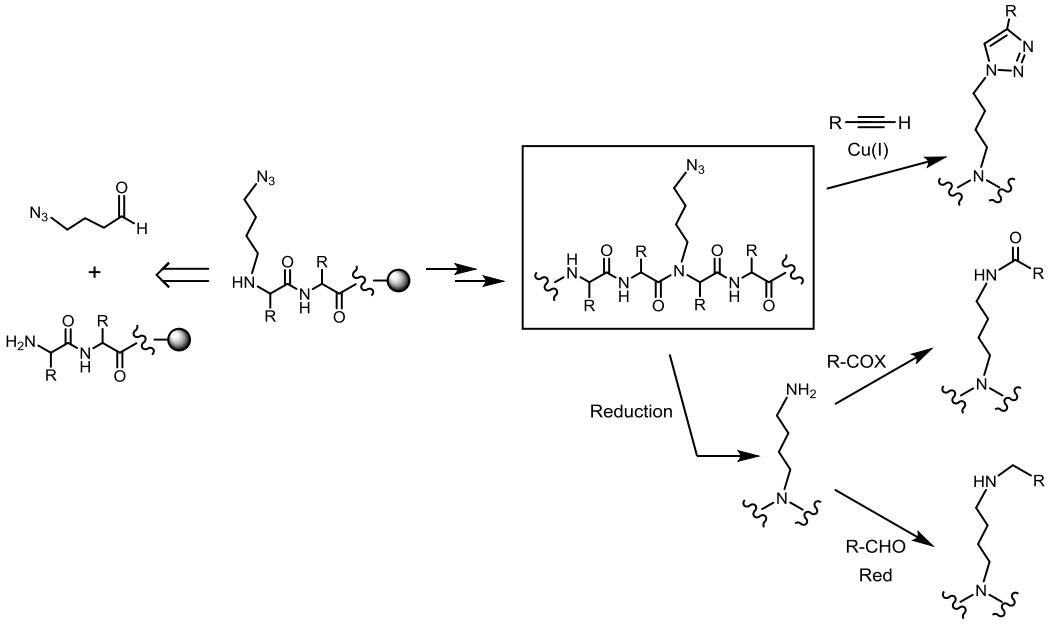

In order to preserve the original peptide conformation, which may be crucial for its biological activity, we propose to use our *N*-(4-azidobutyl) linker as a surrogate for the *N*-Me group, which is a common structural motif in many bioactive peptides isolated from natural sources and is often introduced *de novo* in peptides to optimize their activity or pharmacological properties.[6] As described in Chapter 2, the backbone conformation of the *N*-Me analogs of Sansalvamide A peptide underwent no significant changes upon *N*-Me-for-*N*-TEG substitution. Based on this findings,

we expected that replacement of a backbone *N*-Me group of a cyclic peptide by our linker would provide a minimal influence on its conformational state.

To demonstrate the applicability of our *N*-(4-azidobutyl) linker strategy, we chose Cilengitide[139] (**23**) as a model (see Figure 44). This Arg-Gly-Asp (RGD)-peptide is a good example of the difficulty involved in preparing conjugates of small cyclic peptides that do not offer attachment sites and/or that are not amenable to structural modification whilst preserving biological activity. The RGD-cyclopeptide sequence of Cilengitide, cyclo[RGDf*N*MeV], is the result of systematic research to constrain the RGD motif in its optimum conformation for binding to the $\alpha_v\beta_3$-integrin receptor,[145] which is overexpressed in various malignant cancers and in tumor neovasculature.[140] The functionalization of RGD-cyclopeptide ligands that target this receptor is of great interest, as it allows the conjugation of suitable chemical entities for tumor imaging and therapeutics.[141] Along these lines, PEG polymers have become increasingly important in optimizing the *in vivo* pharmacokinetics of RGD-peptides for specific applications.[142] However, Cilengitide cannot be conjugated as it is. Among the five amino acids in its cyclic structure, three (RGD) are essential for binding to $\alpha_v\beta_3$, D-Phe is involved in hydrophobic interactions with the receptor, and, although the fifth residue does not make contact with the receptor, *N*MeVal has no derivatizable functional group.[144] Substitution of *N*MeVal by Lys led to cyclo[RGDfK], one of the most conjugated peptide ligands and used in a number of biomedical applications (see Figure 44).[141b] However, a decrease in biological activity has to be taken into account when replacing *N*MeVal by Lys, as the *N*-Me group of Val promotes constraints that stabilize the RGD motif in its preferred $\alpha_v\beta_3$-binding conformation.[145]

Figure 44. Structure of cyclo[RGDf*N*MeV] (**23**) and its Lys-containing analog, cyclo[RGDfK].

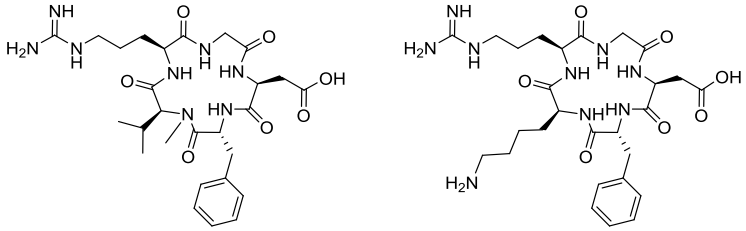

23 cyclo[RGDfK]

We sought to prepare an analog of cyclo[RGDf*N*MeV] in which the *N*-Me group of Val was replaced by an *N*-(4-azidobutyl) group and to study the conformational effect of such replacement. Then, we sought to conjugate this *N*-azidoalkylated cyclopeptide (**27**) with a polydisperse PEG chain of 2 KDa through various chemical transformations. The structures of the target *N*-(4-azidobutylated) cyclopeptide (**27**) and the PEG conjugates (**29-31**) are shown in Figure 45. For these PEG conjugates (**29-31**), we sought to compare their biological activity, lipophilicity and conformational features with those of the non-modified peptide, cyclo[RGDf*N*MeV] (**23**).

Figure 45. Structure of cyclo[RGDf(*N*-$CH_2CH_2CH_2CH_2N_3$)V] (**27**) and the target PEG conjugates (**29-31**).

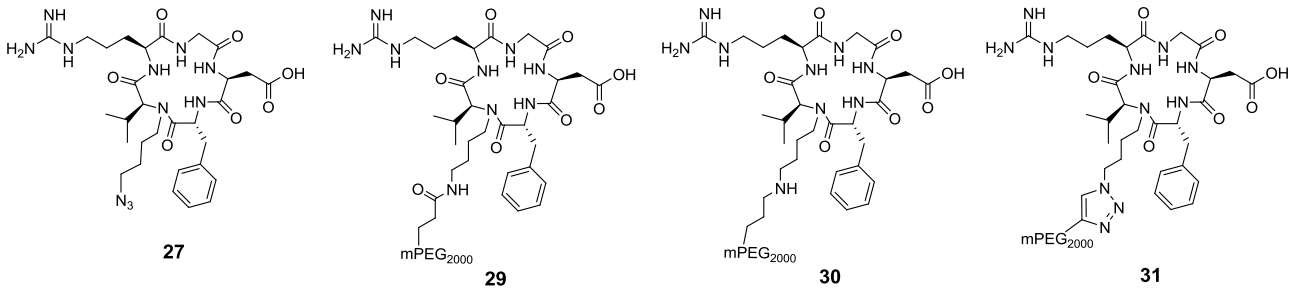

27 **29** **30** **31**

4.2. Objectives

The objectives of this Chapter were:

1. To synthesize an analog of cyclo[RGDf*N*MeV] (**23**) in which the *N*-Me group of Val has been replaced by a *N*-(4-azidobutyl) group and study the conformational effect of such replacement.

2. To use the *N*-(4-azidobutylated) cyclopeptide (**27**) to prepare several conjugates with a polydisperse PEG chain of 2 KDa through different chemical transformations.

3. To compare the PEG conjugates (**29-31**) and the original peptide, cyclo[RGDf*N*MeV] (**23**), with respect to biological activity, hydrophobicity and conformational features.

4.3. Results and discussion

4.3.1. Synthesis of the *N*-(4-azidobutylated) cyclopeptide

4.3.1.1. Synthetic approach

The synthetic strategy to obtain cyclo[RGDf(*N*-$CH_2CH_2CH_2CH_2N_3$)V] (**27**) is shown in Scheme 32. We sought to prepare its linear peptide precursor on a solid support and then cyclize it in solution, followed by removal of side-chain protecting groups.

Scheme 32. Synthetic approach to obtain cyclo[RGDf(*N*-$CH_2CH_2CH_2CH_2N_3$)V] (**27**).

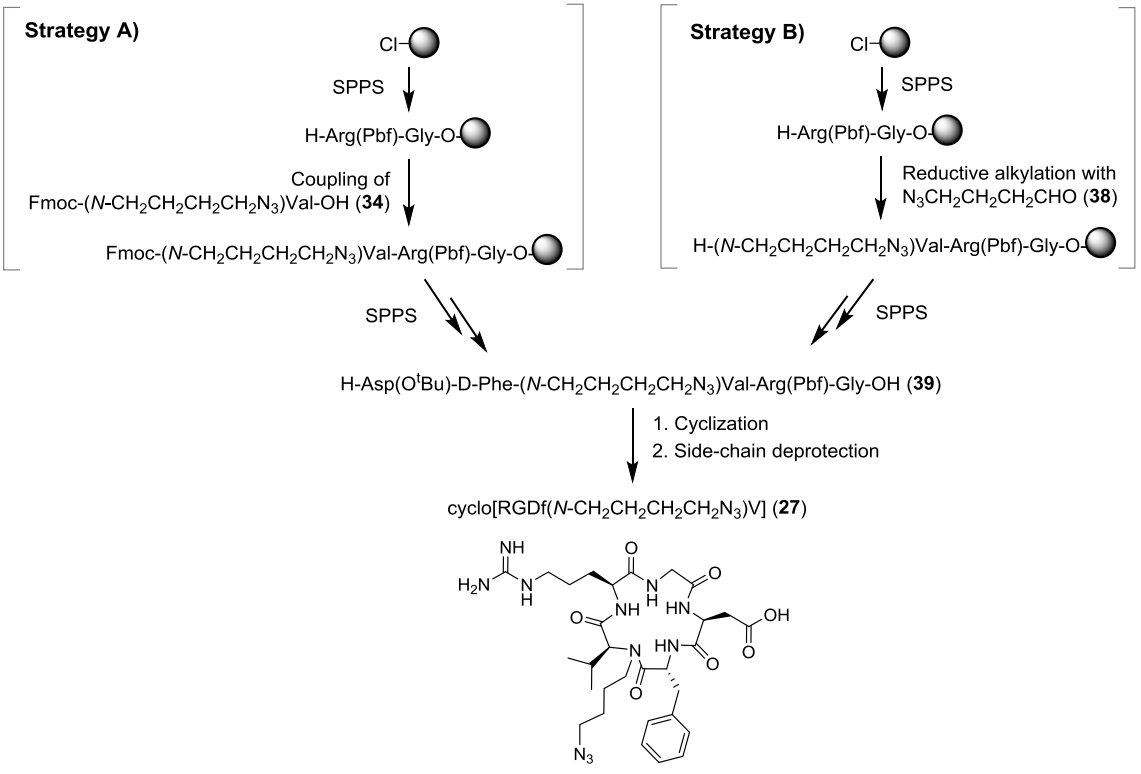

To obtain cyclopeptide **27**, pentapeptide **39** was considered as the most suitable linear precursor. Positioning of *N*-(4-azidobutylated) Val in the middle of the sequence minimizes steric hindrance during cyclization and is expected to facilitate this process due to the turn-inducing properties of *N*-alkyl amino acids.[124] Moreover, this renders Gly at the *C*-terminus, which rules out the possibility of epimerization taking place during the cyclization step.

For the solid-phase synthesis of this pentapeptide (**39**), we initially considered two different strategies. In the first strategy (**A**), the *N*-(4-azidobutyl) group is introduced into the resin-bound peptide by using Fmoc-*N*-(4-azidobutyl) valine (**34**) as building block. In the second strategy (**B**), the *N*-(4-azidobutyl) group is introduced by reductive N^{α}-alkylation of resin-bound Val with 4-azidobutanal (**38**).

4.3.1.2. Synthesis of 4-azidobutanal

Our synthetic approach to introduce the *N*-azidoalkyl group into peptides involves the use of 4-azidobutanal (**38**). Other ω-azido aldehydes could have been chosen for this purpose, but 3-azidopropanal and 2-azidoacetaldehyde are ill-advised due to their high unstability and volatility. Along these lines, 4-azidobutanal (**38**) was preferred to larger ω-azido aldehydes, such as 5-azidopentanal or 6-azidohexanal, since the resulting *N*-azidoalkylated residues would be more difficult to acylate due to increased steric hindrance.

We synthesized 4-azidobutanal (**38**) following a reported procedure (see Scheme 33).[162] The first step was the THF opening by iodide to form 4-iodobutanolate, which was acylated *in situ* with benzoyl chloride yielding **35** in 90% yield. Treatment of this compound with sodium azide gave 4-azidobutylbenzoate (**36**), which was then hydrolyzed to the corresponding alcohol (**37**). Finally, Swern oxydation of **37** furnished 4-azidobutanal (**38**) in 77% yield. The oxidation of 4-azidobutanol (**37**) can alternatively be performed with Dess-Martin periodinane (DMP), which is an efficient method to oxidize alcohols to aldehydes in very mild conditions. However, for the preparation of large amounts of alcohol, the Swern protocol is preferrable due to the high cost of the Dess-Martin reagent.

Scheme 33. Synthesis of 4-azidobutanal (**38**).[a]

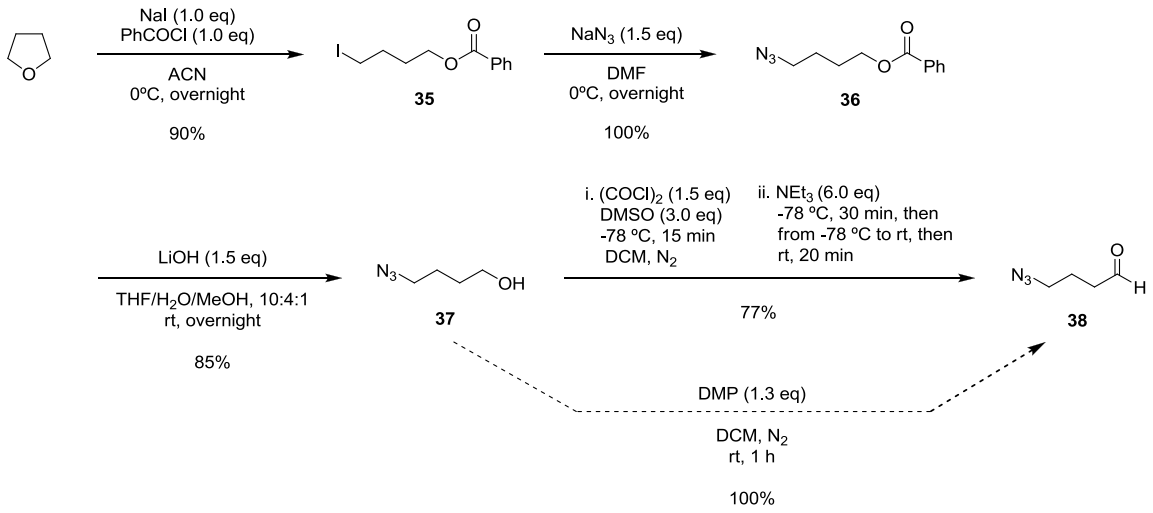

[a] Regular analysis by ^{1}H-NMR showed that aldehyde **38** is stable when kept under argon at -20 ºC.

4.3.1.3. Synthesis of Fmoc-*N*-(4-azidobutyl) valine

For the preparation of Fmoc-*N*-(4-azidobutyl) valine (**34**), we sought to *N*-alkylate the α-amino group of Val with 4-azidobutanal (**38**) in the presence of a reducing agent.

Initially, we investigated the feasibility of carrying out this transformation with no protection at the carboxy group (see Scheme 34). Treatment of unprotected valine with 1.5 equivalents of 4-azidobutanal (**38**) and a excess of $NaBH_3CN$ gave a mixture of the desired *N*-alkylated product and non-alkylated starting material. This mixture was subjected to Fmoc-protection conditions, but the desired product (**34**) and Fmoc-valine were found to be inseparable by flash chromatography.

Scheme 34. Attempt to synthesize Fmoc-*N*-(4-azidobutyl) valine (**34**) starting from unprotected valine.

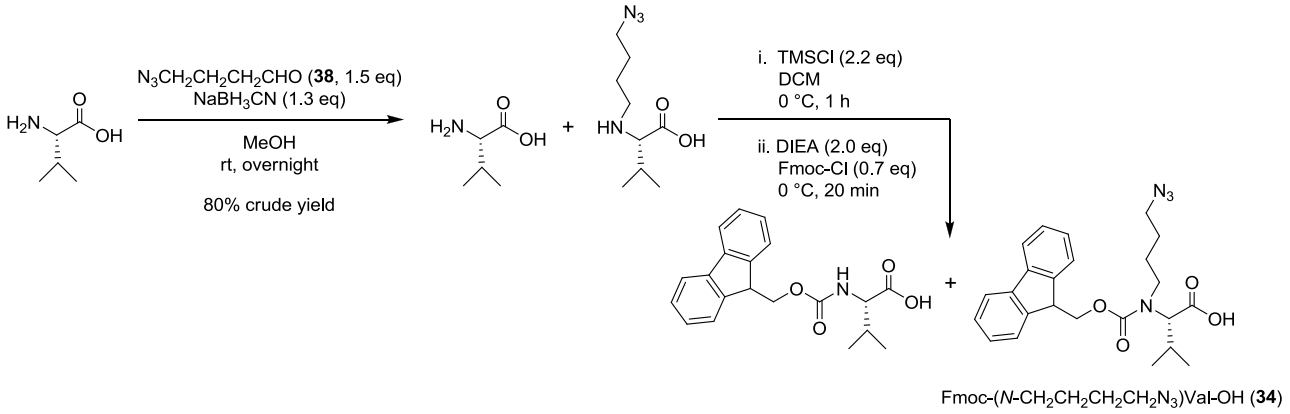

In contrast, Fmoc-*N*-(4-azidobutyl) valine (**34**) was straightforward to obtain from its *tert*-butyl *COOH*-protected precursor (see Scheme 35). Reductive alkylation of valine *tert*-butyl ester with **38** gave a mixture of starting material, *N*-alkylated product (**32**) and *N,N*-dialkylated product. The *N*-alkylated product (**32**) was isolated and acylated with Fmoc-Cl, after which the Fmoc-protected product (**33**) was easily purified. In this Fmoc- protection step, the choice of solvent was a crucial issue. Using dioxane as solvent enabled to obtain the desired product, whereas no product was formed when the reaction was performed in DCM. Finally, acidic cleavage of the *tert*-butyl ester of **33** yielded Fmoc-*N*-(4-azidobutyl) valine (**34**) in 55% overall yield.

Scheme 35. Synthesis of Fmoc-*N*-(4-azidobutyl) valine (**34**) starting from valine *tert*-butyl ester.

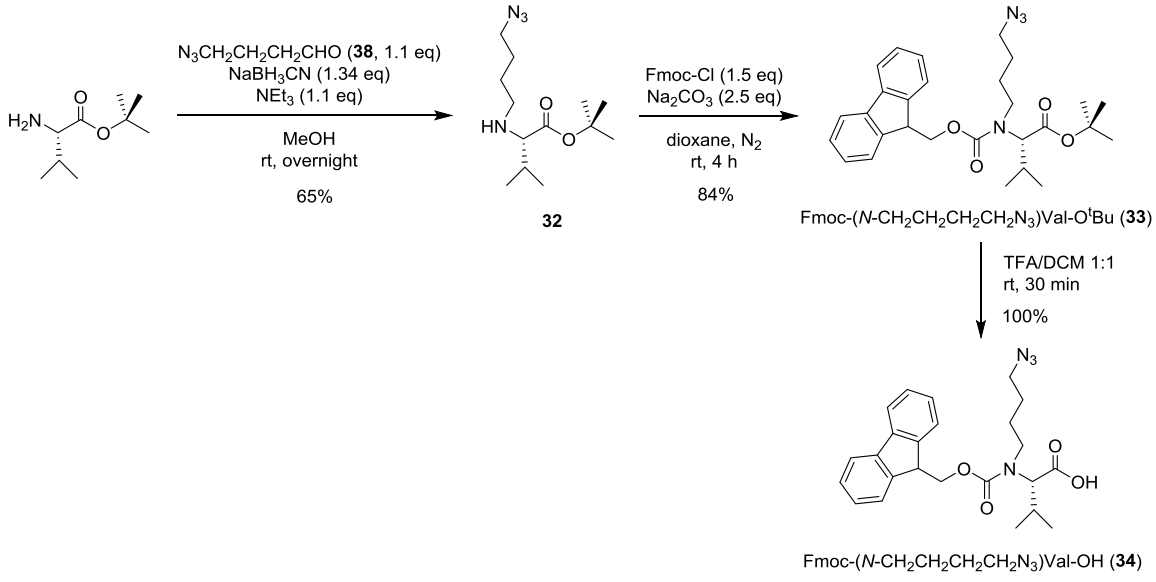

4.3.1.4. Synthesis of H-Asp(O^{t}Bu)-D-Phe-(*N*-$CH_2CH_2CH_2CH_2N_3$)Val-Arg(Pbf)-Gly-OH

The synthesis of pentapeptide **39**, H-Asp(O^{t}Bu)-D-Phe-(*N*-$CH_2CH_2CH_2CH_2N_3$)Val-Arg(Pbf)-Gly-OH, involves a difficult coupling step: the coupling of Fmoc-D-Phe-OH onto *N*-(4-azidobutylated) Val (see Figure 46). This coupling is hampered by the *N*-(4-azidobutyl) group and the β-branched side-chain of Val.

Figure 46. Coupling of Fmoc-D-Phe-OH onto the *N*-(4-azidobutylated) Val residue.

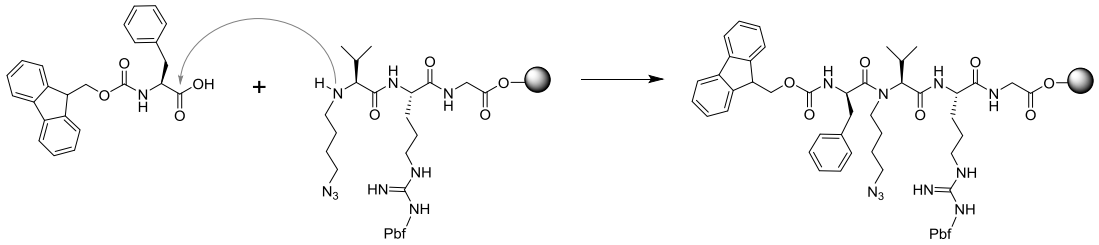

As previously explained, we initially considered two different strategies for the synthesis of this pentapeptide (see Scheme 36). The first strategy (**A**) involves the use of Fmoc-*N*-(4-azidobutyl) valine (**34**) as solid-phase building block, while in the second strategy (**B**) the *N*-(4-azidobutyl) group is introduced into the resin-bound peptide by reductive N^{α}-alkylation of resin-bound Val with 4-azidobutanal (**38**). However, the overall yield of these two strategies was not reproducible when the syntheses were upscaled so, in order to obtain larger amounts of pentapeptide **39**, we had to conceive an alternative synthetic approach (**C**).

Scheme 36. Synthetic strategies to obtain pentapeptide **39**.

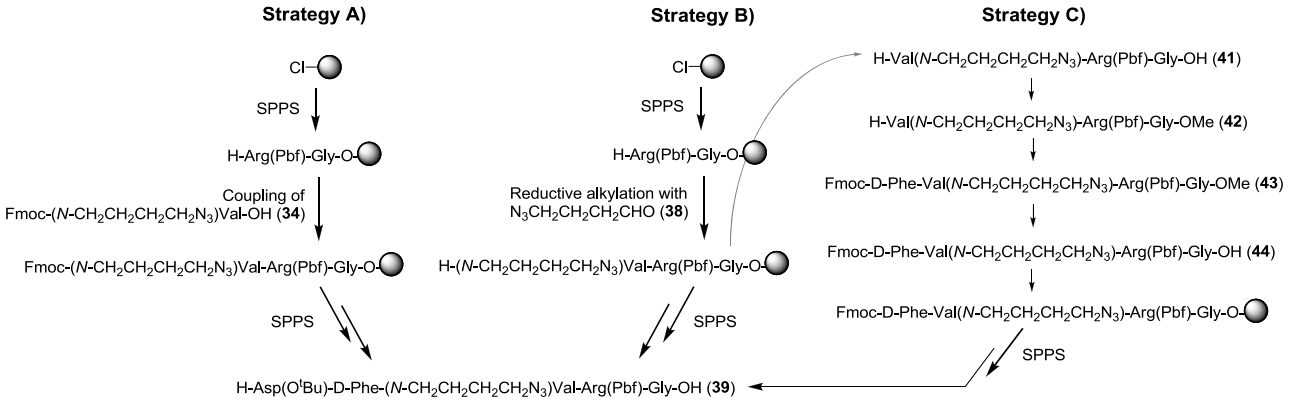

For the three synthetic strategies (**A**, **B** and **C**), we chose the CTC resin as solid support. This resin was chosen because it can be cleaved with very mild acid conditions that enable to obtain fully protected peptide acids. The peptide chain was elongated by stepwise assembly of the Fmoc-protected amino acids and, for standard couplings, we used DIPCDI/OxymaPure activation. In all cases, cleavage was performed with 2% TFA in DCM to obtain the desired peptide (**39**) without removal of the side-chain protecting groups.

Strategy A: SPPS using Fmoc-*N*-(4-azidobutyl) valine

First, we investigated the solid-phase synthesis of pentapeptide **17** using Fmoc-*N*-(4-azidobutyl) valine (**34**) as building block (see Scheme 37). A low resin functionalization was employed, since it may facilitate the hindered coupling step. The coupling **34** onto the Arg(Pbf)-Gly-resin was not efficient under standard conditions. Activation of a 3-fold excess of **34** with DIPCDI/OxymaPure resulted in an uncomplete acylation of the peptidyl-resin, and a second coupling had to

be performed to reach an almost complete conversion. The small amount of unreacted starting material was capped with Ac_2O and we continued with the synthesis.

Scheme 37. Small-scale SPPS of H-Asp(O^{t}Bu)-D-Phe-(*N*-$CH_2CH_2CH_2CH_2N_3$)Val-Arg(Pbf)-Gly-OH (**39**) using Fmoc-*N*-(4-azidobutyl) valine (**34**) as building block (strategy A).

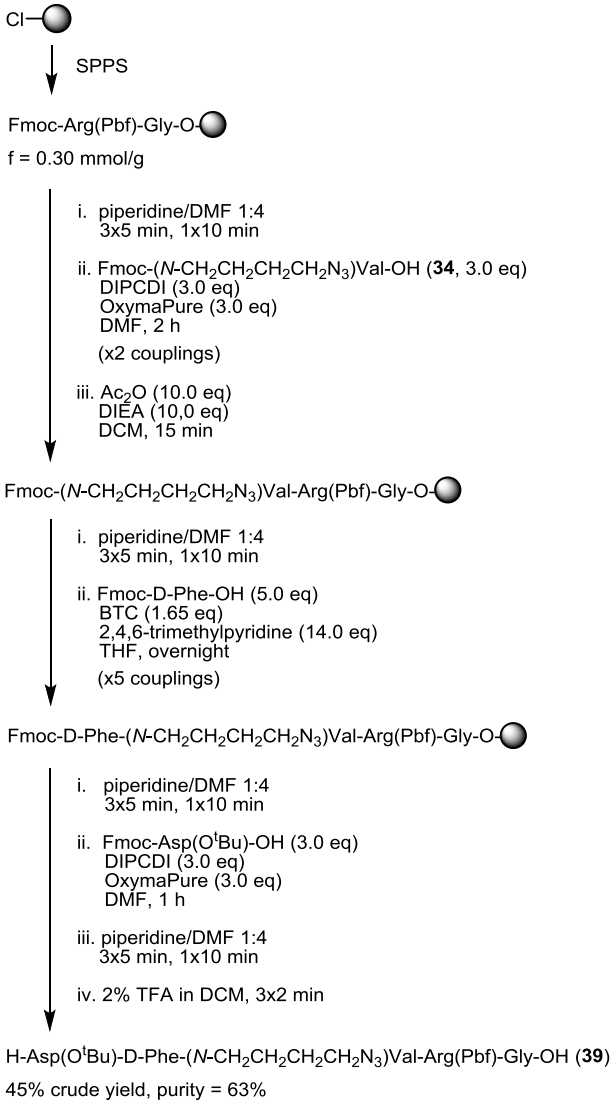

For the coupling of Fmoc-D-Phe-OH onto *N*-(4-azidobutylated) Val, we run a series of experiments with various coupling methods, followed by HPLC analysis with regard to coupling efficiency (data not shown). Activation with DIPCDI/OxymaPure failed to give the desired peptide. When using PyBOP/HOAt or HATU/HOAt, the desired product was not formed either. Attempts failed to achieve this coupling even after several treatments and extended reaction times. The poor reactivity of *N*-azidoalkylated Val was confirmed by treatment of a sample of peptidyl-resin with a mixture of Ac_2O and DIEA in DCM, which resulted in no *N*-acetylation of this residue. At this stage, we investigated if the MW irradiation could promote the coupling. Several experiments were performed using DIPCDI/HOAt activation and under MW heating at 50 ºC, but no conversion was observed. Finally, coupling onto *N*-(4-azidobutylated) Val was found feasible using BTC as activating reagent. After performing 5 treatments with the *in situ*-generated acid chloride (3x3 h, 2x20 h), an 85% conversion was achieved and no epimerization was observed. The rest of the synthesis was continued and, after cleavage from the solid support, the desired pentapeptide (**39**) was obtained in 45% crude yield and 63% purity (see Figure 47).

Figure 47. HPLC analysis of crude pentapeptide **39** obtained by strategy A, linear gradient from 5% to 100% ACN over 8 min.

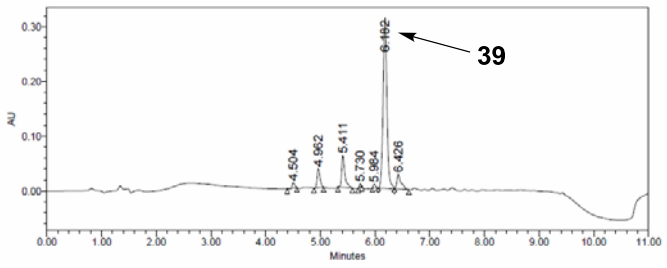

purity = 63%

Strategy B: SPPS by reductive N^{α}-alkylation of resin-bound valine with 4-azidobutanal

The solid-phase synthesis of **17** by using Fmoc-*N*-(4-azidobutyl) valine (**34**) as building block presents some limitations. Coupling of **34** to the peptidyl-resin seems to require a stronger activation method to be efficient. An acceptable conversion can be achieved after two DIPCDI/OxymaPure-mediated couplings, but this requires a considerable amount of **34** (3 equivalents/coupling), which is time-consuming to synthesize. To circumvent these issues, we investigated the introduction of the *N*-(4-azidobutyl) group by reductive alkylation of resin-bound Val with 4-azidobutanal (**38**).

We assembled the Val-Arg(Pbf)-Gly-resin and we tested its reductive alkylation with aldehyde **38** under several conditions (see Table 18). In all the experiments, the resin-bound peptide was first treated with the aldehyde to ensure complete imine formation. Then, the medium was acidified with a few drops of AcOH and 4.0 equivalents of $NaBH_3CN$ were added to reduce the imminium ion. The excess of $NaBH_3CN$ was not found to be relevant and was always kept at 4.0 equivalents. The reaction was tested with different amounts of aldehyde and the desired *N*-alkylated product was formed in all cases. With 0.5 equivalents of aldehyde, a considerable amount of starting material and an unknown species with $[M+57]^+$ (M being the mass of the desired product) were present in the crude (entry 1). With 1.0 equivalent of aldehyde, the amount of unreacted peptide and unknown species decreased, but was still significant (entry 2). When 1.5 equivalents of aldehyde were used, the *N*-alkylated peptide was formed as a major product and the presence of starting material and unknown species was negligible (entry 3). When using 2.0 or more equivalents of aldehyde, all the starting material was converted, but a considerable amount of *N,N*-dialkylated product was formed (entries 4-7). The formation of *N,N*-dialkylated product would not compromise the purification of the final peptide, since the *N*-terminus of the *N,N*-dialkylated product is capped and thus the peptide cannot lead to any deletion sequence. However, *N,N*-dialkylation should be prevented. Therefore, we concluded that the reductive alkylation step should be performed with 1.5 equivalents of aldehyde using THF as solvent (entry 3). THF was preferred to DMF, because the latter seemed to favour over-alkylation when 2.0 equivalents of aldehyde were employed (entries 4 vs. 5 and 6 vs. 7).

Table 18. Conditions investigated for the reductive N^{α}-alkylation of resin-bound Val with 4-azidobutanal (**38**).

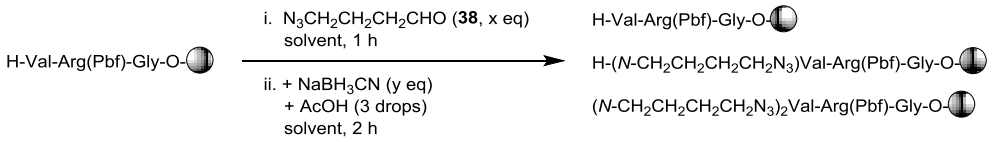

Entry	Solvent	Aldehyde (x eq)	$NaBH_3CN$ (y eq)	Result [a]			
				Starting material	*N*-alkylated product	*N,N*-dialkylated product	Subproduct[b] with $[M_{EP}+57]^+$
1	THF	0.5	4.0	+++	+	-	+++
2	THF	1.0	4.0	++	++	-	++
3	THF	1.5	4.0	+	+++	-	+
4	THF	2.0	4.0	-	+++	++	-
5	DMF	2.0	4.0	-	++	+++	-
6	THF	5.0	4.0	-	++	++++	-
7	DMF	5.0	4.0	-	+	+++++	-

[a] As determined by HPLC and HPLC-MS analysis of cleaved samples of peptidyl-resin.
[b] This unknown species was not found to interfere in the subsequent Fmoc-D-Phe-OH coupling step.

The reason why *N,N*-dialkylation should be prevented is the following (see Scheme 38). Double *N*-alkylation proceeds first at the less hindered sites of the peptidyl-resin bead, and introduces more steric hindrance. Upon *N,N*-dialkylation, certain sites of the resin bead will become less accessible. *N*-alkylated amines located at very hindered sites will be more difficult to acylate in the next coupling step, which is hampered by the *N*-alkyl group. Therefore, conditions that minimize formation of the *N,N*-dialkylated product are preferrable, even if they lead to uncomplete conversion.

Scheme 38. Schematic representation of a bead of Val-Arg(Pbf)-Gly-resin after reductive N^{α}-alkylation with 4-azidobutanal (**38**). **A)** With 1.0-1.5 equiv. of **38**, traces of *N,N*-dialkylated product detected, but reaction not complete. **B)** With 2.0-5.0 equiv. of **38**, almost complete reaction, but considerable *N,N*-dialkylation.

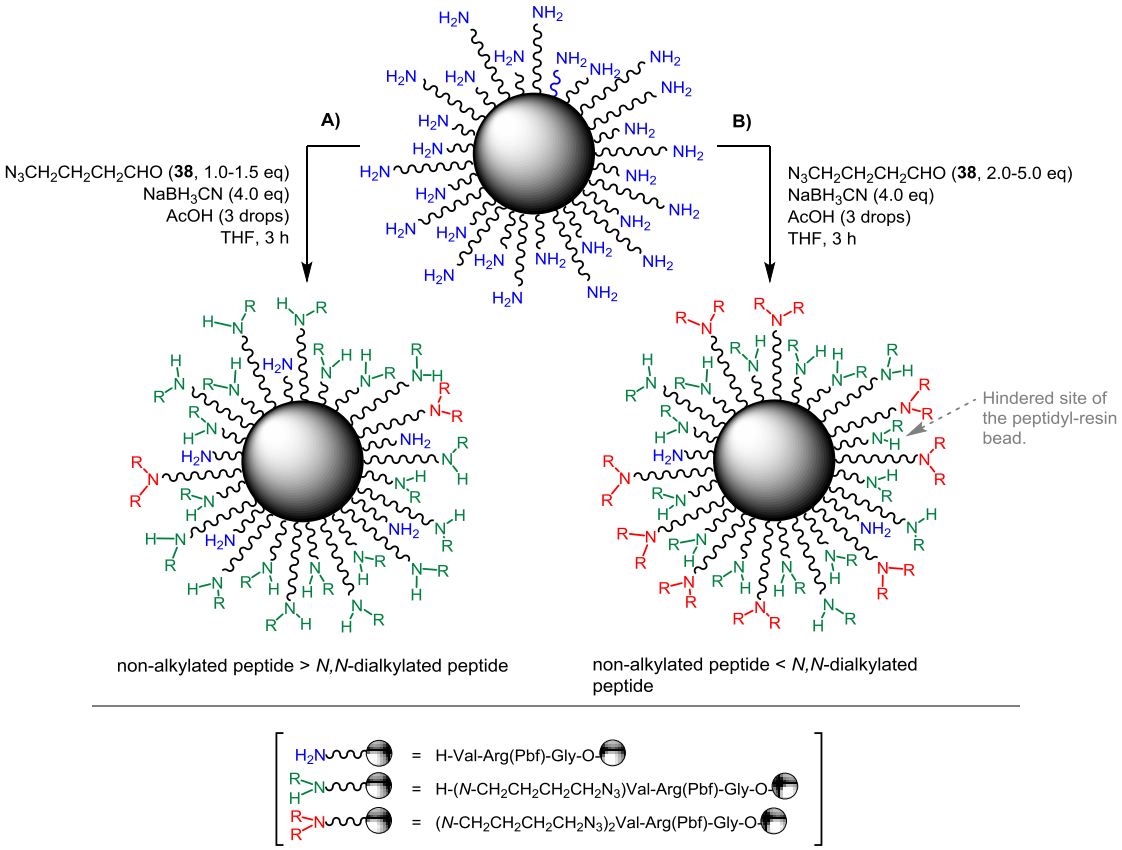

After having optimized the reductive alkylation step, we proceeded to apply this transformation in the solid-phase synthesis of pentapeptide **39** (see Scheme 39). When the resin-bound *N*-terminal Val was treated with 1.5 equivalents of 4-azidobutanal (**38**) and a excess of $NaBH_3CN$, the desired *N*-alkylated product was formed and no *N,N*-dialkylated product was detected. The small amount of unreacted starting material was capped with Ac_2O, and we continued with the synthesis. Fmoc-Phe-OH was coupled onto the *N*-azidoalkylated Val residue with BTC activation. After three overnight treatments, a good conversion was achieved and the lack of racemization was confirmed by HPLC analysis. The rest of the synthesis was continued without any particular difficulty and, after cleavage from the solid support, the desired pentapeptide (**39**) was obtained in 48% crude yield and 43% purity (see Figure 48).

Scheme 39. Small-scale SPPS of H-Asp(O^{t}Bu)-D-Phe-(*N*-$CH_2CH_2CH_2CH_2N_3$)Val-Arg(Pbf)-Gly-OH (**39**) by reductive alkylation of resin-bound Val with 4-azidobutanal (strategy B).

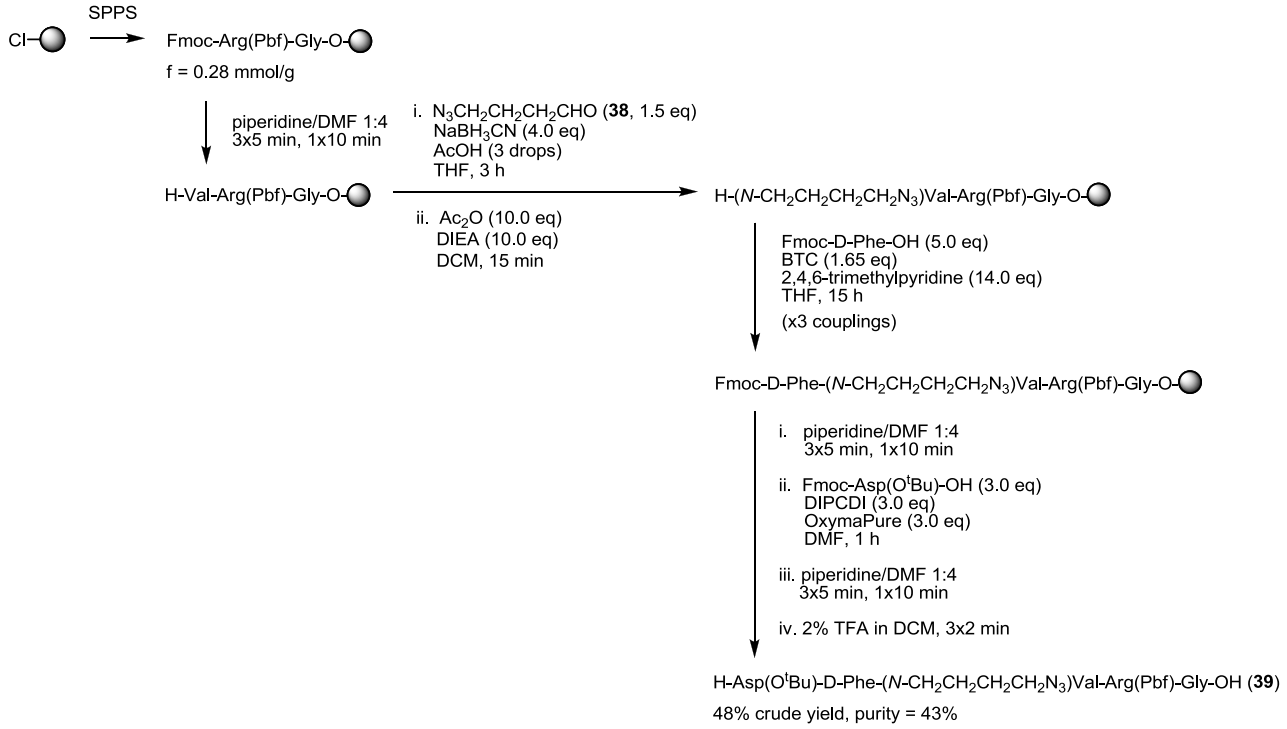

Figure 48. HPLC analysis of crude pentapeptide **39** obtained by strategy B, linear gradient from 5% to 100% ACN over 8 min.

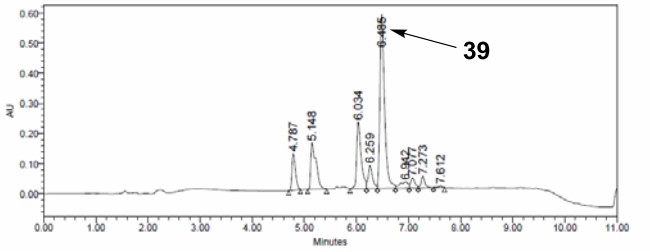

purity = 43%

To sum up, the two solid-phase strategies for the synthesis of **39** (**A** and **B**) enabled us to obtain mg-amounts of this peptide (**39**) with good purities and acceptable crude yields (see Table 19). However, both synthetic approaches required multiple coupling cycles to achieve an efficient coupling onto the *N*-(4-azidobutylated) Val residue.

Table 19. Comparison of the efficiency of the two synthetic strategies (A and B) for the small-scale synthesis of pentapeptide **39**.

Synthetic strategy	Amount of CTC resin	Functionalization (mmol/g)	Amount of crude **39** obtained	Purity of **39**	Crude yield
A	1.4 g	0.30	189 mg	63%	45%
B	1.3 g	0.28	177 mg	43%	48%

Unfortunately, when the solid-phase synthesis of pentapeptide **39** was performed usin a higher amount of resin (>3 g of resin) and/or a higher functionalization (>0.50 mmol/g), the yields were not so satisfactory. Apparently, the efficiency of the BTC-mediated D-Phe-to-[*N*-(4-azidobutyl)Val] coupling is not reproducible on large scale.

Strategy C: Synthesis by a combined solid-phase/solution approach

To obtain larger amounts of pentapeptide **39**, we developed a alternative protocol in which the difficult coupling step is performed in solution and the rest of the peptide elongation in solid-phase (see Scheme 40). In this approach, we sought to prepare *N*-(4-azidobutylated) tripeptide **41** on the CTC resin and cleave it for subsequent acylation with Fmoc-D-Phe-OH. Performing this coupling in solution was expected to be less difficult than in solid-phase, since the reactivity of secondary amines towards activated amino acids is lower when they are bound to a solid support.[147] To perform this coupling in solution, protection at the *C*-terminus of the *N*-azidoalkylated peptide fragment is required and, for our aim, the protecting group of choice should be orthogonal to Fmoc- and Pbf-. In this way, the product obtained in the coupling step can be selectively deprotected at the *C*-terminus and then loaded again onto the solid support for further elongation of the peptide chain.

Scheme 40. Synthesic strategy to obtain **39** by a combined solid-phase/solution approach (strategy C).

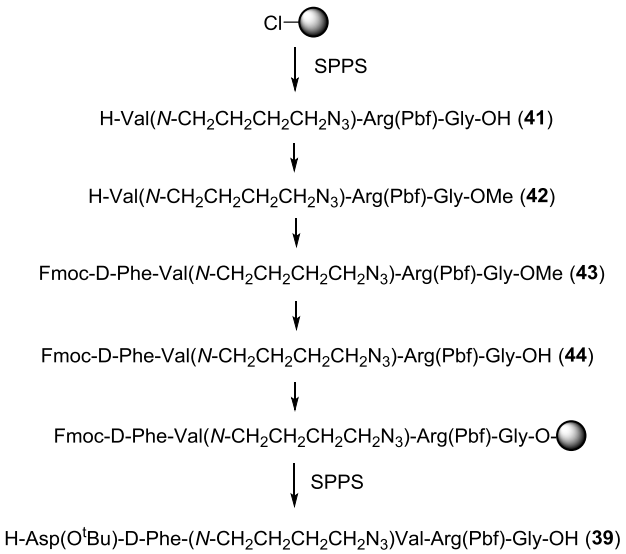

We started off by assembling the Val-Arg(Pbf)-Gly tripeptide on the CTC resin (see Scheme 41). The *N*-(4-azidobutyl) group was incorporated into the growing peptide by reductive N^{α}-alkylation with 4-azidobutanal (**38**), and cleavage from the solid support yielded the *N*-azidoalkylated tripeptide (**41**).

Scheme 41. SPPS of the *N*-azidoalkylated peptide fragment (**41**).

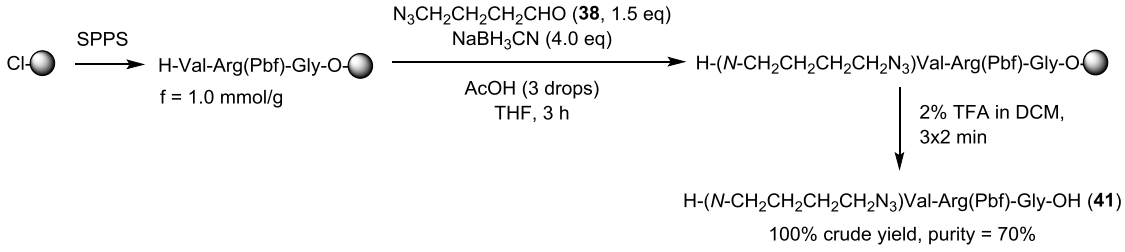

The *C*-terminus of this peptide (**41**) was protected as a methyl ester by treatment with trimethylsilyldiazomethane (see Scheme 42). For the coupling between Fmoc-D-Phe-OH and the *N*-azidoalkylated peptide segment (**42**), we sought to use an acid chloride. In couplings via acid chlorides, the required Fmoc-amino acid chloride is usually prepared in a prior step. We found it more convenient to generate the acid chloride of Fmoc-D-Phe-OH *in situ* by treatment of this amino acid with BTC and 2,4,6-trimethylpyridine. The coupling was allowed to proceed overnight and no epimerization was detected. This procedure enabled us to obtain the desired peptide segment (**43**), which was isolated in 48% yield. Then, the methyl ester of **43** was hydrolyzed under alkaline conditions in the presence of $CaCl_2$, an effective additive to widely suppress base-catalyzed Fmoc- decomposition.[163] Since both the starting methyl ester (**43**) and its saponification product (**44**) can suffer Fmoc- cleavage, the reaction should be monitorized by HPLC and quenched when an acceptable conversion is achieved. After 2 hours, saponification of **34** was almost complete and no side-product from Fmoc- decomposition was detected (as checked by HPLC-MS). Thus, the hydrolisate was neutralized at this point. The desired product (**44**) was straightforward to isolate by simple aqueous extraction.

Scheme 42. Coupling of Fmoc-D-Phe-OH onto *N*-azidoalkylated peptide **42**.

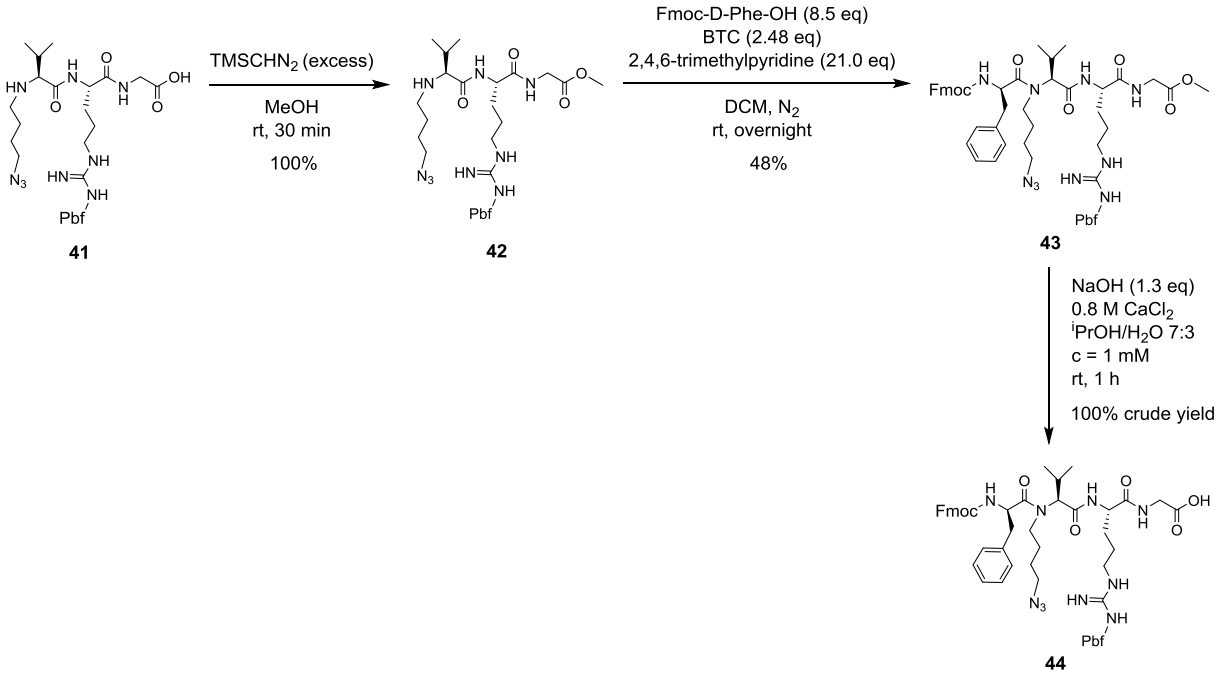

The crude tetrapeptide **44** was loaded again onto the CTC resin (see Scheme 43). The reaction was allowed to proceed overnight to ensure maximum incorporation, and a large excess of DIEA was used. With these conditions, the incorporation of **44** took place with an acceptable efficiency for a low functionalization (*i.e.* 80% peptide incorporation for an expected functionalization of 0.10 mmol/g) and, since **44** has a *C*-terminal Gly, epimerization was not an issue to be assessed. After loading **35** onto the resin, the *N*-terminal residue was deprotected and Fmoc-Asp(O^tBu)-OH was

assembled. Then, the Fmoc- was removed and cleavage of the peptidyl-resin with 2% TFA in DCM yielded pentapeptide **39** in 63% purity (see Figure 49).

Scheme 43. SPPS elongation to obtain **39**.

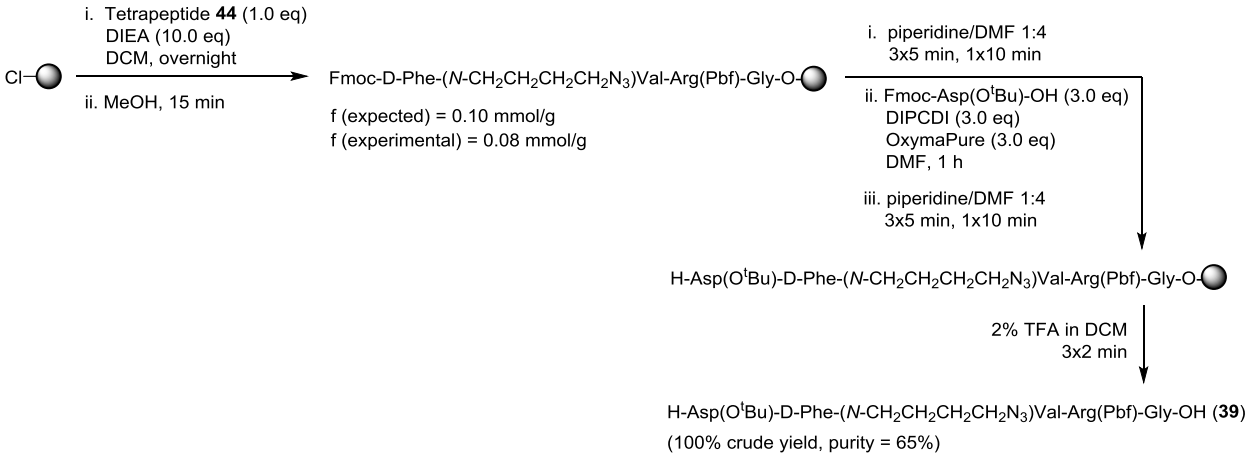

Figure 49. HPLC analysis of crude pentapeptide **39** obtained by strategy C, linear gradient from 20% to 70% ACN over 8 min.

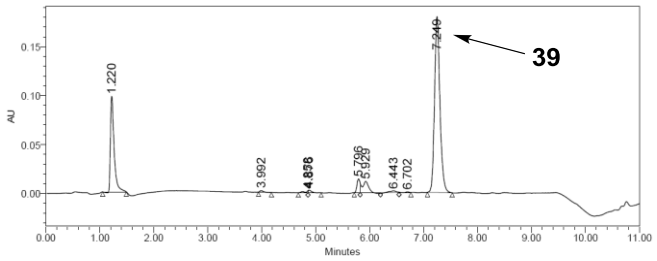

purity = 65%

4.3.1.5. Cyclization and deprotection

The cyclization of pentapeptide **39** was not expected to be difficult. As previously mentioned, the presence of Gly at the *C*-terminus of **39** minimizes steric hindrance during cyclization and rules out the possibility of epimerization taking place. Moreover, the presence of turn-inducing residues -such as *N*-alkyl and D-amino acids in linear peptides favours their cyclization due to backbone preorganization.[124]

For the three synthetic strategies discussed in Section 4.3.1.4., the crude pentapeptide **39** was found to be sufficiently pure to be directly cyclized. In the case of **39** obtained by strategy C (63% purity), cyclization with EDC·HCl/DMAP afforded **40** in 90% crude yield (see Scheme 44). The reaction was complete, almost no by-products were observed and, at a concentration of 1 mM, no cyclodimer was formed (see Figure 50). After cyclization, the Pbf- and ^{t}Bu- groups were removed with TFA:H_2O:TIS 95:5:5. The unprotected cyclopeptide was precipitated with cold *tert*-butyl methyl and isolated by semipreparative RP-HPLC. In this way, the pure *N*-(4-azidobutylated) cyclopeptide (**27**) was obtained in 39% two-step yield, the overall yield of the synthesis being 18% (see Figure 49).

Scheme 44. Cyclization of **39** and deprotection to obtain cyclo[RGDf(*N*-$CH_2CH_2CH_2CH_2N_3$)V] (**27**).

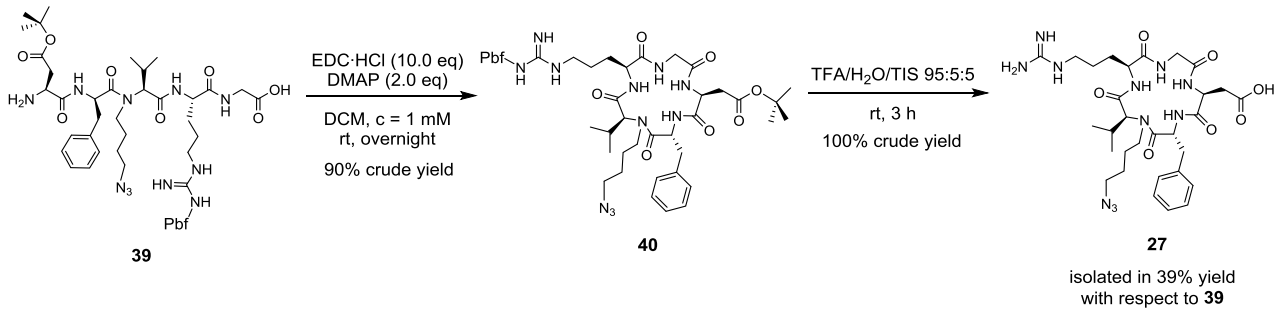

Figure 50. A) HPLC analysis of the cyclization crude, linear gradient from 40% to 100% ACN over 8 min. **B)** HPLC analysis of the deprotection crude, linear gradient from 10% to 50% ACN over 8 min. **C)** HPLC analysis of the purified cyclic peptide (**27**), linear gradient from 10% to 50% ACN over 8 min.

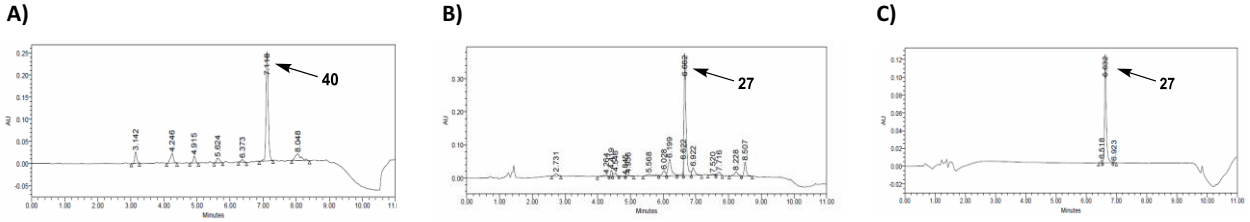

4.3.2. Effect of *N*-(4-azidobutyl) vs. *N*-Me on conformation

In order to investigate if the incorporation of an *N*-(4-azidobutyl) group into a cyclic peptide exerts similar conformational restrictions as a backbone *N*-Me group, we analyzed cyclo[RGDf*N*MeV] (**23**) and its *N*-(4-azidobutylated) analog (**27**) by NMR spectroscopy. For both peptides, ^{1}H- and ^{13}C-NMR data were found to be almost identical. The similarity of their H^N-, H^α- and C^α-chemical shifts, which are sensitive to backbone conformational changes, is outlined in Table 20. The amide protons of **23** and **27** had almost identical temperature coefficients and very similar vicinal scalar coupling constants (see Tables 21 and 22). The close resemblance of these NMR parameters indicates that replacement of the *N*-Me group of cyclo[RGDf*N*MeV] (**23**) by an *N*-(4-azidobutyl) group caused a minimal perturbation of its original conformation, which is reported to stabilize the RGD-motif in its optimum orientation for binding to the $\alpha_v\beta_3$ integrin receptor.[145]

Table 20. H^N-, H^α- and C^α-chemical shifts (ppm) of **23** and **27** in H_2O (pH 6.0) at 288 K.[a]

Peptide	δ (H^N) [ppm]				δ (H^α) [ppm]				
	H^N [Asp]	H^N [Arg]	H^N [D-Phe]	H^N [Gly]	**1:** H^α [*N*MeV] **2**: H^α [(*N*-$CH_2CH_2CH_2CH_2N_3$)V]	H^α [Asp]	H^α [Arg]	H^α [D-Phe]	H^α [Gly]
cyclo[RGDf*N*MeV] (**23**)	8.68	8.47	8.21	8.02	4.37	4.57	3.93	5.21	3.54, 4.14
cyclo[RGDf(*N*-$CH_2CH_2CH_2CH_2N_3$)V] (**27**)	8.68	8.55	8.14	7.83	4.37	4.65	3.86	5.01	3.56, 4.09

Peptide	δ (C^α) [ppm]				
	1: C^α [*N*MeV] **2**: C^α [(*N*-$CH_2CH_2CH_2CH_2N_3$)V]	C^α [Asp]	C^α [Arg]	C^α [D-Phe]	C^α [Gly]
cyclo[RGDf*N*MeV] (**23**)	66.9	52.9	57.6	53.8	46.1
cyclo[RGDf(*N*-$CH_2CH_2CH_2CH_2N_3$)V] (**27**)	67.1	53.2	58.0	54.6	45.9

[a]The complete assignment of all the proton and carbon resonances of **23** and **27** at 288 K is shown in Annex 3.

Table 21. Temperature coefficients (ppb K^{-1}) of the amide protons of **23** and **27** in H_2O (pH 6.0).

Peptide	Δδ/ΔT [ppb K^{-1}]			
	H^N [Asp]	H^N [Arg]	H^N [D-Phe]	H^N [Gly]
23	-7.5	-11.1	-5.5	-5.4
27	-7.5	-10.0	-5.4	-5.1

Table 22. Vicinal scalar coupling constants (Hz) for the amide protons of **23** and **27** in H_2O (pH 6.0) at 288 K.

Peptide	$^3J(H^N\text{-}H^\alpha)$ [Hz]			
	H^N [Asp]	H^N [Arg]	H^N [D-Phe]	H^N [Gly]
23	8.3	7.5	9.6	8.2
27	7.8	7.3	9.1	7.8

On the basis of these results, we can expect that an *N*-(4-azidobutyl) group will exert similar conformational restrictions as a backbone *N*-Me group when incorporated into other cyclic peptides. This finding widens the applicability of the *N*-(4-azidobutyl) group as a linker to support conjugation, as many bioactive cyclopeptides contain *N*-Me residues within their structure. Therefore, replacement of an *N*-Me group present in a cyclopeptide with our linker is a feasible way to functionalize the peptide providing a little impact on its original conformation, which may be crucial for biological activity.

4.3.2. Synthesis of the PEG conjugates

4.3.2.1. Synthetic approach

The synthetic transformations to obtain the PEG conjugates **29-31** are shown in Scheme 45. PEG conjugate **31** can be obtained from **27** by cycloaddition of its azide with an alkyne-functionalized PEG. The preparation of PEG conjugates **29** and **30** requires the prior azide-to-amine reduction of **27** to obtain **28**. Then, reductive *N*-alkylation of **28** with a PEG-aldehyde would yield PEG conjugate **30**, whereas its acylation with an amine-reactive PEG derivative would furnish PEG conjugate **31**.

Scheme 45. Synthetic transformations to obtain PEG conjugates **29-31**.

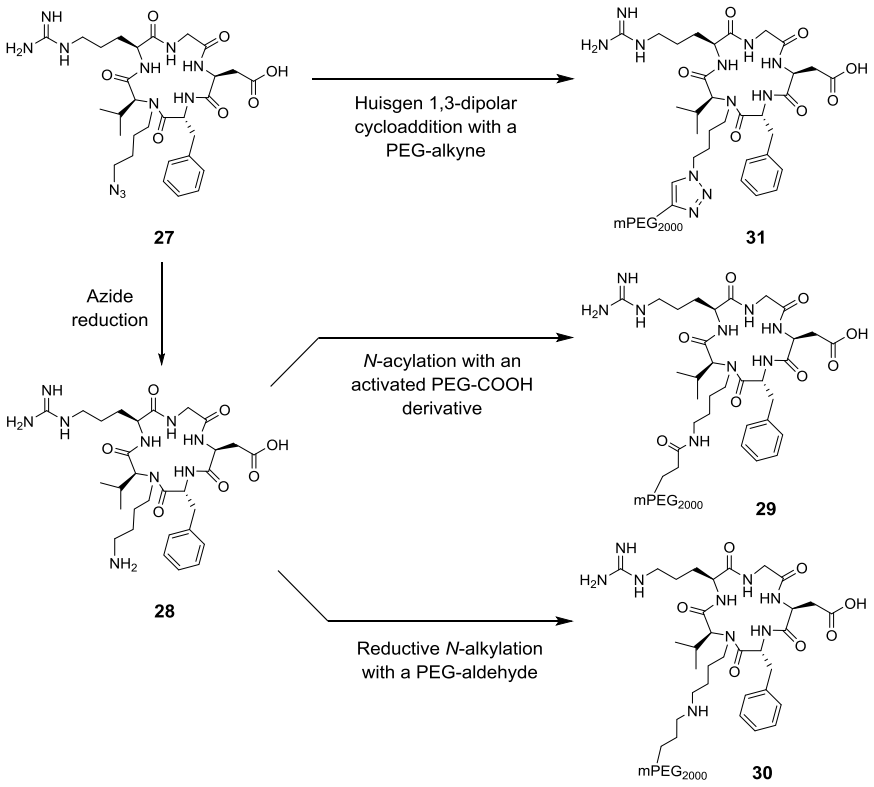

4.3.3.2. Issues in the conjugation of peptides with polydisperse PEG

In conjugation chemistry, the majority of applications of PEG involve the use of a PEG reagent that is polydisperse.[76] Such polydisperse PEG reagents do not have an exact number of repeating ethylene oxide units; what they actually have is a Gaussian distribution of PEG chain lengths. This distribution is characterized by an average MW and a degree of polydispersity.

The conjugation of peptides with polydisperse PEG requires reliable methods for the analysis, purification and characterization of peptide-PEG conjugates (see Table 23).[76] Due to the polydispersity of PEG, several issues have to be considered.

Table 23. Common methods for the detection, characterization and purification of petide-PEG conjugates.

	PEGylating reagents	Peptide-PEG conjugates
Detection	▪ MS detector ▪ Alternatively: RI detector, light scattering techniques	▪ UV detector ▪ MS detector
Characterization	▪ RP-HPLC (MS or RI detection) ▪ MS (for polydisperse PEG, MALDI-TOF preferred to ESI) ▪ ^{1}H-NMR, ^{13}C-NMR	▪ RP-HPLC (UV or MS detection) ▪ MS (for polydisperse PEG, MALDI-TOF preferred to ESI) ▪ ^{1}H-NMR, ^{13}C-NMR
Purification		▪ ultrafiltration/diafiltration ▪ RP-HPLC (UV or MS detection) ▪ For peptide-PEG conjugates of high MW with a size difference with respect to the compounds to be separated, SEC-HPLC may be applicable. ▪ For protein-PEG conjugates with a net charge difference with respect to the compounds to be separated, IEC chromatography and SDS-PAGE may be applicable.

For the monitorization of peptide-PEG conjugates, RP-HPLC is often used due to its high resolution and the possibility of coupling the technique with an online MS detector. PEG-modified peptides can be detected by measuring the UV absorbance at 220 nm. On the contrary, unreacted PEG derivatives do not absorb in the UV-visible and they have to be detected using an MS detector, a refractive index (RI) detector or light scattering techniques.

The MS determination of peptide-PEG conjugates can be difficult because of polymer polydispersity, which leads to a distribution of mass signals in the mass spectra. For such MS determinations, MALDI is the preferred technique because it mainly produces monocharged ions, thus generating mass spectra of low complexity.[164] The MALDI mass spectrum of a PEG-containing compound typically shows a distribution of MW values with the main mass signals spaced apart by $\Delta m/z = 44$, in agreement with the mass of the ethylene oxide monomer unit (see Figure 51).[165] In contrast with MALDI, the electrospray ionization (ESI) method tends to produce multiply charged ions. As a consequence, the ESI mass spectra of polydisperse PEG conjugates show several distributions of mass signals and are very difficult to interpretate.

Figure 51. MALDI-TOF analysis of the polydisperse PEG reagents used in the present work.

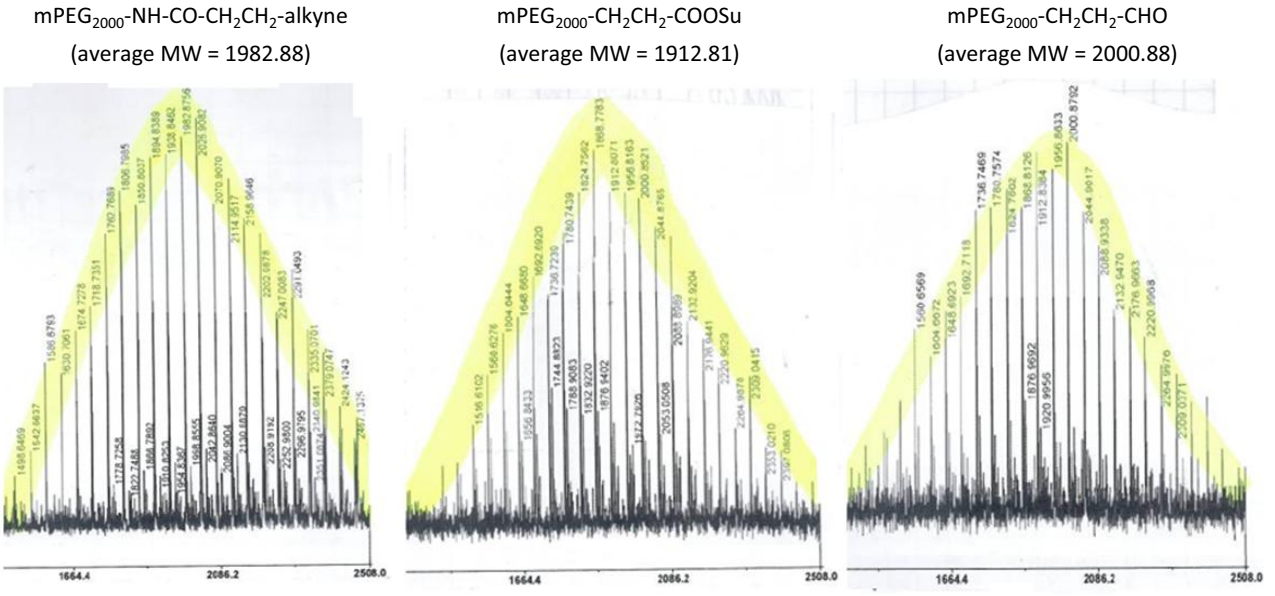

Despite MALDI is the preferred technique for the MS determination of polydisperse PEG conjugates, it presents some limitations. First, MALDI shows a poor ionization efficiency for molecules containing large polymers, which decreases the sensitivity of the method. Second, the presence of salts in the MALDI sample should be avoided, since it may hamper the ionization of the PEG-containing molecules thus impeding their detection.

After conjugating PEG to a peptide, a purification step is always required to eliminate the unreacted starting material, the excess of PEGylating reagent, and possible by-products. Dialysis or ultrafiltration of the reaction mixture may be used to remove low-MW components but, to isolate the the peptide-PEG conjugate in high purity, chromatographic separation is required. For this aim, semipreparative RP-HPLC is the most common technique. Although the method is very rapid, only a limited amount of sample material can be loaded at once. Moreover, the fact that PEG-modified peptides appear as broad HPLC peaks due to polymer polydispersity may compromise their resolution to different extents. Besides, it should be mentioned that the chromatographic instrument should be equipped with an online MS detector in order to ensure that unreacted PEG is well-ressolved from the peptide-PEG conjugate. Otherwise, the absence of residual PEG should be assessed by MS analysis of each of the fractions collected.

Besides semipreparative RP-HPLC, there are other chromatographic techniques for the purification of PEG-modified compounds. Ion-exchange (IEX) chromatography may be applicable in those cases in which the net charge of the conjugate is altered with respect to the original molecule. Size-exclusion (SEC)-HPLC may be applied in those cases in which there is considerable difference in size between the non-modified compound, the conjugation product and the unreacted PEG. These two chromatographic methods are widely used for the purification of PEGylated proteins, but they are not suitable for the purification of peptide-PEG conjugates of low MW.

After purification of a peptide-PEG conjugate, determination of the net peptide content (g pure peptide·100/g sample) by amino acid analysis is highly recommended. Since PEG is a very hygroscopic polymer, samples PEGylated peptides may contain a considerable amount of residual water and thus have a relatively low net peptide content. To obtain reproducible results in quantitative studies, the net peptide content of the sample should be assessed.

For the characterization of a peptide-PEG conjugate, determination of the average MW by MALDI-TOF mass spectrometry and determination of the purity by RP-HPLC are mandatory. Assessment of the lack of impurities by ^{1}H-NMR spectroscopy is highly recommended. Size-exclusion (SEC)-HPLC can be used to evaluate the homogeneicity of

the conjugate; however, this technique cannot provide an accurate determination of the average MW of the PEG-modified peptide. Since PEG is transparent to light at UV-visible wavelenght, circular dichroism may be applied to characterize the secondary structure.

4.3.3.3. Azide reduction

We investigated conditons to reduce the azido group of cyclo[RGDf(*N*-$CH_2CH_2CH_2CH_2N_3$)V] (**27**). Among the various protocols reported for azide reduction,[166] we decided to use Zn and NH_4Cl. This method enables to reduce azides to amines in very mild conditions and is compatible with a variety of functional groups.[167]

The reduction of **27** with 1.3 equivalents of Zn and 2.3 equivalents of NH_4Cl was very slow. When performing the reaction at room temperature, it took several days for the reaction to be complete. When the reduction was carried out at 60 ºC, unreacted **27** remained after 4 hours. After refluxing overnight, complete conversion was achieved. However, elimination of the azido group took place (see Scheme 46). In addition to the N_3-elimination side-product (**I**), another non-desired product (**II**) was also formed, having $[M+H]^+$ = 647. HPLC monitorization showed that the N_3-elimination side-product was progressively transformed into this unknown species (see Figure 52). Thus, this species was assumed to be the side-product from hydration of the double bond that is formed upon N_3-elimination.

Scheme 46. Undesired side-reactions during the azide reduction step.[a]

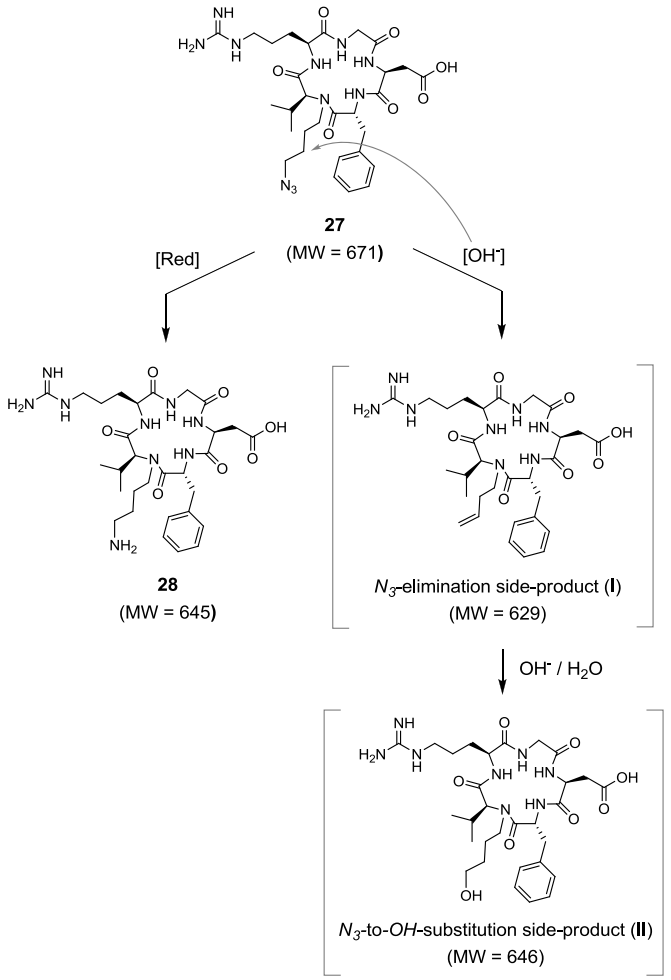

[a] As depicted in this Scheme, OH^- is considered as the base that abstracts the β-proton in the N_3-elimination side-reaction. Such OH- anions pressumably result from the oxidation of Zn in aqueous media: Zn + H_2O → Zn^{2+} + 2 OH^-.

Figure 52. HPLC monitorization of the azide reduction step, linear gradient from 10% to 50% ACN over 8 min.

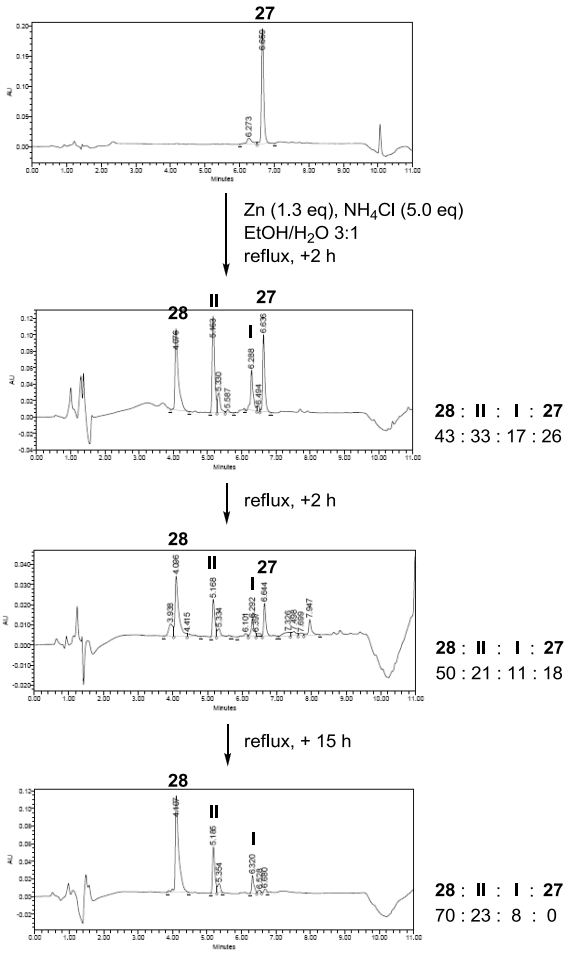

The degree of formation of these two side-products did not decrease when the reaction was performed at room temperature. Therefore, we found it preferrable to perform the azide reduction step at 60 ºC. With these conditions and using a higher excess of NH_4Cl (5.0 equivalents) to ensure acidic media, the desired peptide (**28**) was formed as major product (70%), whereas the N_3-elimination side-product and the species with $[M+H]^+$ = 647 were present in a 8% and 23% proportion, respectively (as determined by HPLC). After semipreparative RP-HPLC purification, we isolated **28** in 24% yield (see Scheme 47).

Scheme 47. Azide reduction to obtain **28**.

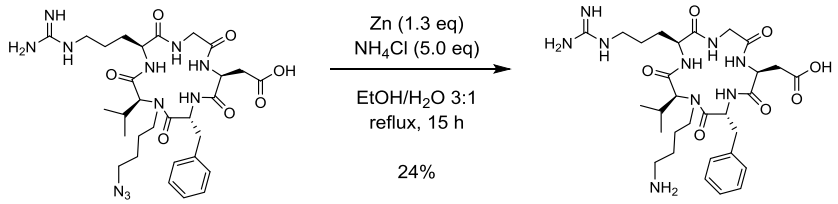

27 **28**

4.3.3.4. Conjugation with PEG via amide bond formation

The conjugation of PEG onto an amine moiety is commonly achieved by using an *N*-hydroxysuccinimidyl ester PEG derivative (PEG-COOSu) as acylating PEG. Several PEG-COOSu derivatives are commercially available and they differ in the distance between the active ester (-COOSu) and the first ethylene oxide monomer unit. This distance affects the reactivity of the active ester towards nucleophiles, such as amines and water (see Table 24).

Table 24. Reactivity (hydrolysis and aminolysis in 0.1 M phophate buffer, pH 8.0) of various *N*-hydroxysuccinimidyl ester PEG derivatives.[168]

PEG-$(CH_2)_n$-COOSu	Name	Hydrolysis[a] $t_{1/2}$ at 25 ºC (min)	Hydrolysis[a] $t_{1/2}$ at 10 ºC (min)	Aminolysis[b] $t_{1/2}$ at 10 ºC (min)
PEG-CH_2-COOSu	PEG-carboxymethyl succinimidyl ester	0.75	2	0.4
PEG-CH_2CH_2-COOSu	PEG-propionate succinimidyl ester	17.1	67	9.5
PEG-$CH_2CH_2CH_2$-COOSu	PEG-butyrate succinimidyl ester	23.3	100	10.3
PEG-$CH_2CH_2CH_2CH_2$-COOSu	PEG-valerate succinimidyl ester	33.6	n.a.	n.a.

[a] Hydrolysis half lives were calculated assuming a pseudo first-order mechanism with respect to -COOSu.

[b] Aminolysis half life was calculated on a low-MW substrate (*N*-acetyl-L-lysine methyl ester 0.3 mM) and using a 10- or 20-fold excess of reactive PEG to mimic a first-order mechanism.

For the conjugation of cyclo[RGDf(*N*-$CH_2CH_2CH_2CH_2NH_2$)V] (**28**) with PEG, we used a polydisperse PEG-propionate succinimidyl ester (PEG-CH_2CH_2-COOSu) of 2 KDa. The reaction was investigated in a basic aqueous buffer using different amounts of activated PEG (see Table 25). Basic media is required to prevent the ω-amino group from being protonated and consequently no reactive towards the activated PEG (pKa of the ε-amine of Lys = 10.5, pKa of the α-amino group at the *N*-terminus of a peptide = 8.0).[169] In aqueous solution, the coupling should be complete in about 30 minutes to 1 hour, since the hydrolysis half-life of PEG-CH_2CH_2-COOSu at pH 8.0 and 25 ºC is around 17.1 minutes.[168] When we used an excess of PEG-CH_2CH_2-COOSu (5.0 equivalents), there was no starting material (**28**) after 1 hour at room temperature (entry 1). The PEG conjugate (**29**) appeared as a broad HPLC peak with the expected average MW (as confirmed by MALDI-TOF analysis). However, the hydrolized PEG derivative and the conjugation product (**29**) were hardly separable by semipreparative RP-HPLC, since their HPLC peaks overlapped with each other for a variety of conditions. Even when using a stoichometric amount of PEG-CH_2CH_2-COOSu (entry 2), the desired

product (**29**) could not be isolated from residual PEG-CH_2CH_2-COOH. Moreover, the fact that the hydrolized PEG derivative is not detectable by UV complicated the purification; since we did not have a semipreparative RP-HPLC apparatus equipped with an MS detector, the presence of hydrolized PEG in the collected fractions had to be assessed by MALDI-TOF analysis.

Table 25. Conditions investigated for the *N*-acylation of **28** with PEG-CH_2CH_2-COOSu.

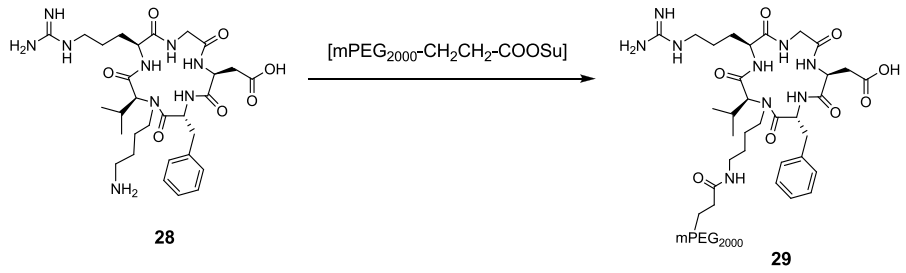

Entry	PEG-CH_2CH_2-COOSu (eq)	Solvent	c(peptide)	Conditions	Result
1	5.0	EtOH/0.2 M borate buffer (pH 8.5) 1:1	2 mg/mL	rt, 2 h	Complete conversion. Considerable amount of hydrolyzed PEG derivative, difficult to separate from **29** by RP-HPLC.
2	1.0	EtOH/0.2 M borate buffer (pH 8.5) 1:1	2 mg/mL	rt, 2 h	Complete conversion. Considerable amount of hydrolyzed PEG derivative, difficult to separate from **29** by RP-HPLC.
3	0.5	EtOH/0.2 M borate buffer (pH 8.5) 1:1	2 mg/mL	rt, 2 h	Around 50% of unreacted peptide. Low amount of hydrolized PEG derivative, difficult to separate from **29** by RP-HPLC.

A possible way to circumvent this problem is to use an excess of peptide substrate (**28**) to ensure that most of the activated PEG is consumed (entry 3). Although this approach implies a sacrifice of **28**, which is time-consuming to synthesize, it enables to minimize the presence of PEG-CH_2CH_2-COOH in the conjugation product (**29**).

Wishing to obtain the pure PEG conjugate (**29**), we reacted 2.0 equivalents of **28** with 1.0 equivalent of PEG-CH_2CH_2-COOSu (see Scheme 48). After 1 hour, the reaction mixture contained the desired product (**29**), unreacted **28** and a certain amount of hydrolized PEG derivative (as confirmed by HPLC-MS analysis). No more conversion took place after stirring for a further 1 hour-period, so the reaction was quenched at this stage. The unreacted peptide (**28**) was easy to separate from the product (**29**) by semipreparative RP-HPLC. However, a certain amount of residual PEG-CH_2CH_2-COOH was still present in the **29**-containing fraction and this fraction had to be re-purified. In this way, we were able to isolate the pure PEG conjugate (**29**) in 99% purity (see Figure 53), but a low amount of product was obtained.

Scheme 48. *N*-acylation of **28** with PEG-COOSu.

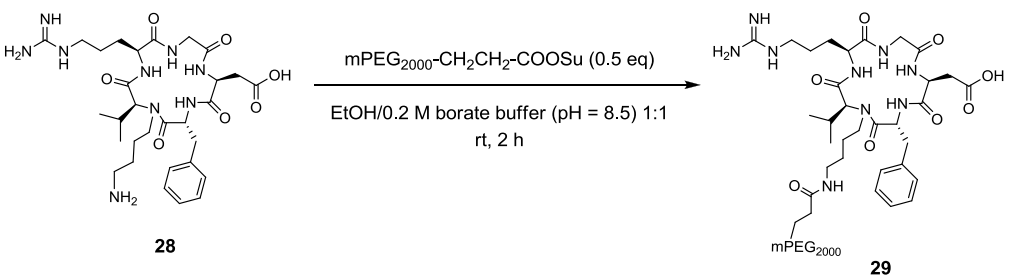

Figure 53. A) HPLC analysis of pure PEG conjugate **29**, linear gradient from 10% to 50% ACN over 8 min. **B)** MALDI-TOF analysis of pure PEG conjugate **29** showed a distribution of MW values around 2421.38 (average MW), with the main mass signals spaced apart by Δm/z = 44.

A)

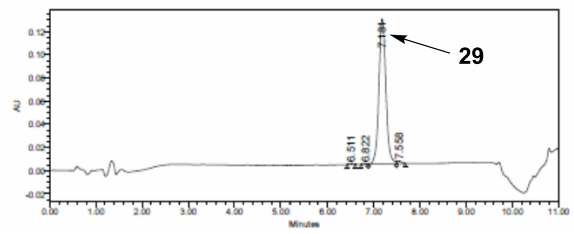

purity = 99%

B)

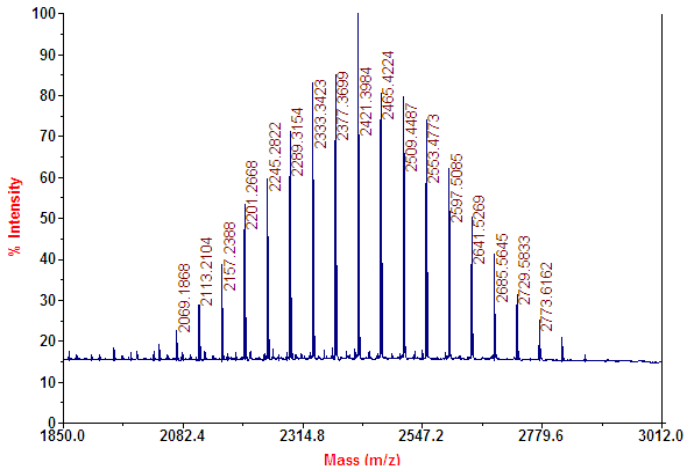

4.3.3.5. Conjugation with PEG via reductive alkylation

For the conjugation of cyclo[RGDf(*N*-$CH_2CH_2CH_2CH_2NH_2$)V] (**28**) with PEG by reductive alkylation, we used a polydisperse PEG-propionaldehyde (PEG-CH_2CH_2-CHO) of 2 KDa. This aldehyde was preferred to PEG-acetaldehyde (PEG-CH_2-CHO) because the latter is reported to undergo rapid decomposition in basic media, pressumably by aldol condensation. In contrast, PEG-propionaldehyde (PEG-CH_2CH_2-CHO) is reported to be stable in basic aqueous solutions, and yet enough reactive for an efficient reductive alkylation.[170]

We investigated the *N*-alkylation of **28** with PEG-CH_2CH_2-CHO using $NaBH_3CN$ as reducing agent (see Table 26). In our initial experiments, we used 2.0 equivalents of PEG-CH_2CH_2-CHO (entries 1-4). Since this aldehyde is stable in basic and acidic media, reactions were allowed to proceed overnight. When the reaction was carried out in a pH 6.0 aqueous buffer, no *N*-alkylated product (**30**) was detected (entry 1). When performing the reaction at pH 8.5, the desired PEG conjugate (**30**) was formed, but a considerable amount of unreacted **28** was present in the reaction mixture (entry 2). Better results were obtained when using MeOH as solvent in the presence of AcOH or NEt_3 (entries 3-4). In both cases, the HPLC profile of the reaction mixture was identical: the PEG conjugate (**30**) was formed, but the reaction was not complete and conversion did not increase after stirring for a further 15 hour-period. To achieve a quantitative yield, more than 2.0 equivalents of PEG-aldehyde are required (entries 5-6). However, a minimum excess should be used, because the marginal HPLC retention time difference between the residual PEG-aldehyde and the PEG conjugate (**30**) jeopardizes the purification of **30** by RP-HPLC.

Table 26. Conditions investigated for the reductive *N*-alkylation of **28** with PEG-CH_2CH_2-CHO.

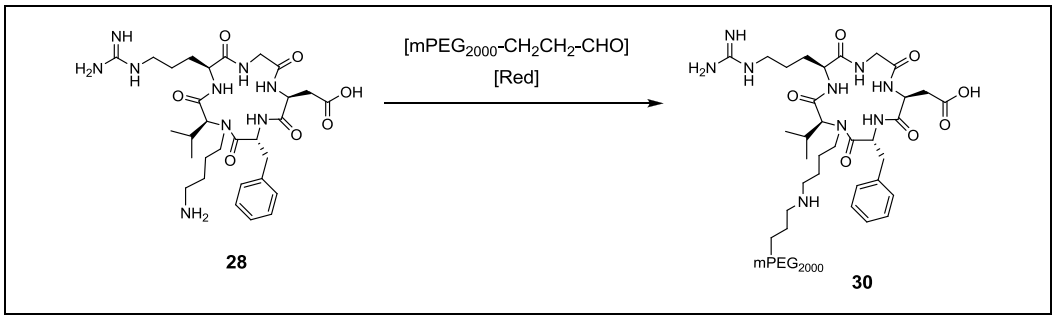

Entry	PEG-aldehyde (eq)	$NaBH_3CN$ (eq)	Solvent	c(peptide)	Conditions	Result
1	2.0	4.0	EtOH/50 mM phosphate buffer (pH 6.0) 1:1	2 mg/mL	rt, 15 h	Product not formed.
2	2.0	4.0	EtOH/0.2 M borate buffer (pH = 8.5) 1:1	2 mg/mL	rt, 15 h	Very low conversion.
3	2.0	4.0	MeOH/AcOH 99:1	2 mg/mL	rt, 15 h	Poor conversion.
4	2.0	4.0	MeOH + NEt_3 (1.2 eq)	2 mg/mL	rt, 15 h	Poor conversion.
5	3.0	6.0	MeOH + NEt_3 (1.2 eq)	2 mg/mL	rt, 15 h	Higher conversion, though not complete.
6	4.0	8.0	MeOH + NEt_3 (1.2 eq)	8 mg/mL	rt, 15 h	Complete conversion.

For obtaining PEG conjugate **30**, we decided to use 3.0 equivalents of PEG-aldehyde; the use of only 2.0 equivalents provides a low conversion, and the use of a higher excess would severely hamper the purification step. With this amount of aldehyde, reductive alkylation of **28** gave a mixture of the desired product (**30**), a little amount of unreacted peptide (**28**), and unreacted PEG-aldehyde (see Scheme 49). After semipreparative RP-HPLC purification, we obtained a fraction of **30** that still contained a certain amount of PEG-aldehyde and had to be re-purified. The whole purification process was very tedious and, since certain fractions of non-pure **30** were discarded, a low amount of pure PEG conjugate (**30**) was obtained (see Figure 54).

Scheme 49. Reductive *N*-alkylation of **28** with PEG-CH_2CH_2-CHO.

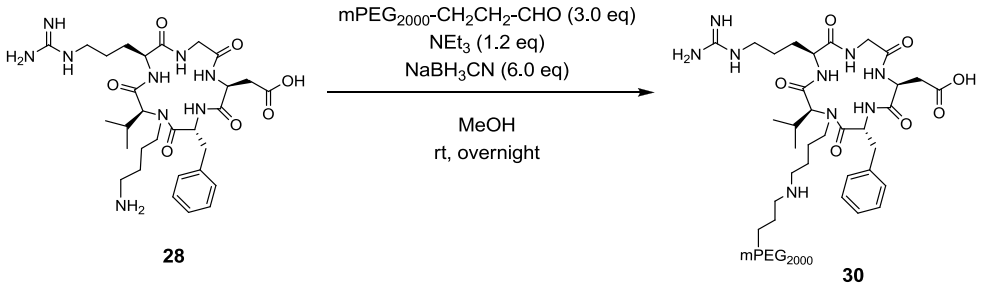

Figure 54. A) HPLC analysis of pure PEG conjugate **30**, linear gradient from 10% to 50% ACN over 8 min. **B)** MALDI-TOF analysis of pure PEG conjugate **30** showed a distribution of MW values around 2654.85 (average MW), with the main mass signals spaced apart by Δm/z = 44.

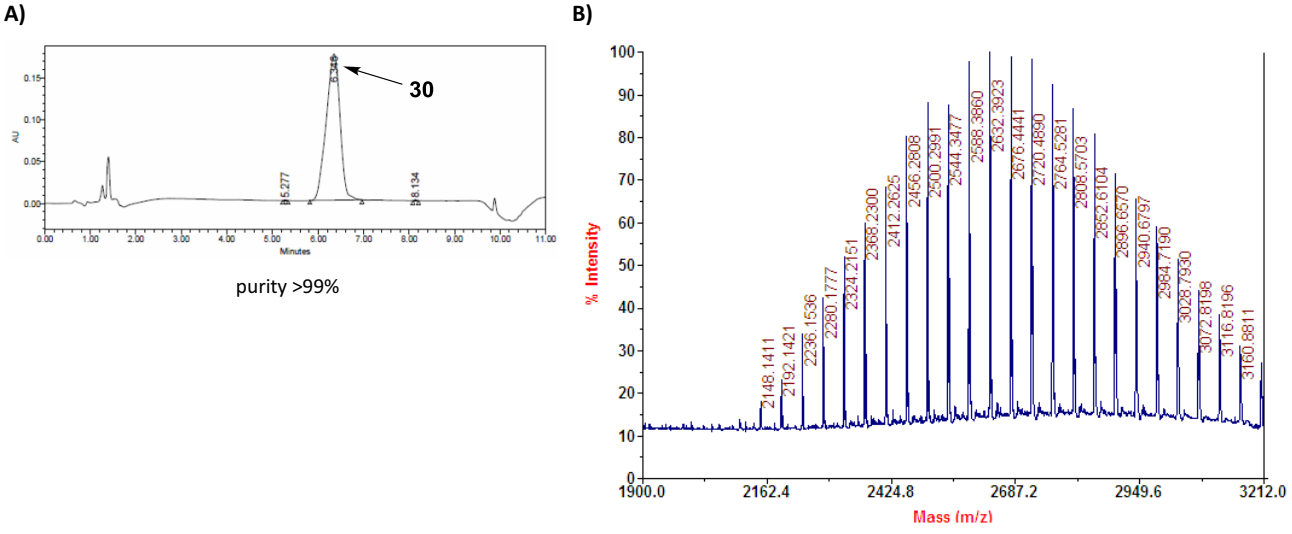

4.3.3.6. Conjugation with PEG via azide-alkyne cycloaddition

The Cu(I)-catalyzed Huisgen 1,3-dipolar cycloaddition between azides and alkynes to form 1,2,3-triazoles[171] belongs to a group of reactions referred to as *click chemistry*.[172] This reaction is regiospecific, yielding exclusively the 1,4-substituted product (see Scheme 50). It has a large thermodynamic driving force and proceeds as much as 10^7 times faster than the uncatalyzed version. In general, quantitative yields are obtained in mild conditions, and the reaction can be performed over a wide range of temperatures (0-160 ºC), in a variety of solvents (including water), and over a wide range of pH values (5-12). Several variations are tolerated in both the azide and the alkyne components. Other convenient features of this reaction are experimental simplicity, reliability, and ease of product purification. Most importantly, azides and alkynes are stable under standard conditions and are largely inert towards other functionalities, thereby avoiding the requirement for protecting groups.[161]

Scheme 50. Cu(I)-catalyzed Huisgen 1,3-dipolar cycloaddition between an azide and a terminal alkyne.

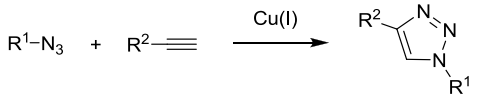

Because of all these reasons, the Cu(I)-catalyzed azide-alkyne cycloaddition has found many applications in a variety of research areas, including polymer chemistry, materials sciences and medicinal chemistry.[171c] This reaction has also drawn a lot of attention in the field of peptide and protein chemistry. Noteworthily, the 1,2,3-triazole moiety is an isostere of a *trans* peptide bond with the advantage of being stable to hydrolytic and proteolytic cleavage.[173]

For the generation of the active Cu(I) catalytic species, several methods are reported. The most common is the *in situ*-reduction of a Cu(II) salt, such as $CuSO_4 \cdot 5H_2O$, to form Cu(I). Sodium ascorbate is typically used as the reducing agent in a 2- to 10-fold excess,[174] but other reducing agents, such as tris(2-carboxyethyl)phosphine (TCEP)[175] and hydrazine,[176] can also be employed. The advantages of the *in situ*-generation strategy over the direct use of Cu(I) are that it does not require a deoxygenated atmosphere, and it allows the use of water as solvent, which removes the need for a base. The main inconvenience is that the reducing agent may reduce Cu(II) down to Cu(0), but this can be prevented by using a proper ratio of reducing agent to catalyst and/or by adding a copper stabilizing agent.

We sought to apply the Cu(I)-catalyzed Huisgen 1,3-dipolar cycloaddition for the conjugation of PEG with cyclo[RGDf(*N*-$CH_2CH_2CH_2CH_2N_3$)V] (**27**). For this aim, we used a polydisperse PEG-NH-CO-CH_2CH_2-alkyne of 2 KDa as alkyne moiety. The presence of an amide group between the PEG chain and the terminal triple bond does not respond to any particular purpose; PEG-NH-CO-CH_2CH_2-alkyne was the only commercially available PEG-alkyne with an average MW of 2 KDa.

We investigated conditions for the Cu(I)-catalyzed reaction between the *N*-azidoalkylated peptide (**27**) and the aforementioned PEG-alkyne (see Table 27). The Cu(I) that is required to catalyze the reaction was generated by *in situ* reduction of $CuSO_4$ with sodium ascorbate. This method was preferred over the direct use of Cu(I) due to the ease with which this species is oxidized to non-catalytic Cu(II). Initial optimisation experiments were performed in dioxane/H_2O 1:1 (entries 1-2), but our **27** was poorly soluble in this solvent mixture. Using ^{t}BuOH/H_2O 1:1 was found to be preferrable. In preliminary experiments, we observed that after a certain period of time (1-2 hours), no more conversion takes place. This means that there is no more active Cu(I)-catalytic species in the media and more $CuSO_4$ and sodium ascorbate should be added. When stoichometric amounts of PEG-alkyne and peptide (**27**) were reacted in the presence of 0.2 equivalents of $CuSO_4$ and 0.5 equivalents of sodium ascorbate (entry 3), the click product (**31**) was formed after 1 hour, though in low conversion, and our attempts to drive the reaction to completion by adding more $CuSO_4$/sodium ascorbate were not successful. The presence of unreacted peptide (**27**) in the reaction mixture should

be avoided, because its HPLC peak overlaps with the broad HPLC peak of the PEG conjugate (**31**) and its purification by semipreparative RP-HPLC is not feasible.

Table 27. Conditions investigated for the click reaction between **27** and the PEG-alkyne.

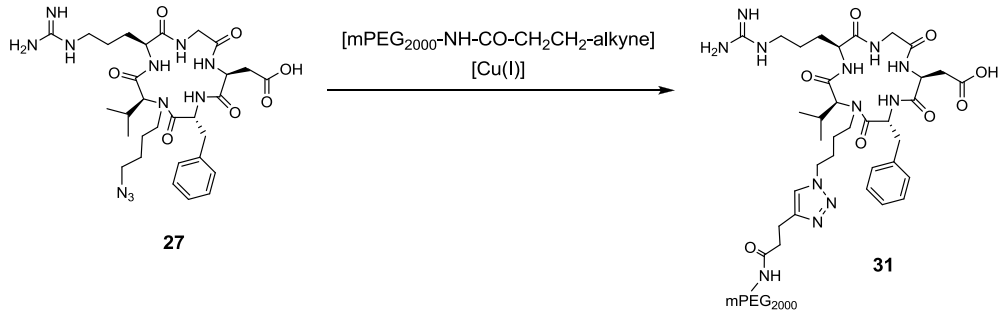

Entry	PEG-alkyne (eq)	$CuSO_4$ (eq)	NaAsc	Solvent	c(peptide)	Conditions	Result
1	1.0	0.1	0.2	dioxane/H_2O 1 :1	4.5 mM	rt, overnight	Poor solubility of the peptide substrate.
2	1.0	1.0	2.0	dioxane/H_2O 1 :1	4.3 mM	rt, overnight	Poor solubility of the peptide substrate.
3	1.0	0.2	0.5	^{t}BuOH/H_2O 1:1	4.3 mM	rt, overnight	Low conversion.
4	2.0	0.2	0.5	^{t}BuOH/H_2O 1:1	4.3 mM	rt, overnight	Low conversion.
5	2.0	1.0	2.0	^{t}BuOH/H_2O 1:1	4.3 mM	rt, 6 h	Complete conversion.
6	1.5	1.0	2.0	^{t}BuOH/H_2O 1:1	4.3 mM	rt, 6 h	Complete conversion.
7	2.0	1.0	2.0	^{t}BuOH/H_2O 1:1	4.3 mM	60 ºC, 2 h	Uncomplete conversion.
8	2.0	1.0	2.0	DMF/H_2O 95:5	4.3 mM	MW, 100 ºC, 15 min	Complete conversion. Side-product formation.

In order to achieve the total conversion of **27**, we sought to use an excess of PEG-alkyne. While investigating our click reaction with 2.0 equivalents of PEG-alkyne (entry 4), we realized that a higher amount of catalyst was required. By increasing the amount of Cu_2SO_4 up to 1.0 equivalent, the reaction was complete after stirring for 6 hours at room temperature (entry 5), and the amount of PEG-alkyne could be lowered to 1.5 equivalents without affecting conversion (entry 6). This amount of copper is unusual for a click reaction between an alkyne and an azide. We think that our peptide may bind to Cu(I) and Cu(II) species through the backbone amide groups and/or through the formed triazole ring, thereby lowering the activity of the catalyst.[177]

We investigated if the reaction could be accelerated by heating. However, after stirring for 2 hours at 60 ºC, a little amount of unreacted peptide (**27**) was still present in the reaction mixture (entry 7). The use of MW heating (100 ºC, 15 min) led to complete conversion, but an unidentified side-product was formed in a considerable proportion (entry 8). This side-product had distribution of mass signals in its MS spectra, indicating polydispersity, and did not evolve after addition of more $CuSO_4$/sodium ascorbate.

Since heating did not prove to be advantageous, we decided to obtain PEG conjugate **31** using the cycloaddition conditions shown in entry 6. The *N*-azidoalkylated peptide (**27**) and 1.5 equivalents of PEG-alkyne were reacted at room temperature in the presence of 1.0 equivalents of $CuSO_4$ and 2.0 equivalents of sodium ascorbate (see Scheme 51). After stirring overnight, complete conversion was achieved. The excess of PEG-alkyne could be separated from the click product (**31**) by semipreparative RP-HPLC, as their HPLC peaks are sufficiently apart from each other. This enabled us to obtain the desired PEG conjugate (**31**) in 100% purity, though in low amount (see Figure 55).

Scheme 51. Click reaction between **27** and the PEG-alkyne.

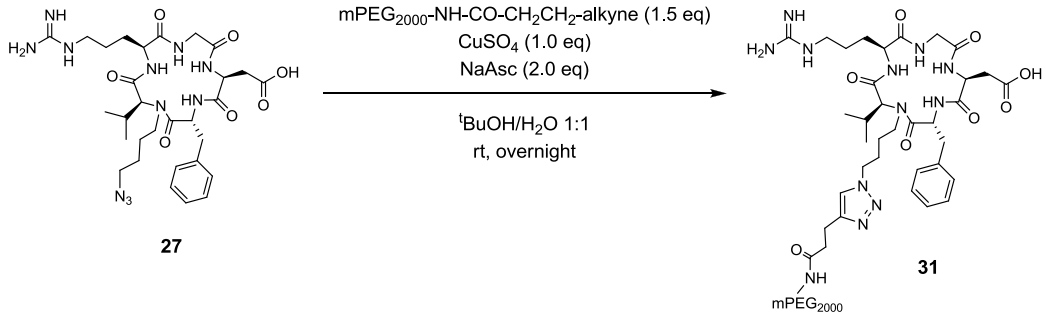

Figure 55. A) HPLC analysis of pure PEG conjugate **31**, linear gradient from 10% to 50% ACN over 8 min. **B)** MALDI-TOF analysis of pure PEG conjugate **31** showed a distribution of MW values around 2676.45 (average MW), with the main mass signals spaced apart by Δm/z = 44.

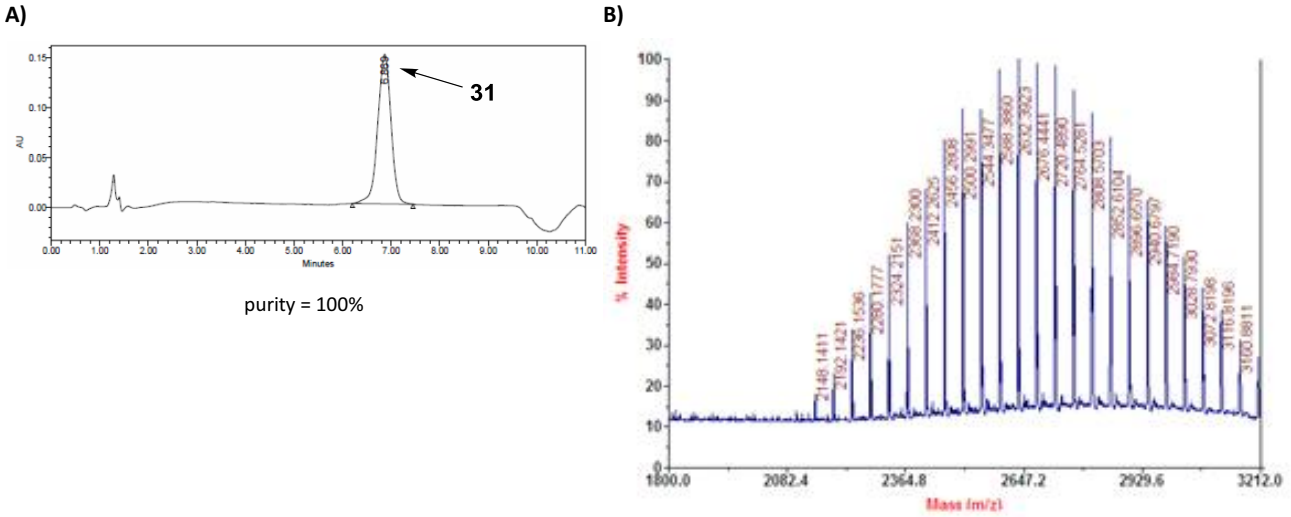

4.3.3.7. A possible strategy to circumvent purification problems

As explained in Sections 4.3.3.4., 4.3.3.5. and 4.3.3.6., we were able to attach a 2 KDa PEG moiety onto the amino group of cyclo[RGDf(*N*-$CH_2CH_2CH_2CH_2NH_2$)V] (**28**) via amide bond formation or reductive alkylation, and we were able to graft a 2 kDa PEG-alkyne onto the azido group of cyclo[RGDf(*N*-$CH_2CH_2CH_2CH_2N_3$)V] (**27**) via click chemistry (see Scheme 52). However, the desired PEG conjugates (**29**-**31**) were obtained in low amount due to problems encountered during their purification. In the case of PEG conjugates **29** and **30**, the marginal retention time difference between the conjugation product and the corresponding PEG reagent did not allow to separate the unreacted PEG by semipreparative RP-HPLC. In contrast, the PEG conjugate obtained via click chemistry (**31**) was easy to separate from the unreacted PEG-alkyne, but its HPLC peak overlapped with that of the unreacted peptide (**27**).

Scheme 52. Synthesis of PEG conjugates **29**-**31**.

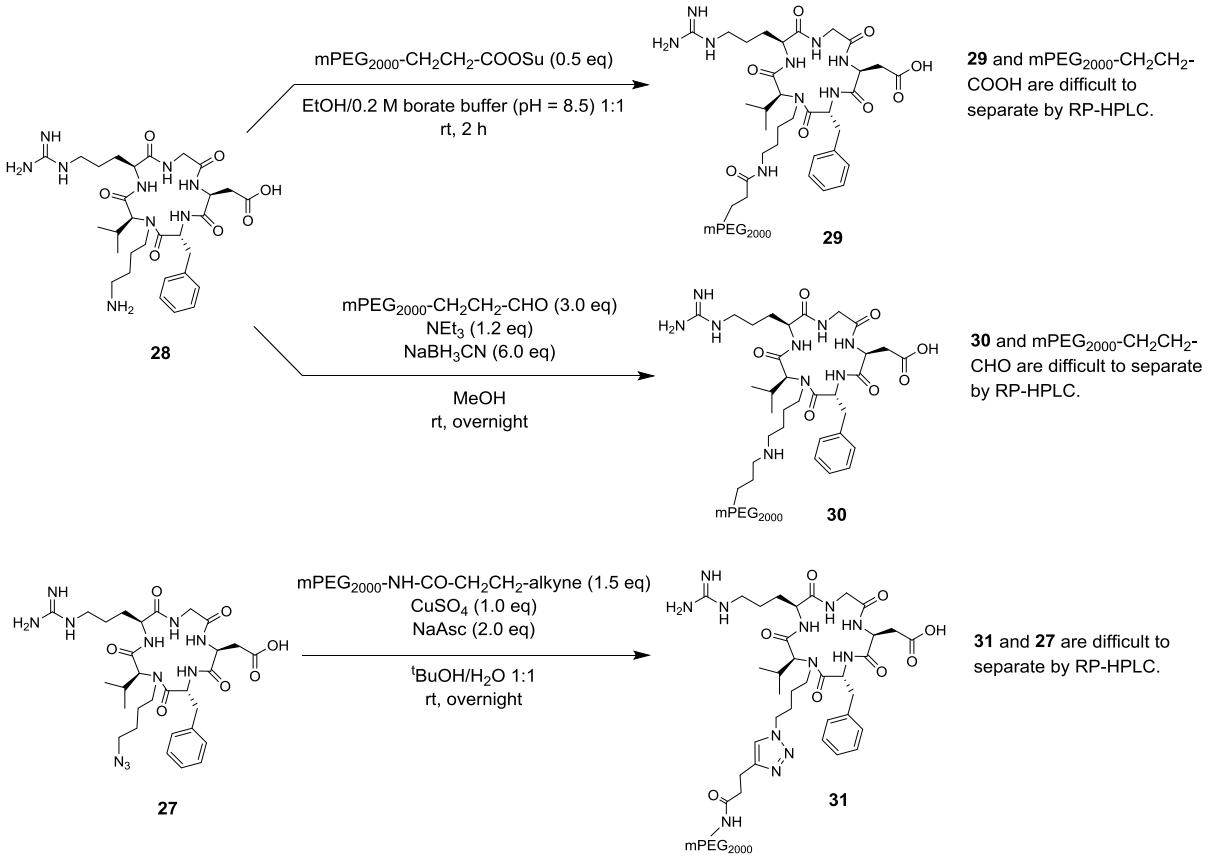

To minimize the presence of residual PEG in PEG conjugates **29** and **30**, we used a minimum amount of PEGylating reagent in the conjugation step. For PEG conjugate **29**, we only used 0.5 equivalents of PEG-COOSu, but the presence of hydrolized PEG-CH_2CH_2-COOH in the conjugation product was still an issue. In the case of PEG conjugate **30**, a 3-fold excess of PEG-aldehyde was required to achieve an acceptable conversion, and thus the unreacted PEG was difficult to separate.

Separation of the unreacted PEG from a PEG-modified molecule is often achieved by dialysis/ultrafiltration of the reaction mixture, but this technique was not applicable in our case. The smallest MW cuttoff available for diafiltration centrifugal devices is 1000 Da. Such a device does not allow to separate the excess of PEG reagent (average MW = 2000 Da) from the PEG conjugate (**29** or **30**, average MW around 2600 Da), because their average MW's are not sufficiently different. Using a 1000 Da-diafiltration device may allow to separate the unreacted peptide (**28**, MW = 645) from the conjugation product (**29** or **30**, average MW around 2600 Da) but, in any case, separation of the unreacted peptide (**28**) was not problematic and, after diafiltration, purification by RP-HPLC would still be required to isolate the desired products in high purity.

To isolate the PEG conjugates **29** and **30** in good overall yields, the final purification step should be revised or an alternative synthetic approach should be conceived. A possible solution would be to perform the conjugation reaction in the presence of side-chain protecting groups (see Scheme 53). Protection of the Arg and Asp side-chains should change the HPLC retention time of the conjugates, thereby facilitating their isolation from unreacted PEG. Nevertheless, we had already obtained enough amount of the target products, and we did not investigate this strategy.

Scheme 53. Synthetic strategy to obtain **29**-**31** performing side-chain deprotection at the last stage.

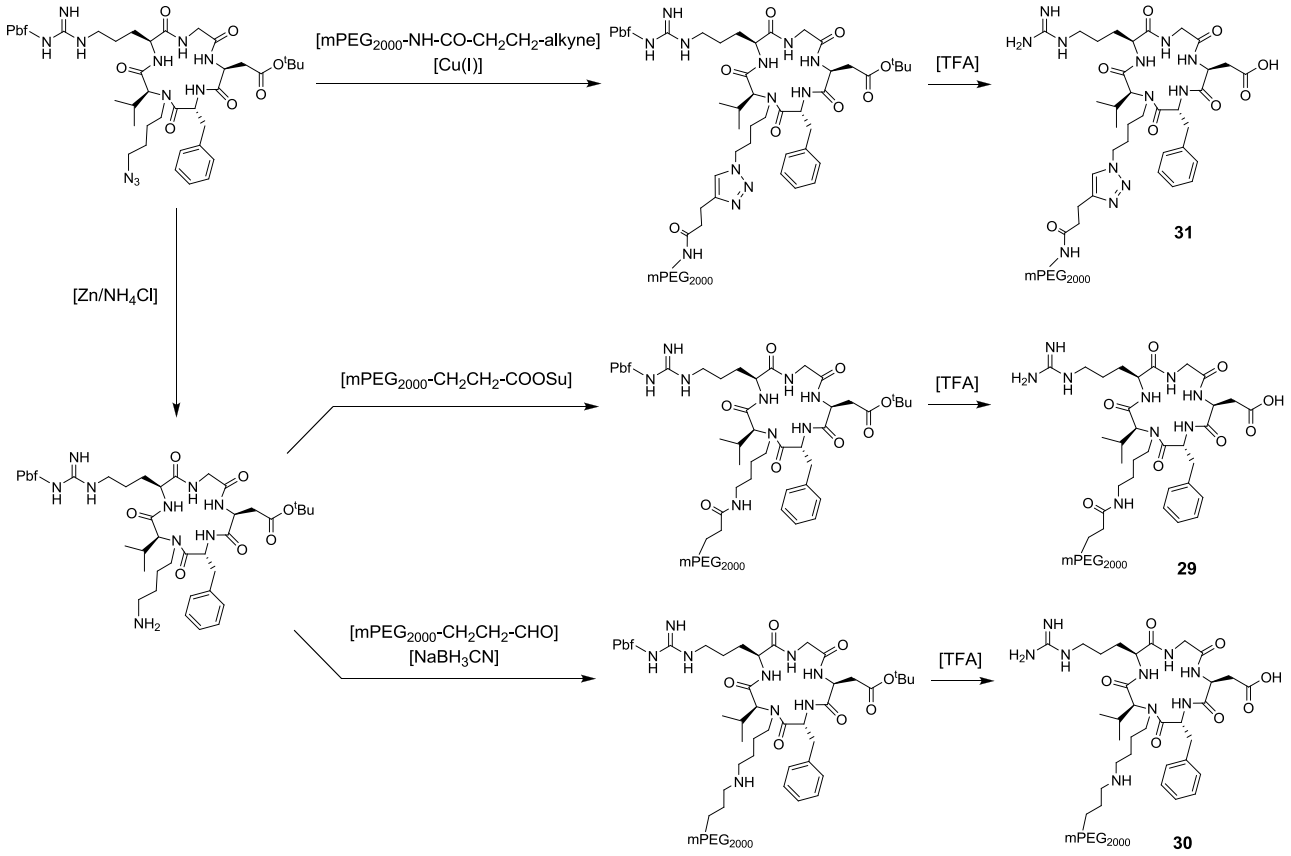

4.3.4. Evaluation of the biological activity of the PEG conjugates

For the synthesized PEG conjugates (**29-31**) and cyclo[RGDf*N*MeV] (**23**), we tested their biological activity such as inhibition of cell adhesion using two different cell types and two integrin ligands for each cell line: vitronectin (VN) and fibrinogen (FB).[150] The cell lines of study were HUVEC endothelial and DAOY glioblastoma cells, both of which overexpress the $\alpha_v\beta_3$ and $\alpha_v\beta_5$ receptors of the α_v-integrin family. These assays were performed by Dr. Jaume Adan, from Leitat technological center, and the results are summarized in Table 28.

Table 28. Adhesion inhibition assays of cyclo[RGDf*N*MeV] (**23**) and PEG conjugates **29-31**. IC_{50} values are given in µM. Standard deviations are between parentheses.[a]

Compound	Vitronectin (VN) $\alpha_v\beta_3 + \alpha_v\beta_5$		Fibrinogen (FB) $\alpha_v\beta_3$	
	HUVEC on VN	DAOY on VN	HUVEC on FB	DAOY on FB
cyclo[RGDf*N*MeV] (**23**)	0.37 (0.05)	2.69 (0.09)	0.076 (0.06)	0.44 (0.05)
PEG conjugate **29**	3.06 (0.03)	28.76 (0.01)	0.23 (0.09)	1.77 (0.03)
PEG conjugate **30**	3.40 (0.06)	49.56 (0.03)	0.41 (0.11)	2.71 (0.03)
PEG conjugate **31**	8.90 (0.05)	75.21 (0.02)	0.53 (0.04)	4.36 (0.04)

[a] The original peptide, cyclo[RGDf*N*MeV] (**23**), was used as reference control in all the assays performed and, its activity correlated well with existing data.[151] Cell adhesion inhibition curves are shown in Annex 4.

For all the cell/ligand systems, all the compounds inhibited cell adhesion in a concentration-dependent manner, resulting in the expected sigmoid curves. In the adhesion of HUVEC and DAOY cells to VN, which is mediated by

integrins $\alpha_v\beta_3$ and $\alpha_v\beta_5$, PEG conjugates **29** and **30** showed IC_{50} values in the low μM range, albeit 1 order of magnitude lower than that of the original peptide (**23**). PEG conjugate **31** also inhibited cell adhesion, but with less potency than **29** and **30**. In the experiments with FB, in which the adhesion is only $\alpha_v\beta_3$-dependent, compounds **29-31** showed the same pattern of inhibitory potency as for the HUVEC/DAOY-to-VN system.

The decreased inhibitory activities of the PEG conjugates (**29-31**) with respect to the unmodified peptide (**23**) indicates their binding affinities towards integrins $\alpha_v\beta_3$ and $\alpha_v\beta_5$ are lower, which is probably due to an interference of their PEG chains with the RGD-receptor interaction. This hypothesis is consistent with the assays of the *N*-OEG cyclopeptide analogs (**24-26**) from Chapter 3, in which those cyclopeptides bearing a longer *N*-OEG chain were considerably less active. Along these lines, CD data seems to indicate that the PEG conjugates (**29-31**) and cyclo[RGDf*N*MeV] (**23**) adopt the same backbone conformation (see Section 3.3.6.). Thus, no evidence has been found to attribute the lowered activity of the PEG conjugates (**29-31**) to a distinct conformational state in which the RGD motif is not optimally oriented for integrin binding.

A reduction in biological activity upon attachment of a PEG chain has been reported for several peptides[178] and proteins.[152] For instance, in the case of PEG-interferon α2a (Pegasys), used in the treatment of hepatitis C, only 7% of the interferon α2a activity remains after PEG modification.[179] The cause of this is postulated to be interference in receptor binding due to PEGylation, either through steric crowding efects or through hydrophobic-hydrophobic interactions between the amphiphilic PEG and the hydrophobic domains within the protein. As for other PEGylated proteins, the reduced *in vitro* biological activity of PEG-interferon α2a is more than counterbalanced by its enhanced *in vivo* half-life due to PEGylation. However, in many PEGylated peptides, the improved pharmacokinetics upon PEGylation do not offset the biological activity loss.

4.3.5. Evaluation of the lipophilicity of the PEG conjugates

In order to evaluate the relative hydrophobicity of PEG conjugates **29-31** with respect to cyclo[RGDf*N*MeV] (**23**), we compared their RP-HPLC retention times (see Table 29). The retention times of the PEG conjugates were found to be superior to that of the unmodified peptide, indicating a higher hydrophobic character. This is consistent with our previous findings for the *N*-OEG cyclopeptide analogs (**24-26**) from Chapter 3 (see Section 3.3.9). Such analogs were increasingly more hydrophobic upon increasing the OEG chain length. Herein, all the PEG conjugates (**29-31**) result from the attachment of a 2 KDa polydisperse PEG chain. Consistently, PEG conjugates **29** and **31** showed similar retention times. PEG conjugate **30** displayed a lower retention, but this can be attributed to the presence of an amine between the *N*-butyl chain and the PEG moiety, whereas in **29** and **31** the linking units are an amide and a triazole, respectively.

Table 29. RP-HPLC retention times cyclo[RGDf*N*MeV] (**23**), the *N*-OEG cyclopeptides (**24-26**), and the PEG conjugates (**29-31**), linear gradient from 10% to 60% ACN over 8 min, C18 column.

Compound	t_r (min)
cyclo[RGDf*N*MeV] (**23**)	4.79
cyclo[RGDf(*N*-OEG_2)V] (**24**)	5.17
cyclo[RGDf(*N*-OEG_{11})V] (**25**)	5.74
cyclo[RGDf(*N*-OEG_{23})V] (**26**)	5.93

Compound	t_r (min)
PEG conjugate **29**	6.11
PEG conjugate **30**	5.53
PEG conjugate **31**	6.02

For cyclo[RGDf*N*MeV] (**23**), the *N*-OEG cyclopeptides (**24-26**), and the PEG conjugates (**29-31**), we plotted their RP-HPLC retention time versus their MW (see Figure 56). The resulting graphic suggests that the influence of OEG chain

length on hydrophobicity is limited: the retention of the *N*-OEG analogs does not increase linearly with OEG chain length. Along these lines, the retention times of PEG conjugates **29** and **31** (average MW = 2421.38 and 2676.45, respectively) do not substantially differ from that of the *N*-OEG_{23} cyclopeptide (**26**, MW = 1659.94).

Figure 56. Plotting of the RP-HPLC retention times (linear gradient from 10% to 60% ACN over 8 min, C18 column) of cyclo[RGDf*N*MeV] (**23**), the *N*-OEG cyclopeptides (**24-26**), and the PEG conjugates (**29-31**) vs. their MW.

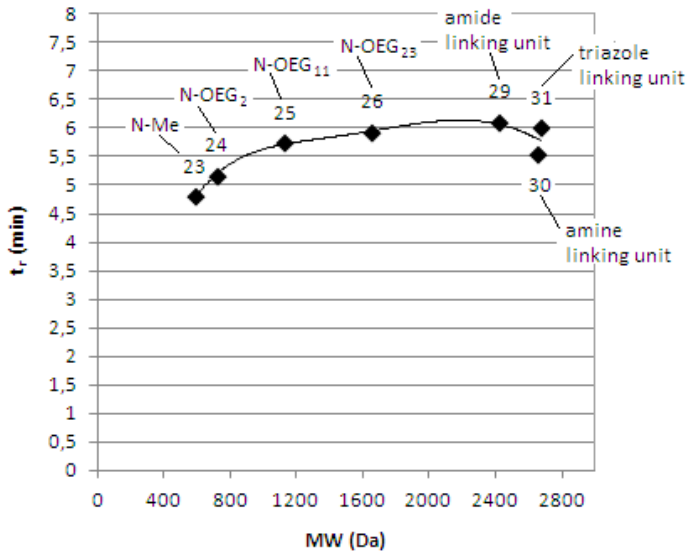

This observation is compatible with our previously formulated hypothesis for the higher hydrophobicity of *N*-OEG vs. *N*-Me peptide analogs. As explained in Section 3.3.9, we reasoned that *N*-Me-for-*N*-OEG substitution may lead to an interaction between the oxygen atoms of the OEG chain (hydrogen bond acceptors) and the backbone amide protons (hydrogen bond donors). This intramolecular interaction should decrease the potential for hydrogen-bonding with the aqueous RP-HPLC mobile phase, thereby resulting in a higher retention time, which –in turn– indicates a higher hydrophibicity. According to this hypothesis, it is reasonable to expect that a limit will be reached, in which all the backbone amide protons are shielded by the ether oxygen atoms.

To estimate the lipophilicity of cyclo[RGDf*N*MeV] (**23**), the *N*-OEG cyclopeptides (**24-26**), and the PEG conjugates (**29-31**), we determined their logP values in octanol/water (see Table 30). No significant differences were found. The parent peptide (**23**), which is known to be highly hydrophilic, consistently showed a logP value of -1.91. The rest of compounds had logP values between -1.24 and -2.15, which are typical of hydrophilic RGD-derivatives.[180] Reported logP values of PEG-modified RGD-cyclopeptides are also within this range.[181]

Table 30. LogP values of cyclo[RGDf*N*MeV] (**23**), the *N*-OEG cyclopeptides (**24-26**), and the PEG conjugates (**29-31**) in octanol/water, determined by the shake-flask method.[a]

Compound	logP
cyclo[RGDf*N*MeV] (**23**)	-1.91 ± 0.02
cyclo[RGDf(*N*-OEG_2)V] (**24**)	-2.15 ± 0.01
cyclo[RGDf(*N*-OEG_{11})V] (**25**)	-1.53 ± 0.10
cyclo[RGDf(*N*-OEG_{23})V] (**26**)	-1.83 ± 0.04

Compound	logP
PEG conjugate **29**	-1.88 ± 0.26
PEG conjugate **30**	-1.98 ± 0.13
PEG conjugate **31**	-1.24 ± 0.03

[a] LogP determination experiments were performed as triplicates using a 1:1 octanol/water proportion.

The similarity among the logP values of our compounds is compatible with the trends observed in RP-HPLC retention data. Two things should be pointed out. First, the fundamental properties responsible for RP-HPLC retention are

different to those responsible for partition between octanol and water, especially the contribution from hydrogen bonding interactions.[128c,132] This is specially true for RP-HPLC measurements on chemically bonded stationary phases, such as C18. Second, for highly hydrophilic compounds, logP determination by the shake flask method is not very accurate: if the compound is extremely hydrophilic or hydrophobic, its concentration in one of the phases will be exceedingly small and thus difficult to quantify.[131]

In conclusion, the higher retention times of **24-26** and **29-31** with respect to cyclo[RGDf*N*MeV] (**23**) indicate that replacement of a backbone *N*-Me group of a peptide by an *N*-OEG chain or an *N*-linker-attached PEG chain provides a higher hydrophobicity.

4.3.6. Study of conformational features of the PEG conjugates

We sought to investigate if the PEG conjugates (**29-31**) have a similar backbone conformation as cyclo[RGDf*N*MeV] (**23**). The conformation of RGD-cyclopeptide ligands is of interest, as it determines their affinity towards integrin receptors.[182]

The conformation of cyclo[RGDf*N*MeV] (**23**) in aqueous solution is characterized by a fast equilibrium between two inverse γ (γ_i)-turns centered at Arg and Asp, and a permanent γ-turn centered at Gly (see Figure 57).[145] This conformation is different from that of cyclo[RGDfV], the lead RGD-cyclopeptide from which **23** was discovered by *N*-Me scan.[145] Cyclic pentapeptides of the LDLDL-series usually exhibit a βII'/γ conformation in which the D-amino acid residues are placed at the *i*+1 positions of the turns. Since Gly can act as a D-amino acid, cyclo[RGDfV] also adopts this typical conformation: a βII' turn with an internal hydrogen bond between H^N [Arg] and CO [Asp] and a γ turn centered at Gly. However, in cyclo[RGDf*N*MeV] (**23**), the formation of the hydrogen bond between H^N [Arg] and CO [Asp] is blocked by the *N*-Me group of Val, and thus a βII'-turn can no longer be present. Furthermore, the conformation of cyclo[RGDf*N*MeV] (**23**) differs to that of cyclo[RGDfV] in the following feature: to avoid steric clash with the *N*-Me group, the Asp-D-Phe and *N*MeVal-Arg amide bonds are placed in a more perpendicular orientation with respect to the plane of the peptide backbone. As a result, the Asp and Arg side-chains of **23** move towards a more pseudoequatorial orientation, whereas in cyclo[RGDfV] these side-chains are placed in a pseudoaxial conformation.[145]

Figure 57. Chemical structure of cyclo[RGDfV] and cyclo[RGDf*N*MeV] (**23**). Adapted from [139]. Dashed lines represent the essential hydrogen bonds required to stabilize the γ_i and γ turns of **23**, and the βII'/γ conformation of cyclo[RGDfV].

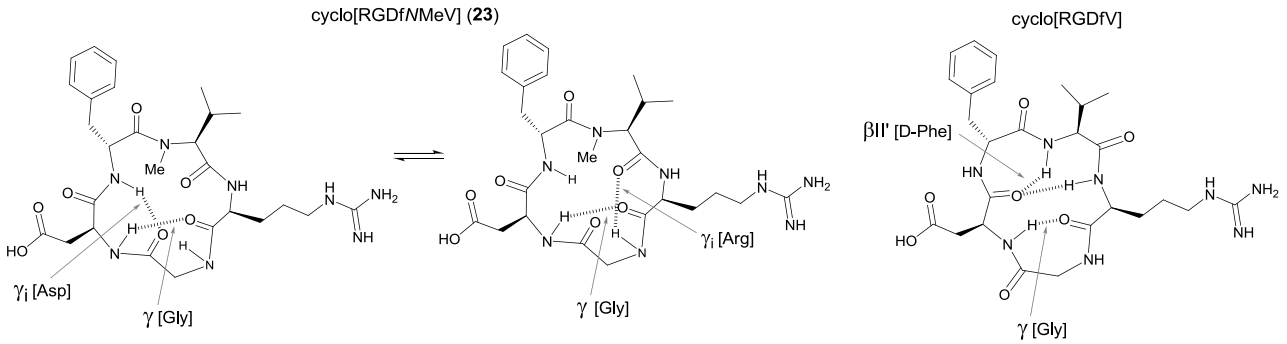

In order to investigate if the PEG conjugates (**29-31**) adopt the same backbone conformation as cyclo[RGDf*N*MeV] (**23**), we analyzed our compounds by CD spectroscopy, a sensitive technique to monitor changes in a peptide secondary structure.[183] The different types of chiral secondary elements found in peptides give rise to characteristic features in the far UV region of their CD spectra (see Figure 58). Because CD reflects the overall conformational

ensemble, one cannot simply correlate a measured CD spectra with any specific backbone conformation. Nevertheless, CD is a valid tool to compare the secondary structures of a series of modified peptide analogs.

Figure 58. CD features of various peptide secondary structures. Adapted from [184].

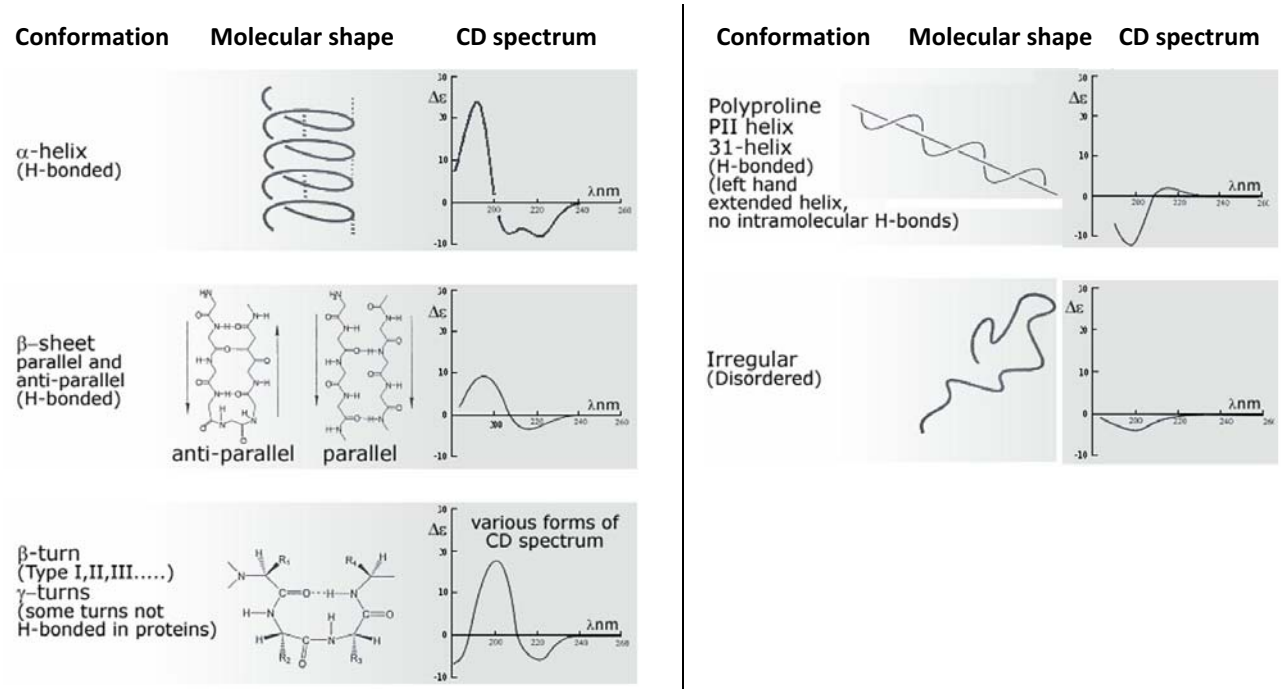

In order to determine the optimal parameters for acquiring the CD spectra of our compounds, we performed preliminary experiments with the original peptide, cyclo[RGDf*N*MeV] (**23**) (see Figure 59). CD spectra were recorded in the range from 190 to 250 nm using water as solvent. In these first experiments, we studied the effect of having different percentages of trifluoroethanol (TFE) on the sample (0%, 10%, 20% and 50%). This solvent is frequently used in CD experiments due to its ability to stabilize helical or β-turn like structures.[185] However, in our case, the magnitude of CD decreased upon increasing the amount of TFE, and when using 50% TFE the secondary structure of the peptide was totally destabilized. We also studied the effect of having the peptide at different concentrations (0.25 mM, 0.5 mM and 1.0 mM). Within this range of concentrations, the molar ellipticities per residue remained unchanged.

Figure 59. CD spectra of cyclo[RGDf*N*MeV] (**23**) in H_2O at various % TFE and various concentrations.

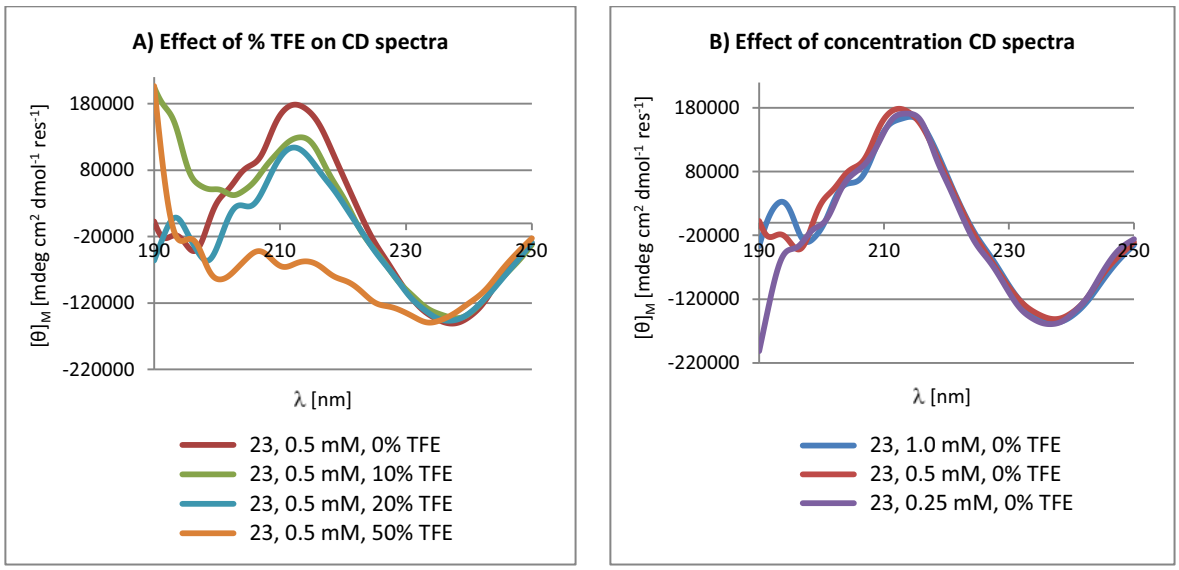

The CD spectrum of cyclo[RGDf*N*MeV] (**23**) showed a negative band at 238 nm (λ_{min}) and a positive band at 212 nm (λ_{max}). The CD spectra of the PEG conjugates (**28-31**) were very similar to that of **23**, which indicates that all the compounds have a similar backbone conformation (see Figure 60).

Figure 60. CD spectra of cyclo[RGDf*N*MeV] (**23**) and the PEG conjugates (**29**-**31**) in H_2O at a 0.5 mM concentration.

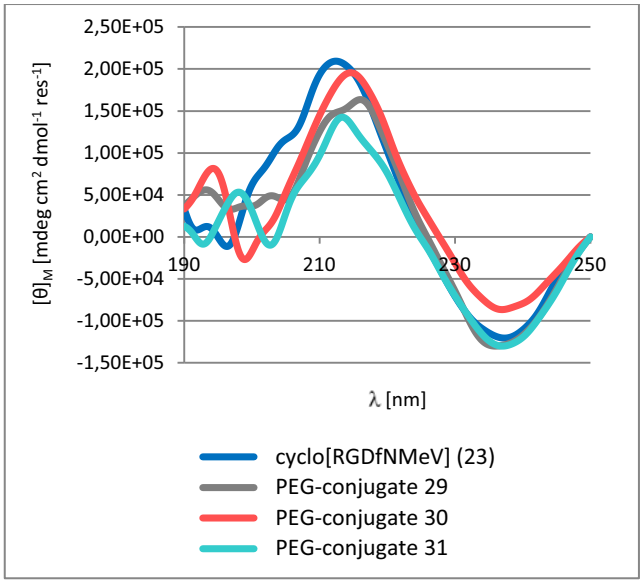

These CD measurements are consistent with a conformation featuring two inverse γ (γ_i)-turns in conformational exchange and a γ-turn, as compared with recently published CD data of three model γ-turn peptides**:** cyclo[Ala-β-Ala-Pro-β-Ala], cyclo[Pro-β-Ala-Pro-β-Ala] and cyclo[Ala-β-Ala-Ala-β-Ala].[186] CD analysis of these peptides, which are reported to exist as one predominant conformer with two inverse γ (γ_i)-turns, revealed a negative band near 230 nm (λ_{min}) and a positive band below 200 nm (λ_{max}) with a long wavelength shoulder.

It is important to note that for peptides for which structural information from NMR is lacking, the CD spectrum can only be taken as a *hint* that a chiral secondary structure is present, since an unambiguous assignment of a CD spectrum to a specific backbone conformation is currently impossible.[187] Also worth to note is that there is almost no data on the CD spectroscopic properties of γ-turn-containing peptides. Whereas the CD features of α-helix and β-sheet structures are well-defined, the CD characterization of γ-turns is still uncertain, and their distinction from β-turns is difficult.[188]

Despite these issues, CD data indicates that replacement of the backbone *N*-Me group of cyclo[RGDf*N*MeV] (**23**) by an *N*-butyl-linked PEG chain caused a minimal perturbation of its backbone conformation.

4.4. Summary and conclusions

In this Chapter, we have developed a methodology to introduce a backbone *N*-(4-azidobutyl) group into peptides. The introduction of this linker allows conjugation in peptides that do not have suitable attachment sites.

We found that the *N*-(4-azidobutyl) group can be introduced into a growing peptide by reductive alkylation of its α-amino group with 4-azidobutanal, which proceeds efficiently and in a reproducible manner. This method is preferrable to using an Fmoc-*N*-(4-azidobutylated) building block, as this derivative has to be previously prepared and then

coupled in excess. The subsequent acylation of the *N*-(4-azidobutylated) amine can be achieved in solid-phase using BTC as activating reagent. However, several coupling cycles are required for an optimum conversion, and the efficiency of such BTC-mediated couplings may not be reproducible when the synthesis is upscaled. To prepare of *N*-(4-azidobutylated) peptides on large scale, we developed an efficient protocol in which the difficult coupling step is performed in solution via an acid chloride. This protocol is based on a *double SPPS scheme* in which the CTC is used for peptide elongation, de- and re-attachment of the fully protected peptide, and final elongation again.

To demonstrate the applicability of our strategy, we synthesized an analog of cyclo[RGDf*N*MeV] (Cilengitide) in which the *N*-Me group of Val was replaced by the *N*-(4-azidobutyl) group. With the synthesis of this peptide, we show that *N*-(4-azidobutylated) peptides are accessible using standard SPPS protocols that are compatible with common protecting groups used in peptide synthesis. Taking into account that the acylation of the *N*-alkylated residue was achieved on a small scale using BTC, we consider that the detour from solid-phase to solution chemistry in the synthesis of cyclo[RGDf(*N*-$CH_2CH_2CH_2CH_2N_3$)V] was necessary because of the additional steric hindrance exerted by the β-branched side-chain of Val, and that this alternate route may not be a general requirement for the synthesis of other *N*-(4-azidobutylated) peptides.

Comparison of NMR data of cyclo[RGDf*N*MeV] and its *N*-(4-azidobutylated) analog indicated that replacement of the *N*-Me group by our linker caused a minimal perturbation of its original conformation. On the basis of this finding, we can expect that an *N*-(4-azidobutyl) group will exert the same conformational restrictions as a backbone *N*-Me group when incorporated into other cyclic peptides. This is potentially useful, since backbone *N*-Me groups are common structural motifs in many bioactive peptides. Therefore, for a given *N*-methylated cyclopeptide, replacement of a backbone *N*-Me group by our linker is expected to have little influence on its conformation, which may be crucial for biological activity.

Next, we used cyclo[RGDf(*N*-$CH_2CH_2CH_2CH_2N_3$)V] to prepare several conjugates with a polydisperse PEG chain of 2 KDa. On one hand, an alkyne-functionalized PEG was conjugated with our azidoalkylated-peptide via Cu(I)-catalyzed Huisgen 1,3-dipolar cycloaddition. On the other hand, the azide function was reduced to an amine with the mild Zn/NH_4Cl reducing system, and the resulting aminoalkylated-peptide was either reductively *N*-alkylated with a PEG-aldehyde or *N*-acylated with a PEG-COOSu derivative. All the conjugation reactions took place in high yield but, due to the polydispersity of PEG, conditions had to be optimized to facilitate the purification of the PEG conjugates by RP-HPLC. With the preparation of these conjugates, we show that our linker allows conjugation through several chemical transformations.

The PEG conjugates and cyclo[RGDf*N*MeV] had similar logP values that were within the typical range of hydrophilic molecules. Interestingly, the PEG conjugates were found to be more hydrophobic than the unmodified peptide, as indicated by their higher RP-HPLC retention times. For all the RGD-cyclopeptide derivatives, we evaluated their antagonistic activity towards integrins $\alpha_v\beta_3$ and $\alpha_v\beta_5$ in cell adhesion inhibition assays, which were performed with two different cell types and two integrin ligands for each cell line. In all cases, the PEG conjugates inhibited integrin-mediated cell adhesion in a concentration-dependent manner, though with less potency than the original peptide. Their decreased inhibitory activity is probably due to an interference of the PEG chain with the RGD-receptor interaction, resulting in lower binding affinities. This hypothesis is consistent with the results of the assays with the *N*-OEG cyclopeptide analogs (Chapter 3), in which those cyclopeptides bearing a longer *N*-OEG chain were considerably less active. Furthermore, CD data indicated that the PEG conjugates and cyclo[RGDf*N*MeV] have the same backbone conformation. Thus, we found no evidence to attribute the lowered activity of the PEG conjugates to a distinct conformational state in which the RGD-sequence is not optimally oriented for binding.

In conclusion, we have shown that a backbone *N*-(4-azidobutyl) group can be incorporated into a peptide using standard SPPS techniques and allows conjugation at a late stage of the synthesis. Due to the orthogonal properties of the azide, our linker is compatible with protecting groups, linkers and resins commonly used in peptide synthesis.

Moreover, the chemical versatility of the azide function, which can be reduced to an amine prior to conjugation, allows for flexibility in the design of peptide conjugates. Along these lines, the possibility of using click chemistry in the conjugation step is an advantageous feature, since it permits conjugation in the presence of side-chain functional groups and thus implies a minimal requirement for protection.

More importantly, modification of peptides with our *N*-(4-azidobutyl) linker is a useful strategy to allow conjugation in peptides that do not have derivatizable groups. In contrast to other strategies used for this purpose, such as the introduction of Lys or Cys, our approach allows conjugation under full conservation of the amino acid side-chains, which may be essential for biological activity, and with a minimal requirement of protecting groups.

On the basis of all these considerations, we strongly believe that our *N*-(4-azidobutyl) linker will have broad utility in peptide chemistry and will widen the application of established conjugation methods.

GLOBAL CONCLUSIONS

The present Thesis was devoted to the synthesis of novel backbone *N*-substituted peptides, and to the study of their properties in comparison to *N*-Me peptides.

In **Chapter 1**, we investigated Fmoc-*N*-triethylene glycol (*N*-TEG) amino acids as building blocks for the SPPS of backbone *N*-substituted peptides. We found that Fmoc-*N*-TEG amino acids can be easily prepared through a 3-step protocol that involves reductive alkylation of the α-amino group with 3,6,9-trioxadecanaldehyde. The main difficulty for the incorporation of these building blocks into peptides is the acylation of the *N*-TEG amine. Several coupling conditions reported as efficient for the acylation of *N*-Me amino acids in solid-phase failed to provide good yields in the case of couplings onto *N*-TEG amino acids, but these couplings were found feasible using BTC as activating reagent. This activation method, which leads to the *in situ*-generation of a highly reactive acid chloride, is compatible with the acid-labile CTC resin.

Chapter 2 describes then the synthesis of *N*-Me and *N*-TEG analogs of Sansalvamide A peptide with the methodology established in Chapter 1. NMR data indicated that the incorporation of *N*-Me and *N*-TEG groups into this cyclic pentapeptide imposes similar constraints to its backbone conformation. The biological activities of all the *N*-Me and *N*-TEG analogs of Sansalvamide A peptide were found to be quite low, but -interestingly- the RP-HPLC retention times of the *N*-TEG analogs were found to be slightly superior to those of their *N*-Me homologues, indicating a higher hydrophobicity for the *N*-TEG peptides. With these observations, we reasoned that the *N*-TEG group can be used as surrogate for the *N*-Me group to provide a slightly more lipophilic peptide with a minimal perturbation of the backbone conformation.

In **Chapter 3**, we chose Cilengitide as model peptide, and we replaced its *N*MeVal constituent by (*N*-OEG)Val derivatives of increasing size. We observed that there is a cutting edge for the stepwise SPPS of *N*-OEG peptides with respect to the OEG chain length: upon a certain length, the solid-phase acylation of an *N*-OEG amine becomes impossible even with the BTC activation method. The two *N*-OEG cyclopeptides bearing the larger OEG chains were obtained by segment condensation. The RP-HPLC retention times of the *N*-OEG analogs were found to be superior to that of parent *N*-Me cyclopeptide, and increased with the OEG chain length. We reasoned that *N*-Me-for-*N*-OEG substitution leads to an interaction between the oxygen atoms from the OEG chain (hydrogen bond acceptors) and the backbone amide protons (hydrogen bond donors). This intramolecular interaction decreases the potential for hydrogen-bonding with the aqueous RP-HPLC mobile phase, thereby resulting in a higher retention time, which -in turn- indicates an enhanced lipophilicity. Remarkably, the *N*-TEG analog displayed the same biological activity as Cilengitide, whereas the analogs having larger *N*-OEG chains were found to be less active. With these observations, we reasoned that substitution of the *N*-Me group of a peptide by the *N*-TEG group is a feasible strategy to confer lipophilicity whilst preserving biological activity, whereas for larger *N*-substituents synthetic yields drop and receptor binding may be hampered.

In **Chapter 4**, we studied the *N*-(4-azidobutyl) group as a backbone linker to permit conjugation in peptides that lack suitable sites for the attachment of molecules. We synthesized an analog of Cilengitide in which its backbone *N*-Me group was replaced by the *N*-(4-azidobutyl) group, and we used this *N*-(4-azidobutylated) analog to prepare several PEG conjugates having different linking moieties. It was shown that the *N*-(4-azidobutyl) linker can be introduced into peptides by reductive alkylation of their α-amino group in solid phase. Although the subsequent coupling onto the *N*-azidoalkylated residue can be achieved in small-scale SPPS, the preparation of larger amounts of peptide required a deattachment step to perform the dificult coupling in solution, and a subsequent reattachment of the peptide segment onto the resin to continue with the elongation. NMR data indicated that Cilengitide and its *N*-(4-azidobutylated) analog have the same backbone conformation. Therefore, substitution of a backbone *N*-Me group by our *N*-(4-azidobutyl) linker is a valuable strategy provide a bioorthogonal conjugation site without altering the original amino acid side-chains and conformation of the parent *N*-Me peptide.

EXPERIMENTAL SECTION

INDEX FOR THE EXPERIMENTAL SECTION

Materials and methods 141

1. Solvents and reagents 141
2. General instrumentation 142
3. Chromatographic methods 142
4. Structural determination techniques 143
5. Experimental procedures for SPPS 144

Experimental procedures for Chapter 1 150

1.1. Synthesis of starting materials 150
1.2. Synthesis of the Fmoc-*N*-TEG amino acids 151
1.3. Use of Fmoc-*N*-TEG amino acids in SPPS 153

Experimental procedures for Chapter 2 156

2.1. Synthesis of the Fmoc-*N*-TEG amino acids 156
2.2. SPPS of the linear *N*-TEG and *N*-Me pentapeptides 156
2.3. Cyclization of the linear *N*-TEG and *N*-Me pentapeptides 158
2.4. Cell culture protocols and biological activity evaluation 161
2.5. Attempts to determine logP by the shake-flask method 164
2.6. NMR studies of peptides **1**, **5a** and **5b** 165

Experimental procedures for Chapter 3 165

3.1. Synthesis of the *N*-OEG building blocks 165
3.2. SPPS of the linear *N*-OEG pentapeptides 169
3.3. Cyclization and deprotection to obtain the *N*-OEG cyclopeptides 172
3.4. Biological activity evaluation 175
3.5. Serum stability assays 175

Experimental procedures for Chapter 4 173

4.1. Synthesis of 4-azidobutanal 174
4.2. Synthesis of Fmoc-*N*-(4-azidobutyl) valine 174
4.3. Synthesis of the *N*-azidoalkylated pentapeptide 178
4.4. Cyclization and deprotection to obtain the *N*-azidoalkylated cyclopeptide 183
4.5. Synthesis of the PEG conjugates 184
4.6. NMR studies of peptides **23** and **27** 185
4.7. Biological activity evaluation 186
4.8. Determination of logP by the shake-flask method 186

MATERIALS AND METHODS

1. SOLVENTS AND REAGENTS

Solvents

Solvent	Quality	Commercial brand
ACN	HPLC analysis	SDS
Acetone	Synthesis	SDS
AcOEt	Synthesis	SDS
AcOH	Synthesis	SDS
$CHCl_3$	Analysis	SDS
Dioxane	Analysis	SDS
DCM	Synthesis	SDS
DMF	Peptide synthesis	SDS
DMSO	ACS	Panreac
Et_2O	Synthesis	SDS
EtOH	Absolute	Panreac
Hexane	Synthesis	SDS
H_2O	MilliQ	-
MeOH	HPLC analysis	SDS
^tBuOMe	Synthesis	SDS
TFA	Analysis	Fluorochem
TFA	HPLC analysis	Fluorochem
THF	Analysis	Scharlau
Toluene	Synthesis	Scharlau

Reagents

Fmoc-protected amino acids were purchased from Iris Biotech GmbH (Marktredwitz, Germany) or Bachem (Basel, Switzerland), except for Fmoc-protected *N*-methyl amino acids, which were purchased from Sigma-Aldrich (Milwaukee, USA). Amino acid *tert*-butyl ester hydrochlorides were also purchased from Sigma-Aldrich (Milwaukee, USA).

2-chlorotrityl chloride (CTC) resin was purchased from Iris Biotech GmbH (Marktredwitz, Germany) or Novabiochem (Läufelfingen, Switzerland).

OxymaPure, HOAt, HOBt and HATU were obtained from Luxembourg Industries (Tel Aviv, Israel).

Piperidine was purchased from SDS (Peypin, France).

Monodisperse CH_3-O-$(CH_2CH_2O)_{11}$-CH_2CH_2-CHO and CH_3-O-$(CH_2CH_2O)_{23}$-CH_2CH_2-CHO were purchased from Iris Biotech (Marktredwitz, Germany). Polydisperse $mPEG_{2000}$-CH_2CH_2-COOSu (average MW = 2 KDa) and polydisperse $mPEG_{2000}$-CH_2CH_2-CHO (average MW = 2 KDa) were purchased from Nanocs Inc. (NY, USA). Polydisperse $mPEG_{2000}$-NH-CO-CH_2CH_2-alkyne (average MW = 2 KDa) was purchased from Iris Biotech (Marktredwitz, Germany).

The rest of chemicals used in the present Thesis were purchased from Sigma-Aldrich (Milwaukee, USA).

2. GENERAL INSTRUMENTATION

Instrument	Trading house, model
centrifuges	Eppendorf, models 5415D and 5415R
	Beckman Coulter, model Allegra 21R
freeze dryer	Virtis, model Freezemobile 12 EL; connected to an Edwards RV12 vacuum pump
IR spectrometer	Termo Nicolet, model 510FT
magnetic stirrer	IKA, model RCT basic
MilliQ water	Millipore, model Milli-Q A10
MW system	CEM corporation, model CEM Discover
pH meter	Crison, model GLP21
orbital shaker	Heidolph, model Unimax 1010
polarimeter	Perkin-Elmer, model 241
rotatory evaporator	Heidolph, model Laborota 4003; connected to a Boc Edwards vacuum pump or to a Vacuubrand MZ 2C vacuum pump
scales	Mettler Toledo, model PB303-S (2 significant digits, precision 1.0 mg)
	Mettler Toledo, model AB204-S (4 significant digits, precision 0.1 mg)
	Mettler Toledo, model AT-261 (5 significant digits, precision 0.01 mg)
spectropolarimeter	Jasco, model J-810
stove	Selecta, model Digitronic
sonicator baths	Branson, models 250 and 1510
UV-VIS spectrometer	Shimadzu, model mini 1240

3. CHROMATOGRAPHIC METHODS

Thin layer chromatography (TLC)

Analytical TLC was carried out on Merck Kieselgel 60 F_{254} plates. Compound spots were visualized by UV light (254 nm) and/or using the following staining solutions:

- Anisaldehyde solution. The spray solution was prepared by dissolving 9.2 mL of 4-methoxybenzaldehyde in a mixture of 338 mL of EtOH, 3.8 mL of AcOH and 12.5 mL of $H_2SO_{4\ (conc.)}$. When the TLC plate is sprayed and heated at 110 ºC for 1 min, the presence of compounds is evidenced by the appearance of coloured spots.
- Vainilline solution. The spray solution was prepared by dissolving 0.05 g of vanillin in a mixture of 8.5 mL of MeOH, 1 mL of AcOH and 0.5 mL of $H_2SO_{4\ (conc.)}$. When the TLC plate is sprayed and heated at 110 ºC for 1 min, the presence of compounds is evidenced by the appearance of coloured spots.
- Phosphomolibdic acid solution. The spray solution was prepared by dissolving 12 g of phosphomolibdic acid in 100 mL of EtOH. When the TLC plate is sprayed and heated at 110 ºC for 1 min, the presence of compounds is evidenced by the appearance of coloured spots.
- Ninhidrine solution. The spray solution was prepared by dissolving 0.5 g of ninhydrine in 100 mL of EtOH. The TLC plate was sprayed and heated at 110 ºC for 1 min. When the TLC plate is sprayed and heated at 110 ºC for 1 min, the presence of primary amine groups is evidenced by the appearance of violet spots.

- Basic $KMnO_4$ solution. The spray solution was prepared by dissolving 3 g of $KMnO_4$ and 20 g of K_2CO_3 in a mixture of 300 mL of H_2O and 5 mL of 5% NaOH $_{(aq.)}$. When the TLC plate is sprayed and heated at 110 ºC for 1 min, the presence of alcohols and/or double bonds is evidenced by the appearance of yellow spots.

Flash chromatography

Flash chromatography was performed on silica gel (60 mesh, 35-70 μm), which was purchased from SDS (Pepypin, France). Separations were performed manually using glass columns of variable size.

Analytical HPLC

Analytical HPLC was carried out on a Waters instrument comprising a Sunfire™ C18 reversed-phase analytical column (3.5 μm, 4.6 x 100 mm), a separation module (Waters 2695), automatic injector, and photodiode array detector (Waters 2298). Data were managed with Empower 2 software (Waters). UV detection was performed at 220 nm, and linear gradients of ACN (+0.036% TFA) into H_2O (+0.045% TFA) were run at a flow rate of 1.0 mL/min over 8 min.

Semipreparative HPLC

For compounds **1**, **1a-5a** and **1b-5b** [from Chapter 2], cyclo[RGDf*N*MeV] (**23**), cyclo[RGDf(*N*-OEG_2)V] (**24**) and cyclo[RGDf(*N*-$CH_2CH_2CH_2CH_2N_3$)V] (**27**) [from Chapters 3 and 4], **s**emipreparative HPLC was carried out on a Waters instrument comprising a Sunfire™ C18 reversed-phase semipreparative column (5.0 μm, 18 x 100 mm), a separation module (Waters Delta 600), Waters 600 controller, automatic injector, and a dual absorbance detector (Waters 2487). Data were managed with Millenium 3.2 software (Waters). UV detection was at 220 nm, and linear gradients of ACN (+0.036% TFA) into H_2O (+0.045% TFA) were run at a flow rate of 15.0 mL/min or in the conditions specified for each case. Fractions were collected with a Waters Fraction Collector II.

For cyclo[RGDf(*N*-OEG_{11}) V] (**25**) and cyclo[RGDf(*N*-OEG_{23})V] (**26**) [from Chapter 3], semipreparative HPLC was carried out on a Waters instrument comprising an Xbridge™ C18 reversed-phase column (5.0 μm, 10 x 100 mm), a separation module (Waters 2695), an automatic injector, and a photodiode array detector (Waters 2298). Data were managed with Empower 2 software (Waters). UV detection was performed at 220 nm, and linear gradients of ACN (+0.036% TFA) into H_2O (+0.045% TFA) were run at a flow rate of 3.0 mL/min in the conditions specified for each case. Fractions were collected manually.

For cyclo[RGDf(*N*-$CH_2CH_2CH_2CH_2NH_2$)V] (**28**) and PEG conjugates **29**-**31** [from Chapter 4], semipreparative HPLC was carried out on a Waters instrument comprising a SunFire™ C18 reversed-phase column (5.0 μm, 10 x 150 mm), a separation module (Waters 2545), a Waters 2767 sample manager, an automatic injector, photodiode array detector (Waters 2998), and mass detector (Waters 3100). Data were managed with MassLynx V4.1 software (Waters). UV detection was performed at 220 nm, and linear gradients of ACN (+0.1% TFA) into H_2O (+0.1% TFA) were run at a flow rate of 3.0 mL/min in the conditions specified for each case.

4. STRUCTURAL DETERMINATION TECHNIQUES

NMR spectroscopy

^{1}H-NMR (400 MHz) and ^{13}C-NMR (100 MHz) spectroscopy were performed on a Varian Mercury 400 MHz spectrometer. ^{1}H-NMR (500 MHz) and ^{13}C-NMR (125 MHz) spectroscopy were performed on a Varian VNMRS 500

MHz spectrometer. ^{1}H-NMR (600 MHz) and ^{13}C-NMR (150 MHz) spectroscopy were performed on a Bruker Digital Avance 600 MHz spectrometer**.** Chemical shifts (δ) are expressed in parts per million and the deuterated solvent signal was used as reference (unless otherwise stated). Coupling constants are expressed in Hertz. The following abbreviations are used to indicate multiplicity: s, singlet; d, doublet, dd, double doublet; t, triplet; dt, double triplet; m, multiplet; and bs, broad signal.

Mass spectrometry

- HPLC coupled to an MS detector (HPLC-MS). HPLC-MS analyses of samples were carried out on a Waters instrument comprising a Sunfire™ C18 reversed-phase analytical column (3.5 µm, 4.6 x 100 mm), a separation module (Waters 2695), automatic injector, photodiode array detector (Waters 2298), and a Waters micromass ZQ unit. Data were managed with MassLynx V4.1 software (Waters). UV detection was performed at 220 nm, and linear gradients of ACN (+0.07% formic acid) into H_2O (+0.1% formic acid) were run at a flow rate of 0.3 mL/min over 8 min.

- High-resolution mass spectrometry (HRMS). High resolution mass spectra (HRMS) were obtained with an Agilent 1100 series LC/MSD trap spectrometer using the electrospray ionization (ESI-MS) method in positive or negative mode (as indicated).

- MALDI-TOF spectrometry. MALDI-TOF mass spectra were obtained with a 4700 Proteomics Analyzer (Applied Biosystems) spectrometer using the α-cyano-4-hydroxycinnamic acid (ACH) matrix. Acquisition of mass spectra was performed in the MS reflector positive ion mode. For the acquisition of mass spectra of the PEG conjugates (**29**-**31**), typical parameters were set to source and grid voltages 20 and 14 kV, respectively, fixed laser intensity of 3300, signal-to-noise threshold 50, and noise window width 200. In all cases, data handling was performed using the Data Explorer 4.0 programme (Applied Biosystems). [*Sample preparation:* 1 µL of sample solution (a solution of the sample in ACN/H_2O 1:1) was mixed with 1 µL of α-cyano-4-hydroxycinnamic acid (ACH) matrix (a 2 mg/mL solution of ACH in ACN/H_2O 1:1 with 0.5% TFA). 1 µL of this mixture was overlaid on each spot and the plate was analyzed.]

IR spectroscopy

IR spectra were recorded with a Termo Nicolet 510FT spectrometer and processed with the Omnic 6.0 program (Termo Nicolet Corporation). Samples were prepared by the film technique, which consists in placing a dry film of the compound over the KBr disk.

Polarimetry

Optical rotation measurements were performed with a 241 Perkin-Elmer polarimeter using the sodium D-line at 589 nm of. Measurements were done at 22 ºC using a cell of 10 cm path length and 1 mL capacity.

CD spectroscopy

CD spectroscopy was performed on a Jasco J-810 spectropolarimeter fitted with a thermostatted cell holder. Measurements were done at room temperature using a quartz cell of 1 mm path length. CD spectra were recorded from 190 nm to 250 nm at a scanning speed of 50 nm/min. The spectra were obtained with a time response of 4 s and a step resolution of 0.2 nm. Each CD spectrum was the average of 4 accumulations. Data were processed with *Jasco's Spectra Manager* software (Jasco). All measurements were taken in ellipticities (θ) and converted to molar ellipticities ($[\theta]_M$) according to the following formula:

$$[\theta]_M = (\theta) / (c \cdot l)$$

where: $[\theta]_M$: molar ellipticity (mdeg cm^2 $dmol^{-1}$ res^{-1}), θ: ellipticity (mdeg cm^2 res^{-1}), c: concentration (M), l: path length (cm).

5. EXPERIMENTAL PROCEDURES FOR SPPS

General considerations for SPPS

All the SPPS described in this Thesis were performed on the CTC resin using Fmoc-/^{t}Bu- chemistry. SPPS were performed in polypropylene syringes provided with a porous polyethylene filter and attached to a vacuum manifold. The syringes volumes used were 2, 5, 10 or 20 mL, depending on the scale of the synthesis. Reagents and solvents were added to the syringe containing the resin and the mixture was stirred in an orbital shaker. After each treatment, the solvent and the excess of reagents were removed by filtration through the vacuum system. After each synthetic step, the resin was washed with DCM (3x1 min), DMF (3x1 min) and DCM (3x1 min) unless otherwise stated.

Colorimetric tests

The following colorimetric tests were used for qualitative monitoring of couplings performed on solid phase:

- Ninhydrin test.[189] The ninhydryn test allows the detection of primary amine groups on the resin. This test was used to monitor conventional couplings during the elongation of the peptide in solid phase. To perform the ninhydryn test, the peptidyl-resin was washed with appropriate solvents and dried. A small amount of peptidyl-resin (0.5-2 mg) was transferred to a small glass tube. To this tube were added 6 drops of the reagent solution A and 3 drops of the reagent solution B. The mixture was heated at 100 ºC for 3 min. The formation of a blue color on the beads or the supernatant is indicative of the presence of free primary amines (positive test) and thus of an uncomplete coupling. Conversely, a yellow coloration indicates the absence of free primary amines (negative test). The method is highly sensitive and a negative test ensures an amino acid incorporation higher than 99.5%.
  - Preparation of reagent solution A: Phenol (40 g) was dissolved in EtOH (10 mL) and the mixture was heated until complete dissolution of the phenol. A solution of KCN (65 mg) in H_2O (100 mL) was added to pyridine (freshly distilled over ninhydrin, 100 mL). Both solutions were stirred for 45 min with 40 g of Amberlite MB-3 ion exchange resin, filtered and combined.
  - Preparation of reagent solution B: Ninhydryn (2.5 g) was dissolved in EtOH (50 mL). The resulting solution was kept in a flask protected from light.
- Chloranil test.[190] The chloranyl test allows the detection of primary or secondary amine groups on the resin. This test was sometimes used to monitor couplings onto *N*-alkylated residues. To perform the chloranil test, the peptidyl-resin was washed with appropriate solvents and dried. A small amount of peptidyl-resin (0.5-2 mg) was transferred to a small glass tube. To this tube were added 20 drops of acetone and 5 drops of a saturated chloranil solution (0.75 mg of 2,3,4,5,6-tetrachloro-1,4-benzoquinone in 25 mL of toluene). The mixture was stirred for 5 min at room temperature. The formation of a blue-greenish color is indicative of the presence of free secondary amines (positive test) and thus of an uncomplete coupling. Conversely, a yellow, amber or brown coloration indicates the absence of free secondary amines (negative test). The method is less sensitive than the De Clerq test.

- De Clercq test.[119] The De Clercq test allows the detection of primary or secondary amine groups on the resin. This test was the preferred method to monitor couplings onto *N*-alkylated residues because it is more sensitive than the chloranyl test. To perform the De Clerq test, the peptidyl-resin was washed with appropriate solvents and dried. A small amount of peptidyl-resin (0.5-2 mg) was transferred to a small glass tube. To this tube were added 5 drops of De Clerq reagent (0.002 M *p*-nitrophenyl ester of disperse Red 1 in ACN). The mixture was heated at 70 ºC for 10 min. The resin was washed extensively with MeOH (3x), DMF (3x) and DCM (3x). The formation of a red color on the beads is indicative of the presence of free primary amines (positive test) and thus of an uncomplete coupling. Conversely, colorless beads indicate the absence of free primary amines (negative test).
    - Synthesis of *p*-nitrophenyl ester of Disperse Red 1: *p*-nitrophenyl ester of Disperse Red 1 is readily accessible from commercial Disperse Red 1 by a 3-step procedure. *Step 1.* To a solution of Disperse Red 1 (6.28 mg, 20 mmol) and $Rh_2(OAc)_4$ (150 mg, 0.34 mmol) in a mixture of DCM (100 mL) and toluene (100 mL) is added at 40 ºC a solution of ethyl diazoacetate (8.4 mL, 80 mmol), in toluene (40 mL) over a period of 1 h. After overnight stirring at room temperature, the crude is by flash chromatography. *Step 2.* The product obtained in step 1 (5 g, 12.5 mmol) was dissolved in a mixture of MeOH (300 mL) and toluene (70 mL). To this solution was added KOH (4.062 g, 62.5 mmol) and the resulting mixture was refluxed under N_2 atmosphere for 1.5 h. The desired product was purified by a series of extractions. *Step 3.* The product obtained in step 2 (2.322 g, 6.0 mmol) was dissolved in DCM (120 mL) and a solution of *p*-nitrophenol (0.834 g, 6.0 mmol) in pyridine (100 mL). The resulting mixture was cooled at -15 ºC and a solution of $POCl_3$ (10.8 mmol, 1.00 mL) in DCM (10 mL) was added over a 1 h-period. The desired product was purified by a series of extractions.

General considerations about the CTC resin

In all the SPPS described in this Thesis, the 2-chlorotrityl chloride (CTC) resin[191] was used as solid support. This acid-labile resin is commonly used for the synthesis of peptide acids through Fmoc-/^{t}Bu- chemistry. Since peptide cleavage can be performed with very mild acid conditions (1% TFA in DCM, 3x1 min), CTC resin allows to obtain fully protected peptide acids and minimizes possible side-reactions, such as acid-catalyzed fragmentation of *N*-alkylated amide bonds. The steric bulk of CTC is also useful to prevent side-reactions, such as DKP formation at the dipeptide and tripeptide stage. Furthermore, the incorporation of the first Fmoc-protected amino acid onto the CTC resin takes place with essentially no epimerization.

Since CTC resin is moisture-sensitive, the resin was stored at -20 ºC and was allowed to warm to room temperature before opening. Once opened, the resin was stored in a KOH dessicator.

Initial conditioning of the CTC resin

The CTC resin was swelled in DCM (15 min). Then, the resin was washed with DCM (3x1 min), DMF (3x1 min) and DCM (3x1 min).

Incorporation of the first amino acid onto the CTC resin

Incorporation of the first Fmoc-aa-OH onto the CTC resin is achieved through a nucleophilic substitution. The initial loading of the CTC resin (1.6 mmol/g) is normally decreased in order to prevent interchain aggregation during SPPS. To decrease the initial loading of the CTC resin, less than 1.0 equiv. of the first Fmoc-aa-OH are used.

It should be considered that, in general, incorporation of the first Fmoc-aa-OH onto the CTC is not quantitative. Typically, the use of 0.7 equiv. of Fmoc-aa-OH is expected to give a loading of 0.5 mmol/g. However, the degree of incorporation depends on the steric hindrance of the Fmoc-aa-OH to be incorporated.

Since the use of 1.2 equiv. of Fmoc-aa-OH is expected to give a loading of 1.0 mmol/g, to achieve an approximate loading of 1.0 mmol/g, a solution of the first Fmoc-aa-OH (1.2 equiv.) and DIEA (12.0 equiv.) in DCM was added to the resin and the mixture was shaken for 1 h. Then, MeOH (0.8 mL/g resin) was added to cap the free sites of the resin and the mixture was stirred for 15 min. Finally, the solvent and the excess of reagents were filtered, and then, the resin was washed.

Fmoc- group elimination

The Fmoc- group was removed by treating the resin with piperidine/DMF 1:4 (2x5 min, 1x10 min). Fmoc- removal from *N*-alkylated residues was carried out using an extra treatment with DBU/toluene/piperidine/DMF 5:5:20:70 (1x5 min). After the basic treatments, the resin was washed with DMF (5x1 min), till the filtrate had a neutral pH.

5.7. Determination of the resin loading by quantification of the Fmoc- group

Resin loading was determined by quantification of the UV-absorbance of dibenzofulvene-piperidine adduct measured at 290 nm. After incorporating the first amino acid, the Fmoc- group was removed and the washes of all treatments were collected in a volumetric flask. The piperidine washes were diluted with DMF and the absorbance of the resulting solution was measured at 290 nm. The resin loading was calculated using the following formula:

$$Z = (A \cdot V) / (\varepsilon \cdot Y \cdot l)$$

where: Z: resin loading (mmol/g resin), A: absorbance, V: volume of solvent (mL), ε: molar extinction coefficient of Fmoc- (ε = 5800 L mol^{-1} cm^{1}), Y: weight of resin (g), l: path length (cm).

Peptide chain elongation

Peptide chain elongation was performed following the cycles described in the Table below.

Stage	Operation	Solvents	Treatments
1	Washes	DMF	3x1 min
		DCM	3x1 min
		DMF	3x1 min
2	Deprotection	piperidine/DMF 1:4	2x5 min, 1x10 min
3	Washes	DMF	3x1 min
		DCM	3x1 min
		DMF	3x1 min
4	Coupling	Fmoc-aa-OH Coupling reagent	1x 60 min
5	Washes	DMF	3x1 min
		DCM	3x1 min
		DMF	3x1 min

After the final washings, the resin was filtered and a ninhydryn or a De Clerq test was performed. If the test was positive (*i.e.* uncomplete coupling), then recoupling was required, and the procedure starting from the third stage of the cycle was repeated. If the test was negative (*i.e.* complete coupling), the procedure starting from the first stage of the cycle was repeated to remove the Fmoc- and incorporate the next amino acid residue.

The coupling method was chosen depending on the difficulty of the specific coupling. Carbodiimide activation was used for couplings over unhindered amino acids. In most carbodiimide-mediated couplings, we used OxymaPure as additive to suppress racemization and improve coupling efficiency. In terms of these effects, the performance of OxymaPure is superior to HOBt and comparable to HOAt. Activation with phosphonium and uronium salts was used for some difficult couplings, like for the coupling of hindered amino acids or for the coupling of dipeptidic segments onto a peptidyl-resin. BTC activation was used for couplings onto *N*-alkylated residues. Activation of an Fmoc-amino acid with BTC is likely to proceed through the *in situ*-generation of the corresponding acid chloride, which is a highly reactive acylating species.

- Coupling with DIPCDI/OxymaPure, DIPCDI/HOAt or DIPCDI/HOBt (carbodiimide procedure). The Fmoc-aa-OH (3.0 equiv.) and the additive (3.0 equiv.) were dissoved in DMF. DIPCDI (3.0 equiv.) was added and, after 3 min of preactivation, the solution was poured to the resin. The peptidyl-resin was shaken for 1 h. Then, the excess of reagents was filtered off and the resin was washed.

- Coupling with PyBOP/HOAt/DIEA (phosphonium salts procedure). The Fmoc-aa-OH (3.0 equiv.) and HOAt (3.0 equiv.) were dissolved in DMF in the presence of DIEA (6.0 equiv.). PyBOP (3.0 equiv.) was added and the solution was poured to the resin. The peptidyl-resin was shaken for 1 h (unless otherwise stated). Then, the excess of reagents was filtered off and the resin was washed.

- Coupling with HATU/DIEA or HBTU/DIEA (uronium salts procedure). The Fmoc-aa-OH (3.0 equiv.) was dissoved in DMF and DIEA (6.0 equiv.) was added. In a different vessel, HATU or HBTU (2.9 equiv.) was dissolved in DMF and mixed with the first solution and the final mixture was preactivated for 30 s. The resulting solution was poured to the resin. The peptidyl-resin was shaken for 1 h (unless otherwise stated). Then, the excess of reagents was filtered off and the resin was washed.

- Coupling with BTC.[91a] The peptidyl-resin was pre-swollen in $THF_{(anh.)}$/DIEA 4:1 for 15 min. The Fmoc-aa-OH (5.00 equiv.) and BTC (1.65 equiv.) were weighed in a 2 mL-eppendorf and dissolved in $THF_{(anh.)}$ to a 0.1-0.2 M concentration. 2,4,6-trimethylpyridine (14.0 equiv.) was added and a white precipitate was formed. The suspension was stirred with a Pasteur pippete during 1 min to ensure quantitative formation of the Fmoc-amino acid chloride. This supension was added to the peptidyl-resin and the mixture was shaken for 3 h or overnight (as specified for each case). The resin was washed with MeOH (3x1 min), DCM (2x1 min), MeOH (2x1 min), DCM (2x1 min), DMF (2x1 min) and DCM (3x1 min). [*Hazard:* BTC is highly toxic and may cause death by inhalation. This substance should be handled in well-ventilated hood with extreme caution.]

_N_-acetylation of unreacted amino groups

In general, when a coupling is uncomplete, another coupling should be performed in hope that all the free amino groups will be *N*-acylated. However, if free amino groups are still present after repeating the coupling or if the amino acid to be coupled is very valuable, then a possible solution is to *N*-acetylate the unreacted peptide. This technique avoids the occurrence of mistmatch sequences in the final peptide, which would hamper the purification of the final peptide product.

Our procedure for capping unreacted *N*-terminal amino groups was the following. The resin was washed with DCM (5x1 min). Then, a solution of Ac_2O (10.0 equiv.) and DIEA (10.0 equiv.) in DCM was added to the resin. After shaking for 15 min, the excess of reagents was filtered and the resin was washed.

Solid-phase reductive alkylation of the *N*-terminal amino group

The reaction was carried out in THF unless otherwise stated. The peptidyl-resin was pre-swollen in THF for 15 min. A solution of the aldehyde (x equiv.) in THF was added to the resin. The resin was shaken for 1 h to ensure complete imine formation. Then, $NaBH_3CN$ (2x equiv.) was added, 2-3 drops of AcOH were added and the reaction mixture was shaken for a further 2 h-period. Finally, the excess of reagents was filtered off and the resin was washed.

Mini-cleavage and HPLC/HPLC-MS analysis

The progress of solid-phase reactions can be monitored by HPLC and HPLC-MS. To do so, a small amount of resin (1-2 mg) was cleaved with a solution of 2% TFA in DCM, the filtrate was concentrated under a stream of N_2, redissolved in ACN/H_2O 1:1 and injected into the chromatographic instrument.

Peptide cleavage from the CTC resin

Peptides were cleaved from resin using a solution of 2% TFA in DCM (3x2 min). After cleavage, TFA was removed under reduced pressure by coevaporation with toluene. The residue was redissolved in ACN/H_2O 1:1 and lyophilized.

Determination of peptide purity

Purities of the peptides synthesized were determined by analytical HPLC using the area percentage method on the UV trace recorded at a wavelength of 220 nm.

Determination of the net peptide content

The net peptide content of a given sample is the fraction of peptidic material relative to counter-ions, residual water and non-peptidic impurities. It can be determined by amino acid analysis.

Net peptide content = (g pure peptide/g sample) · 100

It should be noted that there is an important difference between peptide content and peptide purity. Peptides inevitably contain both counter-ions and residual water as they are often isolated as salts (such as acetates) after lyophilization. So, even if a peptide is 98% pure, the net amount of peptide may only represent 70-85% of the total weight of the peptide sample (depending on its amino acid composition, last purification step and lyophilization).

In the case of PEG-modified peptides, a relatively low peptide content can be expected. Since PEG is a very hygroscopic polymer, PEG-modified peptides isolated after semipreparative RP-HPLC may retain a considerable amount of water. Therefore, determination of their net peptide content is highly recommended to obtain reproducible results in quantitative studies.

Amino acid analysis

Amino acid analysis was carried out by acid hydrolysis of the peptide sample and analysis of the individual amino acid constituents by RP-HPLC after precolumn derivatization with 6-aminoquinolyl-*N*-hydroxysuccinimidyl carbamate (AQC).

i. Acid hydrolysis. An exact amount of dry peptide sample (1-5 mg) was placed in a dry hydrolysis tube. The sample was dissolved in $HCl_{(aq.)}$ 6 M (200-300 µL) and a known amount of 2-aminobutyric acid was added [This compound is used as internal standard to correct for physical and chemical losses that may take place during amino acid analysis]. The sample was hydrolyzed at 120 ºC for 20 h. Then, the acid was removed under reduced pressure and the hydrolyzed sample was redissolved in $HCl_{(aq.)}$ 20 mM (1000 µL). The resulting solution was filtered and diluted with more $HCl_{(aq.)}$ 20 mM to an estimated amino acid concentration of 0.1-0.2 M and final known 2-aminobutyric acid concentration of 0.1 M.

ii. Amino acid derivatization. The amino acids present in the hydrolyzed sample were derivatized using an AccQ-Fluor™ reagent kit (Waters). Amino acid derivatization was conducted according to the manufacturer's protocol. Briefly, 10 µL of the diluted hydrolyzed sample were placed in a nynhydrin tube and mixed with *AccQ·Tag ultra* borate buffer (70 µL). *AccQ·Tag™ reagent* (20 µL) was added. The reaction was allowed to proceed for 10 min at 55 ºC. Finally, the derivatized amino acid solution was mixed with AccQ·Tag™ Ultra concentrate solvent A (100 µL) prior to injection into the RP-HPLC apparatus.

iii. RP-HPLC analysis. RP-HPLC analysis was performed on a Waters 600 instrument, equipped with a delta 600 pump, a Waters 717 automatic injector and a Waters 2487 UV detector. The separation column was a Waters AccQ•Tag™ amino acid analysis column Nova-pak C_{18} (4.0 µm, 3.9 × 150 mm). A gradient of AccQ·Tag™ Ultra concentrate solvent A into ACN was run at a flow rate of 1.0 mL/min over 45 min. Data were managed with MassLynx software (Waters). The concentrations of the individual derivatized amino acids present in the injected sample were calculated from calibration curves.

EXPERIMENTAL PROCEDURES FOR CHAPTER 1

1.1. SYNTHESIS OF STARTING MATERIALS

1.1.1. Synthesis of 3,6,9-trioxadecanaldehyde

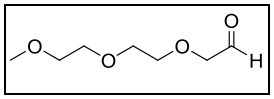

A solution of oxalyl chloride (222.8 mmol, 25.0 mL) in $DCM_{(anh.)}$ (75 mL) was prepared under N_2 and cooled in a dry ice-acetone bath. To this solution was carefully added a solution of DMSO (445.5 mmol, 31.6 mL) in $DCM_{(anh.)}$ (40 mL). The resulting mixture was stirred at -78 ºC for 10 min, and then a solution of triethylene glycol monomethyl ether (148.5 mmol, 25.0 mL) in $DCM_{(anh.)}$ (50 mL) was added slowly. After stirring for 15 min, NEt_3 (891.0 mmol, 91.1 mL) was added dropwise over a period of 20 min. The reaction mixture was left for 30 min at -78 ºC and then allowed to reach room temperature. The reaction was quenched with $NaHCO_{3\ (sat.)}$ (100 mL). Phases were separated. The organic phase was washed with $NaCl_{(sat.)}$ (2x50 mL). Aqueous phases were combined and further extracted with DCM (2x50 mL). The combination of organic phases was dried over $MgSO_{4\ (anh.)}$, filtered and concentrated under reduced pressure. The crude product was purified by flash chromatography (AcOEt/MeOH, 95:5) affording 16.91 g (70%) of pure aldehyde (**0**). ^{1}H-NMR and ^{13}C-NMR spectral data matched literature values.[117] ^{1}H-NMR analysis of the purified product left for 48 h in an open flask

showed that 3,6,9-trioxadecanaldehyde (**0**) is very susceptible to polymerize via aldol condensation, as has been described for mPEG-acetaldehyde.[74] To prevent decomposition, the aldehyde should be stored at -20 ºC under N_2 atmosphere.

1.1.2. Synthesis of Fmoc-Ala-Cl

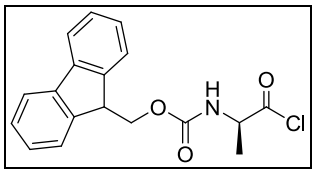

A solution of Fmoc-Ala-OH (2.50 mmol, 0.78 g) in DCM (10 mL) was treated with $SOCl_2$ (25.00 mmol, 1.81 mL) and the mixture was refluxed for 2 h under N_2 atmosphere. Solvents and excess of $SOCl_2$ were removed under reduced pressure and the resulting residue was dissolved in DCM (2 mL). Addition of hexane (12 mL) precipitated 0.78 g (95%) of pure Fmoc-Ala-Cl, which was obtained as a white solid. To assess the identity of this product, a small amount of recristallized Fmoc-Ala-Cl (1 mg) was added to dry methanol to form its methyl ester derivative. HPLC-MS analysis upon esterification showed 99% of Fmoc-Ala-OMe along with 1% of Fmoc-Ala-OH, which indicates that recristallized Fmoc-Ala-Cl contained a negligible amount of residual acid.

1.2. SYNTHESIS OF THE FMOC-*N*-TEG AMINO ACIDS

1.2.1. General procedure for reductive alkylation + Fmoc- protection

To a solution of 3,6,9-trioxadecanaldehyde (**0**, 11.26 mmol, 1.421 g) and amino acid *tert*-butyl ester hydrochloride (10.23 mmol) in MeOH/AcOH 99:1 (80 mL) was added $NaBH_3CN$ (13.71 mmol, 0.862 g) over a period of 30 min. The resulting solution was stirred at room temperature for 2.5 h and then poured into 30 mL of $NaHCO_{3\ (sat.)}$. The product was extracted with AcOEt (2x50 mL). The combination of organic phases was washed with $NaCl_{\ (sat.)}$ (2x50 mL), dried over $MgSO_{4\ (anh.)}$, filtered and concentrated under reduced pressure. The resulting residue consisted of an unseparable mixture of the expected product and *N,N*-dialkylated amino acid. This residue was dissolved in DCM (60 mL) and treated with Fmoc-Cl (12.28 mmol, 3.177 g) in the presence of DIEA (20.46 mmol, 2.93 mL) under N_2 atmosphere. After overnight stirring at room temperature, the solvent was removed under reduced pressure and the residue was redissolved in AcOEt (100 mL). The organic phase was washed with $HCl_{\ (aq.)}$ 1 M (2x40 mL), dried over $MgSO_{4\ (anh.)}$, filtered and concentrated under reduced pressure. The crude was purified by flash chromatography (Hexane/AcOEt 75:25) to give the desired product.

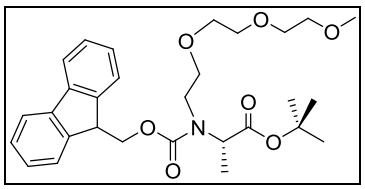

Fmoc-(*N*-TEG)Ala-O^{t}Bu (1). Following the general procedure described above with alanine *tert*-butyl ester hydrochloride (5.50 mmol, 1.000 g), compound **1** (1.977 g, 70%) was obtained as colorless oil. ^{1}H-NMR (400 MHz, $CDCl_3$): δ 1.38-1.46 (m, 12H), 3.13-3.75 (m, 15H), 4.38 (m, 4H), 7.31 (t, *J* = 7.4 Hz, 2H), 7.39 (t, *J* = 7.3 Hz, 2H), 7.59 (d, *J* = 7.4 Hz, 2H), 7.75 (d, *J* = 7.5 Hz, 2H); ^{13}C-NMR (100 MHz, $CDCl_3$): δ 15.3, 15.9, 27.9, 45.7, 46.1, 47.2, 56.1, 56.6, 58.9, 67.0, 67.6, 69.5, 69.7, 70.3, 70.4, 71.8, 81.1, 81.3, 119.8, 124.7, 127.0, 127.5, 141.2, 141.2, 143.9, 143.9, 155.8, 156.0, 171.0, 171.0; IR (KBr): ν = 2876.88, 1734.65, 1704.72, 1451.07, 1415.02, 1367.99, 1287.42, 1245.49, 1150.10, 1103.05, 761.38, 737.59 cm^{-1}; $[\alpha]_D$ -20.2 ($CHCl_3$, 0.01 g/mL); HRMS (ES$^+$): calc. for $[C_{29}H_{39}NO_7 + NH_4]^+$ 531.3064, found 531.3065.

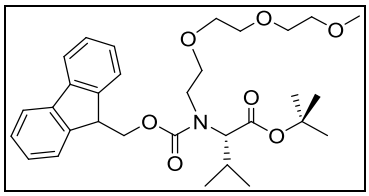

Fmoc-(*N*-TEG)Val-O^{t}Bu (2). Following the general procedure described above with valine *tert*-butyl ester hydrochloride (11.00 mmol, 2.500 g), compound **2** (4.090 g, 69%) was obtained as colorless oil. ^{1}H-NMR (400 MHz, $CDCl_3$): δ 0.66-0.81 (m, 3H), 0.84-0.99 (m, 3H), 1.41 (s, 9H), 1.98-2.23 (m, 1H), 3.20-3.72 (m, 15H), 3.82-4.14 (m, 1H), 4.23 (m, 1H), 4.28-4.63 (m, 2H), 7.31 (t, *J* = 7.4 Hz, 2H), 7.39 (t, *J* = 7.4 Hz, 2H), 7.59 (d, *J* = 7.4 Hz, 2H), 7.75 (d, *J* = 7.5 Hz, 2H); ^{13}C-NMR (100 MHz, $CDCl_3$): δ 19.3, 20.2, 28.2, 44.7, 47.6, 47.7, 59.2, 66.6, 66.3, 67.2, 67.6, 68.9, 69.3, 70.5, 70.7, 72.1, 81.5, 81.6, 120.2, 125.0, 125.1, 125.2, 127.3, 127.4, 127.9, 141.6, 144.1, 144.2, 156.5, 156.8, 170.0, 170.3; IR (KBr): ν = 2965.39, 2928.51, 1730.75, 1703.74, 1451.78, 1416.11, 1368.26, 1279.93, 1140.40, 1129.49, 759.78, 741.14 cm^{-1}; $[\alpha]_D$ -32.5 (MeOH, 0.01 g/mL); HRMS (ES$^+$): calc. for $[C_{31}H_{43}NO_7 + NH_4]^+$ 559.3378, found 559.3374.

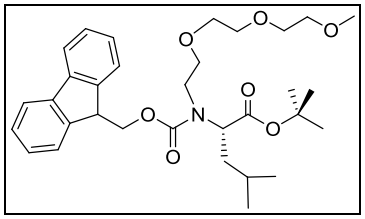

Fmoc-(*N*-TEG)Leu-O^{t}Bu (3). Following the general procedure described above with leucine *tert*-butyl ester hydrochloride (10.23 mmol, 2.290 g), compound **3** (3.410 g, 60%) was obtained as colorless oil. ^{1}H-NMR (400 MHz, $CDCl_3$): δ 0.77-0.95 (m, 6H), 1.41 (bs, 9H), 1.45-1.74 (m, 3H), 3.00-3.73 (m, 15H), 4.22 (m, 1H), 4.30-4.62 (m, 3H), 7.31 (t, *J* = 7.4 Hz, 2H), 7.39 (t, *J* = 7.4 Hz, 2H), 7.59 (d, *J* = 7.4 Hz, 2H), 7.75 (d, *J* = 7.4 Hz, 2H); ^{13}C-NMR (100 MHz, $CDCl_3$): δ 21.4, 21.6, 22.8, 22.9, 24.6, 27.8, 38.1, 38.4, 45.2, 45.5, 47.2, 47.3, 58.8, 58.8, 66.7, 67.3, 69.0, 69.3, 70.2, 70.3, 71.7, 81.1, 81.3, 119.8, 124.6, 124.7, 126.9, 127.5, 141.1, 141.2, 141.2, 143.6, 143.7, 143.8, 143.9, 156.3, 170.8; IR (KBr): ν = 2955.29, 2870.64, 1732.09, 1704.06, 1451.60, 1413.68, 1367.73, 1277.06, 1244.55, 1145.61, 1111.21, 759.30, 740.88 cm^{-1}; $[\alpha]_D$ -31.0 (MeOH, 0.01 g/mL); HRMS (ES$^+$): calc. for $[C_{32}H_{45}NO_7 + NH_4]^+$ 573.3534, found 573.3535.

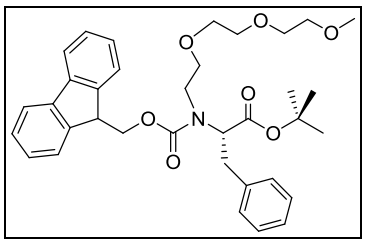

Fmoc-(*N*-TEG)Phe-O^{t}Bu (4). Following the general procedure described above with phenylalanine *tert*-butyl ester hydrochloride (17.88 mmol, 4.564 g), compound **4** (4.219 g, 40%) was obtained as colorless oil. ^{1}H-NMR (400 MHz, $CDCl_3$): δ 1.35-1.46 (m, 9H), 2.60-3.15 (m, 2H), 3.21-3.71 (m, 15H), 4.17-4.30 (m, 2H), 4.32-4.43 (m, 1H), 4.48-4.84 (m, 1H), 6.89-7.27 (m, 5H), 7.31 (m, 2H), 7,39 (m, 2H), 7.58 (m, 2H), 7.75 (m, 2H); ^{13}C-NMR (100 MHz, $CDCl_3$): δ 28.2, 35.5, 36.0, 47.5, 47.8, 28.0, 48.1, 59.2, 67.1, 67.3, 69.3, 69.4, 70.5, 70.7, 70.7, 72.1, 120.2, 120.2, 120.3, 125.0, 125.1, 125.2, 126.6, 127.3, 127.3, 127.9, 128.0, 128.6, 129.3, 129.4, 129.4, 138.3, 138.6, 141.6, 141.7, 144.0, 144.2, 155.8, 156.3, 169.8, 170.0; IR (KBr): ν = 2928.03, 2875.22, 1732.26, 1703.89, 1452.02, 1418.10, 1367.92, 1280.44, 1244.34, 1138.27, 758.43, 740.98 cm^{-1}; $[\alpha]_D$ -62.7 (MeOH, 0.01 g/mL); HRMS (ES$^+$): calc. for $[C_{35}H_{43}NO_7 + NH_4]^+$ 607.3378, found 607.3378.

1.2.2. General procedure for *tert*-butyl ester acidic cleavage

The *tert*-butyl protected amino acid (5.00 mmol) was dissolved in DCM (25 mL) and TFA (25 mL) was added. After stirring for 1 h at room temperature, the mixture was concentrated under reduced pressure. The remaining TFA was removed by co-evaporation with toluene at 50 ºC.

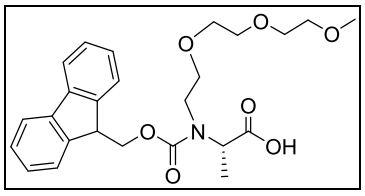

Fmoc-(*N*-TEG)Ala-OH (5). Following the general procedure described above with **1** (0.319 g, 0.62 mmol) compound **5** (0.300 g, 100%) was obtained as yellowish oil. ^{1}H-NMR (400 MHz, $CDCl_3$): δ 2.97 (d, *J* = 7.1 Hz, 3H), 3.17-3.73 (m, 15H), 4.24 (t, *J* = 5.9 Hz, 1H), 4.45 (m, 2H), 4.57 (d, *J* = 5.3 Hz, 1H), 7.31 (t, *J* = 7.3 Hz, 2H), 7.39 (t, *J* = 7.4 Hz, 2H), 7.59 (m, 2H), 7.75 (d, *J* = 7.5 Hz, 2H); ^{13}C-NMR (100 MHz, $CDCl_3$): δ 14.6, 15.2, 45.8, 46.3, 47.2, 55.9, 56.2, 58.8, 67.1, 67.8, 69.9, 70.0, 70.2, 70.3, 71.8,

119.9, 125.2, 128.2, 129.0, 141.3, 143.9, 155.8, 156.0, 173.7, 174.2; IR (KBr): ν = 2924.05, 1732.09, 1701.88, 1451.50, 1417.58, 1288.00, 1199.99, 1100.90, 762.67, 739.88 cm^{-1}; $[\alpha]_D$ -26.2 ($CHCl_3$, 0.01 g/mL); HRMS (ES^+): calc. for $[C_{25}H_{31}NO_7 + NH_4]^+$ 475.2439, found 475.2439.

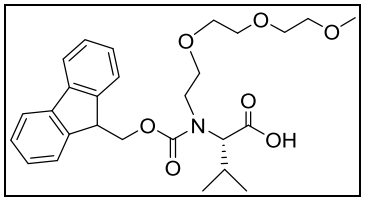

Fmoc-(*N*-TEG)Val-OH (6). Following the general procedure described above with **2** (3.999 g, 7.36 mmol) compound **6** (3.576 g, 100%) was obtained as yellowish oil. ^{1}H-NMR (400 MHz, $CDCl_3$): δ 0.67-0.77 (m, 3H), 0.94-1.20 (m, 3H), 2.11-2.39 (m, 1H), 3.00-3.74 (m, 15H), 3.94 (d, *J* = 10.7 Hz, 1H), 4.25 (m, 1H), 4.32-4.70 (m, 2H), 7.30 (t, *J* = 7.4 Hz, 2H), 7.37 (t, *J* = 7.4 Hz, 2H), 7.60 (m, 2H), 7.73 (d, *J* = 7.5 Hz, 2H), 8.8 (bs, 1H); ^{13}C-NMR (100 MHz, $CDCl_3$): δ 18.6, 18.7, 20.2, 20.5, 27.1, 27.5, 46.7, 47.2, 47.3, 58.6, 58.7, 66.2, 67.0, 67.5, 69.1, 69.2, 69.8, 69.9, 70.1, 70.2, 70.4, 71.6, 119.8, 124.6, 127.1, 127.6, 141.3, 141.3, 141.4, 143.7, 143.8, 143.8, 143.9, 155.9, 156.5, 171.7, 171.1; IR (KBr): ν = 3063.88, 2890.62, 1739.90, 1703.63, 1451.94, 1419.21, 1274.55, 1243.43, 1138.12, 1107.59, 758.96, 741.78 cm^{-1}; $[\alpha]_D$ -29.4 (MeOH, 0.01 g/mL); HRMS (ES^+): calc. for $[C_{27}H_{35}NO_7 + Na]^+$ 508.2306, found 508.2303.

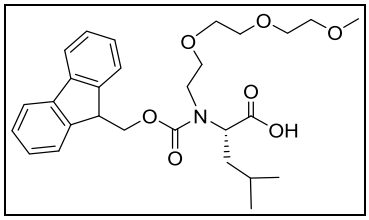

Fmoc-(*N*-TEG)Leu-OH (7). Following the general procedure described above with **3** (2.000 g, 3.60 mmol), compound **7** (1.799 g, 100%) was obtained as yellowish oil. ^{1}H-NMR (400 MHz, $CDCl_3$): δ 0.79-0.93 (m, 6H), 1.39-1.84 (m, 3H), 3.00-3.72 (m, 15H), 4.22 (m. 1H), 4.30-4.62 (m, 3H), 7.30 (t, *J* = 7.4 Hz, 2H), 7.37 (m, 2H), 7.58 (m, 2H), 7.73 (d, *J* = 7.4 Hz, 2H), 8.71 (bs, 1H); ^{13}C-NMR (100 MHz, $CDCl_3$): δ 21.5, 22.9, 24.4, 37.4, 37.8, 45.6, 47.0, 47.1, 58.3, 58.6, 66.8, 67.4, 69.3, 69.7, 69.9, 70.0, 71.6, 119.7, 124.5, 124.5, 124.6, 126.8, 126.9, 127.4, 141.1, 141.1, 143.6, 143.6, 143.7, 156.1, 156.3, 174.0, 174.4; IR (KBr): ν = 2955.10, 2871.21, 1738.72, 1703.09, 1451.09, 1415.57, 1285.96, 1232.62, 1146.95, 1110.04, 759.38, 741.11 cm^{-1}; $[\alpha]_D$ -24.9 (MeOH, 0.01 g/mL); HRMS (ES^+): calc. for $[C_{28}H_{37}NO_7 + NH_4]^+$ 517.2908, found 517.2907.

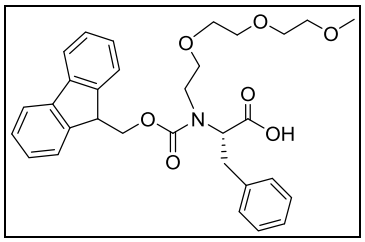

Fmoc-(*N*-TEG)Phe-OH (**8**). Following the general procedure described above with **4** (3.688 g, 6.26 mmol), compound **8** (3.340 g, 100%) was obtained as yellowish oil. ^{1}H-NMR (400 MHz, $CDCl_3$): δ 2.55-2.81 (m, 2H), 3.00-3.70 (m, 15H), 4.15-4.34 (m, 2H), 4.44-4.56 (m, 1H), 4.58-4.72 (m, 1H), 6.82-7.25 (m, 5H), 7.26-7.42 (m, 4H), 7.50 (m, 2H), 7.63 (m, 2H), 7.73 (m, 2H), 9.39 (bs, 1H); ^{13}C-NMR (100 MHz, $CDCl_3$): δ 34.2, 34.7, 46.7, 46.8, 47.9, 58.1, 58.1, 63.3, 66.6, 66.7, 68.7, 68.8, 69.4, 69.5, 69.6, 71.2, 119.4, 119.5, 124.2, 124.3, 125.9, 126.0, 126.6, 126.7, 127.1, 127.2, 127.9, 128.0, 128.5, 128.6, 137.3, 137.5, 140.8, 140.8, 140.9, 143.2, 143.3, 143.4, 154.5, 155.0, 172.3, 172.6; IR (KBr): ν = 2925.17, 2739.77, 1703.16, 1451.45, 1417.01, 1282.94, 1244.52, 1143.83, 1113.31, 759.62, 741.20 cm^{-1}; $[\alpha]_D$ -82.2 (MeOH, 0.01 g/mL); HRMS (ES^+): calc. for $[C_{31}H_{35}NO_7 + Na]^+$ 556.2306, found 556.2300.

1.3. USE OF Fmoc-*N*-TEG AMINO ACIDS IN SPPS

1.3.1. Preparation of peptidyl-resin H-(*N*-TEG)Leu-Leu-Phe-O-ClT (0.25 mmol/g)

The CTC resin (1.0 g, 1.6 mmol/g) was placed in a polypropylene syringe, swollen and washed. The first amino acid, Fmoc-Phe-OH (116 mg, 0.30 mmol), was incorporated in the presence of DIEA (513 µL, 3.00 mmol), the Fmoc- group was removed and a 0.25 mmol/g. resin loading was assessed. Then, Fmoc-Leu-OH (265 mg, 0.75 mmol) was coupled using DIPCDI (116 µL, 0.75 mmol) and OxymaPure (110 mg, 0.75 mmol) as activating reagents, and the Fmoc- group

was removed. Fmoc-(*N*-TEG)Leu-OH (**7**, 500 mg, 0.75 mmol) was coupled using DIPCDI (116 µL, 0.75 mmol) and OxymaPure (110 mg, 0.75 mmol) as activating reagents, the Fmoc- group was removed and the resin was dried. All these steps were carried out following the previously described SPPS procedures.

1.3.2. General procedure for the coupling tests onto the resin-bound (*N*-TEG)Leu residue

The H-(*N*-TEG)Leu-Leu-Phe-O-ClT (0.100 g, 0.25 mmol/g) was placed in a polypropylene syringe and swollen in the solvent of choice for 15 min. After filtering off the solvent, the amino acid to be coupled was activated with the reagents of choice and added to the peptidyl-resin. The peptidyl-resin was shaken for the time specified for each case. Then, the solvent and the excess of reagents were filtered off, the resin was washed and a De Clerq test was performed to check for unreacted amino groups. For the Fmoc- protection step, the peptidyl-resin was swollen in DCM, DIEA (32 µL, 0.19 mmol) was added, and then a solution of Fmoc-Cl (16 mg, 0.063 mmol) in DCM was added. The peptidyl-resin was shaken overnight. The solvent and excess of reagents were filtered off, the resin was washed and a small sample of peptidyl-resin (1-2 mg) was cleaved and analyzed by HPLC.

1.3.3. General procedure for the coupling tests onto the resin-bound (*N*-TEG)Leu residue under MW heating

The H-Leu(*N*-TEG)-Leu-Phe-O-ClT (0.100 g, 0.25 mmol/g) was placed in a polypropylene syringe and swollen in the solvent of choice for 15 min. Then, the solvent was filtered off and the resin was transferred to a MW vessel (*i.e.* a heavy-walled glass vial sealed with an aluminium crimp cap fitted with a silicon septum, the inner diameter of the vial being 1.3 cm). The amino acid to be coupled was activated with the reagents of choice and added to the peptidyl-resin. The reaction mixture was irradiated in the MW apparatus using the PowerMAX irradiation mode (*i.e.* non-continuous irradiation power). During the irradiation (time and temperature specified for each case), reaction mixtures were stirred with a magnetic bar. The temperature, pressure and irradiation power were monitored. The average pressure for reactions run in DMF was 1-2 bar, whereas for reactions run in THF it was 5-6 bar. After completed irradiation, the reaction tube was cooled with high-pressure air until the temperature had fallen below 39 ºC. Then, the peptidyl-resin was tranferred back to the original propylene syringe using a Pasteur pipette. The solvent and the excess of reagents were filtered off, the resin was washed and a De Clerq test was performed to check for unreacted amino groups. For the Fmoc- protection step, the peptidyl-resin was swollen in DCM, DIEA (32 µL, 0.19 mmol) was added, and then a solution of Fmoc-Cl (16 mg, 0.063 mmol) in DCM was added. The peptidyl-resin was shaken overnight. The solvent and excess of reagents were filtered off, the resin was washed and a small sample of peptidyl-resin (1-2 mg) was cleaved and analyzed by HPLC.

1.3.4. Coupling procedures tested

- Coupling with DIPCDI/OxymaPure, DIPCDI/HOBt or DIPCDI/HOAt (carbodiimide procedure). The Fmoc-aa-OH (5.0 equiv.) and the additive (5.0 equiv.) were dissoved in DMF. DIPCDI (5.0 equiv.) was added and, after 3 min of preactivation, the solution was poured to the resin.
- Coupling with HATU/HOAt. The Fmoc-aa-OH (5.0 equiv.) and HOAt (5.0 equiv.) were dissoved in DMF and DIEA (10.0 equiv.) was added. In a different vessel, HATU (4.9 equiv.) was dissolved in DMF and mixed with the first solution and the final mixture was preactivated for 30 s. The resulting solution was poured to the resin.
- Coupling with COMU. The Fmoc-aa-OH (5.0 equiv.) and COMU (5.0 equiv.) were dissoved in DMF. DIEA (10.0 equiv.) was added and the resulting solution was poured to the resin.

- Coupling via a symmetrical anhydride. The Fmoc-aa-OH (10.0 equiv.) was dissolved in DCM and DIPCDI (5.0 equiv.) was added. The resulting solution was stirred for 10 min to ensure quantitative formation of the symmetrical anhydride and then poured to the resin.

- Coupling via a symmetrical anhydride in the presence of DMAP. The Fmoc-aa-OH (10.0 equiv.) was dissolved in DCM, DIPCDI (5.0 equiv.) was added and the mixture was stirred for 10 min to ensure quantitative formation of the symmetrical anhydride. Then, DMAP (0.2 equiv.) was added and the resulting solution was poured to the resin.

- Coupling via a pre-made Fmoc-amino acid chloride. The pre-made Fmoc-aa-Cl (5.0 equiv.) was dissolved in DCM, DIEA (5.0 equiv.) was added and the resulting solution was immediately poured to the resin.

- Coupling via a pre-made Fmoc-amino acid chloride in the presence of HOBt. The pre-made Fmoc-aa-Cl (5.0 equiv.) was added to a solution of HOBt (5.0 equiv.) and DIEA (5.0 equiv.) in DCM. The resulting solution was poured to the resin.

- Coupling via an *in situ*-generated Fmoc-amino acid chloride. The Fmoc-aa-OH (5.0 equiv.) was dissolved in DCM in the presence of DIEA (5.0 equiv.). TCFH (5.0 equiv.) was added and the mixture was stirred for 15 min to ensure quantitative formation of the acid fluoride. To this solution DIEA (5.0 equiv.) was added and the resulting solution was poured to the resin.

- Coupling via an *in situ*-generated Fmoc-amino acid fluoride.

  a. Coupling in the absence of base. The Fmoc-aa-OH (5.0 equiv.) was dissolved in DCM in the presence of DIEA (5.0 equiv.). TFFH (5.0 equiv.) was added and the mixture was stirred for 15 min to ensure quantitative formation of the acid fluoride. Then, this solution was poured to the resin.

  b. Coupling in the presence of base. The Fmoc-aa-OH (5.0 equiv.) was dissolved in DCM in the presence of DIEA (5.0 equiv.). TFFH (5.0 equiv.) was added and the mixture was stirred for 15 min to ensure quantitative formation of the acid fluoride. To this solution DIEA (2.0 equiv.) was added and the resulting solution was poured to the resin.

- Coupling via an *in situ*-generated Fmoc-amino acid fluoride after prior *N*-silylation of the resin-bound peptide. The resin was swollen in DCM and treated with BTSA (5.0 equiv.). *N*-silylation was allowed to proceed overnight prior to perform the coupling. In a separate vessel, the Fmoc-aa-OH (5.5 equiv.) was dissolved in DCM in the presence of DIEA (5.0 equiv.). TFFH (5.0 equiv.) was added and the mixture was stirred for 15 min to ensure quantitative formation of the acid fluoride. Then, this solution was poured to the resin.

- Coupling with BTC. The peptidyl-resin was pre-swollen in $THF_{(anh.)}$ for 15 min. The Fmoc-aa-OH (5.00 equiv.) and BTC (1.65 equiv.) were weighed in a 2 mL-eppendorf and dissolved in $THF_{(anh.)}$ to a 0.1-0.2 M concentration. 2,4,6-trimethylpyridine (14.0 equiv.) was added and a white precipitate was formed. The suspension was stirred with a Pasteur pippete during 1 min to ensure quantitative formation of the amino acid chloride. This supension was added to the peptidyl-resin and the mixture was shaken for 3 h or overnight. The resin was washed with MeOH (3x1 min), DCM (2x1 min), MeOH (2x1 min), DCM (2x1 min), DMF (2x1 min) and DCM (3x1 min). [*Hazard:* BTC is highly toxic and may cause death by inhalation. This substance should be handled in well-ventilated hood with extreme caution.]

EXPERIMENTAL PROCEDURES FOR CHAPTER 2

2.1. SYNTHESIS OF THE FMOC-*N*-TEG AMINO ACIDS

The synthesis and characterization of Fmoc-(*N*-TEG)Val-O^{t}Bu (**2**), Fmoc-(*N*-TEG)Leu-O^{t}Bu (**3**), and Fmoc-(*N*-TEG)Phe-O^{t}Bu (**4**) is described in the experimental procedures for Chapter 1 (see Subsection "1.1. General procedure for reductive alkylation + Fmoc- protection").

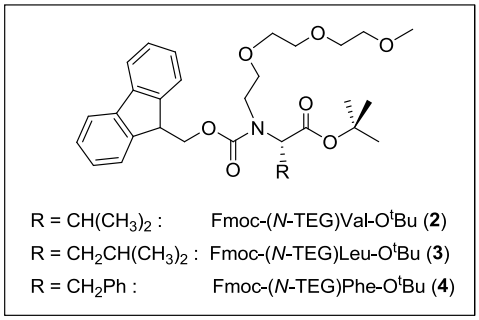

R = $CH(CH_3)_2$: Fmoc-(*N*-TEG)Val-O^{t}Bu (**2**)
R = $CH_2CH(CH_3)_2$: Fmoc-(*N*-TEG)Leu-O^{t}Bu (**3**)
R = CH_2Ph : Fmoc-(*N*-TEG)Phe-O^{t}Bu (**4**)

The synthesis and characterization of Fmoc-(*N*-TEG)Val-OH (**6**), Fmoc-(*N*-TEG)Leu-OH (**7**), and Fmoc-(*N*-TEG)Phe-OH (**8**) is described in the experimental procedures for Chapter 1 (see Subsection "1.2. General procedure for *tert*-butyl ester acidic cleavage").

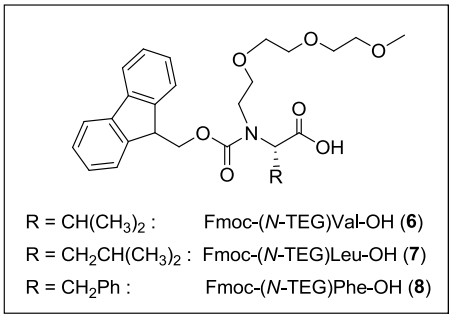

R = $CH(CH_3)_2$: Fmoc-(*N*-TEG)Val-OH (**6**)
R = $CH_2CH(CH_3)_2$: Fmoc-(*N*-TEG)Leu-OH (**7**)
R = CH_2Ph : Fmoc-(*N*-TEG)Phe-OH (**8**)

2.2. SPPS OF THE *N*-TEG AND *N*-Me LINEAR PENTAPEPTIDES

Pentapeptides **p1**, **p1a-p5a** and **p1b-p5b** were synthesized as shown in Scheme 54. The SPPS were performed on the CTC resin at a 0.50 mmol scale. For each of the syntheses, the CTC resin (2.00 g, 1.60 mmol/g) was swollen in DCM for 15 min. A solution of the first amino acid (1.2 equiv., 0.60 mmol) and DIEA (12.0 equiv., 60.0 mmol, 10.5 mL) was poured onto the resin and the mixture was shaken for 1 h. After this time, the free sites of the resin were capped with MeOH (4.0 mL, 15 min) and the resin was washed. The Fmoc- group was removed and the resin loading was determined to be 0.25 mmol/g. Elongation of the peptide chain was accomplished by stepwise assembly of the following Fmoc-protected amino acids. Standard couplings were performed with DIPCDI/OxymaPure using a 3-fold excess of amino acid (1.50 mmol). Couplings onto *N*-alkyl amino acids were performed via the corresponding amino acid chloride, which was generated *in situ* by the BTC method and left to react overnight. In the case of couplings onto the *N*-TEG residues, two overnight couplings were performed. After cleavage from solid support, the crude pentapeptides were lyophilized and obtained in purities between 53% and 89%.

Scheme 54. SPPS of pentapeptides **p1**, **p1a-p5a** and **p1b-p5b**.

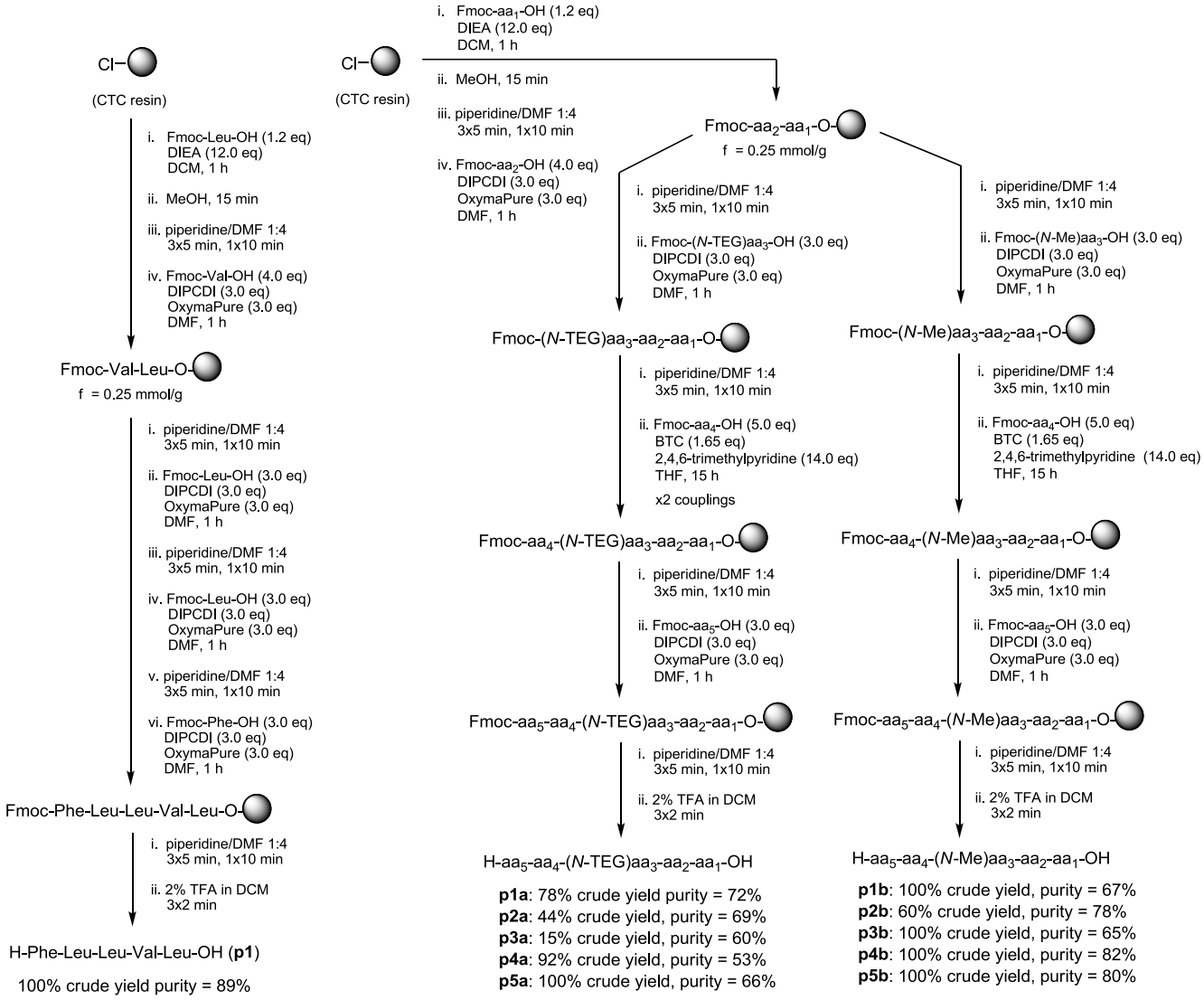

- **H-Phe-Leu-Leu-Val-Leu-OH (p1**, 301 mg, quant. crude yield**)**. HPLC (linear gradient from 10% to 90% ACN over 8 min): t_r = 4.98 min, purity = 89%; HPLC-MS (linear gradient from 0% to 60% ACN over 8 min): t_r = 8.09 min, $[M+H]^+$ = 604.48.

- **H-Phe-Leu-(*N*-TEG)Leu-Val-Leu-OH (p1a**, 291 mg, 78% crude yield**)**. HPLC (linear gradient from 10% to 90% ACN over 8 min): t_r = 5.42 min, purity = 72%; HPLC-MS (linear gradient from 0% to 60% ACN over 8 min): t_r = 8.81 min, $[M+H]^+$ = 750.41.

- **H-Leu-Leu-(*N*-TEG)Val-Leu-Phe-OH (p2a**, 165 mg, 44% crude yield**)**. HPLC (linear gradient from 10% to 90% ACN over 8 min): t_r = 5.36 min, purity = 69%; HPLC-MS (linear gradient from 0% to 60% ACN over 8 min): t_r = 8.79 min, $[M+H]^+$ = 750.41.

- **H-Leu-Val-(*N*-TEG)Leu-Phe-Leu-OH (p3a**, 55 mg, 15% crude yield**)**. HPLC (linear gradient from 10% to 90% ACN over 8 min): t_r = 5.56 min, purity = 60%; HPLC-MS (linear gradient from 0% to 60% ACN over 8 min): t_r = 9.09 min, $[M+H]^+$ = 750.41.

- **H-Val-Leu-(*N*-TEG)Phe-Leu-Leu-OH (p4a**, 346 mg, 92% crude yield**)**. HPLC (linear gradient from 10% to 90% ACN over 8 min): t_r = 5.58 min, purity = 53%; HPLC-MS (linear gradient from 0% to 60% ACN over 8 min): t_r = 9.03 min, $[M+H]^+$ = 750.41.

- **H-Leu-Phe-(*N*-TEG)Leu-Leu-Val-OH (p5a**, 438 mg, quant. crude yield**)**. HPLC (linear gradient from 10% to 90% ACN over 8 min): t_r = 5.45 min, purity = 66%; HPLC-MS (linear gradient from 0% to 60% ACN over 8 min): t_r = 9.01 min, $[M+H]^+$ = 750.41.

- **H-Phe-Leu-*N*MeLeu-Val-Leu-OH (p1b**, 497 mg, quant. crude yield**)**. HPLC (linear gradient from 10% to 90% ACN over 8 min): t_r = 5.20 min, purity = 67%; HPLC-MS (linear gradient from 10% to 70% ACN over 8 min): t_r = 5.40 min, $[M+H]^+$ = 618.11.

- **H-Leu-Leu-*N*MeVal-Leu-Phe-OH (p2b**, 541 mg, 60% crude yield**)**. HPLC (linear gradient from 10% to 90% ACN over 8 min): t_r = 5.10 min, purity = 77.9%. HPLC-MS (linear gradient from 0% to 60% ACN over 8 min): t_r = 8.37 min, $[M+H]^+$ = 618.43.

- **H-Leu-Val-*N*MeLeu-Phe-Leu-OH (p3b**, 541 mg, quant. crude yield**)**. HPLC (linear gradient from 10% to 90% ACN over 8 min): t_r = 5.22 min, purity = 65%; HPLC-MS (linear gradient from 10% to 70% ACN over 8 min): t_r = 5.40 min, $[M+H]^+$ = 618.15.

- **H-Val-Leu-*N*MePhe-Leu-Leu-OH (p4b**, 403 mg, quant. crude yield**)**. HPLC (linear gradient from 10% to 90% ACN over 8 min): t_r = 5.41 min, purity = 82%; HPLC-MS (linear gradient from 10% to 70% ACN over 8 min): t_r = 5.46 min, $[M+H]^+$ = 618.16.

- **H-Leu-Phe-*N*MeLeu-Leu-Val-OH (p5b**, 456 mg, quant. crude yield**)**. HPLC (linear gradient from 10% to 90% ACN over 8 min): t_r = 5.22 min, purity = 80%; HPLC-MS (linear gradient from 10% to 70% ACN over 8 min): t_r = 5.39 min, $[M+H]^+$ = 618.15.

2.3. CYCLIZATION OF THE *N*-TEG AND *N*-Me LINEAR PENTAPEPTIDES

The crude linear pentapeptide (approx. 0.036 mmol) was dissolved in DCM/DMF 9:1 (72 mL). EDC·HCl (0.36 mmol, 69 mg) and DMAP (0.072 mmol, 9 mg) were added to the solution. After stirring overnight at room temperature, the mixture was concentrated to 25 mL and washed with 2% citric acid (2x15 mL), $Na_2CO_{3\ (sat.)}$ (2x15 mL) and $NaCl_{\ (sat.)}$ (2x15 mL). The organic phase was dried over $MgSO_{4\ (anh.)}$, filtered and concentrated under reduced pressure at 50 ºC for 30 min to remove the maximum amount of DMF. The residue was purified by semipreparative RP-HPLC using a Sunfire™ C18 column (linear gradient from 30:70 to 60:40 ACN/H_2O in 15 min, flow rate = 15 mL/min; alternatively: isocratic 60:40 ACN/H_2O in 20 min, flow rate = 15 mL/min). Fractions were collected, pooled and lyophilized to afford the pure cyclic peptides. [*Note:* The isolated yields herein described correspond to the cyclization reactions performed in small scale (*i.e*. 0.036 mmol of linear pentapeptide substrate). For the cyclization reactions performed on a larger scale (*i.e.* 0.45 mmol of linear pentapeptide substrate), the isolated yields could not be properly determined due to problems with the HPLC equipment during the purification.]

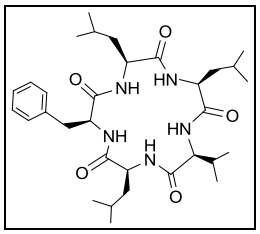

cyclo[Phe-Leu-Leu-Val-Leu] (1). Crude pentapeptide **p1** (22 mg, 89% purity, approx. 0.036 mmol) was cyclized and purified following the general procedure described above. This afforded cyclic peptide **c1** (12 mg, 58%). HPLC (linear gradient from 40% to 100% ACN over 8 min): t_r = 5.97 min, purity = 100%; ^{1}H-NMR (400 MHz, $CDCl_3$): δ 0.78 (d, *J* = 6.5 Hz, 6H), 0.88 (d, *J* = 6.5 Hz, 3H), 0.90-1.01 (m, 15H), 1.26-1.49 (3H), 1.49-1.74 (m, 4H), 1.87 (m, 1H), 2.02 (m, 2H), 2.95 (dd, *J* = 14.0, 8.9 Hz, 1H), 3.16 (dd, *J* = 14.0, 6.0 Hz, 1H), 3.91 (dd, *J* = 14.2, 6.8 Hz, 1H), 4.59-4.80 (m, 3H), 4.66 (dd, *J* = 14.4, 7.7 Hz, 1H), 6.88 (bs, 1H), 7.12 (bs, 1H), 7.15-7.30 (m, 5 H), 7.67 (bs, 1H), 7.80 (m, 2H); ^{13}C-NMR (100 MHz, $CDCl_3$): δ 18.6, 19.3, 22.0, 22.2, 22.3, 22.4, 22.6, 22.7, 24.6, 24.9, 25.4, 37.7, 38.6, 39.0, 39.7, 51.7, 53.7, 55.3, 57.9, 58.8, 127.0, 128.6, 129.0, 136.2, 171.2, 172.0, 172.6, 173.2, 173.4; HRMS (ES^+): calc. for $[C_{32}H_{51}N_5O_5 + H]^+$ 586.3963, found 586.3940.

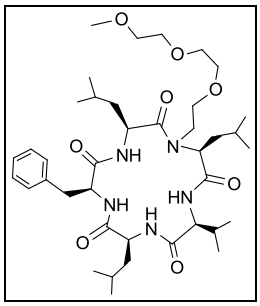

cyclo[Phe-Leu-(*N*-TEG)Leu-Val-Leu] (1a). Crude pentapeptide **p1a** (27 mg, 72% purity, approx. 0.036 mmol) was cyclized and purified following the general procedure described above. This afforded cyclopeptide **1a** (14 mg, 53%). HPLC (linear gradient from 40% to 100% ACN over 8 min): t_r = 7.53 min, purity = 95%; ^{1}H-NMR (400 MHz, $CDCl_3$): δ 0.63-1.04 (m, 24H), 1.05-1.74 (m, 7H), 1.87-2.22 (m, 2H), 3.19-3.48 (m, 6H), 3.45-3.90 (m, 12H), 3.91 (m, 1H), 4.01-4.27 (m, 2H), 4.47 (m, 1H), 4.95 (m, 1H), 6.28 (bs, 1H), 6.97 (bs, 1H), 7.11-7.36 (m, 5H), 7.38-7.68 (m, 1H), 7.78 (bs, 1H); ^{13}C-NMR (100 MHz, $CDCl_3$): δ 19.0, 19.1, 21.9, 22.4, 22.6, 22.7, 22.7, 23.0, 24.5, 24.8, 25.7, 29.7, 31.9, 34.2, 37.2, 39.8, 41.6, 48.6, 50.5, 52.6, 56.1, 58.9, 59.8, 66.4, 68.6, 70.2, 70.7, 71.6, 127.4, 128.8, 129.0, 136.0, 170.2, 172.6, (2C), 173.0 (2C); HRMS (ES^+): calc. for $[C_{39}H_{65}N_5O_8 + H]^+$ 732.4906, found 732.4910.

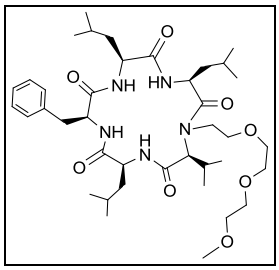

cyclo[Leu-Leu-(*N*-TEG)Val-Leu-Phe] (2a). Crude pentapeptide **p2a** (27 mg, 69% purity, approx. 0.036 mmol) was cyclized and purified following the general procedure described above. This afforded cyclopeptide **2a** (14 mg, 53%). HPLC (linear gradient from 40% to 100% ACN over 8 min): t_r = 7.22 min, purity = 98%; ^{1}H-NMR (400 MHz, $CDCl_3$): δ 0.75 (d, *J* = 6.6 Hz, 3H), 0.64 (d, *J* = 6.4 Hz, 3H), 0.84-0.97 (m, 18H), 1.17-1. 83 (m, 9H), 2.92-3.24 (m, 3H), 3.38 (s, 3 H), 3.50-3.72 (m, 12H), 3.67 (m, 1H), 3.97 (m, 1H), 4.27 (m, 1H), 4.46 (m, 1H), 4.97 (dd, *J* = 16.2 Hz, 7.6 Hz, 1H), 5.74 (bs, 1H), 6.51 (d, *J* = 8.6 Hz, 1H), 7.12-7.33 (m, 6H), 8.15 (d, *J* = 8.9 Hz, 1H); ^{13}C-NMR (100 MHz, $CDCl_3$): δ 19.1, 20.1, 21.1, 21.9, 22.6, 22.8, 22.9, 23.0, 24.4, 24.7, 24.8, 27.3, 29.7, 31.9, 34.2, 36.8, 39.5, 40.4, 41.3, 48.3, 50.4, 50.9, 53.5, 56.6, 59.0, 66.4, 68.5, 70.3, 70.4, 71.9, 127.1, 128.8, 128.9, 135.9, 170.8, 171.6 (2C), 173.0, 173.7; HRMS (ES^+): calc. for $[C_{39}H_{65}N_5O_8 + H]^+$ 732.4906, found 732.4920

.

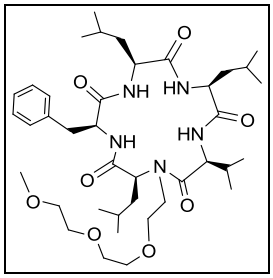

cyclo[Leu-Val-(*N*-TEG)Leu-Phe-Leu] (3a). Crude pentapeptide **p3a** (27 mg, 60% purity, approx. 0.036 mmol) was cyclized and purified following the general procedure described above. This afforded cyclopeptide **3a** (11 mg, 42%). HPLC (linear gradient from 40% to 100% ACN over 8 min): t_r = 6.98 min, purity = 100%; ^{1}H-NMR (400 MHz, $CDCl_3$): δ 0.77-1.01 (m, 24H), 1.24-2.02 (m, 8H), 2.02-2.17 (m, 2H), 2.94 (dd, *J* = 13.7, 8.0 Hz, 1H), 3.04-3.24 (m, 1H), 3.30-3.41 (m, 4H), 3.45-3.67 (m, 11H), 3.63-3.83 (m, 1H), 4.13-4.23 (m, 2H), 4.52-4.64 (m, 2H), 6.40 (d, *J* = 5.1 Hz, 1H), 6.45 (d, *J* = 9.5 Hz, 1H), 7.11-7.34 (m, 5H), 6.82 (d, *J* = 7.5 Hz, 1H), 8.42 (d, *J* = 9.4 Hz, 1H); ^{13}C-NMR (100 MHz, $CDCl_3$): δ 18.1, 19.4, 21.4, 22.2, 22.3, 22.4, 22.7, 22.8, 24.5, 25.2, 25.4, 29.7, 31.1, 36.9, 38.5, 39.8, 40.9, 51.2, 51.9, 53.9, 54.4, 55.4, 59.0, 67.9, 69.0, 70.3, 70.5, 70.6, 71.9, 126.7, 128.5, 129.1, 136.7, 171.5, 171.6, 171.7, 172.0, 173.5; HRMS (ES^+): calc. for $[C_{39}H_{65}N_5O_8 + H]^+$ 732.4906, found 732.4919.

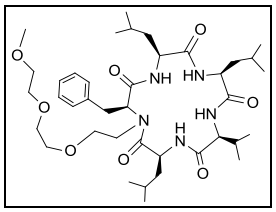

cyclo[Val-Leu-(*N*-TEG)Phe-Leu-Leu] (4a). Crude pentapeptide **p4a** (27 mg, 53% purity, approx. 0.036 mmol) was cyclized and purified following the general procedure described above. This afforded cyclopeptide **4a** (14 mg, 53%). HPLC (linear gradient from 40% to 100% ACN over 8 min): t_r = 7.34 min, purity = 100%; ^{1}H-NMR (400 MHz, $CDCl_3$): δ 0.88-1.09 (m, 24H), 1.33-1.79 (m, 9H), 2.22-2.39 (m, 1H), 3.05-3.22 (m, 2H), 3.22-3.33 (m, 3H), 3.34-3.44 (m, 4H), 3.49-3.61 (m, 7H), 3.68 (dd, *J* = 13.2, 10.2 Hz, 1H), 3.79 (dd, *J* = 9.9, 6.3 Hz, 1H), 4.13 (dd, *J* = 7.3, 5.8 Hz, 1H), 4.22 (dd, *J* = 14.6, 7.7 Hz, 1H), 4.42 (dd, *J* = 15.7, 7.1 Hz, 1H) , 4.87 (dd, *J* = 15.8, 7.2 Hz, 1H), 6.35 (bs, 1H), 6.65 (d, *J* = 6.8 Hz, 1H), 7.05 (bs, 1H), 7.13-7.29 (m, 5H), 8.10 (bs, 1H); ^{13}C-NMR (100 MHz, $CDCl_3$): δ 17.8, 19.5, 22.2, 22.2, 22.6, 22.6, 22.8, 22.9, 24.8, 24.8, 24.9, 29.4, 35.2, 39.7, 39.9, 41.5, 48.5, 51.0, 51.5, 52.8, 59.0, 60.2, 68.4, 70.3, 70.8, 71.9, 126.9, 128.5, 129.1, 137.3, 170.0, 171.2, 171.8, 173.5, 173.6; HRMS (ES$^+$): calc. for $[C_{39}H_{65}N_5O_8 + H]^+$ 732.4906, found 732.4917.

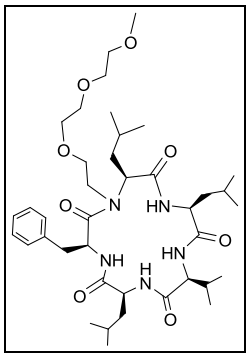

cyclo[Leu-Phe-(*N*-TEG)Leu-Leu-Val] (5a). Crude pentapeptide **p5a** (27 mg, 66% purity, approx. 0.036 mmol) was cyclized and purified following the general procedure described above. This afforded cyclopeptide **5a** (11 mg, 42%). HPLC (linear gradient from 40% to 100% ACN over 8 min): t_r = 7.05 min, purity = 100%; ^{1}H-NMR (400 MHz, $CDCl_3$): δ 0.83 (d, *J* = 6.6 Hz, 3 H), 0.84-1.01 (m, 21H), 1.20-1.35 (m, 1H), 1.35-1.50 (m, 1H), 1.49-1.69 (m, 4H), 1.92 (m, 1H), 2.01 (m, 2H), 2.10 (bs, 2H), 2.88 (dd, *J* = 13.1, 5.8 Hz, 1H), 3.08 (dd, *J* = 13.1, 9.0 Hz, 1H), 3.17-3.29 (m, 1H), 3.32-3.43 (m, 4 H), 3.45 (m, 1H), 3.45-3.66 (m, 9H), 3.79 (t, *J* = 8.9 Hz, 1H), 4.20 (m, 1H), 4.45 (dd, *J* = 16.3, 7.3 Hz, 1H), 5.10 (td, *J* = 8.9, 6.0 Hz, 1H), 6.37 (bs, 1H), 6.74 (d, *J* = 8.6 Hz, 1H), 7.13 (bs, 1H), 7.14-7.33 (m, 5H), 8.08 (d, *J* = 9.1 Hz, 1H); ^{13}C-NMR (100 MHz, $CDCl_3$): δ 19.1, 19.1, 21.1, 22.3, 22.3, 22.6, 22.8, 22.9, 24.9, 25.0, 25.3, 29.5, 38.3, 38.5, 40.1, 40.5, 51.2, 51.2, 51.3, 53.6, 58.9, 60.6, 68.0, 68.8, 70.3, 70.4, 70.5, 71.9, 126.6, 128.6, 129.6, 136.8, 171.1, 171.5, 171.7, 172.7, 173.4. HRMS (ES$^+$): calc. for $[C_{39}H_{65}N_5O_8 + H]^+$ 732.4906, found 732.4908.

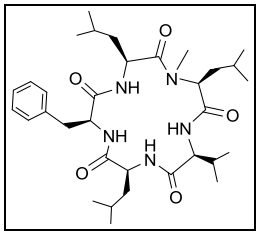

cyclo[Phe-Leu-*N*MeLeu-Val-Leu] (1b). Crude pentapeptide **p1b** (22 mg, 67% purity, approx. 0.036 mmol) was cyclized and purified following the general procedure described above. This afforded cyclopeptide **1b** (13 mg, 60%). HPLC (linear gradient from 40% to 100% ACN over 8 min): t_r = 7.36 min, purity = 95%; ^{1}H-NMR (400 MHz, $CDCl_3$): δ 0.63-1.04 (m, 24H), 1.05-1.74 (m, 7H), 1.87-2.22 (m, 2H), 3.19-3.48 (m, 6H), 3.45-3.90 (m, 12H), 3.91 (m, 1H), 4.01-4.27 (m, 2H), 4.47 (m, 1H), 4.95 (m, 1H), 6.28 (bs, 1H), 6.97 (bs, 1H), 7.11-7.36 (m, 5H), 7.38-7.68 (m, 1H), 7.78 (bs, 1H); ^{13}C-NMR (100 MHz, $CDCl_3$): δ 19.0, 19.1, 21.9, 22.4, 22.6, 22.7, 22.7, 23.0, 24.5, 24.8, 25.7, 29.7, 31.9, 34.2, 37.2, 39.8, 41.6, 48.6, 50.5, 52.6, 56.1, 58.9, 59.8, 66.4, 68.6, 70.2, 70.7, 71.6, 127.4, 128.8, 129.0, 136.0, 170.2, 172.6, (2C), 173.0 (2C); HRMS (ES$^+$): calc. for $[C_{33}H_{53}N_5O_5 + H]^+$ 600.4119, found 600.4131.

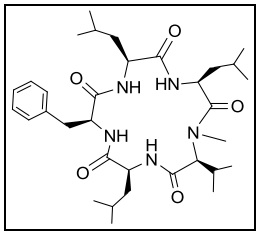

cyclo[Leu-Leu-*N*MeVal-Leu-Phe] (2b). Crude pentapeptide **p2b** (22 mg, 78% purity, approx. 0.036 mmol) was cyclized and purified following the general procedure described above. This afforded cyclopeptide **2b** (10 mg, 46%). HPLC (linear gradient from 40% to 100% ACN over 8 min): t_r = 7.07 min, purity = 100%; ^{1}H-NMR (400 MHz, $CDCl_3$): δ 0.62 (d, *J* = 5.0 Hz, 3 H), 0.73 (m, 3H), 0.84-0.99 (m, 18H), 1.20-1.34 (m, 2H), 1.34-1.51 (m, 2H), 1.45-1.79 (m, 5H), 2.84-3.14 (m, 6 H), 3.68 (m, 1H), 3.97 (m, 1H), 4.20 (m, 1H), 4.47 (m, 1H), 4.85 (d, *J* = 6.8 Hz, 1H), 5.71 (bs. 1H), 6.87 (bs, 1H), 7.04-7.31 (m, 5H), 8.04 (bs, 1H), 8.14 (bs, 1H); ^{13}C-NMR (100 MHz, $CDCl_3$): δ 19.1, 19.9, 21.0, 21.9, 22.6, 22.6, 22.7, 23.1, 24.2, 24.6, 25.0, 27.4, 29.7, 31.9, 34.2, 36.5, 39.3, 40.3, 40.9, 48.3, 51.5, 53.2, 57.5, 65.1, 127.1, 128.8, 128.9, 136.0, 170.6, 171.6, 172.2, 172.4, 174.3; HRMS (ES$^+$): calc. for $[C_{33}H_{53}N_5O_5 + H]^+$ 600.4119, found 600.4112.

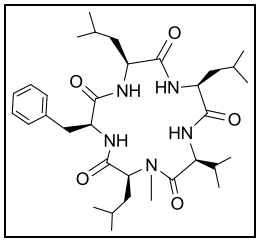

cyclo[Leu-Val-*N*MeLeu-Phe-Leu] (3b). Crude pentapeptide **p3b** (22 mg, 65% purity, approx. 0.036 mmol) was cyclized and purified following the general procedure described above. This afforded cyclopeptide **3b** (11 mg, 51%). HPLC (linear gradient from 40% to 100% ACN over 8 min): t_r = 6.82 min, purity = 100%; ^{1}H-NMR (400 MHz, $CDCl_3$): δ 0.77 (d, *J* = 6.3 Hz, 3H), 0.84 (d, *J* = 6.4 Hz, 6H), 0.95-0.82 (m, 12H), 0.97 (d, *J* = 6.2 Hz, 3H), 1.22-1.36 (m, 2H), 1.36-1.51 (m, 2H), 1.51-1.90 (m, 4H) 2.14 (m, 2H), 2.92-3.02 (m, 1H), 3.02-3.13 (m, 1H), 3.07 (s, 3H), 3.44 (t, *J* = 7.6 Hz, 1H), 4.05-4.27 (m, 2H), 4.49 (t, *J* = 9.4 Hz, 1H), 4.58 (dd, *J* = 16.7, 8.5 Hz, 1H), 6.54 (bs, 1H), 6.73 (bs, 1H), 7.03 (bs, 1H), 7.07-7.58 (m, 5H), 8.13 (bs, 1H); ^{13}C-NMR (100 MHz, $CDCl_3$): δ 18.1, 19.6,21.3, 21.9, 22.0, 22.5, 22.7, 22.8, 24.4, 25.2, 25.5, 29.7, 30.6, 31.9, 34.2, 36.7, 37.7, 39.8, 40.6, 52.1, 54.3, 54.6, 55.3, 68.9, 126.8, 128.5, 129.1, 136.6, 171.9, 172.1, 172.4, 172.6, 174.3; HRMS (ES^+): calc. for $[C_{33}H_{53}N_5O_5 + H]^+$ 600.4119, found 600.4109.

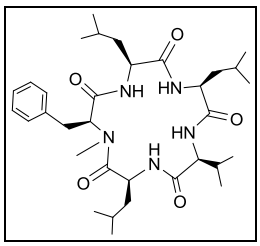

cyclo[Val-Leu-*N*MePhe-Leu-Leu] (4b). Crude pentapeptide **p4b** (22 mg, 83% purity, approx. 0.036 mmol) was cyclized and purified following the general procedure described above. This afforded cyclopeptide **4b** (11 mg, 51%). HPLC (linear gradient from 40% to 100% ACN over 8 min): t_r = 6.97 min, purity = 100%; ^{1}H-NMR (400 MHz, $CDCl_3$): δ 0.84 (d, *J* = 6.6 Hz, 6 H), 0.87-0.99 (m, 18 H), 1.27-1.73 (m, 9H), 2.33 (m, 1H), 2.74 (s, 3 H), 3.22 (dd, *J* = 11.6, 7.3 Hz, 1H), 3.69 (m, 1H), 3.70 (m, 1H), 4.11 (m, 1H), 4.24 (d, *J* = 6.9 Hz, 1H), 4.45 (dd, *J* = 15.5 Hz, 7.3 Hz, 1H), 4.73 (dd, *J* = 15.3 Hz, 7.2 Hz, 1H), 6.38 (bs, 1H), 6.85 (d, *J* = 8.3 Hz, 1H), 7.05-7.35 (m, 6H), 8.04 (bs, 1H); ^{13}C-NMR (100 MHz, $CDCl_3$): δ 17.6, 19.5, 22.2, 22.3, 22.4, 22.5, 22.5, 22.7, 24.6, 24.8, 24.9, 29.1, 29.7, 34.9, 39.6, 40.0, 41.2, 48.3, 51.7, 53.0, 60.2, 72.1, 127.0, 128.6, 128.8, 137.0, 170.1, 171.3, 172.6, 172.8, 173.6; HRMS (ES^+): calc. for $[C_{33}H_{53}N_5O_5 + H]^+$ 600.4119, found 600.4130.

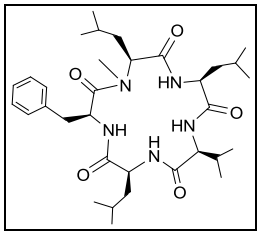

cyclo[Leu-Phe-*N*MeLeu-Leu-Val] (5b). Crude pentapeptide **p5b** (22 mg, 80% purity, approx. 0.036 mmol) was cyclized and purified following the general procedure described above. This afforded cyclopeptide **5b** (10 mg, 46%). HPLC (linear gradient from 40% to 100% ACN over 8 min): t_r = 6.86 min, purity = 100%; ^{1}H-NMR (400 MHz, $CDCl_3$): δ 0.78 (d, *J* = 6.4 Hz, 3 H), 0.92-0.97 (m, 21 H), 1.07-1.26 (m, 1H), 1.33-1.48 (m, 1H), 1.45-1.80 (m, 5H), 1.99 (m, 1 H), 2.23 (m, 1H), 3.10 (m, 1 H), 3.41 (m, 1H), 3.74 (m, 1H), 4.21 (m, 1H), 4.45 (m, 1H), 5.06 (m, 1H), 6.49 (bs, 1H), 6.99 (bs, 1H), 7.09-7.37 (m, 5H), 7.45 (bs, 1H), 7.86 (bs, 1H); ^{13}C-NMR (100 MHz, $CDCl_3$): δ 19.1, 19.2, 20.9, 21.5, 22.3, 22.5, 23.0, 23.1, 24.9, 25.0, 25.1, 29.4, 29.7, 36.3, 38.0, 39.8, 40.3, 51.3, 51.6, 53.5, 61.2, 69.3, 126.7, 128.3, 129.6, 137.0, 171.1, 172.0, 172.1, 173.0, 173.9; HRMS (ES^+): calc. for $[C_{33}H_{53}N_5O_5 + H]^+$ 600.4119, found 600.4125.

2.4. CELL CULTURE PROTOCOLS AND BIOLOGICAL ACTIVITY EVALUATION

2.4.1. Cell culture protocols

- Cancer cell lines. The cancer cell lines used in this study were: GLC-4 (small cell lung cancer), MDA-MB-231 (breast cancer) and SW-480 (colon cancer). All of them proceeded from the American Type Culture Collection (ATCC).

- Cryopreservation of cell lines. Cells were centrifuged to remove medium. Then, they were re-suspended its culture medium supplemented with 10% sterile DMSO at a concentration between 1 and $2{\cdot}10^6$ cells/mL. 2 mL aliquotes of this suspension were transferred to sterile cryovials conveniently placed on a freezing rack. These

cryovials were kept at -80 ºC during 24 h and then transferred to a liquid nitrogen tank for permanent storage at this temperature.

- Defrosting of cell lines. The appropriate cell culture medium was warmed up to 37 ºC. The cryovial containing cells in frozen medium was taken from the nitrogen tank and placed in a 37 ºC water bath. When the content of the tube was almost defrosted, it was transferred to a 15 mL falcon containing a 10-fold volume of warm culture medium. Cells were centrifuged 5 min at 800 rpm to remove the DMSO-containing medium. Then they were re-suspended in fresh medium and seeded in a plate or flask. After initial cell cultivation, it is recommended to freeze 3 to 4 vials for each vial of cells thawed as soon as possible.

- Growing of cell lines. GLC-4 cancer cells were grown in suspension, while MDA-MB-231 and SW-480 cancer cells were grown as an adherent culture. As indicated in the following table, cells were grown in RPMI 1640 (Roswell Park Memorial Institute medium), DMEM (Dubelco's modified Eagle's medium) or L-15 (Leibovitz medium). In all cases, the medium was supplemented with 10% fetal bovine serum, 2 mM L-glutamine, 100 u/mL penicillin and 100 µg/mL streptamicin. The medium was changed every few days. Cells were maintained at 37 ºC in humidified 5% CO_2.

Cell line	Description	Medium	Serum	L-Glutamine	Penicillin	Streptamicin
GLC-4	SCLC	RPMI	10% FBS	2 mM	100 u/mL	100 µg/mL
MDA-MB-231	Breast adenocarcinoma	DMEM	10% FBS	2 mM	100 u/mL	100 µg/mL
SW-480	Colon adenocarcinoma	L-15	10% FBS	2 mM	100 u/mL	100 µg/mL

Suspension cells were regularly seeded into 25 cm^2 or 75 cm^2 flasks. Adherent cells were regularly seeded into 60 mm or 100 mm plates. Cell growth was monitorized every few days under a phase-contrast microscope. When an 80% confluence was reached, cells were split. In case of adherent cell cultures, they have to be digested with trypsin prior to split.

- Change of medium.
  - Suspension cells. The appropriate medium and the PBS were warmed up to 37 ºC. Cells were centrifuged 5 min at 800 rpm and the supernatant was removed. Cells were re-suspended in PBS (5 mL) and centrifuged 5 min at 800 rpm. The PBS was removed and the cells were re-suspended in fresh medium (5 mL for a 25 cm^2 flask, 20 mL for a 75 cm^2 flask)
  - Adherent cells. The appropriate medium and the PBS were warmed up to 37 ºC. The cell-culture medium was removed. Cells were washed with PBS (2x3 mL for a 60 mm plate, 2x5 mL for a 100 mm plate). Fresh medium was added to the plate (5 mL for a 60 mm plate, 10 mL for a 100 mm plate).

- Trypsinization of adherent cells. Trypsinization is the process of using trypsin to dissociate adherent cells from the vessel in which they are being cultured. When added to a cell culture, trypsin breaks down the proteins which enable the cells to adhere to the vessel. Our protocol to trypsinize an adherent cell culture was the following. The appropriate medium, the PBS and the trypsin were warmed up to 37 ºC. The cell-culture medium was removed. Cells were washed with PBS (2x3 mL for a 60 mm plate, 2x5 mL for a 100 mm plate). Trypsin-EDTA 0.25% was added (0.5 mL for 60 mm plate, 1 mL for a 100 mmm plate) ensuring that trypsin covered the entire surface ion which cells were adhered. The plate was incubated for 2 or 3 minutes. The cell culture was observed under a phase-contrast microscope. If detachment was low, the plate was incubated for another minute and detachment was checked every minute thereafter (trypsinization time varies depending on the cell type). When the cells had rounded up and were coming off the plate, they were re-suspended in an excess of serum-containing medium (4 mL for a 60 mm plate, 10 mL for a 100 mmm plate) to inactivate trypsin.

- Determination of cellular density. The density of our cell suspensions (cells/mL) was determined using a hemocytometer. This device consists of a thick glass microscope slide with a rectangular indentation that creates a chamber. The chamber is engraved with a laser-etched grid of perpendicular lines. The device is carefully crafted so that the chamber's volume is exactly known. The chamber is filled with a sample of the cell suspension and the cells in the chamber are counted. By dividing the number of cells in the chamber between the chamber's volume, the concentration of the cells in the original sample can be determined.

  i. Filling the chamber. The chamber is carefully cleaned with lens paper with ethanol to remove any grease. The appropriate coverslip is positioned over chamber. A 10 µL sample of cell suspension (which has been just gently shaken to ensure homogeneicity) is withdrawn with a pipette. The pipette should be held at a 45 º angle to the chamber. The cell suspension is applied to the edge of the coverslip. The sample quickly fills the chamber by capillary action.

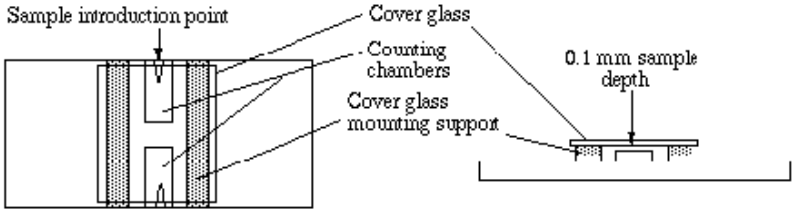

  ii. Cell counting. The chamber is observed through a phase-contrast microscope. The chamber has four 4 corner squares and each of them has 4x4 subdivisions. The number of cells in each of the 4 squares is counted, scanning the subdivisions from left to right updown. Different kinds of cells are counted separately as long as they are visually distinguishable. After counting the number of cells in each square, the average number of cells/square is calculated.

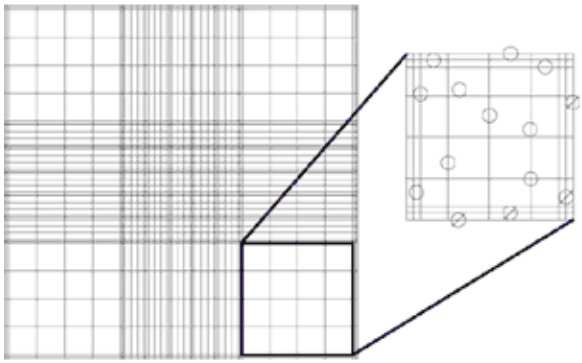

  iii. Determination of the cellular density. The volume overlying each of the 4 squares is 0.1 µl. Therefore, the number of cells/mL in the mixture where the sample comes from can be calculated by multiplying the average number of cells/square per 10^4.

$$(\text{cells/mL}) = (\text{average number of cells/square}) \cdot 10^4$$

2.4.2. Determination of cell viability through MTT assay

The cytotoxicity of our compounds was evaluated by treating the cancer cells with our compounds and monitoring cell viability through MTT assay. This assay is a colorimetric method to determine cell growth.[192] It is frequently used to evaluate the cytotoxity of potential therapeutic agents, since these agents would stimulate or inhibit cell viability and

growth. The test is based on the reduction of the yellow tetrazolium salt MTT to purple formazan crystals. This transformation only takes place in viable cells, because mitochondrial succinic dehydrogenase -the enzyme that metabolyzes MTT- is only active in living cells. In the MTT assay, the purple formazan crystals are dissolved in isopropanol and the absorbance at 570 nm is measured in an spectrophotometer. The net absorbance is directly proportional to the number of metabolically active cells. However, it should be pointed out that a decrease in cell growing determined by the MTT assay can be due to cell death, due to a decrease in cell proliferation of drug-treated cells (in comparison with untreated cells), or due to both.

- Procedure for MTT assay. To each well (containing a volume of 100 µL), 10 µL of MTT reagent (*i.e.* a 5 mg/mL solution of MTT in PBS) were added and the plate was incubated for 4 h. Then, the purple formazan crystals were dissolved by adding 100 µL of isopropanol/HCl $_{(aq.)}$ 1 M 24:1. The absorbance at 570 nm was measured in an ELISA plate reader. 100% cell viability was given to the net absorbance of the untreated cells, which were used as a control, and the % of cell viability was expressed as a percentage of the untreated control cells.

- Evaluation of compound cytotoxicity against various cancer cell lines. GLC-4 cells were seeded into 96-well plates at a concentration of 20000 cells/well. MDA-MB-231 and SW-480 cells were seeded into 96-well plates at a concentration of 5000 cells/well and incubated at 37 ºC during 24 h prior to drug addition. The different compounds were added at a 10 or 50 µM concentration (depending on the experiment), the final volume in each well being 100 µL. The DMSO concentration was kept constant at 1% in all wells. Cells were cultured with and without the compounds for 24, 48 and/or 72 h (depending on the experiment). After this time, the MTT assay was performed using the above-described procedure. The % of cell viability was expressed as a percentage of the untreated control cells. Each experiment was performed three times, seeding the three plates three different times and, for each plate, all test conditions were assayed in triplicate wells. Results were averaged and expressed with the corresponding standard deviation.

- Determination of the IC_{50} (72 h) of the most potent compounds. Cells were seeded into 96-well plates at a concentration of 20000 cells/well. The compound was added at different concentrations between 5 and 100 µM (final volume in each well = 100 µL). The DMSO concentration was kept constant at 1% in all wells. Cells were incubated with and without the compound for 72 h. After this time, MTT assay was performed using the above-described procedure. The % of cell viability was plotted for the different concentrations of the compound. IC_{50} was calculated by interpolation from the dose-reponse curve. All test conditions were assayed in triplicate wells and results were averaged.

2.5. ATTEMPTS TO DTETERMINE logP BY THE SHAKE-FLASK METHOD

Our procedure to try to determine logP by the shake-flask method was the following. 0.03 mmol (or 500 µg) of the compound of study were placed in a 1.5 mL eppendorf. The compound was redissolved in 200 µL of octanol (previously saturated with H_2O) and 200 µL of H_2O (previously saturated with octanol) were added, so that the final concentration of the compound was 75 µM (1.25 µg/µL). The mixture was shaken in a mechanical shaker for 2 days to ensure that equilibrium between both phases was reached. Then, the eppendorfs were centrifuged, phases were separated and an aliquot of each phase was injected into the HPLC apparatus. UV detection was performed at 220 nnm. The relation between the HPLC peak areas of the compound in each phase was used to calculate logP. Since the initial compound concentration is known, retention of compound of study in the interphase can be detected. [*Presaturation of the solvent:* Before partition experiments, the two phases of the solvent system were mutually

saturated. For doing this, two large stock bottles of octanol and H_2O with a sufficient quantity of the other solvent were stirred for 2 days. Then, phases were separated using an extraction funnel.]

2.6. NMR STUDIES OF PEPTIDES 1, 5a AND 5b

- Variable temperature ^{1}H-NMR experiments: For compounds **1**, **5a** and **5b**, ^{1}H-NMR spectra were acquired in the range from 278 K to 318 K with a step size of 10 K. All spectra were recorded on a Bruker Digital Avance 600 MHz spectrometer equipped with a TCI cryoprobe. Measurements were done with 5-20 mM sample solutions in $CDCl_3$. Calibration was performed with reference to the residual solvent signal (^{1}H, 7.26 ppm). Under these conditions, a single set of H^N- and H^α-signals was observed for each peptide and no evidence of conformational equilibria was found.

- Assignment of the H^N-, H^α- and C^α-signals: For compounds **1**, **5a** and **5b**, two-dimensional NMR experiments (COSY, HSQC, TOCSY and NOESY) were carried out. All spectra were recorded at 298 K on a Bruker Digital Avance 600 MHz spectrometer. Measurements were done with 5-20 mM sample solutions in $CDCl_3$. Calibration was performed with reference to the residual solvent signal (^{1}H, 7.26 ppm; ^{13}C, 77.0 ppm). TOCSY spectra were recorded with a mixing time of 70 ms, and NOESY spectra with a mixing time of 500 ms. The assignment of the H^N-, H^α- and C^α- ressonances was accomplished using by through-bond connectivities from the two-dimensional spectra. In particular, we used the $(H^\alpha)_i$-$(H^N)_{i+1}$ cross-peaks from the NOESY spectra, the $(H^\alpha)_i$-$(H^\beta)_i$ cross-peaks from the COSY spectra, the $(H^\alpha)_i$-$(H^\beta)_i$-$(H^\beta)_i$-$(H^N)_i$ the cross-peaks from the TOCSY spectra, and the $(H^\alpha)_i$-$(C^\alpha)_i$ cross-peaks from the HSQC spectra. All the signals could be unequivocally assigned.

- Determination of temperature coefficients for the amide protons: For compounds **1**, **5a** and **5b**, the temperature coefficients for the amide protons were determined from the variable temperature ^{1}H-NMR experiments. The H^N-chemical shifts were plotted versus the acquisition temperature (278 K, 288 K, 298 K, 308 K, 318 K) and the data points were adjusted to a linear fit using an Excel software package. In all cases, a good linear correlation was observed.

EXPERIMENTAL PROCEDURES FOR CHAPTER 3

3.1. SYNTHESIS OF THE *N*-OEG BUILDING BLOCKS

3.1.1. Synthesis of Fmoc-D-Phe-Cl

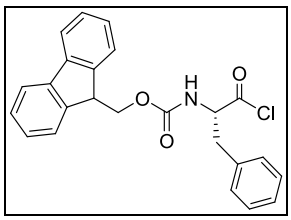

A suspension of Fmoc-D-Phe-OH (3.87 mmol, 1.50 g) and $SOCl_2$ (38.71 mmol, 2.81 mL) in DCM (10 mL) was stirred at room temperature under N_2 atmosphere. After 6 h a clear solution had formed but subsequently the acid chloride began to precipitate. The mixture was stirred overnight and then concentrated under reduced pressure. The resulting yellow solid was triturated and washed onto a filter funnel with hexane. The precipitate was dissolved in DCM (4 mL) and addition of hexane (12 mL) precipitated the pure Fmoc-D-Phe-Cl. Recrystallization from Hexane/DCM 3:1 afforded 1.57 g (100%) of pure product, which was obtained as a white solid. ^{1}H-NMR spectral data matched literature values.[193] To check for any residual acid content, a

small amount of recristallized Fmoc-D-Phe-Cl (1 mg) was added to dry methanol and analyzed by HPLC-MS, which reveals the ratio of acid chloride (as methyl ester) and free acid. HPLC-MS analysis upon esterification showed 100% of Fmoc-D-Phe-OMe ($[M+4]^+$ = 402.61) and no residual acid.

3.1.2. General procedure for reductive alkylation + Fmoc- protection

To a solution of aldehyde (1.1 equiv.) and amino acid *tert*-butyl ester hydrochloride (1.0 equiv.) in MeOH/AcOH 99:1 (aprox. 8 mL/mmol of substrate) was added $NaBH_3CN$ (1.34 equiv.) over a period of 30 min. The resulting solution was stirred at room temperature for 2.5 h and then was poured into 30 mL of $NaHCO_{3\ (sat.)}$. The product was extracted with AcOEt (2x50 mL). The combination of organic phases was washed with $NaCl_{\ (sat.)}$ (2x50 mL), dried over $MgSO_{4\ (anh.)}$, filtered and concentrated under reduced pressure. The resulting residue consisted of an unseparable mixture of the expected product and *N,N*-dialkylated amino acid. This residue was dissolved in DCM (50 mL) and treated with Fmoc-Cl (1.5 equiv.) in the presence of DIEA (2.5 equiv.) under N_2 atmosphere. After overnight stirring at room temperature, the solvent was removed under reduced pressure and the residue was redissolved in AcOEt (100 mL). The organic phase was washed with $HCl_{\ (aq.)}$ 1M (2x40 mL), dried over $MgSO_{4\ (anh.)}$, filtered and concentrated under reduced pressure. The residue was purified by flash chromatography (**9**: Hexane/AcOEt 75:25; **10** and **11**: AcOEt/MeOH/AcOH 90:10:1), which afforded the desired product.

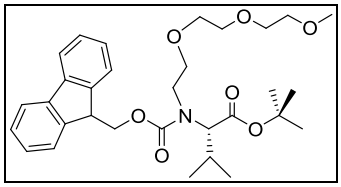

Fmoc-(*N*-OEG$_2$)Val-O^{t}Bu (9). Following the general procedure described above with 3,6,9-trioxadecanaldehyde (1.421 g, 11.26 mmol) and valine *tert*-butyl ester hydrochloride (2.325 g, 10.23 mmol), compound **9** (2.992 g, 54%) was obtained as colorless oil. ^{1}H-NMR (400 MHz, $CDCl_3$): δ 0.66-0.81 (m, 3H), 0.84-0.99 (m, 3H), 1.41 (s, 9H), 1.98-2.23 (m, 1H), 3.20-3.72 (m, 15H), 3.82-4.14 (m, 1H), 4.23 (m, 1H), 4.28-4.63 (m, 2H), 7.31 (t, *J* = 7.4 Hz, 2H), 7.39 (t, *J* = 7.4 Hz, 2H), 7.59 (d, *J* = 7.4 Hz, 2H), 7.75 (d, *J* = 7.5 Hz, 2H); ^{13}C-NMR (100 MHz, $CDCl_3$): δ 19.3, 20.2, 28.2, 44.7, 47.6, 47.7, 59.2, 66.6, 66.3, 67.2, 67.6, 68.9, 69.3, 70.5, 70.7, 72.1, 81.5, 81.6, 120.2, 125.0, 125.1, 125.2, 127.3, 127.4, 127.9, 141.6, 144.1, 144.2, 156.5, 156.8, 170.0, 170.3; IR (KBr): ν = 2965.39, 2928.51, 1730.75, 1703.74, 1451.78, 1416.11, 1368.26, 1279.93, 1140.40, 1129.49, 759.78, 741.14 cm^{-1}; $[\alpha]_D$ -32.5 (MeOH, 0.01 g/mL); HRMS (ES$^+$): calc. for $[C_{31}H_{43}NO_7 + NH_4]^+$ 559.3378, found 559.3374. [*Note:* This compound is the same as Fmoc-(*N*-TEG)Val-O^{t}Bu (**2**) from Chapters 1 and 2.]

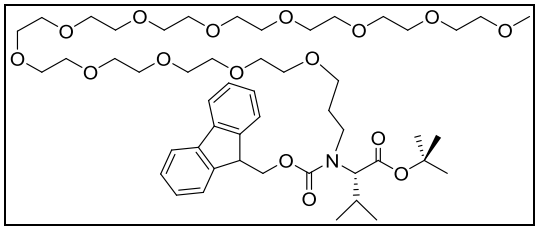

Fmoc-(*N*-OEG$_{11}$)Val-O^{t}Bu (10). Following the general procedure described above with CH_3-O-$(CH_2CH_2O)_{11}$-CH_2CH_2-CHO (320 mg, 0.56 mmol) and valine *tert*-butyl ester hydrochloride (106 mg, 0.51 mmol), compound **10** (232 mg, 48%) was obtained as a colorless oil. ^{1}H-NMR (400 MHz, $CDCl_3$): δ 0.67-0.79 (m, 3H), 0.86-0.97 (m, 3H), 1.42 (s, 9H), 2.89-3.73 (m, 52H), 3.85-4.08 (m, 1H), 4.23 (t, *J* = 5.9 Hz, 1H), 4.27-4.62 (m, 2H), 7.30 (t, *J* = 7.1 Hz, 2H), 7.38 (t, *J* = 7.4 Hz, 2H), 7.60 (m, 2H), 7.75 (d, *J* = 7.4 Hz, 2H); ^{13}C-NMR (100 MHz, $CDCl_3$): δ 19.0, 19.9, 28.0, 29.7, 31.9, 42.9, 47.4, 59.0, 65.7, 65.8, 66.7, 67.2, 69.1, 69.2, 69.9, 70.5, 71.9, 81.2, 119.9, 124.7, 127.0, 127.6, 141.4, 144.1, 156.6, 170.2; IR (KBr): ν = 2921.06, 2868.70, 1729.81, 1700.55, 1451.62, 1418.07, 1367.81, 1348.92, 1282.12, 1249.81, 1108.94, 741.64 cm^{-1}; $[\alpha]_D$ -20.5 ($CHCl_3$, 0.01 g/mL); HRMS (ES$^+$): calc. for $[C_{50}H_{81}NO_{16} + NH_4]^+$ 969.5894, found 969.5895.

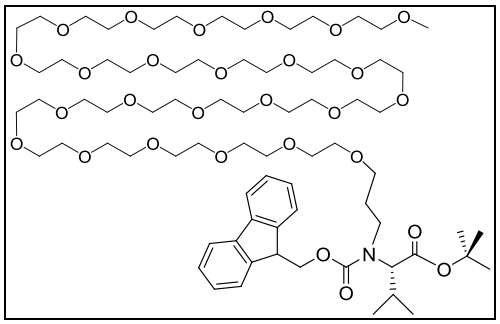

Fmoc-(*N*-OEG$_{23}$)Val-O^{t}Bu (11). Following the general procedure described above with CH_3-O-$(CH_2CH_2O)_{23}$-CH_2CH_2-CHO (66 mg, 0.06 mmol) and valine *tert*-butyl ester hydrochloride (11 mg, 0.05 mmol), compound **11** (31 mg, 44%) was obtained as a colorless oil. ^{1}H-NMR (400 MHz, $CDCl_3$): δ 0.67-0.79 (m, 3H), 0.86-0.97 (m, 3H), 1.42 (s, 9H), 2.95-3.95 (m, 100H), 3.88-4.10 (m, 1H), 4.23 (t, *J* = 5.8 Hz, 1H), 4.29-4.62 (m, 2H), 7.31 (t, *J* = 7.4 Hz, 2H), 7.39 (t, *J* = 7.3 Hz, 2H), 7.61 (m, 2H), 7.75 (d, *J* = 7.5 Hz, 2H); ^{13}C-NMR (100 MHz, $CDCl_3$): δ 19.0, 19.9, 27.9, 28.0, 28.5, 42.9, 47.4, 59.0, 65.6, 65.8, 66.7, 67.2, 69.0, 69.2, 69.9, 70.5, 71.9, 81.2, 81.3, 119.9, 124.7, 124.9, 127.0, 127.6, 141.3, 144.0, 144.0, 156.0, 156.6, 169.9, 170.2; IR (KBr): ν = 2870.59, 1728.69, 1700.91, 1451.42, 1418.04, 1368.10, 1349.48, 1282.68, 1250.22, 1110.59, 740.90 cm^{-1}; $[\alpha]_D$ -25.1 ($CHCl_3$, 0.01 g/mL); HRMS (ES$^+$): calc. for $[C_{74}H_{129}NO_{28} + NH_4]^+$ 1497.9039, found 1497.9010.

3.1.3. General procedure for reductive alkylation + acylation with Fmoc-D-Phe-OH

To a solution of aldehyde (1.1 equiv.) and amino acid *tert*-butyl ester hydrochloride (1.0 equiv.) in MeOH/AcOH 99:1 (aprox. 8 mL/mmol of substrate) was added $NaBH_3CN$ (1.34 equiv.) over a period of 30 min. The resulting solution was stirred overnight at room temperature and then poured into 30 mL of $NaHCO_{3\ (sat.)}$. The product was extracted with AcOEt (2x50 mL). The combination of organic phases was washed with $NaCl_{\ (sat.)}$ (2x50 mL), dried over $MgSO_{4\ (anh.)}$, filtered and concentrated under reduced pressure. The resulting residue consisted of an unseparable mixture of the expected product and *N,N*-dialkylated amino acid. This residue was dissolved in DCM (aprox. 5 mL/mmol of substrate) and treated with Fmoc-D-Phe-Cl (1.5 equiv.) in the presence of DIEA (2.5 equiv.) under N_2 atmposhere. The mixture was stirred overnight at room temperature. Then, the solvent was removed under reduced pressure and the residue and redissolved in AcOEt (100 mL). The organic phase was washed with $HCl_{\ (aq.)}$ 1M (2x40 mL) and then $NaHCO_{3\ (sat.)}$ (2x40 mL), dried over $MgSO_{4\ (anh.)}$, filtered and concentrated under reduced pressure. The resulting residue was purified by flash chromatography (AcOEt/MeOH/AcOH 90:10:1), which afforded the desired product.

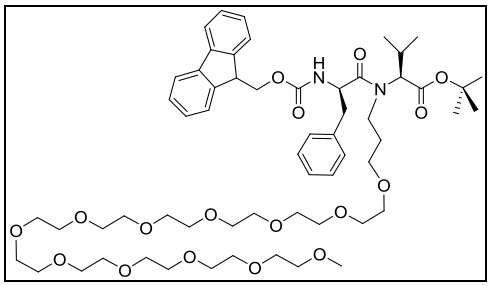

Fmoc-D-Phe-(*N*-OEG$_{11}$)Val-O^{t}Bu (15). Following the general procedure described above with CH_3-O-$(CH_2CH_2O)_{11}$-CH_2CH_2-CHO (1.000 g, 1.75 mmol) and valine *tert*-butyl ester hydrochloride (333 mg, 1.59 mmol), compound 1**5** (638 mg, 37%) was obtained as a colorless oil. ^{1}H-NMR (400 MHz, $CDCl_3$): δ 0.60-1.05 (m, 6H), 1.34-1.52 (m, 9H), 1.57-2.40 (m, 2H), 2.85-3.11 (m, 1H), 3.12-3.82 (m, 53H), 3.90-4.43 (m, 4H), 4.96 (m, 1H), 6.12-6.42 (m, 1H), 7.15-7.31 (m, 7H), 7.36 (t, *J* = 7.4 Hz, 2H), 7.54 (d, *J* = 7.4 Hz, 2H), 7.72 (d, *J* = 7.3 Hz, 2H); ^{13}C-NMR (100 MHz, $CDCl_3$): δ 19.1, 19.2, 27.5, 27.6, 27.9, 28.0, 29.6, 29.8, 39.1, 41.2, 46.9, 47.0, 52.5., 52.6, 66.8, 66.9, 67.0, 67.0, 68.2, 68.2, 69.3, 69.8, 70.1, 70.3, 70.4, 71.8, 81.3, 81.4, 125.1, 125.1, 125.2, 126.8, 126.9, 126.9, 127.5, 128.3, 128.4, 129.4, 129.5, 136.0, 136.3, 141.1, 141.1, 143.7, 143.8, 155.6, 155.9, 168.9, 169.0, 172.9, 173.1; IR (KBr): ν = 3287.94, 2871.78, 1782.00, 1639.03, 1532.42, 1452.26, 1351.58, 1250.12, 1110.62, 1037.62, 952.33, 800.76, 760.61, 742.44, 703.60 cm^{-1}; $[\alpha]_D$ -16.9 ($CHCl_3$, 0.01 g/mL); HRMS (ES$^+$): calc. for $[C_{59}H_{90}N_2O_{17} + NH_4]^+$ 1116.6578, found 1116.6573.

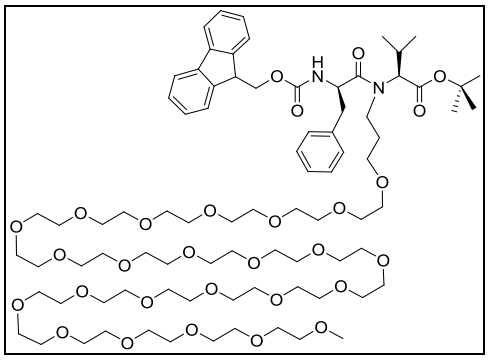

Fmoc-D-Phe-(*N*-OEG$_{23}$)Val-O^{t}Bu (16). Following the general procedure described above with CH_3-O-$(CH_2CH_2O)_{23}$-CH_2CH_2-CHO (1.000 g, 0.91 mmol) and valine *tert*-butyl ester hydrochloride (174 mg, 0.83 mmol), compound 1**6** (374 mg, 28%) was obtained as a colorless oil. ^{1}H-NMR (400 MHz, $CDCl_3$): δ 0.65-1.06 (m, 6H), 1.38-1.53 (m, 9H), 1.61-2.36 (m, 2H), 2.83-3.26 (m, 1H), 3.27-3.85 (m, 101H), 3.94-4.45 (m, 4H), 4.95 (m, 1H), 5.58 (m, 1H), 7.11-7.34 (m, 7H), 7.38 (m, 2H), 7.52 (m, 2H), 7.75 (m, 2H); ^{13}C-NMR (100 MHz, $CDCl_3$): δ 18.5, 19.2, 19.3, 20.5, 27.6, 27.7, 27.9, 29.6, 30.0, 38.4, 39.6, 41.1, 47.0, 47.1, 51.8, 52.4, 59.0, 66.7, 66.8, 66.9, 68.4, 69.3, 69.9, 70.1, 70.2, 70.5, 70.8, 71.9, 81.3, 82.7, 119.9, 125.0, 125.2, 126.9, 127.0, 127.6, 128.3, 128.5, 129.4, 129.6, 135.9, 136.3, 141.2, 141.2, 143.7, 143.8, 143.8, 155.4, 155.5, 168.9, 169.7, 171.5, 172.3; IR (KBr): ν = 3287.15, 2868.84, 1723.24, 1648.89, 1529.73, 1451.39, 1349.20, 1248.17, 1107.27, 1036.50, 950.48, 848.61, 760.21, 742.19, 701.78 cm^{-1}; $[\alpha]_D$ -28.2 (MeOH, c = 0.01 g/mL); HRMS (ES$^+$): calc. for $[C_{83}H_{138}N_2O_{29} + NH_4]^+$ 1644.9724, found 1644.9714.

3.1.4. General procedure for *tert*-butyl ester acidic cleavage

The *tert*-butyl protected amino acid (approx. 5.0 mmol) was dissolved in DCM (25 mL) and TFA (25 mL) was added. After stirring for 30 min at room temperature, the mixture was concentrated under reduced pressure. The remaining TFA was removed by co-evaporation with toluene at 50 ºC.

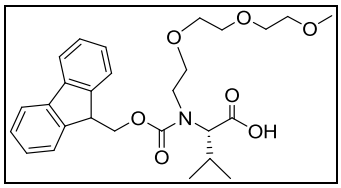

Fmoc-(*N*-OEG$_2$)Val-OH (12). Following the general procedure described above with **9** (2.992 g, 5.52 mmol), compound **12** (2.682 g, 100%) was obtained as yellowish oil. ^{1}H-NMR (400 MHz, $CDCl_3$): δ 0.67-0.77 (m, 3H), 0.94-1.20 (m, 3H), 2.11-2.39 (m, 1H), 3.00-3.74 (m, 15H), 3.94 (d, *J* = 10.7 Hz, 1H), 4.25 (m, 1H), 4.32-4.70 (m, 2H), 7.30 (t, *J* = 7.4 Hz, 2H), 7.37 (t, *J* = 7.4 Hz, 2H), 7.60 (m, 2H), 7.73 (d, *J* = 7.5 Hz, 2H), 8.8 (bs, 1H); ^{13}C-NMR (100 MHz, $CDCl_3$): δ 18.6, 18.7, 20.2, 20.5, 27.1, 27.5, 46.7, 47.2, 47.3, 58.6, 58.7, 66.2, 67.0, 67.5, 69.1, 69.2, 69.8, 69.9, 70.1, 70.2, 70.4, 71.6, 119.8, 124.6, 127.1, 127.6, 141.3, 141.3, 141.4, 143.7, 143.8, 143.8, 143.9, 155.9, 156.5, 171.7, 171.1; IR (KBr): ν = 3063.88, 2890.62, 1739.90, 1703.63, 1451.94, 1419.21, 1274.55, 1243.43, 1138.12, 1107.59, 758.96, 741.78 cm^{-1}; $[\alpha]_D$ -29.4 (MeOH, 0.01 g/mL); HRMS (ES$^+$): calc. for $[C_{27}H_{35}NO_7 + Na]^+$ 508.2306, found 508.2303. [*Note:* This compound is the same as Fmoc-(*N*-TEG)Val-OH (**6**) from Chapters 1 and 2.]

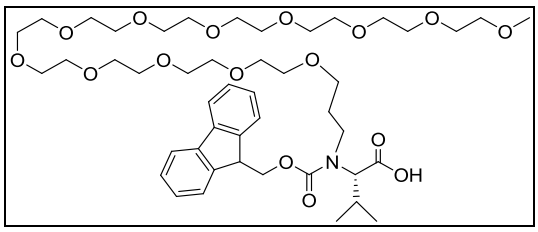

Fmoc-(*N*-OEG$_{11}$)Val-OH (13). Following the general procedure described above with **10** (170 mg, 0.179 mmol), compound **13** (159 mg, 100%) was obtained as yellowish oil. ^{1}H-NMR (400 MHz, $CDCl_3$): δ 0.68-0.79 (m, 3H), 0.92-1.00 (m, 3H), 2.89-3.73 (m, 52H), 3.87-4.10 (m, 1H), 4.23 (m, 1H), 4.29-4.70 (m, 2H), 5.26 (bs, 1H), 7.31 (t, *J* = 7.1 Hz, 2H), 7.39 (t, *J* = 7.4 Hz, 2H), 7.62 (m, 2H), 7.75 (d, *J* = 7.5 Hz, 2H); ^{13}C-NMR (100 MHz, $CDCl_3$): δ 18.6, 18.9, 19.9, 20.2, 27.5, 27.7, 27.9, 28.5, 44.9, 47.3, 58.9, 67.1, 67.6, 68.3, 68.6, 69.9, 70.4, 71.8, 119.9, 124.6, 125.2, 127.1, 127.6, 128.1, 128.9, 141.4, 143.8, 157.3, 171.8; IR (KBr): ν = 2921.85, 1735.56, 1699.53, 1451.75, 1419.92, 1349.59, 1287.42, 1249.66, 1109.80, 751.24, 742.20 cm^{-1}; $[\alpha]_D$ -12.3 ($CHCl_3$, 0.01 g/mL); HRMS (ES$^+$): calc. for $[C_{46}H_{73}NO_{16} + NH_4]^+$ 913.5268, found 913.5270.

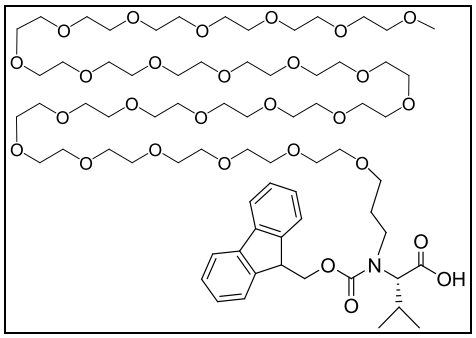

Fmoc-(*N*-OEG$_{23}$)Val-OH (14). Following the general procedure described above with **11** (36 mg, 0.024 mmol), compound **14** (34 mg, 100%) was obtained as yellowish oil. ^{1}H-NMR (400 MHz, $CDCl_3$): δ 0.67-0.81 (m, 3H), 0.90-1.10 (m, 3H), 1.49 (m, 1H), 1.86-2.30 (m, 1H), 2.95-3.95 (m, 100H), 3.88-4.88 (m, 4H), 5.02 (bs, 1H), 7.31 (t, *J* = 7.2 Hz, 2H), 7.39 (t, *J* = 7.3 Hz, 2H), 7.61 (m, 2H), 7.75 (d, *J* = 7.3 Hz, 2H); ^{13}C-NMR (100 MHz, $CDCl_3$): δ 18.8, 19.8, 27.5, 28.4, 44.1, 47.2, 47.4, 58.9, 67.0, 68.4, 70.3, 71.8, 119.9, 124.6, 125.1, 127.1, 127.6, 141.4, 143.9, 157.2, 169.4; IR (KBr): ν = 3374.41, 2917.17, 1737.11, 1462.40, 1377.46, 1259.67, 1105.54, 709.00 cm^{-1}; $[\alpha]_D$ -15.7 ($CHCl_3$, c = 0.01 g/mL); HRMS (ES$^+$): calc. for $[C_{70}H_{121}NO_{28} + NH_4]^+$ 1441.8413, found 1441.8374.

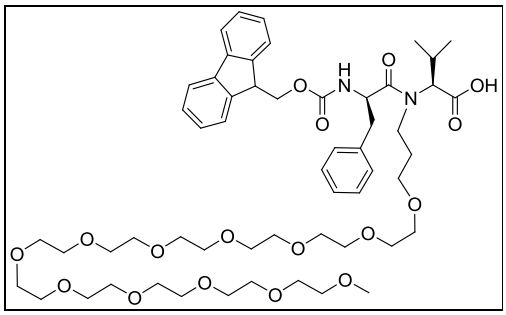

Fmoc-D-Phe-(*N*-OEG$_{11}$)Val-OH (18). Following the general procedure described above with **15** (638 mg, 0.58 mmol), compound **18** (605 mg, 100%) was obtained as yellowish oil. ^{1}H-NMR (400 MHz, $CDCl_3$): δ 0.69-1.05 (m, 6H), 1.22-2.59 (m, 2H), 2.87-3.17 (m, 1H), 3.12-3.82 (m, 53H), 3.98-4.50 (m, 4H), 4.97 (m, 1H), 5.69-5.97 (m, 1H), 5.90 (bs, 1H), 7.15-7.33 (m, 7H), 7.39 (t, *J* = 7.4 Hz, 2H), 7.54 (m, 2H), 7.76 (d, *J* = 7.4 Hz, 2H); ^{13}C-NMR (100 MHz, $CDCl_3$): δ 19.0, 19.1, 20.1, 20.1, 26.9, 27.2, 29.1, 29.6, 39.2, 39.3, 47.0, 47.0, 52.8, 52.9, 58.9, 66.9, 67.0, 67.7, 68.0, 69.7, 70.1, 70.1, 70.2, 70.3, 70.4, 70.6, 71.8, 119.9, 125.0, 125.1, 125.2, 126.8, 127.0, 127.6, 127.6, 128.5, 128.6, 129.4, 129.4, 136.0, 136.1, 143.7. 143.8, 143.8, 155.5, 155.6, 172.2, 174.1; IR (KBr): ν = 3290.79, 2917.41, 1720.36, 1645.83, 1532.30, 1452.05, 1351.31, 1254.69, 1107.03, 1034.42, 952.05, 797.90, 761.07, 742.72, 703.06 cm^{-1}; $[\alpha]_D$ -5.0 ($CHCl_3$, 0.01 g/mL); HRMS (ES$^+$): calc. for $[C_{55}H_{82}N_2O_{17} + NH_4]^+$ 1060.5952, found 1060.5948.

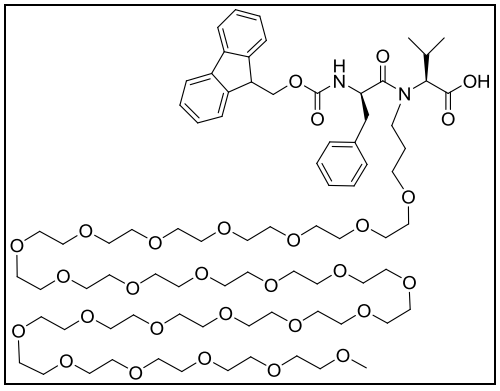

Fmoc-D-Phe-(*N*-OEG$_{23}$)Val-OH (18). Following the general procedure described above with **16** (374 mg, 0.23 mmol), compound **18** (362 mg, 100%) was obtained as yellowish oil. ^{1}H-NMR (400 MHz, $CDCl_3$): δ 0.69-1.14 (m, 6H), 1.48-2.38 (m, 2H), 2.83-3.26 (m, 1H), 3.25-3.94 (m, 101H), 4.04-4.52 (m, 4H), 4.97 (m, 1H), 5.76 (m, 1H), 6.46 (bs, 1H), 7.15-7.32 (m, 7H), 7.38 (t, *J* = 7.4 Hz, 2H), 7.53 (m, 2H), 7.75 (d, *J* = 7.6 Hz, 2H); ^{13}C-NMR (100 MHz, $CDCl_3$): δ 18.4, 19.0, 19.7, 20.1, 26.9, 27.2, 29.1, 29.6, 38.6, 39.3, 41.2, 47.0, 47.0, 52.0, 52.9, 58.9, 66.9, 67.0, 67.7, 68.1, 68.6, 69.7, 70.4, 71.8, 119.8, 119.9, 124.9, 125.0, 125.1, 125.2, 126.8, 127.0, 127.1, 127.6, 127.6, 128.2, 128.6, 129.3, 129.6, 135.7, 136.1, 141.2, 143.6, 143.6, 143.7, 143.8, 155.5, 155.6, 171.2, 171.3, 174.1, 174.2; IR (KBr): ν = 3300.02, 2877.07, 1784.02, 1644.60, 1525.29, 1452.68, 1352.33, 1298.25, 1211.99, 1165.74, 1109.70, 953.54, 847.05, 809.96, 761.07, 743.14, 699.88 cm^{-1}; $[\alpha]_D$ -7.2 (MeOH, c = 0.01 g/mL); HRMS (ES$^+$): calc. for $[C_{79}H_{130}N_2O_{29} + NH_4]^+$ 1588.9098, found 1588.9077.

3.2. SPPS OF THE *N*-OEG LINEAR PENTAPEPTIDES

The pentapeptides **p19-p22** were synthesized on the CTC resin as described for each case. Standard couplings were performed using DIPCDI/OxymaPure and a 3-fold excess of Fmoc-amino acid. In the SPPS of pentapeptides **p19**-**p21**

using an *N*-substituted Val derivative, Fmoc-D-Phe-OH was coupled onto *N*-alkylated Val using BTC activation. In the SPPS of pentapeptides **p21** and **p22** using a dipeptidic building block (**17** and **18**, respectively), the dipeptide was coupled onto the peptidyl-resin using PyBOP/HOAt. After cleavage from the solid support and lyophilization, the crude pentapeptides were obtained in >49% crude yield and they were found to be enough pure to be directly cyclized.

Scheme 55. SPPS of pentapeptides **p19-p21** using an *N*-substituted Val derivative.

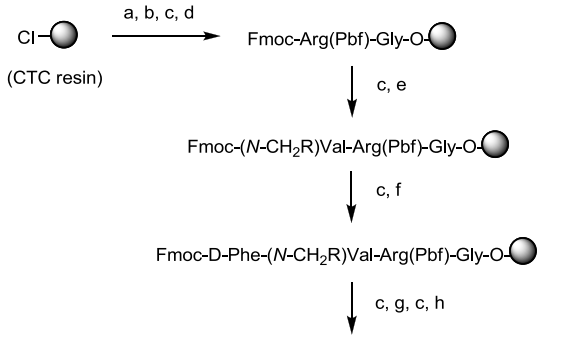

Reagents and conditions: a. Fmoc-Gly-OH (1.2 equiv.), DIEA (12.0 equiv.), DCM, 1 h; b. MeOH, 15 min; c. piperidine/DMF 1:4, 3x5 min, 1x10 min; d. Fmoc-Arg(Pbf)-OH (3.0 equiv.), DIPCDI (3.0 equiv.), OxymaPure (3.0 equiv.), DMF, 1 h; e. Fmoc-(*N*-CH_2R)Val-OH (Fmoc-*N*MeVal-OH or **12-13**, 3.0 equiv.), DIPCDI (3.0 equiv.), OxymaPure (3.0 equiv.), DMF, 2 h; f. Fmoc-D-Phe-OH (5.0 equiv.), BTC (1.65 equiv.), 2,4,6-trimethylpyridine (14.0 equiv.), THF, 15 h, double coupling; g. Fmoc-Asp(O^{t}Bu)-OH (3.0 equiv.), DIPCDI (3.0 equiv.), OxymaPure (3.0 equiv.), DMF, 1 h; h. 2% TFA in DCM, 3x2 min. *Note:* For the synthesis of **p19**: f. Fmoc-D-Phe-OH (3.0 equiv.), HATU (3.0 equiv.), HOAt (3.0 equiv.), DIEA (3.0 equiv.), DMF, 2 h, double coupling.

Scheme 56. SPPS of pentapeptides **p21-p22** using a dipeptidic building block.

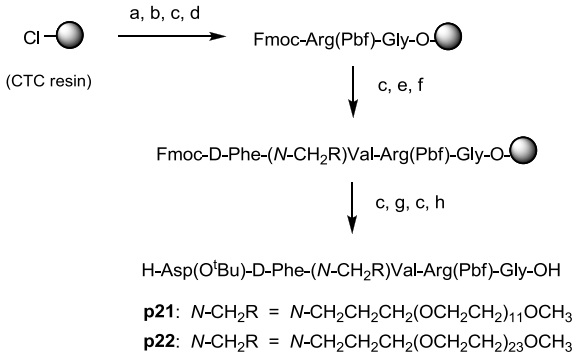

Reagents and conditions: a. Fmoc-Gly-OH (1.2 equiv.), DIEA (12.0 equiv.), DCM, 1 h; b. MeOH, 15 min; c. piperidine/DMF 1:4, 3x5 min, 1x10 min; d. Fmoc-Arg(Pbf)-OH (3.0 equiv.), DIPCDI (3.0 equiv.), OxymaPure (3.0 equiv.), DMF, 1 h; e. Fmoc-D-Phe-Val(*N*-CH_2R)-OH (**17** or **18**, 1.0 equiv.), PyBOP (1.0 equiv.), HOAt (1.0 equiv.), DIEA (2.0 equiv.), DMF, 3 h; then + PyBOP (1.0 equiv.), + DIEA (1.0 equiv.), 15 h; f. Ac_2O (10.0 equiv.), DIEA (10.0 equiv.), DCM, 15 min; g. Fmoc-Asp(O^{t}Bu)-OH (3.0 equiv.), DIPCDI (3.0 equiv.), OxymaPure (3.0 equiv.), DMF, 1 h; h. 2% TFA in DCM, 3x2 min.

- **H-Asp(O^{t}Bu)-D-Phe-*N*MeVal-Arg(Pbf)-Gly-OH (p19).** The SPPS was carried out as shown in Scheme 55 using Fmoc-*N*MeVal-OH as building block and working at a 0.93 mmol scale. Starting from 1.0 g of CTC resin (1.6 mmol/g), the first Fmoc-amino acid was incorporated and the resin loading was determined to be 0.93 mmol/g. Elongation of the peptide chain was performed by stepwise assembly of the Fmoc-protected amino acids as shown in Scheme 55. After cleavage and liophilization, pentapeptide **p19** was obtained (240 mg, quant. crude yield). HPLC (linear gradient from 5% to 100% ACN over 8 min): t_r = 6.02 min, purity = 67%; HPLC-MS (linear gradient from 5% to 100% ACN over 8 min): t_r = 7.36 min, $[M+H]^+$ = 915.70.

- **H-Asp(O^{t}Bu)-D-Phe-(*N*-OEG_2)Val-Arg(Pbf)-Gly-OH (p20).** The SPPS was carried out as shown in Scheme 55 using Fmoc-(*N*-OEG_2)Val-OH (**12**) as building block and working at a 0.81 mmol scale. Starting from 1.7 g of CTC resin (1.6 mmol/g), the first Fmoc-amino acid was incorporated and the resin loading was determined to be 0.27 mmol/g. Elongation of the peptide chain was performed by stepwise assembly of the Fmoc-protected amino acids as shown in Scheme 55. For the acylation of the *N*-OEG_2 Val residue with Fmoc-D-Phe-OH, two BTC-mediated

couplings were performed, which lead to an an almost complete conversion (traces of unreacted *N*-OEG_2 peptide were detected by HPLC-MS). After cleavage and liophilization, pentapeptide **p20** was obtained (950 mg, quant. crude yield). HPLC (linear gradient from 20% to 70% ACN over 8 min): tr = 5.88 min, purity = 62%; HPLC-MS (linear gradient from 20% to 70% ACN over 8 min): tr = 7.58 min, $[M+H]^+$ = 1047.77.

- **H-Asp(O^{t}Bu)-D-Phe-(*N*-OEG_{11})Val-Arg(Pbf)-Gly-OH (p21).**

  a. Using Fmoc-(*N*-OEG_{11})Val-OH (**13**) as building block. The SPPS was carried out as shown in Scheme 55 using Fmoc-(*N*-OEG_{11})Val-OH (**13**) as building block and working at a 0.03 mmol scale. Starting from 150 mg of CTC resin (1.6 mmol/g), the first Fmoc-amino acid was incorporated and the resin loading was determined to be 0.20 mmol/g. Elongation of the peptide chain was performed by stepwise assembly of the Fmoc-protected amino acids as shown in Scheme 55. For the acylation of the *N*-OEG_{11} Val residue with Fmoc-D-Phe-OH using BTC, acylation was not complete after two treatments with the *in situ*-generated acid chloride, and performing a third BTC-mediated coupling did not improve conversion. Final cleavage and liophilization afforded a crude residue (17 mg, 37% crude yield) containing pentapeptide **p21**. This crude residue also contained a considerable amount of unacylated H-(*N*-OEG_{11})Val-Arg(Pbf)-Gly-OH. HPLC (linear gradient from 20% to 70% ACN over 8 min): t_r = 6.99 min, purity = 31%; HPLC-MS (linear gradient from 20% to 70% ACN over 8 min): t_r = 7.45 min, $[M+3]^+$ = 1459.2.

  b. Using Fmoc-D-Phe-(*N*-OEG_{11})Val-OH (**17**) as building block. The SPPS was carried out as shown in Scheme 56 using Fmoc-D-Phe(*N*-OEG_{11})Val-OH (**17**) as building block and working at a 0.19 mmol scale. Starting from 0.95 g of CTC resin (1.6 mmol/g), the first Fmoc-amino acid was incorporated and the resin loading was determined to be 0.20 mmol/g. Elongation of the peptide chain was performed by stepwise assembly of the Fmoc-protected amino acids as shown in Scheme 56. For the coupling of the dipeptidic segment (**17**) onto the peptidyl-resin using PyBOP/HOAt, the procedure was the following. To a solution of dipeptide (2.0 equiv.), HOAt (1.0 equiv.) and DIEA (2.0 equiv.) in DMF, PyBOP (1.0 equiv.) was added and the resulting mixture was poured onto the peptidyl-resin; after 3 h shaking, further PyBOP (1.0 equiv.) and DIEA (1.0 equiv.) were added and the coupling was allowed to proceed overnight. The unreacted resin-bound peptide was acetylated, and the occurrence of epimerization was confirmed by the appearance of two peaks having the mass of the desired product in the HPLC spectra of a cleaved peptidyl-resin sample. These two peaks were present in a 34:56 proportion, and the major one was associated to the desired product by comparison with HPLC data from the SPPS of **p21** using Fmoc-(*N*-OEG_{11})Val-OH (**13**), in which no epimerization was observed. After final cleavage and liophilization, a mixture of pentapeptide **p21** and its epimer at the Val residue (**p21***) was obtained (138 mg, 50% crude yield). HPLC (linear gradient from 20% to 70% ACN over 8 min): t_r = 6.78 min (pressumably the desired stereoisomer), 7.15 min (pressumably the Val-epimer); HPLC-MS (linear gradient from 20% to 70% ACN over 8 min): t_r = 7.00-7.90 min, $[M+3]^+$ = 1459.2 (stereoisomers do not separate).

- **H-Asp(O^{t}Bu)-D-Phe-(*N*-OEG_{23})Val-Arg(Pbf)-Gly-OH (p22).** The SPPS of was carried out as shown in Scheme 56 using Fmoc-D-Phe(*N*-OEG_{23})Val-OH (**14**) as building block working at a 0.06 mmol scale. Starting from 0.30 g of CTC resin (1.6 mmol/g), the first Fmoc-amino acid was incorporated and the resin loading was determined to be 0.20 mmol/g. Elongation of the peptide chain was performed by stepwise assembly of the Fmoc-protected amino acids as shown in Scheme 56. For the coupling of the dipeptidic segment (**18**) onto the peptidyl-resin using PyBOP/HOAt, the procedure was the following. To a solution of dipeptide (2.0 equiv.), HOAt (1.0 equiv.) and DIEA (2.0 equiv.) in DMF, PyBOP (1.0 equiv.) was added and the resulting mixture was poured onto the peptidyl-resin; after 3 h shaking, further PyBOP (1.0 equiv.) and DIEA (1.0 equiv.) were added and the coupling was allowed to proceed overnight. The unreacted sresin-bound peptide was acetylated, and the occurrence of epimerization was confirmed by the appearance of two peaks having the mass of the desired product in the HPLC spectra of a

cleaved peptidyl-resin sample. After final cleavage and liophilization, a mixture of pentapeptide **p22** and its epimer at the Val residue (**p22***) was obtained (59 mg, 49% crude yield). HPLC (linear gradient from 20% to 70% ACN over 8 min): t_r = 7.59 min, purity = 45% (stereoisomers do not separate); HPLC-MS (linear gradient from 20% to 70% ACN over 8 min): t_r = 7.46 min, $[M+4]^+$ = 1989.31 (stereoisomers do not separate).

3.3. CYCLIZATION AND DEPROTECTION TO OBTAIN THE *N*-OEG CYCLOPEPTIDES

3.3.1. General procedure for the cyclization of the linear pentapeptides

The crude linear pentapeptide (1.0 equiv.) was dissolved in DCM (*c* = 1 mM). EDC·HCl (10.0 equiv.) and DMAP (2.0 equiv.) were added to the solution. After stirring at room temperature overnight, the mixture was concentrated and washed with 2% citric acid (2x20 mL), $Na_2CO_{3\ (sat.)}$ (2x20 mL) and $NaCl_{\ (sat.)}$ (2x20 mL). The organic phase was dried over $MgSO_{4\ (anh.)}$, filtered and concentrated under reduced pressure.

- **cyclo[Asp(O^{t}Bu)-D-Phe-*N*MeVal-Arg(Pbf)-Gly] (19)**. Crude pentapeptide **p19** (240 mg, 67% purity, approx. 0.18 mmol) was cyclized with EDC·HCl (345 mg, 1.80 mmol) and DMAP (44 mg, 0.36 mmol) following the general procedure. This afforded cyclopeptide **19** (157 mg, 95% crude yield). HPLC (linear gradient from 5% to 100% ACN over 8 min): t_r = 7.73 min, purity = 39%; HPLC-MS (linear gradient from 30 to 100% over 11 min): t_r = 8.42 min, $[M+H]^+$ = 897.66.

- **cyclo[Asp(O^{t}Bu)-D-Phe-(*N*-OEG$_2$)Val-Arg(Pbf)-Gly] (20)**. Crude pentapeptide **p20** (690 mg, 62% purity, approx. 0.41 mmol) was cyclized EDC·HCl (786 mg, 4.10 mmol) and DMAP (100 mg, 0.82 mmol) following the general procedure. This afforded cyclopeptide **20** (384 mg, 92% crude yield). HPLC (linear gradient from 40% to 100% ACN over 8 min): t_r = 4.99 min, purity = 28%; HPLC-MS (linear gradient from 60% to 100% ACN over 11 min): t_r = 6.55 min, $[M+H]^+$ = 1028.93.

- **cyclo[Asp(O^{t}Bu)-D-Phe-(*N*-OEG$_{11}$)Val-Arg(Pbf)-Gly] (21)**.

  a. From crude pentapeptide **p21** obtained as a single stereoisomer. The crude pentapeptide **p21** (17 mg, 31% purity, approx. 0.01 mmol) was cyclized with EDC·HCl (19 mg, 0.10 mmol) and DMAP (2 mg, 0.02 mmol) following the general procedure. This afforded cyclopeptide **21** (21 mg, quant. crude yield). HPLC (linear gradient from 40% to 100% ACN over 8 min): t_r = 4.57 min, purity = 28%; HPLC-MS (linear gradient from 40% to 100% ACN over 8 min): t_r = 6.91 min, $[M+H]^+$ = 1028.93.

  b. From the crude mixture of pentapeptide **p21** and its Val-epimer (**p21***). The crude diastereomeric mixture of pentapeptides **p21** and **p21*** (138 mg, approx. 0.03 mmol) was cyclized with EDC·HCl (56 mg, 0.30 mmol) and DMAP (7 mg, 0.06 mmol) following the general procedure. This afforded a mixture of the corresponding diasteretereomeric cyclopeptides, **21** and **21*** (158 mg, quant. crude yield). HPLC (linear gradient from 40% to 100% ACN over 8 min): t_r = 5.68 min (pressumably the desired stereoisomer), 5.93 min (pressumably the Val-epimer); HPLC-MS (linear gradient from 40% to 100% ACN over 11 min): t_r = 7.46 min, $[M+3]^+$ = 1441.1 (stereoisomers do not separate).

  Note: The retention time of stereopure **21** (4.57 min) differs from the retention of the desired stereoisomer of **21** (5.68 min) that was present in the mixture of diastereomeric cyclopeptides, although the two crude residues obtained cyclization were analyzed under the same HPLC conditions. Such a retention time difference is because stereopure **21** was analyzed in a distinct HPLC apparatus that had a shorter connector between the column and the detector.

- **cyclo[Asp(O^{t}Bu)-D-Phe-(*N*-OEG$_{23}$)Val-Arg(Pbf)-Gly] (22)**. The crude diastereomeric mixture of pentapeptides **p22** and **p22*** (59 mg, 37% purity, approx. 0.06 mmol) was cyclized with EDC·HCl (115 mg, 0.60 mmol) and DMAP (15 mg, 0.12 mmol) following the general procedure. This afforded a mixture of the corresponding diasteretereomeric cyclopeptides, **22** and **22*** (97 mg, 81% crude yield). HPLC (linear gradient from 40% to 100% ACN over 8 min): t_r = 5.69 min, purity = 18% (stereoisomers do not separate); HPLC-MS (linear gradient from 40% to 100% ACN over 11 min): t_r = 6.72 min, $[M+4]^+$ = 1971.35 (steroisomers do not separate at a base-line level, but two peaks can be distinguished at 6.46 min and 6.72 min).

3.3.2. General procedure for ^{t}Bu- and Pbf- removal

The crude obtained from the cyclization was dissolved in TFA/H_2O/TIS 95:5:5 (0.03 mL/mg of crude). After stirring for 3 h, the reaction mixture was concentrated under reduced pressure. Traces of TFA were removed by co-evaporation with toluene at 50 ºC. The deprotected peptide was precipitated two times by addition of cold *tert*-butyl methyl ether and subsequent centrifugation (3500 rpm, 5 min). The precipitate was redissolved in ACN/H_2O 1:1 and lyophilized. The resulting residue was purified by semipreparative RP-HPLC. Fractions were collected, pooled and lyophilized to afford the pure cyclopeptides. The peptides were redissolved in 1% AcOH in H_2O and lyophilized again.

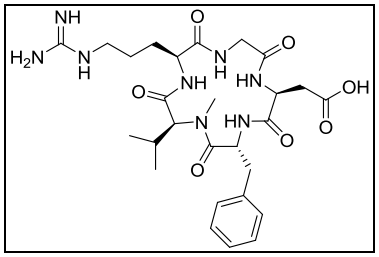

cyclo[RGDf*N*MeV] (23). Following the general procedure with crude cyclopeptide **19** (157 mg, 39% purity) afforded the pure peptide **23** (36 mg, 34% two-step yield with respect to pentapeptide **p19**) after RP-HPLC purification using a Sunfire™ 18 reversed-phase semipreparative column (linear gradient from 0:100 to 70:30 ACN/H_2O over 15 min, flow rate = 15 mL/min). HPLC (linear gradient from 10% to 50% ACN over 8 min): t_r = 5.39 min, purity = 100%; HPLC-MS (linear gradient from 30% to 100% ACN over 8 min): t_r = 2.29 min, $[M+H]^+$ = 589.51; ^{1}H-NMR (500 MHz, CD_3OD): δ 0.48 (d, *J* = 6.6 Hz, 3H), 0.91 (d, *J* = 6.6 Hz, 3H), 1.60 (m, 2H), 1.99 (m, 2H), 2.04 (m, 1H), 2.61 (dd, *J* = 16.7 Hz, *J* = 6.6 Hz, 1H), 2.92 (dd, *J* = 16.8 Hz, *J* = 7.6 Hz, 1H), 2.84 (s, 3H), 2.96 (dd, *J* = 13.0 Hz, *J* = 7.6 Hz, 1H), 3.08 (dd, *J* = 13.0 Hz, *J* = 7.6 Hz, 1H), 3.19 (m, 2H), 3.48 (d, *J* = 14.5 Hz, 1H), 3.85 (dd, *J* = 8.6 Hz, *J* = 6.3 Hz, 1H), 4.06 (d, *J* = 14.3 Hz, 1H), 4.34 (d, *J* = 10.6 Hz, 1H), 4.70 (dd, *J* = 7.6 Hz, 6.7 Hz, 1H), 5.12 (dd, *J* = 10.1 Hz, *J* = 5.3 Hz, 1H), 7.14-7.27 (m, 5H); ^{13}C-NMR (125 MHz, CD_3OD): 19.9, 20.2, 27.3, 27.7, 31.8, 35.3, 39.5, 42.1, 44.7, 51.1, 52.5, 56.4, 65.3, 127.9, 129.6, 130.5, 138.1, 158.7, 171.7, 172.1, 172.8, 173.6, 174.0, 174.4; HRMS (ES^+): calc. for $[C_{27}H_{40}N_8O_7 + H]^+$ 589.3093, found 589.3086; NPC = 74%.

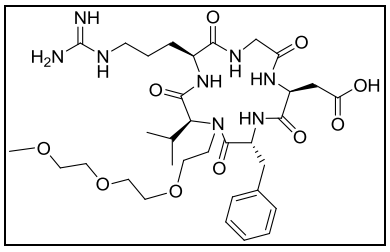

cyclo[RGDf(*N*-OEG$_2$)V] (24). Following the general procedure with crude cyclopeptide **20** (384 mg, 28% purity) afforded the pure peptide **24** (79 mg, 27% two-step yield with respect to pentapeptide **p20**) after RP-HPLC purification using a Sunfire™ C18 semipreparative column (linear gradient from 15:85 to 60:40 ACN/H_2O over 20 min, flow rate = 15 mL/min). HPLC (linear gradient from 10% to 50% ACN over 8 min): t_r = 5.81 min, purity = 99%; HPLC-MS (linear gradient from 10% to 60% ACN over 8 min): t_r = 7.65 min, $[M+H]^+$ = 721.24; ^{1}H-NMR (500 MHz, CD_3OD): δ 0.64 (d, *J* = 6.6 Hz, 3H), 0.95 (d, *J* = 6.6 Hz, 3H), 1.60 (m, 2H), 1.81 (m, 1H), 1.90 (m, 1H), 2.02 (m, 1H), 2.62 (dd, *J* = 16.6 Hz, *J* = 5.2 Hz, 1H), 2.92 (dd, *J* = 16.8 Hz, *J* = 7.9 Hz, 1H), 3.00 (d, *J* = 7.6 Hz, 2H), 3.18 (m, 2H), 3.26 (m, 3H), 3.40 (m, 2H), 3.45 (d, *J* = 14.5 Hz, 1H), 3.50-3.70 (m, 10H), 4.03 (d, *J* = 14.5 Hz, 1H), 4.04 (d, *J* = 10.5 Hz, 1H), 4.34 (dd, *J* = 9.2 Hz, *J* = 5.6 Hz, 1H), 4.78 (dd, J = 8.2 Hz, *J* = 6.4 Hz, 1H), 5.12 (dd, J = 8.4 Hz, *J* = 7.6 Hz, 1H), 7.19-7.30 (m, 5H); ^{13}C-NMR (125 MHz, CD_3OD): 20.2, 21.8, 27.0, 27.6, 29.3, 41.0, 42.0, 44.6, 44.8, 51.0, 52.9, 55.2, 59.2, 68.4, 71.3, 71.4, 71.4, 71.7, 73.0, 128.2, 129.8, 130.6, 137.8, 158.6, 171.8, 172.0, 173.8, 173.9, 175.2; HRMS (ES^+): calc. for $[C_{33}H_{52}N_8O_{10} + H]^+$ 721.3879, found 721.3875; NPC = 67%.

cyclo[RGDf(*N*-OEG$_{11}$)V] (25).

a. From crude cyclopeptide **21** obtained as a single stereoisomer. Following the general procedure with crude cyclopeptide **21** (21 mg, 28% purity) afforded the pure peptide **25** (3 mg) after RP-HPLC purification using an XBridge™ C18 semipreparative column (linear gradient from 15:85 to 40:60 ACN/H_2O over 20 min, flow rate = 3 mL/min). HPLC (linear gradient from 40% to 100% ACN over 8 min): tr = 6.55 min, purity = 100%; HPLC-MS (linear gradient from 40% to 100% ACN over 8 min): tr = 6.92 min, $[M+H]^+$ = 1132.7.

b. From the crude mixture of cyclopeptide **21** and its Val-epimer (**21***). Following the general procedure with the crude mixture of **21** and **21*** (158 mg) afforded a residue containing the desired *N*-OEG$_{11}$ cyclopeptide (**25**) and its Val-epimer (**25***). The two stereoisomeric products (**25** and **25***) were isolated by RP-HPLC purification using an XBridge™ C18 semipreparative column (linear gradient from 25:75 to 33:66 ACN/H_2O over 8 min, flow rate = 3 mL/min). The isolated *N*-OEG$_{11}$ cyclopeptide with the lower retention time (**25**) was identified as the product with the desired stereochemistry, as it was found to co-elute with a sample of stereopure **25**. HPLC (linear gradient from 10% to 50% ACN over 8 min): t_r = 6.45 min, purity = 97%; HPLC-MS (linear gradient from 0% to 60% ACN over 8 min): t_r = 7.79 min, $[M+2]^+$ = 1132.55.

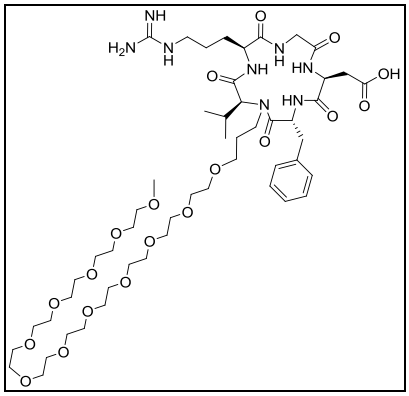

^{1}H-NMR (500 MHz, CD_3OD): δ 0.53 (d, *J* = 6.5 Hz, 3H), 0.93 (d, *J* = 6.6 Hz, 3H), 1.53 (m, 2H), 1.62 (m, 1H), 1.99 (m, 1H), 2.04 (m, 1H), 2.61 (dd, *J* = 16.9 Hz, *J* = 6.1 Hz, 1H), 2.94 (m, 1H), 2.92 (dd, *J* = 16.8 Hz, *J* = 6.3 Hz, 1H), 3.11 (dd, *J* = 12.3 Hz, *J* = 10.3 Hz, 1H), 3.19 (m, 2H), 3.36 (s, 3H), 3.36-3.73 (m, 49H), 3.78 (dd, *J* = 8.6 Hz, *J* = 7.3 Hz, 1H), 4.03 (d, *J* = 14.5 Hz, 1H), 4.33 (d, *J* = 10.6 Hz, 1H), 4.76 (dd, *J* = 8.3 Hz, *J* = 6.1 Hz, 1H), 5.04 (dd, *J* = 10.3 Hz, *J* = 4.9 Hz, 1H), 7.17-7.32 (m, 5H); ^{13}C-NMR (125 MHz, CD_3OD): δ 20.2, 20.6, 27.3, 27.5, 27.8, 31.8, 34.7, 40.5, 42.2, 43.0, 44.5, 51.1, 53.1, 56.9, 59.2, 66.0, 69.7, 71.0, 71.1, 71.2, 71.3, 71.4, 71.5, 73.0, 128.1, 129.7, 130.6, 138.0, 158.6, 171.8, 172.3, 173.3, 174.0, 174.9; HRMS (ES^+): calc. for $[C_{52}H_{90}N_8O_{19} + H]^+$ 1131.6395, found 1131.6379; HRMS (ES^+): calc. for $[C_{52}H_{90}N_8O_{19} + H]^+$ 1131.6395, found 1131.6379; NPC = 69%.

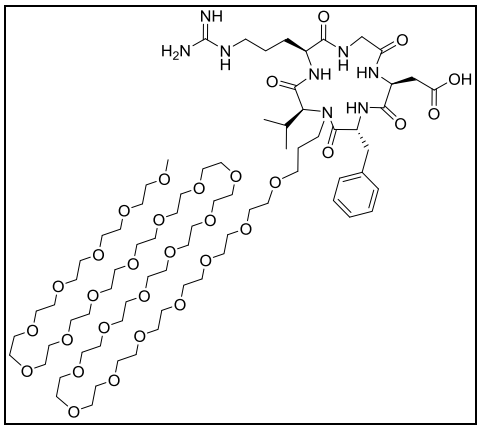

cyclo[RGDf(*N*-OEG$_{23}$)V] (26). Following the general procedure with the crude mixture of **22** and **22*** (97 mg, 18% purity) afforded a residue containing the desired *N*-OEG$_{23}$ cyclopeptide (**26**) and its Val-epimer (**26***). The two stereoisomeric products (**26** and **26***) were isolated by RP-HPLC purification using an XBridge™ C18 semipreparative column (linear gradient from 25:75 to 33:66 ACN/H_2O over 8 min, flow rate = 3 mL/min). We assumed that the isolated *N*-OEG$_{23}$ cyclopeptide with the lower retention time (**26**) was the product with the desired stereochemistry, as we had confirmed for cyclo[RGDf(*N*-OEG$_{11}$)V] (**25**). This assumption is reasonable, based on the *N*-OEG$_{23}$ vs. *N*-OEG$_{11}$ ressemblance of: i. HPLC spectra of the crude mixture of stereoisomeric cyclopeptides obtained after cyclization and deprotection (crude mixture of **25** and **25*** vs. crude mixture of **26** and **26***), ii. ^{1}H-NMR data of the different isolated cyclopeptides (**25** vs. **26***, and **25*** vs. **26***). [*Note:* see "Stereochemical validation of the *N*-OEG$_{23}$ cyclopeptide", in Section 3.3.6.] HPLC (linear gradient from 10% to 50% ACN over 8 min): t_r = 7.27 min, purity = 90%; HPLC-MS (linear gradient from 10% to 60% ACN over 8 min): t_r = 6.96 min, $[M+4]^+$ = 1662.55; HRMS (ES^+): calc. for $[C_{76}H_{138}N_8O_{31} + NH_4 + H]^{2+}$ 838.9939, found 839.9910; NPC = n.d.

3.6. BIOLOGICAL ACTIVITY EVALUATION

Cell adhesion inhibition assays. Cells were grown at 37 ºC and 5% CO_2 and expanded when they reached 90% confluence. For DAOY and HT-29 cells, the medium was DMEM High Glucose, supplemented with 10% FCS; for HUVEC cells, the medium was EBM, supplemented with 10% FCS. Non-tissue culture treated ELISA plates were coated with the appropriate concentration of the ligand (for HUVEC: vitronectin at 0.75 µg/mL and fibrinogen at 10 µg/mL, for DAOY: vitronectin at 0.5 µg/mL and fibrinogen at 40 µg/mL, for HT-29: vitronectin at 4 µg/mL) and incubated overnight at room temperature. Plates were then washed two times with PBS and incubated with the blocking solution (PBS containing 1.5% BSA; 60 min at 37 ºC) to block unspecific interaction sites. The blocking solution was discarded by flicking and serial dilutions of the compounds were plated in duplicates. Immediately, harvested cells were seeded into the same plate at a given concentration (for DAOY and HUVEC: 600000 cells/well, for HT-29: 1000000 cells/well). Plates were incubated for 90 min at 37 ºC to allow cell adhesion and spreading of the ligands. Plates were then washed three times with PBS to remove non-adhered cells and 60 µL/well of hexosaminidase substrate solution (*p*-nitrophenol-*N*-acetyl-*ß*-D-glucosaminide 3.75 mM, containing 50 mM of sodium citrate at pH 5.0) was added. The plates were incubated at 37 ºC during 4 h and then 60 µL of stop solution (0.2 M NaOH, 5 mM EDTA at pH 10.4) was added. The number of cells that remained attached to the plate was evaluated by measuring the absorbance of the plates at 405 nm with a spectrophotometer. Each plate contained positive and negative controls and compounds were tested as duplicates. The adhesion inhibition IC_{50} was calculated using the Prism-4 software based on the sigmoidal dose-response (variable slope) equation. Standard deviations were at the most in the same order of the IC_{50} values.

3.7. SERUM STABILITY ASSAYS

Stability assays in human serum. Stability in human serum (from human male AB) was carried out by incubation at 37 ºC of the peptides with the serum (diluted 9:1 in HBSS buffer). The peptides were assayed at a final concentration of 20-50 µM. Aliquots (30 µL) were periodically taken at 0 to 120 h and then ACN (150 µL) was added in order to precipitate the proteins and cooled to 4 ºC. After 30 min, the sample was centrifuged at 12000 rpm for 5 min, the supernatant was filtered and analyzed 20 µL were injected into the HPLC apparatus. For the blank sample, the procedure used as the same described above, except that H_2O was used instead of human serum. For each of the aliquots analyzed, the area of the HPLC peak corresponding to the peptide was plotted versus time.

EXPERIMENTAL PROCEDURES FOR CHAPTER 4

4.1. SYNTHESIS OF 4-AZIDOBUTANAL[162]

i. 4-iodobutyl benzoate (35). To a suspension of NaI (27.66 g, 185.0 mmol) in THF (15.0 mL, 185.0 mmol) and ACN (7.5 mL), cooled at 0 ºC, was added benzoyl chloride (21.5 mL, 185.0 mmol) in one portion. The reaction mixture was stirred overnight in the absence of light and was then diluted with H_2O (100 mL) and Et_2O (100 mL). Phases were separated and the aqueous phase was extracted with Et_2O (3x30 mL). The combination of organic phases were washed with $NaHCO_{3\ (sat.)}$ (50 mL), then with $Na_2CO_{3\ (sat.)}$ (50 mL), dried over $MgSO_{4\ (anh.)}$ and filtered. The solvent was then removed under reduced pressure to give 50.6 g (90%) of 4-iodobutyl benzoate (**35**), which was obtained as brown oil. ^{1}H-NMR (400 MHz, $CDCl_3$): δ 1.9-2.0 (m, 4H), 3.2 (t, 2H), 4.3 (t, 2H), 7.5 (t, 1H), 7.4 (t, 2H), 8.0 (m, 2H).

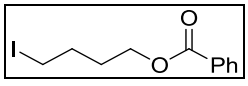

ii. 4-azidobutyl benzoate (36). NaN_3 (16.36 g, 251.5 mmol) was added portion wise to a solution of 4-iodobutyl benzoate (**35**, 50.60 g, 166.0 mmol), in DMF (25 mL) cooled at 0 ºC. The reaction mixture was stirred overnight in absence of light, then diluted with Et_2O (100 mL) and H_2O (100 mL). The organic phase was separated and the aqueous layer was further extracted with Et_2O (3x50 mL), the combined organic phases were concentrated *in vacuo*. The resulting residue was redissolved in hexane (50 mL), washed with H_2O (25 mL), $NaHCO_{3\ (sat.)}$ (15 mL) dried over $MgSO_{4\ (anh.)}$ and filtered. The solvent was then removed under reduced pressure to give 32.93 g (100%) of 4-azidobutyl benzoate (**36**), which was obtained as a colorless oil. ^{1}H-NMR (400 MHz, $CDCl_3$): δ 1.7-2.0 (m, 4H), 3.4 (t, 2H), 4.3 (t, 2H), 7.4 (t, 2H), 7.5 (dt, 1H), 8.0 (dd, 2H).

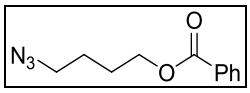

iii. 4-azidobutanol (37). LiOH (7.52 g, 179.1 mmol) was added to a solution of 4-azidobutyl benzoate (**36**, 32.93 g, 123.0 mmol) in THF (100 mL), H_2O (40 mL) and MeOH (10 mL). The reaction mixture was stirred overnight and then was diluted with H_2O (50 mL). The layers were then separated and the aqueous layer was further extracted with Et_2O (3x50 mL). The combined organic layers were washed with $NaHCO_{3\ (sat.)}$ (50 mL), dried over $MgSO_{4\ (anh.)}$ and filtered. The solvent was then removed under reduced pressure to give 13.6 g (85% crude yield) of 4-azidobutanol (**37**), which was obtained as a pale yellow oil. ^{1}H-NMR (400 MHz, $CDCl_3$): δ 1.7-1.6 (m, 4H), 3.3 (t, 2H), 3.7 (t, 2H).

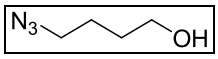

iv. 4-azidobutanal (38)

a. Oxidation with DMP. 4-azidobutanol (**37**, 1.00 g, 8.7 mmol) was added to a solution of Dess-Martin periodinane (4.70 g, 11.1 mmol) in DCM $_{(anh.)}$ (85 mL) under N_2 atmosphere. After stirring 1 h at room temperature, the mixture was and filtered through a thick pad of celite, which was thoroughly washed with CH_2Cl_2. The filtrate was concentrated under reduced pressure. The crude was purified by flash chromatography (AcOEt/Hx, 2:3) affording 0.70 g (100%) of 4-azidobutanal (**38**). Regular ^{1}H-NMR analysis showed that this aldehyde was stable when kept under argon at -20 ºC.

b. Swern oxidation. A solution of oxalyl chloride (4.50 mL, 52.2 mmol) in DCM $_{(anh.)}$ (65 mL) was prepared under N_2 and cooled in a dry ice-acetone bath. To this solution was carefully added a solution of DMSO (8 mL, 113 mmol) in DCM $_{(anh.)}$ (13.0 mL). The resulting premix was stirred at -78 ºC for 30 min, and then a solution of 4-azidobutanol (**37**, 5.00 g, 43.5 mmol) in DCM $_{(anh.)}$ (17.4 mL) was added slowly. The mixture was stirred for 30 min and then NEt_3 (30.2 mL, 217.5 mmol) was added dropwise. The reaction mixture was left for 30 min at -78 ºC and then allowed to reach room temperature. The reaction was quenched with H_2O (50 mL). Phases were separated. The organic phase was washed with NaCl $_{(sat.)}$ (1x50 mL). The aqueous phase was extracted with DCM (3x50 mL). The combination of organic phases was dried over $MgSO_{4\ (anh.)}$, filtered and concentrated under reduced pressure. The crude was purified by flash chromatography (Hexane/AcOEt 1:1), affording 3.79 g (77%) of 4-azidobutanal (**38**). Regular ^{1}H-NMR analysis showed that this aldehyde was stable when kept under argon at -20 ºC. ^{1}H-NMR (400 MHz, $CDCl_3$): δ 1.9 (dt, 2H,), 2.6 (q, 2H), 3.4 (t, 2H), 9.8 (s, 1H).

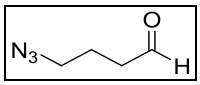

4.2. SYNTHESIS OF FMOC-*N*-(4-AZIDOBUTYL) VALINE

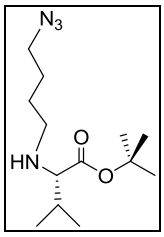

i. H-(*N*-$CH_2CH_2CH_2CH_2N_3$)Val-O^{t}Bu (32). To a solution of valine *tert*-butyl ester hydrochloride (871 mg, 4.1 mmol) in 40 mL of MeOH was added NEt_3 (0.57 mL, 4.1 mmol). 4-azidobutanal (**38**, 500 mg, 4.6 mmol) dissolved in MeOH was then added and the reaction mixture was stirred at room temperature for 1 h. To this solution, was added $NaBH_3CN$ (0.29 g, 4.6 mmol) and stirring was continued for 12 h at room temperature. After, the solvent was removed under reduced pressure and the residue was extracted with AcOEt, washed with 5% $KHSO_4$, $NaHCO_{3\ (sat.)}$, and $NaCl_{\ (sat.)}$ solution. The organic phase was dried over $MgSO_{4\ (anh.)}$ and the solvent was removed by evaporation under reduced pressure. The crude product was obtained as a viscous oil, which was purified by flash chromatography (Hexane/AcOEt 3:1) to give 700 mg (65%) of the desired product (**33**). ^{1}H-NMR (400 MHz, $CDCl_3$): δ 0.93 (d, *J* = 6.8 Hz, 6H), 1.47 (s, 9H,), 1.52 (m, 2H), 1.65 (m, 2H), 1.84 (d7, *J* = 6.9 Hz, *J* = 6.8 Hz ,1H), 2.42 (dt, *J* = 11.3 Hz, *J* = 6.9 Hz , 1H), 2.64 (dt, *J* = 11.3 Hz, *J* = 6.9 Hz , 1H), 2.80 (d, *J* = 6.1 Hz, 1H), 3.28 (t, *J* = 6.9 Hz, 2H); ^{13}C-NMR (100 MHz, $CDCl_3$): δ 18.7, 19.2, 16.6, 27.3, 31.7, 47.9, 51.3, 67.8, 80.8, 174.7; IR (KBr): ν = 2965.91, 2934.35, 2096.37, 1724.38, 1367.81, 1252.13, 1149.95, 771.69 cm^{-1}; $[\alpha]_D$ -33.3 (MeOH, 0.01 g/mL); HRMS (ES$^+$): calc. for $[C_{13}H_{26}N_4O_2 + H]^+$ 271.2129, found 271.2122.

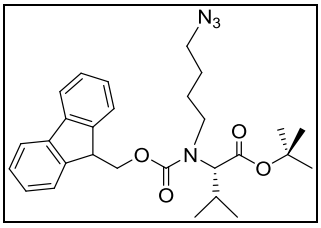

ii. Fmoc-(*N*-$CH_2CH_2CH_2CH_2N_3$)Val-O^{t}Bu (33). To a suspension of compound **32** (1.81 g, 6.6 mmol) in dioxane (100 mL) was added Na_2CO_3 (0.69 g, 6.6 mmol) in H_2O (80 mL) to achieve pH = 9. Then, Fmoc-Cl (2.19 g, 8.5 mmol) was added. The solution was stirred at room temperature for 4 h. Then, the solvent was removed under reduced pressure and the residue was extracted with AcOEt. The resulting residue was purified by flash chromatography (Hexane/AcOEt 3:1) to give 2.50 g (84%) of the desired product (**33**), which was obtained as a colorless oil. ^{1}H-NMR (400 MHz, $CDCl_3$): 0.67-0.72 (m, 3H), 0.85-0.96 (m, 3H), 1.12-1.23 (m, 2H), 1.36-1.52 (m, 9H), 1.50-1.91 (m, 4H), 2.71-2.92 (m, 1H), 2.94-3.05 (m, 1H), 3.11-3.42 (m, 2H), 4.00-4.07 (m, 1H), 4.16-4.81 (m, 2H), 7.33 (t, *J* = 7.4 Hz, 2H), 7.41 (t, *J* = 7.6 Hz, 2H), 7.69 (m, 2H), 7.78 (m, 2H); ^{13}C-NMR (100 MHz, $CDCl_3$): 18.8, 19.7, 26.2, 26.2, 27.9, 28.1, 44.2, 47.6, 50.9, 51.2, 65.2, 67.2, 81.3, 124.5, 127.0, 127.6, 141.4, 144.0, 156.5, 170.2; IR (KBr): ν = 2967.02, 2095.81, 1729.62, 1701.22, 1451.02, 1368.48, 1276.96, 1155.87, 1137.38, 770.94, 741.23 cm^{-1}; $[\alpha]_D$ -18.2 (MeOH, 0.01 g/mL); HRMS (ES$^+$): calc. for $[C_{28}H_{36}N_4O_4 + H]^+$ 493.2809, found 493.2811.‡

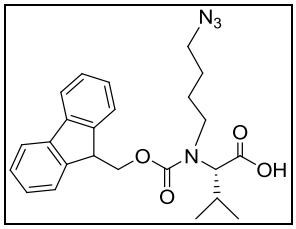

iii. Fmoc-(*N*-$CH_2CH_2CH_2CH_2N_3$)Val-OH (34). Compound **33** (1.50 g, 3.1 mmol) was dissolved in DCM (25 mL) and TFA (25 mL) was added. After stirring for 30 min at room temperature, the mixture was concentrated under reduced pressure. The remaining TFA was removed by co-evaporation with toluene at 50 ºC. This gave compound **34** (1.41 g, 100%) as colorless oil. ^{1}H-NMR (400 MHz, $CDCl_3$): δ 0.56-1.07 (m, 6H), 0.81-2.00 (m, 4H), 2.19-2.82 (m, 2H), 2.89-2.09 (m, 2H), 3.12-3.47 (m, 1H), 3.50-3.87 (m, 1H), 4.17-4.26 (t, 1H), 4.39-4.82 (m, 2H), 7.33 (t, *J* = 7.3 Hz, 2H), 7.41 (t, *J* = 7.2 Hz, 2H), 7.57 (d, *J* = 7.3 Hz, 2H), 7.78 (d, *J* = 7.6 Hz, 2H), 8.28 (bs, 1H); ^{13}C-NMR (100 MHz, $CDCl_3$): δ 19.0, 19.8, 25.7, 25.9, 27.5, 28.0, 47.4, 50.8, 67.6, 69.9, 120.0, 124.4, 127.2, 127.7, 141.4, 143.6, 151.2, 174.2; IR (KBr): ν = 2967.03, 2095.68, 1729.80, 1701.66, 1470.88, 1451.09, 1277.19, 155.75,

‡ *Note:* The ^{1}H- and ^{13}C-NMR spectra of **33** were difficult to interpretate, since most signals were split due to the existence of rotamers. For the ^{1}H-NMR spectrum, the peaks herein described correspond to all the signals appearing in the spectrum. For the ^{13}C-NMR spectrum, the peaks herein described correspond to those signals associated to the major rotamer. All the signals appearing in the spectrum are the following: 18.8, 19.7, 25.7, 26.2, 26.2, 26.5, 27.9, 28.1, 44.2, 44.5, 47.3, 47.6, 50.9, 51.2, 64.8, 65.2, 65.5, 66.1, 67.1, 67.2, 81.3, 119.9, 124.5, 124.8, 124.9, 127.0, 127.6, 141.4, 141.4, 144.0, 144.0, 156.5, 170.2.

1137.03, 741.08 cm^{-1}; $[\alpha]_D$ -33.4 (MeOH, 0.01 g/mL); HRMS (ES^+): calc. for $[C_{24}H_{28}N_4O_4 + H]^+$ 437.2183, found 437.2182. §

4.3. SYNTHESIS OF THE *N*-AZIDOALKYLATED PENTAPEPTIDE

4.3.1. Small-scale SPPS of pentapeptide 39 using Fmoc-*N*-(4-azidobutyl) valine (34) (strategy A)

The small-scale synthesis of pentapeptide **39** through strategy A was performed as shown in Scheme 57.

Scheme 57. Small-scale SPPS of pentapeptide **39** through strategy A.

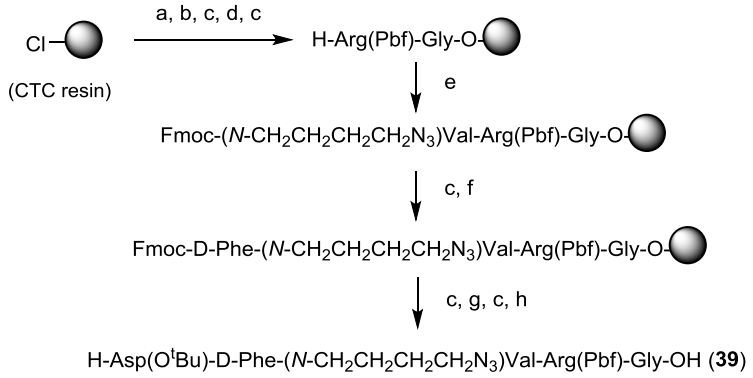

Reagents and conditions: a. Fmoc-Gly-OH (1.2 equiv.), DIEA (12.0 equiv.), DCM, 1 h; b. MeOH, 15 min; c. piperidine/DMF 1:4, 3x5 min, 1x10 min; d. Fmoc-Arg(Pbf)-OH (3.0 equiv.), DIPCDI (3.0 equiv.), OxymaPure (3.0 equiv.), DMF, 1 h; e. Fmoc-(*N*-$CH_2CH_2CH_2CH_2$ N_3)Val-OH (**34**, 3.0 equiv.), DIPCDI (3.0 equiv.), OxymaPure (3.0 equiv.), DMF, 2 h, x2 couplings; f. Fmoc-D-Phe-OH (5.0 equiv.), BTC (1.65 equiv.), 2,4,6-trimethylpyridine (14.0 equiv.), THF, 15 h, x3 couplings; g. Fmoc-Asp(O^tBu)-OH (3.0 equiv.), DIPCDI (3.0 equiv.), OxymaPure (3.0 equiv.), DMF, 1 h; h. 2% TFA in DCM, 3x2 min.

The CTC resin (1.4 g, 1.6 mmol/g) was swollen in DCM for 15 min. A solution of Fmoc-Gly-OH (153 mg, 0.50 mmol) in DIEA (872 µL, 5.00 mmol) was poured onto the resin and the mixture was shaken for 1 h. After this time, the free sites of the resin were capped with MeOH (1.8 mL, 15 min) and the resin was washed. The Fmoc- group was removed and the resin loading was determined to be 0.30 mmol/g. The peptide chain was elongated with the two following amino acids, Fmoc-Arg(Pbf)-OH and then Fmoc-*N*-(4-azidobutyl) valine (**34**), which were coupled in a 3-fold excess (1.26 mmol) using DIPCDI (204 µL, 1.26 mmol) and OxymaPure (188 mg, 1.26 mmol) as described in the general procedure. After a first coupling of **34**, the peptidyl-resin was not completely acylated, and a second coupling had to be performed to reach an almost complete conversion. At this stage, the Fmoc- group was removed, and Fmoc-D-Phe-OH (813 mg, 2.10 mmol) was activated with BTC (206 mg, 0.69 mmol) in the presence of 2,4,6-trimethylpyridine (777 µL, 5.88 mmol) and coupled onto the *N*-(4-azidobutylated) Val residue following the general procedure. This coupling was repeated three times. The small amount of unreacted resin-bound was capped by a 15 min-treatment with a solution of Ac_2O (398 µL, 4.20 mmol) and DIEA (735 µL, 4.20 mmol) in DCM. [*Note:* The poor reactivity of resin-bound *N*-(4-azidobutylated) Val was confirmed by treatment of a small sample of peptidyl-resin with Ac_2O/DIEA, wich resulted in

§ *Note:* The ^{1}H- and ^{13}C-NMR spectra of **34** were difficult to interpretate, since most signals were split due to the existence of rotamers. For the ^{1}H-NMR spectrum, the peaks herein described correspond to all the signals appearing in the spectrum. For the ^{13}C-NMR spectrum, the peaks herein described correspond to those signals associated to the major rotamer. All the signals appearing in the spectrum are the following: 19.0, 19.8, 25.7, 25.9, 27.5, 28.0, 47.4, 50.8, 67.6, 69.9, 120.0, 124.4, 127.2, 127.7, 141.4, 143.6, 151.2, 174.2.

no *N*-acetylation of this residue.] Then, the Fmoc- group was removed and Fmoc-Asp(O^tBu)-OH was assembled in a 3-fold excess (1.26 mmol) using DIPCDI (204 µL, 1.26 mmol) and OxymaPure (188 mg, 1.26 mmol) as described in the general procedure. The excess of reagents was filtered off, the Fmoc- group was removed, the resin was washed, and the peptide was cleaved from the solid support. After liophilization, pentapeptide **39** (189 mg, 45% crude yield) was obtained. The crude peptide was found to be enough pure to be cyclized without prior purification. HPLC (linear gradient from 5% to 100% ACN over 8 min): t_r = 6.18 min, purity = 63%; HPLC-MS (linear gradient from 5% to 100% ACN over 8 min): t_r = 7.36 min, $[M+H]^+$ = 999.51.

4.3.2. Small-scale SPPS of pentapeptide 39 by reductive N^{α}-alkylation with 4-azidobutanal (strategy B)

The small-scale synthesis of pentapeptide **39** through strategy B was performed as shown in Scheme 58.

Scheme 58. Small-scale SPPS of pentapeptide **39** through strategy B.

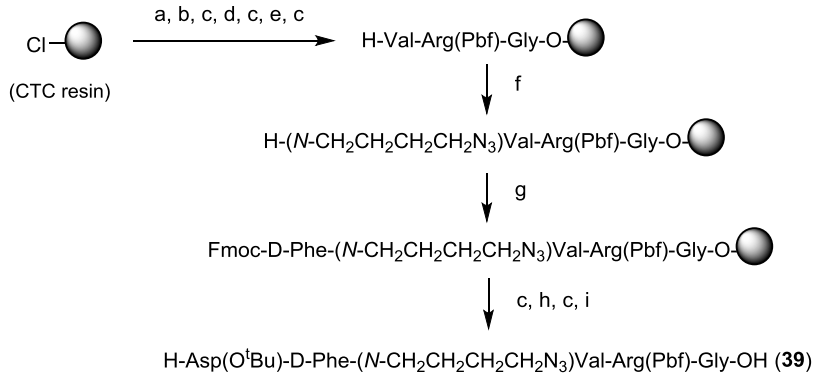

Reagents and conditions: a. Fmoc-Gly-OH (1.2 equiv.), DIEA (12.0 equiv.), DCM, 1 h; b. MeOH, 15 min; c. piperidine/DMF 1:4, 3x5 min, 1x10 min; d. Fmoc-Arg(Pbf)-OH (3.0 equiv.), DIPCDI (3.0 equiv.), OxymaPure (3.0 equiv.), DMF, 1 h; e. Fmoc-Val-OH (3.0 equiv.), DIPCDI (3.0 equiv.), OxymaPure (3.0 equiv.), DMF, 2 h; f. $N_3CH_2CH_2CH_2CHO$ (**38**, 1.5 eq), $NaBH_3CN$ (4.0 eq), 1% AcOH, THF, 3 h; g. Fmoc-D-Phe-OH (5.0 equiv.), BTC (1.65 equiv.), 2,4,6-trimethylpyridine (14.0 equiv.), THF, 15 h, x3 couplings; h. Fmoc-Asp(O^tBu)-OH (3.0 equiv.), DIPCDI (3.0 equiv.), OxymaPure (3.0 equiv.), DMF, 1 h; i. 2% TFA in DCM, 3x2 min.

The CTC resin (1.2 g, 1.6 mmol/g) was swollen in DCM for 15 min. A solution of Fmoc-Gly-OH (86 mg, 0.29 mmol) in DIEA (502 µL, 2.88 mmol) was poured onto the resin and the mixture was shaken for 1 h. After this time, the free sites of the resin were capped with MeOH (1.8 mL, 15 min) and the resin was washed. The Fmoc- group was removed and the resin loading was determined to be 0.25 mmol/g. The peptide chain was elongated with the two following amino acids, Fmoc-Arg(Pbf)-OH and then Fmoc-Val-OH, which were coupled in a 3-fold excess (0.90 mmol) using DIPCDI (146 µL, 0.90 mmol) and OxymaPure (134 mg, 0.90 mmol) as described in the general procedure. After Fmoc- removal, the *N*-terminal Val of the resin-bound peptide was subjected to reductive alkylation with 4-azidobutanal (**38**, 51 mg, 0.45 mmol) in the presence of $NaBH_3CN$ (75 mg, 1.20 mmol) as described in the general procedure. The resin was washed and the small amount of non-alkylated starting material was capped by a 15 min-treatment with a solution of Ac_2O (284 µL, 3.00 mmol) and DIEA (525 µL, 3.00 mmol) in DCM. [*Note:* The poor reactivity of resin-bound *N*-(4-azidobutylated) Val was confirmed by treatment of a small sample of peptidyl-resin with Ac_2O/DIEA, wich resulted in no *N*-acetylation of this residue.] At this stage, the Fmoc- group was removed, and Fmoc-D-Phe-OH (581 mg, 1.50 mmol) was activated with BTC (149 mg, 0.50 mmol) in the presence of 2,4,6-trimethylpyridine (555 µL, 4.20 mmol) and coupled onto the *N*-(4-azidobutylated) Val residue following the general procedure. This coupling was repeated

three times. The Fmoc- group was removed and Fmoc-Asp(O^{t}Bu)-OH was assembled in a 3-fold excess (0.90 mmol) using DIPCDI (146 µL, 0.90 mmol) and OxymaPure (134 mg, 0.90 mmol) as described in the general procedure. The excess of reagents was filtered off, the Fmoc- group was removed, the resin was washed, and the peptide was cleaved from the solid support. After liophilization, pentapeptide **39** (260 mg, 78% crude yield) was obtained. The crude peptide was found to be enough pure to be cyclized without prior purification. HPLC (linear gradient from 5% to 100% ACN over 8 min): t_r = 5.65 min, purity = 52%; HPLC-MS (linear gradient from 5% to 100% ACN over 11 min): t_r = 7.52 min, $[M+H]^+$ = 998.56.

4.3.3. Synthesis of pentapeptide 39 in a larger scale by a combined solid-phase/solution approach (strategy C)

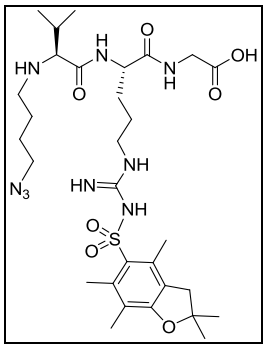

i. SPPS of H-(*N*-$CH_2CH_2CH_2CH_2N_3$)Val-Arg(Pbf)-Gly-OH (41). Tripeptide **41** was synthesized as described in Scheme 59. The CTC resin (6.00 g, 1.6 mmol/g) was swollen in DCM for 15 min. A solution of Fmoc-Gly-OH (2.140 g, 7.20 mmol) and DIEA (12.5 mL, 72.0 mmol) in DCM was poured onto the resin and the mixture was shaken for 1 h. After this time, the free sites of the resin were capped with MeOH (5.0 mL, 15 min) and the resin was washed. The Fmoc-group was removed and the resin loading was determined to be 1.00 mmol/g. The peptide chain was elongated with the two following amino acids, Fmoc-Arg(Pbf)-OH and then Fmoc-Val-OH, which were coupled in a 3-fold excess (18.0 mmol) using DIPCDI (2818 µL, 18.0 mmol) and OxymaPure (2.588 g, 18.0 mmol) as described in the general procedure. After Fmoc- removal, the α-amino group of the resin-bound peptide was subjected to reductive alkylation with 4-azidobutanal (**38,** 1.018 g, 9.0 mmol) in the presence of $NaBH_3CN$ (1.508 g, 24.0 mmol) as described in the general procedure. The excess of reagents was filtered off, the resin was washed, and the peptide was cleaved from the solid support. After liophilization, tripeptide **31** (4.72 g, quant. crude yield) was obtained. HPLC (linear gradient from 30% to 70% ACN over 8 min): t_r = 3.53 min, purity = 70%; HPLC-MS (linear gradient from 30% to 70% ACN over 11 min): t_r = 2.53 min, $[M+H]^+$ = 680.91; HRMS (ES^+): calc. for $[C_{30}H_{49}N_9O_7 + H]^+$ 680.3548, found 680.3565.

Scheme 59. SPPS of H-(*N*-$CH_2CH_2CH_2CH_2N_3$)Val-Arg(Pbf)-Gly-OH (**41**).

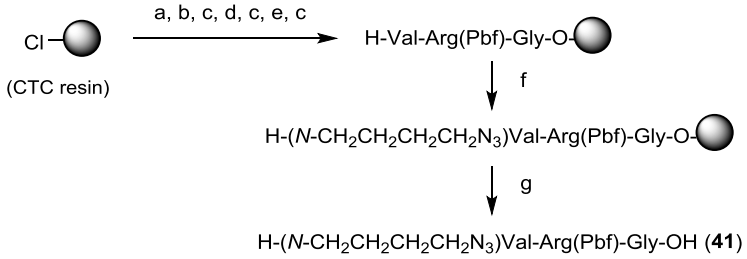

Reagents and conditions: a. Fmoc-Gly-OH (1.2 equiv.), DIEA (12.0 equiv.), DCM, 1 h; b. MeOH, 15 min; c. piperidine/DMF 1:4, 3x5 min, 1x10 min; d. Fmoc-Arg(Pbf)-OH (3.0 equiv.), DIPCDI (3.0 equiv.), OxymaPure (3.0 equiv.), DMF, 1 h; e. Fmoc-Val-OH (3.0 equiv.), DIPCDI (3.0 equiv.), OxymaPure (3.0 equiv.), DMF, 2 h; f. $N_3CH_2CH_2CH_2CHO$ (**38**, 1.5 eq), $NaBH_3CN$ (4.0 eq), 1% AcOH, THF, 3 h; g. 2% TFA in DCM, 3x2 min.

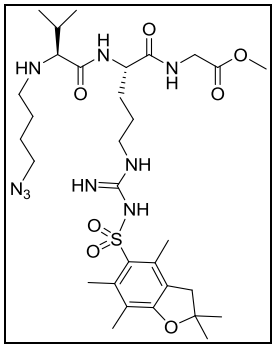

ii. Methyl esterification to obtain H-(*N*-$CH_2CH_2CH_2CH_2N_3$)Val-Arg(Pbf)-Gly-OMe (42). The crude tripeptide (**41**, 4.72 g, 70% purity) was dissolved in MeOH (25 mL) and an excess of $TMSCHN_2$ (6.0 mL of $TMSCHN_2$ 2.0 M in hexane, 12.0 mmol) was added. The mixture was allowed to react for 30 minutes at room temperature. Then, unreacted $TMSCHN_2$ was destroyed by adding AcOH (700 µL, 12.0 mmol) and stirring for a further period of 30 minutes. Next, the reaction mixture was concentrated under reduced pressure. The resulting residue was purified by flash chromatography (AcOEt/MeOH/AcOH 90:10:1) affording 4.19 g (100% yield) of the desired product (**42**), which was obtained as a white solid. HPLC (linear gradient from 30% to 70% ACN over 8 min): t_r = 3.85 min, purity = 93%; HPLC-MS (linear gradient from 30% to 50% ACN over 8 min): t_r = 0.95 min, $[M+H]^+$ = 695.00; HRMS (ES^+): calc. for $[C_{31}H_{51}N_9O_7S + H]^+$ 694.3705, found 694.3721.

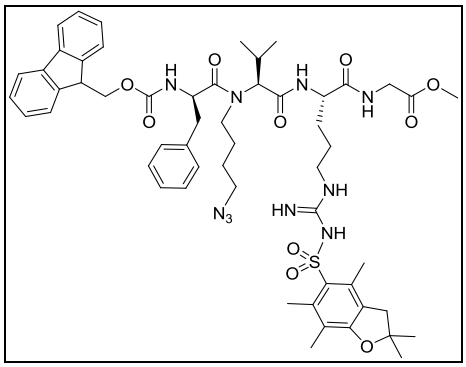

iii. Acylation with Fmoc-D-Phe-OH to obtain Fmoc-D-Phe-(*N*-$CH_2CH_2CH_2CH_2N_3$)Val-Arg(Pbf)-Gly-OMe (43). Fmoc-D-Phe-OH (8.949 g, 23.1 mmol) and BTC (2.257 g, 7.61 mmol) were weighed in a 100 mL-rounded flask and dissolved in THF $_{(anh.)}$ (50 mL). The system was purged with N_2 and cooled at 0 ºC. 2,4,6-trimethylpyridine (8.6 mL, 64.5 mmol) was added in three portions and a white precipitate was formed. The suspension was stirred for 3 min to ensure quantitative formation of the amino acid chloride. This supension was filtered and the filtrate was added to a solution of **42** (3.20 g, 4.61 mmol) in THF $_{(anh.)}$ (50 mL) under N_2 atmosphere. The resulting mixture was allowed to reach room temperature and stirred overnight. Then, the reaction was quenched with MeOH (10 mL). The crude was concentrated under reduced pressure and redissolved in AcOEt (150 mL). The organic phase was washed with $HCl_{(aq.)}$ 1M (2x60 mL) and then $NaHCO_{3\ (sat.)}$ (2x60 mL), dried over $MgSO_{4\ (anh.)}$, filtered and concentrated under reduced pressure. The obtained residue was purified by flash chromatography (Hexane/AcOEt/AcOH 50:50:1, then AcOEt/MeOH/AcOH 90:10:1) affording 2.10 g (52% yield) of the desired product (**43**), which was obtained as a white solid. HPLC (linear gradient from 40% to 100% ACN over 8 min): t_r = 8.56 min, purity = 100%; HPLC-MS (linear gradient from 40% to 100% ACN over 8 min): t_r = 10.36 min, $[M+H]^+$ = 1063.65; HRMS (ES^+): calc. for $[C_{55}H_70N_{10}O_{10}S + H]^+$ 1063.5070, found 1063.5037.

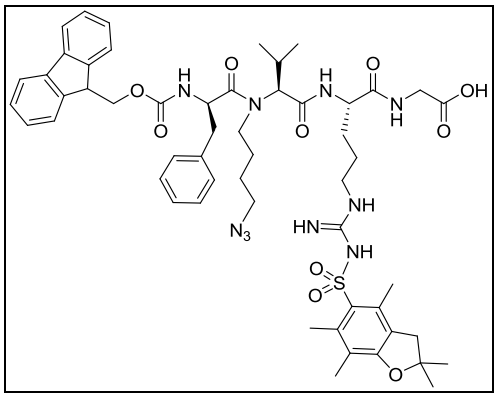

iv. Saponification to obtain Fmoc-D-Phe-(*N*-$CH_2CH_2CH_2CH_2N_3$)Val-Arg(Pbf)-Gly-OH (44). Compound **43** (2.410 g, 2.27 mmol) was dissolved in a 0.8 M solution of $CaCl_2$ in $^iPrOH/H_2O$ 7:3 (1135 mL). To this solution was added NaOH (109 mg, 2.72 mmol) and the mixture was stirred at room temperature (HPLC monitorization). HPLC analysis showed almost no remaining starting material after 1 h. At this point, the crude was acidified to pH = 4-5 by addition of AcOH (a few drops). AcOEt (50 mL) was added, phases were separated, and the aqueous phase was extracted with AcOEt (3x30 mL) and DCM (3x30 mL). The combination of organic phases was dried over $MgSO_{4\ (anh.)}$, filtered and concentrated under reduced pressure. This gave 2.74 g (quant. crude yield) of the desired product (**44**), which was obtained as a yellowish oil. This compound (**44**) was found to be enough pure to be directly used in further steps without prior purification. HPLC (linear gradient from 40% to 100% ACN over 8 min): t_r = 8.00 min, purity = 76%; HPLC-MS (linear gradient from 40% to 100% ACN over 8 min): t_r = 10.15 min, $[M+H]^+$ = 1049.50. HRMS (ES^+): calc. for $[C_{54}H_{68}N_{10}O_{10}S + H]^+$ 1049.4913, found 1049.4904.

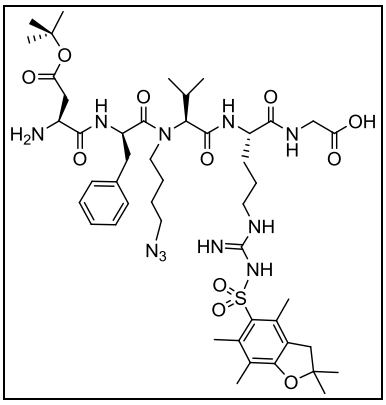

v. Peptide chain elongation in solid-phase and cleavage to obtain H-Asp(O^{t}Bu)-D-Phe-(*N*-$CH_2CH_2CH_2CH_2N_3$)Val-Arg(Pbf)-Gly-OH (39). Pentapeptide **39** was synthesized as described in Scheme 60. The CTC resin (5.5 g, 1.6 mmol/g) was swollen in DCM for 15 min. A solution of tetrapeptide **44** (0.58 g, 0.55 mmol) and DIEA (958 μL, 2.50 mmol) in DCM was poured onto the resin and the mixture was stirred overnight. After this time, the free sites of the resin were capped with MeOH (6.0 mL, 15 min) and the resin was washed. The Fmoc- group was removed and the resin loading was determined to be 0.08 mmol/g (expected 0.10 mmol/g), which corresponds to an 80% incorporation of **44** onto the resin. Next, Fmoc-Asp(O^{t}Bu)-OH (543 mg, 1.32 mmol) was activated with DIPCDI (207 μL, 1.32 mmol) and OxymaPure (188 mg, 1.32 mmol) in DMF in a separate vessel. This solution was poured onto the peptidyl-resin and, after stirring for 1 h, the ninhydrin test indicated a complete coupling. The excess of reagents was filtered off, the Fmoc- group was removed, the resin was washed, and the peptide was cleaved from the solid support. After lyophilization, pentapeptide **39** (0.815 g, quant. crude yield) was obtained. The crude peptide was found to be enough pure to be cyclized without prior purification. HPLC (linear gradient from 20% to 70% ACN over 8 min): t_r = 7.37 min, purity = 65%; HPLC-MS (linear gradient from 5% to 100% ACN over 8 min): t_r = 7.36 min, $[M+H]^+$ = 999.51.

Scheme 60. SPPS of H-(*N*-$CH_2CH_2CH_2CH_2N_3$)Val-Arg(Pbf)-Gly-OH (**41**).

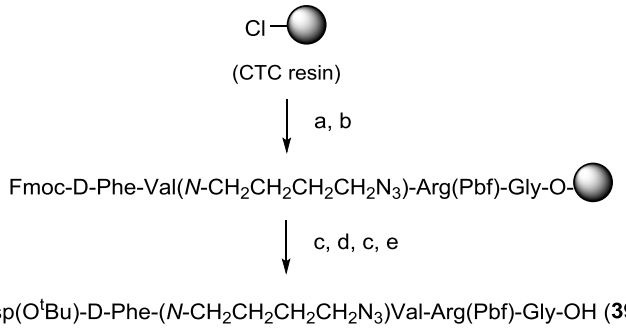

Reagents and conditions: a. Fmoc-D-Phe-(*N*-$CH_2CH_2CH_2CH_2N_3$)Val-Arg(Pbf)-Gly-OH (**44**, 1.0 equiv.), DIEA (10.0 equiv.), DCM, 15 h; b. MeOH, 15 min; c. piperidine/DMF 1:4, 3x5 min, 1x10 min; d. Fmoc-Asp(O^{t}Bu)-OH (3.0 equiv.), DIPCDI (3.0 equiv.), OxymaPure (3.0 equiv.), DMF, 1 h; e. 2% TFA in DCM, 3x2 min.

4.4. CYCLIZATION AND DEPROTECTION TO OBTAIN THE *N*-AZIDOALKYLATED CYCLOPEPTIDE

Note: The reactions described below correspond to the cyclization and deprotection of the crude pentapeptide **39** that was obtained in a larger scale following synthetic strategy C. For the crude pentapeptides **39** prepared through the synthetic strategies A and B, their cyclization and deprotection was performed under the same conditions herein described, and crude yields and purities were reproduced.

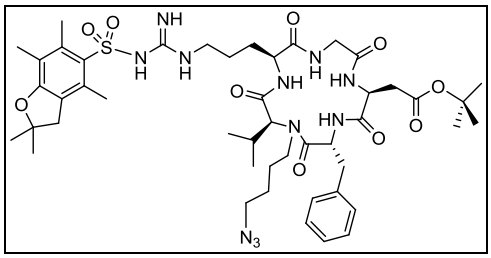

i. cyclo[Arg(Pbf)-Gly-Asp(O^{t}Bu)-D-Phe-(*N*-$CH_2CH_2CH_2CH_2N_3$)Val] (40). Crude pentapeptide **39** (0.767 g, 65% purity, 0.50 mmol) was dissolved in DCM (500 mL). EDC·HCl (0.958 g, 5.00 mmol) and DMAP (122 mg, 1.00 mmol) were added to the solution. After stirring at room temperature overnight, the mixture was concentrated to 100 mL and washed with 2% citric acid (2x30 mL), $Na_2CO_{3\ (sat.)}$ (2x30 mL) and NaCl $_{(sat.)}$ (2x30 mL). The organic phase was dried over $MgSO_{4\ (anh.)}$, filtered and concentrated under reduced pressure. This afforded 0.955 g (quant. crude yield) of cyclopeptide **40**. HPLC (linear gradient from 40% to 100% ACN over 8 min): t_r = 7.04 min, purity = 42%; HPLC-MS (linear gradient from 40% to 100% ACN over 15 min): t_r = 10.17 min, $[M+H]^+$ = 981.35.

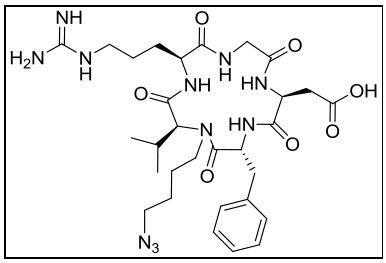

ii. cyclo[RGDf(*N*-$CH_2CH_2CH_2CH_2N_3$)V] (27). Crude cyclopeptide **40** (0.955 g, 42% purity) was dissolved in TFA/H_2O/TIS 95:5:5 (8.0 mL). After stirring for 3 h, the reaction mixture was concentrated under reduced pressure. Traces of TFA were removed by co-evaporation with toluene at 50 ºC. The deprotected peptide was precipitated two times by addition of cold *tert*-butyl methyl ether and subsequent centrifugation (3500 rpm, 5 min). The precipitate was redissolved in ACN/H_2O 1:1 and lyophilized. The resulting residue was purified by semipreparative RP-HPLC using a Sunfire™ C18 column (linear gradient from 30:70 to 45:55 ACN/H_2O over 10 min, flow rate = 3 mL/min). Fractions were collected, pooled and lyophilized to afford the pure cyclic peptide (**27**). which was redissolved in 1% AcOH in H_2O and lyophilized again. This afforded 131 mg (39% yield with respect to linear pentapeptide **39**) of cyclopeptide **27**. HPLC (linear gradient from 10% to 50% ACN over 8 min): t_r = 7.01 min, purity = 97%; HPLC-MS (linear gradient from 10% to 60% ACN over 8 min): t_r = 6.55 min, $[M+H]^+$ = 672.90; ^{1}H-NMR (500 MHz, D_2O): δ 0.62 (d, *J* = 6.3 Hz, 3H), 0.92 (d, *J* = 6.5 Hz, 3H), 1.26 (m, 2H), 1.51 (m, 2H), 1.61 (m, 2H), 2.00 (m, 3H), 2.76 (dd, *J* = 17.0 Hz, *J* = 6.5 Hz, 1H), 2.98 (m, 1H), 2.99 (dd, *J* = 17.0 Hz, *J* = 6.5 Hz, 1H), 3.18 (m, 1H), 3.22 (m, 2H), 3.22 (m, 2H), 3.29 (m, 2H), 3.59 (d, *J* = 14.8 Hz, 1H), 3.87 (dd, *J* = 9.4 Hz, *J* = 5.5 Hz, 1H), 4.12 (d, *J* = 14.7 Hz, 1H), 4.39 (d, *J* = 10.6 Hz, 1H), 4.67 (dd, *J* = 7.2 Hz, *J* = 7.2 Hz, 1H), 5.02 (dd, *J* = 10.1 Hz, *J* = 5.3 Hz, 1H), 7.25-7.41 (m, 5H); ^{13}C-NMR (500 MHz, D_2O): δ 18.5, 19.2, 24.9, 25.3, 25.4, 26.2, 27.7, 33.5, 38.0, 40.5, 43.0, 43.6, 49.9, 50.5, 51.7, 55.1, 64.4, 127.1, 128.8, 129.3, 136.3, 156.6, 170.4, 171.5, 171.7, 172.7, 173.4, 174.4; HRMS (ES^+): calc. for $[C_{30}H_{45}N_{11}O_7 + H]^+$ 672.3576, found 672.3577.

4.5. SYNTHESIS OF THE PEG CONJUGATES

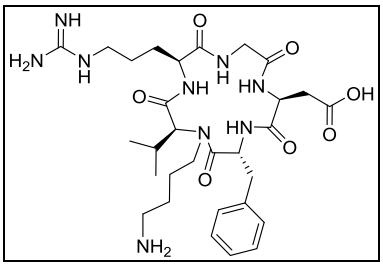

4.5.1. Azide reduction. To a solution of cyclopentapeptide **27** (72 mg, 0.11 mmol) and NH_4Cl (29 mg, 0.55 mmol) in H_2O/EtOH 3:1 (30 mL), zinc powder (9 mg, 0.14 mmol) was added. The mixture was stirred vigorously at 60 ºC and left to react overnight. Then, the mixture was filtered and the filtrate was concentrated under reduced pressure, redissolved in ACN/H_2O 1:1 and lyophilized. The resulting residue was purified by semipreparative RP-HPLC using a Sunfire™ C18 column (linear gradient from 10:90 to 55:45 ACN/H_2O over 15 min, flow rate = 3 mL/min). Fractions were collected, pooled and lyophilized to afford 17 mg (24% yield) of cyclo[RGDf(*N*-$CH_2CH_2CH_2CH_2NH_2$)V] (**28**) as a white solid. HPLC (linear gradient from 10% to 50% ACN over 8 min): t_r = 4.14 min, purity = 97%; HPLC-MS (linear gradient from 10% to 60% ACN over 8 min): t_r = 1.80 min, $[M+H]^+$ = 646.38; ^{1}H-NMR (500 MHz, CD_3OD): δ 0.45 (d, *J* = 6.4 Hz, 3H), 0.92 (d, *J* = 6.5 Hz, 3H), 1.43 (m, 2H), 1.53 (m, 2H), 1.63 (m, 2H), 1.94 (m, 1H), 2.13 (m, 2H), 2.64 (dd, *J* = 16.9 Hz, *J* = 6.4 Hz, 1H), 3.05 (dd, *J* = 17.0 Hz, *J* = 6.9 Hz, 1H), 3.18 (m, 1H), 2.84-3.16 (m, 6H), 3.51 (d, *J* = 14.5 Hz, 1H), 3.67 (dd, *J* = 7.8 Hz, *J* = 5.6 Hz, 1H), 4.13 (d, *J* = 14.6 Hz, 1H), 4.23 (d, *J* = 11.0 Hz, 1H), 4.56 (dd, *J* = 7.7 Hz, *J* = 6.5 Hz, 1H), 5.05 (dd, *J* = 10.2 Hz, *J* = 5.0 Hz, 1H), 7.15-7.35 (m, 5H); ^{13}C -NMR (500 MHz, CD_3OD): δ 20.03, 20.24, 25.65, 26.68, 27.49, 28.10, 30.81, 34.59, 40.27, 40.85, 42.11, 43.90, 44.18, 51.81, 52.85, 57.53, 66.01, 28.14, 129.81, 130.50, 137.85, 158.67, 163.22, 171.53, 171.69, 172.83, 173.10, 174.32, 174.68; HRMS (ES^+): calc. for $[C_{30}H_{47}N_9O_7 + H]^+$ 646.3671, found 646.3681.

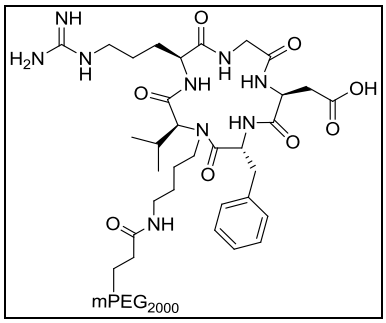

4.5.2. Conjugation of 27 with $mPEG_{2000}$-CH_2CH_2-COOSu. Pure cyclopentapeptide **28** (4 mg, 6 µmol) was dissolved in EtOH/0.2 M borate buffer pH = 8.5 1:1 (1 mL, c = 2 mg/mL) and $mPEG_{2000}$-CH_2CH_2-COOSu (6 mg, 3 µmol) was added while stirring. Complete conversion was observed after stirring for 2 h at room temperature, as confirmed by HPLC. Then, the mixture was concentrated under reduced pressure and the resulting crude was purified by semipreparative RP-HPLC using a Sunfire™ C18 column (linear gradient from 10:90 to 55:45 ACN/H_2O over 15 min, flow rate = 3 mL/min). Fractions were collected, pooled and lyophilized to afford PEG conjugate **29**, which was obtained as a white solid. HPLC (linear gradient from 10% to 50% ACN over 8 min): t_r = 7.18 min, purity = 99%; MALDI-TOF: Distribution of MW values around 2421.38 (average MW), with the main mass signals spaced apart by Δm/z = 44 (in agreement with the mass of the ethylene oxide monomer unit); NPC = 22%.

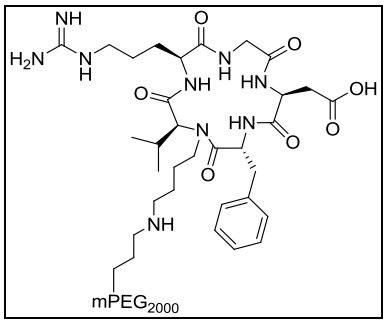

4.5.3. Conjugation of 27 with $mPEG_{2000}$-CH_2CH_2-CHO. Pure cyclopentapeptide **28** (7 mg, 11 µmol) was dissolved in MeOH (3.5 mL, c = 2 mg/mL) and, to this solution, NEt_3 (2 µL, 13 µmol) and $mPEG_{2000}$-CH_2CH_2-CHO (66 mg, 33 µmol) were added. After stirring for 30 minutes, $NaBH_3CN$ (4 mg, 65 µmol) was added to the mixture. The pH was checked to be around 8.0-9.0 and the reaction was allowed to proceed overnight. Then, the mixture was concentrated under reduced pressure and the resulting crude was purified by semipreparative RP-HPLC using a Sunfire™ C18 column (linear gradient from 10:90 to 55:45 ACN/H_2O over 15 min, flow rate = 3 mL/min). Fractions were collected, pooled and lyophilized to afford PEG conjugate **30**, which was obtained as a white solid. HPLC (linear gradient from 10% to 50% ACN over 8 min): t_r = 6.35 min, purity >99%; MALDI-TOF: Distribution of MW values around 2421.38 (average MW), with the main mass signals spaced apart by Δm/z = 44 (in agreement with the mass of the ethylene oxide monomer unit); NPC = 27%.

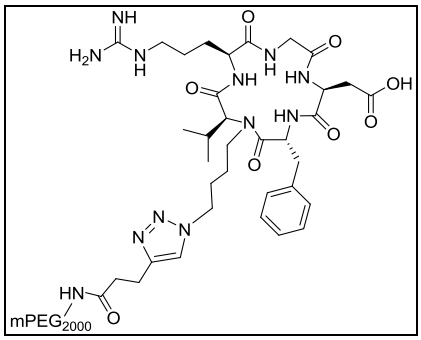

4.5.4. Conjugation of 26 with mPEG$_{2000}$-NH-CO-CH$_2$CH$_2$-alkyne. To a solution of cyclopentapeptide **27** (12 mg, 18 µmol) in ^{t}BuOH/H$_2$O 3:1 (1805 µL) was added mPEG$_{2000}$-NH-CO-CH$_2$CH$_2$-alkyne (54 mg, 27 µmol). Then, CuSO$_4$ (357 µL CuSO$_{4\,(aq)}$ 0.05 M, 18 µmol) and NaAsc (72 µL NaAsc $_{(aq)}$ 0.5 M, 36 µmol) were added (the final concentration of the substrate being 8 mM). The reaction was complete after overnight stirring at room temperature, as confirmed by HPLC. The mixture was concentrated under reduced pressure, redissolved in ACN/H$_2$O 1:1 and lyophilized. The resulting residue was purified by HPLC using a Sunfire™ C18 reversed-phase semipreparative column (linear gradient from 10:90 to 55:45 ACN/H$_2$O over 15 min, flow rate = 3 mL/min). Fractions were collected, pooled and lyophilized to afford PEG conjugate **31**, which was obtained as a yellowish solid. HPLC (linear gradient from 10% to 50% ACN over 8 min): t_r = 6.89 min, purity = 100%; MALDI-TOF: Distribution of MW values around 2654.85 (average MW), with the main mass signals spaced apart by Δm/z = 44 (in agreement with the mass of the ethylene oxide monomer unit); NPC = 70%.

4.6. NMR STUDIES OF PEPTIDES 23 AND 27

- Variable temperature ^{1}H-NMR experiments: For cyclo[RGDf*N*MeV] (**23**) and cyclo[RGDf(*N*-CH$_2$CH$_2$CH$_2$CH$_2$N$_3$)V] (**27**), ^{1}H-NMR spectra were acquired in the range from 278 K to 318 K with a step size of 10 K. All spectra were recorded on a Bruker Digital Avance 600 MHz spectrometer equipped with a TCI cryoprobe. Measurements were done with 7 mM sample solutions in 20 mM phosphate buffer (pH = 6.0) containing 10% D$_2$O for lock adjustament and 0.7 mM sodium 4,4-dimethyl-4-silapentane-1-sulfonate (DSS) as internal standard. Calibration was performed with reference to the DSS signal (^{1}H, 0.00 ppm). Under these conditions, a single set of H^N- and H$^\alpha$-signals was observed for each peptide and no evidence of conformational equilibria was found.

- Assignment of the H^N-, H$^\alpha$- and C$^\alpha$-signals: For cyclo[RGDf*N*MeV] (**23**) and cyclo[RGDf(*N*-CH$_2$CH$_2$CH$_2$CH$_2$N$_3$)V] (**27**), two-dimensional NMR experiments (COSY, HSQC, TOCSY and NOESY) were carried out. All spectra were recorded at 298 K on a Bruker Digital Avance 600 MHz spectrometer. Measurements were done with 7 mM sample solutions in 20 mM sodium phosphate buffer (pH = 6.0) containing 10% D$_2$O for lock adjustament and 0.7 mM 4,4-dimethyl-4-silapentane-1-sulfonic acid (DSS) as internal standard. Calibration was performed with reference to the DSS signal (^{1}H, 0.00 ppm; ^{13}C, 0.00 ppm). TOCSY spectra were recorded with a mixing time of 70 ms, and NOESY spectra with a mixing time of 500 ms. The assignment of the H^N-, H$^\alpha$- and C$^\alpha$- ressonances was accomplished using by through-bond connectivities from the two-dimensional spectra. In particular, we used the $(H^\alpha)_i$-$(H^N)_{i+1}$ cross-peaks from the NOESY spectra, the $(H^\alpha)_i$-$(H^\beta)_i$ cross-peaks from the COSY spectra, the $(H^\alpha)_i$-$(H^\beta)_i$-$(H^\beta)_i$-$(H^N)_i$ the cross-peaks from the TOCSY spectra, and the $(H^\alpha)_i$-$(C^\alpha)_i$ cross-peaks from the HSQC spectra. All the signals could be unequivocally assigned.

- Determination of temperature coefficients for the amide protons: For cyclo[RGDf*N*MeV] (**23**) and cyclo[RGDf(*N*-CH$_2$CH$_2$CH$_2$CH$_2$N$_3$)V] (**27**), the temperature coefficients for the amide protons were determined from the variable temperature ^{1}H-NMR experiments. The H^N-chemical shifts were plotted versus the acquisition temperature (278 K, 288 K, 298 K, 308 K, 318 K) and the data points were adjusted to a linear fit using an Excel software package. In all cases, a good linear correlation (R^2 >0.98) was observed.

4.7. BIOLOGICAL ACTIVITY EVALUATION

Cell adhesion inhibition assays. Cells were grown at 37 ºC and 5% CO_2 and expanded when they reached 90% confluence. For DAOY cells, the medium was DMEM High Glucose, supplemented with 10% FCS; for HUVEC cells, the medium was EBM, supplemented with 10% FCS. Non-tissue culture treated ELISA plates were coated with the appropriate concentration of the ligand (for HUVEC: vitronectin at 0.75 µg/mL and fibrinogen at 10 µg/mL, for DAOY: vitronectin at 0.5 µg/mL and fibrinogen at 40 µg/mL) and incubated overnight at room temperature. Plates were then washed two times with PBS and incubated with the blocking solution (PBS containing 1.5% BSA; 60 min at 37° C) to block unspecific interaction sites. The blocking solution was discarded by flicking and serial dilutions of the compounds were plated in duplicates. Immediately, harvested cells were seeded into the same plate at a concentration of 600000 cells/well. Plates were incubated for 90 min at 37 ºC to allow cell adhesion and spreading of the ligands. Plates were then washed three times with PBS to remove non-adhered cells and 60 µL/well of hexosaminidase substrate solution (*p*-nitrophenol-*N*-acetyl-*ß*-D-glucosaminide 3.75 mM, containing 50 mM of sodium citrate at pH 5.0) was added. The plates were incubated at 37 ºC during 4 h and then 60 µL of stop solution (0.2 M NaOH, 5 mM EDTA at pH 10.4) was added. The number of cells that remained attached to the plate was evaluated by measuring the absorbance of the plates at 405 nm with a spectrophotometer. Each plate contained positive and negative controls and compounds were tested as duplicates. The adhesion inhibition IC_{50} was calculated using the Prism-4 software based on the sigmoidal dose-response (variable slope) equation. Standard deviations were at the most in the same order of the IC_{50} values.

4.8. DETERMINATION OF logP BY THE SHAKE-FLASK METHOD

Our shake-flask procedure to determine the logP values of **23**, **24-26** and **29-31** was the following. The compounds of study were tested as triplicates. 500 µg of compound were weighed in a 1.5 mL eppendorf and dissolved in 600 µL of octanol (previously saturated with H_2O). The sample solution was divided in 3 samples of 200 µL, each of which was placed in a 1.5 mL eppendorf. To each triplicate, 200 µL of H_2O (previously saturated with octanol) were added, so that the final concentration of the compound was 0.42 µg/µL. The resulting mixtures were shaken in a mechanical shaker for 2 days, which ensures that partition equilibrium is reached. Then, the eppendorfs were centrifuged, phases were separated, and an aliquot of each phase was injected into the HPLC apparatus. UV detection was performed at 220 nnm. The relation between the HPLC peak areas of the compound in each phase was used to calculate logP. The given logP values are the average of the logP values calculated for each triplicate. [*Presaturation of the solvent:* Before partition experiments, the two phases of the solvent system were mutually saturated. For doing this, two large stock bottles of octanol and H_2O with a sufficient quantity of the other solvent were stirred for 2 days. Then, phases were separated using an extraction funnel.] [*Note*: Since the initial compound concentration is known, retention of compound of study in the interphase can be detected.]

RESUM DE LA MEMÒRIA

Introducció

En química medicinal, la *N*-metilació de l'esquelet peptídic és una de les modificacions més atractives de l'estructura d'un pèptid.[6] La introducció de grups *N*-Me ha permès optimitzar l'activitat i selectivitat de nombrosos lligands peptídics mitjançant restriccions conformacionals. D'altra banda, la introducció de grups *N*-Me en pèptids millora certes propietats farmacològicament rellevants (*i.e*. lipofilicitat, estabilitat proteolítica, permeabilitat a través de membranes), i és una estratègia cada cop més utilitzada per a guanyar *biodisponibilitat* en pèptids d'interès terapèutic.

Sorprenentment, a la literatura existeixen molts pocs exemples en els quals s'hagin sintetizat pèptids *N*-substituïts amb d'altres grups diferents de *N*-Me. Deixant de banda els peptòids (*i.e*. oligòmers de Gly *N*-substituïts),[8] els pocs exemples de pèptids *N*-alquilats descrits es limiten a *N*-substituents de petit tamany: *N*-etil,[14,63] *N*-al·lil,[14,65] *N*-butil,[64] *N*-guanidilbutil,[68] i grups *N*-alquil functionalitzats per a *backbone cyclization.*[7]

Aquesta escassetat de precedents es pot atribuir a la dificultat sintètica de preparar pèptids *N*-alquilats.[70] La principal dificultat és l'acilació dels residus *N*-alquilats, que està impedida per raons estèriques. En general, els acoblaments sobre aminoàcids *N*-alquilats tenen lloc amb baix rendiment quan s'utlitzen mètodes d'acoblament estàndard. S'han descrit diversos reactius per a l'acilació de residus *N*-Me, però aquests reactius sovint no resulten eficients quan els residus involucrats presenten cadenes laterals voluminoses. A més, en incrementar el tamany del grup *N*-alquil, la formació de l'enllaç amida *N*-alquilat esdevé més difícil a causa del major impediment estèric. D'altra banda, cal esmentar que els aminoàcids *N*-alquilats tenen tendència a epimeritzar en activar el seu grup carboxil i que, un cop incorporats a la cadena peptídica, afavoreixen la formació de DKPs. Aquestes i d'altres reaccions secundàries esdevenen especialment problemàtiques durant acoblaments lents.

L'objectiu principal de la present Tesi ha estat investigar la viabilitat sintètica de modificar l'esquelet peptídic amb *N*-substituents més grans que *N*-Me. Depenent de la naturalesa del *N*-substituent, la seva introducció en un pèptid pot ser útil per a modificar les seves propietats fisicoquímiques, o bé per a funcionalitzar-lo amb un grup reactiu que permeti la unió covalent d'una molècula desitjada.

En general, la modificació de l'esquelet peptídic indueix canvis en la seva conformació. Quan s'introdueix un grup *N*-alquil en un pèptid, s'afavoreix una configuració *cis* a l'enllaç amida *N*-alquilat[15] i es disminueix el nombre de ponts d'hidrogen que el pèptid pot formar. Això modifica les preferències torsionals de l'esquelet peptídic i/o el seu patró de ponts d'hidrogen intramoleculars, alterant la conformació original del pèptid. A més, la introducció de grups *N*-alquil en un pèptid pot disminuir la seva flexibilitat conformacional a causa d'interaccions estèriques locals.[16]

Donat que existeixen pocs precedents en la síntesi de pèptids *N*-alquilats, no s'ha investigat si, per a una mateixa posició *N*-alquilada, diferents grup *N*-alquil exerceixen restriccions conformacionals semblants independentment de la seva naturalesa. Així doncs, durant la realització de la present Tesi, ens vam plantejar un segon objectiu: investigar si els grup *N*-Me presents en un pèptid es poden reemplaçar per altres *N*-substituents sense pertorbar la conformació del pèptid.

Capítol 1

L'objectiu del treball que constitueix aquest Capítol va ser establir una metodologia per a la preparació de Fmoc-aminoàcids *N*-substituïts amb una cadena de *N*-trietilenglicol (*N*-TEG) i per a la seva la utilització com a *building blocks* en síntesi de pèptids en fase sòlida (SPPS).

En primer lloc, vam desenvolupar un protocol robust per a la preparació de Fmoc-*N*-TEG aminoàcids (veure Esquema 61). Aquests derivats es poden obtenir a partir dels seus corresponents aminoàcids *tert*-butil-protegits en tres etapes: i. N^{α}-alquilació reductora amb 3,6,9-trioxadecanaldehid, ii. Fmoc-protecció del grup amino *N*-alquilat, iii. trencament acidolític de l'ester *tert*-butílic. Amb aquest fàcil protocol, vam sintetitzar diversos Fmoc-*N*-TEG derivats amb rendiments satisfactoris i a una escala de 5 g.

Esquema 61. Síntesi de Fmoc-*N*-TEG aminoàcids.

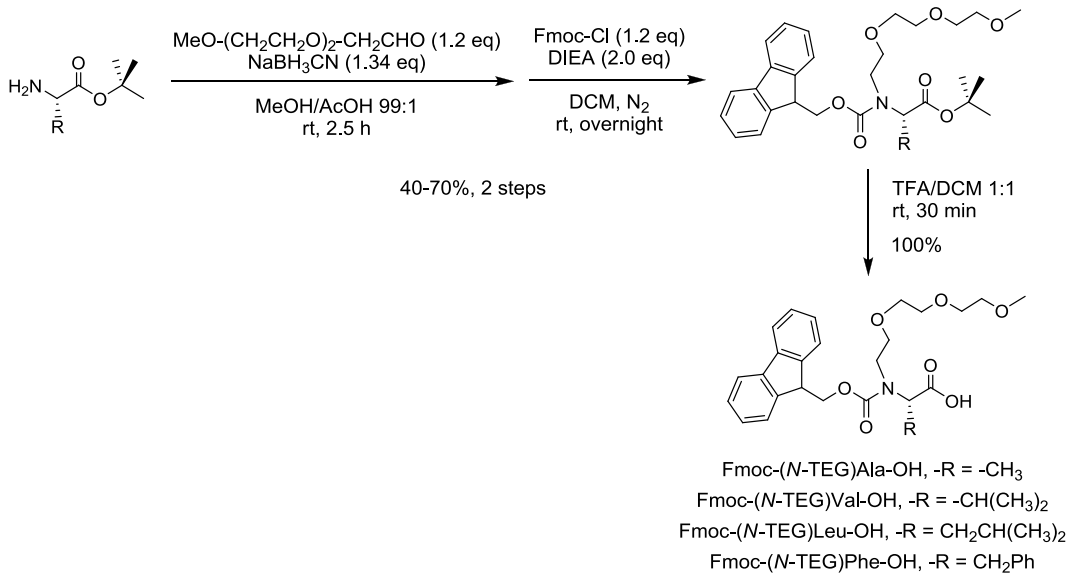

A continuació, vam investigar condicions per a la utilització dels Fmoc-*N*-TEG aminoàcids en SPPS. Vam trobar que aquests derivats es poden acoplar a una peptidil-resina utilitzant condicions estàndard. No obstant, l'acoblament del següent aminoàcid sobre el residu *N*-TEG està impedit estèricament i requereix un mètode d'activació més potent.

Per tal de trobar condicions per a l'acilació de *N*-TEG aminoàcids en fase sòlida, vam estudiar l'acoblament de Fmoc-Ala-OH sobre una (*N*-TEG)Leu-peptidil-resina. Per a aquesta reacció model, vam realitzar una sèrie de proves amb diversos reactius d'acoblament i paràmetres de reacció (*i.e*. temps, temperatura, excés de reactius, additius, irradiació amb MW, etc.). Després de cada prova d'acoblament, vam estimar la conversió de la següent manera: i. Fmoc-protecció dels grup α-amino no acilats presents a la peptidil-resina, ii. anàlisi d'una mostra de la peptidil-resina resultant per HPLC, iii. determinació del % material de partida a partir de la relació entre les àrees d'integració dels pics HPLC corresponents al producte i al material de partida Fmoc-protegit. Això ens va permetre avaluar l'eficiència dels diferents mètodes d'acoblament provats (veure Taula 31).

Taula 31. Avaluació de l'eficiència de diferents mètodes d'acoblament per a l'acilació de (*N*-TEG)Leu-peptidil-resina.

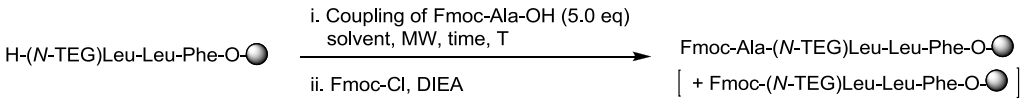

Coupling method	solvent	MW	T (ºC)	time (h)	Coupling efficiency
DIPCDI (5.0 eq)/OxymaPure (5.0 eq)	DMF	-	rt	1	2%
	DMF	-	rt	15	33%
	DMF	MW	50	1	51%
DIPCDI (5.0 eq)/HOAt (5.0 eq)	DMF	-	rt	1	10%
	DMF	-	rt	15	63%
	DMF	MW	50	1	**82%**
HATU (5.0 eq)/HOAt (5.0 eq)/DIEA (10.0 eq)	DMF	-	rt	1	8%
	DMF	-	rt	15	27%
	DMF	MW	50	1	11%
COMU (5.0 eq)/DIEA (10.0 eq)	DMF	-	rt	1	0%
	DMF	-	rt	15	14%
	DMF	MW	50	1	13%
DIPCDI (5.0 eq)/DMAP (0.2 eq)	DCM	-	rt	1	0%
	DCM	-	rt	15	0%
	DMF	MW	50	1	25%
TFFH (5.0 eq)/DIEA (5.0 eq) + DIEA (5.0 eq)	THF	-	rt	15	0%
	THF	MW	50	1	7%
TFFH (5.0 eq)/DIEA (5.0 eq) [*N*-silylation with BTSA (5.0 eq) prior to coupling]	DCM	-	rt	1	0%
	DCM	-	rt	15	0%
Fmoc-Ala-Cl (5.0 eq)/DIEA (5.0 eq)	DMF	-	rt	1	0%
	DMF	-	rt	15	0%
Fmoc-Ala-Cl (5.0 eq)/HOBt (5.0 eq)/DIEA (5.0 eq)	DMF	-	rt	1	3%
	DMF	-	rt	15	28%
TCFH (5.0 eq)/DIEA (5.0 eq) + DIEA (2.0 eq)	THF	-	rt	15	0%
	THF	MW	50	1	25%
BTC (1.65 eq)/2,4,6-trimethylpyridine (14.0 eq)	THF	-	rt	1	59%
	THF	-	rt	15	**87%**
	THF	MW	45	1	51%

Vam trobar que el mètode més eficient per a l'acilació de *N*-TEG aminoàcids en fase sòlida és utilitzar BTC[194] com a reactiu activant i realitzar dos acoblaments overnight a temperatura ambient. Amb aquest mètode, l'acoblament de Fmoc-Ala-OH sobre la (*N*-TEG)Leu-peptidil-resina té lloc amb una conversió del 87%, i s'aconsegueix una acilació completa després del segon acoblament. Vam provar altres reactius recomanats per a l'acilació de grups amino *N*-alquilats. En molts casos, l'escalfament amb MW va promoure l'acoblament i va incrementar la puresa del producte. No obstant, en termes de rendiment, l'activació amb BTC va resultar superior a tots els mètodes que vam provar, incloent l'activació amb HATU/HOAt o l'ús d'un clorur d'àcid com a espècie acilant. Cal esmentar que la utilització de DIPCDI/HOAt en combinació amb MW (1 h, 50 ºC) va donar lloc a una conversió semblant a l'observada amb el mètode BTC (82% vs. 87% després del primer acoblament). No obstant, l'activació amb BTC és preferible, degut al baix cost d'aquest reactiu i la simplicitat experimental del protocol.

L'activació amb BTC també va resultar eficient per a acilar la (*N*-TEG)Leu-peptidil-resina amb altres aminoàcids (*i.e.* Fmoc-Leu-OH, Fmoc-Phe-OH i Fmoc-Val-OH). En tots els casos, l'acilació va ser completa o pràcticament completa després de dos acoblaments.

En conclusió, els Fmoc-*N*-TEG aminoàcids es poden preparar fàcilment en 3 etapes i es poden utilitzar com a *building blocks* en fase sòlida, permetent l'obtenció de *N*-TEG-pèptids de manera ràpida, econòmica i eficient.

Capítol 2

L'objectiu del treball que constitueix aquest Capítol va ser investigar el grup *N*-TEG com a substitut del grup *N*-Me, el qual es troba present en nombrosos pèptids biològicament actius.

Per tal d'investigar això, vam incorporar *N*-TEG i *N*-Me aminoàcids a les diferents posicions del pèptid Sansalvamida A (**1**), un pentapèptid cíclic que presenta activitat anti-tumoral contra diversos tipus de càncers.[123] Vam considerar que aquest ciclopèptid era un bon model per al nostre objecte d'estudi, ja que els seus anàlegs *N*-metilats ja han estat sintetitzats i alguns d'ells són citotòxics contra certes línies cel·lulars canceroses.[123a] Així doncs, vam sintetizar els 5 *N*-TEG i els 5 *N*-Me anàlegs (**1a-5a** i **1b-5b**) del pèptid Sansalvamida A (**1**) i, per a les dues sèries de compostos, vam avaluar la seva activitat biològica, hidrofobicitat, i estat conformacional en comparació amb el pèptid original. Les estructures del pèptid Sansalvamida A (**1**) i dels seus *N*-TEG i *N*-Me anàlegs (**1a-5a** i **1b-5b**) es mostren a la Figura 61.

Figura 61. Estructura del pèptid Sansalvamida A (**1**) i els *N*-TEG i *N*-Me anàlegs (**1a-5a** i **1b-5b**) sintetizats.

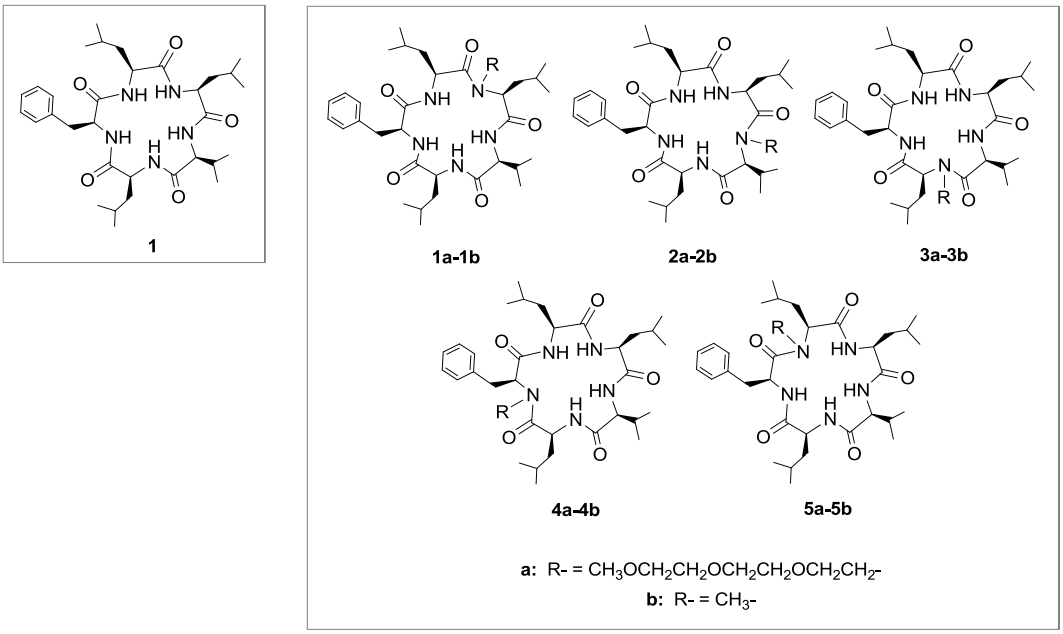

Per tal d'obtenir els *N*-TEG i *N*-Me ciclopèptids (**1a-5a** i **1b-5b**), vam preparar els seus precursors lineals (**p1a-p5a** i **p1b-p5b**) a la resina CTC seguint l'estratègia Fmoc-/^{t}Bu- i utilitzant DIPCDI/OxymaPure com a mètode d'activació per als acoblaments estàndard (veure Esquema 62). En la síntesi dels pentapèptids **p1b-5b** vam utilitzar Fmoc-*N*-Me aminoàcids comercials, mentre que els Fmoc-*N*-TEG aminoàcids requerits per a la síntesi dels pentapèptids **p1a-p5a** es van preparar en solució, emprant la metodologia desenvolupada al Capítol 1. En tots els pentapèptids, els residus *N*-TEG i *N*-Me es van introduir al mig de la seqüència peptídica per tal de minimitzar l'impediment estèric durant l'etapa de ciclació; d'altra banda, és sabut que la presència de grups *N*-alquil en aquesta posició pre-organitza conformacionalment l'esquelet peptídic, afavorint la seva ciclació.[124] Per als acoblaments sobre els residus *N*-alquilats, vam activar el següent aminoàcid amb BTC. Amb aquest mètode vam aconseguir una completa acilació de les diferents *N*-Me i *N*-TEG peptidil-resines, tot i que en el cas dels residus *N*-TEG van ser necessaris dos cicles d'acoblament i, en el cas del pèptid **p2a**, l'acoblament no va ser complet degut a l'impediment estèric addicional exercit per la cadena β-ramificada del residu (*N*-TEG)Val. Després d'allargar la cadena peptídica i escindir els pèptids

de la resina, vam ciclar-los amb EDC·HCl/DMAP i vam aïllar els ciclopèptids resultants per RP-HPLC. D'aquesta manera vam obtenir *N*-TEG i *N*-Me ciclopèptids **1a-5a** i **1b-5b** amb una puresa >95%. En tots els casos, vam obtenir suficients quantitats de pèptid pur en rendiments que són típics per a la síntesi de pentapèptids cíclics. Excepte en el cas del ciclopèptid **2a**, els rendiments globals de les síntesis dels *N*-TEG ciclopèptids (**1a-5a**) no van ser dramàticament inferiors als de les síntesis dels *N*-Me ciclopèptids (**1a-5a**). Així doncs, podem concloure que els pèptids modificats amb el grup *N*-TEG són fàcilment accessibles amb la metodologia establerta per a pèptids *N*-metilats.

Esquema 62. Síntesi dels *N*-TEG i *N*-Me anàlegs **1a-5a** i **1b-5b**.

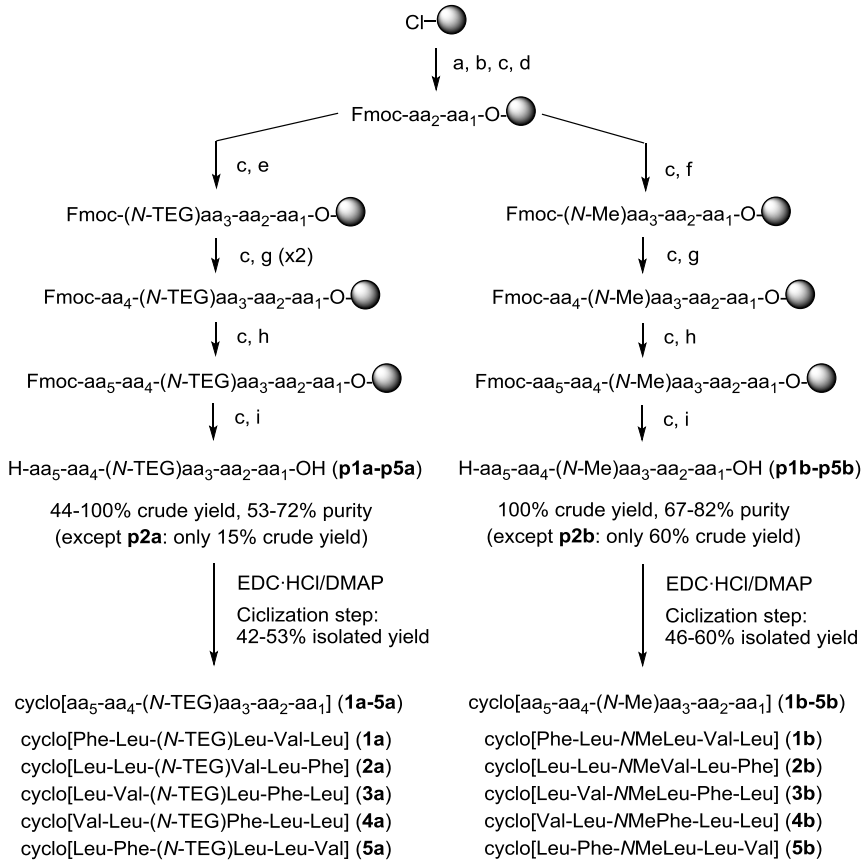

Reactius i condicions: a. Fmoc-aa$_1$-OH, DIEA; b. MeOH; c. piperidine/DMF 1:4; d. Fmoc-aa$_2$-OH, DIPCDI, OxymaPure; e. Fmoc-(*N*-TEG)aa$_3$-OH, DIPCDI, OxymaPure; f. Fmoc-(*N*-Me)aa$_3$-OH, DIPCDI, OxymaPure; g. Fmoc-aa$_4$-OH, BTC, 2,4,6-trimethylpyridine, THF; h. Fmoc-aa$_5$-OH, DIPCDI, OxymaPure; i. 2% TFA in DCM; j. EDC·HCl, DMAP.

Per tal d'investigar com la substitució del grup *N*-Me dels anàlegs **1b-5b** per un grup *N*-TEG afecta la seva activitat anti-cancerígena, vam avaluar la citotoxicitat dels pèptids **1**, **1a-5a** i **1b-5b** contra tres línes cel·lulars canceroses: GLC-4 (pulmó), MDA-MB-231 (mama) i SW-480 (colon). En aquests estudis de citotoxicitat, vam mesurar la viabilitat cel·lular amb l'assaig MTT. El tractament amb 50 µM d'alguns compostos durant 72 h va decréixer la viabilitat de les cèl·lules GLC-4 i MDA-MB-231 fins a un 50-60% (veure Figura 62). Tot i que cap dels compostos va mostrar elevada citotoxicitat envers les línies cel·lulars emprades en aquest estudi, les activitats citotòxiques d'alguns *N*-TEG anàlegs i els seus *N*-Me homòlegs es troben en el mateix rang.

Figura 62. Viabilitat de cèl·lules canceroses GLC-4, MDA-MB-231 i SW-480 després d'un tractament amb 50 μM de **1**, **1a-5a** i **1b-5b** durant 72 h.

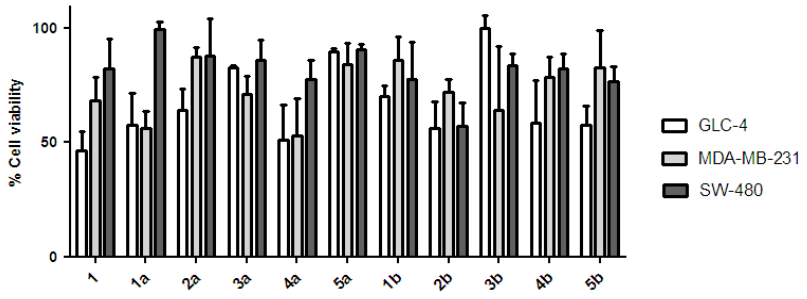

Per tal d'investigar com la modificació d'un pèptid amb el grup *N*-TEG o *N*-Me afecta la seva hidrofobicitat, vam avaluar la hidrofobicitat relativa d'aquest pèptid (**1**) i els seus anàlegs *N*-substituïts (**1a-5a** i **1b-5b**) per comparació dels temps de retenció RP-HPLC (veure Taula 32). La retenció d'un compost en RP-HPLC depèn del seu caràcter hidrofòbic (*i.e.* com més hidrofòbic és un compost, major és la seva retenció en la fase estacionària apolar), i del seu tamany molecular. Així doncs, per a una sèrie d'anàlegs modificats que presenten tamany semblant, la comparació dels seus temps de retenció és un mètode vàlid per a estimar la seva hidrofobicitat relativa.[133] Vam trobar que els temps de retenció dels anàlegs *N*-substituïts (**1a-5a** i **1b-5b**) eren superiors al del pèptid original (**1**), indicant una major hidrofobicitat. Això era d'esperar, ja que la introducció de grups *N*-alquil en un pèptid disminueix el nombre de protons amida, que són donadors de ponts d'hidrogen. Remarcablement, els *N*-TEG anàlegs (**1a-5a**) van resultar ser lleugerament més hidrofòbics que els seus *N*-Me homòlegs (**1b-5b**). La major hidrofobicitat dels *N*-TEG pèptids podria resultar en una major permeabilitat a través de barreres biològiques (*e.g.* epiteli intestinal, pell): el caràcter lipofílic d'una molècula afavoreix la seva difusió passiva a través de les membranes cel·lulars fosfolipídiques,[138] i –per a la majoria de fàrmacs– la difusió passiva transcel·lular és el principal mecanisme de transport. De fet, s'ha postulat que la major permeabilitat intestinal dels pèptids *N*-metilats és deguda –entre d'altres factors– a que són més hidrofòbics i poden formar menys ponts d'hidrogen.[20] Així doncs, la introducció de grups *N*-TEG en pèptids d'interès terapèutic també podria resultar útil per a guanyar permeabilitat intestinal.

Taula 32. Temps de retenció RP-HPLC de **1**, **1a-5a**, **1b-5b**, gradient lineal de 10% a 90% ACN en 8 min, columna C18.

t_r (min)	
1: 5.97	
1a: 7.29	**1b:** 7.12
2a: 7.22	**2b:** 7.07
3a: 6.98	**3b:** 6.82
4a: 7.34	**4b:** 6.97
5a: 7.05	**5b:** 6.86

Per tal d'estudiar si els grup *N*-TEG i *N*-Me exerceixen restriccions conformacionals semblants quan s'incorporen en un pèptid cíclic, vam analitzar dels pèptids **1**, **1a-5a** i **1b-5b** per espectroscòpia RMN de ^{1}H i ^{13}C. La superposició dels seus espectres RMN de ^{1}H es mostra a la Figura 63. Les diferències que s'observen en les regions H^{α} i H^{N} indiquen clarament que la modificació del pèptid Sansalvamida A (**1**) amb *N*-TEG o *N*-Me va perturbar el seu estat conformacional. Depenent de la posició de *N*-alquilació, vam observar diferents patrons de senyals; no obstant, els *N*-TEG i *N*-Me anàlegs (**1a-5a** i **1b-5b**) amb el *N*-substituent a la mateixa posició van presentar desplaçaments químics molts semblants per als protons H^{α} i H^{N}, així com per als carbonis C^{α} (veure Taula 33). La semblança d'aquests desplaçaments químics, que són sensibles a canvis conformacionals en l'esquelet peptídic, indica que els *N*-TEG i *N*-Me pèptids amb el mateix patró de *N*-alquilació presenten una conformació similar, independentent de la naturalesa del

N-substituent. Per als pèptids **5a** i **5b**, vam realitzar un estudi més detallat en comparació amb el pèptid original (**1**). Vam trobar els protons H^N dels homòlegs **5a** i **5b** tenien coeficients de temperatura i patrons de NOEs pràcticament idèntics, alhora que considerablement diferents dels del pèptid Sansalvamida A (**1**). En base a aquests resultats, podem concloure que els grups *N*-TEG i *N*-Me exerceixen restriccions conformacionals semblants quan s'incorporen en un pèptid cíclic.

Figura 63. Espectres de RMN de ^1H (en $CDCl_3$) de **1**, **1a-5a** i **1b-5b** en la regió 8.5-6.0 ppm (A) i en la regió 5.5-3.5 ppm (B).

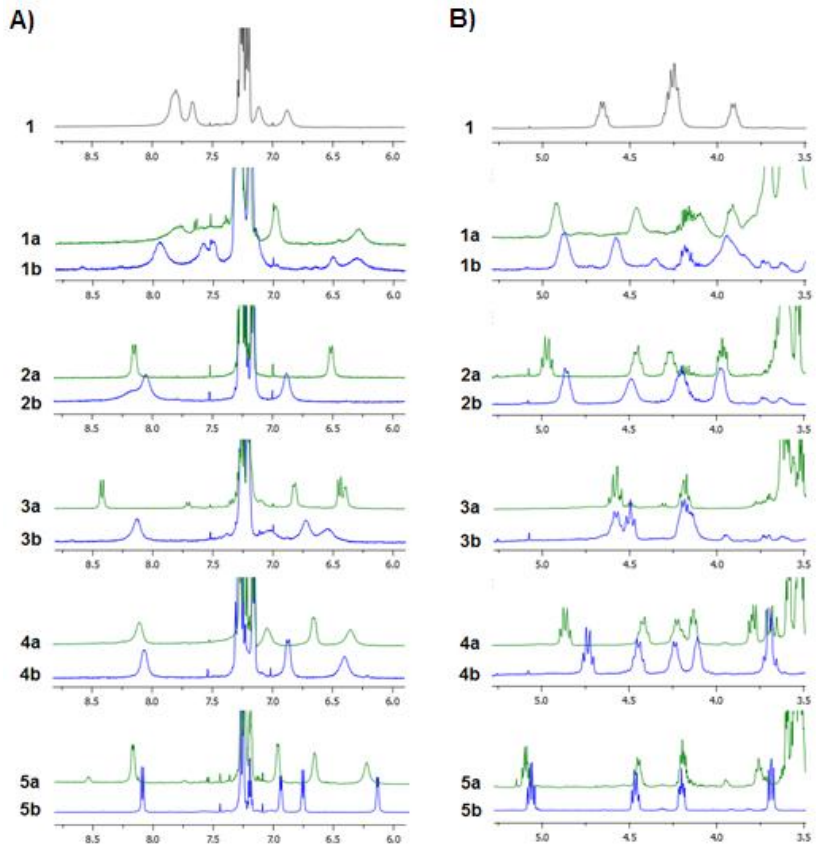

Taula 33. Desplaçaments químics (ppm) dels senyals de C^α de **1**, **1a-5a** i **1b-5b** en $CDCl_3$.

1	1a	1b	2a	2b	3a	3b	4a	4b	5a	5b
51.7	48.6	49.2	48.3	48.3	51.9	52.1	48.5	48.3	51.2	51.2
53.7	52.6	55.0	50.9	51.5	53.9	54.3	51.5	51.7	51.4	51.5
55.3	56.1	56.0	53.5	53.2	54.4	54.6	52.8	53.0	53.6	53.4
57.9	59.8	59.1	56.6	57.5	55.4	55.3	60.2	60.2	60.7	61.2
58.8	66.4	65.0	66.4	65.1	67.9	68.9	70.8	72.1	68.4	70.0

En conclusió, els pèptids modificats amb una cadena de *N*-TEG es poden preparar fàcilment utilitzant metodologia establerta per a la síntesi de pèptids *N*-metilats. En un pèptid cíclic *N*-metilat, és d'esperar que la substitució del seu grup *N*-Me per un grup *N*-TEG no alteri el seu patró de formació de ponts d'hidrogen i provoqui una mínima pertorbació de la seva conformació. No obstant, degut al caràcter amfifílic del grup TEG, els *N*-TEG pèptids són lleugerament més hidrofòbics que els seus homòlegs *N*-metilats. Considerant que el grup *N*-Me es troba present en nombrosos pèptids biològicament actius, reemplaçar els grups *N*-Me presents en un pèptid per altres *N*-substituents és una alternativa viable per a introduir diversitat química o alterar propietats d'interès farmacològic quan no és possible o desitjable modificar estructuralment cap altra posició del pèptid.

Capítol 3

El principal objectiu del treball que constitueix aquest Capítol va ser investigar si la mostra metodologia per a la síntesi de pèptids modificats amb el grup *N*-TEG també permet introduir cadenes de *N*-oligoetilenglicol (*N*-OEG) més grans. Com a segon objectiu, ens vam plantejar investigar com la substitució del grup *N*-Me present en un pèptid bioactiu per grups *N*-OEG de longitud creixent afecta la seva activitat biològica i lipofilicitat.

Per tal d'investigar això, vam escollir Cilengitide (**23**) com a pèptid model. Aquest pèptid, de seqüència ciclo[RGDf*N*MeV], és un ciclopèptid RGD que presenta activitat antagonista envers les integrines de tipus $\alpha_v\beta_3$, $\alpha_v\beta_5$ i $\alpha_v\beta_1$.[139] Vam decidir sintetizar tres anàlegs de **23** en els quals el grup *N*-Me de la Val s'hagués reemplaçat per cadenes *N*-OEG de longitud creixent: *N*-OEG_2, *N*-OEG_{11} i *N*-OEG_{23} (veure Figura 64). La síntesi d'aquests *N*-OEG ciclopèptids (**24-26**) implica la formació de l'enllaç D-Phe-(*N*-OEG)Val. Aquest acoblament no només està dificultat pel substituent *N*-OEG, sinó que la cadena lateral β-ramificada de la Val exerceix un impediment estèric addicional. Així doncs, aquesta reacció és un bon model per a investigar fins a a quina longitud de la cadena OEG l'acilació d'un *N*-OEG aminoàcid és viable.

Figura 64. Estructura del pèptid ciclo[RGDfNMeV] (**23**) i dels *N*-OEG ciclopèptids (**24-26**) sintetitzats.

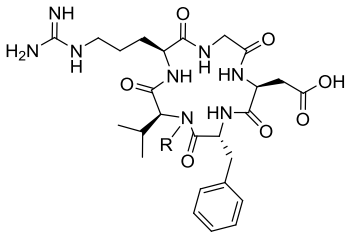

cyclo[RGDf*N*MeV] (**23**): *N*-R = *N*-CH_3

cyclo[RGDf(*N*-OEG_2)V] (**24**): *N*-R = *N*-$CH_2CH_2(OCH_2CH_2)_2OCH_3$

cyclo[RGDf(*N*-OEG_{11})V] (**25**): *N*-R = *N*-$CH_2CH_2CH_2(OCH_2CH_2)_{11}OCH_3$

cyclo[RGDf(*N*-OEG_{23})V] (**26**): *N*-R = *N*-$CH_2CH_2CH_2(OCH_2CH_2)_{23}OCH_3$

La nostra estratègia per a introduir el grup *N*-OEG en un pèptid és utilitzar un Fmoc-*N*-OEG aminoàcid com a *building block*. Així doncs, vam preparar els derivats Fmoc-(*N*-OEG_2)Val-OH (**12**), Fmoc-(*N*-OEG_{11})Val-OH (**13**) i Fmoc-(*N*-OEG_{23})Val-OH (**14**). Aquests compostos es van obtenir en 3 etapes a partir de *tert*-butil valinat, tal i com es mostra a l'Esquema 63. Remarcablement, la superior llargada de les cadenes *N*-OEG_{11} i *N*-OEG_{23} no va impedir l'acilació del residu *N*-alquilat amb Fmoc-Cl, i no va dificultar la purificació dels compostos per cromatografia *flash*.

Esquema 63. Síntesi dels derivats Fmoc-(*N*-OEG)Val-OH (**12-14**).

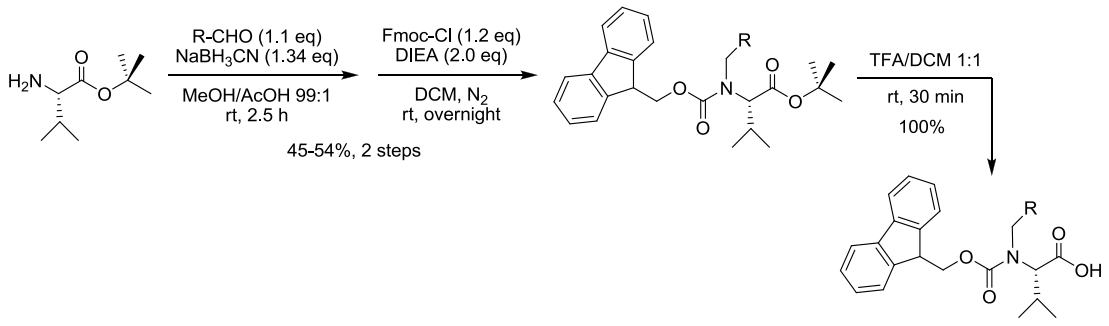

Fmoc-(*N*-OEG_2)Val-OH (**12**), R- = $CH_3O(CH_2CH_2O)_2CH_2$-

Fmoc-(*N*-OEG_{11})Val-OH (**13**), R- = $CH_3O(CH_2CH_2O)_{11}CH_2CH_2$-

Fmoc-(*N*-OEG_{23})Val-OH (**14**), R- = $CH_3O(CH_2CH_2O)_{23}CH_2CH_2$-

Per tal d'investigar l'acoblament D-Phe-(*N*-OEG)Val en fase sòlida, vam incorporar els Fmoc-aminoàcids **12-14** a una Arg(Pbf)-Gly-resina (veure Esquema 64). L'acoblament de Fmoc-(*N*-OEG_2)Val-OH (**12**) i Fmoc-(*N*-OEG_{11})Val-OH (**14**) activats amb DIPCDI/OxymaPure va tenir lloc amb bon rendiment. En canvi, l'acoblament de Fmoc-(*N*-OEG_{23})Val-OH (**15**) amb les mateixes condicions no va procedir eficientment, indicant que aquest aminoàcid requereix un mètode d'activació més potent. Després d'haver preparat les tres *N*-OEG tripeptidil-resines, vam investigar l'acoblament de Fmoc-D-Phe-OH sobre els diferents residus (*N*-OEG)Val. En el cas del residu (*N*-OEG_2)Val, la realització de dos acoblaments utilitzant BTC va permetre una completa acilació. En canvi, per als residus (*N*-OEG_{11})Val i (*N*-OEG_{23})Val, no vam poder trobar unes condicions per a les quals l'acoblament de Fmoc-D-Phe-OH fos eficient. En el cas de (*N*-OEG_{11})Val, el mètode que va donar millors resultats va ser l'activació amb BTC, tot i que l'acoblament va tenir lloc amb baix rendiment i en realitzar un tercer acoblament la conversió ja no va millorar. En el cas de (*N*-OEG_{23})Val, el producte desitjat no es va formar amb cap dels mètodes d'activació provats. Amb impediment estèric d'aquesta magnitud es sobrepassa el límit per al qual l'acoblament d'un Fmoc-aminoàcid és viable en fase sòlida.

Esquema 64. Avaluació de l'eficiència del reactiu BTC per a l'acoblament de Fmoc-D-Phe-OH sobre (*N*-CH_2R)Val en fase sòlida.

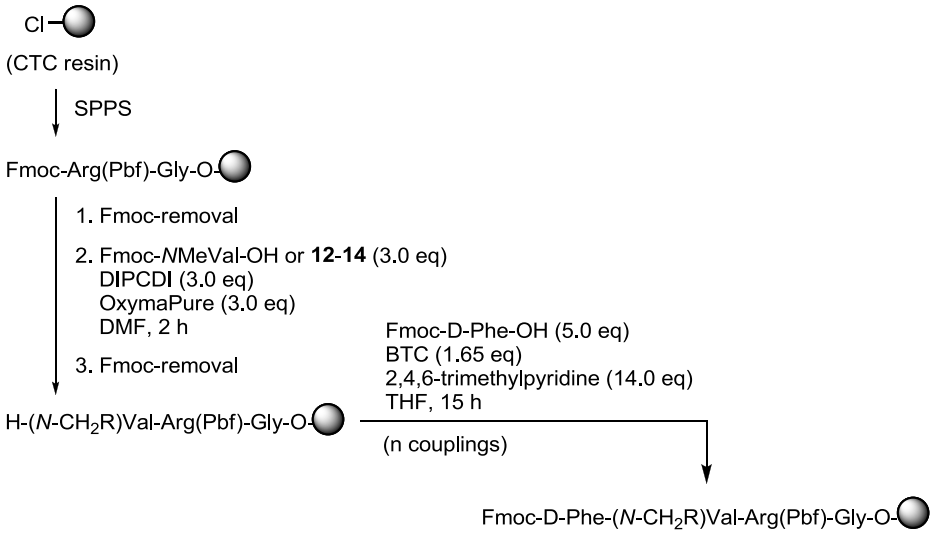

N-CH_2R	Result
N-CH_3	Complete conversion after a single coupling.
N-$CH_2CH_2(OCH_2CH_2)_2OCH_3$	Complete conversion after two couplings.
N-$CH_2CH_2CH_2(OCH_2CH_2)_{11}OCH_3$	Poor conversion after two couplings and did not increase after a third coupling cycle.
N-$CH_2CH_2CH_2(OCH_2CH_2)_{23}OCH_3$	No coupling achieved after several coupling cycles.

Havent trobat que l'acoblament D-Phe-(*N*-OEG_{23})Val no té lloc en fase sòlida, la síntesi del *N*-OEG_{23} ciclopèptid (**26**) utilitzant Fmoc-(*N*-OEG_{23})Val-OH com a *building block* no resulta viable. Per tal d'obtenir ciclo[RGDf*N*MeV] (**23**) i els altres dos *N*-OEG ciclopèptids (**24** i **25**), vam preparar els seus precursors lineals en fase sòlida i els vam ciclar en solució (veure Esquema 65). En tots els pentapèptids lineals (**p19-p21**), els residus *N*-substituïts es van introduir al mig de la seqüència peptidídica. D'aquesta manera, el residu de Gly queda a la posició *C*-terminal, la qual cosa minimitza l'impediment estèric en l'etapa de ciclació i evita el risc d'epimerització durant aquest procés. La síntesi dels pentapèptids **p19-p21** es va dur a terme a la resina CTC seguint l'estratègia Fmoc-/^{t}Bu-. Vam utilitzar una funcionalització baixa (0.2-0.3 mmol/g), ja que una major accessibilitat del grup α-amino pot facilitar acoblaments impedits.[146] Per als acoblaments estàndard, vam utilitzar DIPCDI/OxymaPure i un triple excés de reactius. Amb aquestes condicions, Fmoc-*N*MeVal-OH, Fmoc-(*N*-OEG_2)Val-OH (**12**) i Fmoc-(*N*-OEG_{11})Val-OH (**13**) es van acoblar eficientment. Per al subsequent acoblament de Fmoc-D-Phe-OH, aquest aminoàcid es va activar amb BTC. En el cas del residu (*N*-OEG_{11})Val, l'acoblament de Fmoc-D-Phe-OH va tenir lloc amb un rendiment molt baix, i en realitzar un

tercer acoblament ja no va millorar la conversió. Per a les tres peptidil-resines, vam continuar amb l'elongació del pèptid, vam escindir els pèptids de la resina, i els vam ciclar amb EDC·HCl/DMAP sense prèvia purificació. Després de la ciclació, vam eliminar els grups protectors amb TFA/H_2O/TIS 95:5:5 i vam purificar el cru resultant per RP-HPLC, obtenint els ciclopèptids desitjats (**23-25**). No obstant, en el cas del *N*-OEG_{11} ciclopèptid (**25**), vam aïllar molt poca quantitat de producte, degut a que l'acoblament D-Phe-(*N*-OEG_{11})Val no havia estat complet.

Esquema 65. Síntesi de ciclo[RGDf*N*MeV] (**23**) i els *N*-OEG ciclopèptids **24** i **25** utilitzant Fmoc-*N*MeVal-OH, Fmoc-(*N*-OEG_2)Val-OH (**12**) i Fmoc-(*N*-OEG_{11})Val-OH (**13**) com a *building blocks*.

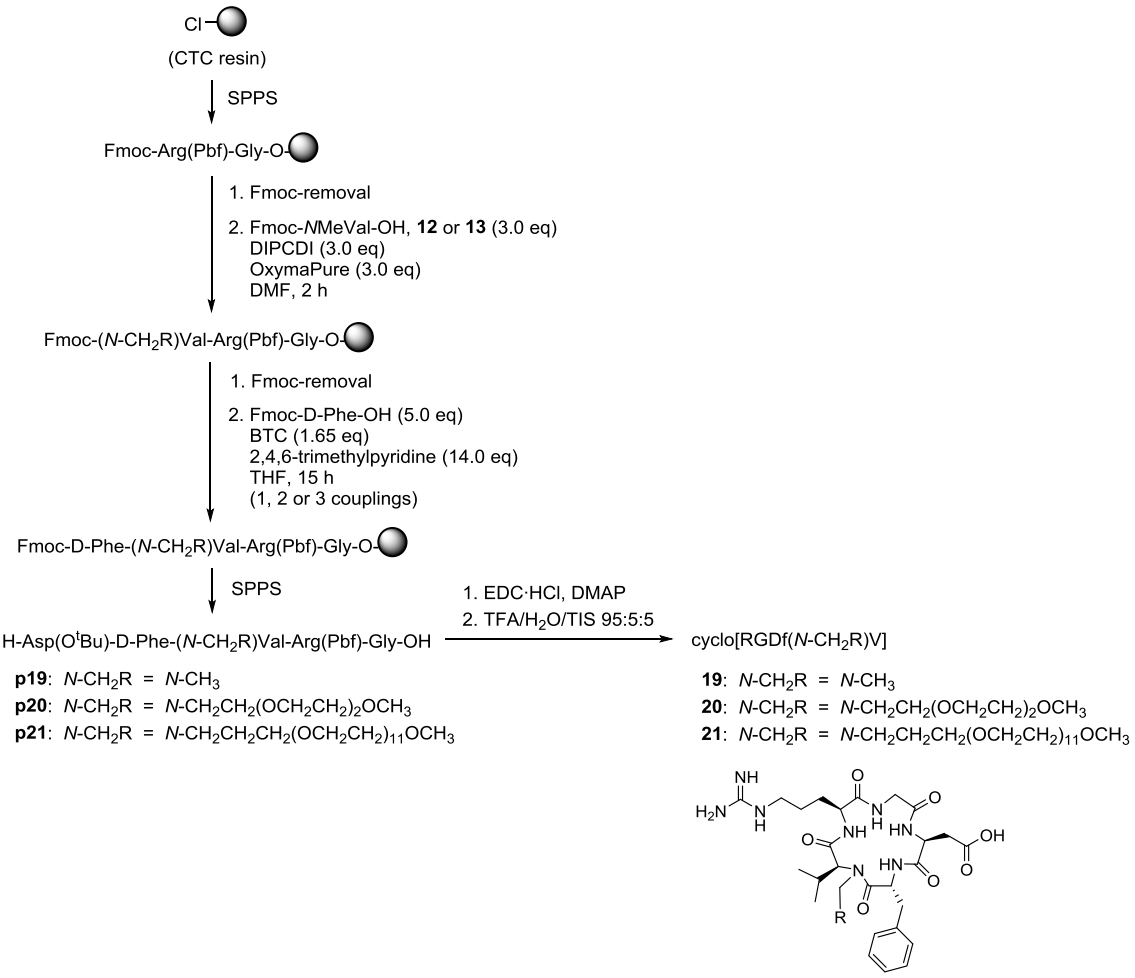

Per tal d'evitar la difícil formació dels enllaços D-Phe-(*N*-OEG_{11})Val or D-Phe-(*N*-OEG_{23})Val en fase sòlida, vam decidir preparar un dipèptid en solució i utilitzar-lo com a *building block*. Vam preveure que els acoblaments D-Phe-(*N*-OEG)Val resultarien més fàcils en solució, ja que les amines secundàries són menys reactives envers aminoàcids activats quan es troben unides a un suport sòlid.[147] Per tal de preparar els Fmoc-dipèptids requerits (**17** i **18**), vam partir de *tert*-butil valinat i el vam sotmetre a condicions de N^{α}-alquilació reductora amb el OEG-aldehid adequat per a obtenir els *N*-OEG_{11} i *N*-OEG_{23} derivats (veure Esquema 66). Per a l'acoblament entre aquests derivats i Fmoc-D-Phe-OH, vam utilitzar el clorur d'àcid d'aquesta espècie, ja que els clorurs d'àcid són altament reactius i s'han utilitzat en solució per a acoblaments entre residus *N*-metilats estèricament impedits.[83b] Aquest mètode ens va permetre formar el dipèptid desitjat sense epimerització, tot i que la conversió de la reacció va ser baixa. Finalment, el trencament acidolític de l'ester *tert*-butílic va fornir els dipèptids desitjats (**17** i **18**).

Esquema 66. Síntesi dels dipèptids Fmoc-D-Phe-(*N*-OEG$_{11}$)Val-OH (**17**) i Fmoc-D-Phe-(*N*-OEG$_{23}$)Val-OH (**18**).

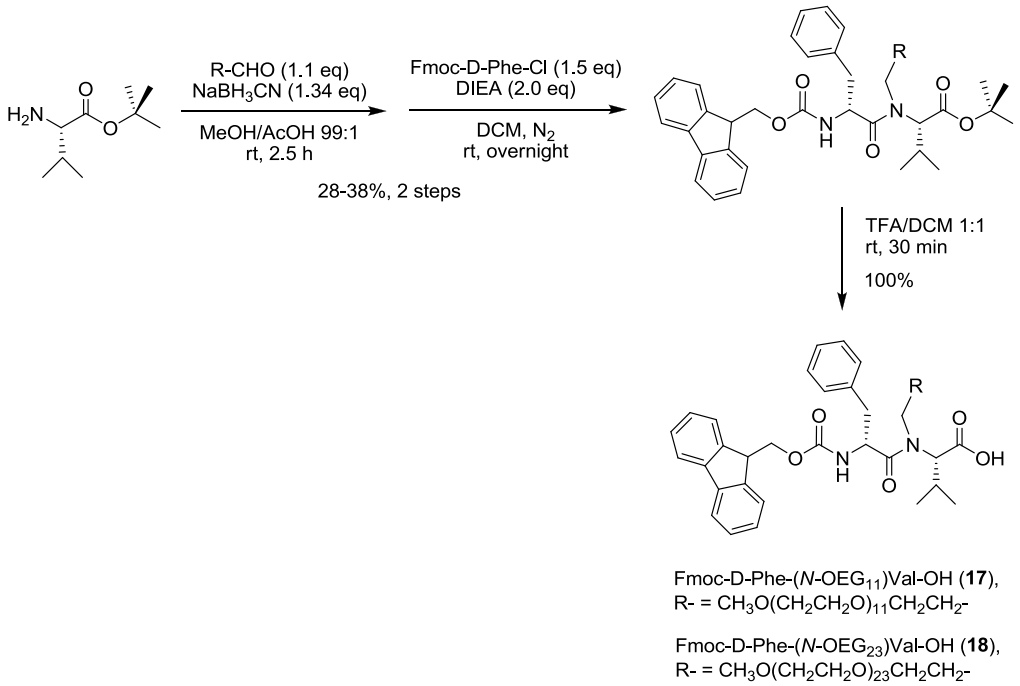

En la síntesi dels *N*-OEG$_{11}$ i *N*-OEG$_{23}$ pentapèptids lineals (**p21 i p22**), vam activar els dipèptids **17** i **18** amb PyBOP/HOAt i els vam acoblar a la peptidil-resina (veure Esquema 67). Aquests acoblaments van tenir lloc amb una eficiència acceptable, però el residu *C*-terminal dels dipèptids va epimeritzar considerablement. Així doncs, després de continuar amb l'elongació de la cadena i escindir els pèptids del suport sòlid, es van obtenir els pentapèptids **p21** i **p22** epimeritzats en el residu de Val *N*-substituït. Després de la ciclació i desprotecció, vam separar els *N*-OEG$_{11}$ i *N*-OEG$_{23}$ ciclopèptids desitjats (**25** i **26**) dels seus Val-epímers mitjançant RP-HPLC. En el cas de ciclo[RGDf(*N*-OEG$_{11}$)V] (**25**), l'estereoquímica dels dos productes aïllats es va determinar per co-injecció HPLC amb una mostra de **25** estereomèricament pur, el qual s'havia obtingut en petita quantitat utilitzant Fmoc-(*N*-OEG$_{11}$)Val-OH (**13**) com a *building block*. Aquests experiments van confirmar que el producte amb un temps de retenció més baix era l'estereoisòmer desitjat. En el cas de ciclo[RGDf(*N*-OEG$_{23}$)V] (**26**), no vam poder identificar l'estereoisòmer desitjat per co-elució HPLC, ja que no disposàvem de cap mostra de **26** estereopur. No obstant, vam assumir que el producte amb un temps de retenció més baix era el desitjat, tal i com havíem observat per a **25**. La comparació dels espectres HPLC dels diferents *N*-OEG$_{11}$ i *N*-OEG$_{23}$ pèptids crus (**p21** vs. **p22**, **25** vs. **26**) sostè aquesta hipòtesi, i també la comparació dels espectres RMN de ^{1}H dels diferents ciclopèptids aïllats (**25** el seu Val-epímer, **26** i el seu Val-epímer).

Esquema 67. Síntesi dels *N*-OEG ciclopèptids **25** i **26** utilitzant els *building blocks* dipeptídics **17** i **18**, respectivament.

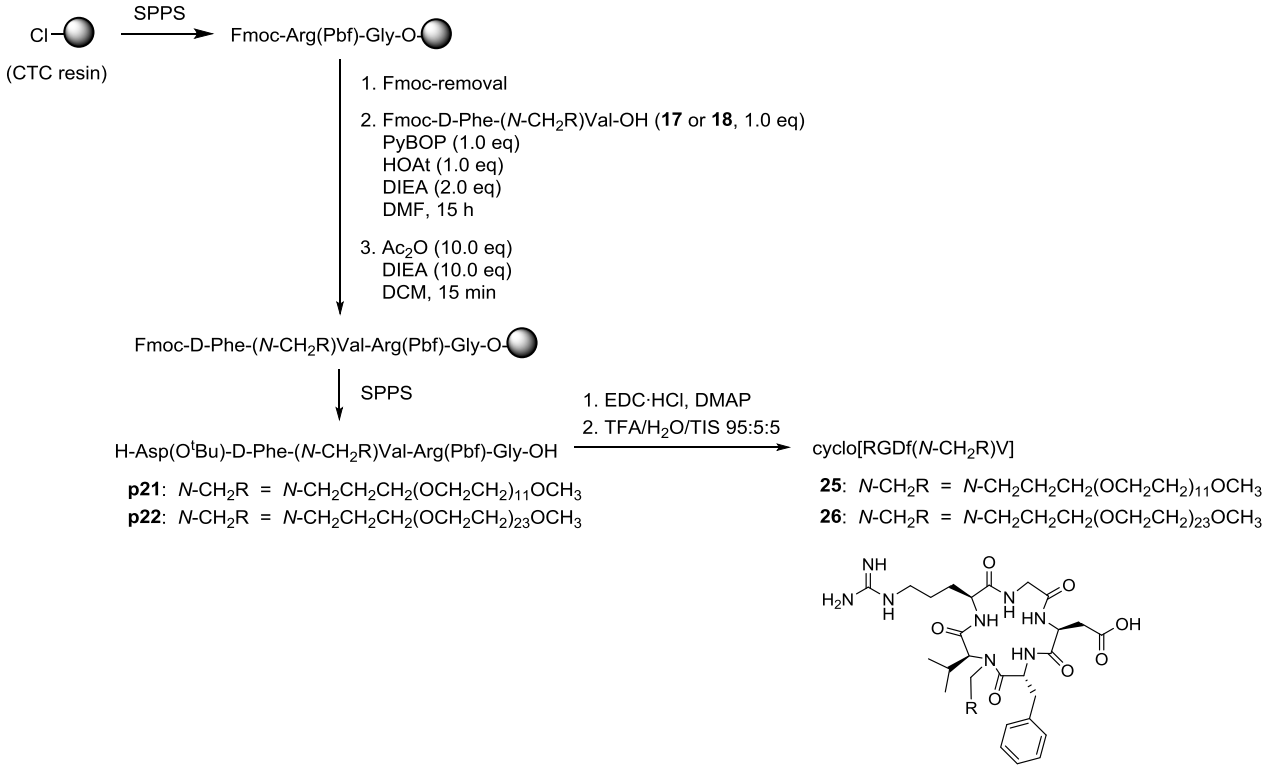

El risc d'epimerització durant l'acoblament dels dipèptids **17** i **18** era previsible. Els dipèptids activats tenen molta tendència a epimeritzar en el seu residu *C*-terminal. Això és degut a que l'aminoàcid activat d'un dipèptid està *N*-acilat, la qual cosa afavoreix la formació d'una oxazolona que és molt susceptible d'epimeritzar en medi bàsic.[110] En canvi, en un Fmoc-aminoàcid activat, el grup *N*-carbamat prevé la seva conversió en oxazolona. D'altra banda, cal esmentar que la presència d'un grup *N*-alquil en un aminoàcid (lliure o constituent d'un segment peptídic) facilita l'abstracció del H^{α} a causa de dues raons: i. el carbanió resultant està estabilitzat per hiperconjugació, ii. s'indueix la seva configuració *cis* en l'enllaç amida *N*-alquilat, la qual és més fàcilment α-desprotonable.[109] Tenint en compte que els dipèptids **17** i **18** contenen un residu *N*-alquilat, el grau d'epimerització observat no resulta sorprenent.

Per als tres *N*-OEG ciclopèptids (**24-26**) i el pèptid original, ciclo[RGDf*N*MeV] (**23**), vam avaluar la seva hidrofobicitat relativa a partir dels seus temps de retenció RP-HPLC. Vam trobar que els temps de retenció RP-HPLC dels *N*-OEG ciclopèptids (**24-26**) eren superiors al de **23**, i que augmentaven de forma proporcional a la llargada de la cadena *N*-OEG, indicant una major hidrofobicitat (veure Figura 65). En canvi, per a Fmoc-*N*MeVal-OH i els seus *N*-OEG derivats (**12-14**), vam observar l'efecte oposat: la substitució *N*-Me-per-*N*-OEG va disminuir la seva hidrofobicitat, i cadenes *N*-OEG de longitud creixent van donar lloc a un caràcter creixentment hidrofílic (veure Figura 66). Per tal d'explicar aquests resultats aparentment contradictoris, vam formular la següent hipòtesi. En el cas dels derivats de ciclo[RGDf*N*MeV] (**23**), la substitució *N*-Me-per-*N*-OEG dóna lloc a una interacció entre els àtoms d'oxigen de la cadena OEG (acceptors de ponts d'hidrogen) i els protons amida de l'esquelet peptídic (donadors de ponts d'hidrogen). Aquesta interacció intramolecular disminueix el nombre de ponts d'hidrogen que es poden formar amb la fase mòbil RP-HPLC aquosa, i això resulta en un major temps de retenció. En canvi, en el cas dels derivats de Fmoc-*N*MeVal-OH, la introducció d'àtoms d'oxigen en substituir el grup *N*-Me per *N*-OEG augmenta el potencial de formació de ponts d'hidrogen amb la fase mòbil RP-HPLC aquosa, i això resulta en una menor retenció.

Figura 65. Co-injecció de ciclo[RGDf*N*MeV] (**23**) i els *N*-OEG ciclopèptids (**24-26**) a l'aparell RP-HPLC, gradient lineal de 10% a 50% ACN en 8 min, columna C18.

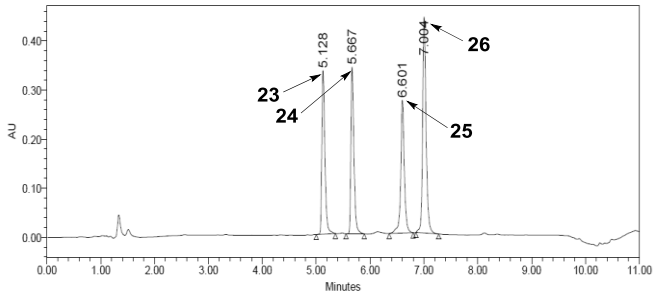

Figura 66. Co-injecció de Fmoc-*N*MeVal-OH i els derivats Fmoc-(*N*-OEG)Val-OH (**12-14**) a l'aparell RP-HPLC, flux isocràtic de 50% ACN durant 15 min, columna C18.

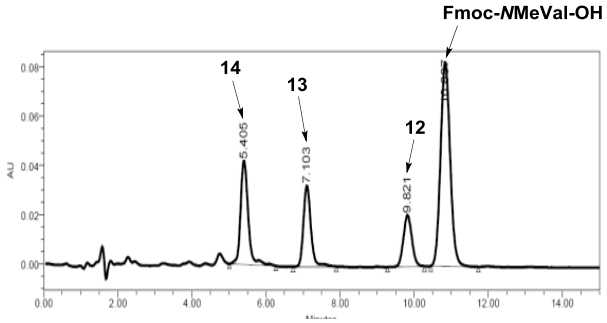

Cal esmentar que l'efecte de la substitució *N*-Me-per-*N*-OEG en ciclo[RGDf*N*MeV] (**23**) en el seus temps de retenció RP-HPLC és consistent amb les nostres observacions per als *N*-Me vs. *N*-TEG anàlegs del Sansalvamida A (**1**), descrites al Capítol 2: per a tots dos pèptids model, el reemplaçament d'un grup *N*-Me per una cadena *N*-OEG dóna lloc a una major hidrofobicitat. La nostra hipòtesi per a explicar la major hidrofobicitat dels *N*-OEG anàlegs de **23**, que presenta dues cadenes laterals ionitzables, tambe serveix per als *N*-TEG anàlegs de **1**, que és un pèptid totalment alifàtic.

Per als tres *N*-OEG ciclopèptids (**24-26**) i el pèptid original, ciclo[RGDf*N*MeV] (**23**), vam avaluar la seva activitat biològica en assajos d'inhibició adhesió cel·lular. En aquests assajos, vam mesurar la capacitat dels compostos per a inhibir l'adhesió de diferents línies cel·lulars sobre vitronectina (VN) i fibrinogen (FN).[150] Aquests dos lligands d'integrina es van immobilitzar en una matriu, i les cèl·lules emprades van ser: HUVEC (endotelials), DAOY (glioblastoma), i HT-29 (càncer de colon). En els experiments amb VN, les cèl·lules HUVEC i DAOY utilitzen les integrines $\alpha_v\beta_3$ i $\alpha_v\beta_5$ per a adherir-se a aquest lligand, mentre que les cèl·lules HT-29 només utilitzen $\alpha_v\beta_5$. En els experiments amb FB, l'adhesió de les cèl·lules HUVEC i DAOY a aquest lligand només està mediada per la integrina $\alpha_v\beta_3$. Així doncs, aquests assajos d'inhibició d'adhesió cel·lular permeten avaluar de forma indirecta l'activitat antagonista d'un pèptid envers les integrines $\alpha_v\beta_3$ i $\alpha_v\beta_5$. Els resultats d'aquests assajos es mostren a la Taula 34. Per a tots els sistemes cèl·lula/lligand, tots els ciclopèptids van inhibir l'adhesió de forma dependent de la concentració, donant lloc a corves d'adhesió sigmoidees. Els pèptids ciclo[RGDf(*N*-OEG_2)V] (**24**) i ciclo[RGDf*N*MeV] (**23**) van mostrar activitats inhibitòries molt semblants, la qual cosa indica que la substitució del grup *N*-Me de **23** per una curta cadena *N*-OEG_2 no afecta la seva afinitat envers les integrines $\alpha_v\beta_3$ i $\alpha_v\beta_5$. En canvi, els pèptids ciclo[RGDf(*N*-OEG_{11})V] (**25**) i ciclo[RGDf(*N*-OEG_{23})V] (**26**) van inhibir l'adhesió cel·lular amb menor potència. Aquesta disminució d'activitat es pot atribuir a una interferència de les seves cadenes *N*-OEG, de major tamany, amb la interacció RGD-receptor. De fet, existeixen nombrosos exemples a la literatura en els quals la unió covalent de OEG a un pèptid provoca una disminució de la seva activitat biològica a causa de raons estèriques, especialment si es tracta d'un pèptid de tamany petit.[152]

Taula 34. Assajos d'inhibició d'adhesió cel·lular amb ciclo[RGDf*N*MeV] (**23**) i els conjugats **29-31**. Els valors de IC_{50} estan expressats en μM.[a,b]

Compost	Vitronectina (VN) $\alpha_v\beta_3 + \alpha_v\beta_5$			Fibrinogen (FB) $\alpha_v\beta_3$	
	HUVEC en VN	DAOY en VN	HT-29 en VN (només $\alpha_v\beta_5$)	HUVEC en FB	DAOY en FB
23	0.37	2.69	3.11	0.076	0.44
24	0.42	3.62	2.17	0.036	0.14
25	12.42	171.5	n.d.	1.38	4.55
26	22.30	143.1	n.d.	0.28	2.31

[a] Les cèl·lules HUVEC i DAOY sobreexpressen els receptors integrina $\alpha_v\beta_3$ i $\alpha_v\beta_5$, mentre que les cèl·lules HT-29 només sobreexpressen el subtipus $\alpha_v\beta_5$.
[b] Aquests assajos biològics van ser realitzats pel Dr. Jaume Adan, del centre tecnològic Leitat.

En conclusió, hem observat que la SPPS de *N*-OEG-pèptids de forma *stepwise* presenta un límit respecte la longitud de la cadena de OEG: a partir d'una certa longitud, l'acilació del *N*-OEG-aminoàcid resulta impossible en fase sòlida, fins i tot amb el mètode d'activació BTC. Per a cadenes *N*-OEG llargues, l'acilació del residu *N*-substituït es pot aconseguir en solució utilitzant un clorur d'àcid. El segments peptídic resultant es pot acoblar a una peptidil-resina per a obtenir el *N*-OEG pèptid desitjat. No obstant, aquesta aproximació no resulta eficient, ja que l'acoblament de segments peptídics té lloc amb considerable epimerització i, en conseqüència, l'aïllament dels productes per RP-HPLC requereix una purificació exhaustiva.

Els nostres resultats indiquen que, per al *N*-Me ciclopentapèptid Cilengitide (**23**), la substitució del seu grup *N*-Me per una cadena curta de *N*-OEG dóna lloc a un anàleg més lipofílic amb la mateixa activitat biològica. En incrementar el tamany del grup *N*-OEG augmenta la hidrofobicitat dels anàlegs, però la síntesi esdevé ineficient i el major impediment estèric comporta una pèrdua d'activitat biològica. En base a aquestes observacions, podem concloure que el reemplaçament d'un grup *N*-Me per una cadena curta de *N*-OEG pot ser una estratègia útil per a augmentar la lipofilicitat d'un pèptid sense afectar la seva activitat biològica, sempre i quan el residu *N*-metilat no sigui essencial per a la interacció pèptid-receptor.

Capítol 4

L'objectiu del treball que constitueix aquest Capítol va ser establir una metodologia per a la introducció del grup *N*-(4-azidobutil) en pèptids i demostrar la utilitat d'aquest *linker* per a permetre la conjugació en pèptids que no tenen grups derivatitzables.

Moltes aplicacions biomèdiques requereixen la conjugació d'un pèptid amb una molècula d'interès (*e.g.* fluoròfor, agents quelant, polímer, marcador radioactiu).[158] En general, la unió covalent d'una molècula a un pèptid s'aconsegueix per reacció d'aquesta amb l'extrem *N*-terminal del pèptid o amb els grups funcionals de les cadenes laterals.[159] En pèptids que no presenten funcionalitats reactives, cal modificar la seva estructura per tal de permetre la conjugació. Normalment, això s'aconsegueix reemplaçant un dels residus constituents per un aminoàcid que possseeixi un grup funcional reactiu (*e.g.* Lys, Cys, un aminoàcid no natural amb una funció bioortogonal). No obstant, la modificació de les cadenes laterals d'un pèptid pot afectar desfavorablement la seva activitat biològica.

Vam pensar que la modificació de l'esquelet peptídic amb un *N*-substituent funcionalitzat podria ser una estratègia útil per a permetre la conjugació en pèptids sense grups derivatitzables. Com a *N*-substituent functionalitzat, vam investigar el grup *N*-(4-azidobutil). Aquest *N*-substituent es pot introduir en una peptidil-resina per N^{α}-alquilació

reductora amb 4-azidobutanal, i permet la conjugació d'una molècula mitjançant diverses transformacions químiques (veure Esquema 68). La funció azida és estable a la majoria de protocols utilitzats en síntesi de pèptids i és químicament inert als grups funcionals de les cadenes laterals.[161] Això minimitza possibles reaccions secundàries i simplifica els esquemes de protecció.

Esquema 68. Modificació de pèptids via el *linker N*-(4-azidobutil).

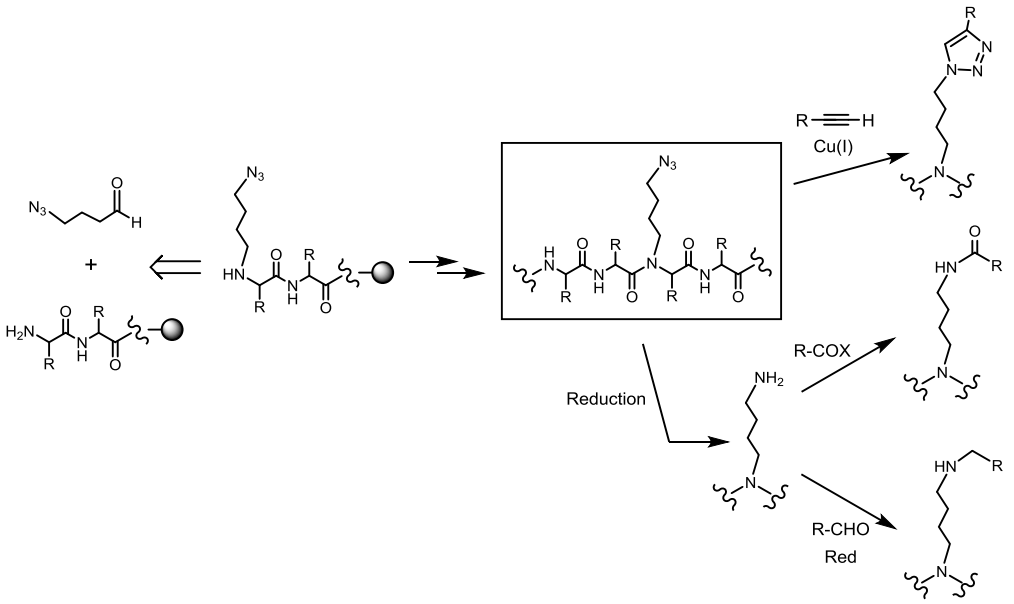

Per tal de demostrar l'aplicabilitat del nostre *linker N*-(4-azidobutil), vam escollir Cilengitide[139] (**23**) com a pèptid model (veure Figura 67). Aquest pèptid RGD és un bon exemple de la dificultat de preparar conjugats bioactius a partir de pèptids cíclics que no poseeixen grups funcionals reactius i/o no són susceptibles de ser modificats estructuralment preservant l'activitat biològica. La seqüència cíclica de Cilengitide, ciclo[RGD*N*MeV], és el resultat d'un estudi conformacional sistemàtic per a restringir la subestructura RGD en una orientació òptima per a interaccionar amb el receptor integrina $\alpha_v\beta_3$, que es troba sobreexpressat en diversos tipus de càncers malignes i en la neovasculatura dels tumors.[140] La funcionalització de ciclopèptids RGD que s'uneixen a aquest receptor és d'interès, ja que permet la conjugació d'entitats químiques per a la visualització i/o tractament de tumors.[141] En aquest tipus d'aplicacions biomèdiques, freqüentment s'uneix una cadena de polietilenglicol (PEG) al lligand RGD-ciclopeptídic per tal d'optimitzar les seves propietats farmacocinètiques.[142] No obstant, l'estructura de Cilengitide no permet la preparació de conjugats que presentin elevada afinitat envers $\alpha_v\beta_3$. Dels seus 5 aminoàcids constituents, tres residus (RGD) són essencials per a la unió al receptor, D-Phe participa en interaccions hidrofòbiques que estabilitzen aqueta unió, i el residu *N*MeVal no presenta cap grup funcional reactiu.[139] La substitució de *N*MeVal per Lys dóna lloc a ciclo[RGDfK], un lligand per a integrines que sí que permet la conjugació (veure Figura 67). Aquest ciclopèptid s'ha conjugat amb una varietat d'entitats químiques i s'ha utilitzat en nombroses d'aplicacions biomèdiques.[141b] No obstant, la modificació de l'estructura de Cilengitide substituïnt *N*MeVal per Lys resulta en una pèrdua d'activitat i selectivitat cap a la integrina $\alpha_v\beta_3$, ja que les restriccions conformacionals exercides pel residu *N*MeVal estabilitzen la subestructura RGD en la seva conformació òptima per a interaccionar amb $\alpha_v\beta_3$.[145]

Figura 67. Estructura de ciclo[RGDf*N*MeV] (**23**) i el seu anàleg amb Lys, ciclo[RGDfK].

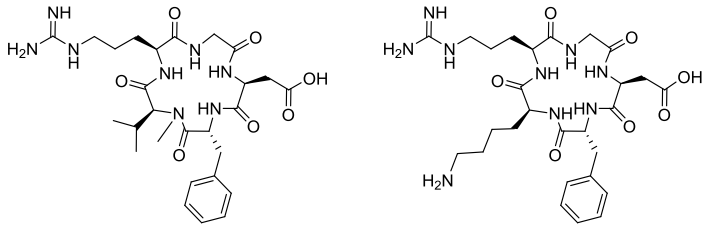

23 cyclo[RGDfK]

Així doncs, ens vam plantejar com a objectiu sintetitzar un anàleg de ciclo[RGDf*N*MeV] (**23**) en el qual el grup *N*-Me de la Val s'hagués reemplaçat per un grup *N*-(4-azidobutil), i a continuació conjugar-lo amb una cadena de PEG polidispers mitjançant diferents transformacions químiques. L'estructura del ciclopèptid *N*-(4-azidobutilat) (**27**) es mostra a la Figura 68. Per als diferents PEG-conjugats, vam comparar la seva activitat biològica, hidrofobicitat i característiques conformacionals amb les del pèptid original (**23**).

Figura 68. Estructura de ciclo[RGDf(*N*-$CH_2CH_2CH_2CH_2N_3$)V] (**27**).

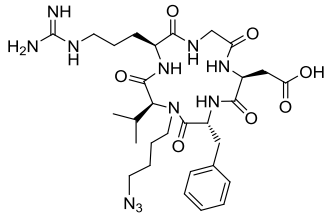

27

Per tal d'obtenir ciclo[RGDf(*N*-$CH_2CH_2CH_2CH_2N_3$)V] (**27**), vam decidir preparar el seu precursor lineal (**39**) a la resina CTC, per a després ciclar-lo en solució (veure Esquema 69). D'entrada, vam sintetitzar el pentapèptid **39** a escala petita seguint dues estratègies diferents. En la primera estratègia, vam utilitzar Fmoc-*N*-(4-azidobutil) valina (**34**) com a *building block* (estratègia A). En la segona estratègia, vam introduir el grup *N*-(4-azidobutil) per N^{α}-alquilació reductora de la Val-Arg(Pbf)-Gly-resina amb 4-azidobutanal (**39**) (estratègia B). Aquesta segona estratègia resulta preferible a la primera, ja que: i. no requereix la preparació prèvia d'un Fmoc-*N*-(4-azidobutil) aminoàcid, ii. l'acilació de la peptidil-resina amb Fmoc-*N*-(4-azidobutil) valina consumeix un excés d'aquest *building block* (*i.e.* cal realitzar dos acoblaments amb 3.0 equivalents per tal que l'acilació sigui completa). Vam trobar que les condicions òptimes per a l'etapa de N^{α}-alquilació reductora són utilitzar $NaBH_3CN$ com a agent reductor i emprar 1.5 equivalents d'aldehid. Amb aquesta quantitat d'aldehid, s'obté el pèptid *N*-alquilat com a producte majoritari, i les quantitats de pèptid *N,N*-dialquilat i pèptid no *N*-alquilat són pràcticament negligibles. Per a les dues síntesis (A i B), l'acilació de *N*-(4-azidobutil)Val amb Fmoc-D-Phe-OH es va aconseguir amb el mètode de BTC, tot i que van ser necessaris diversos cicles d'acoblament per tal d'assolir una bona conversió. Després d'allargar la cadena peptídica i escindir el pèptid de la resina, vam obtenir el pentapèptid **39** amb rendiment i puresa satisfactoris per a totes dues síntesis (rendiment cru = 63% o 43%, puresa = 45% o 48%).

Esquema 69. Síntesi de ciclo[RGDf(*N*-$CH_2CH_2CH_2CH_2N_3$)V] (**27**).

A) SPPS a petita escala utilitzant Fmoc-*N*-(4-azidobutil) valina (**34**) com a *building block*.[a]

B) SPPS a petita escala via N^{α}-alquilació reductora amb 4-azidobutanal (**39**).

C) Síntesi realitzant l'acoblament difícil en solució i la resta de l'elongació en fase sòlida.

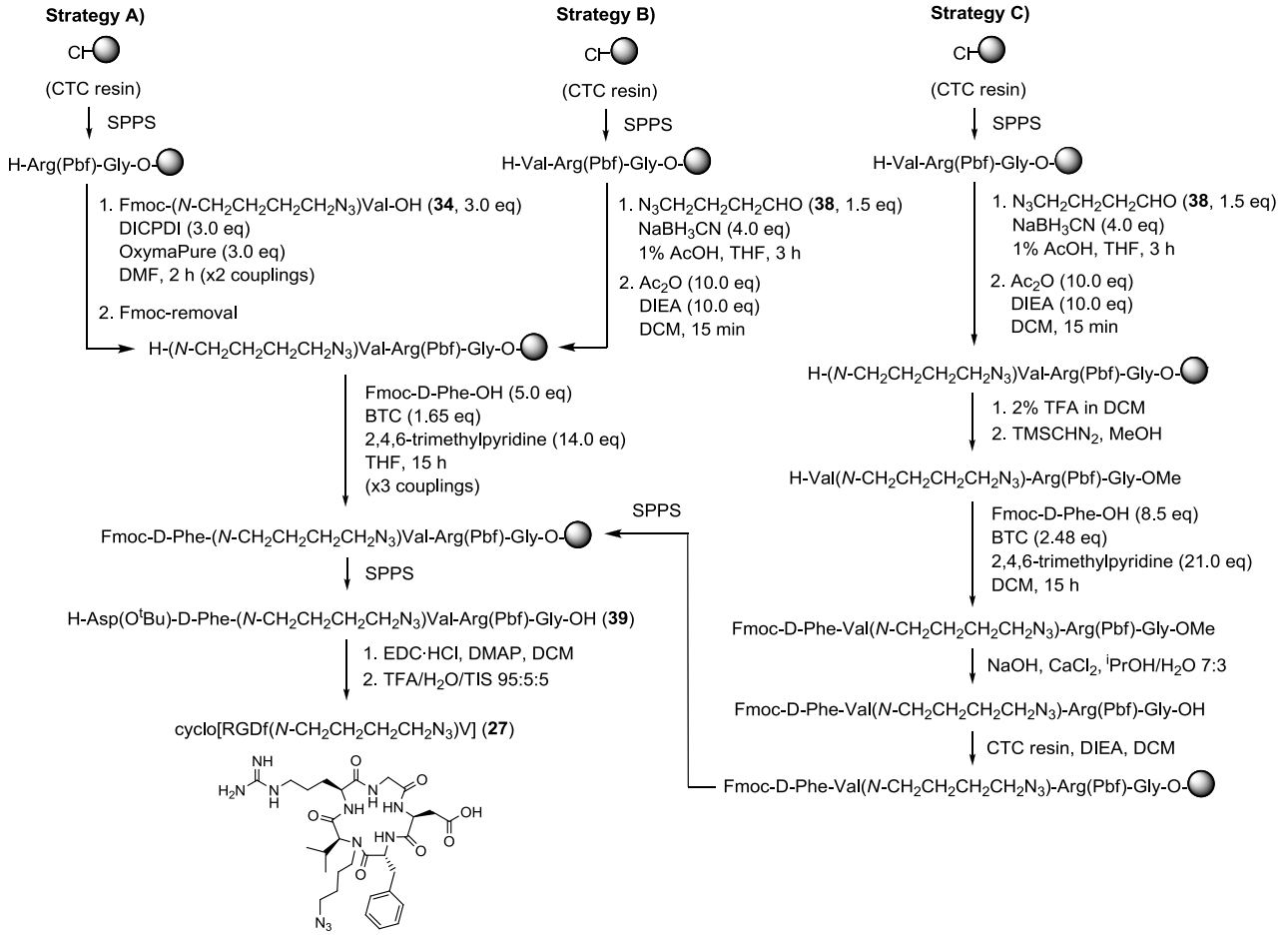

[a] Fmoc-*N*-(4-azidobutil) valina (**38**) és accessible en 3 etapes: i. N^{α}-alquilació reductora de *tert*-butil valinat amb 4-azidobutanal, ii. Fmoc-protecció del grup amino *N*-(4-azidobutilat), iii. trencament acidolític de l'ester *tert*-butílic.

Malauradament, quan vam repetir les síntesis A i B amb una quantitat de resina superior i/o una funcionalització més elevada (*i.e*. >3 g resina, >0.5 mmol/g), vam trobar que els rendiments finals no eren tan satisfactoris, ja que l'eficiència de l'acoblament sobre el residu *N*-(4-azidobutilat) no era reproduïble a escala gran. Per tal d'obtenir quantitats de pentapèptid **39** de l'ordre de g, vam desenvolupar un protocol alternatiu en el qual l'acoblament difícil es realitza en solució i la resta de la síntesi en fase sòlida (estratègia C). En aquesta *doble estratègia de SPPS*, la resina CTC s'utilitza per a l'elongació del pèptid, *escissió i reancoratge* del pèptid completament protegit, i elongació final de la cadena peptídica. L'acoblament D-Phe-[*N*-(4-azidobutil)]Val en solució es va realitzar via un clorur d'àcid, i va fornir el segment peptídic desitjat amb un rendiment acceptable. Després de la desprotecció de l'extrem *C*-terminal, el segment peptídic es va reincorporar a la resina CTC de forma eficient. Aquesta alternativa sintètica ens va permetre obtenir pentapèptid **39** a escala gran i amb un rendiment satisfactori. Després de ciclar-lo, desprotegir-lo, i purificar el cru resultant per RP-HPLC, vam aïllar el ciclopèptid *N*-(4-azidobutilat) (**27**) amb un rendiment global del 18%.

Amb la síntesi de **27** demostrem que els pèptids *N*-(4-azidobutilats) es preparar utilitzant metodologies estàndard de SPPS i que el grup *N*-(4-azidobutil) és compatible amb els grups protectors de l'estratègia Fmoc-/^{t}Bu-. Tenint en compte que l'acilació del residu *N*-(4-azidobutilat) es va aconseguir a escala petita utilitzant BTC com a reactiu

activant, considerem que la síntesi del pentapèptid **39** a escala gran va requerir canviar de fase sòlida a química en solució a causa de l'impediment estèric addicional exercit per la cadena β-ramificada de la Val. Així doncs, creiem que la síntesi d'altres pèptids *N*-(4-azidobutilats) no té perquè requerir aquesta ruta alternativa.

Per tal d'estudiar si els grups *N*-(4-azidobutil) i *N*-Me exerceixen restriccions conformacionals semblants quan s'incorporen en un pèptid cíclic, vam analitzar ciclo[RGDf*N*MeV] (**23**) i el seu anàleg *N*-(4-azidobutilat) (**27**) per espectroscòpia RMN. La Taula 35 mostra la similaritat dels seus desplaçaments químics per als senyals dels H^N, H^α i C^α. La resta de senyals de ^1H i ^{13}C associats a l'esquelet peptídic i a les cadenes laterals també van resultar pràcticament idèntics. D'altra banda, els protons H^N de **23** i **27** van presentar valors molt semblants per als seus coeficients de temperatura i constants escalars d'acoblament veïnal (veure Taula 36). La semblança de tots aquests paràmetres experimentals indica que la substitució del grup *N*-Me de ciclo[RGDf*N*MeV] (**23**) pel grup *N*-(4-azidobutil) provoca una perturbació mínima en el seu estat conformacional. En base a aquest resultat, podem esperar que el grup *N*-(4-azidobutil) també exerceixi les mateixes restriccions que el grup *N*-Me quan s'incorpori en d'altres pèptids cíclics.

Taula 35. Desplaçaments químics (ppm) dels senyals de H^N, H^α i C^α de **23** i **27** en H_2O (pH 6.0) a 288 K.[a]

Peptide	δ (H^N) [ppm]				δ (H^α) [ppm]				
	H^N [Asp]	H^N [Arg]	H^N [D-Phe]	H^N [Gly]	**1:** H^α [*N*MeV] **2**: H^α [(*N*-$CH_2CH_2CH_2CH_2N_3$)V]	H^α [Asp]	H^α [Arg]	H^α [D-Phe]	H^α [Gly]
cyclo[RGDf*N*MeV] (**23**)	8.68	8.47	8.21	8.02	4.37	4.57	3.93	5.21	3.54, 4.14
cyclo[RGDf(*N*-$CH_2CH_2CH_2CH_2N_3$)V] (**27**)	8.68	8.55	8.14	7.83	4.37	4.65	3.86	5.01	3.56, 4.09

Peptide	δ (C^α) [ppm]				
	1: C^α [*N*MeV] **2**: C^α [(*N*-$CH_2CH_2CH_2CH_2N_3$)V]	C^α [Asp]	C^α [Arg]	C^α [D-Phe]	C^α [Gly]
cyclo[RGDf*N*MeV] (**23**)	66.9	52.9	57.6	53.8	46.1
cyclo[RGDf(*N*-$CH_2CH_2CH_2CH_2N_3$)V] (**27**)	67.1	53.2	58.0	54.6	45.9

[a] L'assignació completa de tots els senyals de ^1H i ^{13}C de **23** i **27** a 288 K es troba a l'Annex 3.

Taula 36. Coeficients de temperatura (ppb K^{-1}) i constants escalars d'acoblament veïnal (Hz) dels protons amida de **23** i **27** en H_2O (pH 6.0).

Peptide	Δδ/ΔT [ppb K^{-1}]				$^3J(H^N\text{-}H^\alpha)$ [Hz]			
	H^N [Asp]	H^N [Arg]	H^N [D-Phe]	H^N [Gly]	H^N [Asp]	H^N [Arg]	H^N [D-Phe]	H^N [Gly]
cyclo[RGDf*N*MeV] (**23**)	-7.5	-11.1	-5.5	-5.4	8.3	7.5	9.6	8.2
cyclo[RGDf(*N*-$CH_2CH_2CH_2CH_2N_3$)V] (**27**)	-7.5	-10.0	-5.4	-5.1	7.8	7.3	9.1	7.8

El grup *N*-(4-azidobutil) present a **27** va permetre la unió d'una cadena de PEG polidispers de 2 KDa mitjançant vàries transformacions químiques (veure Esquema 70). El PEG-conjugat **31** es va obtenir a partir de **27** per reacció amb un PEG-alquí (2 KDa) via cicloaddició 1,3-dipolar catalitzada per Cu(I). El Cu(I) catalític es va generar *in situ* a partir de $CuSO_4$ i ascorbat de sodi, i vam trobar que calien 1.0 equivalents de Cu(I) per tal que la reacció fos completa. Per tal d'obtenir els PEG-conjugats **29** i **30**, el grup azido de **27** es va reduir amina. La utilització de Zn/NH_4Cl com a agents reductors va permetre dur a terme aquesta transformació en condicions suaus. El ciclopèptid resultant (**28**) es va acilar amb un derivat PEG-COOSu (2KDa) en medi bàsic aquós, donant lloc al conjugat **29**. Alternativament, l'alquilació reductora de **28** amb un PEG-aldehid (2 KDa) va fornir el conjugat **30**. Totes les reaccions van tenir lloc amb bons rendiments. No obstant, degut a la polidispersitat del polímer PEG, vam haver d'optimitzar l'estequiometria de les reaccions per tal de facilitar la purificació dels PEG-conjugats **29-31** per RP-HPLC.

Esquema 70. Síntesi dels PEG-conjugats **29-31**.

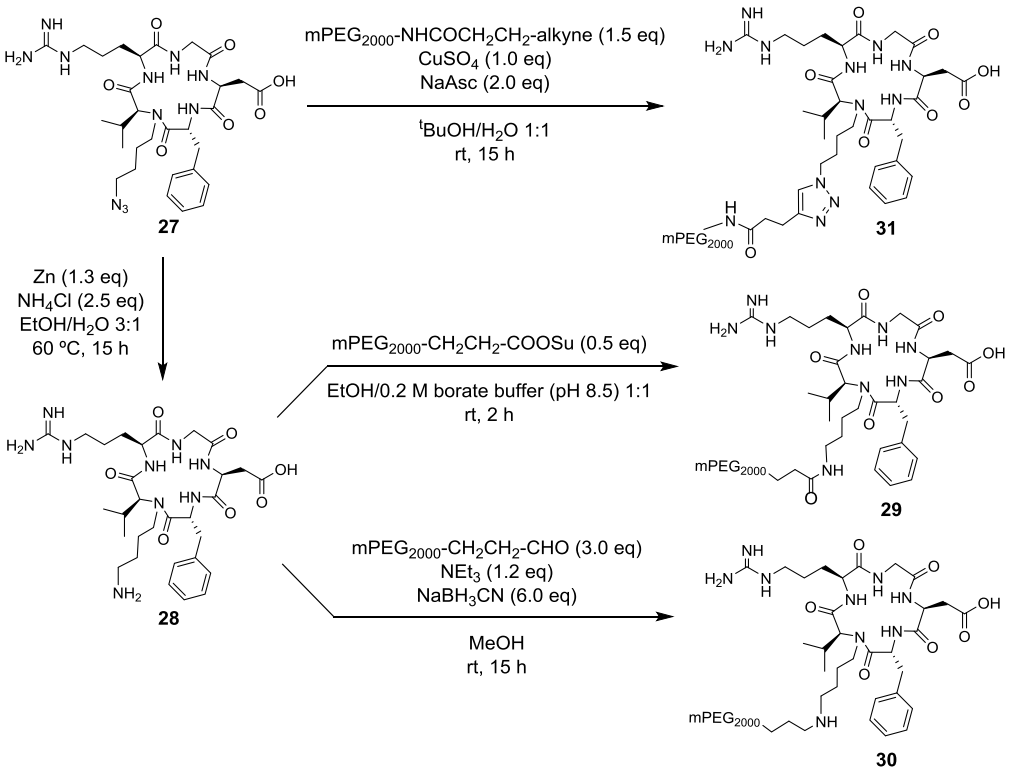

Havent sintetitzat els tres PEG-conjugats (**29-31**), vam investigar si aquests derivats adopten la mateixa conformació que ciclo[RGDf*N*MeV] (**23**). La conformació de **23** en solució aquosa es caracteritza per un gir-γ centrat en el residu de Gly, i un ràpid equilibri dos girs-γ invertits (γ_i) centrats en els residus Arg i Asp.[145] La presència d'aquests elements de quiralitat secundària en un pèptid dóna lloc a bandes característiques en el seu espectre de CD.[183] Tot i que no és possible correlacionar un espectre de CD amb una conformació específica, l'espectroscòpia de CD és una tècnica molt sensible per a detectar canvis en l'estructura secundària d'un pèptid, i és un mètode vàlid per a comparar la conformació d'una sèrie d'anàlegs peptídics modificats. Així doncs, per tal d'estudiar la conformació dels PEG-conjugats **29-31** i la del pèptid no modificat (**23**), vam analitzar-los per espectroscòpia de CD. L'espectre de CD de ciclo[RGDf*N*MeV] (**23**) va presentar una banda negativa a 238 nm (λ_{min}) i una banda positiva a 212 nm (λ_{max}) (veure Figura 69). Els PEG-conjugats **29-31** van donar lloc a espectres de CD molt semblants, indicant que tots aquests derivats presenten una conformació similar a la del pèptid no modificat. Aquestes mesures de CD són compatibles amb una conformació que presenti dos girs-γ_i en ràpid bescanvi conformacional i un gir-γ, ja que per a d'altres pèptids amb girs-γ s'han publicat dades de CD semblants.[186]

Figura 69. Espectres de CD de ciclo[RGDf*N*MeV] (**23**) i els PEG-conjugats **29-31** en H_2O a una concentració de 0.5 mM.

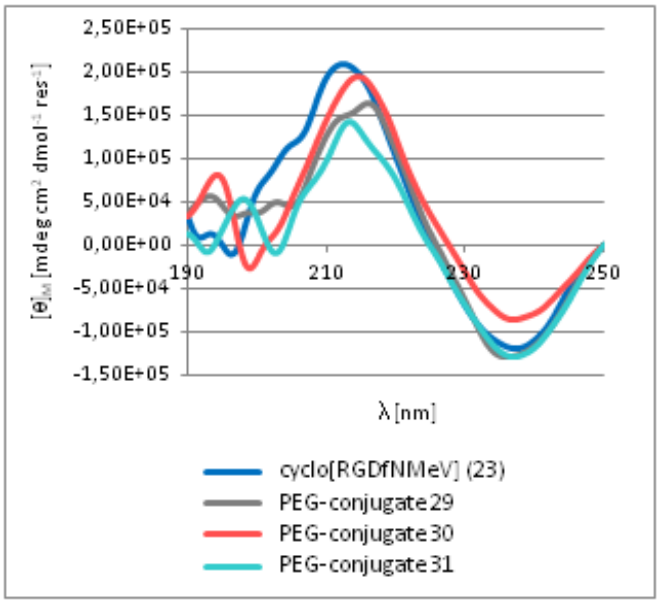

Per als tres PEG-conjugats (**29-31**), vam avaluar la seva activitat biològica en comparació amb el pèptid no modificat, ciclo[RGDf*N*MeV] (**23**) (veure Taula 37). Amb aquest objectiu, vam realitzar assajos d'inhibició d'adhesió cel·lular on vam mesurar la capacitat dels nostres compostos per a inhibir l'adhesió de cèl·lules HUVEC i DAOY sobre dos lligands d'integrina immobilitzats: vitronectina (VN) i fibrinogen (FB).[150] Aquestes cèl·lules s'uneixen a VN i FB a través de les integrines $\alpha_v\beta_3$ i $\alpha_v\beta_5$ que es troben a la seva membrana (només a través de $\alpha_v\beta_3$ en el cas de FB). Així doncs, l'activitat inhibitòria d'adhesió és una mesura indirecta de l'activitat antagonista d'un pèptid RGD envers les integrines $\alpha_v\beta_3$ i $\alpha_v\beta_5$. Per a tots els sistemes cèl·lula/lligand, els conjugats **29-31** van inhibir l'adhesió, tot i que amb menor potència que el pèptid original (**23**). Aquesta disminució d'activitat es pot atribuir a que les seves cadenes de PEG interfereixen amb la interacció RGD-receptor. Aquesta hipòtesi és consistent amb els resultats dels assajos amb els *N*-OEG ciclopèptids **24-26** (Capítol 3), on els derivats amb cadenes de *N*-OEG més llargues van ser considerablement menys actius. D'altra banda, els experiments de CD van indicar que els conjugats **29-31** i ciclo[RGDf*N*MeV] (**23**) tenen la mateixa conformació. Així doncs, no vam trobar cap evidència per a atribuir la menor activitat dels conjugats **29-31** a un estat conformacional diferent en el qual la seqüència RGD no està òptimament orientada per a interaccionar amb els receptors integrina.

Taula 37. Assajos d'inhibició d'adhesió cel·lular amb ciclo[RGDf*N*MeV] (**23**) i els PEG-conjugats **29-31**. Els valors de IC_{50} estan expressats en μM. [a,b]

Compost	Vitronectina (VN) $\alpha_v\beta_3$ + $\alpha v\beta_5$		Fibrinogen (FB) $\alpha v\beta_3$	
	HUVEC en VN	DAOY en VN	HUVEC en FB	DAOY en FB
23	0.37	2.69	0.076	0.44
29	3.06	28.76	0.23	1.77
30	3.40	49.56	0.41	2.71
31	8.90	75.21	0.53	4.36

[a] Les cèl·lules HUVEC i DAOY sobreexpressen els receptors integrina $\alpha_v\beta_3$ i $\alpha_v\beta_5$. [b] Aquests assajos biològics van ser realitzats pel Dr. Jaume Adan, del centre tecnològic Leitat.

Finalment, també vam avaluar la hidrofobicitat relativa dels tres PEG-conjugats (**29-31**) i ciclo[RGDf*N*MeV] (**23**). Tots els ciclopèptids van mostrar coeficients de partició octanol/aigua (logPs) molt semblants. Els seus valors de logP es trobaven en el mateix rang que els valors descrits per a d'altres RGD-ciclopèptids modificats amb PEG[181] i derivats RGD-ciclopeptídics considerats com a hidrofílics.[180] Els tres PEG-conjugats (**29-31**) van presentar temps de retenció RP-HPLC superiors al del pèptid no modificat (**23**), indicant un major caràcter hidrofòbic.

En conclusió, el grup *N*-(4-azidobutil) es pot introduir en un pèptid utilitzant tècniques estàndard de SPPS i permet la conjugació del pèptid al final de la síntesi. Gràcies a les propietats ortogonals de l'azida, el nostre *linker* és compatible amb els grups protectors i resines freqüentment utilitzats en síntesi de pèptids. D'altra banda, la versatilitat química de la funció azida, que es pot reduir amina abans de l'etapa de conjugació, permet un disseny flexible de conjugats peptídics. En relació amb això, la possibilitat d'utilitzar *click chemistry* en l'etapa de conjugació resulta un avantatge, ja que permet la conjugació en presència de grups funcionals a les cadenes laterals i, en conseqüència, implica un requeriment mínim de grups protectors. En base a totes aquestes consideracions, creiem que el nostre *linker* resultarà d'utilitat en química de pèptids i ampliarà l'aplicació de mètodes de conjugació establerts.

D'altra banda, els nostre estudis mitjançant RMN i CD suggereixen que el grup *N*-(4-azidobutil) exerceix les mateixes restriccions que un grup *N*-Me quan s'incorpora en un pèptid cíclic. Això amplia la utilitat del grup *N*-(4-azidobutil) com a *linker* per a la preparació de conjugats peptídics, ja que el grup *N*-Me es troba present en nombrosos pèptids cíclics biològicament actius. Així doncs, reemplaçar el grup *N*-Me d'un ciclopèptid *N*-metilat pel nostre *linker* és una alternativa viable per a funcionalitzar el pèptid sense alterar la seva conformació i sense modificar les cadenes laterals dels seus aminoàcids constituents, en molts casos essencials per a l'activitat biològica.

BIBLIOGRAPHY

[1] N. Sewald and H.-D. Jakubke. *Peptides: chemistry and biology*, *2nd edition*, Wiley-VCH Verlag GmbH & Co, Weinheim (Germany), **2009**.

[2] For detailed statistics about peptide therapeutics, the Peptide Therapeutics Foundation publishes a bi-annual report entitled: "Development Trends for Peptide Therapeutics", which can be found on their website at: http://www.peptidetherapeutics.org/peptide-therapeutics-foundation.htm.

[3] (a) P. Vlieghe, V. Lisowski, J. Martinez and M. Khrestchatisky. Synthetic therapeutic peptides: science and market. *Drug Discov. Today*, **2010**, *15*, 40-46. (b) D. J. Craik, D. Fairlie, Spiros Liras and D. Price. The future of peptide-based drugs. *Chem. Biol. Drug. Des.* **2013**, *81*, 136-147.

[4] S. Royo, K. Gaus and N. Sewald. Synthesis of chemically modified bioactive peptides: recent advances, challenges and developments for medicinal chemistry. *Future Med. Chem.* **2009**, *1,* 1289-1310.

[5] (a) R. Finking and M. A. Marahiel. Biosynthesis of nonribosomal peptides. *Annu. Rev. Microbiol.* **2004**, *58*, 453-488. (b) S. A. Sieber and M. A. Marahiel. Molecular mechanisms underlying nonribosomal peptide synthesis: approaches to new antibiotics. *Chem. Rev.* **2005**, *105*, 715-738.

[6] (a) J. Chatterjee, C. Gilon, A. Hoffman and H. Kessler. *N*-methylation of peptides: a new perspective in medicinal chemistry. *Acc. Chem. Res.* **2008**, *10*, 1331-1342. (b) J. Chatterjee, F. Rechenmacher and H. Kessler. *N*-Methylation of peptides and proteins: an important element for modulating biological functions. *Angew. Chem., Int. Ed.* **2013**, *52*, 254-269.

[7] C. Gilon, D. Halle, M. Chorev, Z. Selinger and G. Byk. Backbone cyclization: a new method for conferring conformational constraint on peptides. *Biopolymers* **1991**, *31*, 745-750.

[8] C. A. Olsen. Peptoid-peptide hybrid backbone architectures. *ChemBioChem*, **2010**, *11*, 152-160.

[9] J. G. Beck, J. Chatterjee, B. Laufer, M. U. Kiran, A. O. Frank, S. Neubauer, O. Ovadia, S. Greenberg, C. Gilon, A. Hoffman and H. Kessler. Intestinal permeability of cyclic peptides: common key backbone motifs identified. *J. Am. Chem. Soc*. **2012**, *134*, 12125−12133.

[10] For methods for the chemical synthesis of *N*-Me amino acid derivatives, refer to: S. Sagan, P. Karoyan, O. Lequin, G. Chassaing and S. Lavielle. *N*- and *Cα*-methylation in biologically active peptides: synthesis, structural and functional aspects. *Curr. Med. Chem.* **2004**, *11*, 2799-2822.

[11] E. Biron and H. Kessler. Convenient synthesis of *N*-methylamino acids compatible with Fmoc solid-phase peptide synthesis. *J. Org. Chem.* **2005**, *70*, 5183-5189.

[12] S. C. Miller and T. S. Scanlan. Site-selective *N*-methylation of peptides on solid support. *J. Am. Chem. Soc.* **1997**, *119*, 2301-2302.

[13] E. Biron, J. Chatterjee and H. Kessler. Optimized selective *N*-methylation of peptides on solid support. *J. Pept. Sci.* **2006**, *12*, 213-219.

[14] J. F. Reichwein and R. M. J. Liskamp. Site-specific *N*-alkylation of peptides on the solid phase. *Tetrahedron Lett.* **1998**, *39*, 1243-1246.

[15] (a) H. Kessler. Detection of hindered rotation and inversion by NMR spectroscopy. *Angew. Chem., Int. Ed.* **1970**, *9*, 219-235. (b) P. Manavalan and F. A. Momany. Conformational energy studies on *N*-methylated analogs of thyrotropin releasing hormone, enkephalin, and luteinizing hormone-releasing hormone. *Biopolymers* **1980**, *19*, 1943-1973. (c) H. Kessler, U. Anders and M. Schudok. An unexpected *cis* peptide bond in the minor conformation of a cyclic hexapeptide containing only secondary amide bonds. *J. Am. Chem. Soc.* **1990**, *112*, 5908-5912.

[16] (a) F. Piriou, K. Lintner, S. Fermandjian, P. Fromageot, M. C. Khosla, R. R. Smeby and F. M. Bumpus. Amino acid side chain conformation in angiotensin II and analogs: correlated results of circular dichroism and ^{1}H nuclear magnetic resonance. *Proc. Natl. Acad. Sci. U.S.A.* **1980**, *77*, 82-86. (b) A. C. Bach, C. J. Eyermann, J. D. Gross, M. J. Bower, R. L. Harlow, P. C. Weber and W. F. Degrado. Structural studies of a family of high affinity ligands for GP IIb/IIIa. *J. Am. Chem. Soc.* **1994**, *116*, 3207-3219.

[17] Several examples are reviewed in: (a) S. Sagan, P. Karoyan, O. Lequin, G. Chassaing and S. Lavielle. *N*- and *Cα*-methylation in biologically active peptides: synthesis, structural and functional aspects. *Curr. Med. Chem.* **2004**, *11*, 2799-2822. [ref. 10] (b) J. Chatterjee, C. Gilon, A. Hoffman and H. Kessler. *N*-methylation of peptides: a new perspective in medicinal chemistry. *Acc. Chem. Res.* **2008**, *10*, 1331-1342. [ref. 5a] (c) J. Chatterjee, F. Rechenmacher and H. Kessler. *N*-Methylation of peptides and proteins: an important element for modulating biological functions. *Angew. Chem., Int. Ed.* **2013**, *52*, 254-269. [ref. 5b]

[18] (a) O. Ovadia, S. Greenberg, J. Chatterjee, B. Laufer, F. Opperer, H. Kessler, C. Gilon and A. Hoffman. The effect of multiple *N*-methylation on intestinal permeability of peptides. *Mol. Pharmaceutics* **2011**, *8*, 479-487. (b) Q. G. Dong, Y. Zhang, M. S. Wang, J. Feng, H. H. Zhang, Y. G. Wu, T. J. Gu, X. H. Yu, C. L. Jiang, Y. Chen, W. Li and W. Kong. Improvement of enzymatic stability and intestinal permeability of deuterohemin-peptide conjugates by specific multi-site *N*-methylation. *Amino Acids* **2012**, *43*, 2431-2441.

[19] (a) E. Biron, J. Chatterjee, O. Ovadia, D. Langenegger, J. Brueggen, D. Hoyer, H. A. Schmid, R. Jelinek, C. Gilon, A. Hoffman and H. Kessler. Improving oral bioavailability of peptides by multiple *N*-methylation: somatostatin analogues. *Angew. Chem. Int. Ed.* **2008**, *45*, 2595-2599. (b) T. R. White, C. M. Renzelman, A. C. Rand, T. Rezai, C. M. McEwen, V. M. Gelev. On-resin *N*-methylation of cyclic peptides for discovery of orally bioavailable scaffolds. *Nat. Chem. Biol.* **2011**, *7*, 810-817.

[20] (a) R. A. Conradi A. R. Hilgers, N. F. H. Ho and P. S. Burton. The influence of peptide structure on transport across Caco-2 cells. II. Peptide bond modification which results in improved intestinal permeability. *Pharm. Res.* **1992**, *9*, 435-439. (b) P. S. Burton, R. A. Conradi, N. F. H. Ho, A. R. Hilgers and R. T. Borchardt. How structural features influence the biomembrane permeability of peptides. *J. Pharm. Sci.* **1996**, *85*, 1336-1340.

[21] J. Chatterjee, D. F. Mierke and H. Kessler. Conformational preference and potential templates of *N*-methylated cyclic pentaalanine peptides. *Chem. Eur. J.* **2008**, *14*, 1508-1517.

[22] B. Laufer, J. Chatterjee, A. O. Frank and H. Kessler. Can *N*-methylated amino acids serve as substitutes for prolines in conformational design of cyclic pentapeptides? *J. Pept. Sci.* **2009**, *15*, 141-146.

[23] (a) J. Chatterjee, O. Ovadia, G. Zahn, L. Marinelli, A. Hoffman, C. Gilon and H. Kessler. Multiple *N*-methylation by a designed approach enhances receptor selectivity. *J. Med. Chem.* **2007**, *50*, 5878-5881. (b) J. Chatterjee, O. Ovadia, G. Zahn, L. Marinelli, A. Hoffman, C. Gilon and H. Kessler. *N*-Methylated sst2 selective somatostatin cyclic peptide analogue as potent candidate for treating neurogenic inflammation. *ACS Med. Chem. Lett.* **2011**, *2*, 2509-514.

[24] L. Doedens, F. Opperer, M. Cai, J. G. Beck, M. Dedek, E. Palmer, V. Hruby and H. Kessler. Multiple *N*-methylation of MT-II backbone amide bonds leads to melanocortin receptor subtype hMC1R selectivity: pharmacological and conformational studies. *J. Am. Chem. Soc.* **2010**, *132*, 8115-8128.

[25] O. Ovadia, S. Greenberg, B. Laufer, C. Gilon, A. Hoffman and H. Kesser. Improvement of drug-like properties of peptides: the somatostatin paradigm. *Expert Opin. Drug Discov.* **2010**, *5*, 655-671.

[26] S. Hess, O. Ovadia, D. E. Shalev, H. Senderovich, B. Qadri, T. Yehezkel, Y. Salitra, T. Sheynis, R. Jelinek, C. Gilon and A. Hoffman. Effect of structural and conformation modifications, including backbone cyclization, of hydrophilic hexapeptides on their intestinal permeability and enzymatic stability. *J. Med. Chem.* **2007**, 50, 6201-6211.

[27] Reported methods for the preparation of *N*-functionalized amino acid derivatives for backbone cyclization include: (a) G. Byk and C. Gilon. Building units for *N*-backbone cyclic peptides. 1. Synthesis of protected *N*-(ω-aminoalkylene) amino acids and their incorporation into dipeptide units. *J. Org. Chem*. **1992**, *57*, 5687-5692. (b) S. Reissmann, G. Greiner, J. Jezek, C. Amberg, B. Müller, L. Seyfarth, L. F. Pineda de Castro and I. Paegelow. Design, synthesis and characterization of bradykinin antagonists via cyclization of the modified backbone. *Biomed*. *Pept*. *Proteins Nucleic Acids,* **1994**, *1*, 51-56. (c) K. Kaljuste and A. Unden. A new general solid-phase method for the synthesis of backbone-to-backbone cyclized peptides. *Int*. *J. Pept*. *Protein Res*. **1994**, *43*, 505-511. (d) G. Bitan and C. Gilon. Building units for *N*-backbone cyclic peptides. 2. Synthesis of protected *N*-(ω-thioalkylene) amino acids and their incorporation into dipeptide units. *Tetrahedron* **1995**, *51*, 10513-10522. (e) D. Muller, I. Zeltser, G. Bitan and C. Gilon. Building units for *N*-backbone cyclic peptides. 3. Synthesis of protected *N*-(ω-aminoalkyl) amino acids and *N*-(ω-carboxyalkyl) amino acids. *J*. *Org*. *Chem*. **1997**, *62*, 411-416. (f) G. Bitan, D. Muller, R. Kasher, E. V. Gluhov and C. Gilon. Building units for *N*-backbone cyclic peptides. Part 4. Synthesis of protected *N*-α-functionalized alkyl amino acids by reductive alkylation of natural amino acids. *J. Chem. Soc., Perkin Trans. 1* **1997**, *1,* 1501-1510. (g) G. Gellerman, A. Elgavi, Y. Salitra and M. Kramer. Facile synthesis of orthogonally protected amino acid building blocks for combinatorial *N*-backbone cyclic peptide chemistry. *J. Peptide Res.* **2001**, *57*, 277-291.

[28] F. Falb, T. Yechezkel, Y. Salitra and C. Gilon. *In situ* generation of Fmoc-amino acid chlorides using bis-(trichloromethyl)carbonate and its utilization for difficult couplings in solid-phase peptide synthesis. *J. Pept. Res.* **1999**, 53, 507-517.

[29] C. Gilon, D. Muller, G. Bitan, Y. Salitra, I. Goldwasser and V. Hornik. *Proceedings of the 24th European Peptide Symposium*, edited by R. Ramage and R. Epton, **1996**, 423-424.

[30] For example: (a) G. Byk, D. Halle, I. Zeltser, G. Bitan, Z. Selinger and C. Gilon. Synthesis and biological activity of NK-1 selective, *N*-backbone cyclic analogs of the C-terminal hexapeptide of Substance P. *J. Med. Chem.* **1996**, *39,* 3174-3178. (b) G. Bitan, I. Sukhotinsky, Y. Mashriki, M. Hanani, Z. Selinger and C. Gilon. Synthesis and biological activity of novel backbone-bicyclic Substance-P analogs containing lactam and disulfide bridges. *J. Pept. Res.* **1997**, *49*, 421-426. (c) C. Gilon, M. Huenges, B. Matha, G. Gellerman, V. Hornik, M. Afargan, O. Amitay, O. Ziv, E. Feller, A. Gamliel, D. Shohat, M. Wanger, O. Arad and H. Kessler. A backbone-cyclic, receptor 5-selective Somatostatin analogue: synthesis, bioactivity, and nuclear magnetic resonance conformational analysis. *J. Med. Chem.* **1998**, *41,* 919-929. (d) S. Gazal, G. Gelerman, O. Ziv, O. Karpov, P. Litman, M. Bracha, M. Afargan and C. Gilon. Human Somatostatin receptor specificity of backbone-cyclic analogues containing novel sulfur building units. *J. Med. Chem.* **2002**, *45*, 1665-1671. (e) Y. Linde, O. Ovadia, E. Safrai, Z. Xiang, F. P. Portillo, D. E. Shalev, C. Haskell-Luevano, A. Hoffman and C. Gilon. Structure-activity relationship and metabolic stability studies of backbone cyclization and *N*-methylation of melanocortin peptides. *Byopolymers*, **2008**, *90*, 671-682. (f) Y. Tal-Gan, M. Hurevich, S. Klein, A. Ben-Shimon, D. Rosenthal, C. Hazan, D. E. Shalev, M. Y. Niv, A. Levitzki and C. Gilon. Backbone cyclic peptide inhibitors of protein kinase B (PKB/Akt). *J. Med. Chem.* **2011**, *54*, 5154-5164.

[31] M. Altstein, O. Ben-Aziz, S. Daniel, I. Schefler, I. Zeltser and C. Gilon. Backbone cyclic peptide antagonists, derived from the insect pheromone biosynthesis activating neuropeptide, inhibit sex pheromone biosynthesis in moths. *J. Biol. Chem.* **1999**, *274,* 17573-17579.

[32] M. Afargan, E. T. Janson, G. Gelerman, R. Rosenfeld, O. Ziv, O. Karpov, A. Wolf, M. Bracha, D. Shohat, G. Liapakis, C. Gilon, A. Hoffman, D. Stephensky and K. Oberg. Novel long-acting somatostatin analog with endocrine selectivity: potent suppression of growth hormone but not of insulin. *Endocrinology* **2001**, *142*, 477-486.

[33] A. Friedler, D. Friedler, N. W. Luedtke, Y. Tor, A. Loyter and C. Gilon. Development of a functional backbone cyclic mimetic of the HIV-1 Tat arginine-rich motif. *J. Biol. Chem.* **2000**, *275,* 23783-23789.

[34] S. Hess, Y. Linde, O. Ovadia, E. Safrai, D. E. Shalev, A. Swed, E. Halbfinger, T. Lapidot, I. Winkler, Y. Gabinet, A. Faier, D. Yarden, Z. Xiang, F. P. Portitlo, C. Haskell-Luevano, C. Gilon and A. Hoffman. Backbone cyclic peptidomimetic melanocortin-4 receptor agonist as a novel orally administrated drug lead for treating obesity. *J. Med. Chem.* **2008**, *51*, 1026-1034.

[35] (a) A. Friedler, N. Zakai, O. Karni, Y. C. Broder, L. Baraz, M. Kotler, A. Loyter and C. Gilon. A backbone cyclic peptide which mimics the nuclear localization signal of HIV-1 MA inhibits nuclear import and HIV-1 production in non-dividing cells. *Biochemistry*, **1998**, *37*, 5616-5622. (b) Kasher, R., Oren, D., Barda, Y., and Gilon, C. Miniaturized proteins: the backbone cyclic peptidomimetic approach. *J. Mol. Biol.* **1999**, *292*, 421-429. (c) M. Hurevich, M. Ratner-Hurevich, Y. Tal-Gan, D. E. Shwlev, S. Z. Ben-Sasson and C. Gion. Backbone cyclic helix mimetic of chemokine (C-C motif) receptor 2: a rational approach for inhibiting dimerization of G protein-coupled receptors. *Bioorg. Med. Chem.* **2013**, *21*, 3958-3966.

[36] R. J. Simon, R. S. Kania, R. N. Zuckermann, V. D. Huebner, D. A. Jewell, S. Banville, S. Ng, L. Wang, S. Rosenberg, C. K. Marlowe, D. C. Spellmeyer, R. Tan, A. D. Frankel, D. V. Santi, F. E. Cohen and P. A. Bartlett. Peptoids: a modular approach to drug discovery. *Proc. Natl. Acad. Sci. U.S.A.* **1992**, *89*, 9367-9371.

[37] R. N. Zuckermann, J. M. Kerr, S. B. H. Kent and W. H. Moos. Efficient method for the preparation of peptoids [oligo(*N*-substituted) glycines] by submonomer solid-phase synthesis. *J. Am. Chem. Soc*. **1992**, 114, 10646-10647.

[38] S. A. Fowler and H. E. Blackwell. Structure-function relationships in peptoids: recent advances toward deciphering the structural requirements for biological function. *Org. Biomol. Chem.* **2009**, *7*, 1508-1524.

[39] S. M. Miller, R. J. Simon, S. Ng, R. N. Zuckermann, J. M. Kerr and W. H. Moos. Comparison of the proteolytic susceptibilities of homologous L-amino acid, D-amino acid, and *N*-substituted glycine peptide and peptoid oligomers. *Drug Dev. Res.* **1995**, *35*, 20-32.

[40] (a) P. A. Wender, D. J. Mitchell, K. Pattabiraman, E. T. Pelkey, L. Steinman and J. B. Rothbard. The design, synthesis, and evaluation of molecules that enable or enhance cellular uptake: peptoid molecular transporters. *Proc. Natl. Acad. Sci. U.S.A.* **2000**, *97*, 13003-13008. (b) Y.-U. Kwon and T. Kodadek. Quantitative evaluation of the relative cell permeability of peptoids and peptides. *J. Am. Chem. Soc.* **2007**, *129*, 1508-1509.

[41] (a) P. Armand, K. Kirshenbaum, R. A. Goldsmith, S. Farr-Jones, A. E. Barron, K. T. V. Truong, K. A. Dill, D. F. Mierke, F. E. Cohen, R. N. Zuckermann and E. K. Bradley. NMR determination of the major solution conformation of a peptoid pentamer with chiral side chains. *Proc. Natl. Acad. Sci. U.S.A.* **1998,** *95*, 4309-4314. (b) C. W. Wu, K. Kirshenbaum, T. J. Sanborn, J. A. Patch, K. Huang, K. A. Dill, R. N. Zuckermann and A. E. Barron. Structural and spectroscopic studies of peptoid oligomers with achiral aliphatic side chains. *J. Am. Chem. Soc.* **2003**, *125*, 13525-13530.

[42] For example: (a) T. Hara, S. R. Durell, M. C. Myers and D. H. Appella. Probing the structural requirements of peptoids that inhibit HDM2-p53 interactions. *J. Am. Chem. Soc.* **2006**, *128*, 1995-2004. (b) N. Chongsiriwatana, J. A. Patch, R. N. Zuckermann, Y. Marcano, A. Czyzewski and A. E. Barron. Peptoids that mimic the structure, function, and mechanism of helical antimicrobial peptides. *Proc. Natl. Acad. Sci. U.S.A.* **2008**, *105*, 2794-2799.

[43] J. P. Meyer, P. Davis, K. B. Lee, F. Porreca, H. Yamamura and V. J. Hruby. Synthesis using a Fmoc-based strategy and biological activities of some reduced peptide-bond pseudopeptide analogs of dinorphin A(1). *J. Med. Chem.* **1995**, *38*, 3462-3468.

[44] (a) H. Jang, A. Fafarman, J. M. Holub and K. Kirshenbaum. Click to fit: versatile polyvalent display on a peptidomimetic scaffold. *Org. Lett.* **2005**, *7*, 1951-1954. (b) J. M. Holub, H. Jang and K. Kirshenbaum. Clickity-click: highly functionalized peptoid oligomers generated by sequential conjugation reactions on solid-phase support. *Org. Biomol. Chem.* **2006**, *4*, 1497-1502.

[45] For example: (a) R. N. Zuckermann, E. J. Martin, D. C. Spellmeyer, G. B. Stauber, K. R. Shoemaker, J. M. Kerr, G. M. Figliozzi, D. A. Goff, M. A. Siani, R. Simon, S. C. Banville, E. G. Brown, L. Wang, L. S. Richter and W. H. Moos. Discovery of nanomolar ligands for 7-transmembrane G-protein-coupled receptors from a diverse *N*-(substituted) glycine peptoid library. *J. Med. Chem.* **1994**, *37*, 2678-2685. (b) S. Ng, B. Goodson, A. Ehrhardt, W. H. Moos, M. Siani and J. Winter. Combinatorial discovery process yields antimicrobial peptoids. *Bioorg. Med. Chem.* **1999**, *7*, 1781-1785. (c) B. Liu, P. G. Alluri, P. Yu and T. Kodadek. A potent transactivation domain mimic with activity in living cells. *J. Am. Chem.*

Soc. **2005**, *127*, 8254-8255. (d) M. M. Reddy, R. Wilson, J. Wilson, S. Connell, A. Gocke, L. Hynan, D. German, T. Kodadek. Identification of candidate IgG biomarkers for Alzheimer's disease via combinatorial library screening. *Cell*, **2011**, *144*, 132-142.

[46] R. N. Zuckermann and T. Kodadek. Peptoids as potential therapeutics. *Curr. Opin. Mol. Ther.* **2009***, 11,* 299-307.

[47] D. G. Udugamasooriya, S. P. Dineen, R. A. Brekken and T. Kodadek. A peptoid "antibody surrogate" that antagonizes VEGF receptor 2 activity. *J. Am. Chem. Soc.* **2008**, *130*, 5744-5752.

[48] J. T. Nguyen, C. W. Turck, F. E. Cohen, R. N. Zuckermann and W. A. Lim. Exploiting the basis of proline recognition by SH3 and WW domains: design of *N*-substituted inhibitors. *Science*, **1998**, *282*, 2088-2092.

[49] For example: (a) B. Goodson, A. Ehrhardt, S. Ng, J. Nuss, K. Johnson, M. Giedlin, R. Yamamoto, W. H. Moos, A. Krebber, M. Ladner, M. B. Giacona, C. Vitt, J. Winter. Characterization of novel antimicrobial peptoids. *Antimicrob. Agents Chemother.* **1999**, *43*, 1429-1434. (b) J. A. Patch and A. E. Barron. Helical peptoid mimics of magainin-2 amide. *J. Am. Chem. Soc.* **2003**, *125*, 12092-12093.

[50] For example: (a) C. W. Wu, S. L. Seurynck, K. Y. Lee and A. E. Barron. Helical peptoid mimics of lung surfactant protein C. *Chem. Biol.* **2003**, *10*, 1057-1063. (b) S. L. Seurynck, J. A. Patch and A. E. Barron. Simple, helical peptoid analogs of lung surfactant protein B. *Chem. Biol.* **2005**, *12*, 77-88. (c) N. J. Brown, C. W. Wu, S. L. Seurynck-Servoss and A. E. Barron. Effects of hydrophobic helix length and side chain chemistry on biomimicry in peptoid analogues of SP-C. *Biochemistry*, **2008**, *47*, 1808-1818. (d) N. J. Brown, J. Johansson and A. E. Barron. Biomimicry of surfactant protein C. *Acc. Chem. Res.* **2008**, *41*, 1409-1417.

[51] For example: (a) I. Peretto, R. M. Sanchez-Martin, X. H. Wang, J. Ellard, S. Mittoo and M. Bradley. Cell penetrable peptoid carrier vehicles: synthesis and evaluation. *Chem. Commun.* **2003**, 2312-2313. (b) T. Schroder, N. Niemeier, S. Afonin, A. S. Ulrich, H. F. Krug and S. Brase. Peptoidic amino- and guanidinium-carrier systems: targeted drug delivery into the cell Cytosol or the nucleus. *J. Med. Chem.* **2008**, *51*, 376-379. (c) A. Unciti-Broceta, F. Diezmann, C. Y. Ou-Yang, M. A. Fara and M. Bradley. Synthesis, penetrability and intracellular targeting of fluorescein-tagged peptoids and peptide-peptoid hybrids. *Bioorg. Med. Chem*. **2009**, *17*, 959-966. (d) K. Eggenberger, E. Birtalan, T. Schroder, S. Brase and P. Nick. Passage of Trojan peptoids into plant cells. *Chembiochem*, **2009**, *10*, 2504-2512.

[52] F. Hamy, E. R. Felder, G. Heizmann, J. Lazdins, F. Aboul-ela, G. Varani, J. Karn and T. Klimkait. An inhibitor of the Tat/TAR RNA interaction that effectively suppresses HIV-1 replication. *Proc. Natl. Acad. Sci. U.S.A.* **1997**, *94*, 3548-3553.

[53] (a) T. A. Tran*,* R. H. Mattern*,* M. Afargan*,* O. Amitay*,* O. Ziv*,* B. A. Morgan*,* J. E. Taylor*,* D. Hoyer and M. Goodman. Design, synthesis, and biological activities of potent and selective somatostatin analogues incorporating novel peptoid residues. *J. Med. Chem.* **1998***, 41,* 2679-2685. (b) R. H. Mattern*,* T. A. Tran and M. Goodman. Conformational analyses of somatostatin-related cyclic hexapeptides containing peptoid residues. *J. Med. Chem.* **1998***, 41,* 2686-2692.

[54] (a) J. R. Holder, R. M. Bauzo, Z. Xiang, J. Scott and C. Haskell-Luevano. Design and pharmacology of peptoids and peptide-peptoid hybrids based on the melanocortin agonists core tetrapeptide sequence. *Bioorg. Med. Chem. Lett.* **2003**, *13*, 4505-4509. (b) J. A. W. Kruijtzer, W. A. J. Nijenhuis, N. Wanders, W. H. Gispen, R. M. J. Liskamp and R. A. H. Adan. Peptoid-peptide hybrids as potent novel melanocortin receptor ligands. *J. Med. Chem.* **2005**, *48*, 4224-4230. (c) F. Mutulis, I. Mutule, E. Liepinsh, A. Yahorau, M. Lapinsh, S. Kopantshuk, S. Veiksina, A. Rinken and J. E. Wikberg. *N*-alkylated dipeptide amides and related structures as imitations of the melanocortins' active core. *Peptides* **2005**, *26*, 1997-2016.

[55] (a) B. Biondi, E. Giannini, L. Negri, P. Melchiorri, R. Lattanzi, F. Rosso, L. Ciocca and R. Rocchi. Opioid peptides: synthesis and biological activity of new endomorphin analogs. *Int. J. Pept. Res. Ther.* **2006**, *12*, 145-151. (b) L. Biondi, E. Giannini, F. Filira, M. Gobbo, L. Negri and R. Rocchi. [D-Ala^2]-deltorphin I peptoid and retropeptoid analogues: synthesis, biological activity and conformational investigations. *J. Pept. Sci.* **2004**, *10*, 578-587. (c) L. Biondi, E. Giannini,

F. Filira, M. Gobbo, M. Marastoni, L. Negri, B. Scolaro, R. Tomatisc and R. Rocchi. Synthesis, conformation and biological activity of dermorphin and deltorphin I analogues containing *N*-alkylglycine in place of residues in position 1, 3, 5 and 6. *J. Pept. Sci.* **2003**, *9*, 638-648.

[56] (a) S. C. Shankaramma, K. Moehle, S. James, J. W. Vrijbloed, D. Obrecht and J. A. Robinson. A family of macrocyclic antibiotics with a mixed peptide-peptoid beta-hairpin backbone conformation. *Chem. Commun.* **2003**, 1842-1843. T. S. Ryge, X. Doisy, D. Ifrah, J. E. Olsen and P. R. Hansen. New indolicidin analogues with potent antibacterial activity. *J. Pept. Res.* **2004**, *64*, 171-185. (b) T. S. Ryge and P. R. Hansen. Novel lysine-peptoid hybrids with antibacterial properties. *J. Pept. Sci.* **2005**, *11*, 727-734. (c) T. S. Ryge and P. R. Hansen. Potent antibacterial lysine-peptoid hybrids identified from a positional scanning combinatorial library. *Bioorg. Med. Chem.* **2006**, *14*, 4444-4451. (d) W. L. Zhu, Y. M. Song, Y. Park, K. H. Park, S. T. Yang, J. I. Kim, I. S. Park, K. S. Hahm and S. Y. Shin. Substitution of the leucine zipper sequence in melittin with peptoid residues affects self-association, cell selectivity, and mode of action. *Biochim. Biophys. Acta* **2007**, *1768*, 1506-1517. (e) S. A. Fowler, D. M. Stacy andH. E. Blackwell. Design and synthesis of macrocyclic peptomers as mimics of a quorum sensing signal from *Staphylococcus aureus. Org. Lett.* **2008**, *10*, 2329-2332. (f) M. Gobbo, M. Benincasa, G. Bertoloni, B. Biondi, R. Dosselli, E. Papini, E. Reddi, R. Rocchi, R. Tavano and R. Gennaro. Substitution of the arginine/leucine residues in apidaecin Ib with peptoid residues: effect on antimicrobial activity, cellular uptake, and proteolytic degradation. *J. Med. Chem.* **2009**, *52*, 5197-5206. (g) M. R. Levengood, C. C. Kerwood, C. Chatterjee and W. A. van der Donk. Investigation of the substrate specificity of lacticin 481 synthetase by using nonproteinogenic amino acids. *ChemBioChem* **2009**, *10*, 911-919.

[57] For example: (a) R. Ruijtenbeek, J. A. Kruijtzer, W. van de Wiel, M. J. Fischer, M. Fluck, F. A. M. Redegeld, R. M. J. Liskamp and F. P. Nijkamp. Peptoid-peptide hybrids that bind Syk SH2 domains involved in signal transduction. *Chembiochem*, **2001**, *2*. 171-179. (b) J. Zimmermann, R. Kuhne, R. Volkmer-Engert, T. Jarchau, U. Walter, H. Oschkinat and L. J. Ball. Design of *N*-substituted peptomer ligands for EVH1 domains. *J. Biol. Chem.* **2003**, *278*, 36810-36818. (c) T. S. Ryge and P. R. Hansen. Potent antibacterial lysine-peptoid hybrids identified from a positional scanning combinatorial library. *Bioorg. Med. Chem.* **2006**, *14*, 4444-4451. (d) A. Caporale, E. Schievano and E. Peggion. Peptide-peptoid hybrids based on (1-11)-parathyroid hormone analogs. *J. Pept. Sci.* **2010**, *16*, 480-485. (e) B. C. Lee and R. N. Zuckermann. Protein side-chain translocation mutagenesis via incorporation of peptoid residues. *ACS Chem. Biol.* **2011**, *6*, 1367-1374.

[58] For example: Y. Tal-Gan, N. S. Freeman, S. Klein, A. Levitzki and C. Gilon. Synthesis and structure-activity relationship studies of peptidomimetic PKB/Akt inhibitors: the significance of backbone interactions. *Bioorg. Med. Chem.* **2010**, *18*, 2976-2985.

[59] M. Park, M. Wetzler, T. S. Jardetzky and A. E. Barron. A readily applicable strategy to convert peptides to peptoid-based therapeutics. *PLOS One*, **2013**, *8*, 1-7.

[60] B. Hoffmann, T. Ast, T. Polakowski, U. Reineke and R. Volkmer. Transformation of a biologically active peptide into peptoid analogs while retaining biological activity. *Protein Peptide Let*t. **2006**, *13*, 829-833.

[61] (a) R. M. Freidinger, J. S. Hinkle, D. S. Perlow and B. H. Arison. Synthesis of 9-fluorenylmethyloxycarbonyl-protected *N*-alkyl amino acids by reduction of oxazolidinones. *J. Org. Chem.* **1983**, *48*, 77-81. (b) Y. Ohfune, N. Kurokawa, N. Higuchi, M. Saito, M. Hashimoto and T. Tanaka. An efficient one-step reductive *N*-monoalkylation of α-amino acids. *Chem. Lett.* **1984**, 441-444. (c) W. R. Bowman and D. R. Coghlan. A facile method for the *N*-alkylation of α-amino esters. *Tetrahedron* **1997**, *53*, 15787-15798.

[62] (a) F. M. Chen and N. L. Benoiton. *N*-ethylamino acid synthesis and *N*-acylamino acid cleavage using Meerwein's reagent. *Can. J. Chem.* **1977**, *55*, 1433-1435. (b) D. W. Hansen and D. Pilipauskas. Chemoselective *N*-ethylation of Boc amino acids without racemization. *J. Org. Chem.* **1985**, *50*, 945-950. (c) T. Rückle, B. Dubray, F. Hubler and M. Mutter. Efficient one-pot Synthesis of *N*-ethyl amino acids. *J. Peptide Sci*. **1999**, *5*, 56-58. (d) H. Schedel and K. Burger. Synthesis of α-*N*-ethylamino acids and their derivatives. *Monatsh. Chem.* **2000**, *131*, 1011-1018. (e) E. L. Belsito, R. De Marco, M. L. Di Gioia, A. Liguori, F. Perri and M. C. Viscomi. *N*-(4-Nitrophenylsulfonyl)- and *N*-(fluorenylmethoxycarbonyl)-*N*-ethyl amino acid methyl esters - a practical approach. *Eur. J. Org. Chem.* **2010**, 4245-

4252. (f) R. De Marco, M. L. Di Gioia, A. Liguori, F. Perri, C. Siciliano and M. Spinella. *N*-Alkylation of *N*-arylsulfonyl-α-amino acid methyl esters by trialkyloxonium tetrafluoroborates. *Tetrahedron* **2011**, *67,* 9708-9709.

[63] F. Hubler, T. Rückle, L. Patiny, T. Muamba, J.-F. Guichou, M. Mutter and R. Wenger. Synthetic routes to *N*EtXaa[4]-cyclosporin A derivatives as potential anti-HIV I drugs. *Tetrahedron Lett*. **2000**, 41, 7193-7196.

[64] D. T. S. Rijkers, J. W. M. Höppener, G. Posthuma, C. J. M. Lips and R. M. J. Liskamp. Inhibition of amyloid fibril formation of human amylin by *N*-alkylated amino acid and α-hydroxy acid residue containing peptides. *Chem. Eur. J.* **2002**, *8*, 4285-4291.

[65] A. Patgiri, M. R. Witten and P. S. Arora. Solid phase synthesis of hydrogen bond surrogate derived α-helices: resolving the case of a difficult amide coupling. *Org. Biomol. Chem.* **2010**, *8*, 1773-1776.

[66] J. Liu, D. Wang, Q. Zheng, M. Lu and P. S. Arora. Atomic structure of a short α-helix stabilized by a main chain hydrogen bond surrogate. *J. Am. Chem. Soc.* **2008**, *130*, 4334-4337.

[67] (a) L.K. Henchey, S. Kushal, R. Dubey, R. N. Chapman, B. Z. Olenyuk and P. S. Arora. Inhibition of Hypoxia inducible factor 1-transcription coactivator interaction by a hydrogen bond surrogate α-helix. *J. Am. Chem. Soc.* **2010**, *132*, 941-943. (b) D. Wang, M. Lu and P. S. Arora. Inhibition of HIV-1 fusion by hydrogen-bond-surrogate-based α-helices. *Angew. Chem., Int. Ed.* **2008**, *47*, 1879-1882. (c) D. Wang, W. Liao and P. S. Arora. Enhanced metabolic stability and protein-binding properties of artificial α-helices derived from a hydrogen bond surrogate: application to Bcl-xL. *Angew. Chem., Int. Ed.* **2005**, *44*, 6525-6529.

[68] J. Ying, X. Gu, M. Cai, M. Dedek, J. Vagner, D. B. Trivedi and V. J. Hruby. Design, synthesis, and biological evaluation of new cyclic melanotropin peptide analogues selective for the human melanocortin-4 receptor. *J. Med. Chem.* **2006**, *49,* 6888-6896.

[69] B. Dörner, G. M. Husar, J. M. Ostresh and R. A. Houghten. The synthesis of peptidomimetic combinatorial libraries through successive amide alkylations. *Bioorg. Med. Chem.* **1996**, *4*, 709-715.

[70] M. Teixidó, F. Albericio and E. Giralt. Solid-phase synthesis and characterization of *N*-methyl-rich peptides. *J. Pep. Res.* **2005**, *15*, 153-166.

[71] F. M. Veronese and J. M. Harris. Introduction and overview of peptide and protein PEGylation. *Adv. Drug Deliv. Rev*. **2002**, *54*, 453-456.
[72] (a) J. M. Harris and Robert B. Chess. Effect of PEGylation on pharmaceuticals. *Nature Rev.* **2003**, *2*, 214-221. (b) F. M. Veronese and G. Pasut. PEGylation, successful approach to drug delivery. *Drug Discov. Today* **2005**, *10*, 1452-1458.

[73] G. T. Hermanson. *PEGylation and synthetic polymer modification*, in *Bioconjugate Techniques, 3rd edition*, Academic Press, **2013**, ch. 18, pp. 787-839.

[74] M. Zacchigna, F. Cateni, S. Drioli and G. M. Bonora. Multimeric, multifunctional derivatives of poly(ethylene glycol). *Polymers* **2011**, *3*, 1076-1090.

[75] (a) M. J. Roberts, M. D. Bentley and J. M. Harris. Chemistry for peptide and protein PEGylation. *Adv. Drug. Del. Rev.* **2002**, *54*, 459-476. (b) A. Mero, C. Clementi, F. M. Veronese and G. Pasut. Covalent conjugation of poly(ethylene glycol) to proteins and peptides: strategies and methods. *Methods Mol. Biol.* **2011**, *751*, 95-129.

[76] F. M. Veronese. Peptide and protein PEGylation: a review of problems and solutions. *Biomaterials* **2001**, *22*, 405-417.

[77] R. W. Payne, B. M. Murphy and M. C. Manning. Product development issues for PEGylated proteins. *Pharm. Dev. Technol.* **2011**, *16*, 423-440.

[78] Y. M. Angell, C. Garcia-Echeverria and D. H Rich. Comparative studies of the coupling of *N*-methylated, sterically hindered amino acids during solid-phase peptide synthesis. *Tetrahedron Lett*. **1994**, *35*, 5981-5984.

[79] L. A. Carpino, A. El-Faham, C. A. Minor and F. Albericio. Advantageous applications of azabenzotriazole (triazolopyridine)-based coupling reagents to solid-phase peptide synthesis. *J. Chem. Soc., Chem. Commun*. **1994**, 201-203.

[80] S. Y. Ko and R. M. Wenger. Solid-phase total synthesis of cyclosporine analogues. *Helv. Chim. Acta* **1997**, *80*, 695-705.

[81] Y. M. Angell, T. L. Thomas, G. R. Flentke and D. H. Rich. Solid-phase synthesis of Cyclosporin peptides. *J. Am. Chem. Soc.* **1995**, *117*, 7279-7280.

[82] L. A. Carpino, M. Beyermann, H. Wenschuh and M. Bienert. Peptide synthesis via amino acid halides. *Acc. Chem. Res.* **1996**, *29,* 268-274.

[83] (a) W. J. Colucci, R. D. Tung, J. A. Petri and D. H. Rich. Synthesis of D-Lysine^{8}-cyclosporine A. Further characterization of BOP-Cl in the 2-7 hexapeptide fragment synthesis. *J. Org. Chem.* **1990**, *55*, 2895-2903. [*Note:* The authors used Fmoc-*N*MeLeu-Cl for coupling this amino acid onto the *N*-terminal Val residue of a tripeptide fragment, which was performed in solution. Although this is not an example of the acylation of an *N*-alkylated residue via an acid chloride, it shows the effectiveness of acid chlorides for hindered coupling steps. Indeed, for the aforementioned coupling reaction, the acid chloride method outperformed the rest of activation methods tested.] (b) D. S. Perlow, J. M. Erb, N. P. Gould, R. D. Tung, R. M. Freidinger, P. D. Williams and D. F. Veber. Use of *N*-Fmoc amino acid chlorides and activated 2-(fluorenylmethoxy)-5(4H)-oxazolones in solid-phase peptide synthesis. Efficient syntheses of highly *N*-alkylated cyclic hexapeptide oxytocin antagonists related to L-365,209. *J. Org. Chem*. **1992**, *57*, 4394-4400.

[84] L. A. Carpino, H. G. Chao, M. Beyermann and M. Bienert. ((9-Fluorenylmethyl)oxy)carbonyl amino acid chlorides in solid-phase peptide synthesis. *J. Org. Chem*. **1991**, *56*, 2635-2642.

[85] John W. Lippert. Amide bond formation by using amino acid fluorides. *ARKIVOC*, **2005**, *xiv*, 87-95.

[86] H. Wenschuh, M. Beyermann, E. Krause, M. Brudel, R. Winter, M. Schtimann, L. A. Carpino and M. Bienert. Fmoc amino acid fluorides: convenient reagents for the solid-phase assembly of peptides incorporating sterically hindered residues. *J. Org. Chem.* **1994**, *59,* 3275-3280.

[87] H. Wenschuh, M. Beyermann, H. Haber, J. K. Seydel, E. Krause, M. Bienert, L. A. Carpino, A. El-Faham and F. Albericio. Stepwise automated solid phase synthesis of naturally occurring peptaibols using FMOC amino acid fluorides. *J. Org. Chem.* **1995**, *60*, 405-410.

[88] L. A. Carpino, D. Ionescu, A. El-Faham, P. Henklein, H. Wenschuh and M. Beyermann. Protected amino acid chlorides vs protected amino acid fluorides: reactivity comparisons. *Tetrahedron Lett.* **1998**, *39*, 241-244.

[89] S. Rajeswari, R. J. Jones and M. P. Cava. A new synthesis of amides from acyl fluorides and *N*-silylamines. *Tetrahedron Lett.* **1987**, *28*, 5099-5102.

[90] H. Wenschuh, M. Beyermann, R. Winter, M. Bienert, D. Ionescu and L. A. Carpino. Fmoc amino acid fluorides in peptide synthesis - extension of the method to extremely hindered amino acids. *Tetrahedron Lett.* **1996**, *37,* 5483-5486.

[91] (a) B. Thern, J. Rudolph and G. Jung. Triphosgene as highly efficient reagent for the solid-phase coupling of *N*-alkylated amino acids — total synthesis of cyclosporin O. *Tetrahedron Lett*. **2002**, *43*, 5013-5016. (b) B. Thern, J. Rudolph and G. Jung. Total synthesis of the nematicidal cyclododecapeptide Omphalotin A by using racemization-free triphosgene-mediated couplings in the solid phase. *Angew. Chem., Int. Ed.* **2002**, *41*, 2307-2309.

[92] M. M. Sleebs, D. Scanlon, J. Karas, R. Maharani and A. B. Hughes. Total synthesis of the antifungal depsipeptide Petriellin A. *J. Org. Chem.* **2011**, *76*, 6686-6693.

[93] Y. Barda, N. Cohen, V. Lev, N. Ben-Aroya, Y. Koch, E. Mishani, M. Fridkin and C. Gilon. Backbone metal cyclization: novel ^{99m}Tc-labeled GnRH analog as potential SPECT molecular imaging agent in cancer. *Nuclear Medicine and Biology*, **2004**, *31*, 921-933.

[94] K. G. Jastrzabek, R. Subiros-Funosas, F. Albericio, B. Kolesinska and Z. J. Kaminski. 4-(4,6-Di[2,2,2-trifluoroethoxy]-1,3,5-triazin-2-yl)-4-methylomorpholinium tetrafluoroborate. Triazine-based coupling reagents designed for coupling sterically hindered substrates *J. Org. Chem.* **2011**, 76, 4506-4513.

[95] E. Marcucci, J. Tulla-Puche and F. Albericio. Solid-phase synthesis of *N*Me-IB-01212, a highly *N*-methylated cyclic peptide. *Org. Lett.* **2012**, *14*, 612-615.

[96] R. Roodbeen, S. L. Pedersen, M. Hosseini and K. J. Jensen. Microwave heating in the solid-phase synthesis of *N*-methylated peptides: when is room temperature better? *Eur. J. Org. Chem*. **2012**, 7106-7111.

[97] S. L. Pedersen, A. P. Tofteng, L. Malik and K. J. Jensen. Microwave heating in solid-phase peptide synthesis. *Chem. Soc. Rev.* **2012**, *41*, 1826-1844.

[98] (a) J. M. Collins and N. E. Leadbeater. Microwave energy: a versatile tool for the biosciences. *Org. Biomol. Chem.* **2007**, *5*, 1141-1150. (b) S. A. Palasek, Z. J. Cox and J. M. Collins. Limiting racemization and aspartimide formation in microwave-enhanced Fmoc solid phase peptide synthesis. *J. Pept. Sci.* **2007**, *13*, 143-148. (c) H. Rodríguez, M. Suarez and F. Albericio, A convenient microwave-enhanced solid-phase synthesis of short chain *N*-methyl-rich peptides. *J. Pept. Sci.* **2010**, *16*, 136-140.

[99] (a) M. Erdelyi and A. Gogoll. Rapid microwave-assisted solid-phase peptide synthesis. *Synthesis* **2002**, 11, 1592-1596. (b) F. Rizzolo, G. Sabatino, M. Chelli, P. Rovero and A. M. Papini. A convenient microwave-enhanced solid-phase synthesis of difficult peptide sequences: case study of gramicidin A and SF114(Glc). *Int. J. Pept. Res. Ther*. **2007**, 13, 203-208. (c) S. Coantic, G. Subra and J. Martinez. Microwave-assisted solid phase peptide synthesis on high loaded resins. *Int. J. Pept. Res. Ther*. **2008**, 14, 143-147.

[100] S. L. Pedersen, A. Mehrotra and K. J. Jensen. *Proceedings of the 31st European Peptide Symposium*, edited by M. Lebl, M. Meldal, K. J. Jensen and T. Hoeg-Jensen, **2010**, 174-175.

[101] (a) S. Härterich, S. Koschatzky, J. Einsiedel and P. Gmeiner. Novel insights into GPCR—peptide interactions: mutations in extracellular loop 1, ligand backbone methylations and molecular modeling of neurotensin receptor 1. *Bioorgan. Med. Chem.* **2008**, *16*, 9359-9368. (b) N. S. Freeman, Y. Tal-Gan, S. Klein, A. Levitzki and C. Gilon. Microwave-assisted solid-phase aza-peptide synthesis: aza scan of a PKB/Akt inhibitor using aza-arginine and aza-proline precursors. *J. Org. Chem*. **2011**, *76*, 3078-3085.

[102] F. Albericio. Orthogonal protecting groups for N^{α}-amino and *C*-terminal carboxyl functions in solid-phase peptide synthesis. *Biopolymers* **2000**, *55*, 123-139.

[103] A. Isidro-Llobet, M. Álvarez and F. Albericio. Amino acid-protecting groups. *Chem. Rev*. **2009**, *109*, 2455-2504.

[104] F. Albericio and S. A. Kates. *Solid-phase peptide synthesis, a practical guide*, Marcel Dekker, New York (USA), **2000**, pp. 275-330.

[105] E. Vedejs and C. J. Kongkittingam. Solution-phase synthesis of a hindered *N*-methylated tetrapeptide using Bts-protected amino acid chlorides: efficient coupling and methylation steps allow purification by extraction. *J. Org. Chem*. **2000**, *65*, 2309-2318.

[106] S. C. Miller and T. S. Scanlan. *o*NBS-SPPS: A new method for solid-phase peptide synthesis. *J. Am. Chem. Soc.* **1998**, *120,* 2690-2691.

[107] M. Meldal, M. A. Juliano and A. M. Jansson. Azido acids in a novel method of solid-phase peptide synthesis. *Tetrahedron Lett.* **1997**, *38*, 2531-2534.

[108] C. W. Tornøe, P. Davis, F. Porreca and M. Meldal. α-azido acids for direct use in solid-phase peptide synthesis. *J. Peptide Sci*. **2000**, *6*, 594-602.

[109] P. Gund and D. F. Veber. On the ease of base-catalyzed epimerization of *N*-methylated peptides and diketopiperazines. *J. Am. Chem. Soc.* **1979**, *101*, 1885-1887.

[110] A. El-Faham and F. Albericio. Peptide coupling reagents, more than a letter soup. *Chem. Rev.* **2011**, *111*, 6557-6602.

[111] L. A. Carpino, D. Ionescu and A. El-Faham. Peptide coupling in the presence of highly hindered tertiary amines. *J. Org. Chem.* **1996**, *61*, 2460-2465.

[112] P. Lloyd-Williams, F. Albericio and E. Giralt. *Chemical approaches to the synthesis of peptides and proteins*, CRC, Boca Raton, FL, **1997**.

[113] C. Chiva, M. Vilaseca, E. Giralt and F. Albericio. An HPLC-ESMS study on the solid-phase assembly of *C*-terminal proline peptides. *J. Peptide Sci.* **1999**, *5*, 131-140.

[114] J. Urban, T. Vaisar, R. Shen and M. S. Lee. Lability of *N*-alkylated peptides towards TFA cleavage. *Int. J. Pept. Prot. Res*. **1996**, *47*, 182-189.

[115] C. Van der Auwera and M. J. O. Anteunis. Easy cleavage of *C*-terminal iminoacids from peptide acids through acidic hydrolysis. *Int. J. Pept. Prot. Res.* **1988**, *31*, 186-191.

[116] M. J. O Anteunis and C. Van Der Auwera. The remarkable sensitivity to acid-catalyzed peptolysis of peptide chains (endopeptolysis) having a succession of three *N*-alkylated amino acid residues. *Int. J. Peptide Protein Res*. **1988**, *31*, 301-310.

[117] T. Da Ros and M. Prato. Easy access to water-soluble fullerene derivatives via 1,3-dipolar cycloadditions of azomethine ylides to C60. *J. Org. Chem*. **1996**, *61,* 9070-9072.

[118] J. M. Humphrey and A. R. Chamberlin. Chemical synthesis of natural product peptides: coupling methods for the incorporation of noncoded amino acids into peptides. *Chem. Rev*. **1997**, *97*, 2243-2266.

[119] A. Madder, N. Farcy, N. G. C. Hosten, H. De Muynck, P. J. De Clercq, J. Barry and A. P. Davis. A novel sensitive colorimetric assay for visual detection of solid-phase bound amines. *Eur. J. Org. Chem.* **1999**, *11*, 2787-2791.

[120] H.-O. Kim, B. G. Gardner and M. Kahn. Acylation of sterically hindered secondary amines and acyl hydrazides. *Tetrahedron Lett.* **1995**, *36*, 6013.

[121] S. S. Wang, J. P. Tam, B. S. Wang and R. B. Merrifield. Enhancement of peptide coupling reactions by 4-dimethylaminopyridine. *Int. J. Pept. Protein Res.* **1981**, *18*, 459-467.

[122] L. A. Carpino and A. El-Faham. Tetramethylfluoroformamidinium hexafluorophosphate: a rapid-acting peptide coupling reagent for solution and solid phase peptide synthesis. *J. Am. Chem. Soc.* **1995**, *117*, 5401-5402.

[123] (a) S. Liu, W. Gu, D. Lo, X.-Z. Ding, M. Ujiki, T. E. Adrian, G. A. Soff and R. B. Silverman. *N*-Methylsansalvamide A peptide analogues. Potent new antitumor agents. *J. Med. Chem*. **2005**, *48*, 3630-3638. (b) C. L. Carroll, J. V. C.

Johnston, A. Kekec, J. D. Brown, E. Parry, J. Cajica, I. Medina, K. M. Cook, R. Corral, P.-S. Pan and S. R. McAlpine. Synthesis and cytotoxicity of novel Sansalvamide A derivatives. *Org. Lett*. **2005**, *7*, 3481-3484. (c) T. J. Styers, A. Kekec, R. Rodriguez, J. D. Brown, J. Cajica, P.-S. Pan, E. Parry, C. L. Carroll, I. Medina, R. Corral, S. Lapera, K. Otrubova, C.-M. Pan, K. L. McGuireb and S. R. McAlpine. Synthesis of Sansalvamide A derivatives and their cytotoxicity in the MSS colon cancer cell line HT-29. *Bioorg. Med. Chem.* **2006**, *14*, 5625-5631. (d) P.-S. Pan, K. L. McGuireb and S. R. McAlpine. Identification of Sansalvamide A analog potent against pancreatic cancer cell lines. *Bioorg. Chem. Lett.* **2007**, *17*, 5072-5077. (e) K. Otrubova, G. Lushington, D. V. Velde, K. L. McGuire and S. R. McAlpine. Comprehensive study of Sansalvamide A derivatives and their structure-activity relationships against drug-resistant colon cancer cell lines. *J. Med. Chem.* **2008**, *51*, 530-544. (f) P.-S. Pan, R. C. Vasko, S. A. Lapera, V. A. Johnson, R. P. Sellers, C.-C. Lin, C.-M. Pan, M. R. Davis, Veronica C. Ardi and S. R. McAlpine. A comprehensive study of Sansalvamide A derivatives: the structure–activity relationships of 78 derivatives in two pancreatic cancer cell lines. *Bioorg. Med. Chem*. **2009**, *17*, 5806-5825.

[124] (a) O. Demmer, A. O. Frank and H. Kessler. In *Design of cyclic peptides*, in *Peptide and protein design for biopharmaceutical applications,* edited by K. J. Jensen, John Wiley & Sons, Ltd, Chichester (UK), **2009,** ch. 1, pp. 133-176. (b) C. J. White and A. K. Yudin. Contemporary strategies for peptide macrocyclization. *Nat. Chem.* **2011**, *3*, 509-524.

[125] (a) A. Ehrlich, S. Rothemund, M. Brudel, M. Beyermann, L. A. Carpino and M. Bienert. Synthesis of cyclic peptides via efficient new coupling reagents. *Tetrahedron Lett.* **1993**, *34*, 4781-4784. (b) A. Ehrlich, H.-U. Heyne, R. Winter, M. Beyermann, H. Haber, L. A. Carpino and M. Bienert. Cyclization of all-L-pentapeptides by means of 1-Hydroxy-7-azabenzotriazole-derived uronium and phosphonium reagents. *J. Org. Chem.* **1996**, *61,* 8831-8838. (c) X.-M. Gao, Y.-H. Ye, M. Bernd and B. Kutscher. Studies on the synthesis of cyclic pentapeptides as LHRH antagonists and the factors that influence cyclization yield. *J. Pept. Sci.* **2002***, 8*, 418-430.

[126] T. J. Styers, R. Rodriguez, P.-S. Pan and S. R. McAlpine. High-yielding macrocyclization conditions used in the synthesis of novel Sansalvamide A derivatives. *Tetrahedron Lett.* **2006**, *47*, 515-517.

[127] S. Violtette, L. Poulain, E. Dussaulx, D. Pepin, A.-M. Faussat, J. Chambaz, J.-M. Lacorte, C. Staedel and T. Lesuffleur. Resistance of colon cancer cells to long-term 5-fluoracil exposure is correlated to the relative level of Bcl-2 and Bcl-x_L in addition to Bax and p53 status. *Int. J. Cancer*. **2002**, *98*, 498-503.

[128] B. Testa, P.-A. Carrupt, P. Gaillard and R.-S. Tsai. In *Intramolecular interactions encoded in lipophilicity*, in *Lipophilicity in drug action and toxicology*, edited by V. Pliska, B. Testa and H. van de Waterbeemd, Wiley-VCH Verlag GmbH & Co, Weinheim (Germany), **2008**. (a) ch. 1, pp. 3-4. (b) ch. 4, pp. 49-71. (c) ch. 5, pp. 73-87. (d) ch. 20, pp. 358-360.

[129] (a) *Glossary of terms used in medicinal chemistry*; IUPAC, in press. (b) *Glossary of terms used in computational drug design*, IUPAC, in press.

[130] (a) H. van de Waterbeemd and B. Testa. *The parametrization of lipophilicity and other structural properties in drug design*. In *Advances in drug research,* vol. 16, edited by B. Testa, Academic Press, London (UK), **1987**, pp. 87-227. (b) R. W. Taft, J. L. M. Abboud, M. J. Kamlet and M. H. Abraham. Linear solvation energy relations. *J. Sol. Chem.* **1985**, *14*, 153-155. (c) M. J. Kamlet, R. M. Doherty, M. H. Abraham, Y. Marcus and R. W. Taft. Linear solvation energy relationships. An improved equation for correlation and prediction of octanol water partition-coefficients of organic nonelectrolytes (including strong hydrogen-bond donor solutes). *J. Phys. Chem.-Us.* **1988**, *92*, 5244-5255. (d) N. El Tayar. R. S. Tsai, B. Testa, P. A. Carrupt and A. Leo. Partitioning of solutes in different solvent systems: the contribution of hydrogen-bonding capacity and polarity. *J. Pharm. Sci.* **1991**, *80*, 590-598. (e) N. El Tayar, B. Testa and P. A. Carrupt. Polar intermolecular interactions encoded in partition coefficients: an indirect estimation of hydrogen-bond parameters of polyfunctional solutes. *J. Phys. Chem.* **1992**, *96*, 1455-1459. (f) G. Steyaert, G. Lisa, P. Gaillard, G. Boss, F. Reymond, H. H. Girault et al. Intermolecular forces expressed in 1,2-dichloroethane-water partition coefficients — a solvatochromic analysis. *J. Chem. Soc. Faraday Trans.* **1997**, *93*, 401-406.

[131] L.-G. Danielsson and Y.-H. Zhang. Methods for determining octanol-water partition constants. *Trends Anal. Chem.* **1996**, *15*, 188-196.

[132] Salwa K. Poole, Colin F. Poole. Separation methods for estimating octanol–water partition coefficients. *J. Chromatogr. B* **2003**, *797*, 3-19.

[133] K. Valkó. Application of high-performance liquid chromatography based measurements of lipophilicity to model biological distribution. *J. Chromatogr. A* **2004**, *1037*, 299-310.

[135] (a) V. Gaberc-Porekar, I. Zore, B. Podobnik and V. Menart. Obstacles and pitfalls in the PEGylation of therapeutic proteins. *Curr. Opin. Drug Discov*. **2008**, *11*, 242-250. (b) M.C. Parrott and J. M. De Simone. Relieving PEGylation. *Nat. Chem*. **2012**, *4*, 13-14.

[136] C. Mueller, M. A. H. Capelle, T. Arvinte, E. Seyrek and G. Borchard. Tryptophan-mPEGs: novel excipients that stabilize salmon calcitonin against aggregation by non-covalent PEGylation. *Eur. J. Biopharm.* **2011**, *79*, 646-657.

[137] (a) P. Wirth, J. Souppe, D. Tritsch and J.-F. Biellmann. Chemical modification of horseradish peroxidase with ethanal-methoxypolyethylene glycol: solubility in organic solvents, activity and properties. *Bioorg. Chem.* **1991**, *19*, 133-142. (b) J. Grun, J. D. Revell, M. Conza and H. Wennemers. Peptide-polyethylene glycol conjugates: synthesis and properties of peptides bearing a *C*-terminal polyethylene glycol chain. *Bioorg. Med. Chem.* **2006**, *14*, 6197-6201.

[138] X. Liu, B. Testa and A. Fahr. Lipophilicity and its relationship with passive drug permeation. *Pharm. Res.* **2011**, *28*, 962-977.

[139] C. Mas-Moruno, F. Rechenmacher and H. Kessler. Cilengitide: the first anti-angiogenic small molecule drug candidate. Design, synthesis and clinical evaluation. *Anti-cancer Agents Med*. **2010**, *10*, 753-768.

[140] (a) B. P. Eliceiri and D. A. Cheresh. The role of α_v integrins during angiogenesis: insights into potential mechanisms of action and clinical development. *J. Clin. Invest.* **1999**, *103*, 1227-1230. (b) E. Ruoslahti. Drug targeting to specific vascular sites. *Drug Discovery Today*, **2002**, *7*, 1138-1143. (c) Z. Liu, F. Wang and X. Chen. Integrin $\alpha_V\beta_3$-targeted cancer therapy. *Drug Dev. Res.* **2008**, *69*, 329-339.

[141] (a) A. Meyer, J. Auernheimer, A. Modlinger and H. Kessler. Targeting RGD recognizing integrins: drug development, biomaterial research, tumor imaging and targeting. *Curr. Pharmac. Design*, **2006**, *12*, 2723-2747. (b) M. Schottelius, B. Laufer, H. Kessler and H. J. Wester. Ligands for mapping $\alpha_v\beta_3$-integrin expression *in vivo*. *Acc. Chem. Res.* **2009**, *42*, 969-980. (c) X. Chen. Integrin targeted imaging and therapy. *Theranostics* **2011**, *1*, 28-29, and references cited therein.

[142] Selected examples in which the covalent attachment of PEG improves the in vivo pharmacokinetic properties of RGD-cyclopeptide ligands. *1. PEGylated ^{64}Cu-/^{125}I-/^{18}F-labeled RGD-cyclopeptides [or ^{99m}Tc-/^{111}In- RGD-cyclopeptide multimers] for tumor imaging:* (a) X. Chen, R. Park, A. H. Shahinian, J. R. Bading and P. S. Conti. Pharmacokinetics and tumor retention of 125I-labeled RGD peptide are improved by PEGylation. *Nucl. Med. Biol*. **2004**, *31*, 11-19. (b) X. Chen, R. Park, Y. Hou, V. Khankaldyyan, I. Gonzales-Gomez, M. Tohme, J. R. Bading, W. E. Laug and P. S. Conti. MicroPET imaging of brain tumor angiogenesis with 18F-labeled PEGylated RGD peptide. *Eur. J. Nucl. Med. Mol. Imaging*, **2004**, *31*, 1081-1089. (c) X. Chen, Y. Hou, M.Tohme, R. Park, V. Khankaldyyan, I. Gonzales-Gomez, J. R. Bading, W. E. Laug and P. S. Conti. Pegylated Arg-Gly-Asp peptide: ^{64}Cu labeling and PET Imaging of brain tumor $\alpha_v\beta_3$-integrin Expression. *J. Nucl. Med*. **2004**, *45*, 1776-1783. (d) L. Wang, J. Shi, Y.-S. Kim, S. Zhai, B. Jia, H. Zhao, Z. Liu, F. Wang, X. Chen and S. Liu. Improving tumor-targeting capability and pharmacokinetics of ^{99m}Tc-Labeled cyclic RGD dimers with PEG_4 linkers. *Mol. Pharm*. **2008**, 6, 231-245. (e) J. Shi, Yang Zhou, S. Chakraborty, Y.-S. Kim, B. Jia, F. Wang and S. Liu. Evaluation of ^{111}In-labeled cyclic RGD peptides: Effects of peptide and linker multiplicity on their tumor uptake, excretion kinetics and metabolic stability. *Theranostics* **2011**, *1*, 322-340. *2. PEGylated RGD-cyclopeptide dimer for tumor therapy:* (f) D. Polyaka, C. Ryppab, A. Eldar-Boocka, P. Ofeka, A. Manyc, K. Lichad, F. Kratzb and R. Satchi-Fainaroa. Development of PEGylated doxorubicin-E-[c$(RGDfK)_2$] conjugate for integrin-targeted cancer therapy. *Polym. Adv. Technol.* **2011**, *22*, 103-113.

[143] M. Aumailley, M. Gurrath, G. Müller, J. Calvete, R. Timpl and H. Kessler. Arg-Gly-Asp constrained within cyclic peptides: strong and selective inhibitors of cell adhesion to vitronectin and laminin fragment P1. *FEBS Lett.*, **1991**, *291*, 50-54.

[144] (a) G. Müller, M. Gurrath and H. Kessler. Pharmacophore refinement of gpIIb/IIIa antagonists based on comparative studies of antiadhesive cyclic and acyclic RGD peptides. *J. Comp-Aided Mol. Des*. **1994**, *8*, 709-730. (b) R. Haubner, R. Gratias, B. Diefenbach, S. L. Goodman, A. Jonczyk and H. Kessler. Structural and functional aspects of RGD-containing cyclic pentapeptides as highly potent and selective integrin $\alpha_V\beta_3$ antagonists. *J. Am. Chem. Soc.* **1996**, *118*, 7461-7472.

[145] M. A. Dechantsreiter, E. Planker, B. Mathä, E. Lohof, G. Hölzemann, A. Jonczyk, S. L. Goodman and H. Kessler. *N*-methylated cyclic RGD peptides as highly active and selective $\alpha_V\beta_3$ integrin antagonists. *J. Med. Chem.* **1999**, *42,* 3033-3040.

[146] J. P. Tam and Y.-A. Lu. Coupling difficulty associated with interchain clustering and phase transition in solid phase peptide synthesis. *J. Am. Chem. Soc*. **1995**, *117*, 12058-12063.

[147] J. Coste, E. Frerot, P. Jouin and B. Castro. Oxybenzotriazole free peptide coupling reagents for *N*-methylated amino acids. *Tetrahedron Lett.* **1991**, *32*, 1967-1970.

[148] R. O. Hynes. Integrins: bidirectional, allosteric signaling machines. *Cell* **2002**, *110*, 673-687.

[149] (a) E. Ruoslahti. The Walter Herbert Lecture. Control of cell motility and tumour invasion by extracellular matrix interactions. *Br. J. Cancer* **1992**, *66*, 239-242. (b) F. Giancotti and E. Ruoslahti. Integrin signaling. *Science* **1999**, *285*, 1028-1033.

[150] (a) D. G. Stupack, X. S. Puente, S. Boutsaboualoy, C. M. Storgard and D. A. Cheresh. Apoptosis of adherent cells by recruitment of caspase-8 to unligated integrins. *J. Cell Biol*. **2001**, *155*, 459-470. (b) S. Maubant, D. Saint-Dizier, M. Boutillon, F. Perron-Sierra, P. J. Casara, J. A. Hickman, G. C. Tucker and E. Van Obberghen-Schilling. Blockade of $\alpha_v\beta_3$ and $\alpha_v\beta_5$ integrins by RGD mimetics induces apoptosis and not integrin-mediated death in human endothelial cells. *Blood* **2006**, *108*, 3035-3044.

[151] T. Cupido, J. Spengler, J. Ruiz-Rodriguez, J. Adan, F. Mitjans, J. Piulats and F. Albericio. Amide-to-ester substitution allows fine-tuning of the cyclopeptide conformational ensemble. *Angew. Chem., Int. Ed*. **2010**, *49*, 2732-2737.

[152] F. M. Veronese and A. Mero. The impact of PEGylation on biological therapies. *Biodrugs* **2008**, *22*, 315-329.

[153] J. A. Arnott and S. L. Planey. The influence of lipophilicity in drug discovery and design. *Expert. Opin. Drug. Discov.* **2012**, *7*, 863-875.

[154] M. Goldberg and I. López-Orellana. Challenges for the oral delivery of macromolecules. *Nat. Rev.Drug Disc.* **2003**, *2*, 289-295.

[155] D. A. Reardon, B. Neyns, M. Weller, J. C. Tonn, L. B. Nabors and R. Stupp. Cilengitide: an RGD pentapeptide $\alpha_V\beta_3$ and $\alpha_V\beta_5$ integrin inhibitor in development for glioblastoma and other malignancies. *Future Oncol.* **2011**, *7*, 339-354.

[156] (a) K. Yamada, M. Murakami, A. Yamamoto, K. Takada and S. Muranishi. Improvement of intestinal absorption of thyrotropin-releasing hormone by chemical modification with lauric acid. *J. Pharm. Pharmacol.* **1992**, *44*, 717-721. (b) M. Hashizume, T. Douen, M. Murakami, A. Yamamoto, K. Takada and S. Muranishi. Improvement of large intestinal absorption of insulin by chemical modification with palmitic acid in rats. *J. Pharm. Pharmacol.* **1992**, *44*, 555-559. (c) E. Yodoya, K. Uemura, T. Tenma, T. Fujita, M. Murakami, A. Yamamoto and S. Muranishi. Enhanced permeability of tetragastrin across the rat intestinal membrane and its reduced degradation by acylation with various fatty acids. *J. Pharmacol. Exp. Ther.* **1994**, *271*, 1509-1513. (d) H. Asada, T. Douen, M. Waki, S. Adachi, T. Fujita, A. Yamamoto and S. Muranishi. Absorption characteristics of chemically modified-insulin derivatives with various fatty acids in the small and large intestine. *J. Pharm. Sci.* **1995**, *84*, 682-687. (e) T. Uchiyama, A. Kotani, H. Tatsumi, T. Kishida, A. Okamoto, N.

Okada, M. Murakami, T. Fujita, Y. Fujiwara, Y. Kiso, S. Muranishi and A. Yamamoto. Development of novel lipophilic derivatives of DADLE (leucine enkephalin analogue): intestinal permeability characateristics of DADLE derivatives in rats. *Pharm. Res.* **2000**, *17*, 1461-1467.

[157] (a) Y. Lee, J. H. Nam, H. C. Shin and Y. Byun. Conjugation of low-molecular-weight heparin and deoxycholic acid for the development of a new oral anticoagulant agent. *Circulation* **2001**, *104*, 3116–3120. (b) S. Clement, J. G. Still and G. Kosutic. Oral insulin product hexyl-insulin monoconjugate 2 (HIM2) in type 1 diabetes mellitus: the glucose stabilization effects of HIM2. *Diabetes Technol. Ther.* **2002**, *4*, 459-466.

[158] (a) S. Lee, J. Xie and X. Chen. Peptide-based probes for targeted molecular imaging. *Biochemistry*, **2010**, *49*, 1364-1376. (b) Jessica Y. Shu, Brian Panganiban and Ting Xu. Peptide-polymer conjugates: from fundamental science to application. *Annu. Rev. Phys. Chem*. **2013**, *64*, 631-657.

[159] M. A. Gauthier and H.-A. Klok. Peptide/protein-polymer conjugates: synthetic strategies and design concepts. *Chem. Commun.* **2008**, 2591-2611.

[160] (a) J. M. Antos and M. B. Francis. Transition metal catalyzed methods for site-selective protein modification. *Curr. Opin. Chem. Biol.* **2006**, *10*, 253-262. (b) E. M. Sletten and C. R. Bertozzi. Bioorthogonal chemistry: fishing for selectivity in a sea of functionality. *Angew. Chem., Int. Ed.* **2009**, *48*, 6974-6998.

[161] (a) H. C. Kolb and K. B. Sharpless. The growing impact of click chemistry on drug discovery. *Drug Discov. Today.* **2003**, *8*, 1128-1137. (b) S. Brase, C. Gil, K. Knepper and V. Zimmermann. Organic azides: an exploding diversity of a unique class of compounds. *Angew. Chem., Int. Ed*. **2005**, *44*, 5518-5240.

[162] R. W. Bates and M. R. Dewey. A formal synthesis of swainsonine by gold-catalyzed allene cyclization. *Org. Lett.* **2009**, *16*, 3706-3708.

[163] R. Pascal and R. Sola. Preservation of the Fmoc protective group under alkaline conditions by using $CaCl_2$. Applications in peptide synthesis. *Tetrahedron Lett*. **1998**, *39*, 5031-5034.

[164] S. D. Hanton. Mass spectrometry of polymers and polymer surfaces. *Chem. Rev.* **2001**, *101*, 527-570.

[165] G. Montaudo, F. Samperi and M. S. Montaudo. Characterization of synthetic polymers by MALDI-MS. *Prog. Polym. Sci.* **2006**, *10*, 1016-1020.

[166] (a) E. F. V. Scriven and K. Turnbull. Azides: their preparation and synthetic uses. *Chem. Rev.* **1988**, *88*, 297-368. (b) Y. Pei and B. O.S. Wickham. Regioselective syntheses of 3-aminomethyl-5-substituted isoxazoles: A facile and chemoselective reduction of azide to amine by sodium borohydride using 1,3-propanedithiol as a catalyst. *Tetrahedron Lett.* **1993**, *34*, 7509-7512. (c) C. Goulaouic-Dubois and M. Hesse. Efficient reduction of azides with samarium diiodide. *Tetrahedron Lett.* **1995**, *36*, 7427-7430. (d) L. Benati, P. C. Montevecchi, D. Nanni, P. Spagnolo and M. Volta. Reduction of azides to amines by samarium diiodide. *Tetrahedron Lett*. **1995**, *36*, 7313-7314. (e) A. Kamal, N. V. Rao and E. Laxman. Iodotrimethylsilane: A mild and efficient reagent for the reduction of azides to amines. *Tetrahedron Lett.* **1997**, *38*, 6945-6948. (f) G. V. Reddy, G. V. Rao and D. S. Iyengar. A novel, simple, chemoselective and practical protocol for the reduction of azides using In/NH_4Cl. *Tetrahedron Lett.* **1999**, *40*, 3937-3938. (g) W. Lin, X. Zhang, Z. He, Y. Jin, L. Gong and A. Mi. Reduction of azides to amines or amides with zinc and ammonium chloride as reducing agent. *Synthetic Comm.* **2002**, *32*, 3279-3284. (h) A. Kamal, K. V. Ramana, H. B. Ankati and A. V. Ramana. Mild and efficient reduction of azides to amines: synthesis of fused [2,1-b]quinazolinones. *Tetrahedron Lett*. **2002**, *43*, 6861-6863. (i) Y. J. Jung, Y. M. Chang, J. H. Lee and C. M. Yoon. Chemoselective conversion of azides to t-butyl carbamates and amines. *Tetrahedron Lett.* **2002**, *43*, 8735-8739. (j) J. L. Norcliffe, L. P. Conway and D. R. W. Hodgson. Reduction of alkyl and aryl azides with sodium thiophosphate in aqueous solutions. *Tetrahedron Lett.* **2011**, *52*, 2730-2732.

[167] W. Lin, X. Zhang, Z. He, Y. Jin, L. Gong and A. Mi. Reduction of azides to amines or amides with zinc and ammonium chloride as reducing agent. *Synth. Comm*. **2002**, *32*, 3279-3284.

[168] M. Morpurgo and F. M. Veronese. In *Conjugates of peptides and proteins to polyethylene glycols*, in *Bioconjugation protocols: strategies and methods (Methods in molecular biology, vol. 283)*, edited by C. M. Nyemeyer, Humana Press Inc., Totowa (New Jersey, USA), **2004**, p. 54.

[169] G. R. Grimsley, J. M. Scholtz and C. N. Pace. A summary of the measured pK_a values of the ionizable groups in folded proteins. *Protein Sci.* **2009**, *18*, 247-251.

[170] (a) S. Zalipsky. Functionalized poly(ethylene glycol) for preparation of biologically relevant conjugates. *Bioconjugate Chem.* **1995,** *6*, 150-165. (b) J. M. Harris and M. R. Sedaghat-Herati. Preparation and use of the polyethylene glycol propionadehyde. US Patent 5252714, **1993**.

[171] (a) C. W. Tornøe, C. Christensen and M. J. Meldal. Peptidotriazoles on solid phase: [1,2,3]-triazoles by regiospecific copper(I)-catalyzed 1,3-dipolar cycloadditions of terminal alkynes to azides. *J. Org. Chem.* **2002**, *67*, 3057-3064. (b) V. V. Rostovtsev, L. G. Green, V. V. Fokin and B. K. Sharpless. A stepwise Huisgen cycloaddition process: copper(I)-catalyzed regioselective "ligation" of azides and terminal alkynes. *Angew. Chem., Int. Ed.* **2002**, *41*, 2596-2599. (c) M. Meldal and C. W. Tornøe. Cu-Catalyzed azide-alkyne cycloaddition. *Chem. Rev.* **2008,** *108,* 2952-3015.

[172] H. C. Kolb, M. G. Finn and K. B. Sharpless. Click chemistry: diverse chemical function from a few good reactions. *Angew. Chem., Int. Ed.* **2001**, *40*, 2004-2021.

[173] (a) W. S. Horne , M. K. Yadav , C. D. Stout and M. R. Ghadiri. Heterocyclic peptide backbone modifications in an α-helical coiled coil. *J. Am. Chem. Soc.* **2004**, *126*, 15366-15367. (b) V. D. Bock, D. Speijer, H. Hiemstra and J. H. van Maarseveen. 1,2,3-Triazoles as peptide bond isosteres: synthesis and biological evaluation of cyclotetrapeptide mimics. *Org. Biomol. Chem.* **2007**, *5*, 971-975. (c) Y. L. Angell and K. Burgess. Peptidomimetics via copper-catalyzed azide-alkyne cycloadditions. *Chem. Soc. Rev.* **2007**, *36*, 1674-1689.

[174] V. D. Bock, H. Hiemstra and J. H.-V. Maarseveen. Cu(I)-catalyzed alkyne-azide "click" cycloadditions from a mechanistic and synthetic perspective. *Eur. J. Org. Chem*. **2006**, 51-68.

[175] W. H. Zhan, H. N. Barnhill, K. Sivakumar, H. Tian and Q. Wang. Synthesis of hemicyanine dyes for "click" bioconjugation. *Tetrahedron Lett.* **2005**, 46, 1691-1695.

[176] P. L. Golas, N. V. Tsarevsky, B. S. Sumerlin and K. Matyjaszewski. Catalyst performance in "click" coupling reactions of polymers prepared by ARTP: ligand and metal effects. *Macromolecules* **2006**, *39*, 6451-6457.

[177] *Note:* S. Perrier *et. al.* recently reported that the cycloaddition between a tetraazide-containing RGD-peptide and four alkyne-functionalized polymers required a large excess of copper catalyst (100-1000 times the amount of a typical system). They stated that the peptide may bind to copper through the amide protons or through the formed triazole ring, thus lowering the catalytic activity. (a) R. Chapman, K. A. Jolliffe and S. Perrier. Synthesis of self-assembling cyclic peptide-polymer conjugates using click chemistry. *Aust. J. Chem.* **2010**, *63*, 1169-1172. (b) C. K. Poon, R. Chapman, K. A. Jolliffe and S. Perrier. Pushing the limits of copper mediated azide-alkyne cycloaddition to conjugate polymeric chains to cyclic peptides. *Polym. Chem.* **2012**, *3*, 1820-1826.

[178] (a) A. Guiotto, M. Pozzobon, M. Canevari R. Manganelli, M. Scarin and F. M. Veronese. PEGylation of the antimicrobial peptide nisin A: problems and perspetives. *Il Farmaco* **2003**, *58*, 45-50. (b) Y. Imura, M. Nishida, Y. Ogawa, Y. Takakura and K. Matsuzaki. Action mechanism of tachyplesin I and effects of PEGylation. *Biochim. Bioph. Acta* **2007**, *1768*, 1160-1169. (c) K. J. Lumb, L. B. DeCarr, F. M. Lucinda, M. R. Mays, T. M. Buckholz, S. E. Fisk, C. M. Pellegrino, A. A. Ortiz and C. D. Mahle. Novel selective neuropeptide Y2 receptor PEGylated peptide agonists reduce food intake and body weight in mice. *J. Med. Chem.* **2007**, 50, 2264-2268. (d) Y. S. Youn, D. H. Na and K. C. Lee. High-

yield production of biologically active mono-PEGylated salmon calcitonin by site-specific PEGylation. *J. Control. Release* **2007**, *117*, 371-379.

[179] P. Bailon, A. Palleroni, C. A. Schaffer, C. L. Spence , W.-J. Fung, J. E. Porter, G. K. Ehrlich, W. Pan, Z.-X. Xu, M. W. Modi, A. Farid and W. Berthold. Rational design of a potent, long-lasting form of interferon: a 40 kDa branched polyethylene glycol-conjugated interferon α-2a for the treatment of hepatitis C. *Bioconjugate Chem.* **2001**, *12*, 195-202.

[180] (a) R. Haubner, H.-J. Wester, F. Burkhart, R. Senekowitsch-Schmidtke, W. Weber, S. L. Goodman, H. Kessler and M. Schwaiger. Glycosylated RGD-containing peptides: tracer for tumor targeting and angiogenesis imaging with improved biokinetics. *J. Nucl. Med.* **2001**, *42*, 326-336. (b) R. Haubner, B. Kuhnast, C. Mang, W. A. Weber, H. Kessler, H. J. Wester and M. Schwaiger. ^{18F}Galacto-RGD: synthesis, radiolabeling, metabolic stability, and radiation dose estimates. *Bioconjugate Chem.* **2004**, *15*, 61-69. (c) D.-E. Lee, Y.-D. Hong, K.-H. Choi, S.-Y. Lee, P. H. Park and S.-J. Choi. Preparation and evaluation of ^{99m}Tc-labeled cyclic arginine-glycine-aspartate (RGD) peptide for integrin targeting. *Appl. Radiat. Isot.* **2010**, *68*, 1896-902. (d) S. Mittal, M. Bhadwal, S. Chakraborty, H. D. Sarma, S. Banerjee and M. R. A. Pillai. A novel concept of radiosynthesis of a ^{99m}Tc-labeled dimeric RGD peptide as a potential radiotracer for tumor imaging. *Bioorg. Med. Chem. Lett*. **2013**, *23*, 1808-1812.

[181] (a) X. Chen, Y. Hou, M. Tohme, R. Park, V. Khankaldyyan, I. Gonzales-Gomez, J. R. Bading, W. E. Laug and P. S. Conti. Pegylated Arg-Gly-Asp peptide: ^{64}Cu labeling and PET imaging of brain tumor $\alpha_v\beta_3$-integrin expression. *J. Nucl. Med.* **2004**, *45*, 1776-1783. (b) X. Chen, R. Park, Y. Hou, V. Khankaldyyan, I. Gonzales-Gomez, M. Tohme, J. R. Bading, W. E. Laug and P. S. Conti, Eur. MicroPET imaging of brain tumor angiogenesis with ^{18}F-labeled PEGylated RGD peptide. *J. Nucl. Med. Mol. Imaging*, **2004**, *31*, 1081-1089. (c) X. Chen, R. Park, A. H. Shahinian, J. R. Bading and P. S. Conti. Pharmacokinetics and tumor retention of ^{125}I-labeled RGD peptide are improved by PEGylation. *Nucl. Med. Biol*. **2013**, *40*, 262-272. (d) X. Chen, R. Park, A. H. Shahinian, J. R. Bading and P. S. Conti. Pharmacokinetics and tumor retention of ^{125}I-labeled RGD peptide are improved by PEGylation. *Nucl. Med. Biol*. **2013**, *40*, 262-272.

[182] (a) K.-E. Gottschalk and H. Kessler. The structures of integrins and integrin-ligand complexes: implications for drug design and signal transduction. *Angew. Chem., Int. Ed.* **2002**, *41* -
- . Kessler. The impact of amino acid side chain mutations in conformational design of peptides and proteins. *Chem. Eur. J.* **2010**, *16*, 5385-5390.

[183] N. Sreerama and R. W. Woody. In *Circular dichroism of peptides and proteins*, in *Circular dichroism - Principles and applications*, edited by N. Berova, K. Nakanishi and R. W. Woody, Wiley-VCH, New York (USA), **2000**.

[184] Adapted from: http://www.photophysics.com/tutorials/circular-dichroism-cd-spectroscopy/6-cd-signatures-of-structural-elements.

[185] (a) J. Kemmink and T. E. Creighton. Effects of trifluoroethanol on the conformations of peptides representing the entire sequence of bovine pancreatic trypsin inhibitor. *Biochemistry*, **1995**, *34*, 12630-12635. (b) J. K. Myers, C. N. Pace and J. M. Scholtz. Trifluoroethanol effects on helix propensity and electrostatic interactions in the helical peptide from ribonuclease T1. *Protein Sci.* **1998**, *7*, 383-388. (c) H. Reiersen and A. R. Rees. Trifluoroethanol may form a solvent matrix for assisted hydrophobic interactions between peptide side chains. *Protein Eng.* **2000**, *13*, 739-743.

[186] E. Vass, Z. Majer, K. Kohalmy and M. Hollósi. Vibrational and chiroptical spectroscopic characterization of gamma-turn model cyclic tetrapeptides containing two beta-Ala residues. *Chirality* **2010**, *8*, 762-871.

[187] A. Glättli, X. Daura, D. Seebach and W. F. van Gunsteren. Can one derive the conformational preference of a β-peptide from its CD spectrum? *J. Am. Chem. Soc.* **2002**, *124*, 12972-12978.

[188] A. Perczel and G. D. Faman. Quantitative analysis of cyclic β-turn models. *Protein Sci.* **1992**, *I,* 378-395.

[189] E. Kaiser, R. L. Colescott, C. D. Bossinger and P. I. Cook. Color test for detection of free terminal amino groups in the solid-phase synthesis of peptides. *Anal. Biochem*. **1970**, *348*, 595-598.

[190] C. Thorkild. A qualitative test for monitoring coupling completeness in solid phase peptide synthesis using chloranil. *Acta. Chem. Scand. B* **1979**, *33*, 763-766.

[191] K. Barlos, D. Gatos, J. Kallitsis, G. Papaphotiu, P. Sotiriu, Y. Wenqing and W. Schäfer. Darstellung geschützter peptid-fragmente unter einsatz substituierter triphenylmethyl-harze. *Tetrahedron Lett.* **1989**, *30*, 3943-3946.

[192] J. van Meerloo, G. J. Kaspers and J. Cloos. Cell sensitivity assays: the MTT assay. *Methods Mol Biol.* **2011**, *731*, 237-245.

[193] L. A. Carpino. Methyl ester nonequivalence in the ^{1}H-NMR spectra of diastereomeric dipeptide esters incorporating *N*-terminal α-phenylglycine units*. J. Org. Chem.* **1988**, *53*, 875-878.

[194] *Original BTC activation procedure:* ref. 28. *Modified BTC activation procedure, compatible with CTC resin:* ref. 91.

[195] D. Cox, M. Brennan and N. Moran. Integrins as therapeutic targets: lessons and opportunities. *Nat. Rev. Drug Discov.* **2010**, *9*, 804-820.

[196] (a) J. A. Nemeth, M. T. Nakada, M. Trikha, Z. Lang, M. S. Gordon, G. C. Jayson, R. Corringham, U. Prabhakar, H. M. Davis and R. A. Beckman. Alpha-v Integrins as therapeutic targets. in oncology. *Cancer Invest.* **2007**, *25*, 632-646. (b) A. R. Reynolds, I. R. Hart, A. R. Watson, J. C. Welti, R. G. Silva, S. D. Robinson, G. Da Violante, M. Gourlaouen, M. Salih, Matt C Jones, D. T. Jones, G. Saunders, V. Kostourou, F. Perron-Sierra, J. C. Norman, G. C. Tucker and K. M. Hodivala-Dilke. Stimulation of tumor growth and angiogenesis by low concentrations of RGD-mimetic integrin inhibitors. *Nature Med.* **2009**, *15*, 392-400. (c) A. Carter. Integrins as targets: first Phase III trial launches, but questions remain. *J. Natl. Cancer Inst.* **2010**, *102*, 675-677.

[197] (a) U. Hersel, C. Dahmen and H. Kessler. RGD modified polymers: biomaterials for stimulated cell adhesion and beyond. *Biomaterials* **2003**, *24*, 4385-4415. (b) M. C. Siebers, P. J. Brugge, X. F. Walboomers and J. A. Jansen. Integrins as linker proteins between osteoblasts and bone replacing materials. A critical review. *Biomaterials* **2005**, *26*, 137-146. (22) E. Lieb, M. Hacker, J. Tessmar, L. A. Kunz-Schughart, J. Fiedler, C. Dahmen, U. Hersel, H. Kessler, M. B. Schulz and A. Göpferich. Mediating specific cell adhesion to low-adhesive diblock copolymers by instant modification with cyclic RGD peptides. *Biomaterials* **2005**, *26*, 2333-2341.

ANNEXES

ANNEX 1: TABLES OF AMINO ACIDS, COUPLING REAGENTS AND PROTECTING GROUPS

Table I: Amino acids used in the present Thesis

Name	Code	Structure
glycine	Gly, G	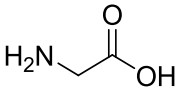
alanine	Ala, A	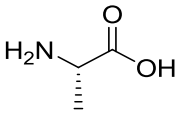
leucine	Leu, L	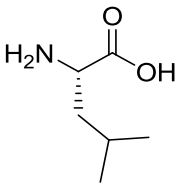
valine	Val, V	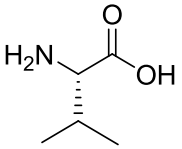
phenylalanine	Phe, F	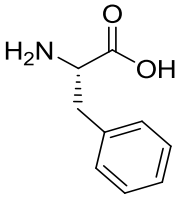
D-phenylalanine	D-Phe, f	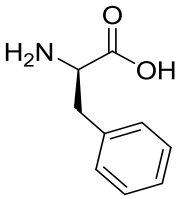
aspartic acid	Asp, D	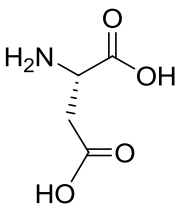
arginine	Arg, R	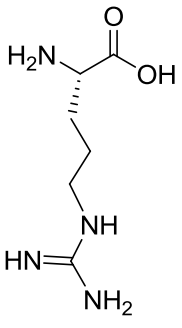

Table II: Protecting groups used in the present Thesis

Common name	Systematic name	Structure	Functional group protected	Stability
Fmoc-	9-fluorenylmethoxycarbonyl	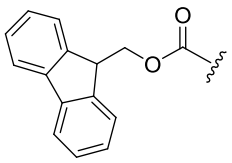	amine	Stable: acid Labile: base
Alloc-	allyloxycarbonyl	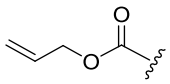	amine	Stable: acid and base Labile: Pd^0
^{t}Bu-	*tert*-butyl		acid	Stable: base Labile: acid
Pnb-	*p*-nitrobenzyl	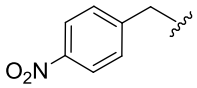	acid	Stable: acid and base Labile: reducing agents or catalytic hydrogenation
Pbf-	2,2,4,6,7-pentamethyl-2,3-dihydrobenzofuran-5-sulfonyl	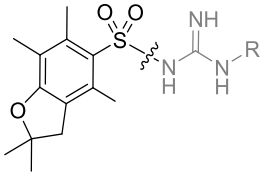	guanidine	Stable: base Labile: acid

Table III: Coupling reagents and additives used in the present Thesis

Common name	Systematic name	Structure
DIPCDI	*N,N'*-diisopropylcarbodiimide	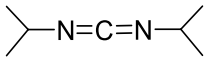
EDC·HCl	*N*-ethyl-*N'*-(3-dimethylaminopropyl)carbodiimide hydrochloride	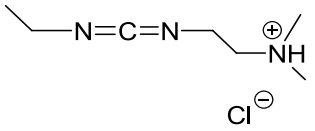
HOAt	1-hydroxy-7-azabenzotriazole	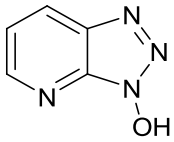
HOBt	1-hydroxybenzotriazole	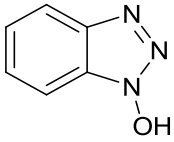
OxymaPure	ethyl 2-cyano-2-(hydroxyimino)acetate	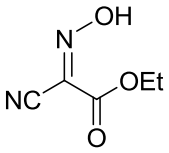
HATU	*O*-(7-azabenzotriazol-1-yl)-*N,N,N',N'*-tetramethyluronium hexafluorophosphate	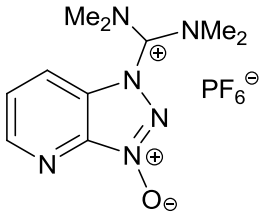
HBTU	*O*-(benzotriazol-1-yl)-*N,N,N',N'*-tetramethyluronium hexafluorophosphate	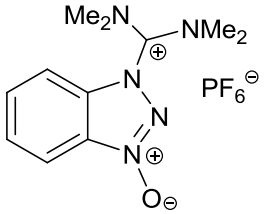
PyBOP	(benzotriazol-1-yl-oxy)tri(pyrrolidino)phosphonium hexafluorophosphate	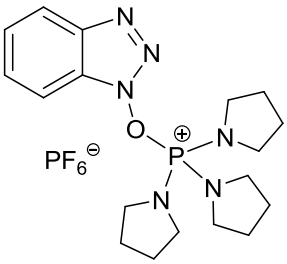
TFFH	tetramethylchloroformamidinium hexafluorophosphate	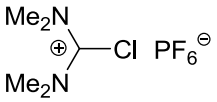
TFFH	tetramethylfluoroformamidinium hexafluorophosphate	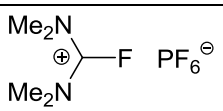

ANNEX 2: ^{1}H AND ^{13}C-NMR ASSIGNMENT OF THE *N*-TEG AND *N*-Me ANALOGS OF SANSALVAMIDE A PEPTIDE

Table IV: ^{1}H-NMR assignment of the *N*-TEG and *N*-Me analogs of Sansalvamide A peptide in $CDCl_3$ at 288 K.

		1a	1b	2a	2b	3a	3b
0.0 -1.2 ppm 24H	2xCH_3 [Leu^1] 2xCH_3 [Leu^2] 2xCH_3 [Leu^3] 2xCH_3[Val]	0.63-1.04 (m, 24H)	0.63-1.04 (m, 24H)	0.75 (d, *J* = 6.6 Hz, 3H) 0.64 (d, *J* = 6.4 Hz, 3H) 0.84-0.97 (m, 18H)	0.62 (d, *J* = 5.0 Hz, 3 H) 0.73 (m, 3H) 0.84-0.99 (m, 18H)	0.77-1.01 (m, 24H)	0.77 (d, *J* = 6.3 Hz, 3H) 0.84 (d, *J* = 6.4 Hz, 6H) 0.95-0.82 (m, 12H) 0.97 (d, *J* = 6.2 Hz, 3H)
1.2-2.5 ppm 9H	γ-CH_2 [Leu^1] γ-CH_2 [Leu^2] γ-CH_2 [Leu^3] β-CH [Leu^1] β-CH [Leu^2] β-CH [Leu^3]	1.05-1.74 (m, 7H) 1.87-2.22 (m, 2H)	1.09-1.83 (m, 6H) 1.80-2.12 (m, 2H) 2.10-2.36 (m, 1H)	1.17-1.83 (m, 9H)	1.20-1.34 (m, 2H) 1.34-1.51 (m, 2H) 1.45-1.79 (m, 5H)	1.24-2.02 (m, 7H) 2.02-2.17 (m, 2H)	1.22-1.36 (m, 2H) 1.36-1.51 (m, 2H) 1.51-1.90 (m, 4H) 2.14 (m, 1H)
2.5-5.5 ppm **1a-5a**: 11H **1b-5b**: 23H	*N*-CH_3 or CH_3O [*N*-TEG]	3.35 (s, 3 H)	3.02 (s, 3H)	3.38 (s, 3 H)	3.01 (s, 3H)	3.34 (s, 3 H)	3.07 (s, 3H)
	N-$\underline{CH_2}CH_2O$ [*N*-TEG] *N*-$CH_2\underline{CH_2}O$ [*N*-TEG] 4xCH_2 [*N*-TEG]	3.48-3.90 (m, 12H)		3.50-3.72 (m, 12H)		3.45-3.67 (m, 12H)	
	β-CH [Val] β-CH_2 [Phe] H^{α}	3.19-3.38 (m, 2H) 3.40-3.48 (m, 1H) 3.91 (m, 1H)	3.18-3.30 (m, 2H) 3.46 (m, 1H) 3.55-4.07 (m, 1H)	2.92-3.24 (m, 3H) 3.67 (m, 1H)	2.84-3.14 (m, 3H) 3.68 (m, 1H)	2.94 (dd, *J* = 13.7, 8.0 Hz, 1H) 3.04-3.24 (m, 1H) 3.37 (m, 1H) 3.63-3.83 (m, 1H)	2.92-3.02 (m, 1H) 3.02-3.13 (m, 1H) 3.44 (t, *J* = 7.6 Hz, 1H)
	4xH^{α}	4.11 (m, 1H) 4.18 (m, 1H) 4.47 (m, 1H) 4.95 (m, 1H)	3.95 (m, 1H) 4.18 (m, 1H) 4.57 (m, 1H) 4.86 (m, 1H)	3.97 (m, 1H) 4.27 (m, 1H) 4.46 (m, 1H) 4.97 (dd, *J* = 16.2 Hz, 7.6 Hz, 1H)	3.97 (m, 1H) 4.20 (m, 1H) 4.47 (m, 1H) 4.85 (d, *J* = 6.8 Hz, 1H)	4.13-4.23 (m, 2H) 4.52-4.64 (m, 2H)	4.05-4.27 (m, 2H) 4.49 (t, *J* = 9.4 Hz, 1H) 4.58 (dd, *J* = 16.7, 8.5 Hz, 1H)
5.5-9.0 ppm 9H	4xH^{N} 5xH^{ar} [Phe]	6.28 (bs, 1H) 6.97 (bs, 1H) 7.11-7.36 (m, 5H) 7.38-7.68 (m, 1H) 7.78 (bs, 1H)	6.50 (bs, 1H) 7.05 (bs, 1H) 7.03-7.40 (m, 5H) 7.58 (bs, 1H) 7.94 (bs, 1H)	5.74 (bs, 1H) 6.51 (d, *J* = 8.6 Hz, 1H) 7.12-7.33 (m, 6H) 8.15 (d, *J* = 8.9 Hz, 1H)	5.71 (bs. 1H) 6.87 (bs, 1H) 7.04-7.31 (m, 5H) 8.04 (bs, 1H) 8.14 (bs, 1H)	6.40 (d, *J* = 5.1 Hz, 1H) 6.45 (d, *J* = 9.5 Hz, 1H) 7.11-7.34 (m, 5H) 6.82 (d, *J* = 7.5 Hz, 1H) 8.42 (d, *J* = 9.4 Hz, 1H)	6.54 (bs, 1H) 6.73 (bs, 1H) 7.03 (bs, 1H) 7.07-7.58 (m, 5H) 8.13 (bs, 1H)

		4a	4b	5a	5b
0.0 -1.2 ppm 24H	2xCH_3 [Leu^1] 2xCH_3 [Leu^2] 2xCH_3 [Leu^3] 2xCH_3[Val]	0.88-1.09 (m, 24H)	0.84 (d, *J* = 6.6 Hz, 6 H) 0.87-0.99 (m, 18 H)	0.83 (d, *J* = 6.6 Hz, 3 H) 0.84-1.01 (m, 21H)	0.78 (d, *J* = 6.4 Hz, 3 H) 0.92-0.97 (m, 21 H)
1.2-2.5 ppm 9H	γ-CH_2 [Leu^1] γ-CH_2 [Leu^2] γ-CH_2 [Leu^3] β-CH [Leu^1] β-CH [Leu^2] β-CH [Leu^3]	1.33-1.79 (m, 9H)	1.27-1.73 (m, 9H)	1.20-1.35 (m, 1H) 1.35-1.50 (m, 1H) 1.49-1.69 (m, 4H) 1.92 (m, 1H) 2.01 (m, 2H)	1.07-1.26 (m, 1H) 1.33-1.48 (m, 1H) 1.45-1.80 (m, 5H) 1.99 (m, 1 H) 2.23 (m, 1H)
2.5-5.5 ppm **1a-5a**: 11H **1b-5b**: 23H	*N*-CH_3 or CH_3O [*N*-TEG]	3.34 (s, 3 H)	2.74 (s, 3 H)	3.36 (s, 3 H)	2.91 (s, 3 H)
	N-$\underline{CH_2}CH_2O$ [*N*-TEG] *N*-$CH_2\underline{CH_2}O$ [*N*-TEG] 4xCH_2 [*N*-TEG]	3.05-3.22 (m, 2H) 3.28-3.44 (m, 3H) 3.49-3.61 (m, 7H)		3.32-3.43 (m, 2 H) 3.45-3.66 (m, 10H)	
	β-CH [Val] β-CH_2 [Phe] H^{α}	2.22-2.39 (m, 1H) 3.29 (dd, *J* = 13.2, 6.1 Hz, 1H) 3.68 (dd, *J* = 13.2, 10.2 Hz, 1H) 3.79 (dd, *J* = 9.9, 6.3 Hz, 1H)	2.33 (m, 1H) 3.22 (dd, *J* = 11.6, 7.3 Hz, 1H) 3.69 (m, 1H) 3.70 (m, 1H)	2.88 (dd, *J* = 13.1, 5.8 Hz, 1H) 3.08 (dd, *J* = 13.1, 9.0 Hz, 1H) 3.17-3.29 (m, 1H) 3.45 (m, 1H)	2.76 (m, 1 H) 2.90 (m, 1 H) 3.10 (m, 1 H) 3.41 (m, 1H)
	4xH^{α}	4.13 (dd, *J* = 7.3, 5.8 Hz, 1H) 4.22 (dd, *J* = 14.6, 7.7 Hz, 1H) 4.42 (dd, *J* = 15.7, 7.1 Hz, 1H) 4.87 (dd, *J* = 15.8, 7.2 Hz, 1H)	4.11 (bs, 1H) 4.24 (d, *J* = 6.9 Hz, 1H) 4.45 (dd, *J* = 15.5 Hz, 7.3 Hz, 1H) 4.73 (dd, *J* = 15.3 Hz, 7.2 Hz, 1H)	3.79 (t, *J* = 8.9 Hz, 1H) 4.20 (m, 1H) 4.45 (dd, *J* = 16.3, 7.3 Hz, 1H) 5.10 (td, *J* = 8.9, 6.0 Hz, 1H)	3.74 (m, 1H) 4.21 (m, 1H) 4.45 (m, 1H) 5.06 (m, 1H
5.5-9.0 ppm 9H	4xH^{N} 5xH^{ar} [Phe]	6.35 (bs, 1H) 6.65 (d, *J* = 6.8 Hz, 1H) 7.05 (bs, 1H) 7.13-7.29 (m, 5H) 8.10 (bs, 1H)	6.38 (bs, 1H) 6.85 (d, *J* = 8.3 Hz, 1H) 7.05-7.35 (m, 6H) 8.04 (bs, 1H)	6.37 (bs, 1H) 6.74 (d, *J* = 8.6 Hz, 1H) 7.13 (bs, 1H) 7.14-7.33 (m, 5H) 8.08 (d, *J* = 9.1 Hz, 1H)	6.49 (bs, 1H) 6.99 (bs, 1H) 7.09-7.37 (m, 5H) 7.45 (bs, 1H) 7.86 (bs, 1H)

Table V: ^{13}C-NMR assignment of the *N*-TEG and *N*-Me analogs of Sansalvamide A peptide in $CDCl_3$ at 288 K.

		1	1a	1b	2a	2b	3a	3b	4a	4b	5a	5b
0-26 ppm	2xCH_3 [Val]	18.6 19.3	19.0 19.1	19.0 19.1	19.1 20.1	19.1 19.9	18.1 19.4	18.1 19.6	17.8 19.5	17.6 19.5	19.1 19.1	19.1 19.2
	2xCH_3 [Leu^1] 2xCH_3 [Leu^2] 2xCH_3 [Leu^3]	22.0 22.2 22.3 22.4 22.6 22.7	21.9 22.4 22.6 22.7 22.7 23.0	20.6 21.9 22.4 22.7 22.8 22.9	21.1 21.9 22.6 22.8 22.9 23.0	21.0 21.9 22.6 22.6 22.7 23.1	21.4 22.2 22.3 22.4 22.7 22.8	21.3 21.9 22.0 22.5 22.7 22.8	22.2 22.2 22.6 22.6 22.8 22.9	22.2 22.3 22.4 22.5 22.5 22.7	21.1 22.3 22.3 22.7 22.8 22.9	20.9 21.6 22.3 22.5 23.0 23.0
	γ-CH [Leu^1] γ-CH [Leu^2] γ-CH [Leu^3]	24.6 24.9 25.4	24.5 24.8 25.7	24.5 24.9 25.7	24.4 24.7 24.8	24.2 24.6 25.0	24.5 25.2 25.4	24.4 25.2 25.5	24.8 24.8 24.9	24.6 24.8 24.9	24.9 25.0 25.4	25.0 25.1 25.2
26-33 ppm	*N*-CH_3 or *N*-CH_2 [*N*-TEG]		(29.1, 29.2, 29.4, 29.4, 29.5, 29.6) 29.7 31.9	(29.1, 29.2, 29.4, 29.4, 29.6, 29.7) 29.7 (31.9)	(27.3) (29.1, 29.3, 29.4, 29.5, 29.6, 29.6) 29.7 31.9	(27.4) (29.1, 29.3, 29.4, 29.5, 29.6) 29.7 (31.9)	29.7 31.1	(29.1, 29.2, 29.4, 29.5, 29.6, 29.6) 29.7 (30.6) 31.9	(29.1, 29.2, 29.3) 29.4 (29.4, 29.6, 29.7) (31.9)	29.1 (29.2, 29.4, 29.5 29.6, 29.6) 29.7 (31.9)	(29.2, 29.1, 29.4, 29.4) 29.4 (29.6, 29.7) 29.7 (31.9)	29.3
33-45 ppm	β-CH_2 [Phe] β-CH_2 [Leu^1] β-CH_2 [Leu^2] β-CH_2 [Leu^3] β-CH [Val]	37.7 38.6 39.0 39.7	34.2 37.2 39.8 41.6	34.2 37.0 38.2 39.8	34.2 36.8 39.5 40.4 41.3	34.2 36.5 39.3 40.3 40.9	36.9 38.5 39.8 40.9	34.2 36.7 37.7 39.8 40.6	35.2 39.7 39.9 41.5	34.9 39.6 40.0 41.2	38.3 38.6 40.2 40.5	38.0 38.1 39.7 40.4
45-80 ppm	5xC^a	51.7 53.7 55.3 57.9 58.8	48.6 52.6 56.1 59.8 66.4	49.2 55.0 56.0 59.1 65.0	48.3 50.4 53.5 56.6 66.4	48.3 51.5 53.2 57.5 65.1	51.2 53.9 54.4 55.4 67.9	52.1 54.3 54.6 55.3 68.9	48.5 51.0 52.8 60.2 70.8	48.3 51.7 53.0 60.2 72.1	51.3 51.4 53.6 60.7 68.4	51.2 51.5 53.4 61.2 70.0
	CH_3O [*N*-TEG] *N*-CH_2-CH_2O [*N*-TEG] 4xCH_2 [*N*-TEG]		50.5 58.9 68.6 70.2 70.7 71.6		50.9 59.0 68.5 70.3 70.4 71.9		51.9 59.0 69.0 70.3 70.5 70.6 71.9		51.5 59.0 68.4 70.3 71.9		53.6 59.0 60.7 68.8 70.3 70.4 (2C) 71.9	
120-140 ppm	4xC_{ar} [Phe]	127.0 128.6 129.0 136.2	127.4 128.8 129.0 136.0	127.4 129.0 129.0 136.0	127.1 128.8 128.9 135.9	127.1 128.8 128.9 136.0	126.7 128.5 129.1 136.7	126.8 128.5 129.1 136.6	126.9 128.5 129.1 137.3	127.0 128.6 128.8 137.0	126.6 128.3 129.6 136.8	126.6 128.3 129.6 136.9
160-180 ppm	5x(C=O)	171.2 172.0 172.6 173.2 173.4	170.2 172.6 (2C) 173.0 (2C)	173.0 173.2 173.9 174.0 174.3	170.8 171.6 (2C) 173.0 173.7	170.6 171.6 172.2 172.4 174.3	171.5 171.6 171.7 172.0 173.5	171.9 172.1 172.4 172.6 174.3	170.0 171.2 171.8 173.5 173.6	170.1 171.3 172.6 172.8 173.6	171.1 171.4 171.8 172.7 173.5	170.9 171.6 171.9 171.9 173.8

Note: For most compounds, the ^{13}C-NMR signal associated to *N*-CH_3 or *N*-CH_2 appeared as two major signals and a set of several signals of considerably lower intensity. Such minor signals are indicated in parentheses.

ANNEX 3: ^{1}H AND ^{13}C-NMR ASSIGNMENT OF cyclo[RGDf*N*MeV] AND ITS *N*-(4-AZIDOBUTYLATED) ANALOG

Table VI: ^{1}H-NMR assignment of cyclo[RGDf*N*MeV] (**23**) and cyclo[RGDf(*N*-$CH_2CH_2CH_2CH_2N_3$)V] (**27**) in H_2O/D_2O 9:1 (pH 6.0) at 288 K.

	cyclo[RGDf*N*MeV] (**23**)	cyclo[RGDf(*N*-$CH_2CH_2CH_2CH_2N_3$)V] (**27**)
N-X [Val]	*N*-CH_3: 2.90 (s, 3H)	*N*-$CH_2CH_2CH_2CH_2N_3$: 1.14 (m, 1H), 1.32 (m, 1H), 1.49 (m, 2H), 3.12 (m, 2H), 3.27 (m, 1H), 3.34 (m, 1H)
γ-CH_3^B [Val]	0.60 (d, *J* = 6.8 Hz, 3H)	0.57 (d, *J* = 6.8 Hz, 3H)
γ-CH_3^A [Val]	0.90 (d, *J* = 6.8 Hz, 3H)	0.89 (d, *J* = 6.8 Hz, 3H)
γ-CH_2 [Arg]	1.56 (m, 1H) 1.60 (m, 1H)	1.55 (m, 1H) 1.60 (m, 1H)
β-CH_2 [Arg]	1.91 (m, 1H) 1.96 (m, 1H)	1.93 (m, 1H) 1.97 (m, 1H)
β-CH [Val]	2.09 (m, 1H)	1.98 (m, 1H)
β-CH_2 [Asp]	2.70 (dd, *J* = 17.4 Hz, *J* = 6.8 Hz, 1H) 2.92 (dd, *J* = 17.4 Hz, *J* = 7.6 Hz, 1H)	2.66 (dd, *J* = 18.5 Hz, *J* = 6.5 Hz, 1H) 2.91 (dd, *J* = 18.5 Hz, *J* = 7.8 Hz, 1H)
β-CH_2 [D-Phe]	2.99 (dd, *J* = 13.5 Hz, *J* = 7.5 Hz, 1H) 3.07 (m, 1H)	2.98 (dd, *J* = 13.8 Hz, *J* = 3.7 Hz, 1H) 3.14 (m, 1H)
δ-CH_2 [Arg]	3.18 (dd, *J* = 13.7 Hz, *J* = 6.9 Hz, 1H) 3.25 (dd, *J* = 13.1 Hz, *J* = 6.5 Hz, 1H)	3.17 (m, 1H) 3.24 (m, 1H)
$H^{\alpha A}$ [Gly]	3.54 (dd, *J* = 15.2 Hz, *J* = 3.5 Hz, 1H)	3.57 (d, *J* = 16.1 Hz, 1H)
H^{α} [Arg]	3.93 (m, 1H)	3.86 (m, 1H)
$H^{\alpha B}$ [Gly]	4.14 (dd, *J* = 15.2 Hz, *J* = 3.5 Hz, 1H)	4.09 (dd, *J* = 16.1 Hz, *J* = 8.1 Hz, 1H)
H^{α} [Val]	4.37 (d, *J* = 11.4 Hz, 1H)	4.37 (d, *J* = 11.7 Hz, 1H)
H^{α} [Asp]	4.57 (m, *J* = 7.5 Hz, 1H)	4.65 (m, *J* = 15.0 Hz, *J* = 6.9 Hz, 1H)
H^{α} [D-Phe]	5.21 (dd, *J* = 17.0 Hz, *J* = 9.6 Hz, 1H)	5.01 (m, 1H)
δ-NH [Arg]	7.28 (m, 1H)	7.28 (m, 1H)
5xH^{ar} [D-Phe]	7.24-7.39 (m, 5H)	7.21-7.40 (m, 5H)
H^{N} [Gly]	8.02 (dd, *J* = 8.2 Hz, *J* = 3.5 Hz, 1H)	7.86 (d, *J* = 7.8 Hz, 1H)
H^{N} [D-Phe]	8.21 (d, *J* = 9.6 Hz, 1H)	8.16 (d, *J* = 9.1 Hz, 1H)
H^{N} [Arg]	8.53 (d, *J* = 7.5 Hz, 1H)	8.60 (d, *J* = 7.3 Hz, 1H)
H^{N} [Asp]	8.68 (d, *J* = 8.3 Hz, 1H)	8.72 (d, *J* = 7.8 Hz, 1H)

Table VII: ^{13}C-NMR assignment of cyclo[RGDf*N*MeV] (**23**) and cyclo[RGDf(*N*-$CH_2CH_2CH_2CH_2N_3$)V] (**27**) in H_2O/D_2O 9:1 (pH 6.0) at 288 K.

	cyclo[RGDf*N*MeV] (**1**)	cyclo[RGDf(*N*-$CH_2CH_2CH_2CH_2N_3$)V] (**2**)
N-X [Val]	*N*-CH_3: 33.4	*N*-$CH_2CH_2CH_2CH_2N_3$: 28.2, 30.4, 46.4, 53.2
γ-CH_3 [Val]	21.0	21.3
γ-CH_3 [Val]	21.2	21.9
γ-CH_2 [Arg]	27.9	27.7
β-CH [Val]	28.0	28.2
β-CH_2 [Arg]	28.6	29.0
β-CH_2 [Asp]	36.8	37.3
β-CH_2 [D-Phe]	40.0	40.8
δ-CH_2 [Arg]	43.4	43.4
C^{α} [Gly]	46.1	45.9
C^{α} [Asp]	52.9	53.2
C^{α} [D-Phe]	53.8	54.6
C^{α} [Arg]	57.6	58.0
C^{α} [Val]	66.9	67.1
4xC^{ar} [D-Phe]	129.7 131.5 132.0 139.3	130.0 131.7 132.1 139.1
H_2N-C(=NH)NH [Arg]	159.6, 165.7	159.6, 165.9
5x(-CONH-)	173.3 173.6 174.6 (x2C) 175.8	173.2 173.7 174.6 175.6 176.2
COOH [Asp]	177.6	178.5

ANNEX 4: CELL ADHESION INHIBITION CURVES OF cyclo[RGDf*N*MeV] AND ITS *N*-SUBSTITUTED ANALOGS

Figure I. Cell adhesion inhibition curves for cyclo[RGDf*N*MeV] (**23**) and its *N*-OEG analogs (**24-26**) in HUVEC and DAOY cells at 3 hours of incubation. **A)** Using vitronectin (VN) as ligand. **B)** Using fibrinogen (FB) as ligand.

A)

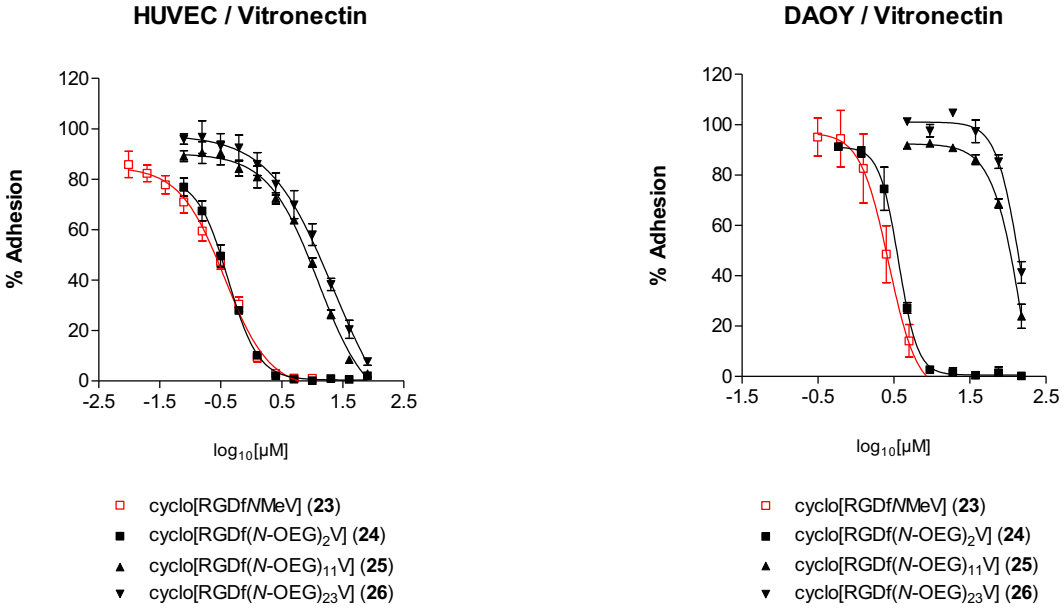

B)

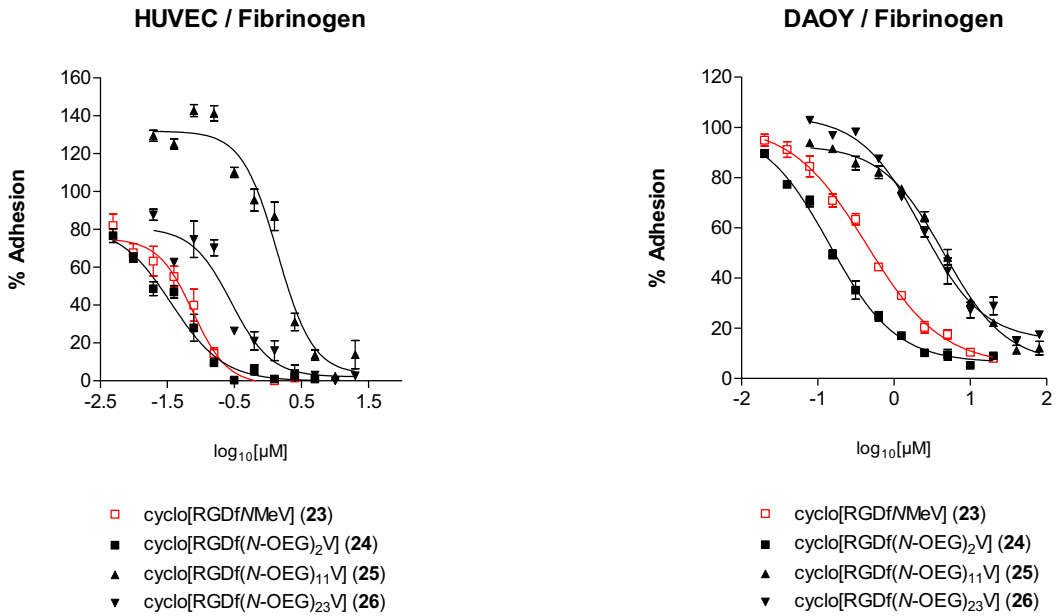

Figure II. Cell adhesion inhibition curves for cyclo[RGDf*N*MeV] (**23**) and its *N*-OEG analog **24** in HT-29 cells at 3 hours of incubation using vitronectin (VN) as ligand.

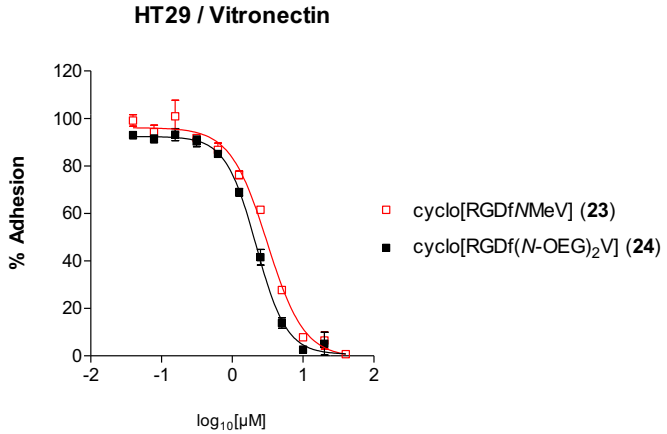

Figure III. Cell adhesion inhibition curves for cyclo[RGDf*N*MeV] (**23**) and the PEG conjugates **29-31** in HUVEC and DAOY cells at 3 hours of incubation. **A)** Using vitronectin (VN) as ligand. **B)** Using fibrinogen (FB) as ligand.

A)

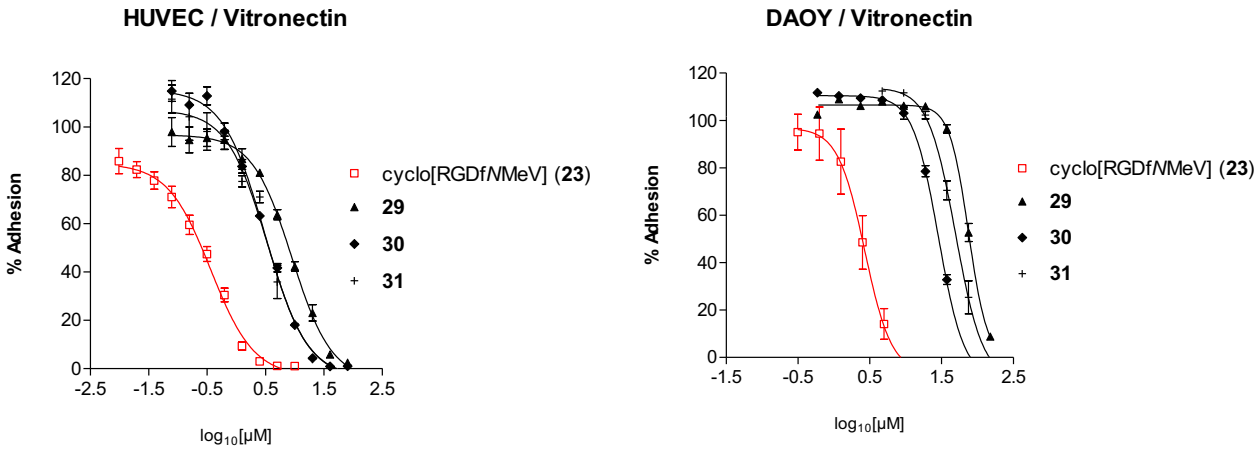

B)

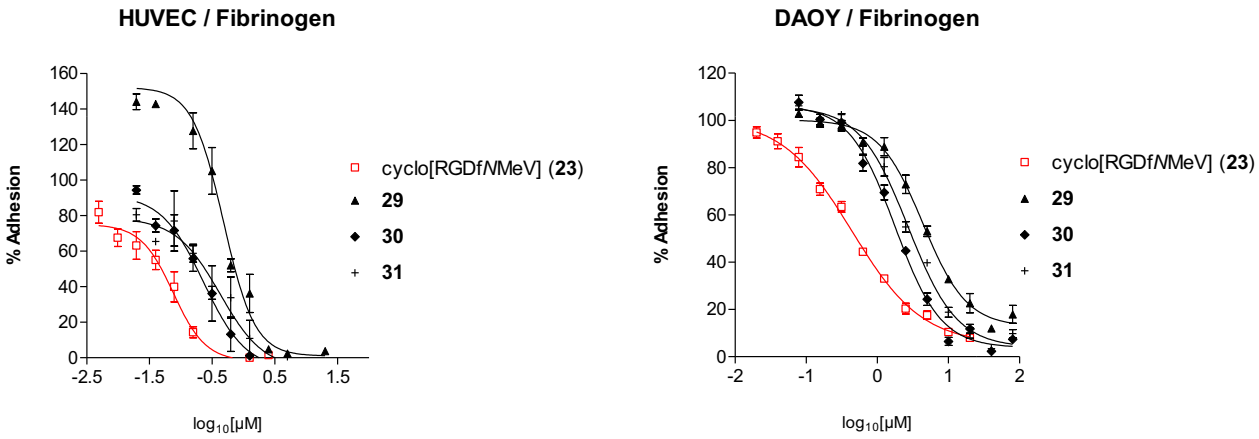

ANNEX 5: PUBLICATIONS

List of publications

Publication I: J. Spengler, A. I. Fernández-Llamazares, J. Ruiz-Rodríguez, K. Burger and F. Albericio. Total regioselective control of tartaric acid. *J. Org. Chem.* **2010**, *75*, 5746-5749. **DOI:** 10.1021/jo101001s. 247

Publication II: J. Spengler, A. I. Fernández-Llamazares and F. Albericio. Use of an internal reference for the quantitative HPLC-UV analysis of solid-phase reactions: a case study of 2-chlorotrityl chloride resin. *ACS Comb. Sci.* **2013**, *15*, 229-234. **DOI:** 10.1021/co4000024. 251

Publication III: A. I. Fernández-Llamazares, J. García, V. Soto-Cerrado, R. Pérez-Tomás, J. Spengler and F. Albericio. *N*-triethylene glycol (*N*-TEG) as a surrogate for the *N*-methyl group: application to Sansalvamide A peptide analogs. *Chem. Commun.* **2013**, *49*, 6430-6432. **DOI:** 10.1039/C3CC41788C. 257

Publication IV: A. I. Fernández-Llamazares, J. García, J. Adan, D. Meunier, F. Mitjans, J. Spengler and F. Albericio. The backbone *N*-(4-azidobutyl) linker for the preparation of peptide chimera. *Org. Lett.* **2013**, *15*, 4572-4575. **DOI:** 10.1021/ol402150m. 261

Paper V: A. I. Fernández-Llamazares, J. Adan, F. Mitjans, J. Spengler and F. Albericio. Tackling lipophilicity of peptide drugs: replacement of the backbone *N*-methyl group of Cilengitide by *N*-oligoethylene glycol (*N*-OEG) chains. Under revision at *Bioconj. Chem*. 265

Paper VI: A. I. Fernández-Llamazares, J. Spengler and F. Albericio. The potential of *N*-alkoxymethyl groups as peptide backbone protectants. Submitted to *Tetrahedron Lett*. 273

Justification of contributions

To date, I am first author and co-author of six research papers, of which four are already published (**publications I, II, III and IV**) and two under revision (**papers V and VI**).

Many of the results described in this Thesis manuscript are published or submitted for publication.

- The results described in Chapters 1 and 2 are published in *Chem. Commun.* **2013**, *49*, 6430-6432. As first author of this publication, I performed the synthetic part and wrote the whole manuscript. The NMR study was performed together with Dr. Jesús García. I also performed the cytotoxicity assays. These assays were carried out at the Cancer Cell Biology Research Group of the UB Faculty of Medicine (Bellvitge campus), under the supervision of Prof. Ricardo Pérez and Dr. Vanessa Soto-Cerrato. [**Publication III**]

- The results described Chapter 3 are under revision at *Bioconj. Chem*. As first author of this paper, I performed the synthetic part and wrote the whole manuscript. We are thankful to Dr. Jaume Adan for performing the cell adhesion inhibition assays. [**Paper V**]

- The results described in Chapter 4 are published in *Org. Lett.* **2013**, *15*, 4572-4575. As first author of this publication, I performed the synthetic part and wrote the whole manuscript. The first studies on the *N*-(4-azidobutyl) linker stemmed from a 3-month research project of David Meunier, a visiting student from ENS Paris.

The NMR study was performed together with Dr. Jesús García. We are thankful to Dr. Jaume Adan for performing the cell adhesion inhibition assays. [**Publication IV**]

During the course of my PhD, I also dedicated considerable time to other projects which are not explained in this Thesis manuscript.

- The paper submitted to *Tetrahedron Lett.* is the outcome of my initial PhD project. This initial project was abandoned because the results were not promising to be further extended. Although this work required significant effort, the results obtained are not described in this Thesis manuscript in order to avoid a fragmentary character (*i.e.* including an extra introduction for the topic). [**Paper VII**]

- The use of an internal reference, as described in *ACS Comb. Sci.* **2013**, *15*, 229-234, would have been very useful for the monitorisation of the difficult coupling steps faced throughthout my PhD, but this method had not yet been established. When we sought to identify conditions for the efficient acylation of *N*-TEG amines (Chapter 1), we realized there was a lack of reliable methods to estimate the conversion of solid-phase reactions. The difficulties we found inspired this pioneer research, to which I contributed perfoming several test experiments. These preliminary experiments are not described in this Thesis manuscript, as this would require a more extensive explication that, in turn, would spoil the presentation of the results related to my main PhD project. [**Publication II**]

- The paper published in *J. Org. Chem.* **2010**, *75*, 5746-5749 describes a synthetic strategy for differentiating the four functionalities of tartaric acid. To this work, I contributed by preparing several compounds. I also contributed with the identification of selective *O*-acetyl deprotection conditions that do not cause β-elimination, which was an issue for obtainig certain target compounds. These results are not described in this Thesis manuscript, as they are not related to the peptide chemistry field. [**Publication I**]

Publication I: J. Spengler, A. I. Fernández-Llamazares, J. Ruiz-Rodríguez, K. Burger and F. Albericio. Total regioselective control of tartaric acid. *J. Org. Chem.* **2010**, *75*, 5746-5749. **DOI:** 10.1021/jo101001s.

JOC*Note*

pubs.acs.org/joc

Total Regioselective Control of Tartaric Acid

Jan Spengler,*[,†,‡] Ana I. Fernández-Llamazares,[†,‡] Javier Ruiz-Rodríguez,[†,‡] Klaus Burger,[§] and Fernando Albericio*[,†,‡,⊥]

[†]*Institute for Research in Biomedicine, Barcelona Science Park, Baldiri Reixac 10, 08028-Barcelona, Spain,* [‡]*CIBER-BBN, Networking Centre on Bioengineering, Biomaterials and Nanomedicine, Barcelona Science Park, Baldiri Reixac 10, 08028-Barcelona, Spain,* [§]*Institut für Organische Chemie, Universität Leipzig, Johannisallee 29, D-04103 Leipzig, Germany, and* [⊥]*Department of Organic Chemistry, University of Barcelona, Martí i Franqués 1-11, 08028-Barcelona, Spain*

jan.spengler@irbbarcelona.org; fernando.albericio@irbbarcelona.org

Received May 27, 2010

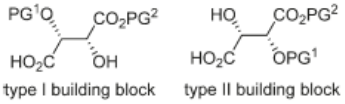

PG[1]: Bzl, *p*-nitrobenzyl, *p*-methoxybenzyl
PG[2]: Me, allyl, *tert*-butyl

An efficient strategy to synthesize tartaric acid building blocks for totally regioselective transformations or derivatizations was disclosed. Starting from L-tartaric acid or L-dimethyl tartrate, respectively, we obtained type I and II building blocks with orthogonal sets of protecing groups (4−8 steps, 38−56% overall yield).

Although tartaric acid is a structurally simple molecule, it is a key chiral pool compound in organic chemistry. It is a very useful starting material for the total synthesis of natural and non-natural products, and it also serves as a core for chirality-inducing ligands.[1] The use of tartaric acid as a chiral building block often requires the appropriate differentiation between the functional groups present in its structure. The distinction between the two pairs of hydroxy and carboxy groups is easy to accomplish. These functionalities can be efficiently monoderivatized by several methods.[2]

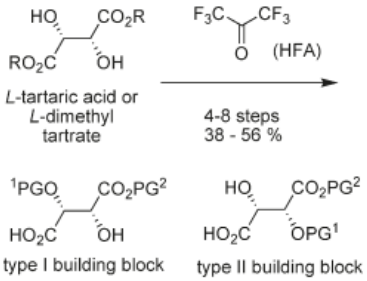

FIGURE 1. Totally regioselective controlled tartaric acid building blocks I and II.

However, what still remains a challenge is the independent modification of the carboxy and the hydroxy group in a regioselective manner, which is crucial for the synthesis of certain products. The strategies reported to date require extensive preparative work, considerable study of reaction conditions, structural assignments, and sometimes cumbersome or impossible separations between regioisomers. For example, the totally regioselective synthesis of tartaric acid derivatives bearing four distinct substituents on the hydroxy and carboxy function requires 12 steps starting from 2-hydroxy-2-(4-[1,3]dioxolanyl)acetate, a building block that is accessible from ascorbic acid in three steps.[3] Apparently, more straightforward is the monosaponification of monoethers of dialkyl tartrates with potassium carbonate or,[4a] alternatively, with pig liver esterase, which has the advantage of providing higher regioselectivity.[4b,c] However, in both cases, the separation of the desired product from the undesired regioisomers and the totally saponified compounds may be difficult to achieve. A few examples of total differentiation have been achieved during the course of multistep syntheses.[5]

While working on the synthesis of anticancer depsipeptides containing tartaric acid as the core unit, we found it highly desirable to develop a general and flexible synthetic route to tartaric acid building blocks of type I and II, in which all four functionalities are differentiated by orthogonal protecting groups. Here we disclose an efficient strategy to synthesize such tartaric acid derivatives on a multigram scale (4−8 steps starting from L-tartaric acid or L-dimethyl tartrate, respectively, with overall yields between 38 and 56%; Figure 1).

Hexafluoroacetone (HFA) is a bidentate protecting/activating reagent with several applications in the chemistry

(1) Comprehensive reviews of applications in organic synthesis: (a) Coppola, G. M.; Schuster, H. F. *Chiral α-Hydroxy Acids in Enantioselective Synthesis*; Wiley-VCH: Weinheim, Germany, 1997. (b) Gawronski, J.; Gawronska, K. *Tartaric and Malic Acids in Synthesis: A Source Book of Building Blocks, Ligands, Auxiliaries, and Resolving Agents*; John Wiley: New York, 1999. Source for chiral auxiliaries: (c) Seebach, D.; Beck, A. K.; Heckel, A. *Angew. Chem.* **2001**, *113*, 96; *Angew. Chem., Int. Ed.* **2001**, *40*, 92. (d) Dieguez, M.; Pamies, O.; Claver, C. *Chem. Rev.* **2004**, *104*, 3189.

(2) Some representative routes not discussed in ref 1: (a) Gonzalez, S. V.; Carlsen, P. *Eur. J. Org. Chem.* **2007**, *21*, 3495. (b) McNulty, J.; Mao, J. *Tetrahedron Lett.* **2002**, *43*, 3857.

(3) (a) Usui, H.; Kagechika, K.; Nagashima, H. European Patent Application EP0949238, 1999. (b) Wei, C. C.; De Bernardo, S.; Tengi, J. P.; Borgese, J.; Weigele, M. *J. Org. Chem.* **1985**, *50*, 3462.

(4) (a) Barton, D. H. R.; Cleophax, J.; Gateau-Olesker, A.; Gero, S. D.; Tachdjian, C. *Tetrahedron* **1993**, *49*, 8381. (b) Gateau-Olesker, A.; Cleophax, J.; Gero, S. D. *Tetrahedron Lett.* **1986**, *27*, 41. (c) Siddiqui, M. A.; Mansoor, U. F.; Reddy, P. A.; Madison, V. S. US Patent Application 2007/0167426, 2007.

(5) (a) Tartaric acid monohydroxamates can be regioselectively O-monosilylated to give the α- or β-hydroxyhydroxamates, depending on the reaction conditions: Kolasa, T.; Miller, M. J. *Tetrahedron* **1989**, *45*, 3071. (b) O-Monobenzylated *tert*-butyl tartrate can be regioselectively reduced with $LiBH_4$ to a 1,3-diol: Nakamura, S.; Hirata, Y.; Kurosaki, T.; Anada, M.; Kataoka, O.; Kitagaki, S.; Hashimoto, S. *Angew. Chem.* **2003**, *115*, 5509; *Angew. Chem., Int. Ed.* **2003**, *42*, 5351.

Published on Web 07/26/2010 DOI: 10.1021/jo101001s

SCHEME 1. Reaction of Tartaric Acid with Hexafluoroacetone (HFA)[a]

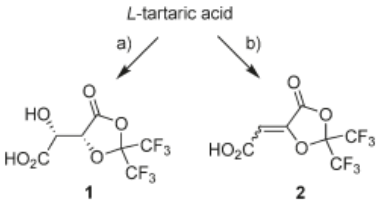

[a]Conditions: (a) ≤3 equiv of HFA, DMSO, 4 days, 64%; (b) ≥4 equiv of HFA, DMSO, 15 h, 64%.

of α-hydroxy acids.[6] HFA reacts with α-hydroxy acids to give five-membered lactones (2,2-bistrifluoromethyl-1,3-dioxolan-4-ones). This reaction also proceeds regioselectively when more carboxy groups are present in the molecule (e.g., in malic acid). In a previous report, structure **1** was proposed as the reaction product of tartaric acid and HFA.[7] To the best of our knowledge, this is the only chemical reaction in which a total differentiation of all four functional groups of tartaric acid can be achieved in one step. Therefore, we considered the dioxolane **1** an ideal key intermediate for the concise preparation of type I and II building blocks (Scheme 1).

First, we had to make a considerable effort to obtain **1** in a reproducible way. We found that the product is contaminated with the inseparable β-elimination product **2** in variable amounts. A more detailed examination of the reaction conditions revealed that both the amount of HFA and the reaction time are crucial factors. The best results were obtained when no more than 3 equiv of gaseous HFA was absorbed by a stirred solution of tartaric acid in DMSO. In the reaction mixture, **1**, unreacted tartaric acid and one major intermediate were detected by ^{1}H and ^{19}F NMR spectroscopy (see Experimental Section). When the reaction mixture was allowed to react in a sealed flask for 4 days, the intermediate disappeared to give **1**, which was isolated by extraction in up to 64% yield (depending on the amount HFA added). However, when more than 4 equiv of HFA was added, only **2** was formed.[8]

Next, we envisaged the introduction of conventional protecting groups into **1** in order to obtain building blocks of type I and II. Nucleophilic ring opening of the dioxolane proceeds with concomitant deprotection of the adjacent hydroxy group.[6] Therefore, to maintain the differentiation of the two hydroxy groups, the free hydroxy group in **1** requires protection before nucleophilic ring opening of the dioxolane. Initially, acetyl was chosen as the OH protecting group because the acetylation of **1** was found to proceed smoothly. The resulting lactone **3** was reacted with methanol to give the methyl ester **4** in excellent yield. The structure of **4**, a type I building block, was confirmed by X-ray spectroscopy (see Supporting Information).[9]

The type II building block **6** was prepared by esterification of the free carboxy group of **3** and subsequent hydrolysis of

SCHEME 2. Synthesis of *O*-Acetyl/Methyl-Ester-Protected Building Blocks 4 and 6[a]

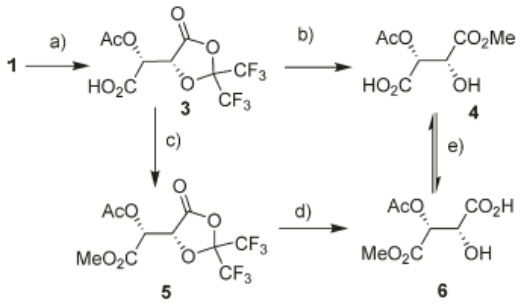

[a]Conditions: (a) AcCl, 15 h, 84%; (b) MeOH/DCM, 15 h, 90%; (c) CH_2N_2 in Et_2O, 15 min, 88%; (d) H_2O/2-PrOH, 15 h, 79%; (e) in aq $NaHCO_3$ at rt, the equilibrium of 2:1 (**4**/**6**) is reached after 3 days.

the lactone **5**. However, **4** and **6** were found to slowly interconvert in aq $NaHCO_3$ solution (^{1}H NMR spectroscopy). Such base-promoted acyl migration[10] is well-known in carbohydrate chemistry and limits the utility of **4** and **6** as totally differentiated tartaric acid building blocks (Scheme 2).

Consequently, the choice of an OH protecting group that does not migrate is mandatory. Silyl ether migration has been reported for tartaric acid derivatives.[5a] Benzyl ethers are not prone to migration and can be cleaved with a broad range of conditions orthogonally to those for the deprotection of methyl esters.[11] Given that the dioxolane **1** decomposes in the presence of bases, the benzylation of **1** was found not to be feasible, and consequently, we changed the strategy. Thus, the monobenzyl (Bzl), *p*-nitrobenzyl (Pnb), and *p*-methoxybenzyl (Mob) ethers of dimethyltartrate (**7a**−**c**) were prepared via a stannylene acetal following efficient protocols cited in the literature.[12] After saponification of **7a**−**c** to the free acids (**8a**−**c**), the differentiation between the carboxylic groups was achieved by reaction with HFA (**8a**−**c** to **9a**−**c**). These reactions required less time than that required for the synthesis of **1** (typically overnight), and no β-elimination was observed.[13] Methanolysis of **9a**−**c** (same conditions as for **3** to **4**) enabled us to obtain the first set of type I building blocks **10a**−**c** with variable O-protection. The set of type II building blocks **12a**−**c** was prepared via the methyl esters **11a**−**c** (Scheme 3).

To introduce further dimensions of orthogonality, building blocks with allyl and *tert*-butyl-ester-protected carboxyl groups were prepared by modified protocols. The allyl ester **13** was obtained by nucleophilic ring opening of the dioxolane **9c** with allyl alcohol. In contrast to the methanolysis, this reaction required heating. To synthesize the regioisomer **15**, the carboxy group of **9c** was activated as acid chloride,

(6) Spengler, J.; Boettcher, C.; Albericio, F.; Burger, K. *Chem. Rev.* **2006**, *106*, 4728.
(7) Weygand, F.; Burger, K. *Chem. Ber.* **1966**, *99*, 2880.
(8) Compound **2** is under current investigation as building block for α-oxo acids.
(9) A sample of *rac*-**4**, prepared from racemic tartaric acid, could be crystallyzed from $CHCl_3$. Crystal data: see Supporting Information.
(10) Roslund, M. U.; Aitio, O.; Warna, J.; Maaheimo, H.; Murzin, D. Y.; Leino, R. *J. Am. Chem. Soc.* **2008**, *130*, 8769. Encouraged by the reported observation that pivaloyl migration takes places considerably more slowly than acetyl migration, we also prepared the pivaloyl analogues. However, migration in aqueous $NaHCO_3$ was also observed in this case.
(11) Greene, T. W.; Wuts, P. G. M. *Protective Groups in Organic Synthesis*, 3rd ed.; John Wiley: New York, 1999.
(12) (a) Nagashima, N.; Ohno, M. *Chem. Lett.* **1987**, 141. (b) Nagashima, N.; Ohno, M. *Chem. Pharm. Bull.* **1991**, *39*, 1972. (c) The protocol used here was adapted from ref 5b.
(13) The formation of six-membered rings, which could give undesired regioisomers, was not observed, and it is known that their formation requires special conditions: Spengler, J.; Ruiz-Rodriguez, J.; Yraola, F.; Royo, M.; Winter, M.; Burger, K.; Albericio, F. *J. Org. Chem.* **2008**, *73*, 2311.

SCHEME 3. Synthesis of *O*-Benzyl/Methyl-Ester-Protected Building Blocks 10a−c and 12a−c (7−12a, R = Bzl; 7−12b, R = Pnb; 7−12c, R = Mob)[a]

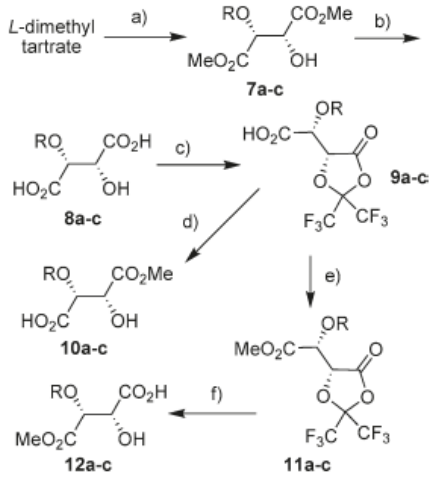

[a]Conditions: (a) $SnOBu_2$, toluene, reflux, 2 h, then CsF, benzylbromide, DMF, 10 h, 80−96%; (b) LiOH, H_2O/dioxane, 1 h, 77−89%; (c) HFA, DMSO, 15 h, 83−98%; (d) MeOH/DCM, 15 h, 81−98%; (e) CH_2N_2 in Et_2O, 15 min, 81−95%; (f) H_2O/2-PrOH, 15 h, 83−100%.

SCHEME 4. Synthesis of *O*-Benzyl/Allyl-Ester-Protected Building Blocks 13 and 15[a]

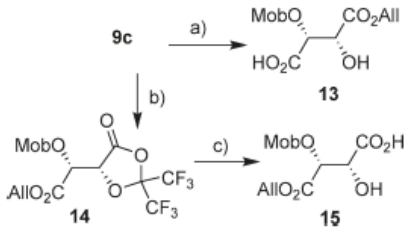

[a]Conditions: (a) allyl−OH/DCM, rt → reflux, 15 h, 93%; (b) $(COCl)_2$, 15 min, then allyl−OH/Et_2O, 4 h, 95%; (c) H_2O/2-PrOH, 15 h, 97%.

which quickly reacted with allyl alcohol at room temperature, affording the ester **14**. Finally, **15** was obtained by hydrolysis of **14** (Scheme 4).

The *tert*-butyl esters **18** and **21** were more difficult to obtain. All of our initial attempts at esterification and nucleophilic ring opening of the dioxolanes **9a−c** with *tert*-butyl alcohol failed. Thus, the methyl esters **10a** and **12a** were, respectively, chosen as an alternative starting point. After acetylating the hydroxy group in both **10a** and **12a**, treatment of the resulting **16** and **19** with *tert*-butyl bromide under phase transfer conditions allowed us to form the *tert*-butyl esters **17** and **20**. The methyl ester and the acetate were then hydrolyzed in one step to give **18** and **21**, respectively. We found that lithium hydroxide in aqueous dioxane promotes the hydrolysis of **17**, yielding **18** exclusively; however, in the case of **20**, considerable amounts of the β-elimination product were formed under the same conditions. We assume that the neighboring CH proton in **17** is protected toward base-mediated abstraction as a result of the steric demand of the adjacent *tert*-butyl group, which hinders elimination. In contrast, acetate hydrolysis becomes more difficult in **20** and, for the same reason, elimination takes place. Elimination was completely

SCHEME 5. Synthesis of *O*-Benzyl/*tert*-Butyl-Ester-Protected Building Blocks 18 and 21[a]

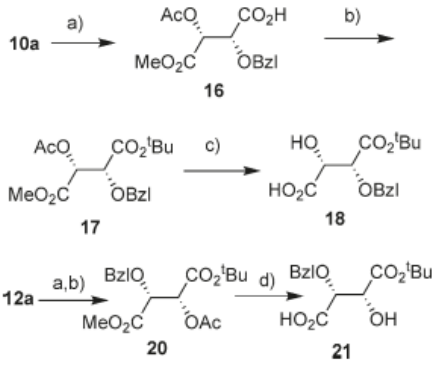

[a]Conditions: (a) AcCl, cat. DMAP, 2 h, 94−96%; (b) ^{t}BuBr, TBACl/DMA, K_2CO_3, 55 °C, 24 h, 80−87%; (c) LiOH, H_2O/dioxane, 2 h, 94%; (d) LiOOH, H_2O/dioxane, 0 °C → rt, 17 h, 97%.

suppressed by using the less basic lithium hydroperoxide instead (Scheme 5).[14]

All of these transformations were robust and proceeded with good overall yields, thus making type I and II building blocks valuable as starting materials for synthesis. These tartaric acid derivatives may contribute to significantly speed up the syntheses of products in which all four functional groups of tartaric acid have to be differentiated. Moreover, the use of these building blocks in some established synthetic routes should now make it possible to obtain products with additional points for structural modification.

Experimental Section

General Procedure A: Reaction of Tartaric Acid and Derivatives with Hexafluoroacetone. ***Caution:*** *Hexafluoroacetone is a toxic gas. All operations must be performed in a well-ventilated fume hood with proper protection of skin and eyes.* A solution of L-tartaric acid or derivative (15−70 mmol, as indicated) in DMSO was stirred in a 250 mL flask equipped with a dry ice condenser and bubbler. The atmosphere in the apparatus was replaced with typically 3 equiv (if not otherwise specified) of hexafluoroacetone gas and stirred for 15 h (if not otherwise indicated). Then, a cold saturated solution of NaCl in water (50−120 mL, prepared by mixing of crushed ice and NaCl) was added to the solution, and it was stirred for 5 min. It was extracted with diethyl ether (3 × 50 mL), and the pooled organic layer was washed with brine and dried over $MgSO_4$. After filtration and evaporation of most of the solvent, it was heated under vacuum (membrane pump) to 50 °C for approximately 30 min in order to remove remaining volatiles from the product.

(2*R*)-(Hydroxy)-{(4*R*)-5-oxo-2,2-bistrifluoromethyl-[1,3]dioxolan-4-yl}acetic acid (1). Compound **1** was prepared following the general procedure A from L-tartaric acid (10.7 g, 71.3 mmol) in DMSO (40 mL) and hexafluoroacetone (3 equiv, 35 g, 210 mmol; added in 5 h). The formation of an intermediate product, which slowly converts into the product, was observed in the reaction mixture. NMR spectra of the reaction mixture after 48 h: ^{1}H NMR (acetone-d_6) δ = 2.59 (s, DMSO, major signal), 4.48 (s, 4.8H, tartaric acid), 4.59 (d, J = 3.0 Hz, 1H, intermediate), 4.71 (d, J = 1.7 Hz, 1.5H, **1**), 4.98 (d, J = 3.0 Hz, 1H, intermediate), 5.53 (m, 1.5H, **1**) ppm; ^{19}F NMR (acetone-d_6) δ = −83.0 (s, 16F, signal HFA*H_2O), −82.31 (q, J = 8.3 Hz,

(14) Evans, D. A.; Britton, T. C.; Ellman, J. A. *Tetrahedron Lett.* **1987**, *28*, 6141.

1.6F, **1**), −80.92 (q, J = 8.77 Hz, 1F, intermediate), −80.48 (m, 2.6F, intermediate and **1**) ppm. It was stirred until the intermediate product has converted into product (~4 days). After addition of the NaCl solution, the product was extracted with diethyl ether (4 × 100 mL) and washed with brine (4 × 50 mL) to give 13.6 g (64%) of **1** as white crystalline mass: mp 162−163 °C (recrystallized from $CHCl_3$); ^{1}H NMR (acetone-d_6) δ = 4.82 (d, J = 1.7 Hz, 1H), 5.58 (m, 1H) ppm; ^{13}C NMR (acetone-d_6) δ = 70.7, 79.3, 99.2 (m), 120.8 (q, J = 286 Hz), 121.9 (q, J = 288 Hz), 167.1, 171.7 ppm; ^{19}F NMR (acetone-d_6) δ = −82.31 (q, J = 8.3 Hz, 3F), −80.56 (q, J = 8.3 Hz, 3F) ppm; IR (KBr) ν = 1866, 1841, 1760, 1752, 981 cm^{-1}; $[\alpha]^{20}_D$ +51.5 (c 2.0, acetone); HRMS (ES$^-$) calcd for $[C_7H_4F_6O_6 - H]^-$ 296.9834, found 296.9830.

(5-Oxo-2,2-bistrifluoromethyl[1,3]dioxolan-4-ylidene)acetic acid (2). Compound **2** was prepared following the general procedure A from L-tartaric acid (4.9 g, 32.6 mmol) in DMSO (20 mL) and hexafluoroacetone (4.3 equiv, 23 g, 140 mmol; added in 1 h). A slight exothermic reaction was observed. It was stirred for 15 h. After addition of the NaCl solution, precipitated product was filtered off and dried in air to give 5.89 g (64%) of crystalline **2**: mp 125 °C; ^{1}H NMR (acetone-d_6) δ = 6.34 (s) ppm; ^{13}C NMR (acetone-d_6) δ = 99.4 (m), 107.0, 120.5 (q, J = 288 Hz), 142.2, 159.1, 163.7 ppm; ^{19}F NMR (acetone-d_6) δ = −81.92 (s) ppm; IR (KBr) ν = 1847, 1726, 1688, 1443, 990 cm^{-1}; HRMS (ES$^-$) calcd for $[C_7H_2F_6O_5 - H]^-$ 278.9728, found 278.9731.

(2*R*)-Benzyloxy-{(4*R*)-5-oxo-2,2-bistrifluoromethyl[1,3]dioxolan-4-yl}acetic acid (9a). Following the general procedure A with **8a** (1.61 g, 6.72 mmol) in DMSO (20 mL) and hexafluoroacetone (added in 1.5 h), **9a** (2.19 g, 83%) was obtained as viscous oil: ^{1}H NMR ($CDCl_3$) δ = 4.44 (d, J = 2.1 Hz, 1H), 4.61 (d, J = 11.2 Hz, 1H), 4.87 (d, J = 11.2 Hz, 1H), 5.13 (d, J = 1.9 Hz, 1H), 7.35 (m, 5H) ppm; ^{13}C NMR ($CDCl_3$) δ = 74.4, 74.5, 76.4, 97.9 (m), 118.4 (q, J = 287 Hz), 119.7 (q, J = 289 Hz), 128.3, 128.5, 128.5, 135.3, 164.9, 171.9 ppm; ^{19}F NMR ($CDCl_3$) δ = −81.4 (q, J = 8.1 Hz), −79.8 (q, J = 8.0 Hz) ppm; IR (film) ν = 1849, 1737, 1319, 1241, 1132, 983 cm^{-1}; $[\alpha]^{20}_D$ +68.6 (c 2.5, $CHCl_3$); HRMS (ES$^-$) calcd for $[C_{14}H_{10}F_6O_6 - H]^-$ 387.0303, found 387.0296.

(2*R*)-(4-Nitrobenzyloxy)-{(4*R*)-5-oxo-2,2-bistrifluoromethyl-[1,3]dioxolan-4-yl}acetic acid (9b). Following the general procedure A with **8b** (4.07 g, 14.26 mmol) in DMSO (25 mL) and hexafluoroacetone (added in 1.5 h), **9b** (6.0 g, 98%) was obtained as dense oil: ^{1}H NMR ($CDCl_3$) δ = 4.52 (d, J = 2.0 Hz, 1H), 4.67 (d, J = 11.9 Hz, 1H), 5.01 (d, J = 11.9 Hz, 1H), 5.21 (d, J = 1.7 Hz, 1H), 7.48 (d, J = 8.6 Hz, 2H), 8.22 (d, J = 8.7 Hz, 2H) ppm; ^{13}C NMR ($CDCl_3$) δ = 73.1, 75.4, 76.3, 97.9 (m), 116.1 (m), 121.9 (m), 123.7, 128.2, 143.0, 147.8, 164.8, 171.5 ppm; ^{19}F NMR ($CDCl_3$) δ = −81.3 (q, J = 7.9 Hz), −79.8 (q, J = 8.0 Hz) ppm; IR (film) ν = 1842, 1738, 1524, 1239, 1131, 983 cm^{-1}; $[\alpha]^{20}_D$ +52.3 (c 2.0, $CHCl_3$); HRMS (ES$^-$) calcd for $[C_{14}H_9F_6NO_8 - H]^-$ 432.0154, found 432.0166.

(2*R*)-(4-Methoxybenzyloxy)-{(4*R*)-5-oxo-2,2-bistrifluoromethyl-[1,3]dioxolan-4-yl}acetic acid (9c). The general procedure A was followed with **8c** (6.93 g, 25.65 mmol) in DMSO (60 mL) and hexafluoroacetone (added in 2 h). After addition of the NaCl solution, the product was extracted with DCM (3 × 100 mL) and then the pooled organic layer was washed with brine (2 × 100 mL), dried over $MgSO_4$, filtered, and concentrated under reduced pressure. After evaporation of most of the solvent, the residue was purified by flash chromatography with hexanes/AcOEt/AcOH 2:1:0.1 (R_f = 0.40, UV) to give 10.7 g (98%) **9c** as dense oil: ^{1}H NMR ($CDCl_3$) δ = 3.81 (s, 3H), 4.40 (d, J = 2.1 Hz, 1H), 4.54 (d, J = 11.1 Hz, 1H), 4.80 (d, J = 11.1 Hz, 1H), 5.12 (d, J = 1.9 Hz, 1H), 6.86 (d, J = 8.7 Hz, 2H), 7.22 (d, J = 8.6 Hz, 2H), 9.61 (br s, 1H) ppm; ^{13}C NMR ($CDCl_3$) δ = 55.2, 73.9, 74.0, 76.5, 97.9 (m), 113.9, 118.4 (q, J = 287.0 Hz), 119.7 (q, J = 288.9 Hz), 127.5, 130.1, 159.8, 165.0, 172.7 ppm; ^{19}F NMR ($CDCl_3$) δ = −81.4 (q, J = 8.1 Hz, 3F), −79.8 (q, J = 8.0 Hz, 3F) ppm; IR (film) ν = 2942. 1857, 1740, 1516, 1320, 1242, 1132, 983, 721 cm^{-1}; $[\alpha]^{20}_D$ +22.9 (c 2.0, $CHCl_3$); HRMS (ES$^-$) calcd for $[C_{15}H_{12}F_6O_7 - H]^-$ 417.0409, found 417.0403.

Acknowledgment. This work was partially supported by CICYT (CTQ2009-07758 and CTQ2008-02856/BQU), the Generalitat de Catalunya (2009SGR 1024, 2009SGR-1472) and the IRB. We thank the Barcelona Science Park (Mass Spectrometry Core Facility, Nuclear Magnetic Resonance Laboratory) and the Universitat de Barcelona (Xavier Alcobé, Mercè Font, Unitat de Difracció de Raigs X Serveis Cientificotècnics) for the facilities.

Supporting Information Available: Full experimental details for the preparation of all other compounds, together with copies of ^{1}H and ^{13}C NMR spectra of compounds **1**−**6**, and crystal X-ray data for compound **4** are provided in the Supporting Information. This material is available free of charge via the Internet at http://pubs.acs.org.

Publication II: J. Spengler, A. I. Fernández-Llamazares and F. Albericio. Use of an internal reference for the quantitative HPLC-UV analysis of solid-phase reactions: a case study of 2-chlorotrityl chloride resin. *ACS Comb. Sci.* **2013**, *15*, 229-234. **DOI:** 10.1021/co4000024.

ACS Combinatorial Science

Technology Note

pubs.acs.org/acscombsci

Use of an Internal Reference for the Quantitative HPLC-UV Analysis of Solid-Phase Reactions: A Case Study of 2-Chlorotrityl Chloride Resin

Jan Spengler,*[,†,‡] Anna-Iris Fernandez-Llamazares,[†] and Fernando Albericio*[,†,‡,§,⊥]

[†]Institute for Research in Biomedicine, Barcelona Science Park, Baldiri Reixac 10, 08028-Barcelona, Spain

[‡]CIBER-BBN, Networking Centre on Bioengineering, Biomaterials and Nanomedicine, Barcelona Science Park, Baldiri Reixac 10, 08028-Barcelona, Spain

[§]Department of Organic Chemistry, University of Barcelona, Martí i Franqués 1-11, 08028-Barcelona, Spain

[⊥]School of Chemistry and Physics, University of KwaZuluNatal, 4001 Durban, South Africa

Supporting Information

ABSTRACT: Here we evaluated the use of internal reference compounds for the rapid assessment of reactions performed in solid-phase. An internal reference compound (commercially available) was bound to the resin, together with the substrate, and cleaved with the products after completion of the reaction. The peak area of the reference compound in the HPLC-UV chromatograms can be correlated directly with those of other compounds present in the reaction mixture, thereby allowing a quantitative interpretation of the chromatograms with respect to conversion and yield. The usefulness of this method was demonstrated by optimization of a protocol for the synthesis of proline-based tripeptides.

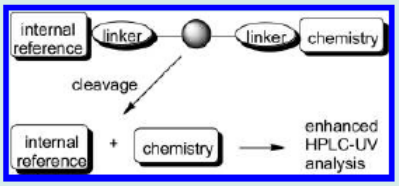

KEYWORDS: *internal standard, reporter compound, analytical construct, Barlos-Resin, DKP-formation*

Solid-phase synthesis is widely used in several fields of chemistry, such as combinatorial sciences, organic, and peptide chemistry.[1,2] However, the optimization of reactions performed on solid-phase requires considerably more effort than when performed in solution. Essential information like the conversion of starting material and product yield cannot normally be obtained directly. NMR, IR, and mass spectroscopy methods applied to compounds on solid supports seldom provide information about quantitative composition.[3] The outcome of organic reactions on solid supports (usually resins of organic polymers) is commonly monitored by HPLC-UV analysis of the products obtained from a cleaved resin sample.

The content of a compound is usually expressed as a percentage of its peak area from the total peak area. However, UV-absorption coefficients can differ from compound to compound. In this case, the relations of the area values of the different peaks do not directly reflect the molar concentrations of the corresponding compounds.[4] This makes it difficult to construe chromatograms from reaction mixtures involving, for example, strongly absorbing protecting groups.

A second limitation of the conventional quantification is that the exact amount of resin the sample was prepared from is not known. Consequently, the peak areas in a chromatogram from a test reaction performed on a resin sample cannot be correlated with the peak areas in a chromatogram obtained from another reaction run on another sample of the same resin.

A theoretically simple solution to these problems might be the cleavage of the samples from resin aliquots and the addition of a fixed amount of (an external) reference compound. However, there is no straightforward way to obtain resin aliquots from reaction mixtures. In the course of a synthesis, the resins are swollen in the solvents and drying until weight constancy causes a significant delay for the evaluation of the outcome of a reaction. Furthermore, the molecular weight of the resin-bonded compounds changes during synthesis, and consequently, so does the resin weight. An alternative solution would be to run the reactions separately on a mini-scale on resin aliquots until an analysis is required. Consequently, all the resin from a reactor has to be cleaved. Prior samples (for intermediate analysis) cannot be taken. Generally, strategies that involve measuring the exact amount of resin subjected to cleavage require much more material than for HPLC-analysis (1−5 mg). Moreover, they are error-prone and imply time-consuming sample preparation for each analysis.

Resins equipped with analytical constructs provide great improvements (Figure 1A). Such a reporter resin can be mixed in a small amount with the resin on which the synthesis is performed. The analytical constructs have two orthogonal cleavage sites. By analytical cleavage, conversion of starting material, yield and identity can be unambiguously determined as a result of the presence of the analytical construct bound to the products, which combine a chromophore that absorbs at a remote wavelength and a mass-sensitizer. For the synthesis, the

Received: August 21, 2012
Revised: February 18, 2013
Published: March 24, 2013

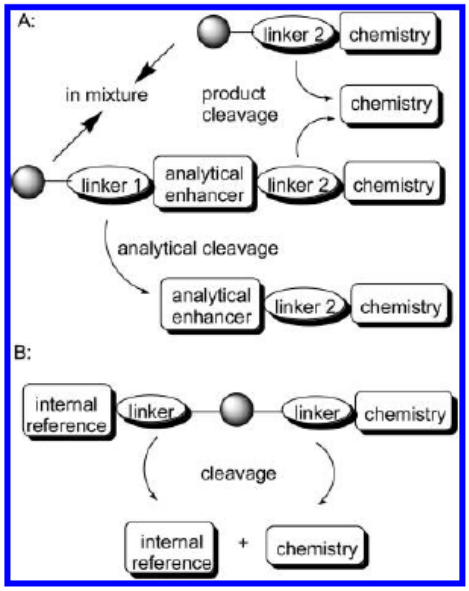

Figure 1. Analytical construct resin with two orthogonal cleavage sites is mixed with the resin used for the synthesis (A). An internal reference can be introduced as "willful contamination", together with the starting material, in the resin-loading step. This resin can be used to optimize the reaction conditions (B).

product can be cleaved without analytical construct. However, such useful tools are not readily available, and so far have been developed for the preparation of carboxamides only.[5,6] It should also be considered that this approach can lead to erroneous results because the outcome of reactions on the reporter-resin with its extra-linker should not be the same as on the resin used for the synthesis.

Here we report a strikingly simple and straightforward method for the quantitative analysis of reactions performed on solid phase (Figure 1B). A reference compound is bound to the resin, together with the starting material, via the same functional group and is cleaved under the same conditions as the products.[7] Commercially available compounds can be used as reference. A suitable reference is chemically inert to the reaction conditions applied. Its HPLC-retention time differs from those of the other compounds and the reference substance can be detected at the same wavelength used for the UV detection of products. This strategy is expected to be applicable to all types of resins and linkers, and the synthetic steps will proceed on the same linker and resin as used for the synthesis. The area of product peaks in HPLC chromatograms can be expressed as multiples of the reference peak area and allows for comparison of chromatograms. Here we describe the use of an internal reference for the straightforward optimization of a protocol for combinatorial synthesis.

■ FOLLOWING A SOLID-PHASE PEPTIDE SYNTHESIS WITH AN INTERNAL REFERENCE

As proof of principle, we synthesized the tripeptide Val-Arg-Phe in the presence of 1-pyreneacetic acid (PAA) as reference compound. PAA is commercially available and can be easily identified because of its characteristic PDA-absorption profile. Its peak retention time was separated from those of the products obtained during the synthesis. As a simple carboxylic acid, PAA was expected to bind to the resin as stably as amino acids and peptides and be cleaved under the same conditions. As solid support, we used 2-chlorotrityl chloride (CTC) resin, a standard support for the synthesis of peptides, pseudopeptides and nonpeptide molecules.[8,9] It was expected that the synthesis of Val-Arg-Phe on this resin would work well under standard conditions.

The solid-phase peptide synthesis (SPPS) started with the loading of CTC resin with Fmoc-Phe containing 10 mol % PAA (Figure 2). A test cleavage from the resulting resin **1** gave

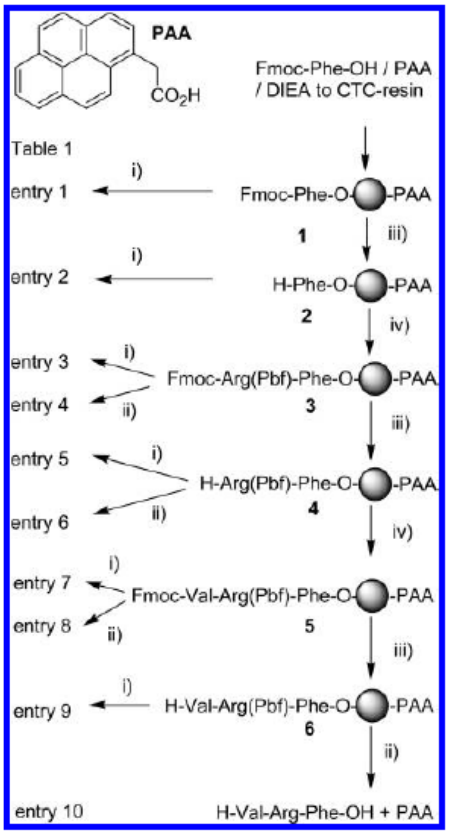

Figure 2. Standard SPPS of the tripeptide Val-Arg-Phe in the presence of PAA as internal reference. The results of intermediate product cleavages are summarized in Table 1. (i) 2% TFA in DCM, 10 min; (ii) TFA/H_2O (95:5), 90 min; (iii) 20% piperidine in DMF, 10 min.; (iv) 4 equiv Fmoc-Xaa, 4 equiv Oxyma, 4 equiv DIPCDI in DMF.

a HPLC-chromatogram with two peaks at 220 nm (a wavelength routinely used for product detection), namely the small PAA peak and the peak of Fmoc-Phe, the latter with a 15-fold area with respect to the former (Table 1, entry 1). We obtained the same result for a repeated test cleavage. The relation between the peak areas remained constant as long as the main peak was not higher than one absorption unit (1 AU). Therefore, we ensured that the main peak did not exceed 1 AU for all the HPLC chromatograms.

The Fmoc-group was removed from resin **1**, and a cleaved sample from the resulting resin **2** showed two peaks, corresponding to Phe and PAA, with nearly equal area values (Table 1, entry 2). The Fmoc-group exerts strong absorbance, and with regard to the reference signal, its impact can now be roughly estimated as a 15-fold increase in the peak area. Throughout this manuscript, we will express the term "*x*-fold multiple of the peak area respectively to the reference peak area" by "area ratio". Thus, an area ratio of 15 implies that the

dx.doi.org/10.1021/co4000024 | ACS Comb. Sci. 2013, 15, 229−234

Table 1. Summary of Product Compositions from Intermediate Cleavages during the Synthesis of Val-Arg-Phe (Figure 3)

		area ratio[b]			
entry[a]	product	Ph, CONH	Ph, CONH, +Fmoc	Ph, CONH, +Pbf	Ph, CONH + Fmoc, +Pbf
1	Fmoc-Phe		15		
2	Phe	1.0			
3	Fmoc-Arg(Pbf)-Phe				46
4	Fmoc-Arg-Phe		14		
5	Arg(Pbf)-Phe			30	
6	Arg-Phe	1.8			
7	Fmoc-Val-Arg(Pbf)-Phe				43
8	Fmoc-Val-Arg-Phe		13		
9	Val-Arg(Pbf)-Phe			30	
10	Val-Arg-Phe	2.2			

[a]See Figure 3. [b]Area ratio means the multiples of the PAA (reference) peak area; for chromatograms see Supporting Information.

peak area of the analyte is 15 times higher than that of the reference compound.

After coupling Fmoc-Arg(Pbf) to **2**, the chromatogram of a sample from the resulting resin **3** shows that the Fmoc-Arg(Pbf)-Phe area ratio was nearly 46 (Table 1, entry 3). This increase resulted from absorption of the Fmoc- and the Pbf-group. The contribution of the former was expected to produce an approximately 15-fold increase in absorption, so we assumed that the additional 30-fold increase was caused by the Pbf-group. To test this notion, resin **3** was treated with 95% TFA. Under these conditions, the Pbf-group was removed to give Fmoc-Arg-Phe with an area ratio of 14 (Table 1, entry 4). The Fmoc-group from **3** was removed to give resin **4**, and the area ratio of Arg(Pbf)-Phe was found to be 30 (Table 1, entry 5). Summing the contributions of the absorbance of the Pbf- and Fmoc-group (30 and 14) gave 44. This value is in good agreement with the 46 found for the dipeptide Fmoc-Arg(Pbf)-Phe (entry 3).

Treatment of resin **4** with 95% TFA yielded the dipeptide Arg-Phe, whose area ratio was 1.8 (Table 1, entry 6). The increase with respect to Phe (entry 2) can be attributed to the additional peptide bond.

Coupling of Fmoc-Val to resin **4** rendered resin **5**. A comparison of the area ratios of Fmoc-Val-Arg(Pbf)-Phe, Fmoc-Val-Arg-Phe, Val-Arg(Pbf)-Phe, and Val-Arg-Phe (entries 7, 8, 9, and 10, respectively) with the those of the products from the previous coupling cycle (Fmoc-Arg(Pbf)-Phe, Fmoc-Arg-Phe, Arg(Pbf)-Phe, and Arg-Phe; entries 3, 4, 5, and 6, respectively) shows that these areas did not increase as expected, but remained constant or even decreased. This finding indicates the loss of some product. In other experiments (vide infra), we found evidence that the activation of amino acids with oxyma/DIPCDI, as used throughout this synthesis, is not optimal for CTC resin.

The synthesis of the tripeptide H-Val-Arg-Phe-OH in the presence of a reference compound (PAA) allowed us to obtain a series of HPLC-UV chromatograms, wherein the products peak areas were quantified as multiples of the peak area of the reference compound. This approach allows for a coherent interpretation of chromatograms during a synthetic sequence that involves strongly absorbing temporary protecting groups.

USE OF AN INTERNAL REFERENCE FOR OPTIMIZING A SOLID-PHASE PROTOCOL FOR COMBINATORIAL SYNTHESIS

Here we demonstrated the use of a reference compound for the optimization of the synthesis of a library of tripeptides type Yaa-Xaa-Pro. The target peptides have Pro at the C-terminus and a rather sterically crowded amino acid (Yaa) at the N-terminus. We aimed to design a straightforward general protocol that works reliably with L- and D-, as well with sterically hindered amino acids in the middle position (Xaa).

Figure 3 shows the envisaged synthesis of three model peptides Fmoc-Aib-Gly-Pro, Fmoc-Aib-D-Leu-Pro, and Fmoc-Aib-Sar-Pro by stepwise SPPS in the presence of a reference compound. Aib represents the sterically crowded amino acid Yaa. The foreseeable critical step in the synthesis is the coupling of Fmoc-Aib to the sequence Xaa-Pro. It is known that dipeptides with C-terminal Pro form diketopiperazines (DKP) and that SPPS of these peptides is often hampered by this unwanted side-reaction, which can cause dramatic reduction in yield.[10] The DKP-prone sequences Gly-Pro and D-Leu-Pro are representative examples for DKP-formation (cyclo-Gly-Pro and cyclo-D-Leu-Pro) under the basic conditions of Fmoc-removal. Furthermore, an appropriate protocol should also give satisfactory results for sterically hindered couplings, which are represented by the coupling of Fmoc-Aib to the sterically hindered *N*-methylamino group on Sar-Pro-resin (Figure 3).

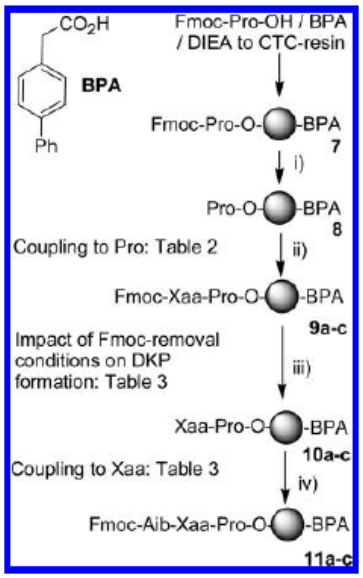

Figure 3. Stepwise SPPS strategy for the synthesis of compounds Fmoc-Aib-Gly-Pro, Fmoc-Aib-D-Leu-Pro, and Fmoc-Aib-Sar-Pro on CTC resin. Intermediate samples for HPLC-UV analysis were cleaved from resins **7**, **9a–c**, and **11a–c** with 2% TFA in DCM for 10 min ((a) Xaa = Gly, (b) Xaa = DLeu, (c) Xaa = Sar). The results (Tables 2 and 3) indicate that the following protocols show the best performance: (i) 2 × 10 min 20% piperidine in DMF, wash with DCM; (ii) 40 min 3 equiv Fmoc-Xaa activated with HBTU/DIEA, wash with DCM; (iii) 5 min 20% piperidine in DMF, wash with DCM; (iv) 40 min 3 equiv Fmoc-Yaa activated with HATU/DIEA, wash with DCM.

dx.doi.org/10.1021/co4000024 | ACS Comb. Sci. 2013, 15, 229–234

We show that an internal reference contributed to obtaining a reliable estimation of the extent of DKP-formation and product yield under a range of coupling conditions, and thus indicates the best protocol for library synthesis.

CTC resin was used as solid support because it prevents DKP formation.[11] Biphenyl acetic acid (BPA) was found to have a peak separable from the product peaks (PAA coelutes with some products). One gram of CTC resin with a maximal capacity of 1.6 mmol/g was loaded with 0.3 mmol BPA and 0.8 mmol Fmoc-Pro. The area ratio between Fmoc-Pro and BPA and was 6.5 in a test cleavage from the test resin 7 (Table 2, entry 1).

Table 2. Coupling Conditions for the Synthesis of Resins 9a−c

entry	protocol applied to 8	area ratio[a] (product)
1		6.5 (Fmoc-Pro from 7)
2	Fmoc-Gly/Oxyma/DIPCDI, 40 min	3.7 (Fmoc-Gly-Pro)
3	Fmoc-Gly/HOAt/DIPCDI, 40 min	3.5 (Fmoc-Gly-Pro)
4	Fmoc-Gly/HBTU/DIEA, 40 min	6.8 (Fmoc-Gly-Pro)
5	Fmoc-Gly/HBTU/DIEA, 40 min	6.8 (Fmoc-Gly-Pro)
6	Fmoc-D-Leu/HBTU/DIEA, 40 min	7.2 (Fmoc-D-Leu-Pro)
7	Fmoc-Sar/HBTU/DIEA, 40 min	6.9 (Fmoc-Sar-Pro)

[a]Area ratios corresponding to BPA.

After removal of the Fmoc-group, a Pro-peak from resin **8** was not observed by HPLC-UV analysis and consequently its conversion to Fmoc-Xaa-Pro could not be followed directly. However, it is reasonable to expect that the area ratio of the subsequent product Fmoc-Gly-Pro from resin **9a** would be similar to that of Fmoc-Pro from **7**. Thus, in this case, the area ratio should be 6.5 or higher due to the additional amide bond. Coupling of Fmoc-Gly activated with oxyma/DIPCDI to resin **8** gave an area ratio of 3.7 (Table 2, entry 2), which did not improve by a repeated coupling. A similar result was obtained for HOAt/DIPCDI activation (area ratio 3.5, Table 2, entry 3). In contrast, by HBTU/DIEA activation, the product was detected with an area ratio of 6.8 (Table 2, entry 4). Since the yield did not increase by longer coupling time or by repeated coupling, we reasoned that the coupling under this condition proceeded quantitatively and that the Oxyma/DIPCDI and HOAt/DIPCDI activation conditions did not work well for coupling to **8**. The first part of the synthesis was then accomplished by coupling Fmoc-Gly, Fmoc-DLeu and Fmoc-Sar activated by HBTA/DIEA to give resins **9a−c**, from which Fmoc-Gly-Pro, Fmoc-D-Leu-Pro, and Fmoc-Sar-Pro were obtained with area ratios higher than the 6.5 (Table 2, entries 5, 6, and 7).

The next step was the removal of the Fmoc-group from the resins **9a−c**. DKP formation can proceed rapidly under these basic conditions (20% piperidine in DMF). It was not possible to obtain area ratios for the products Xaa-Pro from resins **10a−c**, because of the peak shape of the corresponding dipeptides. Fmoc-removal was subsequently followed by coupling of Fmoc-Aib activated by HBTU/DIEA for 40 min over resins **10a−c**. The products Fmoc-Aib-Gly-Pro (from **11a**) and Fmoc-Aib-D-Leu-Pro (from **11b**) were obtained with area ratios lower than the corresponding starting materials and these ratios did not increase with coupling time (Table 3, entries 1 and 2 vs Table 2, entries 5 and 6, respectively). This finding indicates a yield decrease during Fmoc-removal. In contrast, the coupling of Fmoc-Aib over resin **10c** only reached an area ratio of 2.0 after

Table 3. Coupling of Fmoc-Aib over Resins 9a−c

entry	conditions[a,b]	area ratio[c] (product from resin)
1	[a]Fmoc-Aib/HBTU/DIEA, 40 min	6.4 (Fmoc-Aib-Gly-Pro, 11a)
2	[a]Fmoc-Aib/HBTU/DIEA, 40 min	5.9 (Fmoc-Aib-D-Leu-Pro, 11b)
3	[a]Fmoc-Aib/HBTU/DIEA, 40 min	2.0 (Fmoc-Aib-Sar-Pro, 11c)
4	[a]Fmoc-Aib/HBTU/DIEA, 2 h	3.6 (Fmoc-Aib-Sar-Pro, 11c)
5	[a]Fmoc-Aib/HATU/DIEA, 40 min	6.2 (Fmoc-Aib-Gly-Pro, 11a)
6	[a]Fmoc-Aib/HATU/DIEA, 40 min	6.0 (Fmoc-Aib-D-Leu-Pro, 11b)
7	[a]Fmoc-Aib/HATU/DIEA, 40 min	7.4 (Fmoc-Aib-Sar-Pro, 11c)
8	[b]Fmoc-Aib/HATU/DIEA, 40 min	5.3 (Fmoc-Aib-Gly-Pro, 11a)
9	[b]Fmoc-Aib/HATU/DIEA, 40 min	3.1 (Fmoc-Aib-D-Leu-Pro, 11b)
10	[b]Fmoc-Aib/HATU/DIEA, 40 min	7.4 (Fmoc-Aib-Sar-Pro, 11c)

[a]Prior Fmoc-removal by 20% piperidine in DMF for 5 min. [b]Prior Fmoc-removal by 20% piperidine in DMF for 20 min. [c]Area ratios corresponding to BPA.

40 min, but increased after 2 h of reaction time to 3.6 (Table 3, entries 3 and 4). This result indicates a slow coupling between the *N*-methyl group of Sar and Fmoc-Aib.

The activation reagent HBTU was replaced by its more potent aza-analog HATU. The couplings over resins **10a** and **10b** rendered the similar area ratios as when HBTU was used (Table 3, entries 1 vs 5, and entries 2 vs 6, respectively). The coupling of Fmoc-Aib over **10c** gave an area ratio of 7.4 for Fmoc-Aib-Sar-Pro (Table 3, entry 7), which was higher than those obtained for the Gly (6.2) and D-Leu-analogs (6.0) (Table 3, entries 5 and 6). The area ratio did not increase with prolonged coupling. We therefore reasoned that after 40 min the coupling was complete and that the differences between the product area ratios corresponded to the susceptibility of the corresponding Xaa-Pro-sequence on resins **10a−c** to DKP formation under the Fmoc-removal conditions.

To test this, resins **9a−c** were treated for 20 min with 20% piperidine in DMF, and Fmoc-Aib was coupled for 40 min with HATU/DIEA activation. The highest impact of the prolonged basic treatment was observed for the DLeu-Pro sequence, which experienced a 50% reduction in yield (Table 3, entry 6 vs entry 9). The sequence Gly-Pro was also obtained in significantly lower yield (Table 3, entry 5 vs entry 8). However, the same yield was achieved for the sequence Sar-Pro (Table 3, entry 7 vs entry 10).

■ STABILITY OF CARBOXYLIC ACIDS BOUND TO CTC RESIN UNDER A RANGE OF ACYLATION CONDITIONS

Low yields of Fmoc-Gly-Pro were obtained when coupling Fmoc-Gly activated with Oxyma/DIPCDI over resin **8** (Table 2, entry 2). These conditions also caused a yield decrease in the synthesis of Val-Arg-Phe (Table 1). To check the stability of the reference compounds PAA and BPA, and peptides on CTC resin toward different acylation conditions, CTC resin was loaded with an equimolar mixture of BPA, PAA, Fmoc-Gly, Fmoc-Pro, and Fmoc-Leu (0.1 mmol each for 500 mg CTC resin) to give resin **12** (Figure 4).

Aliquots of washed and dried **12** (10 mg) were used to monitor the stability of the resin-bound compounds toward a range of activation conditions for Fmoc-Gly coupling to give **13**. After reaction and cleavage of the corresponding products from the resin aliquot, a fixed volume of an external reference (Z-Gly) solution was added. The area ratios of the products obtained from **13** are shown in Table 4 and refer to the peak area of the external reference (Z-Gly). The area ratios

dx.doi.org/10.1021/co4000024 | ACS Comb. Sci. 2013, 15, 229−234

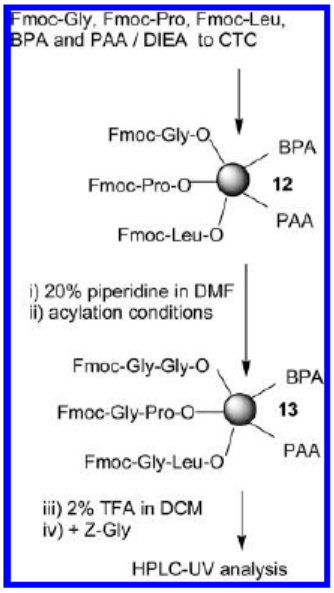

Figure 4. For conditions (ii) see Table 4.

corresponding to the Fmoc-Gly-Xaa-peptides and internal references (BPA, PAA) after coupling of Fmoc-Gly activated with HBTU/DIEA for 40 min were set to 100% (Table 4, entry 1). For all other conditions, the compound peak areas were smaller with respect to the conditions of entry 1 (Table 4, entries 2−8, the losses of compounds from resin with respect to entry 1 are given in parentheses). The yields dropped in all examples during "overnight"-couplings. The reduction in yield was dramatic (up to 60%) when acidic coupling reagents (Oxyma, HOBt and HOAt) were used (Table 4, entries 3−8). The reference compound PAA was found to be the most stable but in contrast, Fmoc-Gly-Pro on CTC showed the lowest stability under the conditions tested. Because of the similar and even higher stability of the reference compounds PAA and BPA with respective to peptides, we were able to detect the decreases in yield in the test reactions described above (Figures 2 and 3). With respect to SPPS on CTC resin, on the basis of our findings we recommend that DIPCDI-mediated HOAt, HOBt, and Oxyma-activation be carefully checked.[12]

SUMMARY

The data presented in this study demonstrate the internal reference method to be a valuable tool for optimizing conditions for solid-phase peptide synthesis and its possible applications in solid-phase synthesis of other compounds. We wish to summarize how to use this method.

First, it must be noted that the internal reference does not improve the chromatographic properties of resin-bound compounds. Its exactness depends on the integration of the peaks. With a suitable internal reference, reaction control by quantitative HPLC-UV analysis proceeds in the same manner as conventional HPLC-UV analysis (taking a resin sample from the reaction mixture, washing it, and running an HPLC chromatogram directly from the cleaved products). The practical value of an internal reference is the rapid sample analysis, which allows comparison of chromatograms from resin samples before and after reaction, or from different reaction conditions. Rather than providing "absolute" values for single chromatograms, the validity of this approach is based on the comparison of chromatograms.

When improvement of a solid-phase synthesis is required, a test resin with internal reference can be designed. There is no "general" internal reference available. However, here PAA and BPA, with high retention times in RP-HPLC, were found to be useful in peptide synthesis on CTC resin. As demonstrated, these compounds bound to the resin more stably or as stable as the peptides by the same functional group. They gave sharp peaks on HPLC-UV which were well separated from product peaks. However, there are no limitations for other compounds that fulfill these key requirements.

For quantification, the main peak should not exceed 1 AU to have a linear relation between the peak areas of the reference and the analyte. As a result, the area ratio between products and the reference should not be too large. The area ratios in this study were between 1 and 50. All analyses should be performed on the same equipment. The peaks have to be clearly distinguished from the baseline. Noisy baselines (caused by UV lamps with long running time) affect the accuracy.

We have demonstrated that such a quantitative analysis provides information rapidly and precisely on the outcome of reactions that would otherwise be difficult to obtain. Once the appropriate protocol is found, the synthesis can then be performed on a resin without a reference. Therefore we consider the internal reference method a valuable addition to the toolbox for solid-phase synthesis.

Table 4. Quantification of Premature Cleavage of Compounds on CTC Resin under a Range of Peptide Coupling Conditions (HBTU/DIEA, 40 min and 15 h, entries 1 and 2; oxyma/DIPCDI, 40 min and 15 h, entries 3 and 4; HOBt/DIPCDI, 40 min and 15 h, entries 5 and 6; HOAt/DIPCDI, 40 min and 15 h, entries 7 and 8)

	area ratio[a] (percent variation respectively to entry 1)				
entry	Fmoc-Gly-Gly	Fmoc-Gly-Pro	BPA	Fmoc-Gly-Leu	PAA
1	3.1 (±0%)	3.2 (±0%)	1.3 (±0%)	3.3 (±0%)	1.9 (±0%)
2	2.9 (−8%)	3.0 (−4%)	1.3 (−4%)	3.2 (−3%)	1.9 (+1%)
3	3.1 (−1%)	2.6 (−19%)	1.4 (+1%)	3.1 (−4%)	1.9 (±0%)
4	2.7 (−13%)	2.3 (−26%)	1.3 (−7%)	2.8 (−14%)	1.9 (±0%)
5	3.0 (−4%)	1.9 (−41%)	1.4 (+1%)	3.0 (−7%)	2.0 (+7%)
6	2.5 (−21%)	1.7 (−47%)	1.2 (−9%)	2.6 (−20%)	1.8 (−3%)
7	2.9 (−8%)	1.9 (−39%)	1.3 (−1%)	2.7 (−18%)	1.9 (+4%)
8	1.8 (−43%)	1.2 (−63%)	0.7 (−50%)	1.7 (−48%)	1.1 (−43%)

[a]Area ratios with respect to the external standard Z-Gly.

dx.doi.org/10.1021/co4000024 | ACS Comb. Sci. 2013, 15, 229−234

■ ASSOCIATED CONTENT

Supporting Information

Experimental procedures and HPLC-UV chromatograms. This material is available free of charge via the Internet at http://pubs.acs.org.

■ AUTHOR INFORMATION

Corresponding Author

*E-mail: jan.spengler@irbbarcelona.org (J.S.); fernando.albericio@irbbarcelona.org (F.A.).

Funding

The work has been partially financed by CICYT (CTQ2009-07758), the Generalitat de Catalunya (2009SGR 1024), the Institute for Research in Biomedicine Barcelona (IRB Barcelona), and the Barcelona Science Park.

Notes

The authors declare no competing financial interest.

■ ACKNOWLEDGMENTS

Peter Fransen (IRB Barcelona, for proposing the use of PAA), Brigitte Morales (MIT, Internship 2011), and Isidro Casals (Barcelona Science Park).

■ REFERENCES

(1) Dörwald, F. Z. *Organic Synthesis on Solid Phase*; Wiley-VCH: Weinheim, Germany, 2002.

(2) *The Power of Functional Resins in Organic Synthesis*; Tulla-Puche, J., Albericio, F., Eds.; Wiley-VCH: Weinheim, Germany, 2008.

(3) Scicinski, J. J.; Congreve, M. S.; Kay, C.; Ley, S. V. Analytical Techniques for Small Molecule Solid Phase Synthesis. *Curr. Med. Chem.* **2002**, *9*, 2103−2127.

(4) Dong, M. W. *Modern HPLC for Practicing Scientists*; John Wiley & Sons, Inc.: Hoboken, NJ, 2006.

(5) Congreve, M. S.; Ley, S. V.; Scicinski, J. J. Analytical Constructs for Analysis of Solid-Phase Chemistry. *Chem.—Eur. J.* **2002**, *8*, 1768−1776.

(6) Congreve, M. S.; Ladlow, M.; Marshall, P.; Parr, N.; Scicinski, J. J.; Sheppard, T.; Vickerstaffe, E.; Carr, R. A. E. Reporter Resins for Solid-Phase Chemistry. *Org. Lett.* **2001**, *3*, 507−510.

(7) We use the term "internal reference" to avoid confusion with the "internal standard" method used predominantly for the analysis of complex biological samples. See ref 4.

(8) Barlos, K.; Gatos, D.; Kallitsis, J.; Papaphotiu, G.; Sotiriu, P.; Yao, W.; Schaefer, W. Preparation of Protected Peptide Fragments Using Triphenylmethyl Resins. *Tetrahedron Lett.* **1989**, *30*, 3943−3946.

(9) Hoekstra, W. J. The 2-Chlorotrityl Resin: A Worthy Addition to the Medicinal Chemists Toolbox. *Curr. Med. Chem.* **2001**, *8*, 715−719.

(10) Fischer, P. M. Diketopiperazines in Peptide and Combinatorial Chemistry. *J. Peptide Sci.* **2003**, *9*, 9−35.

(11) See ref 9.

(12) Subirós-Funosas, R.; El-Faham, A.; Albericio, F. Use of Oxyma as pH Modulatory Agent in the Prevention of Base-Driven Side Reactions and Its Effect on 2-Chlorotrityl Chloride Resin. *Biopolymers* **2012**, *98*, 89−97.

Publication III: A. I. Fernández-Llamazares, J. García, V. Soto-Cerrado, R. Pérez-Tomás, J. Spengler and F. Albericio. *N*-triethylene glycol (*N*-TEG) as a surrogate for the *N*-methyl group: application to Sansalvamide A peptide analogs. *Chem. Commun.* **2013**, *49*, 6430-6432. **DOI:** 10.1039/C3CC41788C.

ChemComm

RSC Publishing

COMMUNICATION

View Article Online
View Journal | View Issue

N-Triethylene glycol (*N*-TEG) as a surrogate for the *N*-methyl group: application to Sansalvamide A peptide analogs†‡

Cite this: *Chem. Commun.*, 2013, **49**, 6430

Received 9th March 2013,
Accepted 24th May 2013

DOI: 10.1039/c3cc41788c

www.rsc.org/chemcomm

Ana I. Fernández-Llamazares,[ab] Jesús García,[a] Vanessa Soto-Cerrato,[c] Ricardo Pérez-Tomás,[c] Jan Spengler*[ab] and Fernando Albericio*[abde]

Here we studied the *N*-triethylene glycol (*N*-TEG) group as a surrogate for the *N*-Me group in Sansalvamide A peptide. The five *N*-TEG and *N*-Me analogs of this cyclic pentapeptide were synthesized, and their biological activity, lipophilicity and conformational features were compared.

The replacement of natural amino acids with *N*-methyl amino acids in biologically active peptides has resulted in analogs with improved pharmacological properties.[1,2] Peptides containing *N*-methyl amino acids show increased metabolic stability and higher hydrophobicity, which can enhance their bioavailability, thus amplifying their therapeutic potential.[2] Furthermore, the incorporation of *N*-methyl amino acids into bioactive peptides can have a substantial impact on their conformation and, as a result, increased biological activity and higher receptor selectivity may be achieved.[3]

Surprisingly, little attention has been devoted to the comparison of the synthesis and properties of *N*-methylated peptides with other *N*-alkylated peptides.[4] We hypothesized that modification of a peptide with an *N*-triethylene glycol (*N*-TEG) group would be comparable to modification with the *N*-Me group in terms of structural and biological effects, while providing some of the features associated with oligoethylene glycol (OEG). To test this notion, we sought to incorporate *N*-TEG amino acids at the different positions of Sansalvamide A peptide (**1**), a cyclic pentapeptide that exhibits anti-tumor activity against a variety of cancer cell lines (Fig. 1).[5,6] This cyclic peptide was considered a reasonable model, since its five *N*-Me analogs (**1b–5b**) have been synthesized, and some of them are cytotoxic against certain cancer cell lines.[6] Replacement of an *N*-Me group with an *N*-TEG group does not alter the amide proton pattern of the cyclic backbone with respect to the *N*-Me analogs; however, due to the amphiphilic nature of OEG, an alteration of certain physicochemical properties, such as hydrophilicity, was expected.

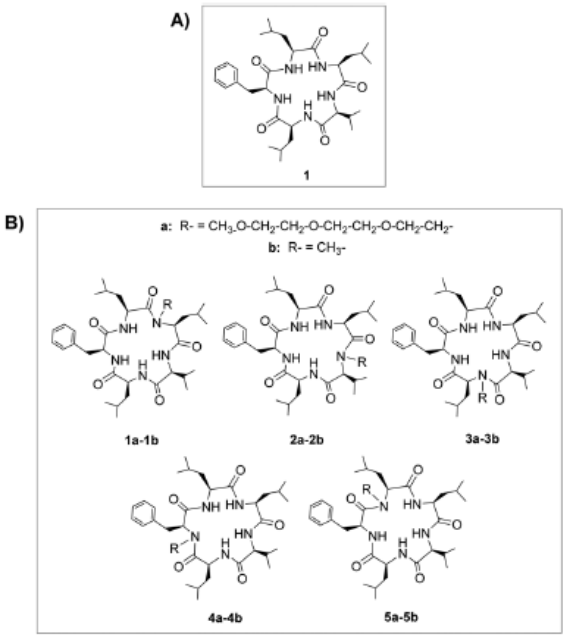

Fig. 1 (A) Structure of Sansalvamide A peptide (**1**). (B) Structure of the *N*-TEG and *N*-Me analogs (**1a–5a** and **1b–5b**).

Here we report on the synthesis of all five *N*-TEG analogs (**1a–5a**) of Sansalvamide A peptide (**1**) (Fig. 1). The five *N*-Me analogs (**1b–5b**) were also synthesized, and both sets of compounds were compared with respect to biological activity, lipophilicity and conformational features.

Our synthetic strategy to prepare the *N*-TEG and *N*-Me analogs of Sansalvamide A peptide (**1a–5a** and **1b–5b**) involved the use of Fmoc-protected *N*-TEG or *N*-Me amino acids as solid-phase building

[a] *Institute for Research in Biomedicine (IRB), Barcelona Science Park (PCB), Baldiri Reixac 10, 08028 Barcelona, Spain. E-mail: albericio@irbbarcelona.org, jan.spengler@irbbarcelona.org*
[b] *CIBER-BBN, Networking Centre on Bioengineering, Biomaterials and Nanomedicine, PCB, Baldiri Reixac 10, 08028 Barcelona, Spain*
[c] *Department of Pathology and Experimental Therapeutics, University of Barcelona, Pavelló Central, LR 5101 C/Feixa Llarga s/n, E-08907 L'Hospitalet, Spain*
[d] *Department of Organic Chemistry, University of Barcelona, Martí i Franqués 1-11, 08028 Barcelona, Spain*
[e] *School of Chemistry & Physics, University of KwaZulua-Natal, 4001 Durban, South Africa*

† To Professor Klaus Burger, a mentor and a friend, on occasion of his 75th anniversary.

‡ Electronic supplementary information (ESI) available: Experimental details, characterization data, and copies of the HPLC, ^{1}H-NMR and ^{13}C-NMR spectra of selected compounds. See DOI: 10.1039/c3cc41788c

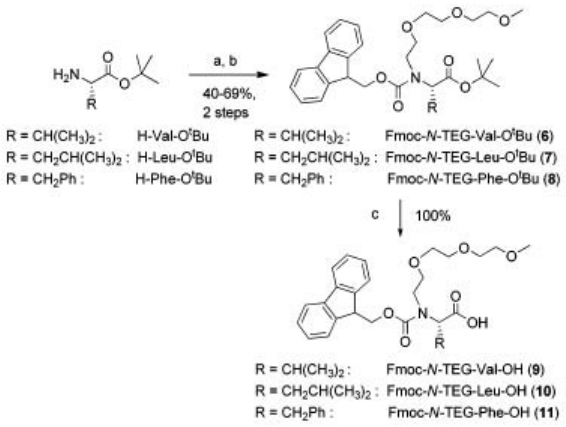

Scheme 1 Synthesis of the Fmoc-*N*-TEG amino acids (**9–11**). Reagents and conditions: (a) CH_3O–$(CH_2CH_2O)_2$–CH_2CHO, $NaBH_3CN$; (b) Fmoc-Cl, DIEA; (c) TFA–DCM 1 : 1.

blocks. All Fmoc-*N*-Me analogs of the proteinogenic amino acids are commercially available. In contrast, we had to prepare the required Fmoc-*N*-TEG amino acids. The Fmoc-*N*-TEG analogs of Val, Leu and Phe (**6–8**) were obtained from their corresponding amino acid *tert*-butyl esters, which were subjected to reductive alkylation with 3,6,9-trioxadecanaldehyde. In all cases, the reaction crude consisted of unreacted starting material, *N*-monoalkylated product and *N*,*N*-dialkylated product. The last two were found to be inseparable; however, after Fmoc-protection of the amino group, the desired products (**6–8**) could be isolated using flash chromatography. Finally, acidic cleavage of the *tert*-butyl ester yielded the required Fmoc-*N*-TEG derivatives (**9–11**) in 40–69% overall yield (Scheme 1).

For the synthesis of the *N*-TEG and *N*-Me analogs of Sansalvamide A peptide (**1a–5a** and **1b–5b**), their corresponding linear precursors (**p1a–p5a** and **p1b–p5b**) were prepared by stepwise solid-phase peptide synthesis (SPPS) on the 2-chlorotrityl resin and then cyclized in solution (Scheme 2). The *N*-substituted residue was placed in the middle of the pentapeptide sequence, which minimizes steric hindrance during cyclization and is expected to facilitate this process due to the turn-inducing properties of *N*-alkyl amino acids.[7]

In the SPPS of the pentapeptides (**p1a–p5a** and **p1b–p5b**), Fmoc-*N*-TEG amino acids (**9–11**) and Fmoc-*N*-Me amino acids were coupled to the peptidyl-resin using DIPCDI–OxymaPure activation. As expected, couplings onto the *N*-TEG residues were a challenging step. These couplings are hampered by the triethylene glycol chain, which is sterically more demanding than a methyl group. Even for the couplings onto *N*-Me residues, special conditions are required to overcome low coupling yields caused by steric hindrance.[3] We checked several protocols that are reported to be efficient for difficult coupling steps, like activation of the subsequent amino acid with HATU or as a symmetrical anhydride using DIPCDI. The best results were obtained using bis(trichloromethyl)carbonate (BTC) as an activating reagent.[8] In the case of BTC-mediated couplings onto the *N*-Me residues, no unreacted peptide was detected in cleaved samples after a single treatment with the activated amino acid (as checked using HPLC-MS). For couplings onto the *N*-TEG residues, complete conversion was achieved after two treatments.

After cleavage from the solid support, the crude pentapeptides (**p1a–p5a** and **p1b–p5b**) were efficiently cyclized, and the desired cyclic

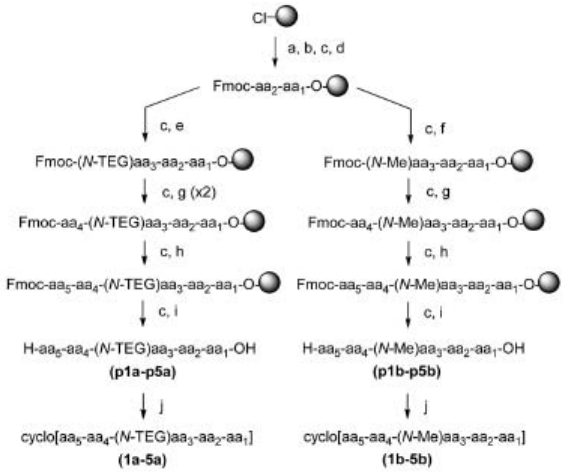

Scheme 2 Synthesis of the *N*-TEG and *N*-Me analogs (**1a–5a** and **1b–5b**). Reagents and conditions: (a) Fmoc-aa_1-OH, DIEA; (b) MeOH; (c) piperidine–DMF 1 : 4; (d) Fmoc-aa_2-OH, DIPCDI, OxymaPure; (e) Fmoc-(*N*-TEG)aa_3-OH, DIPCDI, OxymaPure; (f) Fmoc-(*N*-Me)aa_3-OH, DIPCDI, OxymaPure; (g) Fmoc-aa_4-OH, BTC, 2,4,6-trimethylpyridine, THF; (h) Fmoc-aa_5-OH, DIPCDI, OxymaPure; (i) 2% TFA in DCM; (j) EDC·HCl, 4-DMAP.

peptides (**1a–5a** and **1b–5b**) were easily purified using semi-preparative RP-HPLC. In all cases, sufficient amounts of peptide were obtained in yields that are commonly achieved for cyclic pentapeptides. Except for compound **3a**, the overall yields of the syntheses of the *N*-TEG cyclopeptides were not dramatically lower than those of the *N*-Me cyclopeptides. Thus, *N*-TEG peptides are accessible by the same synthetic repertoire as that already established for *N*-Me peptides.

In order to study how replacement of the *N*-Me group by the *N*-TEG group affects the anti-cancer activities, all compounds (**1**, **1a–5a** and **1b–5b**) were tested for their cytotoxicity against GLC-4 and MDA-MB-231 cancer cells. Treatment with 50 μM of some compounds for 72 h decreased the viability of GLC-4 (**1**, **1a**, **2a**, **4a**, **2b**, **4b**, **5b**) and MDA-MB-231 (**1a**, **4a**, **3b**) cells up to 50–60% (Fig. 2). The cytotoxic activity of the *N*-TEG analogs (**1a–5a**) was found to be within the same range as that of the *N*-Me analogs (**1b–5b**).

The incorporation of *N*-TEG or *N*-Me was expected to affect the lipophilicity of the original peptide (**1**), which is highly hydrophobic. One of the most common parameters to estimate lipophilicity is the octanol/water partition coefficient (log*P*). However, in our attempts to determine the log*P* of our compounds (**1**, **1a–5a** and **1b–5b**) by the shake-flask method, no compound was detected in the aqueous phase, thus impeding calculation of this coefficient. The relative hydrophobicity of **1**, **1a–5a** and **1b–5b** was evaluated by comparison of their RP-HPLC retention times.[9] The increase in the time at which the *N*-TEG

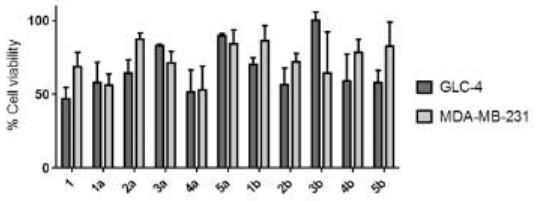

Fig. 2 Cell viability of GLC-4 and MDA-MB-231 cancer cells after 50 μM treatment of **1**, **1a–5a** and **1b–5b** for 72 h.

Table 1 RP-HPLC retention times of **1**, **1a–5a**, **1b–5b**[a]

Entry	t_r (min)	
1	**1**(SA-peptide): 5.97	
2	**1a**: 7.29	**1b**: 7.12
3	**2a**: 7.22	**2b**: 7.07
4	**3a**: 6.98	**3b**: 6.82
5	**4a**: 7.34	**4b**: 6.97
6	**5a**: 7.05	**5b**: 6.86

[a] Linear gradient from 10% to 90% ACN over 8 min, C18 column.

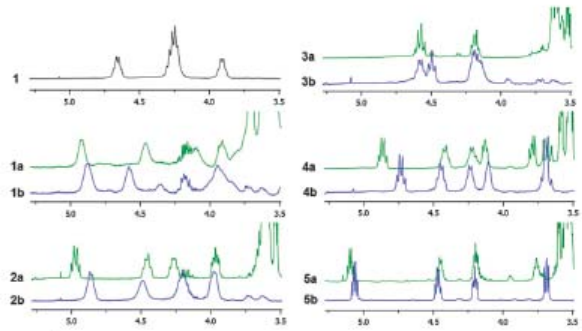

Fig. 3 ^{1}H-NMR spectra (in $CDCl_3$) of **1**, **1a–5a**, **1b–5b** in the 5.5–3.5 ppm region.

and the *N*-Me analogs (**1a–5a** and **1b–5b**) were eluted indicated that the *N*-alkylated analogs were slightly more lipophilic than the original peptide (**1**) (Table 1). Their enhanced lipophilicity can be attributed to the fact that *N*-alkylation of an amide bond decreases the number of potential intermolecular hydrogen bonds that can be formed with the polar solvent (H_2O). Surprisingly, all the *N*-TEG analogs (**1a–5a**) were slightly more hydrophobic than their corresponding *N*-Me counterparts (**1b–5b**), presumably due to the *N*-TEG chain shielding the backbone amide groups from interaction with H_2O. Since the decreased hydrogen-bonding potential and the enhanced lipophilicity upon *N*-methylation are considered to improve membrane permeability,[10] we propose that the incorporation of *N*-TEG may provide a novel modification to gain bioavailability in therapeutic peptides.

The effect of the *N*-TEG group on the conformational state of Sansalvamide A peptide (**1**) was found to be the same as that of the *N*-Me group. An overlay of the ^{1}H-NMR spectra (in $CDCl_3$) of **1**, **1a–5a** and **1b–5b** in the H^N- and H^α-regions clearly showed that *N*-alkylation induced changes in the backbone conformation of the parent peptide (Fig. 3). Depending on the position of *N*-alkylation, different signal patterns were observed; however, the *N*-TEG and the *N*-Me analogs (**1a–5a** and **1b–5b**) bearing the *N*-substituent at the same position were found to have similar H^α-resonances. The resemblance of their C^α-chemical shifts gives further evidence of similar conformational preferences (see ESI‡).

For peptides **5a** and **5b**, a more detailed study was performed in comparison with the parent peptide (**1**) (see ESI‡). For the three peptides, no evidence of conformational equilibria was found using ^{1}H-NMR in the temperature range between 5 and 45 °C. For each peptide, the H^N-, H^α- and C^α-signals were unequivocally assigned, the interproton NOEs were analyzed and the temperature coefficients of the amide protons were determined. These experimental parameters, which are sensitive to conformational changes, were almost identical for the *N*-TEG and *N*-Me analogs **5a** and **5b**, whilst considerably differing from those of the unmodified Sansalvamide A peptide (**1**).

In conclusion, this study shows that peptides in which the backbone *N*-Me group is replaced by a short oligoethylene glycol chain are accessible by the same synthetic repertoire as that already established for *N*-Me peptides. Comparison of the NMR data of *N*-Me and *N*-TEG peptides gives evidence of similar conformational preferences for those peptides with the same *N*-alkylation pattern, and the incorporation of an *N*-TEG chain or an *N*-Me group into a peptide provides a higher lipophilicity. Considering the high abundance of *N*-Me amino acids in biologically active peptides, we contend that modification at this position is a feasible alternative to introduce structural diversity or alter pharmacologically important parameters when modification at any other position of the peptide is not wished or possible.

This work was partially supported by CICYT (CTQ2012-30930), the Generalitat de Catalunya (2009SGR 1024), the Institute for Research in Biomedicine and the Barcelona Science Park. Ana I. Fernández-Llamazares thanks Ministerio de Educación y Ciencia for a FPU fellowship. We thank the Cancer Cell Biology Research group for their support for the cytotoxicity assays and we thank Barcelona Science Park (Mass Spectrometry Core Facility, Nuclear Magnetic Resonance Unit) for the facilities.

Notes and references

1 C. Gilon, M. A. Dechantsreiter, F. Burkhart, A. Friedler and H. Kessler, in *Houben-Weyl, Methods of Organic Chemistry, Synthesis of Peptides and Peptidomimetics*, ed. M. Goodman, A. Felix, L. Moroder and C. Toniolo, Georg Thieme Verlarg, Stuttgart and New York, 2002, vol. E22c, pp. 215–271 and references cited therein.
2 J. Chatterjee, F. Rechenmacher and H. Kessler, *Angew. Chem., Int. Ed.*, 2013, **52**, 254.
3 J. Chatterjee, C. Gilon, A. Hoffman and H. Kessler, *Acc. Chem. Res.*, 2008, **10**, 1331.
4 F. Hubler, T. Ru, L. Patiny, T. Muamba, J.-F. Guichou, M. Mutter and R. Wenger, *Tetrahedron Lett.*, 2000, **41**, 7193.
5 W. Gu, S. Liu and R. B. Silverman, *Org. Lett.*, 2002, **4**, 4171; C. L. Carroll, J. V. C. Johnston, A. Kekec, J. D. Brown, E. Parry, J. Cajica, I. Medina, K. M. Cook, R. Corral, P.-S. Pan and S. R. McAlpine, *Org. Lett.*, 2005, **7**, 3481; T. J. Styers, A. Kekec, R. Rodriguez, J. D. Brown, J. Cajica, P.-S. Pan, E. Parry, C. L. Carroll, I. Medina, R. Corral, S. Lapera, K. Otrubova, C.-M. Pan, K. L. McGuireb and S. R. McAlpine, *Bioorg Med. Chem.*, 2006, **14**, 5625; P.-S. Pan, K. L. McGuireb and S. R. McAlpine, *Bioorg. Med. Chem. Lett.*, 2007, **17**, 5072.
6 S. Liu, W. Gu, D. Lo, X.-Z. Ding, M. Ujiki, T. E. Adrian, G. A. Soff and R. B. Silverman, *J. Med. Chem.*, 2005, **48**, 3630.
7 O. Demmer, I. Dijkgraaf, M. Schottelius, H.-J. Wester and H. Kessler, *Org Lett.*, 2008, **10**, 2015; C. J. White and A. K. Yudin, *Nat. Chem.*, 2011, **3**, 509.
8 E. Falb, T. Yechezkel, Y. Salitra and C. Gilon, *J. Pept. Res.*, 1999, **53**, 507; B. Thern, J. Rudolph and G. Jung, *Angew. Chem., Int. Ed.*, 2002, **41**, 2307; B. Thern, J. Rudolph and G. Jung, *Tetrahedron Lett.*, 2002, **43**, 5013; M. M. Sleebs, D. Scanlon, J. Karas, R. Maharani and A. B. Hugues, *J. Org. Chem.*, 2011, **76**, 6686; J. Spiegel, C. Mas-Moruno, H. Kessler and W. D. Lubell, *J. Org. Chem.*, 2012, **77**, 5271.
9 J. M. R. Parker, D. Guo and R. S. Hodges, *Biochemistry*, 1986, **25**, 5425; T. J. Sereda, C. T. Mant, F. D. Sönnichsen and R. S. Hodges, *J. Chromatogr., A*, 1994, **676**, 139.
10 T. R. White, C. M. Renzelman, A. C. Rand, T. Rezai, C. M. McEwen, V. M. Gelev, R. A. Turner, R. G. Linington, S. S. F. Leung, A. S. Kalgutkar, J. N. Bauman, Y. Z. Zhang, S. Liras, D. A. Price, A. M. Mathiowetz, M. P. Jacobson and R. S. Lokey, *Nat. Chem. Biol.*, 2011, **7**, 810; J. G. Beck, J. Chatterjee, B. Laufer, M. Udaya Kiran, A. O. Frank, S. Neubauer, O. Ovadia, S. Greenberg, C. Gilon, A. Hoffman and H. Kessler, *J. Am. Chem. Soc.*, 2012, **134**, 12125.

Publication IV: A. I. Fernández-Llamazares, J. García, J. Adan, D. Meunier, F. Mitjans, J. Spengler and F. Albericio. The backbone *N*-(4-azidobutyl) linker for the preparation of peptide chimera. *Org. Lett.* **2013**, *15*, 4572-4575. **DOI:** 10.1021/ol402150m.

ORGANIC LETTERS

2013
Vol. 15, No. 17
4572–4575

The Backbone *N*-(4-Azidobutyl) Linker for the Preparation of Peptide Chimera[#]

Ana I. Fernández-Llamazares,[†,‡,§] Jesús García,[†] Jaume Adan,[∥] David Meunier,[†] Francesc Mitjans,[∥] Jan Spengler,[*,†,‡,§] and Fernando Albericio[*,†,‡,§,⊥]

Institute for Research in Biomedicine (IRB), PCB, 08028-Barcelona, Spain, CIBER-BBN, PCB, 08028-Barcelona, Spain, Biomed Division, Leitat Technological Center Institution, PCB, 08028-Barcelona, Spain, Department of Organic Chemistry, University of Barcelona, 08028-Barcelona, Spain, and School of Chemistry, University of KwaZulu Natal, 4001-Durban, South Africa

albericio@irbbarcelona.org; jan.spengler@irbbarcelona.org

Received July 29, 2013

ABSTRACT

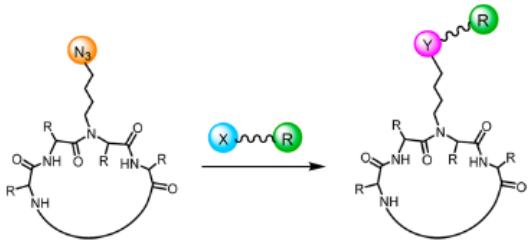

A robust synthetic strategy for the introduction of the *N*-(4-azidobutyl) linker into peptides using standard SPPS techniques is described. Based on the example of Cilengitide it is shown that the *N*-(4-azidobutyl) group exerts similar conformational restraints as a backbone *N*-Me group and allows conjugation of a desired molecule either via click chemistry or—after azide reduction—via acylation or reductive alkylation.

The site-specific covalent attachment of "unnatural" moieties, such as fluorophores, radiolabels, affinity labels, or polymers, to peptides has proven useful for a wide variety of applications.[1] The conjugation of peptides with a desired molecule is typically performed at the *N*-terminus or at naturally occurring side-chain functional groups.[2] Cyclic peptides or even some linear peptides without derivatizable groups often require the introduction of additional residues, such as Lys or Cys, to support side-chain-selective conjugation. In the case of cyclic peptides, additional amino acids cannot be introduced, and finding a suitable position for amino acid replacement is not straightforward. Along these lines, bio-orthogonal conjugation methods that target unnatural amino acids are becoming valuable alternatives to the more commonly used Lys- and Cys-based strategies, as they do not involve cumbersome protection and deprotection protocols.[3] However, each of the techniques currently available for peptide modification have specific drawbacks, and generally there is a lack of widely usable and flexible methods.

We envisaged that modification of the backbone amide groups with a functionalized *N*-substituent may be a valuable addition to the chemist's toolbox to perform peptide conjugation. Kessler's group has shown that the introduction of *N*-Me groups in peptide ligands can optimize their activity and receptor selectivity as a result of conformational modulation.[4] Furthermore, backbone *N*-Me groups are common structural motifs in many bioactive peptides isolated from natural sources.[4]

Here we describe the *N*-(4-azidobutyl) group as linker for the attachment of molecules. This *N*-substituent can be

[#] Dedicated to Professor Klaus Burger on the occasion of his 75th birthday.
[†] Institute for Research in Biomedicine (IRB), PCB.
[‡] CIBER-BBN, PCB.
[∥] Leitat Technological Center Institution, PCB.
[§] University of Barcelona.
[⊥] University of KwaZulu Natal.

(1) (a) Lee, S.; Xie, J.; Chen, X. *Biochemistry* **2010**, *49*, 1364–1376. (b) Shu, J. Y.; Panganiban, B.; Xu, T. *Annu. Rev. Phys. Chem.* **2013**, *64*, 631–657.
(2) Gauthier, M. A.; Klok, H.-A. *Chem. Commun.* **2008**, 2591–2611.
(3) (a) Antos, J. M.; Francis, M. B. *Curr. Opin. Chem. Biol.* **2006**, *10*, 253–262. (b) Sletten, E. M.; Bertozzi, C. R. *Angew. Chem., Int. Ed.* **2009**, *48*, 6974–6998.
(4) Chatterjee, J.; Gilon, C.; Hoffman, A.; Kessler, H. *Acc. Chem. Res.* **2008**, *10*, 1331–1342.

10.1021/ol402150m
Published on Web 08/22/2013

Scheme 1. Peptide Modification through the *N*-(4-Azidobutyl) Linker

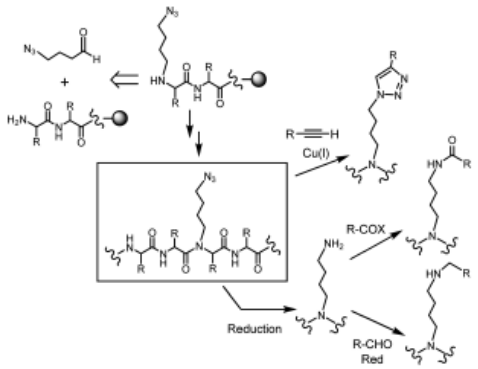

introduced into a resin-bound peptide by reductive alkylation with 4-azidobutanal, providing an azide onto which alkyne-functionalized molecules can be grafted by Cu(I)-catalyzed 1,3-dipolar cycloaddition (Scheme 1). Alternatively, the azide group can be reduced to an amine, onto which molecules can be conjugated via amide bond formation or via reductive alkylation. The azide function is stable to common deprotection protocols used in peptide synthesis and chemically inert to side-chain functional groups,[5] thereby minimizing side reactions and simplifying protection schemes.

A few years back, Kirshenbaum et al. showed that *N*-azidopropyl groups are straightforward to incorporate in peptoid sequences using an azido amine as a submonomer reagent, and that azide-functionalized peptoids can be used as substrates for azide−alkyne cycloaddition reactions.[6] However, the submonomer approach is only efficient for the preparation of *N*-substituted Gly oligomers. Also worth mentioning is that there is no reported example in which a peptide with a backbone *N*-azidoalkyl substituent has been obtained.

To demonstrate the applicability of our *N*-(4-azidobutyl) linker strategy, Cilengitide was chosen as a model. This Arg-Gly-Asp (RGD)-peptide is a good example of the difficulty involved in preparing conjugates of small cyclic peptides that do not offer attachment sites and/or that are not amenable to structural modification while preserving biological activity. The RGD-cyclopeptide sequence of Cilengitide, cyclo[RGDf*N*MeV], is the result of systematic research to constrain the RGD motif in its optimum conformation for binding to the $\alpha_v\beta_3$-integrin receptor, which is overexpressed in various malignant cancers and in tumor neovasculature.[6] The functionalization of RGD-cyclopeptide ligands that target this receptor is of great interest, as it allows the conjugation of suitable chemical entities for tumor imaging and therapeutics.[7] However, Cilengitide cannot be conjugated as it is. Among the five amino acids in its cyclic structure, three (RGD) are essential for binding to the receptor, D-Phe is involved in hydrophobic interactions, and *N*MeVal has no derivatizable functional group.[8] Substitution of *N*MeVal by Lys led to cyclo[RGDfK], one of the most conjugated peptide ligands which is used in a number of biomedical applications.[9] However, a decrease in biological activity has to be taken into account when replacing *N*MeVal by Lys, as the *N*-Me group of Val promotes constraints that stabilize the RGD motif in its preferred $\alpha_v\beta_3$-binding conformation.[10]

We report on the synthesis of an analog of cyclo-[RGDf*N*MeV] (**1**) in which the N-Me group of Val is replaced by the *N*-(4-azidobutyl) group (**2**), with minimal perturbation of the original conformation. By preparing various PEG conjugates from **2**, we show that our linker allows conjugation onto cyclic peptides under full conservation of their amino acid sequence.

To obtain the *N*-azidoalkylated cyclopeptide (**2**), its linear pentapeptide precursor (**3**) was prepared by stepwise solid-phase peptide synthesis (SPPS) on 2-chlorotrityl chloride (CTC) resin and then cleaved for subsequent cyclization and side-chain deprotection (Scheme 2). Positioning of the *N*-alkylated residue in the middle of the sequence of **3** minimizes steric hindrance during cyclization and is expected to facilitate this process as a result of backbone preorganization.[11]

The *N*-(4-azidobutyl) group was introduced into the resin-bound peptide by reductive alkylation with 4-azidobutanal in the presence of $NaBH_3CN$. The reaction was tested with various amounts of aldehyde; with 1.5 equiv, most *N*-terminal Val was exclusively *N*-monoalkylated. Taking advantage of the low reactivity of this secondary amine, the small amount of unreacted resin-bound peptide was capped with Ac_2O in order to facilitate the final purification. The foreseeable challenging step was the coupling of Fmoc-D-Phe onto *N*-(4-azidobutylated) Val. The acylation of this sterically demanding residue did not take place under conditions reported to be efficient for coupling D-Phe onto *N*MeVal. Stronger activation methods, such as PyBOP/HOAt and HATU/HOAt, also failed to form the desired product. Finally, this coupling was achieved by activating Fmoc-D-Phe with bis(trichloromethyl)-carbonate (BTC) in the presence of 2,4,6-trimethylpyridine.[12] After three prolonged couplings (15 h), acylation was almost complete and no epimerization was detected (HPLC). Further peptide elongation and cleavage afforded pentapeptide **3**, which was easy to cyclize with EDC and catalytic amounts of 4-DMAP. The Pbf- and ^{t}Bu- groups were then removed, and RP-HPLC purification rendered **2** in 17% overall yield.

(5) Brase, S.; Gil, C.; Knepper, K.; Zimmermann, V. *Angew. Chem., Int. Ed.* **2005**, *44*, 5518–5240.
(6) (a) Jang, H.; Fafarman, A.; Holub, J. M.; Kirshenbaum, K. *Org. Lett.* **2005**, *7*, 1951–1954. (b) Holub, J. M.; Jang, H.; Kirshenbaum, K. *Org. Biomol. Chem.* **2006**, *4*, 1497–1502.
(7) Liu, Z.; Wang, F.; Chen, X. *Drug Dev. Res.* **2008**, *69*, 329–339.
(8) (a) Schottelius, M.; Laufer, B.; Kessler, H.; Wester, H. J. *Acc. Chem. Res.* **2009**, *42*, 969–980. (b) Chen, X. *Theranostics* **2011**, *1*, 28–29.
(9) Mas-Moruno, C.; Rechenmacher, F.; Kessler, H. *Anti-cancer Agents Med.* **2010**, *10*, 753–768.
(10) Schottelius, M.; Laufer, B.; Kessler, H.; Wester, H.J. *Acc. Chem. Res.* **2009**, *42*, 969–980.
(11) Dechantsreiter, M. A.; Planker, E.; Mathä, B.; Lohof, E.; Hölzemann, G.; Jonczyk, A.; Goodman, S. L.; Kessler, H. *J. Med. Chem.* **1999**, *42*, 3033–3040.
(12) White, C. J.; Yudin, A. K. *Nat. Chem.* **2011**, *3*, 509–524.

Scheme 2. Small-Scale Synthesis of Cyclo[RGDf(*N*-$CH_2CH_2CH_2CH_2N_3$)V] (**2**)

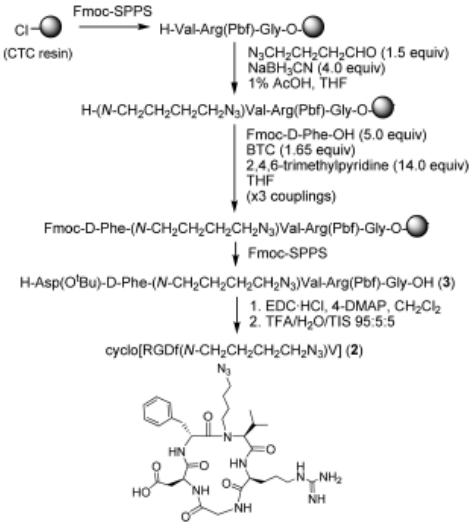

Scheme 3. Large-Scale Synthesis of Cyclo[RGDf(*N*-$CH_2CH_2CH_2CH_2N_3$)V] (**2**)

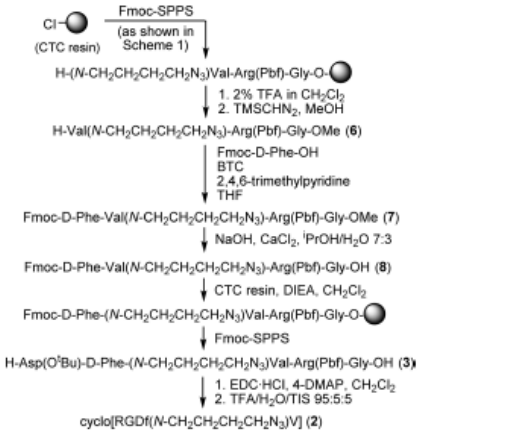

However, when the SPPS of pentapeptide **3** was performed in a larger amount of resin (> 3 g) and/or with a higher functionalization (> 0.50 mmol g^{-1}), the yields were not as satisfactory. To obtain larger amounts of **3**, an efficient *double SPPS* scheme was developed using the CTC resin for elongation, *de- and reattachment* of fully protected peptide, and final elongation again (Scheme 3). In this approach, the Val-Arg(Pbf)-Gly sequence was assembled followed by reductive alkylation of its *N*-terminus with 4-azidobutanal, as previously described. At this stage, the peptide was cleaved with 2% TFA in CH_2Cl_2, and its *C*-terminus was protected as a methyl ester. The coupling between Fmoc-D-Phe and the *N*-azidoalkylated peptide segment (**6**) was performed in solution using the BTC method. This procedure allowed us to obtain the desired peptide (**7**), which was isolated in 48% yield. Then, the methyl ester of **7** was hydrolyzed under basic conditions in the presence of $CaCl_2$, which is reported to suppress Fmoc- decomposition.[13] Using this additive, the methyl ester was saponified with no detectable Fmoc- decomposition (HPLC-MS). The desired peptide (**8**) was isolated by simple aqueous extraction and loaded again onto the CTC resin. The incorporation of **8** took place with an acceptable yield (i.e., 80% peptide incorporation for an expected functionalization of 0.10 mmol g^{-1}). Further peptide chain elongation and cleavage from the resin yielded pentapeptide **3**, which was cyclized and deprotected as described above. After RP-HPLC purification, the *N*-azidoalkylated cyclopeptide (**2**) was obtained in 18% overall yield.

With the synthesis of **2**, we demonstrate that *N*-(4-azidobutylated) peptides are accessible using standard SPPS protocols that are compatible with common protecting groups used in peptide synthesis. Taking into account that the acylation of the *N*-alkylated residue was achieved on a small scale using BTC, we consider that the detour from solid-phase to solution chemistry in the synthesis of **2** was necessary because of the additional steric hindrance exerted by the β-branched side chain of Val and that this change may not be a general requirement for the synthesis of other *N*-(4-azidobutylated) peptides.

It is reasonable to assume that the incorporation of an *N*-(4-azidobutyl) group into a cyclic peptide will exert the same conformational restrictions as a backbone *N*-Me group. The conformation of small cyclic peptides is dictated by their backbone stereochemistry and by the presence of *N*-alkyl groups, rather than by the interactions with or among the amino acid side chains.[14] To test this notion, we performed a detailed NMR study of cyclo[RGDf*N*MeV] (**1**) and its *N*-(4-azidobutylated) analog (**2**). Both peptides had very similar H^N-, H^α-, and C^α-chemical shifts, and their amide protons had almost identical temperature coefficients ($\Delta\delta/\Delta T$) and very similar vicinal scalar coupling constants [$^3J(H^N–H^\alpha)$] (see Supporting Information). The close resemblance of these NMR parameters, which are highly sensitive to conformational changes, indicates that replacement of the *N*-Me group of **1** by our linker provided a minimal perturbation of its conformational state.

To demonstrate the applicability of the *N*-(4-azidobutyl) linker, we prepared several conjugates of **2** with PEG. Conjugate **11** was obtained from **2** by Cu(I)-catalyzed Huisgen 1,3-dipolar cycloaddition with a polydisperse PEG-alkyne (2 KDa). To obtain conjugates **12** and **13**, the azido group of **2** was first reduced to an amine with the mild Zn/NH_4Cl reducing system. The resulting *N*-(4-aminobutylated) cyclopeptide (**10**) was acylated with a polydisperse PEG-COOSu derivative (2 KDa) to yield conjugate **12**, whereas reductive alkylation of **10** with a polydisperse PEG-propionaldehyde (2 KDa) furnished conjugate **13**. The optimized conditions for each transformation are shown in Scheme 4. Due to the polydispersity of PEG,

(13) (a) Thern, B.; Rudolph, J.; Jung, G. *Angew. Chem., Int. Ed.* **2002**, *41*, 2307–2309. (b) Thern, B.; Rudolph, J.; Jung, G. *Tetrahedron Lett.* **2002**, *43*, 5013–5016.

(14) Pascal, R.; Sola, R. *Tetrahedron Lett.* **1998**, *39*, 5031–5034.

Scheme 4. Synthesis of PEG-Conjugates **11**–**13**

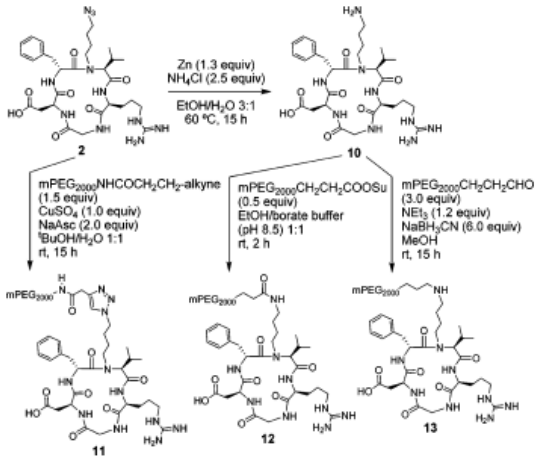

conditions had to be carefully optimized in order to facilitate the RP-HPLC purification of the PEG-conjugates (**11**–**13**).

The PEG-conjugates (**11**–**13**), the *N*-azidoabutylated cyclopeptide (**2**), and cyclo[RGDf*N*MeV] (**1**) were analyzed by circular dichroism (CD), a sensitive technique to monitor changes in a peptide secondary structure. All compounds showed a positive band between 212 and 216 nm (λ_{max}) and a negative band between 230 and 238 nm (λ_{min}) (Figure 1). CD measurements on peptides **2** and **11**–**13** are consistent with data on the peptide **1**, which has a conformation featuring two inverse γ (γ_i) turns and a γ turn.[10]

The biological activity of the PEG-conjugates (**11**–**13**) and cyclo[RGDf*N*MeV] (**1**) was evaluated in cell adhesion inhibition assays. All compounds were tested for their capacity to inhibit the integrin-mediated adhesion of HUVEC endothelial and DAOY glioblastoma cells to their immobilized ligands vitronectin (VN) and fibrinogen (FB) (Table 1). For all the cell/ligand systems, all the compounds inhibited cell adhesion in a concentration-dependent manner, and the same pattern of inhibitory activities was observed. The PEG-conjugates (**11**–**13**) showed IC_{50} values in the low μM range, albeit inferior to those of **1**. The decreased inhibitory activity of **11**–**13** with respect to the parent peptide (**1**) may be attributable to an interference of the PEG chain with the RGD–receptor interaction, resulting in lower binding affinities. Indeed, the reduced biological activity of peptides upon attachment of a bulky PEG chain is an issue of major concern, especially in the case of small peptides.[15]

In conclusion, we have shown that a backbone *N*-(4-azidobutyl) group can be incorporated into a peptide using standard SPPS techniques and allows conjugation at a late stage of the synthesis. Due to the orthogonal properties of the azide, our linker is compatible with side-chain protection strategies, linkers, and resins commonly used in peptide synthesis. Moreover, the chemical versatility of the azide function, which can be reduced to an amine prior to conjugation, allows for the flexible design of peptide conjugates. Along these lines, the possibility of using click chemistry in the conjugation step is an advantageous feature, since it permits conjugation in the presence of side-chain functional groups and thus implies a minimal requirement for protection. On the basis of all these considerations, we strongly believe that our *N*-(4-azidobutyl) linker will have broad utility in peptide chemistry and will widen the application of established conjugation methods.

(15) Chatterjee, J.; Mierke, D. F.; Kessler, H. *Chem.—Eur. J.* **2008**, *14*, 1508–1517.
(16) Veronese, F. M.; Mero, A. *Biodrugs* **2008**, *22*, 315–329.

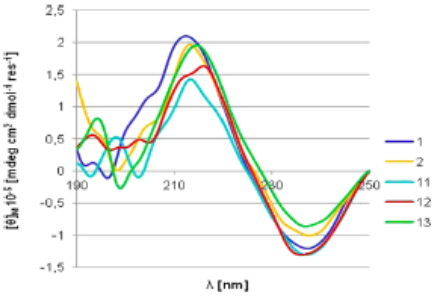

Figure 1. CD spectra of cyclo[RGDf*N*MeV] (**1**), cyclo[RGDf(*N*-$CH_2CH_2CH_2CH_2N_3$)V] (**2**), and compounds **11**–**13** in H_2O at a concentration of 0.5 mM.

Table 1. Adhesion Inhibition Assays of Cyclo[RGDf*N*MeV] (**1**) and Compounds **11**–**13**[a]

	$\alpha_v\beta_3 + \alpha_v\beta_5$		$\alpha_v\beta_3$	
compd	HUVEC on VN	DAOY on VN	HUVEC on FB	DAOY on FB
1	0.37	2.69	0.076	0.44
11	8.90	75.21	0.53	4.36
12	3.06	28.76	0.23	1.77
13	3.40	49.56	0.41	2.71

[a] IC_{50} values are given in μM.

Acknowledgment. This work has been partially supported by CICYT (CTQ2012-30930), the Generalitat de Catalunya (2009SGR 1024), the and the IRB.

Supporting Information Available. Experimental details of the syntheses, cellular assays, characterization data, and copies of the HPLC, HRMS, and NMR spectra of selected compounds. This material is available free of charge via the Internet at http://pubs.acs.org.

The authors declare no competing financial interest.

Paper V: A. I. Fernández-Llamazares, J. Adan, F. Mitjans, J. Spengler and F. Albericio. Tackling lipophilicity of peptide drugs: replacement of the backbone *N*-methyl group of Cilengitide by *N*-oligoethylene glycol (*N*-OEG) chains. Under revision at *Bioconj. Chem.*

Tackling lipophilicity of peptide drugs: replacement of the backbone *N*-methyl group of Cilengitide by *N*-oligoethylene glycol (*N*-OEG) chains

Ana I. Fernández-Llamazares,[†,‡] Jaume Adan,[‖] Francesc Mitjans,[‖] Jan Spengler,*[†,‡] and Fernando Albericio*[†,‡,⊥,§]

[†] Institute for Research in Biomedicine (IRB) Barcelona, Barcelona Science Park, Baldiri Reixac 10, 08028 Barcelona, Spain.

[‡] CIBER-BBN, Networking Centre on Bioengineering, Biomaterials and Nanomedicine, Barcelona Science Park, Baldiri Reixac 10, 08028 Barcelona, Spain.

[‖] Biomed Division, Leitat Technological Center Institution, Barcelona Science Park, Baldiri Reixac 15-21, 08028 Barcelona, Spain.

[⊥] Department of Organic Chemistry, University of Barcelona, Martí i Franqués 1-11, 08028 Barcelona, Spain.

[§] School of Chemistry & Physics, University of KwaZulua-Natal, 4001 Durban, South Africa.

* To whom correspondance may be addressed: albericio@irbbarcelona.org, jan.spengler@irbbarcelona.org
Institute for Research in Biomedicine (IRB) Barcelona, Barcelona Science Park, Baldiri Reixac 10, 08028 Barcelona, Spain.
Phone: (+34) 93 403 70 88, Fax: (+34) 93 403 71 26

TABLE OF CONTENTS GRAPHIC: We synthesized three analogs of cyclo[RGDf*N*MeV] (Cilengitide) in which its backbone *N*-Me group was replaced by *N*-oligoethylene glycol (*N*-OEG) chains of increasing size, leading to an increasingly lipophilic character. The RGD-cyclopeptide with the shorter *N*-OEG chain displayed analogous biological activity as the original peptide, whilst being more lipophilic.

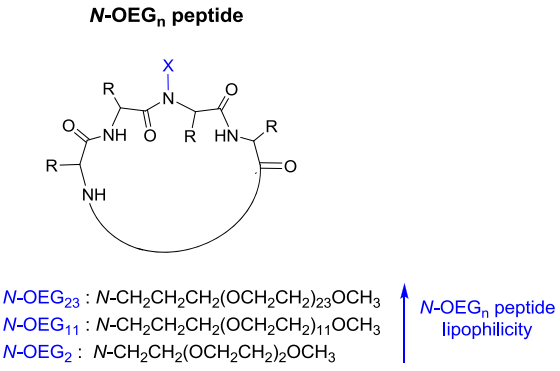

ABSTRACT: Cilengitide is an RGD-peptide of sequence cyclo[RGDf*N*MeV] that was was developed as a highly active and selective ligand for the $\alpha_v\beta_3$ and $\alpha_v\beta_5$ integrin receptors. We describe the synthesis of three analogs of this peptide in which the *N*-Me group has been replaced by *N*-oligoethylene glycol (*N*-OEG) chains of increasing size: namely *N*-OEG_2, *N*-OEG_{11}, and *N*-OEG_{23}, which are respectively composed of 2, 11 and 23 ethylene oxide monomer units. The different *N*-OEG cyclopeptides and the original peptide were compared with respect to lipophilicity and biological activity. The *N*-OEG_2 analog was straightforward to synthesize in solid-phase using an Fmoc-*N*-OEG_2 building block. The syntheses of the *N*-OEG_{11} and *N*-OEG_{23} cyclopeptides are hampered by the increased steric hindrance of the *N*-substituent, and could only be achieved by segment coupling, which takes place with epimerization and thus requires extensive product purification. All the *N*-OEG analogs were found to be more hydrophobic than the parent peptide, and their hydrophobicity was systematically enhanced upon increasing the length of the OEG chain. The *N*-OEG_2 cyclopeptide displayed the same capacity as Cilengitide to inhibit the integrin-mediated adhesion of HUVEC endothelial, DAOY gliobastoma, and HT-29 colon cancer cells to their ligands vitronectin and fibrinogen. The *N*-OEG_{11} and *N*-OEG_{23} analogs also inhibited cell adhesion to these immobilized ligands, but their EC_{50} values dropped one order of magnitude with respect to the parent peptide. These results indicate that replacement of the backbone *N*-Me group of Cilengitide by a short *N*-OEG chain provides a more lipophilic analog with a similar biological activity. Upon increasing the size of the *N*-OEG chain, liophilicity is enhanced, but synthetic yields drop and the longer polymer chains may impede targeted binding.

TEXT

In peptide-based medicinal chemistry, backbone *N*-methylation is an established tool to improve pharmacological properties of peptide drugs. The introduction of backbone *N*-Me groups has allowed to optimize the activity and selectivity of numerous peptide ligands as a result of conformational modulation.[1] Furthermore, the introduction of *N*-Me residues into peptides increases their hydrophobicity, proteolytic resistance, and membrane permeability, which can enhance their bioavailability thus amplifying their therapeutic potential.[1,2] Surprisingly, little research has been conducted on modifiying the peptide backbone with other *N*-alkyl substituents. Besides the so-called peptoids (*N*-substituted glycine oligomers)[3] and the pioneering work carried out by Gilon on *N*-backbone cyclic peptides,[4] only a few examples are reported in which other *N*-alkylated peptides have been accessed, and such examples are limited to modification with small *N*-alkyl groups [*i.e.* *N*-ethyl,[5,6] *N*-allyl,[5,7,8] *N*-butyl,[9] and *N*-guanidylbutyl[10]].

Very recently, we have shown that peptides bearing an *N*-triethylene glycol (*N*-TEG) chain are straighforward to access using standard solid-phase techniques.[11] With our methodology, we synthesized several *N*-TEG analogs of Sansalvamide A peptide, all of which were found to be slightly more lipophilic than their corresponding *N*-Me homologues. Since lipophilicity is a key pharmacological parameter,[12] we found it desirable to know if such an enhancement in lipophilicity would also be observed upon incorporation of an *N*-oligoethylene glycol (*N*-OEG) chain into other peptides. We also sought to evaluate the effect of such structural modification on biological activity more in detail. To investigate this, we chose Cilengitide (**1**) as model peptide. This peptide is an RGD-peptide of sequence cyclo[RGDf*N*MeV] that was developed as a highly active and selective ligand for the $\alpha_v\beta_3$ and $\alpha_v\beta_5$ integrin receptors.[13]

In this work, we have investigated the effect of replacing the backbone *N*-Me group of Cilengitide by different *N*-OEG chains on its lipophilicity and biological activity. Herein we describe synthesis of three analogs of **1** in which the *N*-Me group of Val has been replaced by *N*-OEG chains of increasing length; namely, *N*-OEG_2, *N*-OEG_{11} and *N*-OEG_{23}, which are respectively composed of 2, 11 and 23 repeating ethylene oxide monomer units (Figure 1).

In a first attempt to synthesize cyclopeptides **2-4**, we adopted the strategy that we had employed for the synthesis of the *N*-TEG Sansalvamide A peptide analogs. Such an approach involved the use of Fmoc-protected *N*-TEG building blocks in the solid-phase synthesis of the linear peptide precursors, which were cyclized in solution. To prepare the required Fmoc-*N*-OEG Val derivatives (**6a-6c**), valine *tert*-butyl ester was subjected to reductive alkylation with a suitable aldehyde.[14] In all cases, the reductive alkylation mixture consisted of unreacted starting material, *N*-monoalkylated product, and *N,N*-dialkylated product. The two latter were found to be inseparable, but after Fmoc-protection of the amino group, the desired products (**5a-5c**) could be isolated by flash chromatography. Remarkably, the increased length of the *N*-OEG chain did not prevent the acylation of the secondary amine with Fmoc-Cl and did not hamper the purification of **5a-5c** by flash chromatography. Finally, acidic cleavage of the *tert*-butyl ester yielded **6a-6c** in 45-54% overall yield (Scheme 1).

The solid-phase peptide synthesis (SPPS) of the linear pentapeptides **9a-9c** was performed on the 2-chlorotrityl chloride (CTC) resin by Fmoc-/^{t}Bu- chemistry (Scheme 2). The use of a low functionalization (0.2-0.3 mmol/g) was aimed to facilitate the sterically hindered coupling step.[15] In all the pentapeptides (**9a-9c**), the *N*-OEG Val residue was placed in the middle of the sequence to render Gly at the *C*-terminus, which minimizes steric hindrance during cyclization and rules out the possibility of epimerization in this step. The Fmoc-*N*-OEG Val derivatives (**6a-6c**) were coupled onto the peptidyl-resin in a 3-fold excess using DIPCDI/OxymaPure activation. With these conditions, the coupling of **6a** and **6b** took place efficiently and with no detectable epimerization, whereas the coupling of **6c** was found to be hampered by its longer *N*-OEG_{23} chain and required PyBOP/HOAt as a stronger activation method, although the coupling did not proceed to completion. After having assembled the three *N*-OEG tripeptidyl-resins, we investigated the coupling of Fmoc-D-Phe using bis(trichloromethyl)carbonate (BTC) as activating reagent.[16,17] It is important to note that this coupling is not only hampered by the *N*-substituent, but also by the β-branched side-chain of Val. With this activation method, resin-bound *N*-OEG_2 Val was completely acylated after two treatments (15 h) with the *in situ*-generated acid chloride of Fmoc-D-Phe (as checked by HPLC analysis of a cleaved resin sample). The use of BTC also allowed for coupling Fmoc-D-Phe onto resin-bound *N*-OEG_{11} Val, but the conversion was low and did not improve after a third coupling cycle. However, for the *N*-OEG_{23} peptidyl-resin, no coupling could be achieved. We tested other activation methods, but all of them failed to form the desired amide bond. Thus, we discontinued the synthesis of pentapeptide **9c** by this approach. For the resin-bound *N*-OEG_2 and *N*-OEG_{11} peptides, further peptide chain elongation and cleavage afforded the desired pentapeptides (**9a** and **9b**), which were cyclized with EDC and catalytic amounts of 4-DMAP. Cyclization proceeded smoothly and, after removal of side-chain protecting groups with 95% TFA in the presence of H_2O and TIS, the *N*-OEG_2 and *N*-OEG_{11} cyclopeptides (**2** and **3**) were isolated by semipreparative RP-HPLC.

Thus, the synthetic strategy shown in Scheme 2 allows the efficient preparation of peptides bearing an *N*-OEG chain of 2 ethylene oxide units, and enables to obtain peptides with an 11-monomer unit *N*-OEG chain, though in very low amount. However, the synthesis of our target *N*-OEG_{23} pentapeptide (**9c**) was not found feasible, since no coupling of Fmoc-D-Phe onto resin-bound *N*-OEG_{23} Val could be achieved. To avoid the difficult formation of the D-Phe-(*N*-OEG_{11})Val and D-Phe-(*N*-OEG_{23})Val amide bonds

in solid-phase, we sought to prepare suitable Fmoc-D-Phe-(*N*-OEG)Val dipeptides in solution and use them as solid-phase building blocks. To prepare the required dipeptides (**8b** and **8c**), valine *tert*-butyl ester was subjected to reductive alkylation with a suitable aldehyde, and the resulting *N*-OEG_{11} or *N*-OEG_{23} Val derivatives were reacted with the acid chloride of Fmoc-D-Phe. This procedure enabled us to obtain dipeptides **7b** and **7c** with no detectable epimerization, and acidic cleavage of the *tert*-butyl ester yielded the desired building blocks, **8b** and **8c** (Scheme 3).

In the SPPS of the *N*-OEG_{11} and *N*-OEG_{23} pentapeptides (**9b** and **9c**), dipeptides **8b** and **8c** were coupled onto the peptidyl-resin using PyBOP/HOAt activation (Scheme 4). Since these dipeptides are time-consuming to synthesize, only 1.0 equivalent was coupled. After 3 h coupling, further PyBOP (1.0 equiv.) and DIEA (1.0 equiv.) were added and the reaction was allowed to proceed overnight. These couplings proceeded with acceptable efficiency. However, epimerization of *C*-activated dipeptides can occur through various mechanisms and is known to be a major disadvantage of segment peptide synthesis.[18] In our case, considerable epimerization took place at the dipeptidic *C*-terminal Val residue. The occurrence of epimerization was confirmed by the presence of two peaks with the mass of the desired product in the HPLC spectra of a cleaved peptidyl-resin sample. The high degree of epimerization observed was expectable, as the epimerization of *C*-activated peptides is favoured by itself (no carbamate as protecting group of the *C*-terminal residue) and, in this case, by the presence of D- and/or *N*-alkyl residues.[19-21] Further peptide elongation and cleavage from resin yielded pentapeptides **9b** and **9c** epimerized at Val. After cyclization and deprotection, the desired *N*-OEG_{11} and *N*-OEG_{23} cyclopeptides (**3** and **4**) were separated from their non-desired Val epimers by semipreparative RP-HPLC. For the two isolated *N*-OEG_{11} cyclopeptides, the stereoisomer having a lower retention time was found to co-elute with stereochemically pure cyclo[RGDf(*N*-OEG_{11})V] (**3**), which had been previously prepared using Fmoc-*N*-OEG_{11} Val (**6b**) as building block. Analogously, the isolated *N*-OEG_{23} cyclopeptide with a lower RP-HPLC retention time was assumed to be the product with the desired stereochemistry, cyclo[RGDf(*N*-OEG_{23})V] (**4**) (see Supporting Information).

To study the effect of the *N*-OEG chain on lipophilicity, we co-injected the *N*-OEG cyclopeptides (**2-4**) and cyclo[RGDf*N*MeV] (**1**) onto a C18 column and we compared their RP-HPLC retention times.[22] This is reported as a reliable method to estimate the relative hydrophobicities of a series of modified analogs.[23] The RP-HPLC behaviour of a compound depends on its hydrophobic interactions with the non-polar stationary phase: the more hydrophobic a compound is, the stronger its retention on the column. All the *N*-OEG analogs (**2-4**) were found to be more lipophilic than **1**, and their lipophilicity was systematically enhanced upon increasing the size of the *N*-OEG chain (Figure 2). These results can be explained by the amphiphilic nature of OEG.[24-25] Although OEG-modified peptides often show better aqueous solubility than their corresponding non-modified peptides, this is due to the polymer chain preventing intermolecular aggregation, and not due to an increase in hydrophilicity.[26,27] Along these lines, the attachment of an OEG chain to peptides can improve their solubility in organic solvents.[27-29]

Our findings upon incorporation of *N*-OEG into Cilengitide, which has two ionizable side-chain functionalities, are consistent with our previously reported findings for the *N*-OEG analogs of the totally aliphatic Sansalvamide A peptide: for both model peptides, replacement of a backbone *N*-Me group by an *N*-OEG chain provides a higher lipophilicity. Therefore, we can reasonably expect that *N*-Me-for-*N*-OEG substitution will also increase lipophilicity for other *N*-methylated peptide scaffolds. Such an enhancement in lipophilicity can be conveniently exploited for improving the absorption of peptide drug candidates that are too hydrophilic to cross biological membranes via transcellullar passive diffusion,[30,31] which is the most common transport route for peptides. Indeed, the covalent modification of peptides by attaching lipophilic moieties has proved to be an effective approach to improve their intestinal permeability[32-36] and oral bioavailability.[37,38]

The parent peptide, cyclo[RGDf*N*MeV] (**1**), and its *N*-OEG analogs (**2-4**) showed no degradation when incubated in human serum at 37 ºC over a period of 48 h (see Supporting Information). The high enzymatic stability of **1-4** was expected, since cyclic peptides show increased resistance to proteolytic cleavage, and the presence of D- and *N*-alkyl residues confers them further stability.[39]

The biological activities and selectivities of cyclo[RGDf*N*MeV] (**1**) and the *N*-OEG cyclopeptides (**2-4**) were evaluated in cell adhesion inhibition assays (Table 1). Adhesion studies were carried out with HUVEC endothelial, DAOY glioblastoma and HT-29 colon cancer cells using vitronectin (VN) or fibrinogen (FB) as ligands. For HUVEC and DAOY cells, adhesion to their ligand VN is mediated by integrins $\alpha_v\beta_3$ and $\alpha_v\beta_5$, whereas their adhesion to FB is only mediated by integrin $\alpha_v\beta_3$. In contrast, the adhesion of HT-29 cells to VN is only $\alpha_v\beta_5$-dependent. For all the cell/ligand systems, the compounds inhibited cell adhesion in a concentration-dependent manner, resulting in the expected sigmoid curves. The inhibitory activities of the *N*-OEG_2 cyclopeptide (**2**) were very similar to those of **1**, which indicates that replacement of its *N*-Me group by a short *N*-OEG_2 chain does not affect binding affinity. In contrast, the *N*-OEG_{11} and *N*-OEG_{23} analogs (**3** and **4**) inhibited cell adhesion with less potency, which is probably due their longer OEG chains interfering with the RGD-receptor interaction. Indeed, the reduced biological activity of peptides upon attachment of a bulky polymer chain is an issue of major concern, especially in the case of small peptides.[40]

In summary, the analog of Cilengitide bearing an *N*-OEG_2 chain instead of a backbone *N*-Me group (**2**) was straightforward to synthesize in solid-phase. The acylation of resin-bound *N*-OEG_2 amines can be achieved by activating the following amino acid with

BTC, and the protocol is compatible with the acid-labile CTC resin. However, for resin-bound *N*-OEG_{11} and *N*-OEG_{23} residues, this method does not work. The increased sterical hindrance of their *N*-substituents impedes the acylation in solid-phase (1 and 10 atom-chains for **1** and **2**, versus 38 and 74 atom-chains for **3** and **4**). We were able to obtain the *N*-OEG_{11} and *N*-OEG_{23} cyclopeptides (**3** and **4**) by using a dipeptidic building block, but considerable epimerization took place during dipeptide coupling, and extensive RP-HPLC purification was required to separate the desired cyclic products from their non-desired diastereoisomers.

All the *N*-OEG analogs (**2-4**) were found to be more hydrophobic than the parent peptide (**1**), and their hydrophobicity was systematically enhanced upon increasing the length of the OEG chain. The *N*-OEG_2 cyclopeptide (**2**) displayed the same capacity as Cilengitide (**1**) to inhibit integrin-mediated cell adhesion, but the inhibitory activities of the *N*-OEG_{11} and *N*-OEG_{23} cyclopeptides (**3** and **4**) were one order of magnitude lower. Taken together, the results show that, in the case of the cyclic pentapeptide Cilengitide, substitution of a backbone *N*-Me group by a short *N*-OEG chain provides a more lipophilic analog with a similar biological activity. Upon increasing the length of the OEG chain, lipophilicity is enhanced, but the synthesis is not efficient and steric hindrance may impede targeted binding. Thus, replacement of a backbone *N*-Me group by a short *N*-OEG chain is a feasible way to enhance the lipophilicity of peptide drug candidates, which can result in a better membrane permeability via passive diffusion, and may not have a negative impact on biological activity. Considering that backbone *N*-Me groups are common structural motifs in many biologically active peptides, we want to communicate that modification at this position is a valuable alternative to introduce chemical diversity or alter pharmacologically important parameters when modification at any other position of the peptide is not wished or possible.

ACKNOWLEDGEMENTS. This work was partially supported by CICYT (CTQ2012-30930) and the Generalitat de Catalunya (2009SGR 1024). The Institute for Research in Biomedicine (IRB) Barcelona, the Barcelona Science Park, and Leitat Technological Center are also acknowledged for their support. Ana I. Fernández-Llamazares thanks Ministerio de Educación y Ciencia for a FPU fellowship. We thank Barcelona Science Park (Mass Spectrometry Core Facility, Nuclear Magnetic Resonance Unit) for the facilities.

SUPPORTING INFORMATION AVAILABLE. Experimental details of the syntheses, cellular assays, serum stability assays, characterization data, HPLC traces and HRMS data of the pure cyclopeptides (**1-4**), and copies of the NMR spectra of selected compounds are provided in the Supporting Information. This material is available free of charge via the Internet at http://pubs.acs.org.

ABBREVIATIONS. 4-DMAP, 4-dimethylaminopyridine; ACN, acetonitrile; BTC, bis(trichloromethyl)carbonate; CTC, 2-chlorotrityl chloride; DIEA, *N,N'*-diisopropylethylamine; *N,N'*-diisopropylcarbodiimide; EDC·HCl, 1-ethyl-3-(3-dimethylaminopropyl)carbodiimide hydrochloride; FB, fibrinogen; MeOH, methanol; OEG, oligoethylene glycol; OxymaPure, ethyl-2-cyano-2-(hydroxyimino)acetate; TEG, triethylene glycol; VN, vitronectin.

REFERENCES AND FOOTNOTES

(1) Chatterjee, J., Gilon, C., Hoffman, A., and Kessler, H. (2008) *N*-methylation of peptides: a new perspective in medicinal chemistry. *Acc. Chem. Res. 10*, 1331-1342.

(2) Chatterjee, J., Rechenmacher, F. and Kessler, H. (2013) *N*-Methylation of peptides and proteins: an important element for modulating biological functions. *Angew. Chem., Int. Ed. 52*, 254-269.

(3) Olsen, C. A. (2010) Peptoid-peptide hybrid backbone architectures. *ChemBioChem 11*, 152-160.

(4) Gilon, C., Halle, D., Chorev, M., Selinger, Z., and Byk, G. (1991) Backbone cyclization: a new method for conferring conformational constraint on peptides. *Biopolymers 31*, 745−750.

(5) Reichwein, J. F., and Liskamp, R. M. J. (1998) Site-specific *N*-alkylation of peptides on the solid phase. *Tetrahedron Lett. 39*, 1243-1246.

(6) Hubler, F., Rückle, T., Patiny, L., Muamba, T., Guichou, J.-F., Mutter, M., and Wenger, R. (2000) Synthetic routes to *N*EtXaa4-cyclosporin A derivatives as potential anti-HIV I drugs. *Tetrahedron Lett*. *41*, 7193-7196.

(7) Reichwein, J. F., Versluis, C., and Liskamp, R. M. J. (2000) Synthesis of cyclic peptides by ring-closing metathesis. *J. Org. Chem. 65,* 6187-6195.

(8) Patgiri, A., Witten, M. R., and Arora, P. S. (2010) Solid phase synthesis of hydrogen bond surrogate derived α-helices: resolving the case of a difficult amide coupling. *Org. Biomol. Chem. 8*, 1773-1776.

(9) Rijkers, D. T. S., Höppener, J. W. M., Posthuma, G., Lips, C. J. M., and Liskamp, R. M. J. (2002) Inhibition of amyloid fibril formation of human amylin by *N*-alkylated amino acid and α-hydroxy acid residue containing peptides. *Chem. Eur. J. 8*, 4285-4291.

(10) Ying, J., Gu, X., Cai, M., Dedek, M., Vagner, J., Trivedi, D. B., and Hruby V. J. (2006) Design, synthesis, and biological evaluation of new cyclic melanotropin peptide analogues selective for the human melanocortin-4 receptor. *J. Med. Chem. 49,* 6888-6896.

(11) Fernández-Llamazares, A. I., García, J., Soto-Cerrato, V., Pérez-Tomás, R., Spengler, J., and Albericio, F. (2013) *N*-triethylene glycol (*N*-TEG) as a surrogate for the *N*-methyl group: application to Sansalvamide A peptide analogs. *Chem. Commun. 49*, 6430-6432.

(12) Arnott, J. A., and Planey, S. L. (2012) The influence of lipophilicity in drug discovery and design. *Expert. Opin. Drug. Discov. 7*, 863-875.

(13) Mas-Moruno, C., Rechenmacher, F., and Kessler, H. Cilengitide: the first anti-angiogenic small molecule drug candidate. Design, synthesis and clinical evaluation. (2010) *Anti-cancer Agents. Me*. *10*, 753-768.

(14) $CH_3O(CH_2CH_2O)_2CH_2CHO$ is straightforward to access by oxidation of triethylene glycol monomethyl ether, whereas $CH_3O(CH_2CH_2O)_{11}CH_2CH_2CHO$ and $CH_3O(CH_2CH_2O)_{23}CH2CH_2CHO$ are commercially available.

(15) Tam, J. P., and Lu, Y.-A. Coupling difficulty associated with interchain clustering and phase transition in solid phase peptide synthesis. (1995) *J. Am. Chem. Soc*. *117*, 1058-12063.

(16) Thern, B., Rudolph, J., and Jung, G. (2002) Total synthesis of the nematicidal cyclododecapeptide Omphalotin A by using racemization-free triphosgene-mediated couplings in the solid phase. *Angew. Chem., Int. Ed. 41*, 2307-2309.

(17) Thern, B., Rudolph, J., and Jung, G. (2002) Triphosgene as highly efficient reagent for the solid-phase coupling of *N*-alkylated amino acids - total synthesis of cyclosporin O. *Tetrahedron Lett. 43*, 5013-5016.

(18) Lloyd-Williams, P., Albericio, F., and Giralt, E. (1997) *Chemical approaches to the synthesis of peptides and proteins*, CRC Press (Boca Raton), FL.

(19) El-Faham, A., and Albericio, F. (2011) Peptide coupling reagents, more than a letter soup. *Chem. Rev.111*, 6557-6602.

(20) Gund, P., and Veber, D. F. (1979) On the ease of base-catalyzed epimerization of *N*-methylated peptides and diketopiperazines. *J. Am. Chem. Soc. 101*, 1885-1887.

(21) Steinberg, S., and Bada, J. L. (1981) DKP formation during investigations of amino acid racemization in dipeptides. *Science 213*, 544-545.

(22) In order to evaluate the lipophilicity of our compounds, comparison of their RP-HPLC retention parameters was found to be preferrable to comparison of their octanol/water coefficients determined by the shake-flask method. Determination of the octanol/water coefficients by the shake-flask method is not very accurate and requires a higher amount of sample.

(23) Valkó, K. (2004) Application of high-performance liquid chromatography based measurements of lipophilicity to model biological distribution. *J. Chromatogr. A 1037*, 299-310.

(24) Gaberc-Porekar, V., Zore, I., Podobnik, B., and Menart, V. (2008) Obstacles and pitfalls in the PEGylation of therapeutic proteins. *Curr. Opin. Drug Discov*. *11*, 242-250.

(25) M. C. Parrott and J. M. DeSimone. (2012) Relieving PEGylation. *Nat. Chem*. *4*, 13-14.

(26) Mueller, C., Capelle, M. A. H., Arvinte, T., Seyrek, E., and Borchard, G. (2011) Tryptophan-mPEGs: Novel excipients that stabilize salmon calcitonin against aggregation by non-covalent PEGylation. *Eur. J. Biopharm. 79*, 646-657.

(27) Veronese, F. M. (2001) Peptide and protein PEGylation: a review of problems and solutions. *Biomaterials*, *22*, 405-417. b)

(28) Wirth, P., Souppe, J., Tritsch, D., and Biellmann, J.-F. (1991) Chemical modification of horseradish peroxidase with ethanal-methoxypolyethylene glycol: solubility in organic solvents, activity and properties. *Bioorg. Chem. 19*, 133-142.

(29) Grun, J., Revell, J. D., Conza, M. and Wennemers, H. (2006) Peptide-polyethylene glycol conjugates: synthesis and properties of peptides bearing a C-terminal polyethylene glycol chain. *Bioorg. Med. Chem. 14*, 6197-6201.

(30) Camenisch, G., Alsenz, J., van de Waterbeemd, H., and Folkers, G. (1998) Estimation of permeability by passive diffusion through Caco-2 cell monolayers using the drugs' lipophilicity and molecular weight. *Eur. J. Pharm. Sci. 6*, 313-319.

(31) Goldberg, M., and Gómez-Orellana, I. (2003) Challenges for the oral delivery of macromolecules. *Nat. Rev. Drug Disc. 2*, 289-295.

(32) Yamada, K., Murakami, M., Yamamoto, A., Takada, K., and Muranishi, S. (1992) Improvement of intestinal absorption of thyrotropin-releasing hormone by chemical modification with lauric acid. *J. Pharm. Pharmacol. 44*, 717-721.

(33) Hashizume, M., Douen, T., Murakami M., Yamamoto, A., Takada, K., and Muranishi, S. (1992) Improvement of large intestinal absorption of insulin by chemical modification with palmitic acid in rats. *J. Pharm. Pharmacol. 44*, 555-559.

(34) Yodoya, E., Uemura, K. Tenma, T., Fujita, T., Murakami, M., Yamamoto, A., and Muranishi, S. (1994) Enhanced permeability of tetragastrin across the rat intestinal membrane and its reduced degradation by acylation with various fatty acids. *J. Pharmacol. Exp. Ther. 271*, 1509-1513.

(35) Asada, H., Douen, T., Waki, M., Adachi, S., Fujita, T., Ymamoto, A., and Muranishi, S. (1995) Absorption characteristics of chemically modified-insulin derivatives with various fatty acids in the small and large intestine. *J. Pharm. Sci. 84*, 682-687.

(36) Uchiyama, T., Kotani, A., Tatsumi, H., Kishida, T., Okamoto, A., Okada, N., Murakami, M., Fujita, T., Fujiwara, Y., Kiso, Y., Muranishi, S., and Yamamoto, A. (2000) Development of novel lipophilic derivatives of DADLE (leucine enkephalin analogue): intestinal permeability characateristics of DADLE derivatives in rats. *Pharm. Res. 17*, 1461-1467.

(37) Lee, Y., Nam, J. H., Shin, H. C., and Byun, Y. (2001) Conjugation of low-molecular-weight heparin and deoxycholic acid for the development of a new oral anticoagulant agent. *Circulation 104*, 3116–3120.

(38) Clement, S., Still, J. G., and Kosutic, G. (2002) Oral insulin product hexyl-insulin monoconjugate 2 (HIM2) in type 1 diabetes mellitus: the glucose stabilization effects of HIM2. *Diabetes Technol. Ther. 4*, 459-466.

(39) Royo, S., Gaus, K., and N. Sewald. (2009) Synthesis of chemically modified bioactive peptides: recent advances, challenges and developments for medicinal chemistry. *Future Med. Chem. 1,* 1289-1310.

(40) Veronese, F. M., and Mero, A. (2008) The impact of PEGylation on biological therapies. *Biodrugs 22*, 315-329.

TABULAR MATERIAL AND GRAPHICS

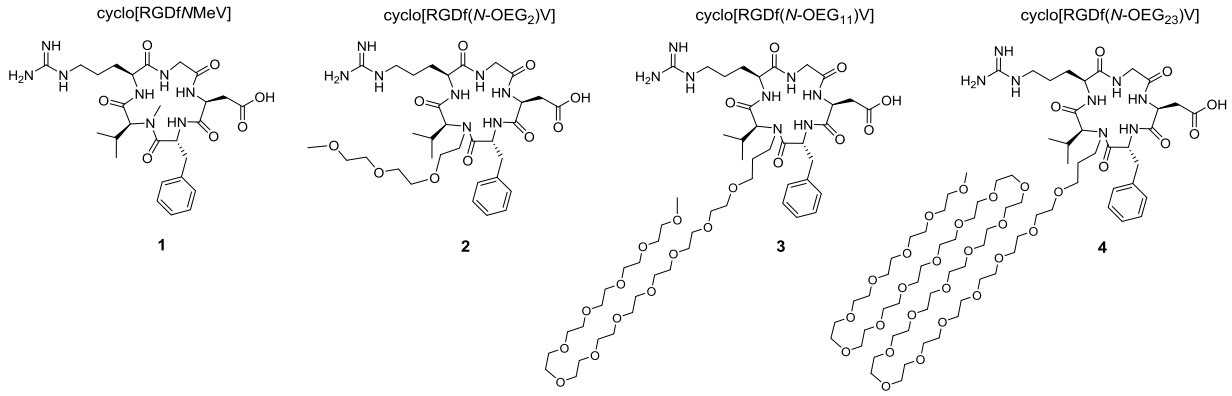

Figure 1. Structure of cyclo[RGDf*N*MeV] (**1**) and the *N*-OEG cyclopeptides (**2-4**) synthesized and tested.

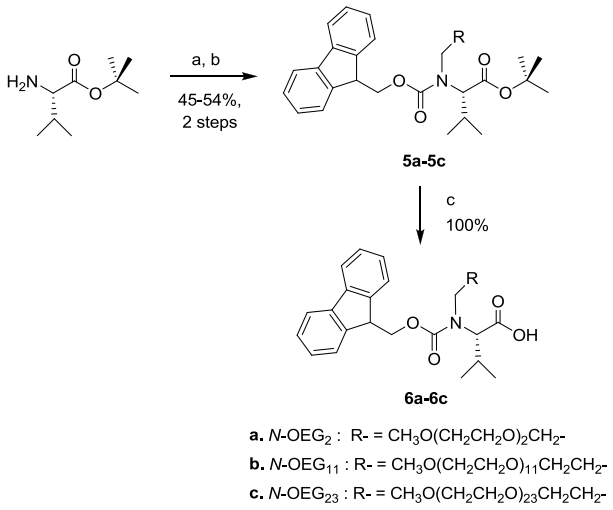

Scheme 1. Synthesis of the Fmoc-*N*-OEG Val derivatives (**6a-6c**). Reagents and conditions: a. R-CHO (1.1 eq), $NaBH_3CN$ (1.34 eq), MeOH/AcOH 99:1; b. Fmoc-Cl (1.2 eq), DIEA (2.0 eq), DCM; c. TFA/DCM 1:1.

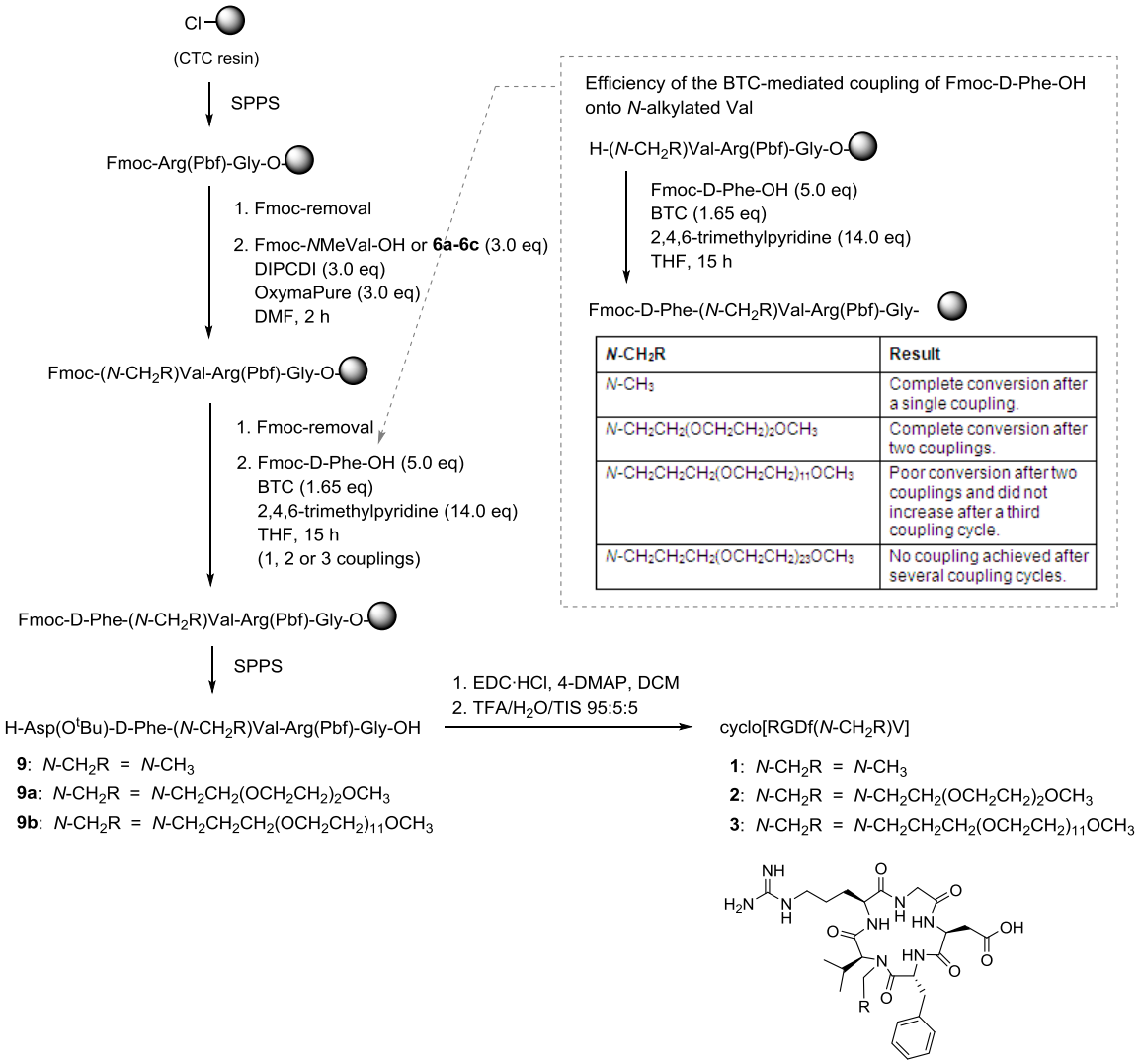

Scheme 2. Synthesis of cyclo[RGDf*N*MeV] (**1**) and the *N*-OEG cyclopeptides **2-3**.

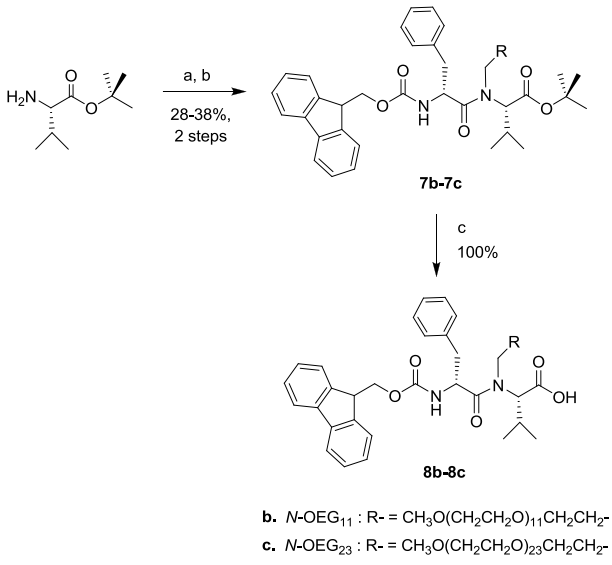

Scheme 3. Synthesis of the Fmoc-D-Phe-(*N*-OEG)Val dipeptides (**8b-8c**). Reagents and conditions: a. R-CHO (1.1 eq), $NaBH_3CN$ (1.34 eq), MeOH/AcOH 99:1; b. Fmoc-D-Phe-Cl (1.5 eq), DIEA (2.5 eq), DCM; c. TFA/DCM 1:1.

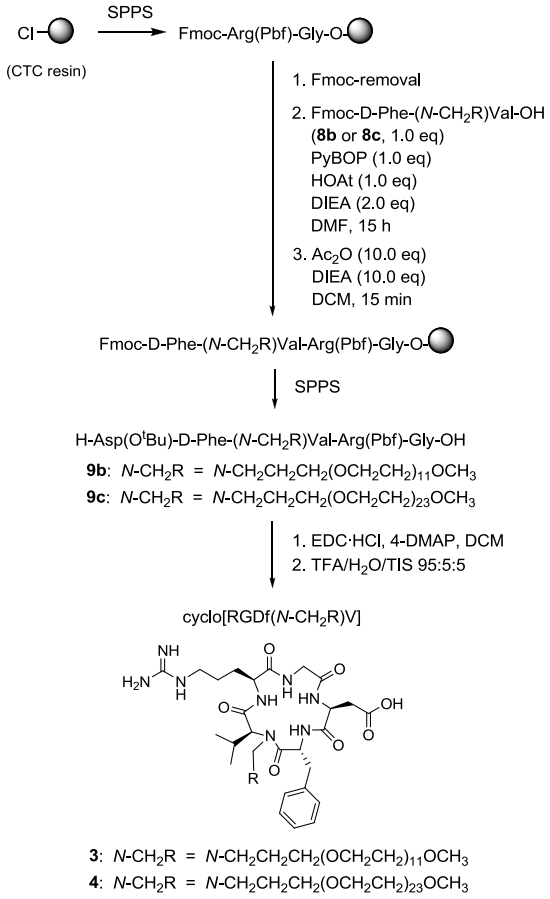

Scheme 4. Synthesis of the *N*-OEG cyclopeptides **3-4** using a dipeptide building block.

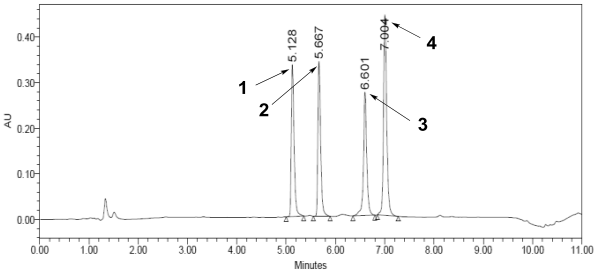

Figure 2. HPLC chromatogram obtained after co-injection cyclo[RGDf*N*MeV] (**1**) and the *N*-OEG cyclopeptides (**2-4**) on a C18 column, linear gradient from 10% to 50% ACN over 8 min.

Table 1. Adhesion inhibition assays of cyclo[RGDf*N*MeV] (**1**) and the *N*-OEG cyclopeptides (**2-4**). IC_{50} values are given in μM.

Compound	Vitronectin (VN)			Fibrinogen (FB)	
	HUVEC on VN $\alpha_v\beta_3 + \alpha_v\beta_5$	DAOY on VN $\alpha_v\beta_3 + \alpha_v\beta_5$	HT-29 on VN $\alpha_v\beta_5$	HUVEC on FB $\alpha v\beta_3$	DAOY on FB $\alpha_v\beta_3$
cyclo[RGDf*N*MeV] (**1**)	0.37	2.69	3.11	0.076	0.44
cyclo[RGDf(*N*-OEG_2)V] (**2**)	0.42	3.62	2.17	0.036	0.14
cyclo[RGDf(*N*-OEG_{11})V] (**3**)	12.42	171.5	n.d.	1.38	4.55
cyclo[RGDf(*N*-OEG_{23})V] (**4**)	22.30	143.1	n.d.	0.28	2.31

Paper VI: A. I. Fernández-Llamazares, J. Spengler and F. Albericio. The potential of *N*-alkoxymethyl groups as peptide backbone protectants. Submitted to *Tetrahedron Lett.*

ELSEVIER

Tetrahedron Letters
journal homepage: www.elsevier.com

The potential of *N*-alkoxymethyl groups as peptide backbone protectants

Ana I. Fernández-Llamazares[a,b], Jan Spengler[*a,b] and Fernando Albericio[*a,b,c,d]

[a] *Institute for Research in Biomedicine, Barcelona Science Park, Baldiri Reixac 10, 08028 Barcelona, Spain.*
[b] *CIBER-BBN, Networking Centre on Bioengineering, Biomaterials and Nanomedicine, PCB, Baldiri Reixac 10, 08028 Barcelona, Spain.*
[c] *Department of Organic Chemistry, University of Barcelona, Martí i Franqués 1-11, 08028 Barcelona, Spain.*
[d] *School of Chemistry & Physics, University of KwaZulu-Natal, 4001 Durban, South Africa.*

ARTICLE INFO

Article history:
Received
Received in revised form
Accepted
Available online

Keywords:
N-alkoxymethyl
Backbone protecting groups
Backbone *N*-alkylation
SPPS
Peptides

ABSTRACT

In this study, the potential of *N*-alkoxymethyl groups as protectants for the peptide backbone has been investigated. These groups were found to be compatible with the standard conditions of Fmoc/^{t}Bu SPPS, and can be cleaved off from the peptide backbone by acids. However, the main issue for their application as protecting groups is the difficulty to incorporate them into the peptide backbone.

1. Introduction

In organic synthesis, alkoxymethyl (Aom) moieties have found many applications as *OH*-protecting groups, and have also been used as *NH*-protectants. Aom groups that have been used for *NH*-protection include methoxymethyl (Mom), benzyloxymethyl (Bom), *tert*-butyloxymethyl (Bum), 2-adamantyloxymethyl (2-Adom), trimethylsilylethoxymethyl (Sem), and (2,2,2,-trichloroethoxy)methyl.[1,2] Due to the extreme sensitivity of *N,O*-acetals to hydrolysis, such Aom groups are not suitable for the protection of simple amines; however, they can be used to protect nitrogen atoms embedded in amides, carbamates, or aromatic heterocycles (*e.g.* indole, pyrrole, imidazole, phtalimide, and derivatives), as the resulting *N*-CH_2-*O* bond is significantly stabilized due to delocalisation and electron withdrawing effects.[2] For such *NH* functionalities, their *N*-Aom derivatives are resistant to bases and nucleophiles, and can generally be cleaved by acids, though certain *N*-Aom substituents also allow for hydrogenolytic or reductive cleavage.

In the literature there are only two examples in which backbone *N*-Aom peptides have been accessed. In one, the authors describe the preparation of Fmoc-(*N*-Mom)Gly by acid-catalyzed condensation of Fmoc-Gly with paraformaldehyde and MeOH. With this building block, the tripeptide Fmoc-(*N*-Mom)Gly-(*N*-Mom)Gly-Val-OBz was obtained in solution, but no yields are given (Scheme 1, entry A).[3] The other reported synthetic route towards backbone *N*-Mom peptides involves *N*-trialkylsilylmethyl amino acids. These intermediates can be acylated in solution, yielding *N*-substituted dipeptides onto which further amino acids can be assembled. Backbone *N*-trimethylsilylmethyl groups can be electrochemically oxidized to *N*-acyliminium ions, which can be trapped with a methanol to yield an *N*-Mom-substituted peptide. Alternatively, (2,4-dimethoxyphenyl)-substituted *N*-silylmethyl groups can be converted to *N*-Mom by chemical oxidation (Scheme 1, entry B).[4]

Although the scope of *N*-Aom groups as peptide backbone protectants is so far not demonstrated, their stability profile should be compatible with the neutral and basic conditions of Fmoc/^{t}Bu SPPS protocols, and should allow for cleavage under the acidic conditions employed for peptide cleavage from resin and/or side chain deprotection. In this study we investigate the feasibility of an alternative access to backbone *N*-Aom peptides, and a first evaluation of their stability under Fmoc/^{t}Bu SPPS conditions.

2. Results and discussion

Since the synthesis of *N*-Aom-substituted peptides through a stepwise strategy (Scheme 1A) appears to be more straightforward than the multistep approach via *N*-silanylmethylated intermediates to be oxidized at a late stage of the synthesis (Scheme 1B), we decided to prepare Fmoc-(*N*-Aom) amino acid building blocks. However, the acid-catalyzed condensation of Fmoc-Gly with paraformaldehyde and MeOH, which is reported as a method to obtain Fmoc-(*N*-Mom)Gly,[3] failed in our hands to give acceptable yields when other amino acids and alcohols were tested. Another possible approach towards Fmoc-(*N*-Aom)Xaa-OH would be the *N*-alkylation of an amino acid ester with an alkyl chloromethyl ether. However, alkyl chloromethyl ether reagents are highly toxic and only few

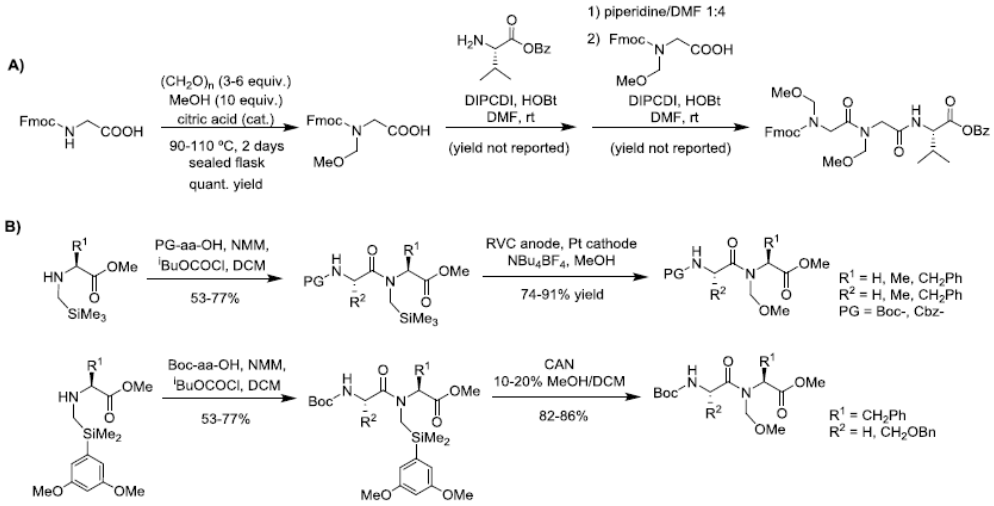

Scheme 1. Reported syntheses of *N*-Aom-substituted peptides. **A)** Synthesis of Fmoc-(*N*-Mom)Gly-(*N*-Mom)Gly-Val-OBz.[3] **B)** Synthesis of *N*-Mom-substituted dipeptides via *N*-silanylmethylated intermediates.[4]

are readily available. An alternative appeared a protocol that involves *N*-chloromethyl amino acid derivatives as reactive intermediates. It is reported that hexafluoracetone (HFA)-protected amino acids, paraformaldehyde, and thionyl chloride undergo a three-component reaction to give *N*-chloromethyl HFA-protected amino acids in excellent yields.[5] These compounds react with *P*-, *C*-, and *H*-nucleophiles to yield *N*-phosphonomethyl,[6] *N*-ethyl,[7] and *N*-methyl derivatives,[5] respectively. Inspired by this, we envisioned that the nucleophilic reaction of an Fmoc-(*N*-chloromethyl) amino acid ester with an alcohol could be a feasible way to prepare Fmoc-(*N*-Aom) building blocks.

We found that Fmoc-amino acid *p*-nitrobenzyl (Pnb) esters are smoothly converted to the corresponding *N*-chloromethyl derivatives upon reaction with paraformaldehyde and thionyl chloride, as observed by ^{1}H-NMR monitorisation of the reaction mixture. Remarkably, the resulting Fmoc-(*N*-CH_2Cl)Xaa-OPnb are sufficiently stable to be isolated by simple aqueous washings and obtained in high purity. The ^{1}H-NMR spectrum of these products features a new signal at 5.4 ppm corresponding to 2H, that replaces the signal corresponding to the carbamate proton.[8] Obviously, this protocol does not tolerate acid-sensitive protecting groups, but allows to obtain the *N*-chloromethyl derivatives of Pnb-esters of Fmoc-Gly, Ala, Leu, and Val in quantitative yields.

The reaction of Fmoc-(*N*-chloromethyl) amino acid esters with alcohols was found to be an efficient way to obtain Fmoc-(*N*-Aom) building blocks. In the presence of $NaHCO_3$ and catalytic amounts of DMAP, this reaction proceeds smoothly upon simple stirring of the *N*-chloromethylated amino acid derivative and the alcohol in DCM at room temperature. The *N*-Aom-substituted compounds derived from *tert*-butanol (*N*-Bum), benzyl alcohol (*N*-Bom), and triethylene glycol monomethyl ether (*N*-Tegom) were obtained in 57-81% isolated yield (flash chromatography). After removal of the Pnb ester group by hydrogenolysis or reduction with $SnCl_2$, the Fmoc-(*N*-Aom)Xaa-OH building blocks can be obtained as stable compounds in good overall yields (Scheme 2).[8]

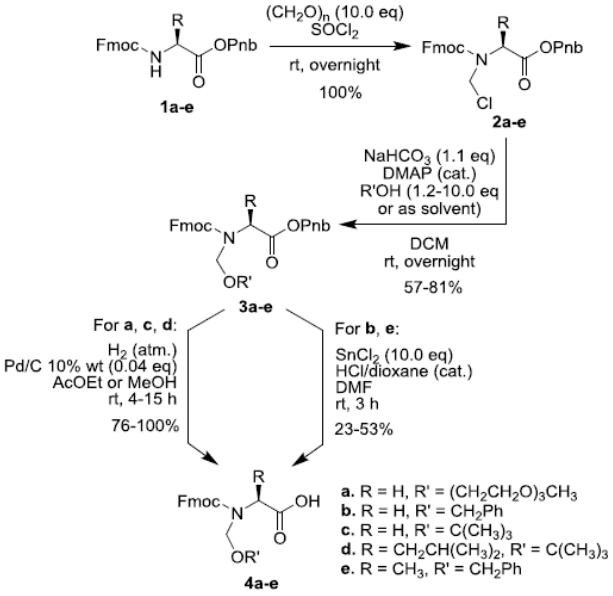

Scheme 2. Synthesis of Fmoc-(*N*-Aom) amino acids.

The usefulness of Fmoc-(*N*-Aom)Xaa-OH building blocks in stepwise SPPS depends on the viability of acylating *N*-Aom amines on solid phase. To investigate this, we chose (*N*-Tegom)Gly. This choice stems from the potential of *N*-Tegom for disrupting intramolecular aggregation throughout the peptide chain.[9] To a Gly-loaded 2-chlorotrityl chloride (CTC) resin was coupled Fmoc-(*N*-Tegom)Gly (**4a**) by DIPCDI/OxymaPure activation. A control cleavage with 2% TFA in DCM confirmed the stability of the *N*-Tegom group under these coupling conditions. After Fmoc-removal, a ninhydrin test did not give the blue color that is usually observed when primary amino groups are present. This indicates that the amine-bound *N*-Tegom moeity is stable to the standard treatments with 20% piperidine in DMF employed for Fmoc-elimination. However, most of the activation methods tested for the coupling of an amino acid (Fmoc-Leu) onto the *N*-Tegom-amine rendered exclusively the peptide without the *N*-Tegom group (Fmoc-Leu-Gly-Gly). Only when

employing an *in situ*-generated Fmoc-amino acid chloride (BTC/2,4,6-trimethylpyridine activation),[10] a partial acylation of the *N*-Tegom amine could be achieved, giving a 4:1 mixture of Fmoc-Leu-Gly-Gly-OH and Fmoc-Leu-Gly-(*N*-Tegom)Gly-OH, as confirmed by HPLC-MS (Scheme 3).

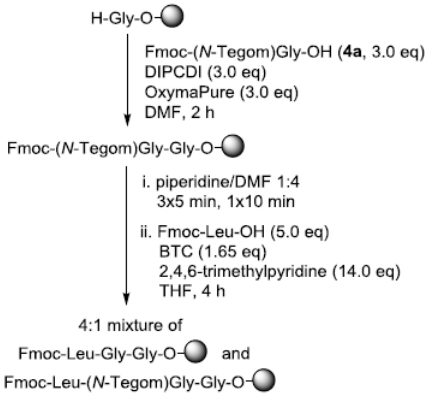

Scheme 3. Loss of the *N*-Tegom group during the coupling of Fmoc-Leu onto an H-(*N*-Tegom)Gly-Gly-resin.

Taken together, these results show that the acylation of a *N*-Tegom amine on solid phase is hampered by the steric hindrance exerted by the *N*-substituent, and that *N*-Aom amines decompose in the coupling reaction mixture prior to acylation. Thus, we reasoned that a stepwise SPPS approach using Fmoc-(*N*-Aom) amino acid building blocks would hardly be a practicable method to introduce *N*-Aom groups into peptides.

In order to circumvent the difficult acylation of *N*-Aom amines, we sought to apply our chloromethylation/substitution protocol to a suitably protected dipeptide segment to obtain Fmoc-(*N*-Aom)Xaa-(*N*-Aom)Yaa-OH. After coupling such a segment to the solid phase, the peptide chain can be further elongated using standard conditions. The *N*-terminal *N*-Aom group will be lost after Fmoc-removal and coupling of the subsequent amino acid, but the *N*-Aom group in the middle position should be preserved, as amide-bound *N*-Aom groups are known to be stable to bases and nucleophiles.

To test this notion, we initially chose Alloc-(*N*-Tegom)Leu-(*N*-Tegom)Gly-OH (**5**) as model segment. We found that Alloc-Leu-Gly-OPnb undergoes double *N*-chloromethylation upon treatment with $SOCl_2/(CH_2O)_n$. This dipeptide was converted into its *N,N'*-dichloromethyl derivative, and subsequent reaction with triethylene glycol monomethyl ether enabled us to obtain Alloc-(*N*-Tegom)Leu-(*N*-Tegom)Gly-OPnb (Scheme 4, entry A). However, a hydrogenolytic removal of the *C*-terminal Pnb ester was not found feasible. Reductive cleavage of Pnb with $SnCl_2$ yielded the desired product (**5**), but its separation from Sn salts and *p*-aminotoluene was difficult. To avoid these contaminations, we changed the *C*-terminal Pnb ester for a methyl ester (Scheme 4, entry B). Alloc-Leu-Gly-OMe (**6**) was subjected to the *N*-chloromethylation conditions, and the *N,N'*-dichloromethylated intermediate (**7**) was reacted with triethylene glycol monomethyl ether. Unfortunately, undesired transesterification at the *C*-terminus took place during this nucleophilic substitution step. In contrast, the use of ethanol as nucleophilic alcohol was found to render the expected dipeptide, Alloc-(*N*-Etom)Leu-(*N*-Etom)Gly-OMe (**8**). Saponification of its methyl ester furnished Alloc-(*N*-Etom)Leu-(*N*-Etom)Gly-OH (**9**), though in low overall yield (20% 3-step yield from dipeptide **6**).

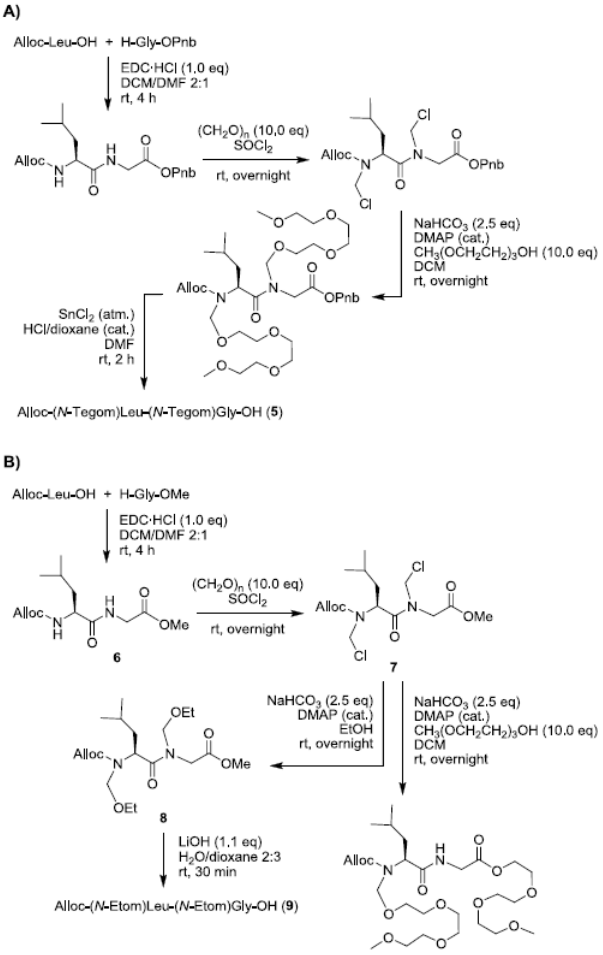

Scheme 4. A) Synthesis of Alloc-(*N*-Tegom)Leu-(*N*-Tegom)Gly-OH (**5**). **B)** Synthesis of Alloc-(*N*-Etom)Leu-(*N*-Etom)Gly-OH (**9**).

We observed that the synthesis of *N,N'*-diAom-substituted dipeptides seems to proceed with lower yields than the synthesis of Fmoc-(*N*-Aom) amino acids. Furthermore, the double *N*-chloromethylation/substitution protocol is limited to dipeptides having a *C*-terminal Gly. Protected Leu-Leu, Gly-Leu, Ala-Ala dipeptides rendered the corresponding mono-*N*-substituted dipeptides as major products.

To investigate the use of *N,N'*-diAom-substituted dipeptides as segments for SPPS, we coupled dipeptide **9** onto a Phe-loaded CTC resin, and the resulting Alloc-(*N*-Etom)Leu-(*N*-Etom)Gly-Phe-resin was subjected to two coupling cycles. In the first cycle, the Alloc- group was removed with catalytic Pd(0) and Fmoc-Leu was coupled. In the second coupling cycle, the *N*-terminus was deprotected with 20% piperidine in DMF and Fmoc-Gly was coupled, which rendered Fmoc-Gly-Leu-Leu-(*N*-Etom)Gly-Phe-OH, as confirmed by HPLC-MS analysis of a cleaved resin sample (Scheme 5). On the basis of these findings, *N*-Aom groups attached to the peptide backbone can be expected to be stable under conditions employed in Fmoc/^{t}Bu SPPS protocols.

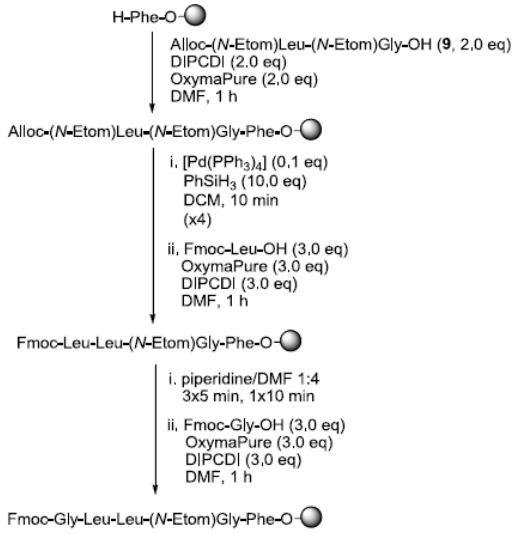

Scheme 5. Synthesis of resin-bound Fmoc-Gly-Leu-Leu-(*N*-Etom)Gly-Phe-OH using using Alloc-(*N*-Etom)Leu-(*N*-Etom)Gly-OH (**9**) as building block.

We observed that cleaved samples (2% TFA) of *N*-Etom-substituted peptides dissolved in ACN/H_2O undergo slow degradation to their corresponding non-substituted peptides, probably due to the presence of acid traces (HPLC-MS). We checked the stability of backbone *N*-Aom groups against acids with Alloc-(*N*-Etom)Leu-(*N*-Etom)Gly-OPnb. This dipeptide was found to be stable over 15 days in aqueous buffers at pH 3.9, 7.0 and 9.2, except for slow hydrolysis of the Pnb ester. In contrast, it undergoes rapid decomposition upon treatment with TFA/DCM or TFA/H_2O 1:1. Even in 5% TFA in DCM, most of the *N,N'*-diEtom-substituted dipeptide is converted within one minute to several intermediate products (presumably *N*-CH_2OH-substituted compounds), which further degrade to Alloc-Leu-Gly-OPnb at a slower rate (see Supporting Information). These results indicate that backbone *N*-Aom groups in peptides can be removed by acid treatment. The formaldehyde released may be trapped with appropriate scavengers to prevent undesired side-reactions.

3. Summary and conclusions

Several *NH*-protecting groups for the peptide backbone are reported, such as 2-hydroxy-4-methoxybenzyl (Hmb-),[11] 2,4-dimethoxybenzyl (Dmb),[12] dicyclopropylmethyl (Dcm-),[13] 3,4-ethylenedioxy-2-thenyl (EDOTn),[14] 1-methyl-3-indolylmethyl (MIM),[14] or pseudoprolines (only for Thr, Ser, and Cys).[15] However, none of them meets the key parameters that would allow for general and routine application. These parameters are: easy incorporation into the peptide chain, to work well with all (or at least many) amino acids, and to be cleavable under mild conditions. In this study we could show that backbone *N*-alkoxymethyl (*N*-Aom) groups are compatible with Fmoc/tBu SPPS conditions, but the main issue for their application as protectants is the difficulty to incorporate them into the peptide backbone and the limitation to *N*-Gly. Despite this issue, we observed that backbone *N*-deprotection proceeds already under mild acidic conditions, which is a unique feature among the known peptide backbone protecting groups. For this reason, we think that *N*-Aom groups hold significant potential as protecting groups for the peptide bond.

Furthermore, we found that Fmoc-(*N*-Aom) amino acids are straightforward to obtain by *N*-chloromethylation of an Fmoc-amino acid ester, followed by nucleophilic reaction with an alcohol. This may be a valuable alternative to the use of alkoxymethyl ethers for amide and/or carbamate protection of other compounds, as long as acidic conditions are tolerated.

Acknowledgements

This work was partially supported by CICYT (CTQ2012-30930), the Generalitat de Catalunya (2009SGR 1024), and IRB-Barcelona. Ana I. Fernández-Llamazares thanks Ministerio de Educación y Ciencia for a FPU fellowship.

Supplementary material

Supplementary data associated with this article (synthetic methods, characterization data, relevant HPLC and HPLC-MS chromatograms, and NMR spectra of selected compounds) can be found, in the online version, at http://dx.doi.org/xxx.

References and notes

[1] *Houben-Weyl Methods in organic chemistry E22, Synthesis of peptides and peptidomimetics*; Goodman, M.; Felix, A.; Moroder, L.; Toniolo, C., Eds.; Thieme: Stuttgart, New York, 2002-2003; Vol. 1 (E22a), ch. 2, pp 338-339.

[2] Kocienski, P. J. *Protecting groups*; Georg Thieme Verlag: Stuttgart, New York, 2000; ch. 8, pp 561-565.

[3] Bartl, R.; Frank, R. International patent WO 92/22566, 1992.

[4] Sun, H.; Martin, C.; Kesselring, D.; Keller, R.; Moeller, K. D. *J. Am. Chem. Soc.* **2008**, *128*, 13761-13771.

[5] Spengler, J.; Burger, K. *Synthesis* **1998**, 67-70.

[6] Spengler, J.; Burger, K. *J. Chem. Soc., Perkin Trans. 1* **1998**, 2091-2093.

[7] Schedel, H.; Burger, K. *Monatsch. Chem.* **2000**, *131*, 1011-1018.

[8] *N*-chloromethyl and *N*-Aom-amino acids show two sets of signals in their NMR spectra due to the formation of rotamers around the *N*-alkylated amide bond.

[9] Kocsis, L.; Bruckdorfer, T.; Orosz, G. *Tetrahedron Lett.* **2008**, *49*, 7015-7017.

[10] a) Falb, F.; Yechezkel, T.; Salitra, Y.; Gilon, C. *J. Pept. Res.* **1999**, *53*, 507-517. b) Thern, B., Rudolph, J.; Jung, G. *Tetrahedron Lett.* **2002**, *43*, 5013-5016.

[11] a) Hyde, C.; Johnson, T.; Owen, D.; Quibell, M.; Sheppard, R. C. *Int. J. Pept. Protein. Res.***1994**, *43*, 431-40. b) Johnson, T.; Quibell, M.; Owen, D.; Sheppard, R. C. *J. Chem. Soc., Chem. Commun.* **1993**, 369-372.

[12] a) Johnson, T.; Packman, L. C.; Hyde, C. B.; Owen, D.; Quibell, M. *J. Chem. Soc. Perkin. Trans. 1* **1996**, 719-728.

[13] Carpino, L. A.; Nasr, D.; Abdel-Maksoud, A. A.; El-Faham, A.; Ionescu, D.; Henklein, P.; Wenschuh, H.; Beyermann, M.; Krause, E.; Bienert, M. *Org. Lett.* **2009**, *11*, 3718-3721.

[14] Isidro-Llobet, A.; Just-Baringo, X.; Álvarez, M.; Albericio, F. *Biopolymers,* **2008**, *90*, 444-449.

[15] a) Haack, T.; Mutter, M. *Tetrahedron Lett.* **1992**, *33*, 1589-1592. b) Mutter, M.; Nefzi, A.; Sato, T.; Sun, X.; Wahl, F.; Wuhr, T. *Pept. Res.* **1995**, *8*, 145-153. c) Wöhr, T.; Wahl, F.; Nefzi, A.; Rohwedder, B.; Sato, T.; Sun, X.; Mutter, M. *J. Am. Chem. Soc.* **1996**, *118*, 9218-9227.

[1] N. Sewald and H.-D. Jakubke. *Peptides: chemistry and biology*, 2nd edition, Wiley-VCH Verlag GmbH & Co, Weinheim (Germany), **2009**.

[2] For detailed statistics about peptide therapeutics, the Peptide Therapeutics Foundation publishes a bi-annual report entitled: "Development Trends for Peptide Therapeutics", which can be found on their website at: http://www.peptidetherapeutics.org/peptide-therapeutics-foundation.htm.

[3] (a) P. Vlieghe, V. Lisowski, J. Martinez and M. Khrestchatisky. Synthetic therapeutic peptides: science and market. *Drug Discov. Today*, **2010**, *15*, 40-46. (b) D. J. Craik, D. Fairlie, Spiros Liras and D. Price. The future of peptide-based drugs. *Chem. Biol. Drug. Des.* **2013**, *81*, 136-147.

[4] S. Royo, K. Gaus and N. Sewald. Synthesis of chemically modified bioactive peptides: recent advances, challenges and developments for medicinal chemistry. *Future Med. Chem.* **2009**, *1*, 1289-1310.

[5] (a) R. Finking and M. A. Marahiel. Biosynthesis of nonribosomal peptides. *Annu. Rev. Microbiol.* **2004**, *58*, 453-488. (b) S. A. Sieber and M. A. Marahiel. Molecular mechanisms underlying nonribosomal peptide synthesis: approaches to new antibiotics. *Chem. Rev.* **2005**, *105*, 715-738.

[6] (a) J. Chatterjee, C. Gilon, A. Hoffman and H. Kessler. *N*-methylation of peptides: a new perspective in medicinal chemistry. *Acc. Chem. Res.* **2008**, *10*, 1331-1342. (b) J. Chatterjee, F. Rechenmacher and H. Kessler. *N*-Methylation of peptides and proteins: an important element for modulating biological functions. *Angew. Chem., Int. Ed.* **2013**, *52*, 254-269.

[7] C. Gilon, D. Halle, M. Chorev, Z. Selinger and G. Byk. Backbone cyclization: a new method for conferring conformational constraint on peptides. *Biopolymers* **1991**, *31*, 745-750.

[8] C. A. Olsen. Peptoid-peptide hybrid backbone architectures. *ChemBioChem*, **2010**, *11*, 152-160.

[9] J. G. Beck, J. Chatterjee, B. Laufer, M. U. Kiran, A. O. Frank, S. Neubauer, O. Ovadia, S. Greenberg, C. Gilon, A. Hoffman and H. Kessler. Intestinal permeability of cyclic peptides: common key backbone motifs identified. *J. Am. Chem. Soc.* **2012**, *134*, 12125-12133.

[10] For methods for the chemical synthesis of *N*-Me amino acid derivatives, refer to: S. Sagan, P. Karoyan, O. Lequin, G. Chassaing and S. Lavielle. *N*- and *C*α-methylation in biologically active peptides: synthesis, structural and functional aspects. *Curr. Med. Chem.* **2004**, *11*, 2799-2822.

[11] E. Biron and H. Kessler. Convenient synthesis of *N*-methylamino acids compatible with Fmoc solid-phase peptide synthesis. *J. Org. Chem.* **2005**, *70*, 5183-5189.

[12] S. C. Miller and T. S. Scanlan. Site-selective *N*-methylation of peptides on solid support. *J. Am. Chem. Soc.* **1997**, *119*, 2301-2302.

[13] E. Biron, J. Chatterjee and H. Kessler. Optimized selective *N*-methylation of peptides on solid support. *J. Pept. Sci.* **2006**, *12*, 213-219.

[14] J. F. Reichwein and R. M. J. Liskamp. Site-specific *N*-alkylation of peptides on the solid phase. *Tetrahedron Lett.* **1998**, *39*, 1243-1246.

[15] (a) H. Kessler. Detection of hindered rotation and inversion by NMR spectroscopy. *Angew. Chem., Int. Ed.* **1970**, *9*, 219-235. (b) P. Manavalan and F. A. Momany. Conformational energy studies on *N*-methylated analogs of thyrotropin releasing hormone, enkephalin, and luteinizing hormone-releasing hormone. *Biopolymers* **1980**, *19*, 1943-1973. (c) H. Kessler, U. Anders and M. Schudok. An unexpected *cis* peptide bond in the minor conformation of a cyclic hexapeptide containing only secondary amide bonds. *J. Am. Chem. Soc.* **1990**, *112*, 5908-5912.

[16] (a) F. Piriou, K. Lintner, S. Fermandjian, P. Fromageot, M. C. Khosla, R. R. Smeby and F. M. Bumpus. Amino acid side chain conformation in angiotensin II and analogs: correlated results of circular dichroism and [1]H nuclear magnetic resonance. *Proc. Natl. Acad. Sci. U.S.A.* **1980**, *77*, 82-86. (b) A. C. Bach, C. J. Eyermann, J. D. Gross, M. J. Bower, R. L. Harlow, P. C. Weber and W. F. Degrado. Structural studies of a family of high affinity ligands for GP IIb/IIIa. *J. Am. Chem. Soc.* **1994**, *116*, 3207-3219.

[17] Several examples are reviewed in: (a) S. Sagan, P. Karoyan, O. Lequin, G. Chassaing and S. Lavielle. *N*- and *C*α-methylation in biologically active peptides: synthesis, structural and functional aspects. *Curr. Med. Chem.* **2004**, *11*, 2799-2822. [ref. 10] (b) J. Chatterjee, C. Gilon, A. Hoffman and H. Kessler. *N*-methylation of peptides: a new perspective in medicinal chemistry. *Acc. Chem. Res.* **2008**, *10*, 1331-1342. [ref. 5a] (c) J. Chatterjee, F. Rechenmacher and H. Kessler. *N*-Methylation of peptides and proteins: an important element for modulating biological functions. *Angew. Chem., Int. Ed.* **2013**, *52*, 254-269. [ref. 5b]

[18] (a) O. Ovadia, S. Greenberg, J. Chatterjee, B. Laufer, F. Opperer, H. Kessler, C. Gilon and A. Hoffman. The effect of multiple *N*-methylation on intestinal permeability of peptides. *Mol. Pharmaceutics* **2011**, *8*, 479-487. (b) Q. G. Dong, Y. Zhang, M. S. Wang, J. Feng, H. H. Zhang, Y. G. Wu, T. J. Gu, X. H. Yu, C. L. Jiang, Y. Chen, W. Li and W. Kong. Improvement of enzymatic stability and intestinal permeability of deuterohemin-peptide conjugates by specific multi-site *N*-methylation. *Amino Acids* **2012**, *43*, 2431-2441.

[19] (a) E. Biron, J. Chatterjee, O. Ovadia, D. Langenegger, J. Brueggen, D. Hoyer, H. A. Schmid, R. Jelinek, C. Gilon, A. Hoffman and H. Kessler. Improving oral bioavailability of peptides by multiple *N*-methylation: somatostatin analogues. *Angew. Chem. Int. Ed.* **2008**, *47*, 2595-2599. (b) T. R. White, C. M. Renzelman, A. C. Rand, T. Rezai, C. M. McEwen, V. M. Gelev. On-resin *N*-methylation of cyclic peptides for discovery of orally bioavailable scaffolds. *Nat. Chem. Biol.* **2011**, *7*, 810-817.

[20] (a) R. A. Conradi, A. R. Hilgers, N. F. H. Ho and P. S. Burton. The influence of peptide structure on transport across Caco-2 cells. II. Peptide bond modification which results in improved intestinal permeability. *Pharm. Res.* **1992**, *9*, 435-439. (b) P. S. Burton, R. A. Conradi, N. F. H. Ho, A. R. Hilgers and R. T. Borchardt. How structural features influence the biomembrane permeability of peptides. *J. Pharm. Sci.* **1996**, *85*, 1336-1340.

[21] J. Chatterjee, D. F. Mierke and H. Kessler. Conformational preference and potential templates of *N*-methylated cyclic pentaalanine peptides. *Chem. Eur. J.* **2008**, *14*, 1508-1517.

[22] B. Laufer, J. Chatterjee, A. O. Frank and H. Kessler. Can *N*-methylated amino acids serve as substitutes for prolines in conformational design of cyclic pentapeptides? *J. Pept. Sci.* **2009**, *15*, 141-146.

[23] (a) J. Chatterjee, O. Ovadia, G. Zahn. *et al.* Multiple *N*-methylation by a designed approach enhances receptor selectivity. *J. Med. Chem.* **2007**, *50*, 5878-5881. (b) J. Chatterjee, O. Ovadia, G. Zahn, L. Marinelli, A. Hoffman, C. Gilon and H. Kessler. *N*-Methylated sst2 selective somatostatin cyclic peptide analogue as potent candidate for treating neurogenic inflammation. *ACS Med. Chem. Lett.* **2011**, *2*, 509-514.

[24] L. Doedens, F. Opperer, M. Cai, J. G. Beck, M. Dedek, E. Palmer, V. Hruby and H. Kessler. Multiple *N*-methylation of MT-II backbone amide bonds leads to melanocortin receptor subtype hMC1R selectivity: pharmacological and conformational studies. *J. Am. Chem. Soc.* **2010**, *132*, 8115-8128.

[25] O. Ovadia, S. Greenberg, B. Laufer, C. Gilon, A. Hoffman and H. Kessler. Improvement of drug-like properties of peptides: the somatostatin paradigm. *Expert Opin. Drug Discov.* **2010**, *5*, 655-671.